

# Beyond the Visible World

Bridging macroscopic and paleohistopathological techniques in the study of periosteal new bone formation in human skeletal remains

A Thesis Submitted to the University of Coimbra in Partial Fulfillment of the Requirements for the Degree of Doctor in Biological Anthropology with supervision of:

**Dr. Ana Luísa Santos**

Department of Life Sciences  
University of Coimbra, Portugal



UNIVERSIDADE DE COIMBRA

**Dr. Anne Keenleyside**

Department of Anthropology  
Trent University, Peterborough  
Ontario, Canada



**Sandra Sofia Domingos Assis**

Department of Life Sciences  
Faculty of Sciences and Technology  
University of Coimbra  
Coimbra |2013

## **COVER**

Histological detail of the pleural-endosteal surface of the 5<sup>th</sup> left rib sample collected from the individual Sk. 332 (Identified Collection of the Bocage Museum, Lisbon, Portugal) who died of pulmonary tuberculosis (Nikon Eclipse 80i® polarized light, magnification 100x). Visceral surface of the rib exhibiting erosive and proliferative lesions and macroscopic view of the thin section prepared.

## TABLE OF CONTENTS

---

LIST OF TABLES	vii
LIST OF FIGURES	xi
ABSTRACT / KEY-WORDS	xxvii
SUMÁRIO / PALAVRAS-CHAVE	xxxix
ACKNOWLEDGEMENTS	xxxv
<b>CHAPTER 1</b>	<b>1</b>
<b>1. INTRODUCTION: A SHORT OVERVIEW</b>	<b>3</b>
1.1. Paleohistopathology: bone disease diagnosis and the challenges of paleopathology	6
1.2. Objectives	13
<b>CHAPTER 2</b>	<b>15</b>
<b>2. PALEOHISTOPATHOLOGY: A LITERATURE REVIEW</b>	<b>17</b>
2.1. Concepts and historical endeavor	17
2.2. Paleohistopathology today: a systematic review of the published data	23
2.3. Limitations and achievements of paleohistopathology	56
<b>CHAPTER 3</b>	<b>61</b>
<b>3. INCURSION TO THE BIOLOGY OF BONE AND DISEASE</b>	<b>63</b>
3.1. The human skeleton: an invisible framework	64
3.1.1. The nature of bone: a double composition with an organic and inorganic substrate	66
3.1.2. The texture of bone: a woven or lamellar arrangement of the matrix	67
3.1.3. The structure of bone: osteons, arch-like bone structures and cell components	69
3.1.4. The microarchitecture of bone: bone dynamics and tissue envelopes	78
3.1.5. The macroarchitecture of bone: a perfect scaffold	84
3.1.6. The human ribs: gross anatomy, development and microstructure	85
3.2. Periosteal new bone formation (PNBF): bony changes at the surface	91
3.2.1. PNBF in the clinical literature	91
3.2.1.1. A Definition	91
3.2.1.2. Mechanisms of regulation and pathophysiology	91
3.2.1.3. Classification and types	108
3.2.2. PNBF in the paleopathological literature	114
3.2.2.1. Macroscopic and histological manifestations	114

<b>CHAPTER 4</b>	<b>123</b>
<b>4. MATERIALS AND METHODS</b>	<b>125</b>
4.1. Material	125
4.1.1. Macroscopic Analysis	125
4.1.2. Paleohistological Analysis	129
4.1.2.1. Identified Bone Samples	130
4.1.2.2. Archaeological Bone Samples	132
4.2. Methods	134
4.2.1. Macroscopic Analysis	134
4.2.2. Paleohistological Analysis	135
<b>CHAPTER 5</b>	<b>145</b>
<b>5. RESULTS</b>	<b>147</b>
5.1. Macroscopic Analysis	147
5.1.1. Representativeness and Preservation of the Skeletal Sample	148
5.1.2. Periosteal New Bone Formation (PNBF): Gross Morphology	152
5.1.2.1. General Distribution by Sex and Age at Death	152
5.1.2.2. Distribution by Cause of Death	152
5.1.2.3. Distribution Pattern within the Skeleton	153
5.1.2.3.1. Distribution of PNBF in the Ribs	156
5.1.2.3.2. Distribution of PNBF in the Appendicular Skeleton	164
5.2. Paleohistopathological Analysis	181
5.2.1. Group 1- Tuberculosis (TB)	181
5.2.2. Group 2 – Non-Tuberculosis (non-TB)	191
5.2.3. Group 3 – Other conditions	196
5.2.4. Group 4 – Archaeological samples	204
<b>CHAPTER 6</b>	<b>211</b>
<b>6. DISCUSSION</b>	<b>213</b>
6.1. Macroscopic Analysis	213
6.1.1. Chest Wall: Ribs	213
6.1.2. Appendicular skeleton	222
6.2. Histological Analysis	239
<b>CHAPTER 7</b>	<b>261</b>
<b>7. CONCLUSION</b>	<b>263</b>

---

<b>CHAPTER 8</b>	<b>271</b>
<b>8. REFERENCES</b>	273
<b>APPENDICES</b>	<b>337</b>



## LIST OF TABLES

---

<b>Table 2.1:</b> List of selected journals used for analysis.	24
<b>Table 2.2:</b> Summary of paleohistopathological studies in the literature.	27
<b>Table 3.1:</b> Different types of bone and their main components.	68
<b>Table 3.2:</b> Summary of the main morphological changes observed on ribs during growth and development.	88
<b>Table 3.3:</b> Summary of the microstructural changes observed on ribs during growth and development.	89
<b>Table 3.4:</b> Regulators of bone metabolism.	93
<b>Table 3.5:</b> List of conditions that frequently manifests new bone deposition.	104
<b>Table 3.6:</b> Different types of abnormal bone formation and resorption.	115
<b>Table 3.7:</b> Different types of new bone abnormalities observed at microscopic level.	117
<b>Table 3.8:</b> List of paleopathological conditions that frequently manifests new bone deposition.	118
<b>Table 4.1:</b> Distribution of individuals by cause of death, sex and age at death intervals.	127
<b>Table 4.2:</b> Maximum, minimum and mean age at death values by cause of death and sex groups.	127
<b>Table 4.3:</b> Grade system used to rank periosteal bone lesions by location and type.	135
<b>Table 5.1:</b> Distribution of the total number of ribs observed by side and for the overall sample.	148
<b>Table 5.2:</b> Number of bones of the appendicular skeleton observed by side and in the overall sample.	150
<b>Table 5.3:</b> Distribution of cases of periosteal new bone formation (PNBF) by sex and age at death.	152
<b>Table 5.4:</b> Distribution of individuals affected and unaffected by PNBF according to the cause of death.	153
<b>Table 5.5:</b> Distribution of individuals affected with PNBF by age and anatomical location.	154
<b>Table 5.6:</b> Distribution of PNBF by cause of death and anatomical location.	155
<b>Table 5.7:</b> Frequency and average number of ribs affected with PNBF by individual, age group and cause of death.	156
<b>Table 5.8:</b> Number of rib lesions by age and cause of death.	158
<b>Table 5.9:</b> Distribution of ribs affected with PNBF by side and cause of death.	159
<b>Table 5.10:</b> Distribution of the lesions observed by rib segment and cause of death.	161
<b>Table 5.11:</b> Distribution of the type of lesions observed in the ribs by cause of death.	163
<b>Table 5.12:</b> Distribution of the bones affected with PNBF in the upper and lower limbs by side and total sample.	165

<b>Table 5.13:</b> Distribution of periosteal reactions in the bones from the upper and lower limb of the individuals affected by age groups.	167
<b>Table 5.14:</b> Distribution of periosteal reactions in the bones from the upper and lower limb of the individuals affected by cause of death.	168
<b>Table 5.15:</b> Distribution of individuals affected with PNBf by cause of death.	173
<b>Table 5.16:</b> Distribution of individuals affected with PNBf in the bones of the lower limb by age range.	174
<b>Table 5.17:</b> Distribution of individuals affected with PNBf in the bones of the lower limb by cause of death.	175
<b>Table 5.18:</b> Distribution of individuals affected with PNBf by cause of death.	176
<b>Table 5.19:</b> Distribution of the type of bone lesions by cause of death (upper limb bones).	178
<b>Table 5.20:</b> Distribution of the type of bone lesions by cause of death (lower limb bones).	180
<b>Table 5.21:</b> Summary of the histological analysis of Group 1 samples.	190
<b>Table 5.22:</b> Summary of the histological analysis of Group 2 samples.	195
<b>Table 5.23:</b> Summary of the histological analysis of Group 3 samples.	203
<b>Table 6.1:</b> Summary of the literature review on cases of chest wall tuberculosis with rib lesions.	215
<b>Table 6.2:</b> Comparative analysis of the distribution of PNBf on ribs of tuberculous individuals from different collections.	219
<b>Table 6.3:</b> Frequency and average age at death of the individuals affected by PNBf in the upper and lower limb bones by cause of death.	223



## LIST OF FIGURES

---

<b>Figure 2.1:</b> Results of the systematic literature review.	25
<b>Figure 2.2:</b> Distribution of the 95 paleohistopathological papers by interval of publication.	49
<b>Figure 2.3:</b> Distribution of the 95 published papers by type of study.	50
<b>Figure 2.4:</b> Distribution of the 95 papers by type of histological study.	51
<b>Figure 2.5:</b> Distribution of the studies recorded by paleopathological condition analysed.	51
<b>Figure 3.1:</b> The five levels of organization of the structure of a long bone.	65
<b>Figure 3.2:</b> Micrography of a rib section of an adult male [SK.1235] from the Lisbon Bocage Museum.	71
<b>Figure 3.3:</b> Schematic diagram of the genesis of osteoblast and osteoclast cells in their role in bone formation and resorption.	73
<b>Figure 3.4:</b> Micrography of a rib sample of an adult female [Sk. 119] from the Lisbon Bocage Museum.	76
<b>Figure 3.5:</b> Classical scheme of bone remodelling process comprising the four stages of cell interplay.	82
<b>Figure 3.6:</b> Example of the morphology of a typical human adult rib.	86
<b>Figure 3.7:</b> Rib cross-section illustrating the location of the cutaneous and pleural surfaces.	87
<b>Figure 3.8:</b> Schematic representation of the three phases of bone fracture healing.	96
<b>Figure 3.9:</b> Schematic representation of bone canaliculi development by woven and lamellar osteocytes during fracture healing.	98
<b>Figure 3.10:</b> The various types of periosteal new bone formations.	113
<b>Figure 4.1:</b> Sample distribution by sex and age at death.	126
<b>Figure 4.2:</b> Storing of the human identified collection at Bocage Museum.	I
<b>Figure 4.3:</b> Chronological distribution of the individuals who show a complete record for birth and death dates.	128
<b>Figure 4.4:</b> Geographic distribution of the sample by Portuguese districts.	129
<b>Figure 4.5:</b> Anatomical distribution of the bone samples collected.	131
<b>Figure 4.6:</b> Bone sectioning at the sternal end of a 5 <sup>th</sup> left rib (Sk. 1383).	I
<b>Figure 4.7:</b> Distal extremity of the right fibula from the skeleton 1534-A.	ii
<b>Figure 4.8:</b> Distribution of bone samples by cause of death groups.	131
<b>Figure 4.9:</b> Examples of bone specimens collected from the three archaeological assemblages.	li
<b>Figure 4.10:</b> Summary of all procedures used in the production of bone histological sections for microscopic analysis.	136
<b>Figure 4.11:</b> Material used to collect the bone samples.	lii
<b>Figure 4.12:</b> Material used to clean the bone samples.	lii
<b>Figure 4.13:</b> Distinct steps and supplies required to embed the bone samples.	lv
<b>Figure 4.14:</b> Sequence of actions taken to sectioning the bone blocks.	v
<b>Figure 4.15:</b> Steps and supplies required to polish the slide samples.	vi
<b>Figure 4.16:</b> Some requirements used during flipping and polishing.	vii
<b>Figure 4.17:</b> Cover slip procedures.	viii

<b>Figure 4.18:</b> Microscope used for sample observation.	Ix
<b>Figure 5.1:</b> Classification of the ribs according to four grades of preservation.	149
<b>Figure 5.2:</b> Lower left ribs from the SK. 488 (male, 26 years old) showing severe postmortem damage at the visceral surface.	X
<b>Figure 5.3:</b> Classification of the bones of the upper and lower limb according to four grades of preservation.	151
<b>Figure 5.4:</b> Some postmortem destruction of the cortical surface observed in the lower extremity of the right humerus of the Sk. 684 (male, 16 years old).	X
<b>Figure 5.5:</b> Massive cortical destruction observed at the surface of the right bones of the hand of the Sk. 1227 (male, 21 years old).	xi
<b>Figure 5.6:</b> Postmortem destruction of the lower extremities of the tibiae of the SK. 1145 (male, 69 years old).	xi
<b>Figure 5.7:</b> Number and frequency of individuals affected with PNBf by anatomical location.	154
<b>Figure 5.8:</b> Number of ribs with PNBf in individuals with varying causes of death.	157
<b>Figure 5.9:</b> Periosteal new bone formation extending from the vertebral end into the shaft of the 6 <sup>th</sup> to 9 <sup>th</sup> left ribs of the SK. 1227, an young male (21 y.o.) who died of TB infection.	Xii
<b>Figure 5.10:</b> New bone deposition alongside the visceral surface of the 6 <sup>th</sup> to 9 <sup>th</sup> right ribs of the SK. 270, an adult male (50 y.o.) who died of bronchopneumonia.	Xii
<b>Figure 5.11:</b> Massive periosteal reaction affecting almost the entire rib cage of the Sk. 457, an adult male (66 y.o.) who died of rectum neoplasm.	Xiii
<b>Figure 5.12:</b> Distribution of ribs affected by PNBf (left and right ribs combined) by their anatomical order in the rib cage.	158
<b>Figure 5.13:</b> Distribution of rib lesions by side and anatomical location in the rib cage.	159
<b>Figure 5.14:</b> Distribution of rib lesions by bony segment and anatomical order in the rib cage.	162
<b>Figure 5.15:</b> New bone formation with a compact appearance at the visceral surface of the 4 <sup>th</sup> right rib of the Sk. 1299, an adult male (26 y.o.) who died from TB infection.	xiii
<b>Figure 5.16:</b> Mixture of reactive and erosive lesions at the visceral surface of the 6 <sup>th</sup> left rib (vertebral end) of the Sk. 470, an elder adult male (68 y.o.) who died from tuberculous infection.	xiv
<b>Figure 5.17:</b> Erosive nodule associated with new bone formation of woven type at the sternal end of the 11 <sup>th</sup> right rib of the young female skeleton (SK. 1583, 9 y.o), who died of tuberculosis.	xiv
<b>Figure 5.18:</b> Thoracic vertebrae (4 <sup>th</sup> -12 <sup>th</sup> ) of the Sk. 1583.	xv
<b>Figure 5.19:</b> Lumbar vertebrae of the young female skeleton 314 (20 y.o.) who died of Pott's disease.	xv
<b>Figure 5.20:</b> Distribution of the ribs affected by type of new bone formed and anatomical order in the rib cage.	164
<b>Figure 5.21:</b> Distribution of the individuals affected with PNBf by bone type (upper and lower limb).	166

<b>Figure 5.22:</b> Distribution of the individuals affected with PNBf by the bones from the upper limb and laterality.	169
<b>Figure 5.23:</b> Symmetric new bone deposition with a smooth and porous appearance at the lower extremity of the radius of the Sk. 1098, an elder female (78 y.o.) who died of bronchopneumonia.	Xvi
<b>Figure 5.24:</b> Symmetric bone deposition of woven type at the lower lateral portion of the humerus of the SK. 8, a young adult female (18 y.o.) who died of acute tuberculosis.	Xvi
<b>Figure 5.25:</b> Distribution of individuals affected with PNBf in the lower limb bones by side.	170
<b>Figure 5.26:</b> Symmetric lesions mixing woven and lamellar bone observed on distinct segments of the tibiae of the Sk. 1192, an adult male (56 y.o.) who died of pulmonary tuberculosis.	Xvii
<b>Figure 5.27:</b> 5 <sup>th</sup> metatarsal bones of the Sk. 1604, an adult female (45 y.o.) who died of TB infection.	xvii
<b>Figure 5.28:</b> Diffuse unilateral lesions more severe at the medial lower portion of the left tibia of the Sk. 307, an adult male (69 y.o.) who died of septicaemia.	xviii
<b>Figure 5.29:</b> Distribution of individuals with two or less affected symmetrical bones by cause of death.	170
<b>Figure 5.30:</b> New bone formation observed in the lower limb bones of the Sk. 507, an adult male (51 y.o.) who died of pulmonary emphysema.	Xix
<b>Figure 5.31:</b> New bone deposition in the ulnae of the SK.491, an adult male (66 y.o.) who died of syphilis.	Xix
<b>Figure 5.32:</b> Tibiae of the Sk. 491 showing slight expansion and longitudinal striation partially remodelled at the upper middle portion.	Xx
<b>Figure 5.33:</b> Symmetric new bone formation observed at the lower extremity of the leg bones of the Sk. 35, an adult male (47 y.o.) who died of leprosy.	Xx
<b>Figure 5.34:</b> Diffuse new bone formation observed in the tibiae of the Sk. 1484, an adult male (73 y.o.) who died of gastric ulcer.	Xxi
<b>Figure 5.35:</b> Periosteal reaction located at the middle lower third of the shaft of the fibulae of the Sk. 1484.	Xxi
<b>Figure 5.36:</b> Distribution of individuals affected with PNBf of the upper limb bones, according to the extent of lesions.	172
<b>Figure 5.37:</b> Distribution of individuals affected with PNBf in the lower limb bones, according to the extent of lesions.	174
<b>Figure 5.38:</b> Distribution of the type of bone response in the bones from individuals affected (upper limb bones).	177
<b>Figure 5.39:</b> Distribution of the type of bone response in the bones from individuals affected (lower limb bones).	179
<b>Figure 5.40:</b> Right innominate bone of the adult male Sk. 1298 (67 y.o.) who died of prostate cancer.	Xxii
<b>Figure 5.41:</b> Rib sample collected from the Sk. 1243 individual and macroscopic view of the thin section prepared.	Xxiii
<b>Figure 5.42:</b> Microscopic view of the rib thin section under polarized light.	Xxiii

<b>Figure 5.42 A:</b> Close-up of a segment of the rib thin section under polarized light showing well-preserved Haversian systems and interstitial lamellae, as well as endosteal resorption spaces or Howship’s lacunae.	Xxiii
<b>Figure 5.42 A1:</b> Close-up of the previous image under transmitted light showing the cortical bone composed of secondary osteons, interstitial lamellar and osteocyte lacunae.	Xxiv
<b>Figure 5.42 B:</b> Close-up of a middle-section of the rib sample under polarized light showing the pleural and the cutaneous surfaces bridged by trabeculae.	xxiv
<b>Figure 5.43:</b> Rib sample collected from the Sk. 102 individual and macroscopic view of the thin section prepared.	xxv
<b>Figure 5.44:</b> Microscopic view of the rib thin section under polarized light showing well defined rib contours, with exception for the damaged inferior border.	xxv
<b>Figure 5.44 A:</b> Close-up of a segment of the rib thin section under transmitted light exhibiting the upper corner with a row of well-preserved osteons in the pleural surface.	xxvi
<b>Figure 5.44 A1:</b> Detail of the previous picture under transmitted light showing a well defined osteon and a denser layer of periosteal bone.	xxvi
<b>Figure 5.44 B:</b> Close-up of a segment of the rib thin section under polarized light showing the cortical bone formed by multiple rows of secondary osteons and interstitial lamellae.	xxvii
<b>Figure 5.44 B1:</b> Detail of the periosteal new bone under transmitted light that partially submerged a cortical osteons.	xxvii
<b>Figure 5.44 C:</b> Close-up of a middle segment of the rib thin section under polarized light exhibiting the pleural cortex with multiple rows of Haversian systems and interstitial lamellae.	xxviii
<b>Figure 5.44 D:</b> Another close-up of a middle segment of the rib thin section under polarized light showing a thinner cortex in relation to the new periosteal bone.	xxviii
<b>Figure 5.44 D1:</b> Detail of the periosteal new bone under polarized light showing spaces of bone resorption that separates the newly formed bone from the cortex.	xxix
<b>Figure 5.45:</b> Rib sample collected from the individual Sk. 154 and macroscopic view of the thin section prepared.	xxx
<b>Figure 5.46:</b> Microscopic view of the rib thin section under polarized light.	xxx
<b>Figure 5.46 A:</b> Close-up of an upper segment of the rib cortex under polarized light showing multiple rows of secondary osteons, interstitial lamellae and Haversian canals.	xxxi
<b>Figure 5.46 B:</b> Close-up of another segment of the rib cortex under polarized light showing some rows of osteons and interstitial lamellae and enlarged Haversian canals.	xxxi
<b>Figure 5.46 B1:</b> Detail of the previous image under polarized light showing an enlarged Haversian canal embedded in interstitial lamellae.	xxxii
<b>Figure 5.46 B2:</b> Detail of the new periosteal bone under polarized light showing the linear orientation of the primary lamellae and osteocytes lacunae.	xxxii
<b>Figure 5.46 C:</b> Close-up of a segment of the rib thin section under polarized light exhibiting the cortical bone with Haversian systems, interstitial lamellae and osteon canals.	Xxxiii

<b>Figure 5.46 C1:</b> Detail of the periosteal new bone under polarized light showing several layers or levels of deposition intersected by primary vascular canals.	Xxxiii
<b>Figure 5.46 D:</b> Magnification of a segment of the lower portion of the thin section under polarized light showing multiple layers of new bone deposition, intersected by primary vascular canals.	Xxxiv
<b>Figure 5.46 E:</b> Detail of the lower portion of the thin section under polarized light showing a clear interface between the newly formed bone and the original cortex formed by osteoclastic resorption.	Xxxiv
<b>Figure 5.46 F:</b> Close-up of a segment of the cutaneous surface under polarized light showing several enlarged Haversian canals and areas of resorption.	Xxxv
<b>Figure 5.46 F1:</b> Detail of the cutaneous cortical bone under polarized light showing enlarged osteons canals.	Xxxv
<b>Figure 5.47:</b> Rib sample collected from the individual Sk. 332 and macroscopic view of the thin section prepared.	Xxxvi
<b>Figure 5.48:</b> Microscopic view of the rib thin section under polarized light.	Xxxvi
<b>Figure 5.48 A:</b> Close-up of a segment of the pleural surface under polarized light showing the endosteal and periosteal layers and two well-preserved osteons with their Maltese crosses.	Xxxvii
<b>Figure 5.48 B:</b> Close-up of a middle segment of the rib under polarized light showing the bone cortex composed of secondary osteons and interstitial lamellae as well as multiple foci of bone resorption (Howship's lacunae).	Xxxvii
<b>Figure 5.48 B1:</b> Detail of a segment of the pleural surface under polarized light highlighting the lack of organization of the fibres of the periosteal new bone.	Xxxviii
<b>Figure 5.48 C:</b> Close-up of a middle segment of the rib cortex under polarized light showing dense lamellae occupying an intracortical position bellow the new periosteal layer.	xxxviii
<b>Figure 5.48 C1:</b> Detail of the intracortical mature lamellae under polarized light exhibiting several Howship's lacunae.	xxxix
<b>Figure 5.48 C2:</b> Detail of a segment of the rib thin section under polarized light showing endosteal and intracortical foci of bone resorption.	xxxix
<b>Figure 5.48 D:</b> Close-up of another segment under polarized light showing a proliferation of osteolytic foci in the endosteal surface of the cortical bone and at the periosteal level.	xl
<b>Figure 5.49:</b> Close-up of a segment of another rib thin section from the Sk. 332 sample under polarized light showing Howship's lacunae on both periosteal and endosteal surfaces.	xl
<b>Figure 5.50:</b> Close-up of a segment of the midsection of the pleural-endosteal surface under polarized light exhibiting multiple foci of bone resorption in the rib cortex and at the endosteal surface.	xli
<b>Figure 5.50 A:</b> Detail of the previous figure under polarized light showing the cortex of the rib diggested by several Howship's lacunae.	xli
<b>Figure 5.51:</b> Rib fragment sampled from the Sk. 470 individual and macroscopic view of the thin section prepared.	xlii
<b>Figure 5.52:</b> Microscopic view of the rib thin section under transmitted light.	xlii

<b>Figure 5.52 A:</b> Close-up of a middle segment of the rib sample under polarized light exhibiting a thick layer of new bone deposited upon the cortical bone.	xliii
<b>Figure 5.52 A1:</b> Detail of the previous image under polarized light showing the dense and haphazard appearance of the layer of new bone.	xliii
<b>Figure 5.52 A1.1:</b> Detail from the previous image under polarized light showing the absence of a line of demarcation between the periosteal new bone and the cortex.	xliv
<b>Figure 5.52 A2:</b> Another close-up of the rib segment under polarized light showing the increased thickness of the periosteal new bone and the proliferation of osteocyte lacunae dispersed in the periosteal layer, cortex and rib trabeculae.	xliv
<b>Figure 5.52 B:</b> Close-up of a segment of the rib section under polarized light showing the thickness of the new bone that surpasses the cortical tissue.	xlv
<b>Figure 5.53:</b> Microscopic view of another rib thin section obtained from the Sk. 470 under polarized light.	xlv
<b>Figure 5.53 A:</b> Close-up of the middle segment under polarized light showing the original cortical bone with osteons, Haversian canals and interstitial lamellae.	xlvi
<b>Figure 5.53 A1:</b> Detail of the previous image under transmitted light exhibiting the cortical bone formed by osteons, Haversian canals and interstitial lamellae.	xlvi
<b>Figure 5.53 A2:</b> Another close-up under transmitted light showing the structure of the periosteal new bone.	xlvii
<b>Figure 5.54:</b> Rib sample collected from the Sk. 1383 individual and macroscopic view of thin section prepared.	xlviii
<b>Figure 5.55:</b> Microscopic view of the rib thin section under transmitted light.	xlviii
<b>Figure 5.55 A:</b> Close-up of a segment of the pleural surface under transmitted light showing the microstructure of the periosteal reaction.	xlix
<b>Figure 5.55 A*:</b> Detail of the previous picture under polarized light.	xlix
<b>Figure 5.55 A*1:</b> Detail of the periosteal reaction under polarized light showing the layer that is in contact with the rib cortex and the ruffled rim.	l
<b>Figure 5.55 B:</b> Close-up of a segment of the periosteal surface under transmitted light showing the clear demarcation between the newly built bone and the rib cortex.	l
<b>Figure 5.55 B*:</b> Detail of the previous picture under polarized light exhibiting the structure of the periosteal new bone formation and the composition of the cortex formed by rows of osteons.	li
<b>Figure 5.55 C:</b> Close-up of another segment of the rib sample under transmitted light presenting the type of bone bridging among periosteal layers.	li
<b>Figure 5.55 D:</b> Close-up of a segment of the cutaneous surface under polarized light showing a regular bone thickness and cortical microstructure.	lii
<b>Figure 5.55 D1:</b> Detail of the previous picture under polarized light showing well defined osteons with their circumferential lamellae and osteocyte lacunae.	lii
<b>Figure 5.56:</b> Rib sample collected from the individual Sk. 1227 and macroscopic view of the thin section prepared.	liii
<b>Figure 5.57:</b> Microscopic view of the thin section under polarized light showing a thicker pleural surface when compared with the cutaneous shell.	liii

<b>Figure 5.57 A:</b> Close-up of a segment of the pleural surface under polarized light showing signs of bone resorption in the endosteal surface and rib cortex.	liv
<b>Figure 5.57 B:</b> Close-up of a lateral rib segment under polarized light showing intracortical lamellae and Haversian systems intersected by Howship's lacunae.	liv
<b>Figure 5.57 B1:</b> Detail of the intracortical lamellae under polarized light.	lv
<b>Figure 5.57 B2:</b> Another detail under polarized light exhibiting a branch layer of periosteal new bone with osteocyte lacunae.	lv
<b>Figure 5.57 C:</b> Close-up of a segment of the cutaneous surface under polarized light showing remains of the periosteal and endosteal lamellae encircling the rib cortex.	lvi
<b>Figure 5.57 C1:</b> Detail of the cortical bone under polarized light showing well preserved osteons with their circumferential lamellae, osteocyte lacunae and Haversian canals.	lvi
<b>Figure 5.58:</b> Partial microscopic view of another thin section of the individual Sk. 1383 under polarized light showing a clear separation formed by Howship's lacunae between the periosteal new bone and the original cortex.	lvii
<b>Figure 5.58 A:</b> Detail of the previous image under polarized light showing the periosteal new bone combining mature lamellae with more haphazard new bone.	lvii
<b>Figure 5.59:</b> Rib sampled collected from the individual Sk. 1235 and macroscopic view of the rib thin section prepared.	lviii
<b>Figure 5.60:</b> Microscopic view of the thin section under polarized light showing well defined contours and an enlargement of the pleural surface in relation to the cutaneous shell.	lviii
<b>Figure 5.60 A:</b> Close-up of a segment of the pleural surface under polarized light showing two distinct layer of bone interconnected by pedestals structures.	lix
<b>Figure 5.60 B:</b> Another detail of the pleural surface under polarized light showing the periosteal new bone with small vascular holes.	lix
<b>Figure 5.60 C:</b> Close-up of a segment of the cutaneous surface under polarized light presenting some rows of cortical osteons.	lx
<b>Figure 5.61:</b> Rib sample collected from the individual Sk. 1299 and macroscopic view of the rib thin section prepared.	lxi
<b>Figure 5.62:</b> Microscopic view of the thin section under polarized light showing a slight thickness in the pleural surface in comparison with the cutaneous shell.	lxi
<b>Figure 5.62 A:</b> Close-up of the lower portion of the rib section under polarized light showing resorption lacunae in the cortical bone.	lxii
<b>Figure 5.62 A1:</b> Detail of the previous image under transmitted light exhibiting resorption spaces, endosteal and periosteal circumferential lamellae, and remains of the cortical bone with partially digested osteons and interstitial lamellae.	lxii
<b>Figure 5.62 B:</b> Close-up of a middle segment of the rib under polarized light showing the cortical bone and some signs of postmortem damage.	lxiii
<b>Figure 5.62 C:</b> Another middle segment of the pleural surface under polarized light exhibiting a dense layer of new bone deposited upon the cortical bone.	lxiii
<b>Figure 5.62 C1:</b> Detail of the previous image under polarized light.	lxiv
<b>Figure 5.62 D:</b> Close-up of another middle section of the pleural surface under polarized light showing a thick layer of new bone deposited above the rib cortex.	lxiv

<b>Figure 5.62 D1:</b> Detail of the previous image under transmitted light showing the periosteal new bone with an irregular and wavy-like appearance.	lxv
<b>Figure 5.62 D2:</b> Another detail of the pleural surface under transmitted light showing two distinct layers.	lxv
<b>Figure 5.63:</b> Rib sample collected from the individual Sk. 1583 and macroscopic view of the thin section prepared.	lxvi
<b>Figure 5.64:</b> Microscopic view of the thin section under transmitted light showing the cutaneous surface relatively well-preserved when compared with the visceral surface.	lxvi
<b>Figure 5.64 A:</b> Close-up of a segment of the thin section under transmitted light showing some postmortem damage in the visceral surface.	lxvii
<b>Figure 5.64 B:</b> Detail of the upper portion of the rib thin section under transmitted light showing the presence of primary vascular canals in the cutaneous surface.	lxvii
<b>Figure 5.64 B1:</b> Detail of the previous figure under transmitted light exhibiting the primary vascular canals and the well defined intracortical primary lamellar bone.	lxviii
<b>Figure 5.65:</b> Microscopic view of the rib thin section under polarized light.	lxviii
<b>Figure 5.65 A:</b> Close-up of a rib segment under polarized light showing the cortex formed by a network of trabeculae with a dense and haphazard appearance and multiple osteocyte lacunae.	lxix
<b>Figure 5.65 B:</b> Detail of a segment of the rib under polarized light showing areas of primary lamellae associated woven bone.	lxix
<b>Figure 5.65 B1:</b> Detail of the previous image under polarized light exhibiting a cortical primary vascular canal encircled by numerous lamellae.	lxx
<b>Figure 5.65 C:</b> Detail of the cutaneous surface under polarized light showing well defined collagen fibres in the primary lamellae.	lxx
<b>Figure 5.66:</b> Distal extremity of the 5 <sup>th</sup> metatarsal bone collected from the individual Sk. 1604 and macroscopic thin section prepared.	lxxi
<b>Figure 5.67:</b> Microscopic view of the 5 <sup>th</sup> metatarsal thin section under polarized light.	lxxi
<b>Figure 5.67 A:</b> Close-up of a segment of the thin section under polarized light showing a well-preserved cortical bone composed of secondary osteons, interstitial lamellae, and intracortical lamellar.	lxxii
<b>Figure 5.67 A1:</b> Detail of the previous image under polarized light showing well defined osteons with their circumferential lamellae, Haversian canals and interstitial lamellae.	lxxii
<b>Figure 5.67 B:</b> Close-up of a mid-segment under polarized light showing the cortical bone composed of erratic secondary osteons and fragments of osteons embedded in dense lamellae.	lxxiii
<b>Figure 5.67 B1:</b> Detail of the previous image under polarized light exhibiting an endosteal osteon partially digested and intracortical osteons embedded in dense lamellae with few osteocyte lacunae.	lxxiii
<b>Figure 5.67 B2:</b> Detail of the periosteal new bone under polarized light showing the point of contact with the underlying cortical bone.	lxxiv
<b>Figure 5.68:</b> Rib sample collected from the individual Sk. 270 and macroscopic view of the thin section prepared.	lxxv



<b>Figure 5.69:</b> Microscopic view of the rib thin section under polarized light.	lxxv
<b>Figure 5.69 A:</b> Close-up of a segment of the pleural surface under polarized light showing the cortical bone encircled by endosteal and periosteal circumferential lamellae.	lxxvi
<b>Figure 5.69 B:</b> Close-up of a middle segment of the pleural surface under polarized light exhibiting multiple resorption spaces in the cortical bone and endosteal surface.	lxxvi
<b>Figure 5.69 C:</b> Close-up of another segment under transmitted light showing the cortex surrounded by endosteal and periosteal circumferential lamellae.	lxxvii
<b>Figure 5.69 C*:</b> Detail of the previous figure under polarized light showing the cortex formed by a row of well defined osteons.	lxxvii
<b>Figure 5.69 D:</b> Close-up of another segment of the pleural surface of the rib under polarized light exhibiting the cortex composed of a row of well-defined osteons.	lxxviii
<b>Figure 5.70:</b> Rib sample collected from the individual Sk.1429 and slide thin section prepared.	lxxix
<b>Figure 5.71:</b> Microscopic view of the rib thin section under polarized light.	lxxix
<b>Figure 5.71 A:</b> Close-up of a segment of the rib thin section under polarized light showing a massive periosteal new bone deposition with an amorphous appearance in the pleural surface.	lxxx
<b>Figure 5.71 B:</b> Detail of the periosteal new bone under polarized light showing a disorganized microstructure and a high concentration of osteocyte lacunae.	lxxx
<b>Figure 5.71 B1:</b> Detail of the previous image under polarized light exhibiting the cortical bone composed of interstitial lamellae, incomplete osteons and intracortical lamellae.	lxxxii
<b>Figure 5.72:</b> Microscopic view of another thin section of the Sk, 1429 sample under transmitted light showing a detail of the periosteal new bone formation.	lxxxii
<b>Figure 5.72 A:</b> Close-up of a segment of the pleural-endosteal surface under transmitted light showing the cortical bone intersected by large spaces of bone resorption.	lxxxiii
<b>Figure 5.72 A*:</b> Detail of the previous image under polarized light showing a major focus of bone resorption and a high concentration of osteocyte lacunae.	lxxxiii
<b>Figure 5.72 B:</b> Detail of the last layers of periosteal new bone under transmitted light showing differences in tissue organization.	lxxxiv
<b>Figure 5.73:</b> Rib sample collected from the individual Sk. 1534-A and macroscopic view of the thin section prepared.	lxxxiv
<b>Figure 5.74:</b> Microscopic view of the rib thin section under polarized light showing a well preserved microanatomy.	lxxxv
<b>Figure 5.74 A:</b> Close-up of a segment of the pleural-cutaneous surface under transmitted light showing a subadult cortical microstructure.	lxxxv
<b>Figure 5.74 A*:</b> Detail of the previous image under polarized light showing the cortical bone composed of essentially by woven bone and the new periosteal layer populated by multiple osteocyte lacunae.	lxxxvi
<b>Figure 5.74 B:</b> Detail of the pleural-endosteal cortex and of periosteal new bone formation.	lxxxvi

<b>Figure 5.74 C:</b> Detail of the cutaneous-endosteal surface under polarized light showing a woven structure combined with foci of bone resorption and primary vascular canals.	lxxxvi
<b>Figure 5.75:</b> Bone sample extracted from the individual Sk.1534-A and thin section prepared.	lxxxvii
<b>Figure 5.76:</b> Microscopic view of the thin section under polarized light showing some lack of bone birefringence.	lxxxvii
<b>Figure 5.76 A:</b> Close-up of a segment of the periosteal-endosteal surface under polarized light showing the newly built bone with an arc-like structure.	lxxxviii
<b>Figure 5.76 B:</b> Close-up of the middle portion under polarized light showing the periosteal new bone and portions of the cortical bone.	lxxxviii
<b>Figure 5.76 C:</b> Another close-up of the periosteal surface under polarized light showing a deposit of new bone with a spiky microstructure and intersected by lacunae.	lxxxix
<b>Figure 5.77:</b> 5th left metatarsal sample collected from the individual Sk. 119 and macroscopic view of the thin section prepared.	xc
<b>Figure 5.78:</b> Microscopic view of the thin section under transmitted light showing a well preserved cortex and a darker and denser layer of periosteal new bone.	xc
<b>Figure 5.78 A:</b> Close-up of a section of the periosteal-endosteal surface under polarized light exhibiting the cortical tissue in excellent state of preservation and with high birefringence.	xci
<b>Figure 5.78 B:</b> Detail of the periosteal new bone formation under transmitted light showing a dense layer clearly demarcated from the rib cortex.	xci
<b>Figure 5.78 C:</b> Detail of another segment of the periosteal-endosteal surface under polarized light exhibiting large areas of localized resorption in the endosteal surface and at the point of contact between the cortical bone and the periosteal reaction.	xcii
<b>Figure 5.78 D:</b> Another detail of the periosteal-endosteal surface under polarized light showing a thick layer of new bone deposited upon a well preserved cortex.	xcii
<b>Figure 5.78 D1:</b> Detail from the previous picture under polarized light exhibiting a thick layer of periosteal new bone with a primary vascular canal.	xciii
<b>Figure 5.79:</b> Fibula sample collected from Sk. 198 and macroscopic view of the slide thin section prepared.	xciv
<b>Figure 5.80:</b> Microscopic view of the thin section under polarized light.	xciv
<b>Figure 5.80 A:</b> Close-up of a segment of the fibula under polarized light showing the cortex formed by a net of lamellae and partially digested Haversian systems.	xcv
<b>Figure 5.80 B:</b> Close-up of another segment of the fibula under polarized light showing a thin rim of periosteal bone bordering the cortex.	xcv
<b>Figure 5.80 C:</b> Detail of a segment of the fibula cortex under polarized light exhibiting a disorganized net of bone lamellae formed after digestion of previous Haversian system and embedded in a blue-grey substance.	xcvi
<b>Figure 5.81:</b> Microscopic view of another thin section of the fibula sample under polarized light.	xcvi

<b>Figure 5.81 A:</b> Close-up of a segment of fibula thin section under polarized light showing partially preserved mature lamellae bordering the outer surface of the bone.	xcvii
<b>Figure 5.81 A1:</b> Detail of the previous image under polarized light showing branches and islands of immature or wove bone connecting preserved systems of mature lamellae and embedded in a blue-grey substance.	xcvii
<b>Figure 5.82:</b> Tibia sample collected from the Sk. 54 and macroscopic view of the thin section prepared.	xcviii
<b>Figure 5.83:</b> Microscopic view of the tibia thin section under polarized light.	xcviii
<b>Figure 5.83 A:</b> Close-up of a segment of the tibia thin section under polarized light showing a regular periosteal surface and a dense and mature cortical bone.	xcix
<b>Figure 5.83 A1:</b> Detail of the previous image under polarized light showing the microstructure of the intracortical lamellae inserted between secondary osteons.	xcix
<b>Figure 5.83 A2:</b> Detail of the periosteal surface under polarized light showing a major resorption space due to osteoclastic activity that digested Haversian systems and interstitial lamellae.	c
<b>Figure 5.83 B:</b> Close-up of another segment of the tibia under polarized light exhibiting the cortical bone composed of multiple secondary osteons of various sizes and shapes and surrounded by interstitial lamellae.	c
<b>Figure 5.83 C:</b> Close-up of a segment of the tibia under polarized light showing a thick layer of dense bone at the periosteal surface that connects with the cortical tissue.	ci
<b>Figure 5.83 D:</b> Detail of another segment of the tibia under polarized light showing a thin rim of bone at the periosteal surface and a cortex composed of densely packed lamellae, small osteons and randomly organized lamellar units.	ci
<b>Figure 5.84:</b> Rib sample collected in the Sk. 119 and macroscopic view of the prepared thin section.	cii
<b>Figure 5.85:</b> Microscopic view of the rib thin section under transmitted light.	cii
<b>Figure 5.85 A:</b> Close-up of a segment of the pleural-endosteal surface under transmitted light showing the endosteal circumferential lamellae and remnants of the periosteal circumferential lamellae encircling the rib cortex.	ciii
<b>Figure 5.85 B:</b> Close-up of another segment of the pleural-endosteal surface under transmitted light exhibiting the cortical tissue formed by several rows of osteons and interstitial lamellae intercalated by sheets of lamellar bone.	ciii
<b>Figure 5.86:</b> Microscopic view of the rib thin section under polarized light.	civ
<b>Figure 5.86 A:</b> Close-up of a segment of the pleural-endosteal surface under polarized light exhibiting the cortical tissue formed by osteons of different sizes and shapes intersected by layers of lamellar tissue.	civ
<b>Figure 5.86 B:</b> Close-up of another segment of the pleural surface under polarized light showing the cortex composed of multiple rows of osteons.	cv
<b>Figure 5.86 B1:</b> Detail of the periosteal new bone under polarized light exhibiting several degrees of bone organization.	cv
<b>Figure 5.87:</b> Rib sample collected from the Sk. 1138 and macroscopic view of the prepared thin section.	cvi
<b>Figure 5.88:</b> Microscopic view of the rib thin section under polarized light.	cvi

<b>Figure 5.88 A:</b> Close-up of a segment of the pleural-endosteal surface under polarized-light showing multiple rows of osteons in the cortex.	cvii
<b>Figure 5.88 B:</b> Close-up of another segment of the pleural-endosteal surface under polarized light presenting rows of osteons and enlarged Haversian canals.	cvii
<b>Figure 5.88 C:</b> Plain illustration of a segment of the pleural-endosteal surface under polarized light presenting a micro-crack of diagenetic origin separating the rib cortex.	cviii
<b>Figure 5.88 D:</b> Close-up of a segment of the lower pleural-endosteal surface under polarized light exhibiting well-defined endosteal circumferential lamellae layering the rib cortex.	cviii
<b>Figure 5.88 D1:</b> Detail of the previous image under polarized light showing the endosteal circumferential lamellae well defined and bordering the cortical tissue in which large resorption spaces are visible.	cix
<b>Figure 5.89:</b> Rib sample collected from Sk. 1196 and macroscopic view of the thin section prepared.	cx
<b>Figure 5.90:</b> Microscopic view of the rib thin section under polarized light.	cx
<b>Figure 5.90 A:</b> Close-up of a segment of the cutaneous-endosteal surface under polarized light showing the rib cortex formed by a thin row of osteons and interstitial lamellae.	cx
<b>Figure 5.90 B:</b> Detail of the upper border of the cutaneous-endosteal surface of the rib thin section under polarized light showing a major space of bone resorption enclosed by a thin rim of bone lamellae.	cx
<b>Figure 5.90 C:</b> Illustration of a segment of the pleural-endosteal surface exhibiting the inner and the outer circumferential lamellae of the cortical bone.	cx
<b>Figure 5.91:</b> Bone sample collected from the right radius of the Sk. 1196 and macroscopic view of the thin section prepared.	cxii
<b>Figure 5.92:</b> General macroscopic view showing the bone callus formed by an intricate net of trabeculae and large resorption spaces.	cxii
<b>Figure 5.92 A:</b> Detail of the type of trabecullae that composes the bone callus under polarized light.	cxiii
<b>Figure 5.92 B:</b> Close-up of a segment of the radius under polarized light showing multiple sheets of new bone with a haphazard appearance and densely populated by osteocyte lacunae.	cxiii
<b>Figure 5.92 B1:</b> Detail of the previous picture under polarized light exhibiting the microstructure of the newly built bone.	cxiv
<b>Figure 5.92 C:</b> Close-up of the anterior cortex of the radius under polarized light showing distinct layers of bone deposition.	cxiv
<b>Figure 5.93:</b> Rib sample collected from the Sk. 1484 and macroscopic view of the rib thin section prepared.	cxv
<b>Figure 5.94:</b> Microscopic view of the rib thin section under polarized light.	cxv
<b>Figure 5.94 A:</b> Close-up of a segment of the pleural-endosteal surface under polarized light showing the rib cortex formed by multiple rows of osteons and interstitial lamellae.	cxv

<b>Figure 5.94 B:</b> Detail of the cutaneous-endosteal surface under polarized light exhibiting the rib cortex formed by several layers of osteons and interstitial lamellae.	cxvi
<b>Figure 5.94 C:</b> Close-up of another segment of the cutaneous-endosteal surface under polarized light highlighting the proliferation of bone diagenetic changes, such as micro-cracks and tissue disintegration.	cxvi
<b>Figure 5.94 D:</b> Close-up of another segment of the rib cutaneous-endosteal surface under polarized light revealing the cortex formed by few rows of osteons with enlarged Haversian canals.	cxvii
<b>Figure 5.94 D1:</b> Detail of the previous image under polarized light showing cortical osteons with enlarged Haversian canals.	cxvii
<b>Figure 5.95:</b> Rib sample collected from Sk. 457 and macroscopic view of the thin section prepared.	cxviii
<b>Figure 5.96:</b> Microscopic view of the rib thin section under polarized light.	cxviii
<b>Figure 5.96 A:</b> Detail of the spiky formations of periosteal new bone under polarized light.	cxix
<b>Figure 5.96 B:</b> Close up of the rib cortex at the interface with the new bone formation under polarized light showing remnants of Haversian systems and interstitial lamellae partially digested by osteoclastic activity.	cxix
<b>Figure 5.96 C:</b> Close-up of the spikes of periosteal new bone under polarized light.	cxx
<b>Figure 5.96 D:</b> Detail of the rib cortex under polarized light showing enlarged Haversian canals and vast resorption spaces due to osteoclast activity.	cxx
<b>Figure 5.97:</b> Femur sample collected from the Sk.135 and macroscopic view of the thin section prepared.	cxxi
<b>Figure 5.98:</b> Microscopic view of the femur thin section under polarized light.	cxxi
<b>Figure 5.98 A:</b> Close-up of a segment of the femur thin section under polarized light showing a microstructure composed of mature bone lamellae and newly built bone.	cxxi
<b>Figure 5.98 A1:</b> Detail of the previous image under polarized light exhibiting a sheet of mature lamellae partially detached from the remaining bone tissue by a major bay of bone resorption.	cxxii
<b>Figure 5.98 B:</b> Close-up of another segment of the femur thin section under polarized light showing densely packed lamellae crossed by layers of new randomly organized bone.	cxxii
<b>Figure 5.98 B1:</b> Detail of the femur thin section under polarized light exhibiting large resorption spaces separating branches of bone.	cxxiii
<b>Figure 5.98 C:</b> Detail of another segment of the femur thin section under polarized light showing branches of newly formed bone intersected by large resorption spaces and some primary vascular canals.	cxxiii
<b>Figure 5.99:</b> Tibia sample collected from the Sk. 1412 and macroscopic view of the thin section prepared.	cxxiv
<b>Figure 5.100:</b> Microscopic view of the thin section prepared under polarized light.	cxxiv
<b>Figure 5.100 A:</b> Close-up of a segment of the periosteal-endosteal surface under polarized light showing multiple rows of osteons and interstitial lamellae surrounded by endosteal and periosteal circumferential lamellae.	cxxiv

<b>Figure 5.100 B:</b> Detail of another segment of the tibia thin section under polarized light showing the cortical bone formed by several layer of osteons and interstitial lamellae.	cxxv
<b>Figure 5.100 C:</b> Close-up of a middle segment of the sample under polarized light exhibiting the tibia cortex composed of multiple rows of osteons and interstitial lamellae.	cxxv
<b>Figure 5.101:</b> Macroscopic view of the thin section of the rib sample showing normal thickness, but with a rim of new bone attached to the cortex of the visceral surface.	cxxvi
<b>Figure 5.102:</b> Microscopic view of the rib sample observed under transmitted light showing multiple vascular holes (Haversian canals), which are particularly numerous and larger in the dorsal surface.	cxxvi
<b>Figure 5.102 A:</b> Close-up of the cutaneous surface of the rib under transmitted light showing the absence of preserved Haversian systems and lamellae.	cxxvii
<b>Figure 5.102 B:</b> Magnification of the periosteal reaction observed on the visceral surface of the rib.	cxxvii
<b>Figure 5.102 B*:</b> Magnification of the periosteal new bone formation on the visceral surface of the rib under polarized light.	cxxviii
<b>Figure 5.102 C:</b> Close-up of the rib trabeculae under polarized light showing a small area of birefringence.	cxxviii
<b>Figure 5.103.</b> Macroscopic view of the thin section extracted from a rib showing extensive areas of bone resorption mainly at the endosteal level.	cxxix
<b>Figure 5.104:</b> Microscopic view of the rib thin section observed under polarized light.	cxxix
<b>Figure 5.104 A.</b> Close-up of a section of the pleural surface of the rib under transmitted light showing massive bone resorption, especially on the endosteal surface.	cxxx
<b>Figure 5.104 B:</b> Close-up of a section of the cutaneous surface of the rib under transmitted light exhibiting bays of bone resorption affecting the endosteal surface and the rib trabeculae.	cxxx
<b>Figure 5.104 C:</b> Close-up of a segment of the cutaneous surface of the rib under transmitted light showing several bays of bone resorption with origin in the endosteal portion.	cxxxii
<b>Figure 5.104 D:</b> Magnification of a lateral segment of the cutaneous surface of the rib under transmitted light showing the contours of two Haversian systems.	cxxxii
<b>Figure 5.104 D*:</b> Magnification of a segment of the cutaneous surface of the rib under polarized light showing a general lack of bone birefringence and multiple areas of bone diagenesis.	cxxxiii
<b>Figure 5.105:</b> Macroscopic appearance of a half thin section of a rib observed under transmitted light.	cxxxiii
<b>Figure 5.106:</b> Microscopic view of a rib sample under polarized light, highlighting the pleural and trabeculae surfaces.	cxxxiii
<b>Figure 5.106 A:</b> Close-up of a segment of the pleural surface of the rib observed under transmitted light showing the original cortical bone and the new bone layer attached to the underlying substrate by bone bridges.	cxxxiv

<b>Figure 5.106 B:</b> Close-up of the deposits of new bone observed under polarized light.	cxxxiv
<b>Figure 5.106 C:</b> Detail of the periosteal new bone formation in relation to the underlying rib cortex observed under transmitted light.	cxxxv
<b>Figure 5.107.</b> Macroscopic view of a thin section of a rib sample with the anatomical contours well defined.	cxxxvi
<b>Figure 5.108:</b> Full microscopic view of the rib sample viewed under polarized light.	cxxxvi
<b>Figure 5.108 A:</b> Close-up of a segment of the cutaneous surface of the rib cortex under polarized light showing some Haversian canals preserved.	cxxxvii
<b>Figure 5.108 B:</b> Magnification of another section under polarized light of the rib's cutaneous surface showing a micro crack that crosses the cortex and runs parallel to the surface.	cxxxvii
<b>Figure 5.108 C:</b> Close-up of a segment of the pleural surface of the rib observed under transmitted light showing massive diagenetic changes comprising of micro-cracks and bone tunnelling.	cxxxviii
<b>Figure 5.108 D:</b> Close-up of the pleural surface under transmitted light showing a layer of periosteal bone clearly demarcated from the cortical bone.	cxxxviii
<b>Figure 5.108 E:</b> Segment of the pleural surface under transmitted light showing the enlargement of the Haversian canals on the endosteal surface.	cxxxix
<b>Figure 5.108 F:</b> Close-up of the pleural surface under transmitted light showing some preserved Haversian canals.	cxxxix
<b>Figure 109:</b> Macroscopic view of the fibula thin section.	cxl
<b>Figure 5.110:</b> General microscopic view of the fibula thin section observed under polarized light.	cxl
<b>Figure 5.110 A:</b> Close-up of a segment of the fibula diaphysis observed under transmitted light exhibiting periosteal bone with a wave-like and round morphology.	cxli
<b>Figure 5.110 B:</b> Magnification of another portion of the fibula diaphysis under polarized light.	cxli
<b>Figure 5.110 C:</b> Close-up of the fibula surface showing the new periosteal bone arranged in a wave-like pattern that is separated from the underlying cortex by bone spaces.	cxlii
<b>Figure 5.110 C*:</b> Close-up of the previous figure under polarized light.	cxlii
<b>Figure 5.110 D:</b> Close-up of the fibula diaphysis under transmitted light showing a smooth layer of new bone and the shadow of some Haversian systems.	cxliii
<b>Figure 5.110 E:</b> Close-up of the fibula diaphysis observed under transmitted light.	cxliii
<b>Figure 5.111:</b> Macroscopic view of a thin section of the diaphysis of the left femur.	cxliv
<b>Figure 5.112:</b> Microscopic view the diaphysis of the left femur under polarized light showing a clear line of separation between the original cortical bone and the subperiosteal hematoma.	cxliv
<b>Figure 5.112 A:</b> Close-up of a segment of the femur diaphysis under polarized light showing a line of separation between the original cortical bone and the new bone formation.	cxlv
<b>Figure 5.112 A1:</b> Close-up of the contact zone under polarized light showing the Haversian systems intercalated by layers of preserved lamellae.	cxlv

<b>Figure 5.112 B:</b> Close-up of the cortex of the femur diaphysis under polarized light.	cxlvi
<b>Figure 5.112 C:</b> Magnification of a segment of the ossified subperiosteal hematoma under polarized light.	cxlvi
<b>Figure 5.112 D:</b> Close-up of the surface of the subperiosteal haematoma under polarized light.	cxlvii
<b>Figure 5.112 E:</b> Close-up of the subperiosteal hematoma under transmitted light showing the contours of several osteons, however with no system of circumferential lamellae preserved due to diagenetic changes.	cxlvii
<b>Figure 5.112 E1:</b> Magnification of the surface of the subperiosteal haematoma under transmitted light showing the new superficial layer of bone with a lamellar appearance and the shadow of one osteon intersected by a taphonomic micro-crack.	cxlviii
<b>Figure 5.112 F:</b> Close-up of a section of the subperiosteal haematoma under transmitted light showing the absence of preserved bone microstructure and the proliferation of worm-like black structures that may be linked with fungi or bacterial activity.	cxlviii
<b>Figure 5.112 F1:</b> Close-up of the previous figure showing the shadow of an osteon.	cxlix
<b>Figure 5.113:</b> Macroscopic view of the bone outgrowth thin section.	cl
<b>Figure 5.114:</b> Microscopic view of a portion of an unspecific bone ossification observed under polarized light.	cl
<b>Figure 5.114 A:</b> Close-up of a segment of the periosteal new bone under polarized light exhibiting some apparent birefringence of lamellar around a Haversian canal.	cli
<b>Figure 5.114 B:</b> Close-up of the new bone formation under polarized light showing some signs of bone birefringence, spaces of bone remodelling, and diagenetic changes.	cli
<b>Figure 5.114 C:</b> Close-up of the new periosteal bone under transmitted light showing some spaces of bone remodelling and the proliferation of diagenetic changes.	clii
<b>Figure 5.115:</b> Macroscopic view of tibia thin section.	cliii
<b>Figure 5.116:</b> Microscopic view of the thin section of the diaphysis of the tibia under polarized light showing some bone birefringence.	cliii
<b>Figure 5.116 A:</b> Close-up of a segment of the tibia diaphysis under transmitted light showing some preserved Haversian systems intersected by micro-cracks.	cliv
<b>Figure 5.116 A1:</b> Close-up of the tibia diaphysis surface under transmitted light showing a partially preserved osteon.	cliv
<b>Figure 5.116 A2:</b> Close-up of a peripheral cortical osteon under transmitted light.	clv
<b>Figure 5.116 B:</b> Close-up of a segment of the tibia diaphysis under transmitted light exhibiting some partially preserved Haversian systems, as well as osteon canals, intersected by some areas with diagenetic changes.	clv
<b>Figure 5.116 C:</b> Close-up of a portion of the cortical bone under polarized light showing an intricate net of bone filaments with preserved lamellae that resemble bone trabeculae.	clvi
<b>Figure 5.116 D:</b> Close-up of a segment of the periosteal surface under polarized light showing extensive areas of bone resorption intersected by filaments of bone composed of lamellae and small primary vascular canals.	clvi



## ABSTRACT

Paleopathology, summarily defined as the study of past diseases, has on the differential diagnosis a major challenge. Taking into account the difficulties faced by paleopathologists on the study of ancient conditions, especially those of infectious origin involving periosteal new bone formation (PNBF), an investigation was conducted combining macroscopic and histological techniques. The purpose of this research was twofold: firstly, to analyze the macroscopic distribution of periosteal reactions by age and cause of death, anatomical location, laterality, symmetry, bone dispersion and type of new bone; and secondly, to microscopically examine and compare thin sections of periosteal new bone, in order to evaluate the existence (or not) of microstructural differences in individuals who died from: (1) tuberculosis infections-TB (Group 1, n=114); (2) non-TB infections (Group 2, n=89); and (3) other conditions (Group 3, n=50).

For the macroscopic analysis an assemblage of 253 individuals from the Human Identified Skeletal Collection from the Bocage Museum (Lisbon, Portugal), 136 males and 117 females, comprising individuals with an age at death ranging from 2.5 months to 94 years old, was chosen. A total of 34 dry bone specimens: 26 belonging to 23 individuals from the Bocage Museum, and eight from eight individuals from archaeological contexts (14<sup>th</sup>-19<sup>th</sup> centuries) were prepared for histological examination under transmitted and polarized light.

Analysis of the macroscopic results revealed a high frequency (71.2%) of PNBF in individuals younger than 45 years old ( $\bar{x}$ =22.64 years old). Deposits of new bone were most commonly found in individuals who died from TB (Group 1=82.5%) in comparison with those who died from non-TB disorders (Group 2=42.7%) or from other conditions (Group 3=46%), and the results were highly significant. Only the PNBF located on ribs had a positive relationship with TB as the cause of death (Group 1). Individuals who died from TB infection were also those who showed a broader involvement of the rib cage. Here periosteal lesions were most frequently observed in the upper to middle segment (R1→R6, 60.2% [405/673]), mainly in the left-side (41.2%). In the ribs, a predominance of diffuse lesions combining *woven* and lamellar foci was recurrently seen. In spite of the apparent relationship between periosteal rib lesions and TB, the presence of similar lesions in individuals who died from other diseases does not allow for the establishment of a definitive association. The frequency of PNBF in the appendicular bones was higher in the tibia (T) and fibula (Fi) of the individuals from Group 2 (T=36.7%; Fi=17.4%) and Group 3 (T=41.2%; Fi=17.1%), and in those older than 45 years of age (T=38.8%; Fi=17.5%). The analysis of the individuals with multiple periosteal bone involvement did not reveal significant differences among cause of death groups. The

younger individuals from Group 1 were those with more deposits of new bone in the humerus, radius and ulna. With regard to the distribution of the periosteal lesions, symmetric foci were most often seen in the scapula and radius (n=5, respectively), whereas left-sided ones more common in the ulna (n=5), and right-sided ones in the humerus (n=4). In the lower limb bones, a predominance of symmetric lesions was observed in the tibia (n=37), femur (n=28) and fibula (n=15). Localized foci of new bone were commonly observed in the upper limb bones. In contrast, a high frequency of diffuse lesions was found on the shaft of the lower limb bones (e.g. tibia and fibula). Only the femur (n=28) showed a high prevalence of localized lesions. Differences in the type of new bones were also found between the upper (predominance of *woven* and *woven/lamellar* foci) and the lower limb bones (*lamellar* and *woven/lamellar* foci). In the appendicular skeleton, the lack of association between new bone formation, particularly in the tibia and fibula, and the underlying cause of death seems to corroborate the non-specificity of periosteal lesions, challenging their usefulness as an indicator of physiological stress. Furthermore, it may point out to the existence of inaccurate records of cause of death, or the coexistence of multiple conditions not identified in the obituary certificate.

The value of the histological analysis on the study of bone lesions was observed at three main levels: (1) diagnosis of pathological conditions; (2) description of bone lesions; and (3) assessment to bone tissue quality. With regard to the diagnosis of pathological conditions, differences in the microstructure of PNB were seen between Group 1 and Group 2 of cause of death and within groups. Multiple layers of “appositional bone” enclosing numerous primary vascular canals were the pattern most commonly observed (n=4) in the samples from Group 1. In contrast, three samples (one from Group 1, two from Group 2) presented a microstructure compatible with subperiosteal hematomas. These observations suggest that beyond pulmonary diseases other mechanisms may stimulate PNB on the visceral surface of ribs. Histological analysis was also fundamental in the description and characterization of bone changes. For example, of the five samples with “consolidated” fracture callus, only two presented a truly mature and remodeled microstructure. This means that the outer surface of a bone lesion may not give a complete picture of the tissues response. In spite of the good preservation of some bone samples, massive diagenetic changes due to the action of bacteria and fungi were observed at microscopic level. This clearly suggests that gross inspection is not a good measure of the bone tissue quality. In contrast, microscopy is essential to differentiate between pseudopathology and physiological or pathological signs.

This study demonstrated the difficulties in using periosteal lesions, especially those of the lower limb bones to ascertain the diagnosis of particular conditions. Furthermore, it also revealed the limitations and possible misinterpretations found in the macroscopic study of

identified skeletal collections. In contrast, the histological analysis showed surprising results that reinforce the pertinence of applying histological techniques in the description and diagnosis of bone changes in human remains.

Future studies based on well-documented collections with accurate medical records and/or samples retrieved from clinical cases will eventually solve some of the problems and limitations detected in this investigation. Increasing the sample size will also improve our understanding of the entire spectrum of new bone variation associated with a particular condition. It is possible that further research in the field of bone biochemistry, immunology and cell communication will shed light on the exact mechanism (or mechanisms) behind PNBf.

**KEY-WORDS:** paleopathology, macroscopic inspection, palaeohistopathology, periosteal new bone formation (PNBF), tuberculosis (TB), bone callus, bone diagenesis



## SUMÁRIO

A paleopatologia, sumariamente definida como o estudo das doenças do passado, tem no diagnóstico diferencial um importante desafio. Com o intuito de atenuar as dificuldades associadas à análise de condições patológicas em material osteológico humano, designadamente as de natureza infecciosa que se manifestam através de reacções periosteas (RP), foi desenvolvida uma investigação que combinou a análise macroscópica com o estudo histológico. Dois objectivos foram definidos: (1) analisar macroscopicamente a distribuição das RP por idade e causa de morte dos indivíduos, distribuição anatómica por tipo de osso, lateralidade, simetria, dispersão óssea e tipo de osso novo produzido; e (2) examinar e comparar, histologicamente, secções de osso contendo RP com o intuito de avaliar a existência (ou não) de diferenças microestruturais em indivíduos que morreram de (i) tuberculose - TB (Grupo 1, n=114); (ii) infecções não tuberculosas (Grupo 2, n=89); e (iii) outras condições (Grupo 3, n=50).

Para o estudo macroscópico foram seleccionados 253 indivíduos de ambos os sexos (136 homens e 117 mulheres) e diferentes idades (2.5 meses a 94 anos) provenientes da Colecção de Esqueletos Identificados do Museu Bocage (Lisboa, Portugal). No que concerne à análise histológica, foram seccionadas 34 amostras ósseas: 26 pertencentes a 23 esqueletos identificados, e oito provenientes de oito indivíduos de contexto arqueológico (séculos XIV-XIX). As amostras foram preparadas para microscopia óptica de transmissão e de polarização.

A análise dos dados macroscópicos revelou uma elevada frequência (71.2%) de RP em indivíduos com idade inferior a 45 anos ( $\bar{x}$ =22.64 anos). Frequência igualmente elevada e significativa foi registada no grupo de indivíduos que morreram de TB (Grupo 1=82.5%), quando comparados com os que morreram de infecções de origem não tuberculosa (Grupo 2= 42.7%), assim como de outras condições (Grupo 3=46%). Apenas as RP observadas nas costelas revelaram uma relação positiva com TB enquanto causa de morte (Grupo 1). Indivíduos que morreram de TB foram também aqueles que apresentaram lesões mais extensas na caixa torácica, designadamente, entre o segmento superior e médio (R1→R6, 60.2% [405/673], e no lado esquerdo (41.2%). Nas costelas foi assinalada uma predominância de lesões difusas do tipo *woven* e lamelar. Não obstante a aparente associação entre RP nas costelas e TB, a presença de alterações semelhantes em indivíduos que morreram de outras condições não permite estabelecer uma relação de casualidade definitiva. No esqueleto apendicular foi observada uma maior frequência de depósitos de osso novo na tibia (T) e fíbula (Fi) no Grupo 2 (T=36.7%; Fi=17.4%) e Grupo 3 (T=41.2%; Fi=17.1%) de causa de morte, e nos indivíduos com idade superior a 45 anos (T=38.8%; Fi=17.5%). A análise dos indivíduos com vários ossos afectados e por causa de morte não revelou resultados estatisticamente

significativos. Indivíduos jovens (< 45 anos) do Grupo 1 exibiram mais RP no úmero, rádio e ulna. Lesões simétricas foram maioritariamente observadas na escápula e rádio (n=5, respectivamente), lesões unilaterais esquerdas na ulna (n=5) e lesões unilaterais direitas no úmero (n=4). No membro inferior, as lesões simétricas foram maioritariamente observadas na tíbia (n=37), femur (n=28) e fíbula (n=15). Depósitos localizados de osso novo foram mais frequentemente registados no membro superior, enquanto que as lesões difusas foram uma constante no membro inferior (ex. tíbia e fíbula). Apenas o fémur apresentou uma maior frequência de lesões localizadas (n=28). No membro superior foi assinalada uma maior frequência de lesões do tipo *woven* e *woven/lamelar*, enquanto que no membro inferior predominou o tipo lamelar e *woven/lamelar*. No esqueleto apendicular, a inexistência de uma clara associação entre a deposição de osso novo e a causa de morte, designadamente para a tíbia e fíbula, parece sugerir a não-especificidade das RP e a sua contra-indicação enquanto indicadores de stress fisiológico. Concomitantemente, parece indicar a existência de possíveis problemas associados ao registo da causa de morte dos indivíduos e/ou à coexistência de outras condições patológicas aquando da morte não descritas no certificado de óbito.

A pertinência da análise histológica no estudo de alterações patológicas foi denotada a três níveis: (1) diagnóstico de condições patológicas, (2) descrição de lesões ósseas, e (3) acesso à qualidade do tecido ósseo. Observaram-se diferenças na microestrutura das RP entre e intra-grupos, particularmente notórias na superfície visceral das costelas. Para além da sobreposição de osso novo sugestiva de infecções crónicas (> Grupo 1), foram observadas lesões compatíveis com hematomas subperiosteos ossificados que sugerem a existência de múltiplas etiologias associadas à produção de osso novo nas costelas. A análise histológica revelou ser determinante para caracterizar lesões (ex. proliferativas) e avaliar a sua remodelação (ex. fraturas). Esta observação sugere que a aparência externa de uma lesão poderá não ilustrar toda a resposta óssea. No que concerne ao acesso à qualidade do tecido ósseo observou-se uma discrepância entre a integridade macroscópica e a condição do tecido ósseo. Amostras com uma arquitetura óssea aparentemente intacta, não preservavam sistemas de Havers, com implicações na análise biomolecular e imagiológica. Estes resultados sugerem que a análise macroscópica é insuficiente na avaliação da qualidade do tecido ósseo. O estudo histológico foi essencial para diferenciar entre alterações diagenéticas e aspectos de natureza fisiológica e patológica do tecido ósseo.

Do presente estudo salientam-se as dificuldades na utilização de RP, nomeadamente as do membro inferior, no diagnóstico de determinadas condições patológicas. Conjuntamente realçam-se algumas limitações e possíveis erros de análise associados ao estudo macroscópico.

A análise histológica, por seu turno, demonstrou resultados surpreendentes que reforçam a pertinência da sua aplicação na descrição e diagnóstico de condições patológicas.

A realização de estudos similares com amostras histológicas mais alargadas e provenientes de colecções identificadas com um registo médico mais completo e/ou provenientes de casos clínicos poderá, futuramente, atenuar algumas das limitações encontradas no presente estudo. Também a conjugação com outras áreas de investigação que se debruçam sobre a dinâmica do tecido ósseo poderá auxiliar na correcta interpretação dos reais mecanismos subjacentes às RP.

**PALAVRAS-CHAVE:** paleopatologia, análise macroscópica, paleohistopatologia, reacções periosteas (RP), Tuberculose (TB), calos ósseos, diagénese óssea.





## ACKNOWLEDGEMENTS

There are many people that I wish to thank for their assistance and advice during the production of this thesis. Without them this thesis would not have been possible:

First and foremost, I would like to express my gratitude to my supervisors Dr. Ana Luísa Santos and Dr. Anne Keenleyside who have provided me guidance and support throughout my research project. Their critical reviews, enthusiasm, encouragement, and dedication greatly improved the quality of this dissertation. I would like to thank Dr. Anne Keenleyside for giving me the opportunity to develop the practical component of my research at the Laboratory of Bioarchaeology from the Department of Anthropology of Trent University, Peterborough, (Ontario, Canada) and for the patient editing of the text. Dr. Keenleyside, thank you for your friendship, hospitality and for so kindly organizing all aspects of my pleasant stay in Canada. I also want to thank the former chair of the Department of Anthropology of Trent University, Dr. Julia Harrison, for her hospitality;

I want to thank the Bocage Museum – Museu Nacional de História Natural e da Ciência da Universidade de Lisboa (Lisbon, Portugal), namely Dr. Maria da Graça Ramalinho, former director, and Dr. Diana Carvalho and Dr. Hugo Cardoso, former curators, for allowing me access to the Human Identified Skeletal Collection used in this research, as well as, for giving me a space to work and perform daily data collection and bone sampling. I would like to thank Dr. Francisca Alves Cardoso from the Universidade Nova de Lisboa (Lisboa, Portugal) for allowing me permission to take bone samples from two archaeological skeletal series (cemetery of the extinct Royal Hospital of All Saints in Lisbon and cemetery from the hospital from the Ordem do Carmo in Oporto). I am in debt with Dr. Hugo Lehmann from the Department of Psychology of Trent University for his suggestions in the digital recording and image processing of the histological bone samples. I want to thank Cynthia Thompson for her help and advices during the early stage of my research at the Laboratory of Bioarchaeology. At the Laboratory of Sediment Geology and Fossil Record of the Department of Earth Sciences of the University of Coimbra, I would like to thank Dr. Helena Henriques for her assistance with the polarized microscope. I thank Mrs. Lina Santos and Mrs. Célia Cardoso, librarians at the Department of Life Sciences (Anthropology) of the University of Coimbra for their kindness and help during my bibliographic search. I am also in debt to Mrs. Teresa Alcobia, librarian at the Library of Health Sciences of the University of Coimbra who so kindly sent me some bibliographic references.

I want to thank to all the friends that I meet in Canada without them my research would not have been so enjoyable! From this side of Atlantic, I would like to acknowledge all my friends (you know who you are!) for always being there when I was over stressed about the data collection or about other everyday issues. Thank you so much for your kindness, patient and support. I hope you can all forgive me for being less available and so reclused during the writing stage of the thesis.

Finally, I would like to thank my family for encouraging me all the time. To my parents, I am eternally grateful for your endless love and support. Thanks for letting me chase my dreams.

This research was funded by the Fundação para a Ciência e Tecnologia, Portugal (Grant reference: SFRH/BD/36739/2007).

**"THE MOMENT YOU DOUBT WHETHER YOU CAN FLY, YOU CEASE FOREVER TO BE ABLE TO DO IT"**

IN *PETER PAN IN KENSINGTON GARDENS*

JAMES MATTHEW BARRIE (1916: 27)

***TO MY PARENTS WHO GAVE ME "WINGS" TO FLY.***

***AND TO THOSE WHO ALWAYS BELIEVED IN ME AND SHOWED ME NOTHING BUT UNCONDITIONAL SUPPORT.***

THANK YOU! | OBRIGADA!



---

# CHAPTER 1

---

*"THERE IS NOWHERE ELSE TO LOOK FOR THE FUTURE BUT IN THE PAST"*

JAMES BURKE (1978) IN BEN-MENACHEM (2009: xi)



## 1. INTRODUCTION: A SHORT OVERVIEW

Beyond the visible world, a new avenue of biological and medical research was opened up with the invention of the microscope in the 17<sup>th</sup> century<sup>1</sup>. With this fascinating instrument the inner face of nature, once closed off to both intuition and direct observations, was revealed to the human eye (Mayr, 1982; Wilson, 1995; Mazzarello, 1999). Hogg (1854) points out that the microscope increased our sensorial perception, enlightening new amazing animal, vegetable and mineral kingdoms where beauty, perfection, adaptation and velocity of reproduction surpassed all of the objects and living organisms known before. The microscope's technical capabilities changed dramatically human concepts about the world with substantial epistemological, metaphysical and methodological implications to science (Wilson, 1995). By

---

<sup>1</sup> According to Hogg (1854), the invention of the microscope cannot be traced with accuracy before the year 1660. However, if we define microscope as an instrument consisting of one single lens, its history is more ancient (Hogg, 1854). In fact, there are written records from the Greek author Aristophanes (4<sup>th</sup> century B.C.) that point to the existence of globular glasses, also called "burning spheres", used to increase visual perception (Hogg, 1854; Croft, 2006). In the first century A.D., Seneca wrote that paper letters could be enlarged by viewing them through a globe of glass filled with water (Croft, 2006). A thousand years before, the Arabian scholar Alhazan wrote about optical principles, describing the eye anatomy and how a lens could improve focusing images (Croft, 2006: 5). In spite of historical data concerning the first proto-microscopes, the invention of a composite microscope is shrouded in uncertainties (Croft, 2006). Both Italians and Dutch claim its invention (Hogg, 1854; Hajdu, 2002). For some authors, Galileo Galilei (1564-1642, Italy) is credited as the father of the microscope (as well as the telescope), whereas for others, it was developed by Hans Jansen and his son Zacharias of Middleburg (1588-1630, Netherland) around 1595 (Hajdu, 2002; Croft, 2006; Ben-Menahem, 2009). The word microscope derives from the Greek terms "small" and "to view", and was introduced in 1625 by the Italian physician Johannes Faber (1574-1629) (Hajdu, 2002). A major contribution to microscopy was made by Robert Hooke (1635-1703, England) with the publication of his book "Micrographia", in which the term "cell" was used for the first time (Hogg, 1854; Mazzarello, 1999; Croft, 2006; Ben-Menahem, 2009). In 1653, Petrus Borellus (1620-1689, France) published a report describing the first application of the microscope to medicine (Lloyd, 1898; Hajdu, 2002). Curiously, one of the greatest contributions to microscopy was made by an amateur, the Dutch draper maker Anthon van Leeuwenhoek (1632-1723, Netherlands) (Mayr, 1982; Mazzarello, 1999; Hajdu, 2002; Croft, 2006; Ben-Menahem, 2009). He was responsible for the discovery and description of bacteria, protozoa, spermatozoa, and blood cells (in 1695), and for the first observations of bone tissue, namely the periosteum (Leeuwenhoek, 1720; Mayr, 1982; Hajdu, 2002). Since then many improvements were made on microscope capabilities with increasing sophistication (see Hogg, 1854), and its use became more frequent, not only in medical diagnosis, but also in biological and geological studies (Croft, 2006).

revealing layer after layer of very small articulated structures, the microscope gave sense to the idea of a non-occult interpretation of natural phenomena, leading to a truly remarkable “recalibration of human knowledge” (Wilson, 1995: 41). In agreement with Wilson (1995), the discovery of such a parallel microcosm offered to metaphysicians the challenge to reconcile the ubiquity of life with contemporary anthropocentric views. Additionally, it revolutionized philosophical thought, shaking the foundations of previous beliefs (Mayr, 1982)<sup>2</sup> and raising questions about the concepts of order and chaos, realism and the unrealistic world, the boundaries of human perception, as well as the role of “instrumentally mediated knowledge”<sup>3</sup> to the improvement of science (Wilson, 1995: 71).

The discovery of an entire world of microscopic living forms comprising algae, bacteria, protozoa, fungi and viruses introduced new doubts about their origin, continuity and possible relationship with human diseases (Mayr, 1982). In fact, it is almost impossible to talk about the findings of Gerhard Hansen (1841-1912, Norway), Robert Koch (1843-1919, Germany) and Louis Pasteur (1822-1895, France) without referring to the value of the microscope (Kato, 1973; Ben-Menahem, 2009; Merrill, 2010).

In the medical domain, the use of the microscope allowed the development of innovative methods for anatomical dissection, as complex body systems could be separated into smaller components, the tissues and the cells (Hogg, 1854; Mayr, 2004). Besides gross anatomy, physicians were now able to examine the physiology of organs and the interaction of cells (Mayr, 2004). For instance, we can emphasize the first descriptions of bone histology published by Anthon van Leeuwenhoek in November 20<sup>th</sup>, 1720: «[i]t is impossible for those, who have not seen this with their own eyes, to conceive the prodigious number of small

---

<sup>2</sup> The discovery of new facts through microscopic analysis gave biology and medicine a new enthusiasm for experiment, observation and comparative studies (Wilson, 1995; Hays, 2009). Such improvements had a negative effect on the dominant philosophies of Aristotle (384-322 BCE, Greece) and Claudius Galen (129-200 CE, Greece and Rome) (Ben-Menahem, 2009; Hays, 2009). The belief that God’s power dominated the universe, and that man occupied a central place in it – or the universe revolved around humankind - started to be questioned (Hays, 2009). In fact renown philosophers from the 17<sup>th</sup> century, such as René Descartes (1596-1650, France) and Francis Bacon (1561-1626, England), came to the radical conclusion that all knowledge accepted in the past as true was uncertain and that new epistemological principles were needed, independently of their deductive or inductive nature (Ben-Menahem, 2009; Hays, 2009). Quoting Hays (2009: 99), «[i]n either case authority – perhaps Aristotle’s, perhaps Galen’s, perhaps Christianity’s – must be set aside».

<sup>3</sup> In the 17th century two explanatory philosophies were debated, one explaining natural events as the result of forces acting upon distances, the opposite justifying natural phenomena on the base of mechanics (Hays, 2009). The first was strongly defended by the empiricists who had a firmly established “first-person view of experience”, rejecting any type of “instrument-assisted sense perception” like the microscope (Wolfe, 2010: 337). The second was represented by mechanistic philosophers who accepted the microscope’s potential with enthusiasm (Wolfe, 2010). To those «(...) the microscope is viewed as extending the sensory powers of the subject, and indeed her intellectual power (...)» (Wolfe, 2010: 337).



vessels, of which the cortical part of the bone consists; which in some places lies no thicker upon the spongy part of the bone, than a thick hair of a man's head (...)» (page 92).

Another important contribution of microscopy was to disease diagnosis (Hays, 2009; Merrill, 2010). The foundations of clinical histology, also called histopathology, can be traced back to the year 1799 when Xavier Bichat (1771-1802, France), a young pathologist, published a book entitled “*Traité des membranes en general et de diverses membranes en particulier*” in which, and for the first time, morbid anatomy and histopathological changes were described (Bichat, 1799; Hajdu, 2002). Focusing the importance of microscopy on disease diagnosis, Hogg (1854: vi) states that: «[t]he smallest portion of a diseased structure, placed under a microscope, will tell more in one minute to the experienced eye than could be ascertained by many days' examination of the gross masses of disease in the ordinary method».

The usefulness of histopathology early surpassed the frontiers of medicine, being incorporated by other sciences. This was the case for paleopathology. The use of histological techniques in paleopathological investigations offered the possibility to look inside the microstructure of both normal and abnormal body tissues (i.e. bone, teeth, mummified bodies) to diagnose diseases that affected past populations. Undeniably, the application of tissue microscopy is, by itself, deeply embedded in the history of paleopathology as a modern science (Aufderheide and Rodríguez-Martín, 1998).

Paleopathology, defined by Sir Marc Armand Ruffer (1859-1917) in 1914 as «(...) the science of the diseases which can be demonstrated in human and animal remains of ancient times» (Moodie, 1921: 374), had a discrete onset at the end of the 18<sup>th</sup> century characterized by punctuated discoveries in mainly non-human remains (Aufderheide and Rodríguez-Martín, 1998; Ortner, 2003a; Mann and Hunt, 2005). In the following century, emphasis was placed on the description and differential diagnosis of pathological cases, which was increasingly improved by the application of new techniques of observation, such as microscopy and radiology (Mendonça de Souza et al., 2003; Grauer, 2008; Ortner, 2011a). After World War II, a new approach to the analysis of the antiquity of disease emerged; instead of describing exciting and rare diseases, researchers re-focused their interest on the study of health patterns of past populations (Aufderheide and Rodríguez-Martín, 1998; Mendonça de Souza et al., 2003; Ortner, 2003a; Mann and Hunt, 2005; Grauer, 2008). The combination of macroscopic examination and descriptive analysis with modern diagnostic techniques, such as radiology, histology, immunology, and more recently ancient DNA, is claimed to be responsible for the

contemporary scientific character of the discipline (Aufderheide and Rodríguez-Martín, 1998; Mann and Hunt, 2005).

## **1.1. PALEOHISTOPATHOLOGY: BONE DISEASE DIAGNOSIS AND THE CHALLENGES OF PALEOPATHOLOGY**

Paleopathology is currently conceived as the study and interpretation of disease and injury that afflicted our ancestors (human and non-human), through a combination of both primary (i.e. mummies, bones, teeth, ashes)<sup>4</sup> and secondary (i.e. paintings, religious statuary, pottery, burial goods, and written documents) sources of evidence (Magner, 1992; Lovell, 2000; Ortner, 2003a; Zimmerman, 2004; Roberts and Manchester, 2005; Buikstra, 2010). It is an interdisciplinary science (Roberts and Manchester, 2005; Perez, 2006) that focuses not only on the study of health conditions of past populations or societies, but also aims to trace the origin and evolution of diseases in a biocultural perspective (Martin, 1991; Lovell, 2000; Zimmerman, 2004; Roberts and Manchester, 2005; Perez, 2006). Additionally, it offers a good measure of the adaptative capabilities of humans to the surrounding environment, being a fundamental step in every bioarchaeological study (Ortner, 2003a; Zimmerman, 2004; Roberts and Manchester, 2005). As pointed out by Roberts (2010: 39): «[e]xploring health and disease in bioarchaeology provides us with a window on how populations have adapted to (or not) changes in their environment». This attempt to draw a global picture of diseases in order to understand their present-day evolution falls within the field of paleoepidemiology (Dutour, 2008).

Nevertheless, in the past two decades pertinent questions have been addressed about the effectiveness of paleopathology, especially in the difficult task of reconstructing the evolutionary history of infectious diseases (Wood et al., 1992; Larsen, 2006). With the re-emergence of ancient diseases such as tuberculosis, paleopathologists have focused their interests on host-pathogen co-evolution in order to understand disease development in the past as a way to predict their “behaviour” in the future (Buikstra, 2010). However, critics have warned that linking community health with skeletal indicators of morbidity is not a

---

<sup>4</sup> Human skeletal remains are a notable source of information, since they represent the last biological testimonies of our ancestors (Larsen, 2002) and in some cases, the only picture of health available (Steckel, 2003).

straightforward exercise due to the effects of selective mortality<sup>5</sup> and hidden heterogeneity<sup>6</sup> in the risk of developing illness (Wood et al., 1992; Wright and Yoder, 2003; Pinhasi and Bourbou, 2008; Larsen, 2010). As a consequence, the mortality pattern observed in a particular sample may not parallel the parameters of the living population from which it is derived (Pinhasi and Bourbou, 2008; Pinhasi et al., 2011). This problem is addressed in the 1992 publication “[t]he osteological paradox: problems of inferring prehistoric health from skeletal samples”, by Wood and co-authors. According to these authors, a high prevalence of skeletal lesions may be a sign of better health, suggesting that individuals survived long enough to develop bone changes (Wood et al., 1992). A year before, Ortner (1991: 10) had noted that in cases where skeletal involvement occurs late in the disease process, individuals must survive in order for bone lesions to appear, indicating «(...) a good immune response and relatively healthy individuals». The publication of the “Osteological paradox” challenged the “conventional” paleopathological interpretation that attributes the absence of bone lesions to a good health (Bennike et al., 2005; Cook and Powell, 2006; Pinhasi and Bourbou, 2008). Simultaneously, it started a broader discussion that is far from being finished (Pinhasi and Bourbou, 2008). Some authors are in agreement with Wood et al.’s (1992) point of view (e.g. Wright and Chew, 1998; Wright and Yoder, 2003); for others (e.g. Goodman, 1993; Cohen et al., 1994; Armelagos and Van Gerven, 2003; Mendonça de Souza et al., 2003; Bennike et al., 2005; Jackes, 2011) the presence of bone lesions continues to be a good measure of the morbidity and mortality profiles of the living populations (Pinhasi et al., 2011). In spite of all critics, the majority of researchers agree that Wood et al.’s (1992) paper was extremely valuable since it forced bioarchaeologists to evaluate previously unexamined biases and interpretations built into paleopathological and paleodemographic research (Sullivan, 2005), as well as to be conscious of the fact that different interpretations of prevalence data are possible (Pinhasi and Bourbou, 2008: 37). Furthermore, it gave bioarchaeologists a powerful lens through which they can critically evaluate their own work without forgetting the role of culture in generating heterogeneity (Wright and Yoder, 2003; Sullivan, 2005). Through Wood et al.’s (1992) work it became clear that the interpretation of bioarchaeological data must be done cautiously given the limitations imposed by skeletal samples (Katzenberg et al., 1996). In the domain of paleopathology, other

---

<sup>5</sup> According to Wood et al. (1992) mortality is selective since it targets those individuals that are at the higher risk of death in the population, instead of killing them all at the same rate.

<sup>6</sup> Hidden heterogeneity refers the individual’s frailty or susceptibility to disease and death. This heterogeneity may be caused by genetic factors, socioeconomic differences, microenvironmental variation, or even from temporal trends in health and disease (Wood et al., 1992).

potential limitations besides selective mortality and hidden heterogeneity can be pinpointed. These are: (1) the representativeness of skeletal assemblages; (2) the importance of differential diagnosis; (3) the reliability of the methods used in bone disease diagnosis; and (4) the low sensitivity and specificity of bone lesions, especially those of infectious origin (Wood et al., 1992; Dutour, 2008).

In accordance with Wright and Yoder (2003), our ability to make inferences about a past population's health depends on the representativeness of archaeological sampling of ancient human remains. This assumption has been addressed by numerous authors (e.g. Wood et al., 1992; Waldron, 1994 and 2007; Kemkes-Grottenthaler, 2002; Roberts and Buikstra, 2003; Dutour, 2008; Milner et al., 2008; Pinhasi and Bourbou, 2008; Ortner, 2011b). For instance, Waldron (1994 and 2007) argues that an assemblage of skeletons is neither a population nor a representative sample of the living because they are "generally small, scattered and badly preserved and probably non-random" (Mendonça de Souza et al., 2003: 24). Considering this subject, Jackes (2011) points out that in bioarchaeology we only can work with what is allowed by the chance of preservation and recovery. Quoting Milner et al. (2008: 571): «[t]he bones we might examine are the ones that survived a complicated winnowing process that might be summarized by the following sequence: living → dead → buried → preserved → found → saved». In fact, there are several factors, both extrinsic (i.e. burial assemblage and cultural practices associated with the body disposal, duration of the inhumation, taphonomic constraints and methods of archaeological excavation) and intrinsic (i.e. structure of the sample in terms of sex and age at death distribution) that can bias our ability to make statements about past populations (Mays, 1998; Chamberlain, 2000; Roberts and Manchester, 2005; Waldron, 2007; Dutour, 2008; Pinhasi and Bourbou, 2008; Stodder, 2008; Jackes, 2011). From the above mentioned factors, taphonomy is considered a powerful disrupting force that obliterates evidence from the paleodemographic and paleopathological record (Stodder, 2008). Several biological, chemical and physical agents play a determining role in the preservation of human remains (Mays, 1998; White and Folkens, 2005; Stodder, 2008; Turner-Walker, 2008). These agents are normally responsible for the differential preservation of bone elements, as they vary in their strength and microstructure (Mays, 1998; Pinhasi and Bourbou, 2008; Jackes, 2011). Furthermore, they can produce postmortem changes mistakenly diagnosed as disease lesions (Ortner, 2003b; Pinhasi and Bourbou, 2008; Turner-Walker, 2008). The presence of a pathological condition at the time of death may also contribute to differential preservation of the skeleton (Pinhasi and Bourbou, 2008). It is important to note

that bone preservation may vary not only between archaeological assemblages, but also within the same cultural layer in the excavated area (Pinhasi and Turner, 2008; Stodder, 2008). Besides taphonomy a variety of socio-cultural, political, economic and religious factors can shape the composition of a certain necropolis, affecting the representativeness of the skeletal assemblage, and consequently, the true prevalence of bone lesions (Jackes, 2011).

The second major issue concerns the differential diagnosis. According to Larsen (2006: 363): «[d]iagnosis is still an important element of understanding disease and health history in an ancient population». As Ortner (2003c and 2011b) notes, differential diagnosis in paleopathology depends on a careful evaluation of the type of bone abnormalities observed, their distribution, as well as some knowledge regarding the disease process and the physiological factors that affect the body's response to disease. However it is well known from the paleopathological literature that the bone response to disease is limited to abnormalities of size, shape, density, bone formation and bone destruction (Ortner, 2003b and 2011b; Roberts and Manchester, 2005). This fact means that disease diagnosis in paleopathology is not as straightforward as in medicine (Larsen, 2002). In a clinical setting, a diagnosis relies on the patient history, symptoms, direct clinical examination and supplementary laboratory tests, whereas in paleopathology it is almost entirely based on the gross observation of skeletal remains (Waldron, 2007). The absence of soft tissues, organs, cells and body fluids broadly limits the accuracy of the paleopathological diagnosis (Ortner, 2003c; Pfeiffer, 1991a). Furthermore, it excludes the chance to establish symptomatology or to follow the progress of the condition (Pfeiffer, 1991a). Thus, in paleopathology the differential diagnosis is silent (no medical records are available to trace the clinical history of individuals), static (no clinic evolution is checked) and limited (mainly to skeletal expression) (Dutour, 2008). As a consequence, many diseases are under-represented or unrecorded since they may not have produced visible bone changes (Zimmerman, 2004; Dutour, 2008; Ortner, 2011a). Even in those disorders that typically involve the skeleton, individuals are not equally affected (Ortner, 2011b). Moreover, a number of different bone conditions may coexist at the time of death, which makes differential diagnosis difficult (Ortner, 2011b).

The reliability of paleopathological diagnosis also depends on the methods used. Although the importance of using multiple lines of inquiry in the analysis of skeletal remains is well recognized, the majority of studies are based on gross inspection (Grauer, 2008). This reality may lead to simplistic and misleading interpretations, since different conditions, acting solely or in synergistic interaction, may produce the same pattern of bone lesions (Wood et al.,

1992; Grauer, 2008). Further limitations are imposed by the fact that diseases are rarely represented by a single typical symptom or trait (Dutour, 2008). In fact, only a few conditions that affect the skeleton leave pathognomonic traits that allow for a positive diagnosis (Waldron, 2007).

Finally, the majority of bone lesions are insensitive indicators of their associated disease processes (Wood et al., 1992). Similarly they present a relatively nonspecific reaction to a variety of stressing agents (Pfeiffer, 1991a). The nature of periosteal bone reactions is a striking example of this phenomenon (Ortner, 1991; Weston, 2008). If periosteal lesions encompass the macroscopic signatures of a particular disease, which include their morphology, types of new bone produced and anatomical distribution, in addition to other types of skeletal evidence, as in the case of tuberculosis, treponemal diseases and leprosy, the diagnosis is more straightforward (Larsen, 2006; Ortner, 2011a). Unfortunately, this ideal scenario is usually absent (e.g. due to taphonomic constraints), which constrains our ability to identify infectious diseases in skeletal remains (Larsen, 2006; Weston, 2008).

Taking into account the challenges faced by paleopathology, what can researchers do to reduce the limitations on the study of past diseases, especially those of infectious origin involving periosteal new bone formation (PNBF)?

The main solution advanced by several authors (e.g. Ortner, 1991 and 2003b; Buikstra, 2010; Ortner, 2011a and 2011b) relies on the application of more accurate methods for the description and diagnosis of pathological conditions. Ortner (2011a and 2011b) states that an effective collaboration between skeletal paleopathology and the medical knowledge derived from orthopaedic pathology and radiology is required to improve the disease description. Furthermore, he highlights the need to develop a proper classificatory system for describing gross bone abnormalities in order to reduce biased interpretations between researchers (Ortner, 1991). This recommendation integrates the three mandatory rules required for the macroscopic description: (1) an unambiguous terminology; (2) a precise identification of the location and distribution of bone abnormalities affecting the component of the bone involved, the aspect of the bone and affected features; and (3) a descriptive summary of the morphology of the bone lesions describing the type of bone formed and its organizational structure (Ortner and Putschar, 1981; Lovell, 2000; Ortner, 2003b; Roberts and Manchester, 2005; Grauer, 2008).

The development and/or improvement of new analytical instruments is another important avenue that may ensure the production of relevant data about past diseases

(Ortner, 1991 and 2011b; Buikstra, 2010). Wood et al. (1992: 357) pointed out that: «(...) we need a better understanding of the details of various pathological processes at the cell, tissue, and organ levels. Specific aspects of pathology that need to be addressed include how long it takes to develop particular hard-tissue lesions, how overall health affects the probability of lesion development, and how frailty and the risk of death vary by stage of lesion development, including the inactive or healed stage» (Wood et al. 1992: 357). Reiterating this statement Wright and Yoder (2003) argue that in addition to the macroscopic observation, the application of biomolecular and histological techniques may be very useful in clarifying the nature of bone changes. According to these authors, the application of histological [or paleohistopathological] methods may be especially important for examining the degrees of bone healing, as well as to identify traces of disease in cases where little bone response occurred prior to death (Wright and Yoder, 2003). This assumption is equally shared by Ragsdale and Lehmer (2012: 227): if cells are the effectors of bone changes, understanding their dynamic interaction is a necessary step for the differential diagnosis.

Bone, as a dynamic and living tissue, has the capability to self-repair throughout life, changing its properties and configuration in response to mechanical demands and stress factors (Ortner, 1991; Garland, 1993; Schultz, 1997; Gosman and Stout, 2010). The paleohistopathological analysis of human remains can provide a wide range of information regarding normal and pathological changes that occurred during an individual's lifespan in response to internal and external stimuli (Martin, 1991). Moreover, it offers a glimpse into the products of cellular activity, such as excessive tissue mineralization, signs of abnormal bone resorption, and residual organics associated with past diseases (Bell and Piper, 2000; Ortner, 2003b). Through the microscope lens, all antemortem and abnormal changes to the bone microstructure can be ascertained, which provides important insight into the vascular and cellular conditions associated with the underlying pathology (Ortner, 2003b). The histological scrutiny provides information on a more subtle level that is otherwise omitted from the bone surface (Martin, 1991). This property can be very useful for differential diagnosis in a way that surpasses both macroscopic and radiological scrutiny alone (e.g. Garland, 1993; Schultz, 1993; 1997; 2001 and 2003; Bell and Piper, 2000; Larsen, 2006). Schultz (2001; 2003 and 2012) emphasizes that regular use of microscopy must be established in order to obtain more reliable diagnoses. As pointed out by Frost (1964 in Martin, 1991: 55): «[b]one at the microscopic level can be used as a tool, that is, a model system or biological “window” into the past giving a view of earlier behaviour and health of the skeletal system».

Studying traces of disease in poorly preserved archaeological remains can also be enhanced by microscopic investigation (Schultz, 1997 and 2001). Even when bone is incomplete and shows taphonomic changes at the macroscopic level, a considerable amount of information about the underlying pathology can be gathered from histological analysis (Uytterschaut, 1993; Bell and Piper, 2000). Differentiation between antemortem and postmortem bone changes is also possible through microscopy (Schultz, 1997), which substantially reduces the amount of bias in the differential diagnosis.

The only point of disagreement concerning the application of paleohistopathological techniques is related to the low sensitivity/specificity of some bone lesions, such as periosteal new bone formation (PNBF). According to Schultz (2001; 2003 and 2012) all diseases that cause bone changes can be studied by microscopy. The author emphasizes that a particular group of conditions (e.g. haematogenous osteomyelitis, treponemal diseases, leprosy, nonspecific and specific osteomyelitis, scurvy, anemia, rickets, and tumours, among others) are only diagnosable by microscopy. Schultz's (2001; 2003 and 2012) assumption is based on the premise that certain diseases such as tuberculosis, treponematosi s and leprosy imprint a characteristic "testimony" on the periosteal microstructure that is different from that caused by nonspecific inflammatory conditions (e.g. haematogenous osteomyelitis). For example, Schultz (2001: 126) argues that the presence of polsters ("pillow-like newly built bone formations") and grenzstreifen ("a very fine or a narrow, band-like structure that represents the original external surface of the bone shaft") are considered a telltale sign of treponemal diseases. With respect to this issue, Pfeiffer and Pinto (2012) are of the opinion that only a few conditions leave a distinct histological signature that allows for a definitive differential diagnosis, for instance osteoporosis, hyperparathyroidism, Paget's disease, treponemal infection and leprosy. Recent studies focusing on the macroscopic (Weston, 2004 and 2009) and the histological (von Hunnius et al., 2006; Weston, 2004 and 2009; Van der Merwe et al., 2010) structure of periosteal reactions similarly show an absence of specific diagnostic traits. Van der Merwe et al. (2010) state that the features associated with treponemal diseases may be not exclusive to these diseases. However, they underline the value of histology in distinguishing between infectious lesions and those of traumatic origin, such as ossified haematomas (Van der Merwe et al., 2010). Researchers also highlight the multiple pathogenesis of periosteal reactions, a fact frequently ignored in population studies, where the assumption of an infectious aetiology of these lesions is common (Weston, 2004). All criticisms reinforce the need to understand the range of variation of periosteal reactions at the



microscopic level, both qualitatively and quantitatively, in order to develop more accurate methods for the differential diagnosis of infectious diseases (von Hunnius et al., 2006; Weston, 2004 and 2009). As Ortner (1991) recommended two decades ago, basic research on the biological significance of many microscopic features is required to develop standards for distinguishing among normal and abnormal histological patterns. This will certainly help in ascertaining the real sensitivity and specificity of bone lesions, and consequently, the true prevalence of disease in skeletal assemblages. In addition to these reliable diagnoses, a better understanding of the aetiology and epidemiology of diseases in ancient populations will be possible (Schultz, 2012).

## 1.2. OBJECTIVES

The chief goal of this research is *to develop diagnostic criteria that can be used to distinguish between infectious disease and other systemic conditions that potentially stimulate the development of periosteal reactions (e.g. tumours and bone trauma), with particular emphasis on the identification of fragmentary bone lesions unearthed from archaeological contexts*. Combining both macroscopic and histological sources, the purpose of this research is twofold: firstly, to analyze the macroscopic distribution of periosteal reactions by age and cause of death, anatomical location, side location, symmetry, bone dispersion and type of new bone; and secondly, to microscopically examine and compare thin sections of periosteal new bone, in order to evaluate the existence (or not) of microstructural differences in individuals who died from: (1) tuberculosis infections-TB; (2) non-TB infections; and (3) other systemic conditions of different aetiologies. To pursue this goal, bone samples were collected from the Human Identified Skeletal Collection of the Museu Bocage (Lisbon, Portugal). For comparison, archaeological samples were collected from three distinct skeletal assemblages (14<sup>th</sup>-19<sup>th</sup> centuries): the Constância necropolis; the cemetery of the hospital of the *Ordem do Carmo* in Oporto; and the cemetery of the Royal Hospital of All Saints in Lisbon.

The study's specific hypotheses are as follows:

1. *Does new bone deposition manifest differently, both macroscopically and histologically, in the different cause-of-death groups?* With respect to both TB and non-TB infectious groups, several macroscopic studies point to a possible association between new bone deposition on the visceral surface of ribs and cases of pulmonary TB (Roberts et al., 1994;

Santos and Roberts, 2001 and 2006; Matos and Santos, 2006). However, this proliferative phenomenon also occurs in other infectious and inflammatory conditions of the lungs (Roberts et al., 1994). So, at the histological level, *are there qualitative differences between pulmonary and non-pulmonary TB conditions that allow for a positive diagnosis?*

2. With respect to TB infectious and other systemic conditions, *are the proliferative lesions of tuberculous origin different from those caused by tumours?* In early stages of fracture healing, the new bone formed may mimic that of infectious origin, which can be particularly problematic when studying fragmentary remains from archaeological contexts. Thus, *to what extent is the new bone produced during fracture remodelling different from that of infectious origin?*

3. *Does bone microstructure remain unaffected in cases where no visible lesions are present?*

4. And finally, considering both identified and archaeological samples, *do histological comparative studies aid in the differential diagnosis of archaeological remains?* Since burial conditions (e.g. soil type, duration of inhumation and others) affect the integrity of bone tissue (Nawrocki, 1995; Ortner, 2003b; Roberts and Manchester, 2005), *what major taphonomic differences are found among identified and archaeological samples and what are the implications for the differential diagnosis?*

---

# CHAPTER 2

---

*"PALAEOHISTOLOGY IS A UNIQUE AND EXCITING TOOL FOR THE STUDY OF EXTANT  
MATERIAL, AND ITS TOTAL POTENTIAL IS, AS YET UNTAPPED"*

GARLAND (1993: 14)



## **2. PALEOHISTOPATHOLOGY: A LITERATURE REVIEW**

The main goal of paleohistopathology (or paleohistology, as referred to by the pioneering researchers) is the description and diagnosis of pathological changes in ancient remains (e.g. Schultz, 1986, 1993, 1997, 2001, 2003 and 2012; Martin, 1991). The long partnership between paleopathology and paleohistology is clear in the literature, as it seems to hold much promise for the improvement of disease diagnosis. However, and contrary to paleopathology whose journey is well-established, in paleohistopathology there are many gaps that need to be filled. This occurrence is probably the result of a nonsystematic and non-standardized approach to the microscopic study of skeletal abnormalities in past human remains.

In the following pages, a critical evaluation of the history of paleohistopathology will be made. Since the usefulness of paleohistopathological diagnosis depends on the methods applied, the state of art of the discipline will be accompanied by a summary of the main technical achievements.

### **2.1. CONCEPTS AND HISTORICAL ENDEAVOR**

The first application of histology to the study of ancient pathological remains can be traced back to the 19<sup>th</sup> century. With respect to the analysis of mummified remains, this technique was pioneered by the Czech physician J. N. Czermak (1828-1873), in 1879, to describe a case of arteriosclerosis in an Egyptian mummy (Aufderheide and Rodríguez-Martín, 1998; Aufderheide, 2003; Denton, 2008). In the beginning of the 20<sup>th</sup> century, Sir Armand Ruffer, a professor of Bacteriology in Cairo (who is also considered the father of

paleopathology) developed revolutionary methods for rehydrating mummified tissues for histological inspection (Sandison, 1967; Swinton, 1981; Auferderheide and Rodríguez-Martín, 1998; Auferderheide, 2003; Denton, 2008). In order to restore the flexibility of tissues, Ruffer's method consisted of embedding sectioned material in several cycles of alkaline salts (sodium carbonate) mixed with alcohol for two to three days, followed by baths in pure reagents (alcohol, chloroform or paraffin) (Moodie, 1921). Through this innovative procedure, several paleopathologies were identified on mummified and bone remains, such as arterial diseases, diffuse anthracosis of lungs, kidney abscesses, spondylitis deformans of vertebrae, among others (Moodie, 1921). In his paper entitled "Histological studies on Egyptian mummies" presented at L'Institut Égyptien in 1911, Ruffer emphasized the importance of the systematic use of histology as a complement to the macroscopic observation of pathological changes (Moodie, 1921). Almost at the same time the eminent British pathologist S. G. Shattock (1852-1924) studied histological sections of an aorta from an Egyptian pharaoh (Lovell, 2000). Since this early beginning, the contribution of histology to the analysis of disease on mummified bodies has been considerable (e.g. Sandinson, 1955; Post and Daniels, 1969; Armitage and Clutton-Brock, 1981; Massa, 1981; Weinstein et al., 1981; Pahl, 1983; Walker et al., 1987; Zimmerman et al., 1998; Ciranni et al., 1999; Lynnerup, 2007; Zweifel et al., 2009). This growing interest was improved by new techniques for the preparation of mummified tissue (e.g. Graf, 1949; Sandinson, 1955; Turner and Holtom, 1981; Hess et al., 1998; Auferderheide, 2003; Mekota and Vermehren, 2005).

Histological examination was also applied by Roy L. Moodie (1880-1934, USA) to the study of bone lesions on nonhuman fossil remains (Moodie, 1918a and 1918b), for example, a rib fracture from a reptile from the Permian of Texas (Moodie, 1918b); a hemangioma observed on two caudal vertebrae from an *Apatosaurus* from the Comanchian (Moodie, 1918a and 1918b); and a case of osteoperiostitis observed on a humerus from a *Mosasaur* from the Cretaceous (Moodie, 1918a and 1918b). Apart from applying this new diagnostic technique, Moodie was also responsible for introducing the concept of paleohistology in 1926 (Garland, 1993). Nevertheless, it was not until 1949 that a proper definition was proposed by Wilhelm Graf (Sweden), who described paleohistology as «(...) the examination of microscopic sections of ancient human beings and the recognizing of tissues and cells in such sections» (Graf, 1949: 236). With regard to the study of archaeological human bone, the first histological analysis was undertaken by the American pathologist Theophil Mitchell Prudden (1849-1924) in 1891 (Garland, 1993). Prudden used microscopy to confirm a possible case of syphilis observed in

two adult tibiae exhumed from the prehistoric site of Animas River, Colorado, whose microstructure revealed chronic periostitis and osteomyelitis. Another historical reference concerning the application of histology to skeletonized remains is attributed to Carl Magnus Fürst (1854-1935, Sweden) who diagnosed, in 1920, a case of periostitis ossificans in the tibia of King Magnus of Sweden, 13<sup>th</sup> century A.D. (Graf, 1949). In 1927, M. Weber (Germany) developed a new microscopic technique to distinguish inflammatory bone lesions linked with presumed syphilitic cases (Graf, 1949; Schultz, 1997). In spite of Weber's efforts to standardize diagnosis, little attention was paid to his work (Schultz, 1997). A year later, H. U. Williams described an experimental method to the study of osteoporotic bones that consisted of embedding fragile bones in celloidin and then decalcifying them in an acid solution (Graf, 1949). Focusing on the preservation of mummified and dry bone remains, Graf (1949) performed a comparative study on three Egyptian mummies and fifteen Swedish skeletons from different chronological periods, concluding that there were no parallels between the chronology and the microscopic preservation of remains (an assertion that is still valid today, see e.g. Stout and Teitelbaum, 1976; Schmidt-Schultz and Schultz, 2007). No pathological indicators were recorded by the author. Besides the comparative histomorphology, Graf also tested different methods. Regarding the preparation of dry bone specimens he adopted the classical histopathological procedures used by clinicians that consisted of bone decalcification (nitric acid), paraffin-embedding and staining techniques (Graf, 1949).

Despite all of the medical improvements on light and polarized microscopy<sup>7</sup>, as well as on techniques for decalcification, paraffin wax embedding<sup>8</sup>, and handgrinding of human bone, the histological analysis of archaeological bone and teeth remained underdeveloped until the

---

<sup>7</sup> Polarized light microscopy allows a detailed picture of cells and tissues by revealing the birefringence (this property is the numerical difference between the maximum and minimum principal refractive indices) of long molecules, such as those that comprise the collagen fibers (Lovell, 2000; Delly, 2008). This type of analysis is achieved adding an analyser and a polarizer on the microscope and orientating polarization planes to a right-angled position in order to reveal bright and black areas (Herrmann, 1993). Introducing tint plates, interference colours may be produced, allowing for the identification of the physical properties of the bone samples (Herrmann, 1993).

<sup>8</sup> Decalcification and paraffin-embedding biopsy is the most common method applied to the histological study of soft tissues, cartilage, and decalcified bone specimens in both experimental and diagnostic histotechnology and histomorphometry (An and Gruber, 2003). Bone decalcification consists of its immersion in an acid solution (hydrochloric acid and nitric acid in an aqueous solution are the most commonly used), a chelating solution (a chelator is an organic chemical, such as ethylenediamine tetraacetic acid – EDTA that bonds with tissue and removes free metal ions from solutions) or a solution consisting of an acid-chelator complex (Skinner, 2003). Paraffin-embedding techniques were introduced by Edwin Klebs in 1869 and are today one of the most suitable methods for embedding soft tissues and decalcified hard tissues. Other methods using waxes and resins have also been developed according to the specificities of the specimens (An et al., 2003).

mid-1990s (Garland, 1993)<sup>9</sup>. Two main reasons may explain this lack of interest: firstly, the emphasis placed on bioanthropological studies during the first half of the 20<sup>th</sup> century, for example, on the description of skull morphology and subsequent “racial” classification (Garland, 1993; Armelagos and Van Gerven, 2003); and secondly, due to technical limitations dictated by the nature of the samples. The physical properties of archaeological bone and teeth fall among those of fresh and fossil origin: they do not possess the elasticity that characterizes living tissues, nor the hardness of fossil remains, a fact that generates substantial difficulties during bone sectioning (Turner-Walker and Mays, 2008).

The situation started to change in the 1950s with the introduction of plastic embedding techniques for the preparation of thin sections and new microscope devices (Herrmann, 1993; Turner-Walker and Mays, 2008). For instance, a simple method consisting of bone fixation in successive alcohol and ether-alcohol baths, and bone infiltration in a solution of ether-alcohol solvated plastic (plasticized nitrocellulose) to increase bone hardness was proposed by Arnold and Jee (1954). A similar procedure, using a plastic substance (methyl methacrylate monomer) was also presented by Jowsey (1955). Shortly afterwards, the feasibility of plastic embedding media started to be investigated, with researchers searching for the quickest and most advantageous method to produce bone samples (Woodruff and Norris, 1955). Focusing on the preparation of thin undecalcified bone sections, Frost published, in 1958, the guidelines of an innovative method characterized by its simplicity, cheapness, rapidity and dependability. Bone, instead of being fixed, embedded, dehydrated and heated as in the previous methods, was simply ground on both sides, using abrasive paper on a plate of glass gently moistened with water (Frost, 1958). Also in 1958, Pugh and Savchuck (1958) presented a new suggestion for undecalcified bone preparation based on plastic embedding (polyvinyl resin), polishing and staining techniques. In 1968, two distinct papers concerning the use of staining-labelling techniques (in vivo) to evaluate the rates of bone formation and resorption in undecalcified bone samples were published by Frost (1968) and Hoyte (1968). Although these innovations were first used in the field of medicine, they were rapidly adapted to the study of ancient remains. In 1969, the result of one of the first applications of the electron microscope<sup>10</sup> to the

---

<sup>9</sup> Even the technique of bone decalcification was revealed to be unfeasible in certain circumstances, since it affects the mineral arrangement and the biochemical components of bone required in some paleopathological studies (Arnold and Jee, 1954; Jowsey, 1955; Franklin and Martin, 1980).

<sup>10</sup> One of the first researchers to apply electron microscopy to the study of ancient bone remains was Barbour (1950). In her pioneering work, she compared fresh and fossil bones with distinct chronologies to evaluate small structures that were beyond the range of light microscopy (Barbour, 1950). Transmission electron microscopy (TEM) is the most powerful technique for evaluating the microstructure and morphology of large molecules, such as those from bone tissue (An and Gruber, 2003). Additionally, certain tissue structures like cell nuclei are revealed



analysis of pathological tissues from Egyptian and Peruvian mummies was presented by Macadam and Sandison (1969). Criticizing the pioneering methods of decalcification of ancient human bone, Stout and Teitelbaum (1976) proposed a new method using plastic embedding substances (methyl methacrylate). According to these authors, this technique provided excellent preservation of bone microstructure, allowing for the diagnosis of many systematic diseases and deficiencies (Stout and Teitelbaum, 1976). Two years later, Pawlicki (1978) described an alternative method combining grinding and staining techniques for the preparation of fossil bone for light and transmission electron microscopy.

Regarding the time-consuming nature of the traditional methods, Wallin et al. (1985: 331) proposed a new “low-speed rim-type diamond cut-off wheel and a slowly advancing table” for carrying the bone specimen that only required dehydration and epoxy resin embedding (grinding was not needed). One year later, Schultz (1986) published an extensive work on the application of light and polarized microscopy to the study of bone lesions in prehistoric skeletons, highlighting the methodology used. In 1988, a rapid method for producing stained undecalcified bone sections was presented by Emmanuel (1988). A similar work based on methyl methacrylate embedding and staining protocols was published by Sterchi and Eurell (1989). In 1991, Maat (1991) used a scanning electron microscope<sup>11</sup> to compare the ultrastructure of both normal and pathological red blood cells with pseudopathological structures. The same technology was applied by Wakely et al. (1991) to the study of rib lesions.

Aiming to discuss the untapped potential of microscopy in bioarchaeology and forensic science, a “Palaeohistology Workshop” was held at the University of Göttingen, Germany, in 1990. After the meeting, a proceedings book entitled “Histology of ancient human bone: methods and diagnosis” was edited by Grupe and Garland (1993). Among the subjects discussed, particular emphasis was placed on the description of the methods used in the study of decomposition phenomena (Grupe and Dreses-Werringloer, 1993), differential diagnosis of

---

(Lovell, 2000). Through TEM analysis, a beam of electrons with a smaller wave-length crosses bone, producing an image with a much higher magnification when compared with light microscopy (Lovell, 2000).

<sup>11</sup> Scanning electron microscopy (SEM) and backscattered electron microscopy (BSEM) are important microscopic techniques for evaluation of the structure and morphology of bone such as the trabecular bone surface, osteoclastic bone interface and vascular structure (An and Gruber, 2003). Scanning electron microscopy is designed to make a scan of the object in a raster pattern, producing an image that is built up serially (Lovell, 2000). With SEM analysis it is possible to observe the bone surface features with a three-dimensional resolution (Lovell, 2000). Compared with SEM, BSEM is more sensitive to subtle differences in sample density, allowing for a more clear observation of the bone elements, such as lamellar bone, osteons, cement lines, reversal lines, amongst others (Turner-Walker and Mays, 2008). Furthermore, it is useful for distinguishing soil components, exogenous minerals and altered bone minerals from normal or pathological bone (Turner-Walker and Mays, 2008).

human and animal bones (Harsányi, 1993) and general observations of the bone microstructure (Heuck, 1993). In 1995, Abou-Arab and co-authors (1995) published a technical note concerning the importance of staining in the study of secondary osteons. A method for bone and teeth slide preparation to be carried out in different microscope modes, namely light and backscattered electron microscopy was accurately described by Goldman and co-authors (1999). Caropreso et al. (2000) made available a simple method based on resin embedding (epoxy resin), cutting and mounting procedures to apply to both modern and archaeological remains. A year later, a revised and modified version of Frost's rapid manual method was proposed by Maat and co-authors (2001). In the same year, an innovative method for the morphological study of fungi and bacteria contaminating ancient human bone, combining resin embedding (Implex "three-phase" polyester resin) and staining techniques was presented by Dore et al. (2001). An extensive handbook focusing on histological methods for bone and cartilage was edited by An and Martin (2003), in which numerous procedures for sample fixation, decalcification, embedding, staining, cutting, grinding and instrumental observation are presented and discussed. In the meantime, several studies were conducted to test the feasibility of the available methods for the study of dry bone samples (e.g. Beauchesne and Saunders, 2006; Martiniaková et al., 2006). In 2007, a guideline manual for teeth sectioning and analysis was developed by FitzGerald and Saunders to be used in the Anthropology Hard Tissue and Light Microscopy Laboratory at McMaster University. Recently a new method for embedding, sawing, grinding and staining was proposed by De Boer et al. (2012a and 2013) to study undecalcified archaeological bone samples, especially when lesions are present. Finally, in the recent book entitled "Bone histology: an anthropological perspective", two chapters are exclusively dedicated to laboratory histology procedures and microscope instrumentation (Cho, 2012; Cooper et al., 2012).

In addition to the improvements in the preparation of samples, other sophisticated microscope techniques were introduced to the study of archaeological remains, namely the atomic force microscope<sup>12</sup> (Thalhammer et al., 2001), the epifluorescence microscope<sup>13</sup>,

---

<sup>12</sup> Also called scanning force microscopy (SFM), the atomic force microscope (ATM) is a high-resolution type of scanning microscope used to image and measure properties of material, chemical and biological surfaces with an accurate resolution ranging from 100µm to less than 1µm (Blanchard, 1996; Galloway Group, 2004; Turner-Walker and Mays, 2008). This new instrument was invented by Gerd Binnig, in 1986, to study and image materials that do not conduct an electric charge (Galloway Group, 2004). In comparison with other techniques it provides extraordinary topographic contrast; three-dimensional images with low expense sample preparation and high resolution (Blanchard, 1996; Galloway Group, 2004; Turner-Walker and Mays, 2008).

<sup>13</sup> Fluorescence microscopy is nowadays an essential tool for medical and biological studies (Spring, 2003). The use of fluorochromes (stain substances that attach themselves to visible or subvisible structures) made possible

microscopic computerized tomography<sup>14</sup>, and the confocal laser scanning microscope<sup>15</sup> (Kuhn et al., 2007; Rühli et al., 2007; Maggiano et al., 2009; Šefčáková et al., 2001).

## 2.2. PALEOHISTOPATHOLOGY TODAY: A SYSTEMATIC REVIEW OF THE PUBLISHED DATA

Despite the improvements made in sample preparation and analysis, the “running for technology” was not pursued by a systematic application to paleopathological studies (Grupe and Garland, 1993). To test this assumption, a literature review was conducted in the main journals of the area (Table 2.1), using the online platform ISI Web of Knowledge/Web of Science and PubMed<sup>16</sup>. Regardless of the apparent simplicity of this task, it was not straightforward as it required the use of several key-words to target the higher number of articles, for instance: paleohistology and paleohistopathology [or palaeohistology and palaeohistopathology], histology, histologic, microscopy, microscope, microscopic<sup>17</sup>. In the case of journals with a broader scientific spectrum such as PLoS One and PNAS, the key-words

---

the identification of molecules and other structures of interest (Spring, 2003). Accordingly to Erben (2003), in bone and teeth the fluorochrome bands are visualized through UV, blue-violet, or blue excitation, which are activated by super pressure mercury vapour lamps or laser devices. In epifluorescence microscopy, the vertical illuminator of the microscope is designed to direct light onto the specimen by first passing it through the objective on the way toward the specimen and then using the same objective to capture the emitted light (Spring, 2003: 549).

<sup>14</sup> According to Cooper et al. (2012), microscopic computerized tomography (or micro-CT) is an extension of computed tomography (CT) applied to the microscopic level. CT is an x-ray non-invasive technique that generates serial cross-sectional images used to visualize the internal structure of organisms in 3D. Micro-CT presents two variants: laboratory micro-CT, built around microfocus x-ray sources; and synchrotron (SR) micro-CT that employs radiation within a synchrotron facility, for example the European Synchrotron Radiation Facility in Grenoble, France (Cooper et al., 2012). SR micro-CT has opened the way for a range of microscopic and analytical techniques at the nanometre level with high resolutions (Turner-Walker and Mays, 2008). This type of micro-CT produces images comparable to BSEM, but without the need for physical sectioning of the specimens (Turner-Walker and Mays, 2008).

<sup>15</sup> Confocal microscopy has a wide range of application in biomedical and orthopedical research (An and Gruber, 2003). It creates image reflecting light off of the surface of the specimen or as an alternative, stimulating fluorescence from special dyes used to stain the specimen (Turner-Walker and Mays, 2008). In bone, the fluorescence can be endogenous or introduced to target a particular structure (Cooper et al., 2012). The Confocal Laser Scanning Microscopy (CLSM) is able to produce focused images of specimens that normally appear distorted in a conventional microscope (Turner-Walker and Mays, 2008). Another advantage is that it can be used on unfixed, wet specimens or cells (An and Gruber, 2003).

<sup>16</sup> This survey only considered complete journal articles published until January 2012. Special volumes or numbers containing abstracts from meetings were not evaluated because in many cases the information available is not sufficient for a complete analysis.

<sup>17</sup> The survey on the *Bulletins et Mémoires de la Société d'Anthropologie de Paris* was made using key-words in English and French.

were always combined with the term “paleopathology” or “bioarchaeology” to narrow the search. The same principle was used during the search on PubMed. The references targeted in each journal were then uploaded to a bibliographical management software, EndNote X3®, and stored in specific libraries. Regarding those journals that are not indexed in the selected platforms (e.g. ASE: Anthropological Science, *Bulletins et Mémoires de la Société d'Anthropologie de Paris* and JASs: Journal of Anthropological Sciences), a consultation was made individually, searching for all of the available articles on the journal’s website. The Journal of Paleopathology was consulted in its paperback version. The steps followed during the selection of the references are summarized in Figure 2.1.

**Table 2.1:** List of selected journals used for analysis.

Journal list	Publishing source	Online database
<b>American Journal of Physical Anthropology</b>	<b>Wiley Online Library</b> [Articles available online: since 1918]	ISI Web of Knowledge
<b>Archaeology, Ethnology and Anthropology of Eurasia</b>	<b>Elsevier Science Direct</b> [Articles available online: since 2008]	ISI Web of Knowledge
<b>ASE: Anthropological Science</b>	<b>J-Stage   Japan Science and Technology Information Aggregator, Electronic</b> [Articles available online: since 1998]	Individual search
<b>Bulletins et Mémoires de la Société d'Anthropologie de Paris</b>	Articles available online: From 1859-1999, <b>Persée</b> From 2000-2010, <b>Revue.org</b> From 2010-present, <b>Springer</b>	Individual search
<b>Forensic Science International</b>	<b>Elsevier Science Direct</b> [Articles available online: since 1978]	ISI Web of Knowledge
<b>HOMO: Journal of Comparative Human Biology</b>	<b>Elsevier Science Direct</b> [Articles available online: since 2002]	ISI Web of Knowledge
<b>International Journal of Osteoarchaeology</b>	<b>Wiley Online Library</b> [Articles available online: since 1991]	ISI Web of Knowledge
<b>International Journal of Paleopathology</b>	<b>Elsevier Science Direct</b> [Articles available online: since 2011]	ISI Web of Knowledge
<b>JASs: Journal Anthropological Sciences</b>	<b>Istituto Italiano di Antropologia</b> [Articles available online: since 2004]	Individual search
<b>Journal of Archaeological Science</b>	<b>Elsevier Science Direct</b> [Articles available online: since 1974]	ISI Web of Knowledge
<b>Journal of Forensic Sciences</b>	<b>Wiley Online Library</b> [Articles available online: since 2006]	ISI Web of Knowledge
<b>Journal of Human Evolution</b>	<b>Elsevier Science Direct</b> [Articles available online: since 1972]	ISI Web of Knowledge
<b>Journal of Paleopathology</b>	<b>Museo Universitario di Chieti</b> [Articles available: from 1987-2009]	Individual search
<b>PLoS One</b>	<b>Public Library of Sciences</b> [Articles available online: since 2006]	Individual search
<b>PNAS</b>	<b>National Academy of Sciences from USA</b> [Articles available online: since 2000]	Individual search
<b>Virchows Archiv</b>	<b>Springer</b> [Articles available online in English: since 1960s]	ISI Web of Knowledge

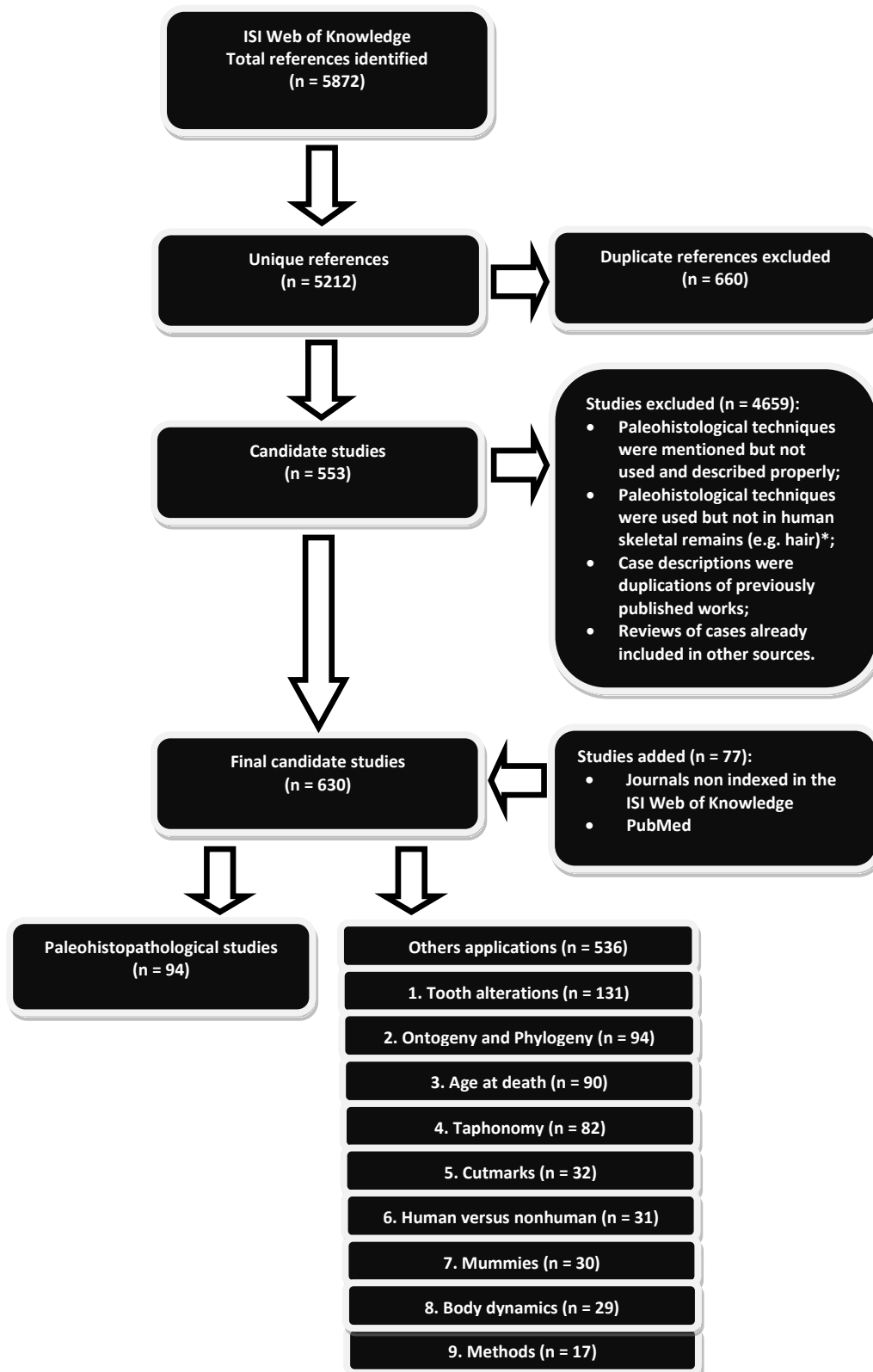


**Figure 2.1:** Results of the systematic literature review (\*references related to mummy histology, calcified tissues and other body substances found in bioarchaeological contexts were included in this survey).

Through key-words scrutiny, a total of 5872 references were targeted in the ISI Web of Knowledge platform. From this assemblage, all duplicate references (n=660) were removed, and some others were eliminated (n=4659) because they did not match the search criteria for the following reasons: (1) paleohistological techniques were mentioned but not used and described; (2) paleohistological techniques were used but not in bone and tooth remains; (3) case descriptions were duplications of previously published works; and (4) some studies were reviews of cases already included in other sources<sup>18</sup>. After the rejection of references, a candidate sample composed of 553 studies was obtained. To this sample were added 77 references collected in journals that are not indexed in the ISI platform and others allocated in PubMed, yielding a total of 630 studies that have used paleohistology as a diagnostic tool.

In spite of the high number of references found, only 94 focused on the paleohistopathological analysis of bone conditions (Table 2.2)<sup>19</sup>.

---

<sup>18</sup> The approval or rejection of the references was done taking into account the title and the abstract contents. When no direct mention of paleohistology techniques was found in the title or abstract, a more in-depth paper review was conducted to eliminate possibilities.

<sup>19</sup> The results presented here are obviously under represented since they are based on a restricted journal selection.

**Table 2.2:** Summary of paleohistopathological studies in the literature.

Authors/year	Study type	Sample ID	Pathological condition	Microscope technique	Paleohistopathological results
Cule and Evans (1968)	Case-study	Skull vault from a non-adult skeleton, National Museum of Wales, U.K. (Bronze Age)	Porotic hyperostosis: iron-deficiency anemia	Light and electron microscopy	Inner and outer tables with intervening cancellous bone with a normal appearance. Absence of any excess of unmineralized bone.
Arnaud and Arnaud (1975)	Case-study B	Skull fragments from a young female from the necropolis of Notre-Dame du Bruse, France (Paleo-Christian period)	Porotic hyperostosis: thalassaemia minor or constitutional haemolytic anemia	Light microscopy	Thickness of the skull vault with expansion of the diploe. Generalized osteoporosis with thinning of the inner table. The limit between the outer and the inner table and diploe is not well defined.
Martin and Armelagos (1979)	Population study	74 adult individuals (40 females, 34 males) from a Prehistoric population from Sudanese Nubia, Sudan (350-550 A.D.)	Osteoporosis	Microradiograph	High cortical bone loss in females (10.7%) when compared with males (4.9%), especially before the third decade of life. In males, a decrease in mineralization of the periosteum and endosteum was observed. Females older than 30 showed a high frequency of resorption spaces and forming osteons. Stress related to childbearing and childrearing may be responsible for the frequencies observed in this population.
Martin et al. (1981a)	A*				
Lagier and Baud (1980)	Case-study B**	Right adult femur from Switzerland (Medieval period) – portion of the diaphysis and the bone overgrowth collected	Myositis ossificans circumscripta	Microradiograph, polarized light microscopy	The bone overgrowth is composed of spongy trabeculae that are thicker than in normal bone. The histological analysis revealed cortical bone with a normal lamellar structure and Haversian systems. The bone overgrowth showed osteons partly remodeled.
Weinstein et al. (1981)	Case-study B	Left hemipelvis from an adult male mummy from the pre-Columbian civilization at Chancay, Peru (400-1600 A.D.)	Metabolic disorder	Microradiograph, light microscopy	The histomorphometric analysis revealed low trabecular bone volume and trabecular atrophy consistent with an unknown metabolic disease. The study questions the negative effect that certain metabolic diseases may have on histological age at death estimation.

Authors/year	Study type	Sample ID	Pathological condition	Microscope Technique	Paleohistopathological results
Lagier et al. (1982)	Case-study B	Two Paleo-Eskimo skulls from St. Lawrence Island, Alaska (1 <sup>st</sup> -14 <sup>th</sup> century A.D.); Case #1: Non-adult individual Case #2: Adult male	Infection and malignant tumor	Light, polarized microscopy and microradiograph	The histological examination showed good preservation of the bone tissue and helped in the differential diagnosis: Case #1: Chronic infection secondary to blunt trauma; Case #2: Malignant tumor, more probably metastatic carcinoma.
Lagier et al. (1983)	Case-study B	Adult male left tibia from the necropolis of Corseaux-sur-Vevey, Switzerland (3200-2500 B.C., Neolithic)	Brodie's abscess	Microradiography	Thickening of cancellous trabeculae surrounding the cavity abscess. Postmortem damage by fungi and bacteria.
Tkocz and Bierring (1984)	Case-study B	Adult male rib from the medieval churchyard of Svendborg (Denmark)	Metastatic carcinoma	Light microscopy	Deeper disarranged bone is seen, consisting of fragments of lamellar bone surrounded of more primitive structures with collagen fibers and patchwork like arrangement.
Martin and Armelagos (1985)	Population study A	Sample composed of 185 adult human femora from Prehistoric Sudanese Nubia	Nutritional deficiency	Light microscopy, microradiograph	The study revealed deficient bone maintenance in young and old females (density and morphology of osteons affected). The results are related to nutritional stress in reproducing females and to age in old females.
Martin et al. (1987)	Population study A	Sample composed of 80 skeletons from Arkansas, USA (1878-1939) – 29 adult femoral thin sections (15 females, 14 males)	Nutritional deficiency	Light microscopy	The histological analysis showed low percent of cortical bone and high rates of resorption when compared to bone formation. The pattern of bone porosity observed is not age dependent but rather the result of nutritional and disease stress.
Stuart-Macadam (1987)	Population study B	Poundbury Camp, Roman-British series and Hodgson collection, East Asian (19 <sup>th</sup> century)	Porotic hyperostosis and <i>cribra orbitalia</i> (anemia?)	Light microscopy	The bone microstructure presents a thinned outer table and cancellous bone with enlarged spaces opening to the surface, which correspond to the external porosities. These changes are consistent with marrow hyperplasia.



Authors/year	Study type	Left Sample ID	Pathological condition	Microscope Technique	Paleohistopathological results
Suzuki (1987)	Case-study B	Young adult female left femur from Oahu Island, Hawaii (precontact Hawaiian)	Osteosarcoma	Light microscopy	Large amount of coarse tissue formation (woven bone) with a poorly organized structure that do not reveal the presence of Haversian lamellae or remodelling osteons.
Cook et al. (1988)	Case-study B	Adult female skeleton from Dakleh Oasis, Egypt (36 B.C.-400 A.D.) – femoral head sampled	Hyperparathyroidism	Polarized, ultraviolet light	Trabecular bone sections showed lamellar bone, fibrous lamellar bone and tunneling resorption. The subchondral plate exhibited scalloping and crenulation of surfaces, features that are consistent with a case of hyperparathyroidism.
Grupe (1988)	Case-study B	Adult male rib sample from Germany	Bronchogenic carcinoma	Light microscopy	Presence of osteolytic lesions originating from the deeper layers of the bone tissue with cortical destruction.
Ripamonti (1988)	Case-study B	Fossil remains from a juvenile <i>Australopithecus africanus</i> from Sterkfontein, South Africa (2.5-3.0 Ma) – alveolar bone sampled	Prepuberal periodontitis	Stereomicroscopy and scanning electron microscopy	The anatomy of the alveolar crest shared the presence of perforating nutrient canals at the bone surface which points to a pathological process of corticalization of the endosteal surface. Presence of a vertical pattern of bone loss.
Grévin et al. (1990)	Case-study B	Cremated skull fragments from a young adult from Seine –et- Marne, France (Late Bronze Age)	Healed trephination or <i>foramina parietalia permagna</i>	Light microscopy	The microscopic analysis revealed postmortem destruction (enlargement of the lacunae spaces with deposition of amorphous material) induced by bacteria. Enlargement of the vascular channels due to the action of fire. The paleopathological analysis revealed an increased thickness of the skull vault composed of compact lamellar bone crossed by vascular channels.
Molto (1990)	Case-study B	Right ribs from an adult male from the LeVesconte burial mound, southern Ontario, Canada (300 B.C. – A.D. 500)	Actinomycosis	Scanning electron microscope	Signs of bone remodelling in the subperiosteal zone with unremodelled periosteal new bone formation on the pleural surface.

Authors/year	Study type	Sample ID	Pathological condition	Histological Technique	Paleohistopathological results
Bell and Jones (1991)	Case-study A	Medieval adult left humerus and radius: Case #1: St. Margaret, Norwich; Case #2: Sandwell Priory, Sandwell	Paget's disease	Scanning electron microscope (SEM) in backscattered electron (BSE)	More than a diagnostic tool, SEM-BSE technique was highly sensitive and informative about the effect of diagenetic processes on the bone microstructure survival.
Strouhal (1991)	Case-study B	Adult male from Sayala, Egyptian Nubia (6 <sup>th</sup> -11 <sup>th</sup> century) – occipito-lateral wall of the left maxillary sinus sampled	Primary carcinoma of the nasal and paranasal cavities	Light, polarized and scanning electron microscopy	Signs of rapid bone resorption in the external and internal wall of the maxillary sinus. Excessive destruction of the lamellar bone structure. Localized osteoclastic activity with well-defined Howship's lacunae.
Wakely et al. (1991)	Case-study A	Rib samples from British Roman and Medieval cemeteries	Respiratory infectious conditions	Scanning electron microscopy	The samples showed active deposition of bone around a network of vascular grooves that vary from slight deepening grooves to the complete enclosure of blood vessels. Several superimposed layers of new bone were observed, indicating a chronic process. Evidence of osteoblastic and osteoclastic activity (Howship's lacunae).
Aaron et al. (1992)	Case-study A	Case #1: Adult male skeleton exhumed from Wells Cathedral, U.K. (16 <sup>th</sup> century); Case #2: Isolated medieval sacrum recovered at Barton-on-Humber, U.K.	Paget's disease	Light, polarized microscopy	The histological analysis confirms the regions of abnormal bone (increasing trabecular width and mosaic woven bone). Without microscopic examination the gross evidence remained insubstantial.
Anderson et al. (1992)	Case-study B	Adult male from medieval Canterbury, U.K. – rib, mandible and skull scrutinized	Metastatic carcinoma	Scanning electron microscopy	The lesions consisted of irregularly arranged flaps and trabeculae of bone, creating a complex network structure. Solid areas are also seen, particularly in the centre of the lesions. New bone was observed encircling small blood vessels, as well as inside the marrow spaces.

Authors/year	Study type	Sample ID	Pathological condition	Histological Technique	Paleohistopathological results
Blondiaux et al. (1992)	Case-study B	Young adult from Les Rues des Vignes, Nord, France (500-700 A.D.) – ulna, femur, and tibia sampled	Hypertrophic osteoarthropathy (HOA)	Microradiograph, instrumental neutron activation	The microradiograph cross-section and the chemical components of bone (Zn) indicated areas of active bone mineralization at the time of death compatible with HOA.
Roberts and Wakely (1992)	Population Study A	Sample of skeletons from the Roman and Medieval period, U.K. – vertebrae and radius sampled	Microfractures associated with osteoporosis	Scanning electron microscope	In the vertebrae, the analysis of the cancellous tissue revealed high horizontal trabecular resorption and loss of connectivity between adjacent trabeculae. Presence of healing microfractures on the vertical trabeculae. The distal end of the radius callus was filled with trabecular bone. A band of dense bone marked the site of the united fracture.
Lazenby and Pfeiffer (1993)	Case-study A	Adult male skeleton (executed criminal Marion “Pegleg” Brown), London, Ontario, Canada (19 <sup>th</sup> century) - femora sampled	Left lower leg amputation	Light microscopy	Marked asymmetry due to bone hypertrophy between femora. The analysis of the left femur from the amputated leg showed a reduction in the normal size and geometric strength of the bone tissue, along with an increase in cortical bone turnover.
Blondiaux et al. (1994)	Case-study A	Case #1: adult female from Neuville-sur-Escaut, northern France; Case #2: adult male from Vaison-la-Romaine, southern France (5 <sup>th</sup> -6 <sup>th</sup> A.D.) – metatarsals sampled	Leprosy	Light microscopy, microradiograph	Replacement of large parts of the normal bone by well-mineralized, irregular and lamellar bone with scattered and abnormally large osteons. In some cases, the erosion of the endosteal and periosteal envelopes destroyed the normal contour of the cortex with numerous disseminated osteoclastic lacunae and no signs of bone remodelling.
Lewis (1994)	Case-study B	Six right tibiae and a metacarpal bone from a Tchefuncte Indian burial site (500 B.C. - 300 A.D)	Treponematosi and Lyme borreliosis	Light microscopy	Resorption and deformation of the bone tissue.

Authors/year	Study type	Sample ID	Pathological condition	Histological Technique	Paleohistopathological results
Parsche et al. (1994)	Case-study B	Right tibia from a young adult male from the site of Pacatnamu, Peru	Periostitis secondary to an injury other than fracture	Polarized microscopy, immunohistology	Evidence of intensive new bone production in the periosteal layer. Signs of intensive osteogenesis leading to local osteosclerosis. Increased bone remodelling in the exterior compacta at the time of the death. Ossifying haematoma, sclerosing osteomyelitis and tumors excluded from the differential diagnosis.
Ricci et al. (1994)	Case-study B	Non-adult from L'Aquila, Abruzzo, Italy (15 <sup>th</sup> century) – skull was sampled	Meningioma or neuroblastoma	Light microscopy	Presence of osteoclastic lacunae in the skull due to bone resorption secondary to tumor infiltration.
De La Rúa et al. (1995)	Case-study B	Adult male exhumed from a mass burial of San Juan Ante Portam Latinam, Laguardia, Spain (5000 B.P.) – iliac blade was sectioned	Metastatic carcinoma	Light, polarized microscopy	Signs of osteoclastic and osteoblastic activity in the iliac blade, causing the total replacement of the original bone. The tumor is arranged in elongated spiculae that are perpendicular to the cortical plates. Absence of normal trabecular bone. The tumor seems completely mineralized.
Foldes et al. (1995)	Case-study B	Adult female ilium from the Negev Desert, Israel (500 A.D.)	Osteoporosis	Light microscopy	Extreme osteopenia. Thin and porous cortex. Eroded surfaces present at the trabecular, endocortical and at the periosteal surfaces. No woven bone was detected.
Wakely et al. (1995)	Case-study B	Adult male from medieval Canterbury (U.K.) – ribs were sampled	Metastatic carcinoma - prostatic	Scanning electron microscopy	The ribs show a mixture of osteoclastic and osteoblastic lesions, forming elongated and irregularly shaped (spikes, bars, smooth areas) patches of abnormal bone on the visceral surface. Osteoblastic deposits also encircle blood vessels. Deposits of trabeculated bone fill the space between the normal spongy bone trabeculae. Osteoclastic lesions are normally located around the margins of the osteoblastic deposits.

Authors/year	Study type	Sample ID	Pathological condition	Histological Technique	Paleohistopathological results
Duhing et al. (1996)	Case-study B	Adult male from the Anglo-Saxon cemetery of Barrington, U.K. (6 <sup>th</sup> -7 <sup>th</sup> centuries) – cranial vault sampled	Osteolytic metastatic carcinoma	Light, scanning electron microscopy	Compact bone with variable thickness and atypical lamellar structure. Spongiotic layer characterized by thickened and deformed trabeculae disrupted by Howship's lacuna.
Malgosa et al. (1996)	Case-study B	Four neonate individuals from the Ermita de la Soledad, Huelva, Spain (16 <sup>th</sup> century). Samples collected from: Case #1: right humifrontal; Case #2: left humerus; Case #3: left humerus; Case #4: left femur	Congenital syphilis and haematogenous osteomyelitis (?)	Light microscopy (?)	Case #1: Bone with a hyperostotic appearance and a porous aspect on its surface; Case #2: Juxtametaphysial detachment of the outer layer of the cortical bone with some periosteal osteolysis; Case #3: Areas of osteolysis on the distal epiphysis; Case #4: The cortical layer has a porotic appearance with signs of remodelling on the borders of the lytic region.
Mays et al. (1996)	Case-study B	Adult male from Wharram Percy, U.K. (11-16 <sup>th</sup> century A.D.) – ribs sampled	Metastatic Carcinoma	Light, scanning electron microscopy	Under light microscopy remnants of osteoblasts cover the surfaces of trabeculae. The distinction between cortical and cancellous bone is obliterated. Normal bone structure was substituted by irregular trabeculae.
Strouhal et al. (1996a)	Case-study B	Three adult male skulls from an ossuary at Křtiny, Czech Republic (13 <sup>th</sup> – 18 <sup>th</sup> centuries)	Malignant tumors	Light and scanning electron microscopy	Case #1: Osteolytic metastatic carcinoma (mixture of trabecular resorption and new lamellae formation); Case #2: Osteolytic metastatic carcinoma (massive destruction of the spongiotic trabecular bone); Case #3: Multiple myeloma (spongiotic trabeculae without signs of Howship lacunae resorption. Localized pathological damage of trabeculae).

Authors/year	Study type	Sample ID	Pathological condition	Histological Technique	Paleohistopathological results
Strouhal et al. (1996b)	Case-study B	Two adult skulls from a male and a female from the ossuary at Křtiny, Czech Republic (13 <sup>th</sup> - 18 <sup>th</sup> centuries)	Female: osteoma or hyperostosis; Male: fibroma or angiofibroma	Light and scanning electron microscopy	Female: regular trabecular bone with a non-lamellar pattern and uneven calcification. No remnants of osteoblastic activity. Male: hypertrophied and densely packed spongiotic trabeculae with remnants of osteoblasts on their surfaces. Some lacunae of osteocytes were observed.
Wapler and Schultz (1996)	Case-study A	Ten skull fragments from 6 non-adults and 4 adults (2 males, 1 female and 1 with sex undetermined) exhumed in Turkey (2500 B.C.), Sudan (Meriotic Period) and Germany (6 <sup>th</sup> -7 <sup>th</sup> A.D.)	<i>Cribrra orbitalis</i> and porotic hyperostosis: Anemia, and infection and postmortem changes	Light and polarized microscopy	Anemia: the skull vault revealed pathological destruction of the outer table and expansion of diploë. The majority of the orbital samples showed enlargement of the medullae with subsequent migration to the outer tables. The supraorbital diploë presented elongation of the porous areas. Infection: the bone remains showed superimposed layers of bone over the inner table with the limits of the original cortex clearly defined. Slight destruction of the diploë.
Zias and Mitchell (1996)	Case-study B	Commingle skeletal remains of nine males and one female from the Byzantine Monastery of Martyrius, Israel (15 <sup>th</sup> century) – phalanges observed	Psoriatic arthritis	Scanning electron microscopy	The analysis revealed erosive cavitations with variable degrees of sclerosis that ranged from shallow erosion in the cortex to severe erosion of the cancellous bone. The lesions are periarticular in some areas, but partially or totally destroyed the joint surface in other areas.
Aufderheide et al. (1997)	Case-study B	Adult female from the Chiribaya people, Southern Peru (1150-1300 A.D.) - right humerus sampled	"Sunburst" osteosarcoma	Scanning electron microscopy	Specimens show the formation of reactive spicular woven bone with a sponge-like structure. The tumor lesion presents a rough-texture, rounded matrix deposits attached to the healthy bone surface.
Blondiaux (1997)	Case-study B	Adult male from Somme, France (12 <sup>th</sup> century) – left femur sampled	Infectious condition (probably associated with a skin condition)	Light microscopy	Three types of periosteal reactions were identified: two composed of a single layer of woven bone and a third formed by remodeled bone. A division line between distinct periosteal appositions was also observed.

Authors/year	Study type	Sample ID	Pathological condition	Histological Technique	Paleohistopathological results
Blondiaux et al. (1997)	Case-study B	Two adult skeletons: a female from the cathedral of Rouen (11 <sup>th</sup> century) and a male from Lisieux (4 <sup>th</sup> century), France – metatarsals and metacarpals sampled	Symmetrical erosive polyarthropathy	Light, polarized microscopy	Female skeleton showed small appositions of woven bone and resorption lacunae in the erosive surfaces. Male skeleton presented generalized erosion with no signs of new bone formation. In front of the bone erosion, Howship's lacunae were observed.
Capasso (1997)	Comparative study A	Case #1: Human skull For comparison: ribs from fish of the Miocene and Pliocene, as well as from mammals	Osteoma	Light microscopy	Case #1: The lesion presents a rock-hard, irregularly nodular or granular mass of bone. Wide trabeculae of mature bone are present in an irregular pattern. Because of the numerous trabeculae and their increased width, the intertrabecular spaces are reduced.
Mays and Nerlich (1997)	Case-study B	Non-adult from Wharram Percy, U.K. (Medieval period) – anterior margin of the mandible sampled	Langerhan's cell histiocytosis	Polarized microscopy	Lack of woven bone or major reactive sclerosis. No major evidence of osteoclastic activity. Only mature lamellar bone was present.
Strouhal et al. (1997)	Case-study B	Young adult male skull exhumed from the Chapel of St. Joseph, Kyjov, Czech Republic (late medieval-early modern)	Osteosarcoma	Light, scanning electron microscopy	The tumor lesion showed newly formed trabeculae composed of less-mineralized bone within areas of well-mineralized tissue. Presence of uneven mineralization consisting of rough thickened and irregularly spaced trabeculae. Presence of osteocyte small lacunae. Howship's lacunae were rare.
Wakely et al. (1998)	Case-study B	Adult female from the Medieval Lay cemetery of Abingdon Vineyard, Oxfordshire, England (13 <sup>th</sup> 16 <sup>th</sup> centuries) – ribs sampled	Multiple myeloma	Light, scanning electron microscopy	The external layer of the rib was uneven thickened. Trabeculae of spongy bone filled the interior of the bone. In some places Howship's lacunae were preserved. No evidence of osteoblastic deposition.
Capasso (1999)	Population study B	Sample of 151 individuals: 16 with signs of brucellosis (12 males; 4 females) from Herculaneum, Italy (79 A.D.) – ribs sampled	Brucellosis	Light microscopy	Ribs exhibited isolated or confluent bone oval masses. The surfaces of the rib lesions were smooth or rough according to their antiquity or remodelling. The bone formations consist of new bone superimposed on the older cortical surface.

Authors/year	Study type	Sample ID	Pathological condition	Histological Technique	Paleohistopathological results
HersHKovitz et al. (1999)	Population study B	3797 adult skulls: 1706 from the Hamann-Todd collection, Cleveland and Terry Collection, Washington, U.S.A. (20 <sup>th</sup> century); 1012 skulls from Native Americans (16 <sup>th</sup> -17 <sup>th</sup> century); 720 from Israel (18 <sup>th</sup> -20 <sup>th</sup> century) and 287 from Hungary historical populations; 72 skulls from cadavers were used for histology analysis	Hyperostosis <i>frontalis interna</i> (HFI)	Light, polarized and scanning electron microscopy	The inner table along with the closely attached dural layer plays a major role in the osteogenesis of HFI. Five osseous layers are observed: A, composed of dense lamellar bone with no evidence of bone remodelling; B, presents normal diploic spaces with trabeculae and associated cavities; C, shows a thin band of remodeled, disorganized, sclerotic lamellar bone with irregular cavities and ill-defined margins; D, consists of numerous thin-walled blood vessels of various diameters and large vascular sinuses; E, composed by a thin shell of organized lamellar bone, traversed by blood vessels.
Katzenberg and Lovell (1999)	Case-study A	Seven bone samples obtained at autopsy at the University of Alberta Hospital, Canada, from individuals with known cause of death. Three samples from individuals with no visible bone changes (2 males, 1 female). Four samples with visible bone changes: 1 male (fibula - periostitis); 1 female (fibula - fracture); 1 female (femur - atrophy); 1 male (tibia - osteomyelitis)	Infection, trauma , idiopathic polyneuritis	Light microscopy	The microscopic analysis revealed: One male (fibula - periostitis) - new bone deposition with a porous appearance. A line between the cortex and the new bone was visible; One female (fibula - fracture) – ossified woven bone showing some degree of remodelling; One female (femur - atrophy) – reduced diaphyseal volume justified by a high number of osteocyte lacunae and a lack of Haversian bone; One male (tibia - osteomyelitis) – endosteal bone apposition observed.



Authors/year	Study type	Sample ID	Pathological condition	Histological Technique	Paleohistopathological results
Schultz (1999)	Case-study A	Ten samples from fossilized bones: Dinosaur -1; <i>Australopithecus africanus</i> - 2; <i>Homo erectus</i> (O.H. 9) - 2; <i>Homo neanderthalensis</i> (Düsseldorf and Krapina) - 3; <i>Homo sapiens</i> - 1; <i>Pan paniscus</i> - 1	Dinosaur: hemangioma <i>Homo erectus</i> : hypervitaminosis A <i>Homo neanderthalensis</i> (Düsseldorf): osteoporosis and fracture <i>Homo neanderthalensis</i> (Krapina): osteoporosis	Light and polarized microscopy	Dinosaur: coarse bone trabeculae in a net-like structure located between enlarged spaces. <i>Homo erectus</i> (O.H.9): regular bone microarchitecture with a well lamellated external structure. <i>Homo neanderthalensis</i> (Düsseldorf): enlarged Haversian canals and an increase in spongy bone in the endosteal area. Evidence of bone atrophy in the fractured bone. <i>Homo neanderthalensis</i> (Krapina): generalized enlargement of the blood vessel canals. Enlarged Haversian systems with small canals. External surface with a smooth appearance.
Vyhnanek et al. (1999)	Case-study B	Right forearm bones from a young adult male from Sqqara, Egypt (664-332 B.C.)	“Kissing” osteochondroma	Light microscopy, scanning electron microscopy (SEM)	Bone outgrowths presented a normal trabecular structure. The bone is immature, fibrous and without a lamellar pattern. The contact trabeculae of the radius and ulna showed many tiny lacunae which may represent the imprints of the original cartilage.
Faerman et al. (2000)	Case-study B	Thin sections were collected from an autopsied individual: frontal portion of a thoracic vertebra and left humerus	Sickle cell anemia	Light, polarized microscopy	The humerus compact bone was replaced by porotic areas, resembling spongy bone. This abnormal tissue contacts the diaphyseal medullary space. The orientation of collagen fibers is a record of successive osteoclastic deletions and osteoblastic apposition events. The vertebral sample revealed thin and long trabeculae (sign of atrophy). The cancellous modules of the vertebral marrow were enlarged.
Djurić-Srejić and Roberts (2001)	Population study B	Sample of 1617 skeletons from later medieval Serbia (11 <sup>th</sup> -19 <sup>th</sup> centuries): Case #1: Adult tibia and fibula; Case #2: Mature male femur and tibia	Treponemal disease or non-specific haematogenous pyogenic infection	Light microscopy (?)	In both cases a thick layer of bone with a rugose porous surface and cavitations was observed. The cortical bone showed a necrotic area with calcified zones. Thin trabeculae with large marrow spaces.

Authors/year	Study type	Sample ID	Pathological condition	Histological Technique	Paleohistopathological results
Šefčáková et al. (2001)	Case-study B	Old male individual from Borovce, Slovakia (8 <sup>th</sup> -9 <sup>th</sup> centuries)	Metastatic carcinoma	Scanning electron microscopy, laser scanning confocal microscopy	The trabeculae of the spongy layer are covered by numerous Howship's lacunae. Trabeculae from the edge of an osteolytic focus display smooth surfaces with irregularly spaced large osteolytic lacunae, whereas the spongy trabeculae from the center of the pathologic process show numerous lacunae of different dimensions.
Alt et al. (2002)	Case-study B	Right femur of a non adult from Sulzburg, Germany (12 <sup>th</sup> century)	Osteosarcoma	Light, reflected electron microscopy	The newly formed tumor bone shows vertical bone tissue, calcified to differing extents. There is also a substantial amount of calcified tumor osteoid, forming the characteristic "chessboard-like" structure.
Bagousse and Blondiaux (2002)	Case-study B	Right tibia of a non adult from Lisieux (Calvados), France (4 <sup>th</sup> - 9 <sup>th</sup> centuries A.D.)	Caffey's disease	Light, polarized microscopy	The transverse section of the right tibial diaphysis showed eroded cortical bone surface, vascular spaces and thick fringe of primary bone.
Blondiaux et al. (2002)	Case-study B	Non adult from Lisieux, Normandy, France (4 <sup>th</sup> century) – tibia and parietal bone sampled	Rickets and trauma	Light, polarized microscopy	The skull parietal fracture presented postmortem erosion of the outer lamina. The inner lamina exhibited well remodeled laminated bone and smooth margins. In the tibia with rickets, and on the periosteum, a thick and extensive peripheral layer of osteonic bone with small and malformed osteons separated by small strips of lamellae bone was observed. The subperiosteal bone was irregular and mostly made of woven bone with large osteocytic cavities.

Authors/year	Study type	Sample ID	Pathological condition	Histological Technique	Paleohistopathological results
Eshed et al. (2002)	Population study A	Sample of 585 human (sex, age at death and race known), 52 gorilla and 52 chimpanzee skulls from the Hammann-Todd Collection, Cleveland, USA	Button osteoma	Light microscopy and scanning electron microscopy (SEM)	Three distinct histological conditions detected: Button osteoma – mushroom-like shaped poorly vascularized and composed of well-organized lamellar bone with homogeneous thickness (onion-skin pattern). Rare osteocyte lacunae. The diploic bone extended beyond the original ectocranial table into the new area of new bone. Reactive post-traumatic event – rich vascularization with plenty of osteocyte lacunae and prominent Haversian systems. Lack of laminated structure. No clear distinction between the lesion and the ectocranial table. Ballooned osteoma – characterized by a dome-shaped bony roof, poorly vascularized and multilaminated in some areas. The trabecular layer is diffuse and forms large spaces. Collapse and extensive remodelling of the ectocranial table not seen externally.
Hershkovitz et al. (2002)	Population study B	Adult skulls (n=1884) from the Hamann-Todd collection (HTH), Cleveland, U.S.A. - 12 skulls sampled	Serpens Endocrania Symmetrica (SES)	Light, scanning electron microscopy	SES process is limited to the most superficial portion of the endocranium. Three zones are observed: juxta-diploic zone with well-developed primary and secondary Haversian systems; intermediate zone, more thickened and characterized by dense, well-organized, laminated bone. It is avascular and presents sporadic Haversian systems on its margins. The third zone does not show a lamellar pattern, presenting osteocytes randomly distributed. The area is notched by several fissures, leading to a denticulated appearance. The space fissure is heavily vascularized. The bone is disorganized with numerous lacunae, but no Haversian systems. Normal thickness and appearance/organization of the ectocranial plate and diploë.

Authors/year	Study type	Sample ID	Pathological condition	Histological Technique	Paleohistopathological results
Roches et al. (2002)	Case-study A	Case #1: Adult female cranium from Lisieux, France (330-340 AD); Case #2: Adult male left femur, pelvis and lumbar vertebra from Saint-Pierre-sur-Dives, France (11 <sup>th</sup> century)	Paget's disease	Light microscopy (?)	Microscopy revealed important skeletal evidences of Paget's disease (mosaic bone, trabecular thickening, excessive bone formation and resorption).
Józsa and Fóthi (2003)	Case-study B	Right tibia and fibula from an adult female from a medieval cemetery from Budapest (14 <sup>th</sup> -15 <sup>th</sup> centuries)	Juxtacortical osteosarcoma	Light, polarized, stereo and scanning electron microscopy	Specimen with a sponge-like appearance. Spiculae with different sizes and thickness. Cortical and cancellous bone with osteolytic lacunae. No signs of bone remodelling in the destroyed areas. Presence of large structures formed by irregular neoplastic new bone trabeculae. Some tumor parts are in close contact with spongy bone remains.
Schamall et al. (2003)	Comparative study A	Lumbar vertebral bodies from 61 individuals with known sex and age-at-death (37 with signs of rickets and osteomalacia) housed at the Federal Museum of Pathological Anatomy, Vienna, Austria (19 <sup>th</sup> century)	Rickets and osteomalacia	Light microscopy, computer-assisted morphometry and scanning electron microscope (SEM)	Both techniques (non-invasive radiology and invasive histology) can be successfully applied in documented and archaeological material.
Strouhal et al. (2003) Strouhal and Němečková (2004)	Case-study B	Adult female from Iufaa, Abusir, Egypt, 26 <sup>th</sup> dynasty (625 B.C.) – remnants of soft tissue preserved on the sacrum sampled	Neurilemmoma	Light microscopy	In the remnants of the soft tissues were observed: spindle-shaped cells (Verocay bodies) surrounded by collagen stroma; microcystic changes, areas of hyalinization and remnants of cells; and Reich granules.
Tamarit et al. (2003)	Case-study B	Case #1: Adult left tibia from Segovia, Spain (11 <sup>th</sup> -12 <sup>th</sup> centuries); Case #2: Adult female left lower limb from El Burgo de Osma, Spain (17 <sup>th</sup> -18 <sup>th</sup> centuries)	Two cases of osteomyelitis: exogenous and haematogenous	Light microscopy	The histological analysis was crucial to determine the origin of the infection.

Authors/year	Study type	Sample ID	Pathological condition	Histological Technique	Paleohistopathological results
Maat (2004)	Population study B	50 Dutch whalers from Spitsbergen Archipelago, The Netherlands (17 <sup>th</sup> -18 <sup>th</sup> centuries)	Scurvy	Immunoenzymatic staining microscopy	The black stain spots observed macroscopically (tip of dental roots and at endofractures of metaphyses of weight-bearing bones) are remnants of denatured hemoglobin. No microscopic repair was denoted. In individuals who recovered several times from scurvy, the new hematomas were replaced, layer by layer, by new bone tissue.
Wapler et al. (2004)	Population study A	Sample composed of 333 skulls (161 females and 172 males) from Missimonia, Northern Sudan (2 <sup>nd</sup> -6 <sup>th</sup> centuries): 33 orbits with <i>cribra orbitalia</i> sampled	<i>Cribra orbitalia</i>	Light, polarized microscopy and polarized combined with a hilfsobject as compensator	Histological analysis revealed that 6% of the individuals suffered from anemia: the marrow spaces were widened and the orbital lamina was opened. The remaining trabeculae tended to lie almost at right angles to the orbital lamina. Signs of inflammation due to osteitis were observed in 4.5%: this process may lead to extensive bone resorption through osteoclast activity. Howship's lacunae were visible. Remodelling (or bone apposition) was also present. Histological analyses showed that 20% of macroscopic <i>cribra orbitalia</i> was due to postmortem erosion.
Canci et al. (2005)	Case-study B	Female skeleton from Montescaglioso, Basilicata, Southern Italy (6 <sup>th</sup> century) – left tibia sampled	Meliorheostosis	Light microscopy	Histological analysis showed a large disorganized distribution of Haversian channels and packed layers of woven bone. Only a thin layer of compact bone with normal Haversian system was seen on the endosteal and periosteal sides.

Authors/year	Study type	Sample ID	Pathological condition	Histological Technique	Paleohistopathological results
Brickley and Ives (2006)	Case-study B	Six non-adults from St. Martin's cemetery, Birmingham, England (18 <sup>th</sup> -19 <sup>th</sup> centuries) – orbits and scapula sampled	Scurvy	Scanning electron microscopy	The mass of porous cortical bone formed a new layer on the top of the existing bone surface. This layer was highly vascular with holes penetrating the cortex. Bone was not formed in normal layers, suggesting a rapid response to inflammation or trauma. The newly formed bone constituted a discrete layer of spongy and irregular tissue when compared with the normal solid cortex. The margins were irregular and spiculated.
Paine and Brenton (2006)	Population study A	Sample composed of 34 individuals (11 females; 23 males from different age groups) from the Raymond Dart Skeletal Collection, Johannesburg, South Africa (20 <sup>th</sup> century) - 4-6 <sup>th</sup> ribs sampled	Pellagra	Light microscopy	Extremely low rate of secondary osteons, namely in young individuals. High degree of cortical bone loss in ribs when compared with other nutritional diseases. Bone remodelling highly affected.
Von Hunnius et al. (2006)	Case-study A	Pre-Columbian skeletons from a medieval Augustinian friary, Kingston upon Hull, England. Case #1: Adult male fibula; Case# 2: Adult male proximal right humerus; Case #3: Adult female tibia and fibula; Case #4: Adult male tibial fragments	Syphilis	Light, polarized microscopy	Signs of syphilis at the microscopy level were found in case #1 and case #3: Grenzstreifen and/or cement lines separating the original bone from the newly formed bone; sinus lacunae; polsters and areas of focal destruction. Grenzstreifen and polsters suggest the presence of a chronic, inflammatory condition. Sinus lacunae indicate the presence of lytic activity (osteitis).
Brickley et al. (2007)	Population study B	291 adult skeletons from the churchyard of St. Martin's, Birmingham, England (18 <sup>th</sup> -19 <sup>th</sup> century) – rib and femur samples were collected from 7 individuals	Osteomalacia	Scanning electron microscopy (SEM)	The study showed areas of bone resorption and defective mineralization of newly formed bone, especially in the areas adjacent to the cement lines in Haversian canals. Small fragments of new bone were left unconnected to pre-existing bone. In some cases, enlarged osteocyte lacunae were observed, sometimes surrounded by poorly mineralized bone.

Authors/year	Study type	Sample ID	Pathological condition	Histological Technique	Paleohistopathological results
Capasso (2007)	Population study B	Sample of 162 skeletons (83 males, 61 females, 18 unsexed adults) from Herculaneum, Italy (1 <sup>st</sup> century A.D.) – 12 samples from distal fibula (8 males, 4 females)	Contamination by natural tetracycline (antibiotic)	Light stereomicroscope, scanning electron microscopy	Fluorescence due to tetracycline contamination was observed in: osteons that were in the remodelling phase at the time of death; lamellar bone; walls of some osteocytic lacunae and in some Volkmann's and Haversian canal walls. The signs of this natural contamination seem to explain the low prevalence of infectious lesions.
Kuhn et al. (2007)	Case-study A	Five postcranial bone samples from the Galler Collection, Switzerland (20 <sup>th</sup> century) : Case# 1: Adult male tibia; Case# 2: Adult femur; Case# 3: Adult female humerus; Case# 4: Young adult male femur; Case# 5: Adult male tibia	Case# 1: Osteomyelitis Case# 2: TB Case# 3: Trauma Case# 4: Osteogenic sarcoma Case# 5: HOA	Light, polarized microscopy, micro-computed tomography	Case# 1: Absence of the external circumferential lamella which was substituted by small osteons with Haversian channels with small lumina. Signs of strong vascularization (large vessels). Howship's lacunae rare. Trabeculae composed mainly of lamellar bone (end of remodelling); Case# 2: Absence of regular external circumferential lamellae. Active remodelling. High number of Howship's lacunae. Large areas of spongy bone composed of woven bone; Case# 3: Bone callus composed mainly of woven bone. Large resorption holes with Howship's lacunae in the compact bone; Case# 4: Large tumor infiltration combining original lamellar bone with irregular structures. No Howship's lacunae are present. Tumor woven bone extended between trabeculae; Case# 5: The original bone surface is covered with new bone (especially woven bone) with a spongy appearance. Blood vessels channels bridge compact and newly formed bone. Secondary replacement of endosteal compact bone by woven bone.

Authors/year	Study type	Sample ID	Pathological condition	Histological Technique	Paleohistopathological results
Mays et al. (2007)	Case-study B	Non-adult from St. Martin's Church, Birmingham, UK (19 <sup>th</sup> century) – distal radius sampled	Hyperparathyroidism	Scanning electron microscopy	Reduction of trabecular size by osteoclast resorption. Areas of dense new bone formation but less well-mineralized. Bite-like defects and eroded surfaces. Enlarged vascular spaces.
Rühli et al. (2007)	Comparative study A	Seven adult skulls from the Galler Collection, Natural History Museum Basel, Switzerland (20 <sup>th</sup> century)	Chronic osteomyelitis; syphilis; hyperostosis <i>frontalis interna</i> ; hyperparathyroidism; trauma; osteomyeloclerosis	Polarized light microscopy, micro-computed tomography ( $\mu$ CT)	The external and internal lamina features of the cranial bone can be visualized by $\mu$ CT and polarized histology. Both techniques permit the observation of Howship's lacunae, assessment of the bone maturity, orientation of the trabeculae and collagen fibers. $\mu$ CT is less time-consuming and the 3D image produced is better to analyze surface changes. Polarized microscopy allows a better image of bone resorption and when the diagnosis by $\mu$ CT is unclear, it is the best way to confirm it.
Schultz et al. (2007)	Case-study A	Adult Scythian King from Arzhan, Siberia, Russia (7 <sup>th</sup> century) –right parietal bone, right humerus and femur, body of the 7 <sup>th</sup> thoracic vertebra and left 4 <sup>th</sup> and 5 <sup>th</sup> rib sampled  Two recent adult males, Department of Anatomy, University of Göttingen, Germany –right femur sampled	Metastasizing prostate carcinoma	Light, polarize, scanning electron microscopy	Archaeological case: no original bone structure was preserved. Signs of irregular rapid bone growth characterized by a primary osteoclastic and a secondary dominating osteoblastic process were observed. In the skull, the original bone was substituted by a bulky, almost compact structure that caused the loss of the diploic module. On the long bones, the compact tissue was largely destroyed by osteoclastic activity, being replaced in some areas by secondary built primitive woven bone. Identical bone changes were observed on vertebrae and ribs.
Djuric et al. (2008)	Population study B	327 individuals (< 14 years old) from Stara Torina, Serbia (9 <sup>th</sup> -11 <sup>th</sup> centuries) – 12 femoral <i>cribra</i> sampled; 12 humeral <i>cribra</i> sampled	Porotic lesions: humeral and femoral <i>cribra</i>	Light, polarized microscopy	The histological analysis revealed thinning of the cortical lamina with porosity in the affected area, enlargement of the intertrabecular space, and growth of the trabeculae perpendicular to the bone surface. In some cases, the compact cortical bone is completely absent in the affected areas.



Authors/year	Study type	Sample ID	Pathological condition	Histological Technique	Paleohistopathological results
Holck (2008)	Case-study B	Adult male from the medieval city of Hamar, Norway (12 <sup>th</sup> century) – occipital bone sampled	Subacute pachymeningeal infection secondary to a trephination	Light microscopy	The microscopic study revealed a rupture of the inner table by an osteolytic process, displaying the diploic trabeculae. Since no significant re-vascularisation in the porotic appearance was observed, the histological features are in accordance with a subacute pachymeningeal infection.
Luna et al. (2008)	Case-study B	Adult male from Chenque I site from Lihué Calel National Park (La Pampa province), Argentina (1030-370 B.P.)	Multiple metastasis	Scanning electron microscopy (SEM)	The trabeculae of the spongy bone showed multiple destructive cavities (Howship's lacunae), irregularly located by osteoclastic activity. The borders of the lesions are smooth without signs of bone remodelling.
Mays and Turner-Walker (2008)	Case-study B	Non adult skeleton from Wharram Percy, U.K. (960-1700 A.D.) – ribs sampled	Renal osteodystrophy	Scanning electron microscopy	The ribs showed an increase in cancellous bone, which differs both in morphology and in quantity. Contrary to the honeycomb structure characteristic of the healthy ribs, the pathological ones showed a chaotic mass of random, finely branching bone spiculae that filled the endosteal space. The rib cortical bone was thicker and showed increased porosity due to the presence of resorptive spaces. The resorption spaces showed scalloped borders of closely-spaced Howship's lacunae. Subperiosteal bone deposition was observed.
D' Anastasio et al. (2009)	Case-study B	<i>Australopithecus africanus</i> (Stw 431) from Sterkfontein, South Africa (1.5-2.5 Ma.) – Lumbar vertebra L4 sampled	Brucellosis	Scanning electron microscopy (SEM)	Granulomatous tissue on the anterior rim of the vertebral body. Bone destruction mediated by osteoclasts was confirmed due to the presence of Howship's lacunae.

Authors/year	Study type	Sample ID	Pathological condition	Histological Technique	Paleohistopathological results
Flohr and Schultz (2009a)	Population study	151 mastoids of 104 individuals from an early medieval Frankish population from Dirmstein, Germany - 12 samples for transmitted light microscopy and 7 samples for SEM analysis were chosen	Mastoiditis	Light, polarized and scanning electron microscopy	Presence of Howship's lacunae associated with spicular structures in the border between the former bone surface and the newly-built bone. Formation of bony layers due to proliferation of pneumatised cells. Slight enlargement of air structures. Plate-like proliferations are present. These structures are attached to the wall of the pneumatised cells by pin-like or spicular structures.
Flohr and Schultz (2009b)	A				
Flohr et al. (2009)	Case-study	Left fifth metacarpal bone from an Iroquoian dog, Cleveland site, Ontario, Canada (16 <sup>th</sup> century)	Hypertrophic osteoarthropathy (HOA)	Light, polarized microscopy	Visible demarcation between the original cortex and the newly pathological bone. Bone changes visible mostly in the periosteal layer: elevated, irregular and scalloped border with lacy interior alterations. Presence of a mesh-like bridging of trabeculae within the newly-built bone.
Von Humnius (2009)	A				
Weston (2009)	Case-study	Diagnosed bone specimens from St. George's Hospital Pathology Museum, London, U.K.	Infectious conditions	Scanning electron microscopy	The analysis revealed that the histological features considered as specific to particular conditions, such as treponemal diseases (e.g. grenzstreifen, polsters and sinuous lacunae) are also found in other inflammatory processes. Their specific diagnostic value is questioned.
Zaki et al. (2009)	Population study	74 adult individuals (43 males, 31 females) representing high officials and workers from the Giza necropolis, Egypt (2687-2191 B.C.) – 22 individuals were sampled (10 normal, 8 osteopenia, 4 osteoporosis)	Osteoporosis	Scanning electron microscopy (SEM)	Osteoporosis was more frequent among male workers and in high official females. Nutritional stress and workload is argued to be responsible for the first result, sedentary lifestyle for the second. SEM analysis revealed that horizontal trabeculae are more affected than vertical trabeculae in osteoporotic cases.
Djurić et al. (2010)	Population study	81 adolescent individuals (21 males, 23 females, 37 unsexed) from Stara Torina, Northern Serbia (9 <sup>th</sup> -13 <sup>th</sup> centuries)	Periosteal inflammatory reactions – acute osteomyelitis	Light, polarized microscopy	Histological sections of the subperiosteal area demonstrated irregular bone arrangement, enlarged Haversian canals and trabeculae perpendicular to the bone surface.
	B				

Authors/year	Study type	Sample ID	Pathological condition	Histological Technique	Paleohistopathological results
Pinto and Stout (2010)	Case-study A	Adult skeletal remains from pre-contact Safety Harbour Briarwoods site, Pasco County, Gulf coast Florida, U.S.A. (1000-1500 A. D.)	Paget's disease	Light microscopy (?)	The histological mosaic pattern characteristic of Paget's disease was not observed due to extensive diagenesis.
Van Der Merwe et al. (2010)	Population study A	107 adult skeletons (86 males, 15, females, 6 unknown sex); 12 non-adult skeletons: 14 adult samples were collected from the anterior tibia	Ossified hematoma, Osteomyelitis, Non-specific periostitis	Light, polarized microscopy	Ossified haematoma: lesions were positioned on the top of normal cortical bone that was not affected by the condition. The original periosteal surface represented by the original external circumferential lamellae was not compromised. The newly formed bone on the outside of the original periosteal surface was composed of radiating trabeculae, perpendicular to the periosteal surface. Newly formed bone in distinct stages of remodelling was observed. Osteomyelitis: intense remodelling of the cortical bone with numerous resorption holes. Porous appearance made distinction between cortical and cancellous bone impossible. No original circumferential lamella was observed. Hemorrhagic bone apposition and inflammatory bone reactions: cortical bone with different degrees of resorption. Maintenance of the original periosteal bone represented by its original circumferential lamellae with radiating appositional bone in the top.
Arnautou et al. (2011)	Case-study B	Commingled bone remains from a Neolithic necropolis from Southern France (3350 B.C.) – rib sampled	Polyostotic Paget's disease	Light, polarized microscopy	Presence of thickened trabeculae with areas containing woven and lamellar bone. Presence of resorption spaces in the trabecular bone. Mixture of resorption and production areas.

Authors/year	Study type	Sample ID	Pathological condition	Histological Technique	Paleohistopathological results
Cho and Stout (2011)	Population study A	149 individuals older than 17 years old (both sexes) were selected from the Isola Sacra necropolis, Italy (100-300A.D.) – ribs and femur sampled	Osteoporosis	Light microscopy	The histological analysis revealed normal age – associated bone loss via increased intracortical porosity and endosteal expansion (bone turnover greater in females than males). Different remodelling rates in ribs and femora, probably reflecting different age of adults or loading environments.
Flohr and Witzel (2011)	Population study B	70 individual from the ancient city of Qatna, Syria (Bronze Age) were studied. Nine revealed hyperostosis <i>frontalis interna</i> (HFI) – only one case analyzed through microscope	Hyperostosis <i>frontalis interna</i> (HFI)	Polarized microscope	The histological analysis revealed the typical traits of the condition: complete remodelling of the internal table; however it is possible to identify its original position. The microstructure of the newly built bone presents a well-organized lamellar structure.
Petrone et al. (2011)	Population study B	76 skeletons from the victims of the Vesuvius, Italy (A.D. 79) – samples extracted from the long bones of adult and juvenile skeletons	Endemic Fluorosis	Light, Polarized microscopy	In the bone ground sections of the juveniles and adult long bones was observed: increased cortical and trabecular thickness; massive formation of exostosis on the periosteal bone margin; lost or poorly formed Haversian lamellar system; and extensive mottled bone matrix and enlarged Haversian canals.
Wade et al. (2011)	Case-study B	Adult male from the Grant Skeletal Collection from the Department of Anatomy from the University of Toronto, Canada (20 <sup>th</sup> century)	Paget's disease	Micro-CT scan	The micro-CT scan of the left pubis showed foci of greatly increased sclerosis, areas of marrow with little or no trabeculation, and areas showing an increase and decrease of radiodensity. In some areas increased cortical thickness and greatly decreased trabeculae were observed.
Wu et al. (2011)	Case-study B	Human skull from Maba, South China (Middle Pleistocene-Late Pleistocene)	Trauma	Stereomicroscopy and high-resolution industrial CT scanner	The lesion on the frontal bone is characterized by a depression in the ectocranial bone that extended through diploë and tables, generating an internal bulge with secondary remodelling of the external table.

An examination of the distribution of the 94 paleohistopathological studies by year of publication revealed that in the past two decades a non linear increase in the number of papers published has occurred (Figure 2.2).

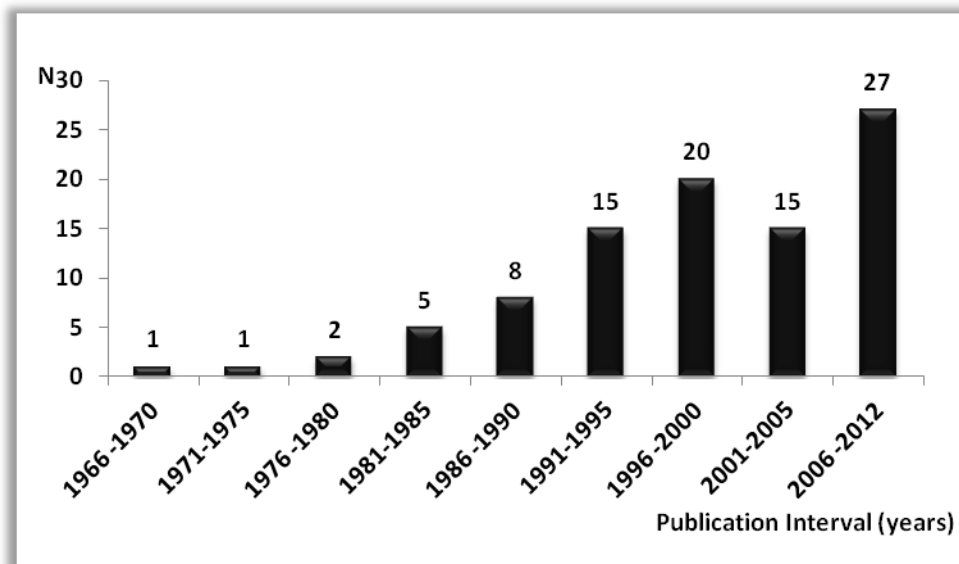


**Figure 2.2:** Distribution of the 94 paleohistopathological papers by interval of publication.

The publication intervals that gathered the high number of references are those between the years of 1996-2000 (20 papers) and 2006-2012 (27 papers). But are these numbers representative? The answer is probably not. For instance, and using the *International Journal of Osteoarchaeology* as a reference, a search of the total number of paleopathological studies published in the interval of 2006-2012 was made. The survey revealed 177 papers; nevertheless, only 12 considered the application of histology to their differential diagnosis, which represents only 6.8%. The period of time with the smallest number of references is located between the years of 1966-1990. This reduced number of publications may not signify an absence of paleohistopathological studies, but a dispersion of references in reviews not indexed or not easily available to the public. It is important to note that this systematic search only included papers in English and French. The paucity of paleohistopathological studies is also observed in the type of research conducted.

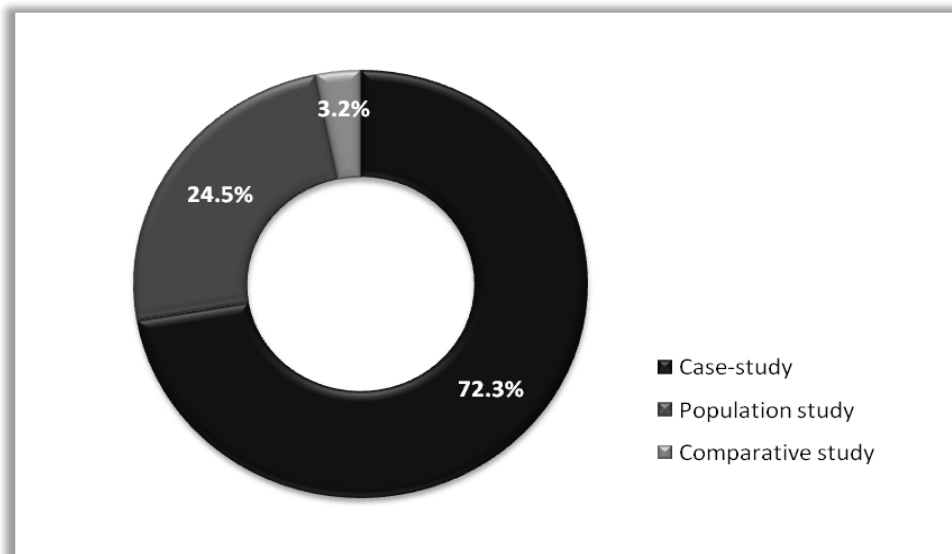


**Figure 2.3:** Distribution of the 94 published papers by type of study.

As portrayed in Figure 2.3, the majority of papers published are case-studies (72.3%, 68/94), followed by population level studies (24.5%, 23/94). Only in 3.2% of the studies (3/94) was microscopy used as a comparative tool. When considering the “weight” of the palaeohistopathological survey it is clear that this technique was mostly used as an auxiliary diagnostic tool and not as a primary source for paleopathological evidence (Figure 2.4). This is particularly evident for case-studies where only 15 papers based their research on histology, compared to 53 that have used this technique as a complement to macroscopic and/or radiologic analysis.

With regard to the type of paleopathological conditions published (Figure 2.5), histology was essentially applied to the study of metabolic conditions (e.g. Paget’s disease, osteoporosis, anemia, amongst others), 34% (32/94), benign and malignant tumors, 27% (25/94), and specific and non-specific infectious diseases, 23%. The analysis of miscellaneous conditions (e.g. Caffey’s disease, melorheostosis, endemic fluoride, psoriatic arthritis, symmetrical erosive polyarthropathy) was recorded in 6.4% of the papers. The lower values were obtained in the analysis of combined pathologies (5.3%) and bone trauma (4.3%).

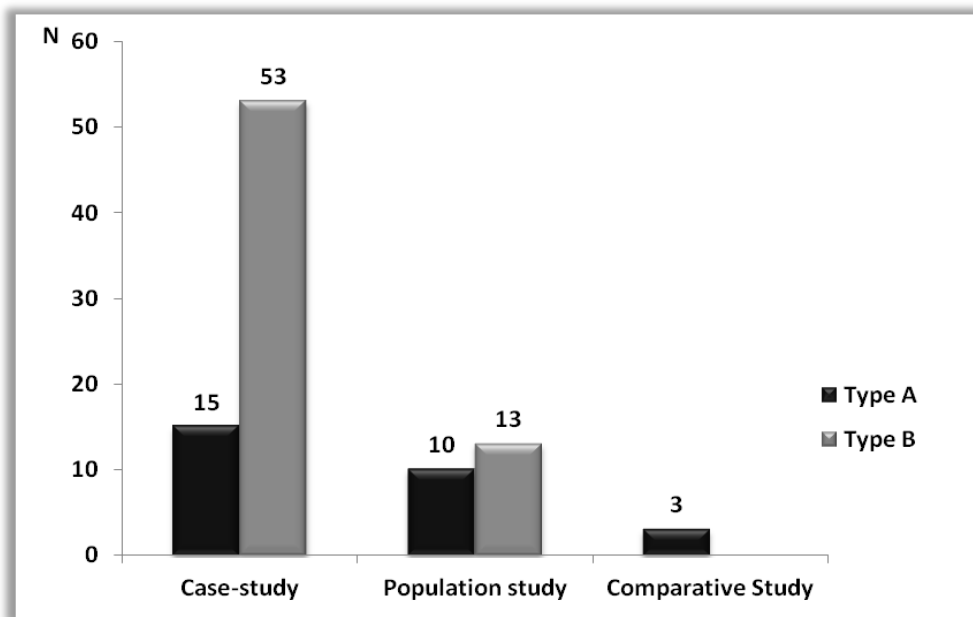


**Figure 2.4:** Distribution of the 94 papers by type of histological study: type A - used as primary source of evidence; Type B - used as a secondary tool.

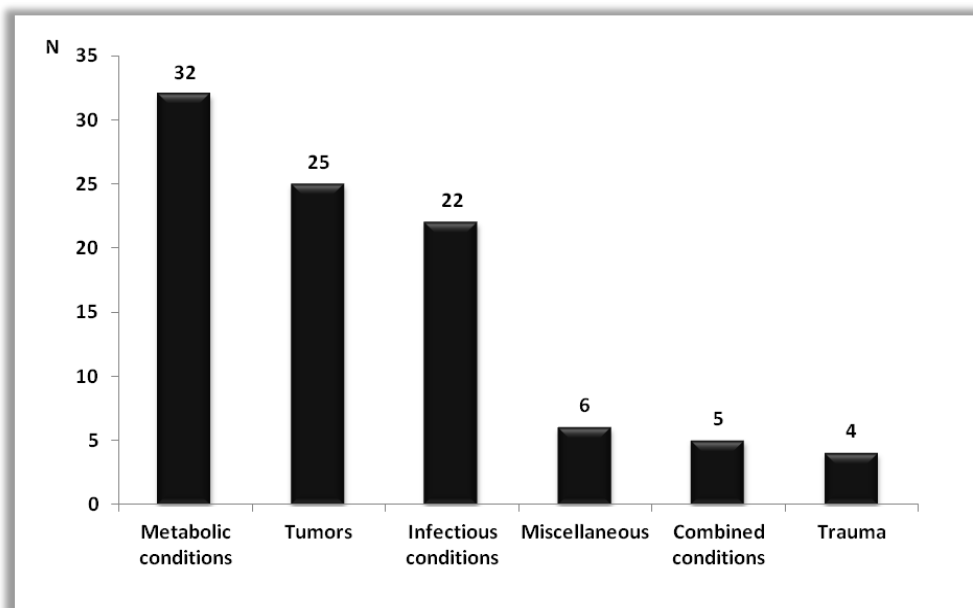


**Figure 2.5:** Distribution of the studies recorded by paleopathological condition analysed.

The remaining papers targeted in this survey (n=536) focused on other applications of paleohistology to bioarchaeology and forensic sciences, such as the study of:

**1. Tooth alterations (n=131).** Histological techniques are applied to the analysis of tooth remains to make inferences about diet, behavior and the impact of physiological stress on an individual's development. Dental microwear texture is studied to assess and compare dietary

habits and seasonal changes in food resources among fossil hominins (e.g. Puech and Albertini, 1984; Lalueza et al., 1996; Pérez-Pérez et al., 1999; Ungar et al., 2006; Estebaranz et al., 2009; Rivals et al., 2009), modern humans (e.g. Bullington, 1991; Teaford and Lytle, 1996; Schmidt, 2001; Macchiarelli et al., 2006; Mahoney, 2006; Patrick, 2006; Mahoney, 2007; Polo-Cerda et al., 2007; Hogue and Melsheimer, 2008; Ma and Teaford, 2010; Schmidt, 2010) and nonhuman primates (e.g. Ryan, 1979; Gordon, 1982; Teaford and Robinson, 1989; Teaford and Runestad, 1992; Teaford et al., 1996; Nystrom et al., 2004; El-Zaatari et al., 2005; Scott et al., 2006; Merceron et al., 2009). Certain patterns of microwear also reveal information about behavioral or “cultural” practices linked to the use of the teeth as a third hand (e.g. Fox and Frayer, 1997; Ungar and Spencer, 1999; Minozzi et al., 2003; Lozano et al., 2008). The microscopic examination of linear enamel defects is also an important tool to understand the physiological mechanisms responsible for growth disruptions during dental development (e.g. Rose, 1977; Rose et al., 1978; Marks and Rose, 1985; Goodman and Rose, 1990; Reid and Dean, 2000; King et al., 2005; FitzGerald et al., 2006; Ritzman et al., 2008; Witzel et al., 2008).

**2. Ontogeny, phylogeny and human evolution skeletal dynamics (n=94).** Histology gives insights into the dynamic of bone growth and remodelling in the course of human ontogeny and evolution (e.g. Martin and Armelagos, 1979; Oyen et al., 1979; Ricqlès, 1993; Abbott et al., 1996; Streeter, 2005; Martínez-Maza et al., 2006; Gosman and Ketcham, 2009; Harrington, 2010; Martínez-Maza et al., 2010). Furthermore, it allows for the development of standards for comparison with other non-human primates (e.g. Schaffler and Burr, 1984; Havill, 2003; Mulhern and Ubelaker, 2003; Mulhern and Ubelaker, 2009; Reinholt et al., 2009). A similar contribution is made by the histological study of dentition (e.g. Molnar and Gantt, 1977; Molnar et al., 1981; Keene, 1982; Hildebolt et al., 1986, Mann et al., 1991; Maas, 1993 and 1994; Anemone et al., 1996; Hillson and Bond, 1997; Darnell et al., 2010).

**3. Age at death estimation (n=90).** Several histological methods have been developed to estimate age at death using bone and dental remains. Bone growth, modelling and remodelling are responsible for a mature cortex with particular features that can be quantifiable through histomorphometric analysis<sup>20</sup> (Schultz, 1997; Meindl and Russell, 1998; Pfeiffer, 2000; Robling and Stout, 2008; Pickering and Bachman, 2009; Shih, 2009). The histological indicators of age are based on the grade of remodelling of osteons and their respective quantification in adult cortical bone (Bass, 1979; Simmons, 1985; Frost, 1987; Stout and Paine, 1992; Schultz, 1997; Meindl and Russell, 1998; Mulhern and Ubelaker, 2003;

---

<sup>20</sup> Quoting Boivin and Meunier (1993: 137): «[h]istomorphometry, or quantitative histology, consists of counting or measuring tissue components: the cells or the extracellular constituents or both».



Pickering and Bachman, 2009). Different skeletal elements have been considered in these studies, namely ribs and clavicle (e.g. Stout and Paine, 1992; Stout et al., 1996; Paine and Brenton, 2006; Crowder and Rosella, 2007; Kim et al., 2007; Cannet et al., 2010; Pavón et al., 2010; Cho and Stout, 2011), long bones (e.g. Kerley, 1965; Singh and Gunberg, 1970; Kerley and Ubelaker, 1978; Pfeiffer, 1980; Stout and Gehlert, 1982; Frost, 1987; Stout and Stanley, 1991; Wallin et al., 1994; Ericksen, 1991 and 1997; Ericksen and Stix, 1991; Thomas et al., 2000; Lynnerup et al., 2006; Maat et al., 2006b; Chan et al., 2007; Keough, 2007; Robling and Stout, 2008; De Donno et al., 2009; Han et al., 2009; Martrille et al., 2009; Villa and Lynnerup, 2010) and ilium (e.g. Boel et al., 2007). The reliability of using weight-bearing bones, as well as the effect of intrinsic (sex and population variability) and extrinsic (adequate bone sampling) factors on age at death estimation has also been discussed in the literature (e.g. Martin et al., 1981b; Neill, 1983; Aiello and Molleson, 1993; Pfeiffer et al., 1995; Drusini, 1996; Iwaniec et al., 1998; Macho et al., 2005; Paine and Brenton, 2006; Robling and Stout, 2008; Henning and Cooper, 2011). Dental histological techniques have been developed based on the study of secondary dentin formation, cementum annulation (e.g. Charles et al., 1986; Martin, 1996; Jankauskas et al., 2001; Kagerer and Grupe, 2001; Wittwer-Backofen et al., 2004; Maat et al., 2006a; Renz and Radlanski, 2006; Roksandic et al. 2009), enamel striae and linear formation (e.g. FitzGerald and Saunders, 2005; Katzenberg et al., 2005; Martin et al., 2008), root dentine translucency (e.g. Chandler and Fyfe, 1997) amongst others (Meindl and Russell, 1998; Hillson and Antoine, 2003). Similar methods have been created for the study of faunal remains (e.g. Beasley et al., 1992; Burke and Castanet, 1995; Wendy, 1998; Dirks et al., 2002; Havill, 2004).

**4. Taphonomic processes and identification of burned remains (n=82).** Microscopy has been used to evaluate the integrity of bone microstructure in different environmental contexts (e.g. Stout, 1978; Hermann, 1986; Hanson and Buikstra, 1987; Garland, 1993; Hedges et al., 1995; Bell et al., 1996; Nicholson, 1998; Nielsen-Marsh and Hedges, 2000; Pfeiffer and Varney, 2000; Roberts et al., 2002; Jans et al., 2004; Guarino et al., 2006; Schmidt-Schultz and Schultz, 2007; Tersigni, 2007; Monsalve et al., 2008; Jans, 2008; Turner-Walker and Jans, 2008; Reiche et al., 2010; Maurer et al., 2011; Bell, 2012; Hollund et al., 2012). When bone is exposed to the burial environment it may experience structural changes induced by physical, chemical or biological agents (Stout, 1978; Garland, 1993; Bell et al., 1996; Schultz, 1997; Collins, 2002; Jans, 2008; Turner-Walker and Jans, 2008; Reiche et al., 2010). The study of postmortem alterations is important to differentiate decomposition phenomena from normal physiological processes or disease lesions (e.g. Stout, 1978; Lynne, 1990; Grupe and Dreses-Werringloer,

1993; Jackes et al., 2001; Turner-Walker and Jans, 2008). Microscopic methods are also of great value in identifying and studying cremated human remains (e.g. Herrmann, 1977; Holden et al., 1995; Hanson and Cain, 2007; Schmidt, 2007; Warren, 2008; Squires et al., 2011) during paleopathological analysis (Schultz, 1997) or to age at death estimation (Hummel and Schutkowski, 1993; Fairgrieve, 2008). In zooarchaeological studies they also help in understanding the diagenetic processes that operate on buried bones and teeth (Haynes et al., 2002; Stutz, 2002).

**5. Cutmarks (n=32).** Distinct microscopic techniques, such as scanning electron microscopy, are employed in the study of cutmarks in human and nonhuman bone remains. These techniques are important to obtain evidence of hacking trauma and dismemberment in past population and forensic contexts (Hutchinson, 1996; Cox and Bell, 1999; Haverkort and Lubell, 1999; Bartelink et al., 2001; Tucker et al., 2001; Orschiedt et al., 2003; Alunni-Perret et al., 2005); traits of defleshing in hominin fossil remains (e.g. White, 1986); and marks of butchering on faunal remains and their role in understanding the evolution of hominin handedness (e.g. Shipman and Rose, 1983; Bromage and Boyde, 1984; Bello and Soligo, 2008; Pickering and Hensley-Marschand, 2008). Cutmark micromorphology is also considered in the study of surgical or ritual bone incisions, such as trephinations, and their differentiation from taphonomic changes (e.g. Stevens and Wakely, 1993; Fabbri et al., 2012).

**6. Differentiation between human and non-human remains (n=31).** Histology is a useful tool to distinguish between human and nonhuman bone remains, especially when bone is fragmentary (Harsányi, 1993; Horni, 2002; Dupras et al., 2006; Klepinger, 2006; Hillier and Bell, 2007; Croker et al., 2009; Greenlee and Dunnell, 2009; Hollund et al., 2012; Mulhern and Ubelaker, 2012). This differentiation is possible because humans have a unique pattern of cortical osteons, as well of primary bone types, when compared with other mature mammals (e.g. Davies and Fearnhead, 1960; Pfeiffer, 2000; Thomas, 2003; Cuijpers, 2006; Klepinger, 2006; Pfeiffer, 2006; Rosado et al., 2007; Cattaneo et al., 2009). The distinguishing features of bone histomorphometry also allow for the taxonomic classification of zooarchaeological remains (e.g. Powell et al., 1973; den Heuvel et al., 1991; Barnes et al., 2000; Miles, 2001; Horni, 2002; Dittmann, 2003; Dittmann et al., 2006; Martiniaková et al., 2007; Paral et al., 2007). Another role of histology is in the identification of strange bodies found associated with human skeletal remains, such as renal and biliary calculus (e.g. Morris and Rodgers, 1989; Sanchez and Etxeberria, 1991), calcified tissues and organisms (e.g. Perry et al., 2008; Quintelier, 2009; Cook and Patrick, 2011), fossilized body fluids and faecal deposits (Maat,

1991; Blondiaux and Charlier, 2008; Shillito et al., 2011), parasites and contaminating substances (e.g. Nelson et al., 2010; Oh et al., 2010).

**7. Mummies (n=30).** The analysis of mummified tissues was one of first applications of histology to the study of ancient remains. Nowadays it continues to fascinate researchers in a variety of subjects that range from the simple identification of soft tissues (e.g. Post and Daniels, 1969; Rabino-Massa and Chiarelli, 1972; Lamendin, 1974; Walker et al., 1987; Shin et al., 2003; Mekota et al., 2005; Kim et al., 2008; Pabst et al., 2009) to the study of abnormal lesions (e.g. Brothwell et al., 1969; Bellard and Cortés, 1991; Ciranni et al., 1999; Ciranni and Fornaciari, 2004; Bianucci et al., 2008), taphomic changes (Aufderheide, 2011) and replication of mummifying techniques (e.g. Zimmerman, 1979; Zimmerman et al., 1998).

**8. Bone tissue dynamics and variability in modern and prehistoric populations (n=29).** The skeleton has the capability to adapt itself to biomechanical stress, increasing bone mass when activity increases or reducing bone tissue due to inactivity (Schultz, 1997; Pearson and Lieberman, 2004; Peck and Stout, 2007). Through histomorphometric analysis it is possible to infer strain levels and bone dynamics within populations or among human groups from different chronologies and geographic provenances (e.g. Martin and Armelagos, 1985; Martin et al., 1987; Mulhern and van Gerven, 1997; Pfeiffer, 1998; Velasco-Vázquez et al., 1999; Mulhern, 2000; Cho et al., 2006; Drapeau and Streeter, 2006; Pfeiffer et al., 2006; Maggiano et al., 2011).

**8. Methods (n=17).** As pointed out previously, the literature review also showed the efforts made in the development of new histological methods and techniques for bone and teeth analysis (e.g. Marks et al., 1996; Scherf and Tilgner, 2009).

The data presented is a clear indicator that paleohistopathology has, in some way, been neglected in paleopathological analysis. Nevertheless, this is not the only sign of its scientific fragility; another indicator is the absence of a clear definition for palaeohistopathology. Contrary to modern medicine where histopathology is a branch of pathology defined as the microscopic examination of a biopsy specimen in order to study and diagnose the manifestation of disease (Bell and Piper, 2000), there is no formal definition of paleohistopathology. An approach is given by Bell and Piper (2000: 258): paleohistopathology is the microscopic study of pathological material in opposition to paleohistology that is the microscopic study of non-pathological skeletal material. Even so, this subdivision is not widely used because in many studies paleohistology and disease appear side by side (e.g. Aaron et al.,

1992). There are also uncertainties about who introduced the concept and when it was introduced in the paleopathological literature. Macadam and Sandison (1969) used the term to emphasize the role of electron microscopy in disease diagnosis. Bianco and Ascenzi (1993) also apply the concept in a mummy case-study. Nevertheless, only after the publication of Schultz's (2001) article entitled "Paleohistopathology of bone: a new approach to the study of ancient diseases" in the *Yearbook of Physical Anthropology*, has the concept acquired a new relevance, being used by other researchers (e.g. Tamarit, 2003; Weston, 2009). In fact, any survey on the *ISI Web of Knowledge*, *Medline* or *PuBMed* databases using the term "paleohistopathology" automatically redirects the search to Schultz's article. Since the early 1980's, Prof. Michael Schultz from the University of Göttingen, Germany, has played an important role in the development of palaeohistopathology, publishing reviews and syntheses of methods used based on the application of light and polarized microscopy (e.g. Schultz, 1993, 1997, 2001, 2003 and 2012).

In the next section the chief reasons that might explain the non-systematic use of paleohistopathology, as well as the unexploited potential of the discipline will be presented and discussed.

### 2.3. LIMITATIONS AND ACHIEVEMENTS OF PALEOHISTOPATHOLOGY

In 1981, Ortner and Putschar proffered, in the monograph "Identification of pathological conditions in human skeletal remains", a non-enthusiastic sentence that reflects the skepticism that surrounded paleohistopathological studies during that time:

«Microscopic study of bone, like chemical analysis, is limited in its application. As a general rule, in archeological skeletal material, microscopic data add little to what can be seen grossly or on X-ray films. Because microscopic examination does involve destruction of some of the bone, it should only be applied when diagnosis is likely to be aided. It should not be considered a routine procedure» (page 52). In the last decades, this skepticism has been progressively reduced. For instance, in the re-edition of the monograph by Ortner (2003) the quoted sentence was removed and a full chapter is dedicated to paleohistopathology. Despite that, the initial point of view shared by Ortner and Putschar (1981) is useful because it enunciates two of the recurring limitations attached to paleohistopathology: (1) its reliability in the differential diagnosis of pathological conditions; and (2) its destructive nature (Bell and

Piper, 2000; Ortner, 2003b; Turner-Walker and Mays, 2008; Pfeiffer and Pinto, 2012). In addition to these limitations, two more can be added: (3) the time consuming and technically high demanding procedures required for thin section preparation; and (4) the high scientific proficiency needed to interpret bone morphology at the microscopic level (Bell and Piper, 2000; Schultz, 2012).

With concern to the first limitation, Schultz (1993, 1997, 2001, 2003, and 2012) strongly suggests that paleohistopathology is a determinant to disease diagnosis in archaeological remains. The author subscribes to the idea that histology, especially light-polarized microscopic investigation, is an indispensable tool to attain reliable diagnoses that are essential for reconstructing the etiology and epidemiology of diseases in the past (Schultz, 2001, 2003 and 2012). Responding to the initial reluctance of Ortner and Putschar (1981), Schultz (2012) emphasizes that in the past years more data have been added to the knowledge of dry bone microarchitecture. Thus, by studying the orientation of collagen fibers; the size, thickness and orientation of trabeculae; the thickness of external and internal circumferential lamellae; the size and number of Haversian systems and their canals; the number of interstitial lamellae and fragmented osteons; the presence of special cement lines and Howship's lacunae, it is possible to identify a disease group or even a particular condition, such as anemia, scurvy, rickets, osteomyelitis, and external periostitis (Schultz, 2012). In seeking a reliable diagnosis in paleohistopathology, a broad difficulty is pinpointed by researchers: the absence of soft tissues, body fluids and cells (Bianco and Ascenzi, 1993; Turner-Walker and Mays, 2008). As pointed out by Schultz (2012), the lack of particular cells, such as granulocytes, osteoblasts, osteoclasts and other macrophages, as well as fibrous connective tissue, makes any cytological and pathophysiological analysis impossible in archaeological skeletal remains. Accordingly, the differential diagnosis conducted by paleohistopathologists must follow a distinct pathway when compared with the evaluation made by clinicians (Bell and Piper, 2000; Turner-Walker and Mays, 2008; Schultz, 2001, 2003 and 2012). For researchers, the future of paleohistopathology, and paleohistology, depends on the development of uniform methods, as well as the application of a proper nomenclature to describe and characterize pathological bone at the microscopic level. This achievement will improve scientific standards and reduce potential errors and/or semantic barriers (Pfeiffer and Pinto, 2012; Schultz, 2012; Stout and Crowder, 2012).

Another drawback attributed to paleohistopathology is its invasive and apparent destructive nature (Grupe and Garland, 1993; Ortner, 2003b). Many museum curators and

osteologists have an understandable reluctance in damaging, or allowing the destruction of skeletonized remains in order to obtain samples (Turner-Walker and Mays, 2008). Bell and Piper (2000) justify this generalized feeling as a result of a misinterpretation of the meaning of invasive and destructive concepts. In many museums' sampling protocols, invasive analysis is used as a synonym for destructive handling, which is not completely true. Quoting Bell and Piper (2000: 258): «While histopathology is undoubtedly invasive, it is not destructive in this way [referring to the total "combustion" of samples during dating or isotopic studies], since a section may be preserved and archived indefinitely. This is an extremely important distinction, not just in terms of the management of skeletal collections, but also as a recoverable resource or archive of paleopathological information». Highlighting the role of histological collections, Spatola and co-authors (2012) have recently published a work describing the potential of using one of the largest bone slide collections in the world (with more than 10,000 slides of stained and undecalcified bone and joint specimens) housed at the Anatomical Division of the National Museum of Health and Medicine (NMHM)<sup>21</sup> at the Armed Force Institute of Pathology (AFIP), Washington, DC, for research in paleopathology, bioarchaeology and forensic science research. Similar histological collections are also curated at European universities and museums, for example, the Collection of the Department of Legal Medicine at the University of Vienna, Austria, and the Collection of the Department of Pathology at the University of Göttingen, Germany (Schultz, 2012). According to Pfeiffer (2000) the progress of paleohistopathology is dependent on a change in the curatorial rules. Before refusing access to skeletal collections, curators and researchers may be aware that the preparation of thin sections represents the transformation of material rather than its destruction (Pfeiffer, 2000). Sampling damaged bones and/or small bone elements such as ribs, metacarpals or metatarsals is regarded as a solution to expedite lab work and reduce the degree of disruption of curated material (Pfeiffer, 2000). To compensate for bone sectioning, Schultz (2012) suggests the use of a true-to-life or a plaster complement to restore the bone pieces that were removed. This procedure was already used by Wapler et al. (2004) after the extraction of skull samples that presented *cribra*

---

<sup>21</sup> This large collection was constituted through donation of other small collections: the Johnson-Sweet Whole-Mount Collection of Orthopedic Pathology was started after World War II by Dr. Donald Sweet and Dr. Bruce Ragsdale and comprises several diagnosed rare cases (e.g. osteosarcoma, chondrosarcoma, giant cell tumor, osteomyelitis, carcinoma, fracture, Paget's disease, amongst others); the Historic Collections (or Codman and Plemister) was donated by the American College of Surgeons in 1953 and is composed of 2.300 bone tumors from the former Codman Registry of Bone Sarcoma; and the Kerley Collection was started as a result of Dr. Ellis Kerley's research on the study of age-related changes in the bone microstructure of humans and chimpanzees. The collection is growing through new acquisitions or donations; the latest included samples of human and nonhuman specimens, namely 300 slides from human long bones (Spatola et al., 2012).

*orbitalia*. In this case, the sample gaps were filled with pieces of tightly adjusted plaster (Wapler et al., 2004).

The third limitation concerns the highly time-consuming nature of the histological techniques, which require expensive and sophisticated supplies (Schultz, 2012). This generalization is not completely true because there are simple methods, like those published by Frost (1958) and Maat et al. (2001) that researchers can easily reproduce. The selection of a particular method is, of course, not random and depends on extrinsic (design and goals of the research) and intrinsic factors (preservation of the bone samples). Whenever bone samples are small or belong to fragile skeletonized pieces, the use of more time-consuming techniques in order to guarantee high quality thin-sections is preferred (Schultz, 2012).

The last, and perhaps, the broader obstacle to paleohistopathological analysis is the lack of training of paleopathologists (Bell and Piper, 2000; Pfeiffer and Pinto, 2012; Schultz, 2012). However, taking into account recent publications (e.g. Schultz, 1986, 1993, 2001 and 2003; Hershkovitz et al., 1999; Eshed et al., 2002; Hershkovitz et al., 2002; Wapler et al., 2004; Von Hunnius et al., 2006; Brickley et al., 2007; Kuhn et al., 2007; Zaki et al., 2009; Weston, 2009; Van Der Merwe et al., 2010; Crowder and Stout, 2012) and the growing expertise in diagnosing disease at the microscopic level, researchers must be encouraged to employ histological techniques (Schultz, 2012). Additionally, a deep understanding of the typical mosaic patterns found in normal and pathological cortical and trabeculae bone throughout life will certainly make the interpretation of dry bone remains easier (Heuck, 1993).

Because macroscopic and radiologic analyses are sometimes obscured by similarities in the macromorphology of lesions, the microscopic inspection of bone tissue is regarded as the remaining solution to produce reliable diagnosis (Schultz, 1993, 2001, 2003 and 2012). In spite of some criticisms (e.g. Weston, 2004 and 2009), this assertion is advanced because certain pathological conditions seem to leave an individual mark on the bone microstructure, such as the radial orientation of trabeculae in subperiosteal hematomas (Van Der Merwe et al., 2010); the *grenzstreifen* in treponematoses and leprosy, or the *fasefilz* in slowly growing primary osteoblastic bone tumors (Schultz, 2001, 2003 and 2012). To demonstrate the importance of histology for the epidemiology of diseases in past population, Schultz (1993) gives the example of an investigation carried out in a sample of individuals with signs of anemia, rickets, osteomyelitis and irritation of meninges from the early Bronze Age site of Ikiztepe, Anatolia. The comparison between macroscopic and histological analysis revealed striking results: three cases macroscopically diagnosed as osteomyelitis were histologically identified as irritation of

meninges; three cases grossly identified as anemia were in fact osteomyelitis, and five cases diagnosed as osteomyelitis were microscopically described as rickets (Schultz, 1993).

Related to the histological analysis of taphonomic changes, two other potentials emerge in disease diagnosis: the ability to differentiate between lesions and pseudopathologies, and its usefulness to assess bone quality in disease rate quantification. Some authors (e.g. Grupe and Dreses-Werringloer, 1993) consider thin sectioning essential to differentiate between decomposition phenomena and physiological or pathological signs; otherwise any attempted diagnosis will be biased. Bianco and Ascenzi (1993) stressed that histology reveals the two-way interaction between bone lesions and taphonomic changes. According to them, histology is important to ascertain the impact of diagenetic factors in the architecture of normal and pathological bone, as it is to infer the role that bone abnormalities have in the non-random progression of diagenesis (Bianco and Ascenzi, 1993). The use of histology to evaluate the preservation of bone remains was broadly discussed by Stout (1978). According to this author, the application of histology as a technique to evaluate bone preservation is fundamental before any differential diagnoses because there is a substantial risk of evaluating differences in preservation instead of the effects of aging or pathology. Turner-Walker (2008) states that diagenesis not only contributes to macroscopic alterations, but also alters the chemistry and microstructure of the tissues, leading to biased diagnosis, for example in the interpretation of radiodensitometry and measurements of bone density. Still on the topic of bone integrity, the histological analysis may reveal surprising results. This happened with Bell and Jones' (1991) study of two possible cases of Paget's disease. The analysis by SEM/BSE techniques revealed that the bone fragment considered poorly preserved macroscopically, had extensive areas unaffected by diagenesis, whereas the piece regarded as in excellent state of macroscopic preservation, showed profound diagenetic changes at the microscopic level (Bell and Jones, 1991). This result reinforces the usefulness of histology in distinguishing between disease and diagenesis.

Despite the limitations currently addressed in palaeohistopathological analysis, it is clear that histological investigation can provide important data that would be otherwise unavailable through other methods (Pfeiffer and Pinto, 2012). In the words of Martin (1991: 58), «(...) it seems timely for histology to enter the mainstream of skeletal analysis in anthropology».



---

# CHAPTER 3

---

*“(...) BONE IS NOT AN IMPENETRABLE SOLID; IT IS A METROPOLIS OF HIGHWAYS AND  
FREEWAYS, TURNPIKES AND UNDERGROUND RAILWAYS; A HOUSE OF MANY ROOMS AND  
CORRIDORS, WITH FLUID-FILLED CANALS AND CANALICULI, WIRED WITH NERVE FIBRES, FED WITH A  
VASCULATURE NO LESS COMPLEX THAN THAT OF THE HEPATOBILIARY, PULMONARY-ALVEOLAR OR  
RENAL GLOMERULOTUBULAR SYSTEMS.”*

(SEEMAN, 2007: 123)



### 3. INCURSION TO THE BIOLOGY OF BONE AND DISEASE

Talking about diseases that affect the human skeleton without mentioning the marvellous architecture of the bone tissue is the same as writing a poem without knowing the meaning of the words.

The interest in understanding the structure and function of the skeleton, especially the disorders that affect it, is remarkably ancient dating nearly five thousand years (Beasley, 1982a). Several iconographic and documentary sources from different chronological periods (e.g. Egyptian and Greek civilizations)<sup>22</sup> corroborate this assumption (Beasley, 1982a; Whiting and Zernicke, 1998). In the 17<sup>th</sup> century, the invention of the microscope was crucial to understanding the ultrastructure of bone in both normal and pathological cases. Even rudimentarily, the “histology of bone” was firstly portrayed in 1691 by Clopton Havers (1657-1702, U.K.) in his book “*Osteologia Nova, or some New observations of the bones, and the parts belonging to them, with the manner of their accretion and nutrition*” (Dobson, 1952; Hall, 2005). Havers identified and described the spaces or canals that traverse the compact bone tissues which now bear his name, the Haversian canals<sup>23</sup> (Dobson, 1952; Beasley, 1986).

---

<sup>22</sup> The first attempt to explain the origin of bone tissue was made by the Greek philosopher Plato (429–347 B.C) in the latter part of the fifth century B.C.. Centuries later, fundamental discoveries regarding the anatomy and physiology of the skeleton based essentially on the dissection of pigs and apes (the study of human cadavers was proscribed at that time) were made by Galen (A.D. 129-199/217, Greece) (Beasley, 1982a; Whiting and Zernicke, 1998). In the fifteenth century, numerous artists such as the Italians Leonardo da Vinci (1452-1519), Michelangelo (1475-1564) and Raphael (1483-1520) contributed actively, not only to the Renaissance of art, but also to the renaissance of the studies on human anatomy, which greatly inspired their works (Beasley, 1982b). This relationship with art was extremely important leading to the publication of the first illustrated books of human anatomy. One of the most impressive monographs entitled *De Humani Corporis Fabrica* was written by Andreas Vesalius of Brussels (1514-1564), who is also considered the reformer of anatomy (Ball, 1910; Whiting and Zernicke, 1998).

<sup>23</sup> «In the bones, thro' and between the plates, are formed pores, besides those which are made for the passage of the blood-vessels, which are of two sorts; some penetrate the laminae, and are transverse, looking from the cavity to the external superficies of the bone; the second sort are form'd between the plates, which are

Almost two decades earlier, Anthon van Leeuwenhoek (1632-1723, Netherlands) had already made some incursions in the microstructure of bone, though paying more attention to the structure of periosteum than to the significance of vessels and canals alike (Beasley, 1986).

Since the very first descriptions many discoveries of bone microstructure have been made. Although all of them enhance our understanding, many issues related to the physiology of bone and cell metabolism remain unresolved.

In the following pages, an introduction to the biology of bone tissue, giving particular attention to the latest discoveries, will be presented. This preamble will be followed by an approach to periosteal new bone formations (PNBFs) or periosteal reactions (PRs) focusing on their clinical meaning, mechanisms of regulation, pathophysiology and classification. Finally, a clinical and paleopathological overview regarding the main conditions that produce periosteal new bone lesions will be provided

### **3.1. THE HUMAN SKELETON: AN INVISIBLE FRAMEWORK**

There are many ways of introducing the bone morphology, microstructure and function. For this thesis, the model of organization for a typical long bone presented by Chappard and co-authors (2011) was selected because it more clearly fits the key components of bone and its distinct roles (Figure 3.1). Since the sample under analysis in the present research is mostly composed of ribs, particular attention will be given to the rib's microstructure and development.

---

longitudinal and straight, tending from one end of the bone towards the other, and observing the course of the bony strings» (Havers, 1691 in Dobson, 1952: 706).

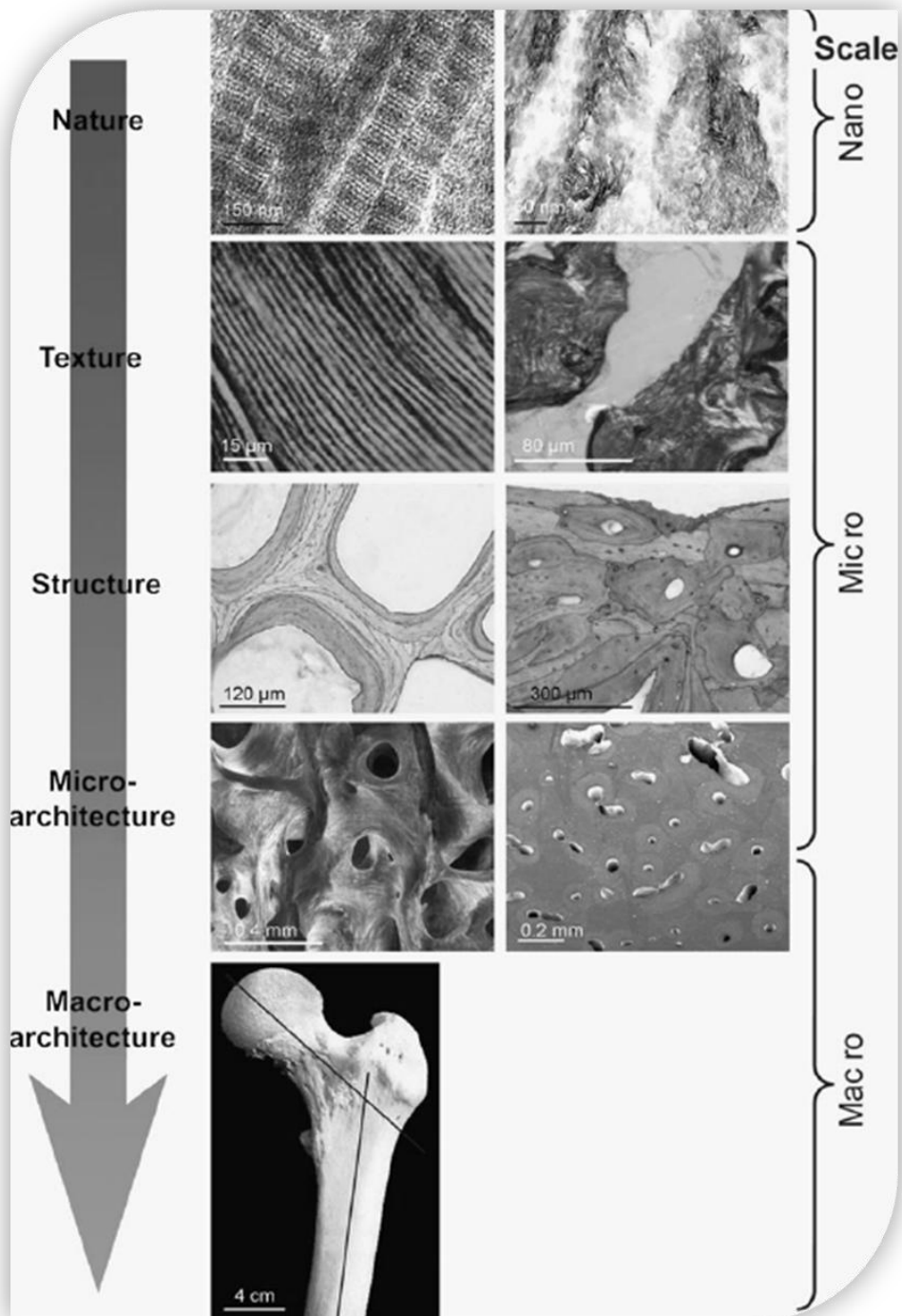


**Figure 3.1:** The five levels of organization of the structure of a long bone (after Chappard et al., 2011: 2227).

### 3.1.1. The Nature of Bone: a Double Composition with an Organic and Inorganic Substrate

Bone is frequently perceived as a static, hard and unchanging structure (Franz-Odenaal et al., 2006; Seeman, 2007), but this is a misleading view since bone is a living, dynamic, and highly specialized type of connective tissue (Martin, 1991; Cullinane and Einhorn, 2002; Marks and Odgren, 2002; Young et al. 2006) composed of an organic matrix (about 30%) that is strengthened by calcium and phosphate minerals (about 70%) (Young et al. 2006). Ninety percent of the organic component of bone is formed by type I collagen (Proff and Römer, 2009), a double chain protein synthesized by osteoblasts and coded by two different genes in chromosomes 17 and 7 (Chappard et al., 2011). The mineral phase is composed of poorly crystalline hydroxyapatite tablets ( $\text{Ca}_{10}[\text{PO}_4]_6[\text{OH}]_2$ ) with hydrogen phosphate ( $\text{HPO}_4$ ) and carbonate ( $\text{CO}_3$ ) groups showing distinct anisotropic shapes, which are claimed to be responsible for the anisotropic<sup>24</sup> properties of bone (Iyo et al., 2004; Chappard et al., 2011). Both components have a well defined function: the inorganic confers the rigidity that characterizes bone, whereas the network of collagen fibres (matrix) allows some degree of flexibility<sup>25</sup> (Lieberman, 1997; Jee, 2001; Marks and Odgren, 2002; Iyo et al., 2004; Seeman, 2007; Young et al. 2006). Furthermore, their interaction is not random. Since deposition of new bone occurs at distinct rates, the process of mineralization is not simultaneous (Chappard et al., 2011). It normally starts 15 days after the deposition of the first collagen fibers and non-collagenous proteins by osteoblasts, forming the osteoid seam (Chappard et al., 2011). In the initial stage, hydroxyapatite appears at the mineralization front in the form of small crystals that will increase in size during calcification and through incorporation of new crystals between the collagen fibrils (Gupta et al., 2006; Chappard et al., 2011). These newly mineralized fibrils are then arranged into different motifs such as fibril arrays and lamellae (Gupta et al., 2006).

---

<sup>24</sup> According to Qin and Zhang (2005: 203), «[B]one is an anisotropic or heterogeneous structure because its basic components are assembled in different ways». Biomechanically, it means that bone strength properties are different for each major direction of load (Knudson, 2007).

<sup>25</sup> The viscoelasticity of materials is related to their mechanical properties. In bones, the mechanical property is strain-rate dependent: if strain increases, the bone tissue become stiffer and stronger. This is possible because bone consists of both solid and fluid components (Qin and Zhang, 2005).

### 3.1.2. The Texture of Bone: a Woven or Lamellar Arrangement of the Matrix

At the microscopic level, two forms of bone exist: immature or woven bone<sup>26</sup> and mature or lamellar bone (Junqueira and Carneiro, 2005) (Table 3.1).

Woven bone is a type of primary bone formed by a matrix with an anarchic texture in which the mineralized collagen fibrils are randomly organized (Ortner and Turner-Walker, 2003; Steiniche and Hauge, 2003; Junqueira and Carneiro, 2005; Young et al., 2006; Chappard et al., 2011). This lack of organization is the result of a rapid and haphazard production of osteoid by osteoblasts, as observed during foetal bone development (Young et al., 2006), and in adults following tumours and some metabolic (e.g. Paget's disease) and infectious conditions, as well as during fracture healing (Steiniche and Hauge, 2003; Ortner and Turner-Walker, 2003; Young et al., 2006). Other features include a lower mineral content, reduced biomechanical properties (Chappard et al., 2011) and a higher number of osteocytes (Ortner and Turner-Walker, 2003; Junqueira and Carneiro, 2005). During normal growth, the woven bone is replaced in adults by a more organized tissue called lamellar bone (Ortner and Turner-Walker, 2003; Junqueira and Carneiro, 2005). The only exceptions are found near the cranial sutures, in the tooth sockets, and at the sites of insertion of tendons and ligaments (Ortner and Turner-Walker, 2003; Junqueira and Carneiro, 2005).

Lamellar bone is a mature, highly organized and densely packed tissue (Su et al., 2003; Junqueira and Carneiro, 2005) characterized by "regular parallel bands [or lamellae] of collagen arranged in sheets" (Young et al., 2006: 191). These lamellae may extend parallel to the bone surface originating in the circumferential lamellar bone (Weiner et al., 1999), or may lie concentrically around the Haversian canal of the osteon (Junqueira and Carneiro, 2005). Within each lamella, the collagen fibres run in opposite directions, crossing between neighbouring lamellae (Schultz, 1997). This typical fibrous network can be identified through polarized light as the "Maltese cross", which is characterized by an alternate pattern of light and dark bands (Schultz, 1997; Ortner and Turner-Walker, 2003). The lamellar bone is found only in adults and is the key component of both compact and spongy tissue (Schultz, 1997).

---

<sup>26</sup> There is some disagreement regarding the best term to describe this type of bone. Ortner and Turner-Walker (2003) note that the word "woven" may lead to some misconceptions since it creates a visual image of organization of the fibrils, similar to fabric that is incompatible with the random orientation that they actually exhibit. As an alternative, Ortner and Turner-Walker (2003: 19) suggest the use of the concept of "fiber bone". Besides woven and immature bone, Pfeiffer (2006: 17) also uses the term "bundle bone" as synonymous.

Although the synthesis of lamellar bone is frequently described as secondary to a pre-existing tissue, it is important to note that it might have a primary origin. Contrary to the secondary type, the primary lamellar bone is produced *de novo* on an existing bone surface (Mulhern and Ubelaker, 2012), being found in the form of superimposed lamellae around the periosteal and endosteal circumferences of long bones (Pfeiffer, 2006).

**Table 3.1:** Different types of bone and their main components (after Pfeiffer, 2006: 17, with additional information added from Pfeiffer, 2000; Ortnier and Turner-Walker, 2003; Hall, 2005; Mulhern and Ubelaker, 2012).

Type of bone	Major macroscopic and histological distinguishing features
<b>Woven bone</b>	<ul style="list-style-type: none"> <li>• Deposited <i>de novo</i></li> <li>• Forms more rapidly than other types</li> <li>• Most disappears by four years of age</li> <li>• Random orientation of collagen fibres</li> <li>• More lacunae per unit volume</li> <li>• Weaker than other types of bone</li> </ul>
<b>Plexiform bone</b>	<ul style="list-style-type: none"> <li>• Must be deposited on a pre-existing substrate</li> <li>• Forms more rapidly than other types, except woven bone</li> <li>• Increased mechanical strength relative to woven bone</li> <li>• Lamellar bone present</li> <li>• Bricklike structure: lamellar bone is sandwiched by non-lamellar bone</li> <li>• Observed in human infants and in children during growth spurts post-infancy</li> </ul>
<b>Primary lamellar bone</b>	<ul style="list-style-type: none"> <li>• Must be deposited on a pre-existing substrate</li> <li>• Forms more slowly than woven or plexiform bone</li> <li>• Superior mechanical strength</li> <li>• Lamellae are organized parallel to endosteal and periosteal surfaces</li> <li>• Can become very dense and can include primary osteons</li> <li>• Includes circumferential lamellar bone, seen in adult cortical bone as thin periosteal and endosteal layers</li> </ul>
<b>Cement line</b>	<ul style="list-style-type: none"> <li>• Formed during bone remodelling (reversal phase)</li> <li>• Corresponds to the initial layer of bone matrix deposited on the walls of the resorption space</li> <li>• High mineralization and high proportion of noncollageneous proteins</li> </ul>
<b>Primary osteon</b>	<ul style="list-style-type: none"> <li>• Requires a vascular space for formation</li> <li>• Fewer concentric lamellae than secondary osteon</li> <li>• Smaller vascular canal (diameter less than 100 <math>\mu\text{m}</math>). No cement (reversal) line</li> <li>• May be found in association with plexiform bone</li> <li>• Formed during rapid growth periods</li> </ul>
<b>Secondary osteon</b>	<ul style="list-style-type: none"> <li>• Requires pre-existing bone for formation</li> <li>• Cement (reversal) line present</li> <li>• Forms more slowly than immature bone types</li> <li>• More concentric lamellae compared to primary osteon</li> <li>• Larger vascular canals crossed by a single blood vessel</li> <li>• Predominant structure within adult cortical bone</li> </ul>
<b>Interstitial bone</b>	<ul style="list-style-type: none"> <li>• Lamellar remnants of pre-existing bone separated from the bone surface and vascular canals by the cement lines</li> <li>• Most commonly found in adult cortical bone</li> </ul>



Primary lamellar bone occupies the greater part of the width of the diaphysis and presents superior biomechanical properties (Pfeiffer, 2006). In this type of bone, the incorporation of vascular spaces may lead to the formation of primary osteons (Martin et al., 1998 in Pfeiffer, 2006). Besides woven and lamellar bone, another type of tissue called plexiform bone can be described. The histology of plexiform bone, also called fibrolamellar bone, is well known for many non-human mammals, especially in those whose body weight increases rapidly during development, requiring their bones to grow quickly in diameter (e.g. bovines, pigs and horses) (Dittmann et al., 2006). This type of bone has also been reported in children associated with major growth spurts (Pfeiffer, 2006). Nevertheless, this relationship is not consistently described, leading some authors to consider its presence or absence as a good way of distinguishing between human and non-human bone remains (Pfeiffer, 2006). Plexiform bone is characterized by a bricklike appearance that forms when woven bone is precipitated on the surface and the gaps fill with lamellar bone (Dittmann et al., 2006; Mulhern and Ubelaker, 2012).

### **3.1.3. The Structure of Bone: Osteons, Arch-like Bone Structures and Cell Components**

The most striking differences between cortical and spongy bone tissue are of a structural and functional nature (Marks and Odgren, 2002).

Structurally, cortical bone is made of columns arranged parallel to its long axis (Schultz, 1997; Young et al., 2006). In each column, several concentric layers (or lamellae) are arranged around a neurovascular channel known as the Haversian canal (Wynsberghe et al., 1995; Schultz, 1997; Pfeiffer, 2000; Young et al., 2006; Chappard et al., 2011). These cylindrical units of calcified bone are named osteons or Haversian systems (Wynsberghe et al., 1995; Young et al., 2006). The osteons are considered the “cornerstones” of the cortical bone (Steiniche and Hauge, 2003: 62) or their structural unit (BSU – Bone Structure Units) (Chappard et al., 2011: 2227), being subdivided into primary and secondary osteons (Table 3.1).

Primary osteons are formed during the first generation of bone (Steiniche and Hauge, 2003). In contrast, secondary osteons result from osteoclastic tunnelling of a mass of compact bone to produce a canal into which blood vessels and nerves grow (Young et al., 2006). These canals are lined internally by active osteoblasts whose function is to deposit concentric lamellae of bone (Young et al., 2006). During the appositional synthesis, the diameter of the osteon canal decreases and the osteoblasts become trapped as osteocytes in the lacunae

(Young et al., 2006). This means that the growth occurs from the periphery to the Haversian canal, with the number of lamellae per osteon varying between 2 and 20 (Schultz, 1997). A typical secondary osteon is demarcated from the surrounding bone by a cement or reversal line (Schultz, 1997; Pfeiffer et al., 2006). This line signifies where bone lysis stopped and osteoblast production occurred (Pfeiffer, 2000; Ortner and Turner-Walker, 2003; Steiniche and Hauge, 2003). Thus, the maximum diameter of an osteon is determined by the resorption process, as well as by the cement line (Pfeiffer, 2000) (Figure 3.2). In the human skeleton, the size of osteons varies from bone to bone (Pfeiffer, 2000). Nevertheless, a diameter that ranges between approximately 180 and 250  $\mu\text{m}$  is commonly found (Ortner and Turner-Walker, 2003)<sup>27</sup>. From the Haversian canal, multiple branches called perforating or Volkmann's canals spread at right angles to extend the system of nerves and vessels outward and inward through the cortical tissue (Wynsberghe et al., 1995; Schultz, 1997; Steiniche and Hauge, 2003), and between periosteal and endosteal spaces (Chappard et al., 2011). As a result of the continuous production and resorption of bone, newly formed osteons are dispersed between partly resorbed systems in a process called internal or osteon remodelling (Schultz, 1997; Pfeiffer, 2000). These remnants of osteons left by osteoclasts during the internal remodelling of bone are usually referred to as interstitial systems or lamellae (Schultz, 1997; Pfeiffer, 2000). Approximately two-thirds of cortical volume is formed by intact secondary osteons, and the remainder is filled with interstitial bone (Steiniche and Hauge, 2003).

Unlike cortical bone, spongy or cancellous tissue has a loosely organized, porous matrix with few vascular channels (Ortner and Turner-Walker, 2003). Despite this, its BSUs are comparable to incomplete osteons with an arch-like appearance. Nevertheless, in developing individuals, intratrabecular Haversian systems are also observed (Chappard et al., 2011). In cancellous tissue, BSUs form two types of trabeculae: large plates (arranged along the stress lines), connected laterally by pillars and rods that ensure cohesion, forming a honeycomb network structure (Chappard et al., 2011). The author points out that this characteristic structure varies, not only between different bones, but also with age. As in cortical bone, the cancellous remodelling occurs through the production of new bone and its deposition onto the surface of trabeculae previously eroded by osteoclasts. Between the newly formed bone, remnants of the eroded tissue persist, constituting the interstitial trabecular bone (Chappard et al., 2011). Thus, the only difference between cortical and trabeculae BSUs is the shape; the

---

<sup>27</sup> Several histomorphometric studies have shown that the size of osteons has changed through time, with past populations exhibiting small osteons when compared with modern groups. Additionally, there is some disagreement about the possible differences observed between sexes (Pfeiffer, 2000).

trabecular osteons are broad-lined because of the parallel lamellae (Steiniche and Hauge, 2003). Additionally, they possess a reduced thickness (approximately 40-45  $\mu\text{m}$ ) and irregular cement lines (Steiniche and Hauge, 2003; Boel et al., 2007; Chappard et al., 2011).

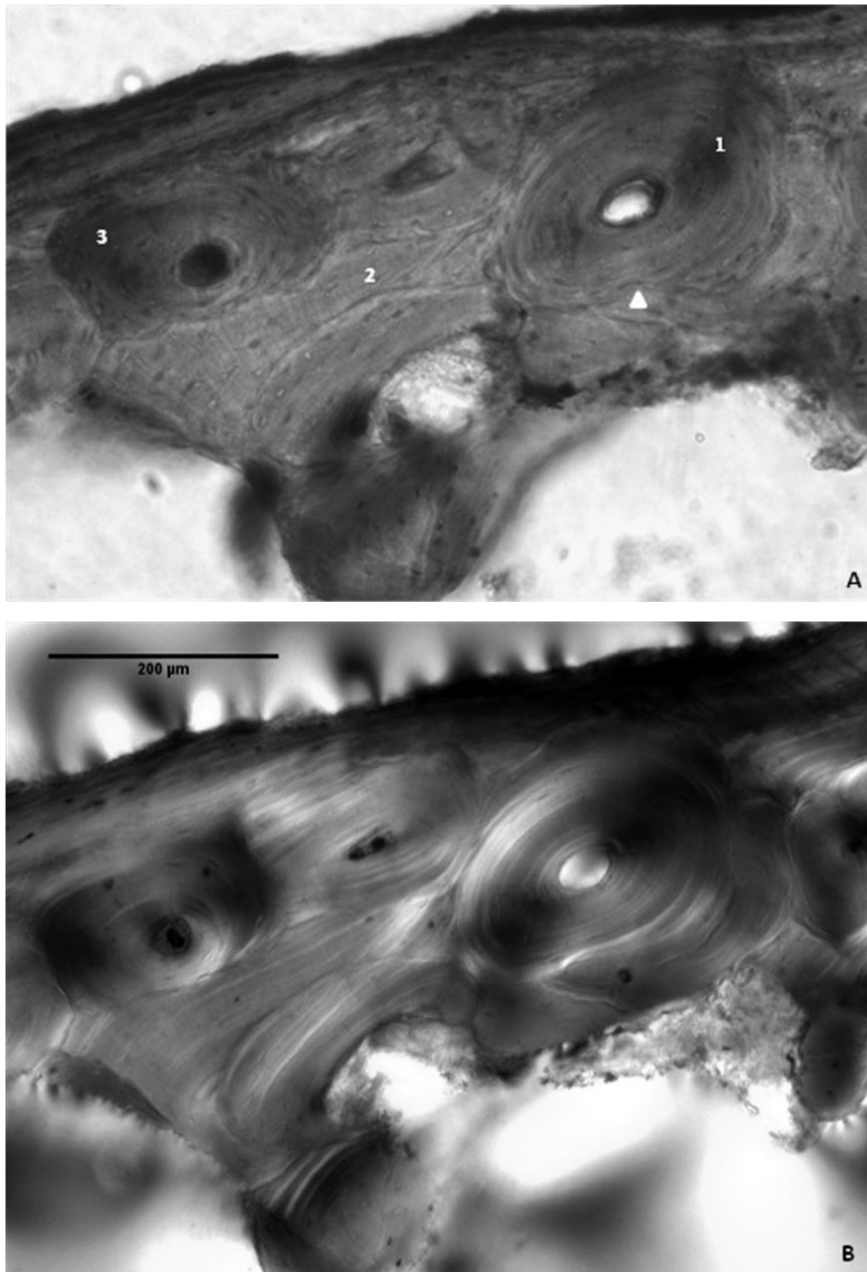


**Figure 3.2:** Micrography of a rib section of an adult male [SK.1235] from the Bocage Museum, Lisbon (Nikon Eclipse 80i®). A: Transmitted microscopy: 1. Secondary osteon with a well-defined cement line (white arrow); 2. Interstitial lamellae; 3. Secondary osteon partially resorbed. B: Same bone microstructure under polarized microscopy. Magnification 40x.

Functionally, the size and thickness of the cortex and the architecture of the spongy bone are optimally designed to support the biomechanical forces that bones must resist (Steiniche and Hauge, 2003), providing «(...) maximum strength for the least weight» (Young et al., 2006: 189). In the compact bone, the structure of osteons is designed to resist compressive forces, while the spongy bone is designed to support shifts in weight distribution (Wynsberghe et al., 1995).

At the microscopic level, five different types of cells populate the bone tissue, namely the osteoprogenitor cells, osteoblasts, osteocytes, bone-lining cells and osteoclasts (Ortner and Turner-Walker, 2003; Robling et al., 2006).

The osteoprogenitor cells are located in the bone marrow and result from the differentiation of non-hematopoietic mesenchymal stem cells (MSCs)<sup>28</sup> (Ortner and Turner-Walker, 2003). They can also be defined as pre-osteoblast precursors, which then differentiate into mature osteoblasts (Ortner and Turner-Walker, 2003). As starting units of the osteogenic process, the osteoprogenitor cells are abundant in growing individuals, decreasing in number with age (Jilka, 2002; Ortner and Turner-Walker, 2003). Jilka (2002: 581) points out that age has a deleterious effect on MSCs number through a reduction in the self-renewal capacity. Although the origin of osteoblasts recruited for bone synthesis in later life is unclear, there is some evidence that these stem cells are also present in the periosteum and endosteum (Ortner and Turner-Walker, 2003) (Figure 3.3).

Osteoblasts are fully differentiated cells responsible for the formation of osteoid - the organic or unmineralized component of bone matrix (type I collagen, proteoglycans, and glycoproteins) (Schultz, 1997; Marks and Odgren, 2002; Ortner and Turner-Walker, 2003; Junqueira and Carneiro, 2005, Young et al., 2006). They are mononucleated cells with a well-developed endoplasmic reticulum, a prominent Golgi apparatus, and numerous ribosomes and mitochondria that reflect the requirement for abundant protein production (Marks and Odgren, 2002; Ortner and Turner-Walker, 2003). When active, osteoblasts have a cuboidal to columnar shape with abundant basophilic cytoplasm (Junqueira and Carneiro, 2005; Young et al., 2006). Once their activity declines, they become flattened (Junqueira and Carneiro, 2005) and “spindle-shaped” (Young et al., 2006: 189). Osteoblasts are exclusively observed on the bone surface (Junqueira and Carneiro, 2005: 190), lying beneath the periosteum and on the

---

<sup>28</sup> Non-hematopoietic mesenchymal stem cells (or MSCs) are pluripotent units that have the ability to differentiate into multilineage cells, forming distinct types of mesenchymal tissues, such as bone, cartilage, ligament or muscle (Gregory et al., 2005; George et al., 2006). Due to its pluripotent nature, these cells are currently used in tissue engineering as a clinical solution to improve tissue and organ transplantation (George et al., 2006).

outer shell of trabeculae (Schultz, 1997). During osteoid synthesis, some osteoblasts may become enclosed by newly formed matrix, turning into osteocytes (Junqueira and Carneiro, 2005). Others may be transformed in bone-lining cells (resting osteoblasts) or undergo apoptosis (Jee, 2001). Another function advanced by researchers is their transdifferentiation into cells that deposit chondroid or chondroid bone (Franz-Odenaal et al., 2006).

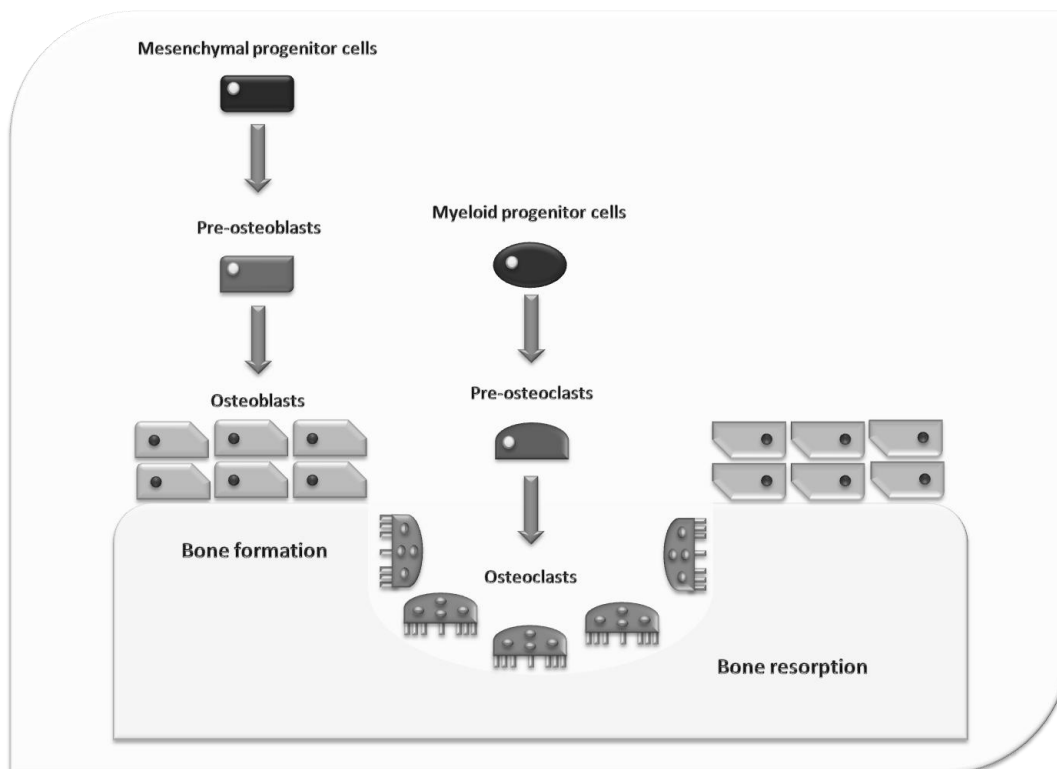


**Figure 3.3:** Schematic diagram of the genesis of osteoblast and osteoclast cells in their role in bone formation and resorption (content from Price et al. 1993; design reproduction by Sandra Assis).

Mature osteocytes are stellated or dendritic-shaped cells formed during the last differentiation stage of the osteoblastic lineage (Nijweide et al., 2002). They can be described as inactive osteoblasts that become trapped in the newly formed bone (Young et al., 2006)

The transformation from osteoblasts to osteocytes is accompanied by several cellular changes (Figure 3.4). At the early stage of cell differentiation, the newly formed osteocytes, also called osteoid-osteocytes, are larger than mature or “older” osteocytes and possess well-developed Golgi apparatus for collagen storage (Franz-Odenaal et al., 2006). After mineralization of the osteoid, the osteocytes undergo structural changes characterized by a reduction in the endoplasmic reticulum and Golgi apparatus due to a decrease in the synthesis of proteins (Franz-Odenaal et al., 2006). The authors also note that the size and shape of the

newly formed osteocytes vary according to the activity and size of the committed osteoblasts, as well as with the type of bone formed; for instance, in woven bone the osteocytes are isodiametric, whereas in lamellar bone they are flattened and oblate with their long axis parallel to the thickness of the lamellae (Franz-Odenaal et al., 2006). Osteocytes are long-living cells (Junqueira and Carneiro, 2005) whose life span is largely determined by bone turnover (Nijweide et al., 2002). They are also the most abundant cell type in bone (Klein-Nulend and Bakker, 2007). Osteocytes reside in oval cavities within the bone matrix that are called lacunae (Marks and Odgren, 2002; Ortner and Turner-Walker, 2003; Young et al., 2006). From the cell bodies, long filopodia-like cytoplasmic processes spread radially through small channels named canaliculi (Marks and Odgren, 2002; Nejweide et al., 2002; Ortner and Turner-Walker, 2003; Young et al., 2006). These cytoplasmic extensions are used by mature cells to communicate with neighbouring osteocytes (Figure 3.4), bone-lining cells, and osteoblasts, forming a complex network or syncytium (Nejweide et al., 2002; Ortner and Turner-Walker, 2003; Klein-Nulend and Bakker, 2007; Qing and Bonewald, 2009). The lacunocanalicular system described allows the transport of nutrients, waste products, and chemical signals between the Haversian blood vessels and the bone cells (Nejweide et al., 2002; Ortner and Turner-Walker, 2003; Young et al., 2006). Two main functions can be ascribed to osteocytes: blood-calcium homeostasis and mechanosensory regulation (Cullinane and Einhorn, 2002; Nejweide et al., 2002). Osteocytes seem to have a key role in the regulation of calcium and phosphorus levels into and out of the bone matrix, and for the bloodstream (Nejweide et al., 2002; Ortner and Turner-Walker, 2003; Klein-Nulend and Bakker, 2007). Additionally, they are considered the mechanosensors of bone, being responsible for the maintenance of its osteonic and trabecular architecture (Nejweide et al., 2002)<sup>29</sup>. Thus, a frequent question is postulated by researchers: «are the osteocytes the “nerve cells” of the mineralized bone matrix?» (Nijweide et al., 2002: 93). Recent studies indicate that osteocytes form a neuralgic centre “(...) where bone is informed about local osteopenia or bone redundancy in relation to its usage” (Nejweide et al., 2002: 103). Nevertheless, and contrary to neurons, this transmission of signals is made by gap junctions instead of synapses (Marotti, 2000; Junqueira and Carneiro, 2005; Young et al., 2006). Specific neurotransmitters like nitric oxide and amino acid glutamate are synthesised as messengers (Marotti, 2000; Cullinane and Einhorn, 2002). According to Seeman (2006: 1443),

---

<sup>29</sup> The apoptosis of osteocytes, which may occur through microdamage, estrogen deprivation, elevated cytokines, glucocorticoid treatment, osteoporosis, osteoarthritis, aging, and after immobilization, has the opposite effect: a decrease in bone mechanoregulation and an activation of bone resorption by osteoclasts (Klein-Nulend and Bakker, 2007).

osteocytes orchestrate focal modelling and remodelling by detecting strain, modify the distribution of bone tissue focally to accommodate stress, and produce the diversity of contours and shapes that characterize bones. To a limited extent, these cells also have the capacity to synthesize and to resorb their perilacunar matrix (Marks and Odgren, 2002; Franz-Odenaal et al., 2006) through a process called osteocytic osteolysis (Qing and Bonewald, 2009). For decades, the “digestive” function of osteocytes was coupled with bone remodelling (Cullinane and Einhorn, 2002). Current understanding is that the lytic activity of these cells plays a role, not in the bone matrix remodelling but in the systemic mineral homeostasis (Cullinane and Einhorn, 2002; Qing and Bonewald, 2009).

Bone-lining cells can be described as flat, elongated and inactive cells that cover the bone surface (Marks and Odgren, 2002; Walsh et al., 2003), laying in close proximity to the osteoblasts (Walsh et al., 2003). Additionally, they have also been identified adjacent to the Haversian canal wall (Miller and Jee, 1987 in Walsh et al., 2003). Apparently the bone-lining cells are not directly involved in bone formation or resorption (Marks and Odgren, 2002; Walsh et al., 2003), since they possess few cytoplasmic organelles (Marks and Odgren, 2002; Ortner and Turner-Walker, 2003). For that reason they have received little attention in the study of bone microstructure. Marotti (2000) claims that one of the biggest mistakes made by researchers was to consider the bone only in its productive and destructive stage (or transient phase), neglecting the intermediate steps where bone-lining cells seem to have an important role. According to Everts et al. (2002: 85): «(...) bone-lining cells exert a series of activities crucial for remodelling of bone: after withdrawal of the osteoclast from the resorption pit, bone-lining cells enter the lacuna and clean its bottom from matrix leftovers. This cleaning proves to be a prerequisite for the subsequent deposition of a first layer of (collagenous) proteins in the resorption pits». Therefore bone-lining cells are important for modulating osteoclast activity (Everts et al., 2002). Other authors, such as Burger and Klein-Nulend (1999), describe bone-lining cells as being part of the osteocyte network that guarantees the functional integrity and mechanical adequacy of a bone organ.

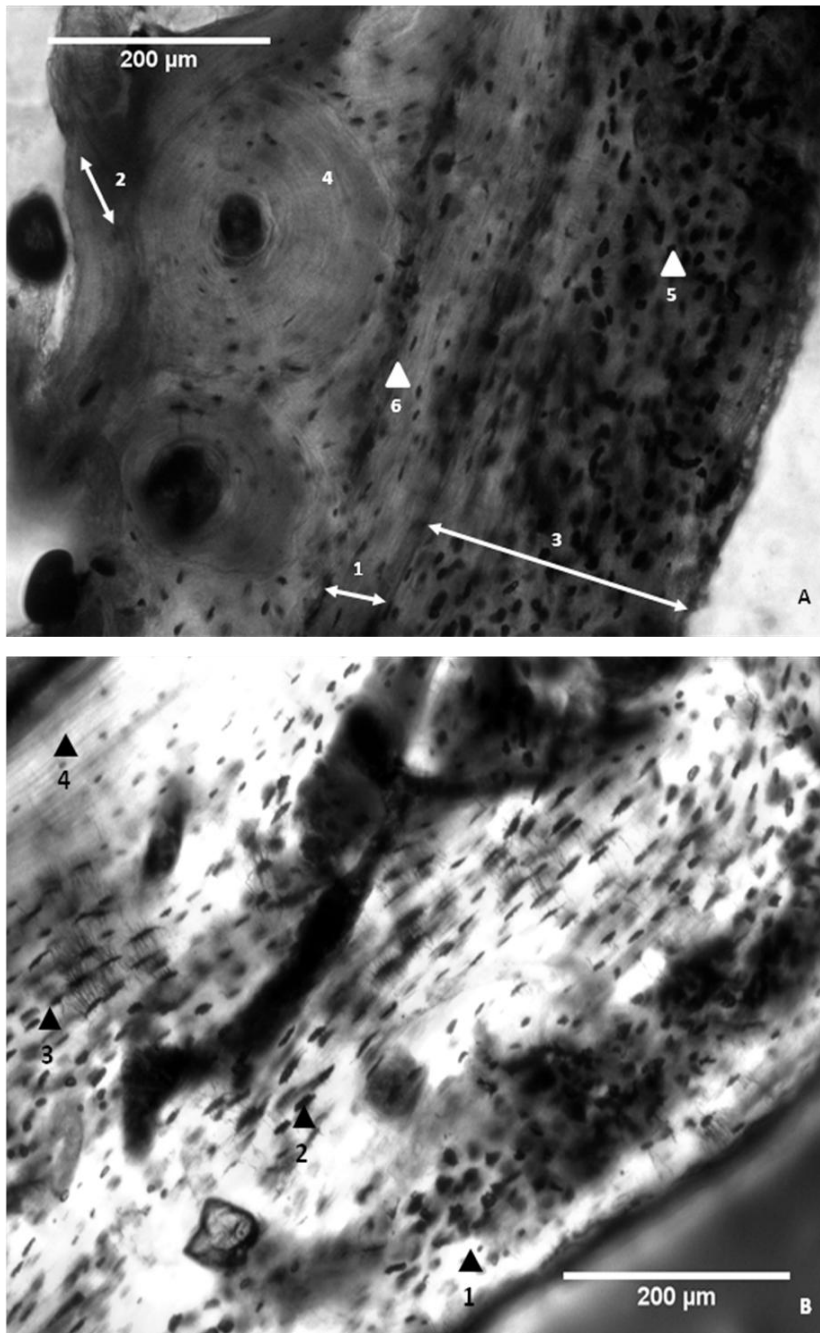


**Figure 3.4:** Micrography of a rib sample of an adult female [Sk. 119] from the Bocage Museum, Lisbon (Nikon Eclipse 80i®). A: Light microscopy. 1. Periosteal circumferential lamellae; 2. Endosteal circumferential lamellae; 3. Abnormal periosteal new bone deposition (woven bone); 4. Secondary osteon; 5. Multiple osteoid-osteocyte lacunae (elliptical black spots); 6. Lamellar osteocyte lacunae (elongated black spots). Magnification 40X B: Polarized microscopy. 1. High concentration of disorganized osteoid-osteocyte lacunae (woven bone); 2. Flattened osteocyte lacunae in an almost linear arrangement; 3. Osteocyte lacunae exhibiting their canaliculi and the formation of a syncytium; 4. Small lamellar osteocytes. Magnification 100X.



Originating from the hematopoietic cells of the monocyte-macrophage lineage, the osteoclasts constitute a group of cells responsible for the breakdown and resorption of bone (Marks and Odgren, 2002; Takahashi et al., 2002; Ortner and Turner-Walker, 2003; Novack and Teitelbaum, 2008; Proff and Römer, 2009). Thus, their differentiation pathway is common to that of macrophages and other cells that practice phagocytosis (Schultz, 1997; Väänänen et al., 2000; Väänänen and Zhao, 2002; Young et al., 2006). Osteoclasts are mobile, multinucleated<sup>30</sup> giant cells that are seen lying in etched depressions in the bone matrix called Howship's lacunae (Schultz, 1997; Junqueira and Carneiro, 2005; Young et al., 2006). Nuclei are typically located toward the antiresorptive surface (Marks and Odgren, 2002; Novack and Teitelbaum, 2008). In the cytoplasm, multiple circumnuclear Golgi stacks, a high density of mitochondria and abundant lysosomal vesicles are present (Marks and Odgren, 2002). The high number of lysosomes reflects the potential of these cells for destruction of bone tissue (Ortner and Turner-Walker, 2003). When active, osteoclasts rest on the bone surface and possess two distinct plasma membranes: a ruffled border and a clear zone (Marks and Odgren, 2002; Junqueira and Carneiro, 2005). The ruffled border is the central, highly infolded area of the plasma membrane composed of fine microvilli (Marks and Odgren, 2002; Young et al., 2006). From this area, several organic acids and lysosomal proteolytic enzymes which will dissolve the mineral and the organic components of bone, respectively, are produced (Young et al., 2006). Therefore, the ruffled border is commonly considered the "resorptive organelle" par excellence (Väänänen and Zhao, 2002; Novack and Teitelbaum, 2008: 462). After migration to the resorption site, a specific membrane domain, the sealing zone or actin ring, forms under the osteoclast body (Väänänen et al., 2000; Novack and Teitelbaum, 2008). This zone is a microfilament-rich, organelle-free structure that serves as the point of attachment of the osteoclast to the underlying bone matrix (Marks and Odgren, 2002; Junqueira and Carneiro, 2005). Additionally, it creates an isolated extracellular microenvironment, sealing the resorption site from its surroundings (Väänänen et al., 2000; Novack and Teitelbaum, 2008). There is an unanimous consensus among biologists that the main physiological function of osteoclasts is to degrade mineralized bone matrix, as well as dentine and calcified cartilage (Väänänen et al., 2000; Väänänen and Zhao, 2002). Proff and Römer (2009) point out that the mineral component of bone and teeth is dissolved through the secretion of hydrochloric acid, whereas the organic phase is degraded by specific enzymes, such as the lysosomal cathepsin K and, to a lesser extent, by the matrix metalloproteinases. Osteoclastic bone resorption is a

---

<sup>30</sup> Each cell may contain from 5 to 50 (or more) nuclei (Junqueira and Carneiro, 2005).

cyclical phenomenon – also called a resorption cycle - in which the cells converge on the target area, degrade the underlying matrix, detach and finally suffer apoptosis or return to their non-resorbing stage to restart the process (Väänänen et al., 2000; Novack and Teitelbaum, 2008). The cycle is regulated by systemic and local chemical signals (Ortner and Turner-Walker, 2003). After matrix degradation, the waste products are removed from the lacuna via the ruffled border and deposited into the extracellular space (Väänänen et al., 2000). Resorption of mineralized tissues is crucial for normal skeletal maturation that includes bone growth and remodelling, as well as tooth eruption and fracture healing (Väänänen et al., 2000; Väänänen and Zhao, 2002). Additionally, this process has an unquestionable role in the maintenance of blood calcium homeostasis (Väänänen et al., 2000; Väänänen and Zhao, 2002; Young et al., 2006).

#### **3.1.4. The Microarchitecture of Bone: Bone Dynamics and Tissue Envelopes**

Bone development and maintenance comprises three distinct but interconnected phases: growth, modelation and remodelation (Robling and Stout, 2008).

During individual growth, bone can be formed through intramembranous ossification that results from the direct mineralization of matrix secreted by osteoblasts, or by endochondral ossification, which occurs by deposition of bone matrix over a pre-existing cartilage matrix (Junqueira and Carneiro, 2005).

Intramembranous ossification has its onset during the embryonic development of the skeleton (Marks and Odgren, 2002) and at the primary centres of ossification (Junqueira and Carneiro, 2005). In these islands of developing bone, the osteoprogenitor cells differentiate into osteoblasts which begin the synthesis of osteoid. Mineralization then follows, converting the trapped osteoblasts into osteocytes (Karaplis, 2002; Young et al., 2006). As a consequence of the radial growth and fusion of neighbouring ossification centres, the primitive mesenchymal tissue is replaced by woven bone (Junqueira and Carneiro, 2005; Young et al., 2006). Finally, the primary bone is extensively remodelled to form mature or lamellar bone (Junqueira and Carneiro, 2005). Intramembranous ossification underlies the formation of most of the flat bones of the skull, maxillary bones and parts of the mandible and clavicle (Karaplis, 2002; Marks and Odgren, 2002; Junqueira and Carneiro, 2005; Young et al., 2006). Additionally, it contributes to the growth of short bones and thickening of long bones (Junqueira and Carneiro, 2005).

In contrast, endochondral ossification occurs within a portion of hyaline cartilage whose shape resembles the bone to be formed (Junqueira and Carneiro, 2005; Young et al., 2006). The process follows a complex and predefined sequence of events that begin in the diaphyseal area, as described below (Wynsberghe *et al.*, 1995; Karaplis, 2002; Junqueira and Carneiro, 2005; Young et al., 2006):

- i. About 6 to 8 weeks after conception, the mesenchymal stem cells of the embryo multiply rapidly and cluster together to form a cartilage model;
- ii. This bone prototype undergoes appositional growth to form a more stretched mass of cartilage composed of a central shaft (pre-diaphysis) and two extremities (pre-epiphyses);
- iii. Soon after, a thin layer of primitive perichondrium appears covering the outer surface of cartilage; this is responsible for the appositional growth, serving as a source for chondroblasts;
- iv. As the cartilage grows, the perichondrium is replaced by a fibrous membrane called periosteum. Beneath periosteum, the osteoprogenitor cells differentiate into osteoblasts, and matrix synthesis occurs. Furthermore, a hollow cylinder of trabecular bone called a bone collar is formed;
- v. In the next step, a primary centre of ossification is produced near the central portion of the cartilage model (diaphysis). This occurs by osteoclast tunnelling of the bone collar that allows not only the spread of capillaries throughout the matrix, but also the transport of osteoprogenitor cells into the middle of the diaphysis, leading to the formation of the marrow cavity;
- vi. After birth, blood vessels enter the extremities of the cartilage model (epiphyseal cartilage), giving rise to the secondary centres of ossification. During their expansion both primary and secondary centres form cavities that are gradually filled with bone marrow;
- vii. Under the influence of biomechanical stress, the remnants of cartilage and the surrounding woven bone are remodelled to form the outer shell of compact bone;
- viii. Nevertheless, some cartilage is retained in joints and at the epiphyseal or growth plate<sup>31</sup>, which is responsible for the longitudinal growth of a long bone. When growth

---

<sup>31</sup> The growth plate is composed of five major zones: (1) resting zone, where chondrocytes are arranged randomly and separated by large amounts of matrix; (2) zone of proliferation, characterized by columns of discoid cells which result from the rapid division of chondrocytes; (3) hypertrophic cartilage zone, which allows the maturation and enlargement of chondrocytes and matrix synthesis; (4) calcified cartilage zone, where after

stops, the epiphysis fuses to the diaphysis leaving an epiphyseal line which eventually disappears.

Endochondral ossification is responsible for the formation of long bones, as well as the vertebrae, pelvis and bones of the base of the skull (Young et al., 2006). Despite the value of endochondral ossification in foetal osteogenesis, the synthesis of ossifying bone on a cartilage scaffold is also an essential part of postnatal growth, bone modelling and fracture repair (Karaplis, 2002). In a growing skeleton, the normal architecture is achieved by bone modelling (Gross and Bain, 1993; Marks and Odgren, 2002; Pfeiffer et al., 2006). This process insures the “transverse and longitudinal bone geometries” (Gross and Bain, 1993: 152), which are crucial to sustaining biomechanical load (Robling et al., 2006; Robling and Stout, 2008; Safadi et al., 2009). During this period, which occurs in the first two decades of life, bone synthesis necessarily precedes and exceeds bone resorption (Marks and Odgren, 2002; Seeman, 2006). All processes that regulate bone development pre- and post-natally are under the influence of a variety of humoral and local factors (Marks and Odgren, 2002). Among these are growth, thyroid, glucocorticoid, vitamin D and sex hormones (Karaplis, 2002; Nijweide et al., 2002; Young et al., 2006: 197). Once skeletal maturity is reached, modelling is reduced to a residual level and remodelling takes place; however, modelling can be activated later in life in association with some diseases or when biomechanical constraints change drastically (Robling et al., 2006).

Bone remodelling, also called bone turnover is a dynamic process not related to growth that may occur simultaneously in different locations of the skeleton (Junqueira and Carneiro, 2005). It is a complex phenomenon responsible for the continuous change of the internal structure of bone, which involves two steps: removal of existing bone by osteoclasts and replacement of new bone by osteoblasts (Ott, 2002; Seeman, 2006). Nevertheless, and in contrast to modelling, the amount of bone formed equals the quantity of bone removed, in a process called bone coupling (Marks and Odgren, 2002). Any change in this perfect equilibrium can lead to several metabolic conditions (Ott, 2002), and other inflammatory processes, since bone remodelling is considered “an inflammatory repair response” (Martin, 2003: 105).

---

mineralization, the chondrocytes undergo apoptosis, leaving irregular lacunae in the ossifying cartilage. These cavities are then invaded by blood vessels originating in the bone marrow; (5) ossification zone, characterized by the formation of endochondral bone. Osteoprogenitor cells lining the lacunae start to differentiate into osteoblasts and osteocytes. The osteoblasts deposit osteoid which calcifies into woven bone, whereas osteoclasts are involved in bone resorption (Wynsberghe et al., 1995; Karaplis, 2002).

Bone is remodelled by a team of cells derived from distinct lineages called the basic multicellular unit (BMU) (Robling et al., 2006). The BMUs are not permanent units (Ott, 2002). They consist of coupled osteoclasts and osteoblasts that act in response to external signals or stimuli, eroding and refilling the bone surface (Ott, 2002; Ortner and Turner-Walker, 2003; Robling et al., 2006; Robling and Stout, 2008). A fundamental property is that remodelling occurs in specific locations following the same sequence: «(...) origination and organization of BMU, activation of osteoclasts, resorption of old bone, recruitment of osteoblasts, formation of new bone matrix, and mineralization» (Ott, 2002: 304). These steps comprise the bone remodelling cycle (Figure 3.5), which takes 4 or 5 years to be completed (Ott, 2002). During a person's lifetime many cycles of bone turnover may occur (Carter and Beaupré, 2001), as the BMUs are responsible for the appositional growth of long bones (Marks and Odgren, 2002). The appositional growth is responsible for the resorption of compact and cancellous bone in the marrow cavity (endosteal surface) and by its addition externally (periosteal surface) (Marks and Odgren, 2002; Ortner and Turner-Walker, 2003). Bone periosteal deposition and endosteal removal must be conducted in balance in order to maintain the mechanical integrity of bone (Ortner and Turner-Walker, 2003). Thus, BMUs can be ascribed as mediator mechanisms that bridge individual cellular activity to whole bone morphology (Robling et al., 2006). The remodelling cycle operates on the periosteal and endosteal surfaces, as well as on the surface of bone trabeculae, and at the linings of vascular channels in compact bone (Ortner and Turner-Walker, 2003: 22). However, there are a number of differences between cortical and cancellous remodelling (Ott, 2002). The renewal of cancellous bone is made along the surface either through bone channelling or by extending out over a certain area (Ott, 2002). This potentially increases the bone volume, a process that cannot occur in cortical tissue (Ott, 2002). In cortical and intracortical remodelling, tunnels are produced throughout the bone cortex (Ott, 2002). Additionally, woven bone can be added to its periosteal surface in response to mechanical loading, an event not observed in cancellous bone (Ott, 2002). Other features of trabecular bone remodelling include the formation of microcalluses and a more ready access to marrow cells (Ott, 2002).

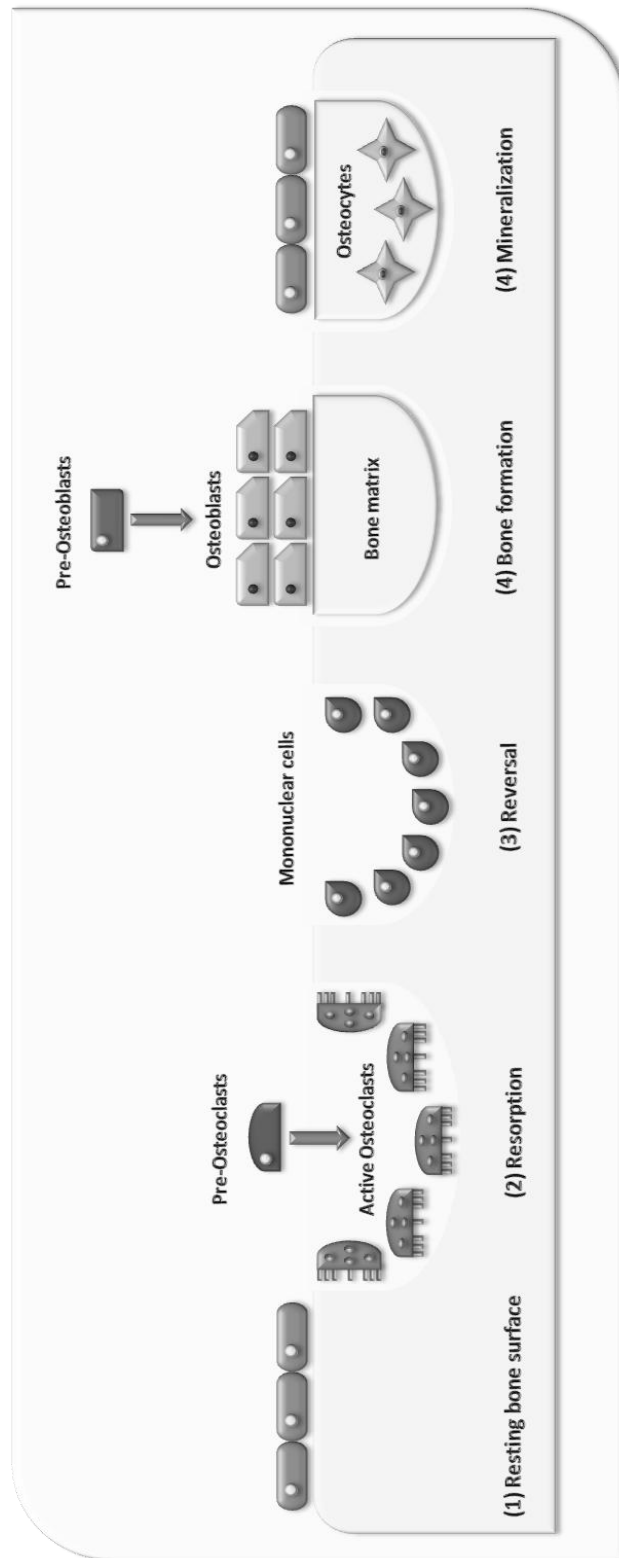


**Figure 3.5:** Classical scheme of bone remodelling process comprising the four stages of cell interplay (content from: <http://www.ns.umich.edu/Releases/2005/Feb05/img/bone.jpg>; design reproduction by Sandra Assis).

Remodelling is essential to repair fatigue microdamage and thus maintain bone strength (Ott, 2002; Martin 2003; Seeman, 2006). In addition, it also contributes to mineral metabolism (Ott, 2002) and ionic balance (Hall, 2005). Histologically, the remodelling cycle produces secondary osteons (Pfeiffer et al., 2006). Foremost, it is a complex process determined by the mutual interaction of osteoblasts and osteoclasts. Any disturbance in this perfect balance will affect remodelling leading to the development of severe bone diseases, such as osteoporosis (Proff and Römer, 2009).

Bone is composed by two envelopes of condensed fibrous tissue: an external, the periosteum; and an internal, the endosteum (Junqueira and Carneiro, 2005; Young et al., 2006). The periosteum<sup>32</sup> is a thin membrane of connective tissue that covers the outer surface of long bones except for tendon insertions, joint surfaces and sesamoid bones (Wynsberghe et al., 1995; McWhinney et al., 2001; Allen et al., 2004). In mature individuals this dynamic tissue is subdivided into two levels: an outer layer named the *stratum fibrosum*, which is composed of a complex network of fibroblasts and collagenous fibers – Sharpey’s fibers that anchor the membrane to the underlying bone; and an inner layer (or *stratum osteogenicum*) that retains a highly osteogenic potential<sup>33</sup> (Schultz, 1997; Junqueira and Carneiro, 2005; Ortner, 2008). This germinative or “cambium” layer (Ito et al., 2001: 215) is composed of cells in distinct stages of maturation, such as mesenchymal progenitor cells, differentiated osteogenic progenitor cells, osteoblasts and fibroblasts, as well as nerves and capillaries that supply the periosteum in a sparse collagenous matrix (Ellender et al., 1988; Squier et al., 1990; Fang and Hall, 1997; Schultz, 1997; McWhinney et al., 2001; Aubin and Triffitt, 2002; Junqueira and Carneiro, 2005;

---

<sup>32</sup> The first description of the microstructure of the periosteum was made by Anthon van Leeuwenhoek (1632-1723, Netherlands). As can be read in his letter to the Royal Society: «[t]o the cortex of the bone, the periosteum is united, not only on the outside, but even by entering in many places into the very substance of the bone, and join’d to it by the vessels, which issue out from the bone, in such at sometimes one cannot determine which is the bone, and which belongs to the membrane investing it, they both appearing in the microscope to consist alike of exceeding small vessels» (Leeuwenhoek, 1720: 93). In 1739, Henri-Louis Duhamel du Monceau (1700-1782, France) recognized the capability of periosteum to form new bone (Dwek, 2010). By embedding silver wires in the bones of growing animals, he found out that after some time the metallic object became completely covered by bone, concluding that periosteum is osteogenetic and operates similarly to the cambium layer of the trees (Dwek, 2010).

<sup>33</sup> The assertion that the periosteum has osteogenic capabilities was not consensual throughout time. In 1800, Baron Guillaume Dupuytren (1777 – 1835, France) suggested that the periosteum plays an important role in fracture repair (Altun, 2008). A century later, Sir William Macewan (1848 – 1924, U.K.) described in his work “The Growth of Bone”, published in 1912, that periosteum cannot be viewed as osteogenic, but merely as a limiting membrane (Gallie and Robertson, 1914; Altun, 2008). In 1928, Emil Geist (U.S.A) published a short report entitled “Does periosteum form bone?”, in which he concludes that the new bone formed during bone repair has a periosteal origin (Geist, 1928). However, only in 1945 were the first impressions of Duhamel definitely confirmed by John Victor Lacroix (Altun, 2008).

Dwek, 2010). According to Schultz (1997: 197) the inner layer of the periosteum is the most important structure for bone regeneration (e.g. following fractures).

The endosteum covers all of the internal cavities within bone, including the trabeculae of spongy bone and the walls of the blood vessels, and is formed by a single layer of flattened cells (Schultz, 1997; Junqueira and Carneiro, 2005). This membrane possesses small amounts of connective tissue and is smaller than periosteum (Junqueira and Carneiro, 2005).

On the cortical bone, the osteons are located between the periosteal and endosteal envelopes forming the circumferential lamellae. Under the periosteum and above the endosteum, the osteon layer is doubled by a number of parallel lamellae that constitute, respectively, the periosteal and endosteal bone tissue (Chappard et al., 2011). The main functions of periosteum and endosteum are to nourish the osseous tissue as well as to restore the number of osteoblasts needed for bone growth, remodelling and repair (Junqueira and Carneiro, 2005; Young et al., 2006), especially during fracture healing (Dwek, 2010).

### **3.1.5. The Macroarchitecture of Bone: a Perfect Scaffold**

A typical long bone is composed of a tubular shaft called the diaphysis, which houses the medullary cavity, and by two roughly spherical extremities called the epiphyses (Wynsberghe et al., 1995; Schultz, 1997). Between the epiphyses and the diaphysis there is a transitional region named the metaphysis (Wynsberghe et al., 1995; Schultz, 1997; Carter and Beaupré, 2001). In the growing individual the epiphysis and metaphysis are separated by the physis (Carter and Beaupré, 2001). The physis (or growing plate) is a cartilage platform that allows for longitudinal growth during an individual's development (Wynsberghe et al., 1995; McGuinnis, 1999; Scheuer and Black, 2000; Carter and Beaupré, 2001; Young et al., 2006).

In cross section, two distinct types of bone are distinguishable: cortical (or compact) and spongy (or cancellous) (Marks and Odgren, 2002; Ortner and Turner-Walker, 2003; Steiniche and Hauge, 2003; Young et al., 2006). Cortical tissue appears as a solid continuous mass that makes up the thick-walled cylinder (diaphysis) of the long bones (Wynsberghe et al., 1995; Ortner and Turner-Walker, 2003; Steiniche and Hauge, 2003). In contrast, spongy bone is a reticulate tissue that consists of thin trabeculae arranged in a three-dimensional (3D) network (Steiniche and Hauge, 2003; Young et al., 2006). This bony tissue is primarily observed in the roughly spherical extremities (epiphyses) of the tubular bones (Wynsberghe et al., 1995; Ortner and Turner-Walker, 2003). Other common places for spongy tissue are the bodies of vertebrae and the flat bones of the pelvis and skull (Ortner and Turner-Walker, 2003).



All bony elements are involved in two important life processes: mechanical and homeostatic (Pfeiffer, 2000; Pfeiffer et al., 2006). The bone tissue supports the soft structures and protects major organs such as those in the cranial and thoracic cavities (Cullinane and Einhorn, 2002; Karaplis, 2002; Hall, 2005; Junqueira and Carneiro, 2005). In addition, other skeletal functions can be highlighted, such as the ability to produce movement and to store calcium and other minerals (Karaplis, 2002; Marks and Odgren, 2002; Junqueira and Carneiro, 2005; Pfeiffer *et al.*, 2006). It also serves an important role in calcium metabolism and in body haematopoiesis<sup>34</sup> (Gross and Bain, 1993; Frassico et al. 1997; Cullinane and Einhorn, 2002; Marks and Odgren, 2002; Karaplis, 2002; Pearson and Lieberman, 2004; Hall, 2005).

In summary, bone is a multifunctional and physiologically dynamic tissue that is in continuous adaptation to the surrounding environment (Gross and Bain, 1993; Lieberman, 1997; Cullinane and Einhorn, 2002; Roberts et al., 2004). An awareness of how the external forces interact with the skeletal tissue is useful to understanding the mechanics of bone lesions (Carter and Beaupré, 2001).

### **3.1.6. The Human Ribs: Gross Anatomy, Development and Microstructure**

In general, an adult individual possesses 12 pairs of ribs (a total of 24) that articulate, on the posterior plane, with the thoracic vertebrae via synovial joints, and on the anterior plane, with the ventral hyaline costal cartilage, encircling the rib cage (Scheuer and Black, 2000). Nevertheless, the number of ribs may vary due to the presence of an additional cervical or lumbar pair, or by the agenesis of the twelfth pair (Scheuer and Black, 2000). Developmental errors during growth and ossification processes can lead to ribs agenesis (Glass et al., 2002; Castriota-Scanderbeg and Dallapiccola, 2005). Despite the apparent singularity, bilateral agenesis of ribs is a common occurrence in a normal individual.

Ribs can be subdivided into typical and atypical according to their morphology. The typical ribs are the most numerous in the chest wall and include the ribs number 3 to 9 (R3-R9). The atypical or special ribs are the 1<sup>st</sup>, 2<sup>nd</sup> and the 10<sup>th</sup> to 12<sup>th</sup> (R1, R2 and R10-R12) (Scheuer and Black, 2000; White and Folkens, 2005). Ribs can also be grouped in relation to the anterior point of articulation. The first seven ribs (R1-R7) articulate directly with the sternal

---

<sup>34</sup> According to Travlos (2006: 549) "hematopoiesis is a compartmentalized process within the hematopoietic tissue (...)" that is responsible for the production of the blood compounds. This type of tissue is found in the bone marrow located in the central cavities of axial and long bones, and is composed by blood cells, barrier cells, adipocytes and macrophages.

costal notches via cartilage. Ribs 8, 9 and 10 are interconnected by common cartilage that anchors them to the sternum. The remaining ribs (R11 and R12), also called free-floating ribs, do not articulate with any anatomical structure (White and Folkens, 2005).

Broadly, ribs are composed of the following anatomical structures (Figure 3.6):

- Head, an enlarged posterior portion that articulates with the thoracic vertebrae by one (R1, R10-12), or two (R2-R9) joints;
- Neck, a short segment between the head and the rib's joint that articulates with the transverse process of the thoracic vertebra;
- Interarticular crest, a bony structure that separates the joint facets;
- Tubercle, located at the posteroinferior corner of each rib, being the point of contact between the shaft and the neck;
- Shaft or body, which constitutes the remaining portion of the rib extending from the tubercle to the sterna end. The shaft of ribs 3 to 6 is thicker and rounder in cross section compared to ribs 7 to 12;
- Body angle, represented by a sharp curve in the bone lateral to the tubercle. On the inferior border of ribs, there is a subcostal groove, which is more pronounced posteriorly, especially between ribs 5-7, and houses the intercostal neurovascular bundle (Scheuer and Black, 2000; White and Folkens, 2005).

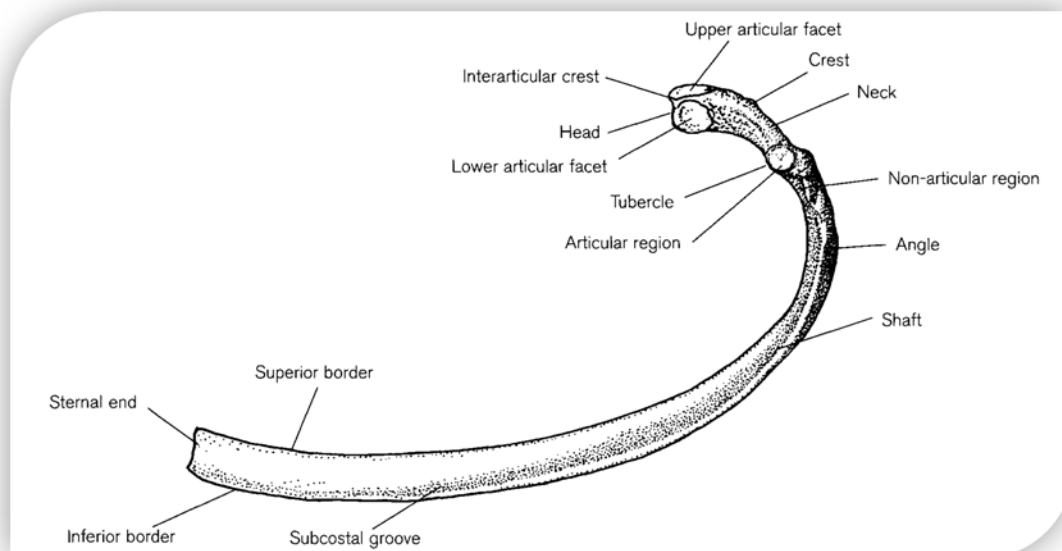


**Figure 3.6:** Example of the morphology of a typical human adult rib (adapted from Scheuer and Black, 2000: 233).

In terms of texture (Figure 3.7), the ribs present an inner smooth surface covered by parietal pleura – the pleural surface, and an outer rugous surface that bears various insertion marks to the attachment of muscles, and the cutaneous surface (Scheuer and Black, 2000).

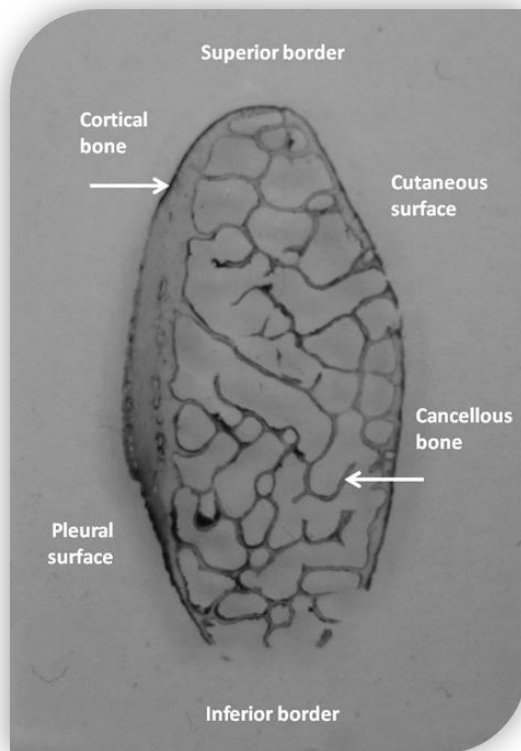


**Figure 3.7:** Rib cross-section illustrating the location of the cutaneous and pleural surfaces (3<sup>rd</sup> right rib from the adult male Sk. 102 from the Bocage Museum, Lisbon).

The growth and development of ribs occur, with the exception of the eleventh and twelfth ribs, from four centres of ossification (White and Folkens, 2005) (Table 3.2). The first centres emerge early in foetal life and are fully developed at birth (Scheuer and Black, 2000; Pfeiffer, 2006). During puberty (12-14 yrs), the secondary centres of ossification appear in the rib's head at the sites of articulation. Additionally, other centres may occur at the non-articulating areas of the tubercle (Scheuer and Black, 2000; White and Folkens, 2005). Also in early puberty, the epiphysis for the articulating region starts to develop (Scheuer and Black, 2000). The costal groove, normally absent at birth, becomes prominent on the inferior border of ribs during childhood (Pfeiffer, 2006). The epiphyses of the head of the ribs are the last to form, being fused around 17 yrs. All epiphyses are fused to the rib body in early adulthood (White and Folkens, 2005).

**Table 3.2:** Summary of the main morphological changes observed on ribs during growth and development (adapted from Scheuer and Black, 2000: 242).

Period	Morphological Changes
<b>Foetal</b>	
<b>Wks 8-9</b>	Primary centres of ossification appear in ribs 5-7
<b>Wks 11-12</b>	All ribs exhibit ossification centres
<b>Non-adults</b>	
<b>Birth</b>	All primary ossification centres are present
<b>12-14 yrs</b>	Epiphyses appear in the non-articular region of the tubercle
<b>Adult</b>	
<b>18 yrs</b>	Epiphyses appear in the articular region of the tubercle
<b>17-25 yrs</b>	Epiphyses appear and fuse in the head region
<b>&gt;25 yrs</b>	Ribs are fully adult

The growth and ossification of the ribs is greatly controlled by the genetic pool of the individuals. Nevertheless, the morphology of ribs may be influenced during development by the surrounding environment. Thus, the upper ribs are modified by the shape of the lung buds and heart, whereas the lower ribs grow to house the abdominal viscera, such as the liver (Scheuer and Black, 2000). According to Pfeiffer (2006), the expansion of the rib cage follows the development of the lungs, with a rapid increase in size after birth, then a slow growth during mid-childhood, and a rapid period of growth at puberty. This evidence indicates that the rib cage not only protects vital organs but is also shaped by them.

At the microscopic level, ribs are composed of cancellous bone surrounded by a thin rim of cortical tissue (Figure 3.7). As in the long bones, the spongy core is composed of plates and columns of trabeculae filled with bone marrow (Cormier, 2003). Similarly, the cortical or compact bone is formed by an array of osteons or Haversian systems connected by lamellar bone (Cormier, 2003). Between birth and adulthood, a set of important transformations occur in the microstructure of ribs, both at the cutaneous and pleural surfaces (Table 3.3).

**Table 3.3:** Summary of the microstructural changes observed on ribs during growth and development (adapted from Streeter, 2012).

Rib phases	Microstructural changes observed on ribs	
Phase I: < 5 yrs	<b>General considerations</b>	The primordial cortex is mostly composed of woven bone. The margins of the medullar cavity initially indistinct become more clearly defined at the end of this phase. Modelling drift <sup>35</sup> is discernible as the deposition of circumferential lamellae replaces the woven bone. This transition starts first at the pleural surface and later in the cutaneous periosteal cortex
	<b>Cutaneous cortex</b>	Thinner, mostly woven bone, many primary vascular canals. Osteoclastic resorption is evident at the scalloped surfaces (Howship's lacunae)
	<b>Pleural cortex</b>	Thicker, some woven bone, primary lamellae initially form endosteally. Presence of many Volkmann's canals. Osteoclastic resorption is evident at the scalloped surfaces (Howship's lacunae).
	<b>Woven bone</b>	Most of both cortices
	<b>Primary lamellar bone</b>	Rare, small areas on pleural endosteal and cutaneous periosteal surfaces initially
	<b>Remodelling</b>	Rare
Phase II: 5-9 yrs	<b>General considerations</b>	Presence of drifting osteons aligned in parallel rows from the periosteum and the endosteum. These osteons are normally incompletely formed and eccentrically orientated. Signs of resorption are indicated by the presence of scalloped Howship's lacunae on the opposite site of the vascular canal
	<b>Cutaneous cortex</b>	Thinner, mostly intracortical woven bone with many primary vascular canals
	<b>Pleural cortex</b>	Thicker (two to three times the width of the cutaneous cortex), largely primary lamellar bone, few drifting osteons, many Volkmann's canals
	<b>Woven bone</b>	In some areas of the cutaneous cortex, rare woven bone on pleural cortex
	<b>Primary lamellar bone</b>	Primarily in pleural cortex
	<b>Remodelling</b>	Intracortical remodelling in the form of large drifting osteons on pleural cortex originating from the primary lamellar bone near the periosteal surface of the pleural cortex
Phase III: 10-17 yrs	<b>General considerations</b>	Primary lamellar bone increasingly remodelled in both cortices with drifting osteons more deeply located. Presence of a thin rind of primary lamellar or woven bone that develop along the cutaneous-periosteal surface. At some points, this unremodelled bone is crossed with primary vascular canals, indicating an accelerated cortical modelling typical of the puberty growth spurt
	<b>Cutaneous cortex</b>	Thinner, mostly lamellar bone with some remodelling, periosteal woven bone, and more porous with large resorptive bays (drifting osteons)
	<b>Pleural cortex</b>	Thicker, denser remodelling, still some areas of primary lamellar bone
	<b>Woven bone</b>	Thin rind on cutaneous periosteal surface
	<b>Primary lamellar bone</b>	Both cortices intracortically and often on cutaneous periosteal surface
	<b>Remodelling</b>	Drifting osteons on both cortices.

<sup>35</sup> Modelling drift, or osseous drift (as enunciated by Enlow in 1962), is the phenomenon that controls the spatial distribution of bone in response to physiological and biomechanical stimuli (Maggiano, 2012: 140). At this stage, the bone moves in anatomical space-time so dramatically to accommodate the rates of formation and resorption along the periosteum and endosteum that its adult position is far removed from its initial immature position (Maggiano, 2012).

<b>Phase IV: 18-21 yrs</b>	<b>General considerations</b>	Rib cortices with a more adult morphology characterized by the presence of secondary osteons (type I)
	<b>Cutaneous cortex</b>	Thinner, dense remodelling, osteons three to four rows deep, rarely primary lamellar bone periosteally
	<b>Pleural cortex</b>	Thicker, dense remodelling, osteons three to five rows deep, occasional areas of primary lamellar bone intracortically
	<b>Woven bone</b>	None or rare
	<b>Primary lamellar bone</b>	Isolated areas on both cortices intracortically
	<b>Remodelling</b>	Both cortices, fewer drifting osteons more type I (secondary) osteons.

The microanatomy of the subadult and adult ribs is substantially different. In subadults, the distinct features observed are closely related with the ongoing process of growth and modelling (Streeter, 2012). During the early stages of growth, ribs are formed by woven bone that is progressively replaced by primary lamellar bone deposited as circumferential lamellae on both the periosteal and endosteal surfaces (Streeter, 2012). Pfeiffer (2006), studying the rib microstructure of an identified juvenile skeletal sample (Spitalfields, U.k., 18<sup>th</sup>-19<sup>th</sup> centuries), concluded that during infancy through mid-childhood, and later in adolescence, structures similar to “plexiform bone” can be observed.

From birth to maturity, important changes also occur at the total area of the rib cross-section (Pfeiffer, 2006). Before the second decade of life, an increase in the cortical thickness is observed through bone formation at the periosteum (Streeter, 2012). When adulthood is reached, the periosteal expansion slows and the rate of marrow cavity expansion increases, leading to a reduction in the cortical area and an increment of the medullary space (Pfeiffer, 2006; Streeter, 2012). This growth dynamic is under rule of a process called “modelling drifts” (Streeter, 2012: 140). This process is responsible for the resorption of older bone at the pleural-endosteal and cutaneous-periosteal surfaces (Streeter, 2012). A similar mechanism occurs for the trabecular bone. Cancellization or trabecularization takes place at the cutaneous-endosteal surface after the partial digestion of peripheral osteons, whose remnants are then converted into cancellous bone (Streeter, 2012). Remodelling of ribs occurs by replacement of primary lamellar bone and formation of secondary osteons, which constitute the dominant feature of the adult ribs (Pfeiffer, 2006; Streeter, 2012).

## **3.2. PERIOSTEAL NEW BONE FORMATION (PNBF): BONY CHANGES**

### **AT THE SURFACE**

Many pathological conditions leave their testimony in human bones. Although a true statement, the precise diagnosis of the numerous conditions that affect the skeleton is far from being easy or even consensual. This reality is the result of the limited response of bone tissue to internal or external assaults. In fact, it is well recognized by researchers that bone only has three types of response: abnormal bone production; excessive bone resorption, or a combination of both (Ortner, 2003b; Ortner, 2008).

The formation of deposits of new bone, also called periosteal new bone formations (PNBF) or periosteal reactions (PR) is a common finding in a large spectrum of conditions (Ortner, 2003d). Nevertheless, the knowledge about this bone response is not proportional to its occurrence. Thus, in the next pages an approach to the study of periosteal new bone formations will be made, attending to its definition, regulation, pathophysiology, classification and etiology.

### **3.2.1. PNBF in the Clinical Literature**

#### **3.2.1.1. A Definition**

Periosteal reaction (PR) constitutes a bone response of the periosteum to a variety of pathological conditions (e.g. osteitis, syphilis, leprosy, tumours, venous lesions, developmental disorders, endocrine disturbances), as well as to normal growth and stress injury (Edeiken et al., 1966; Steinbock, 1976; Burgener et al., 1991; Aufderheide and Rodríguez-Martín, 1998; Gladkowska-Rzeczycka, 1998; Ortner, 2003d; Wenaden et al., 2005; Haun et al., 2006; Tong et al., 2006; Rana et al., 2009; Nogueira-Barbosa et al. 2010).

#### **3.2.1.2. Mechanisms of Regulation and Pathophysiology**

During normal growth and remodelling, new bone is produced through a balanced interplay between the bone-forming (osteoblast) and bone-resorbing (osteoclast) cells (Weston, 2004; Robling et al., 2006; Bielby et al., 2007). This mechanism is extensive to all bone tissue, including the periosteal membrane, and is crucial for maintaining bone strength throughout life, as well as to regulate its metabolic functions (Raisz, 1999; Rauch et al., 2007; Seeman, 2007). An example of the active role of periosteum during early development is given

by a phenomenon called physiological periostitis (or physiological subperiosteal new bone formation). Physiological periostitis is a common finding in paediatric radiology, especially in preterm and newborn individuals aged 1-6 months (with a peak between 2 and 3 months) (Shopfner, 1966). Wrongly interpreted during decades as a component of some diseases (e.g. congenital syphilis and other infections, infantile cortical hyperostosis, unrecognized trauma, hypervitaminosis A, leukemia, and neuroblastoma), it is currently viewed as a manifestation of normal periosteal bone growth (Shopfner, 1966; de Silva et al., 2003) via intramembranous ossification, which leads to the rapid formation of a double cortical layer that is progressively incorporated into the pre-existing cortex (Kwon et al., 2002).<sup>36</sup>

In general, periosteal new bone production occurs by induction of fibroblasts into osteogenic precursor cells, which then suffer progressive modulation to develop into active osteogenic cells in the cambium layer (Wenaden et al., 2005: 439). In contrast, osteoclasts have their origin by migration from the marrow through cortical bone (Vigorita, 2008). Allen et al. (2004) note that the potential of the cambium layer to generate new cells is age dependent, which affects not only the morphology but also the number of cells produced. For example, in immature bone the osteoblasts are cuboidal in shape and quite numerous, whereas in the mature skeleton they are more elongated and less numerous (Allen et al., 2004). The number of fibroblasts and the thickness of the fibrous layer also decrease with age (Allen et al., 2004). Fan and co-authors (2008) studying different aged rats also concluded that the structure and composition of the cells of the periosteum are age-related and site-specific. These age-related changes are also present in the vessel density; however the periosteum retains the capacity to increase the number of vessels when stimulated by mechanical loading (Allen et al., 2004). In addition to age, other systemic factors seem to play an important role in cell metabolism and regulation (Weston, 2004; Karaplis, 2002; Rauch et al., 2007) (Table 3.4).

---

<sup>36</sup> Physiological periostitis is frequently symmetrical and affects more often the diaphysis of the long bones, namely the femur, humerus and tibia (Kwon et al., 2002; de Silva et al., 2003). Usually, it is not concentric, affecting only one aspect of the bone diaphysis (de Silva et al., 2003). The average thickness of the new bone deposition ranges from 0.7 to 0.9 mm, being never higher than 1.8 mm (Kwon et al., 2002). Kwon and co-authors (2002) state that a similar new bone distribution in individuals older than 4 months or with a thickness exceeding 2 mm should be carefully analyzed as a sign of a potential abnormality.



**Table 3.4:** Regulators of bone metabolism (after Weston, 2004: 30, with additions from Raisz, 1999).

Bone regulators	Hormones and minerals	Effect
Calcium-regulating hormones	Parathyroid hormone	Stimulates resorption and has direct inhibitory effect on osteoblasts
	1,25-Dihydroxyvitamin D <sub>3</sub>	Interferes in the differentiation of osteoblasts and osteoclasts
	Calcitonin	Inhibitor of bone resorption
Systemic hormones	Estrogen	Normal bone turnover
	Growth hormone/ Insulin	Bone formation and resorption
	Thyroid hormones	Bone formation and resorption and homeostasis of remodelling
	Glucocorticoids	Inhibit bone formation
Growth factors	insulin-like growth factor (IGF)	Local and physiologic remodelling and skeletal repair
	Fibroblast-derived growth factor	
	Platelet-derived growth factor	
Local factors	Prostaglandin	Stimulator of bone resorption
	Osteoclast activating factor	Periosteal apposition or resorption
	Mechanical load	
Ions	Calcium	Exerts direct effects on the function of osteoblasts and osteoclasts
	Phosphate	
	Magnesium	

Three major calcium-regulating hormones largely serve the metabolic functions of the skeleton: the parathyroid hormone (PTH), 1,25-Dihydroxyvitamin D<sub>3</sub> and calcitonin (Raisz, 1999). PTH has a crucial function in the regulation of the serum calcium concentration, being a potent stimulator of bone resorption (Raisz, 1999; Karaplis, 2002; Safadi et al., 2009). This hormone has a biphasic effect: in high plasma concentrations it inhibits the collagen synthesis, and after long administration it induces bone formation (Raisz, 1999). Besides its importance in the intestinal absorption of calcium and phosphate, 1,25-Dihydroxyvitamin D<sub>3</sub> also has a critical role in the differentiation of both osteoblasts and osteoclasts (Raisz, 1999). Calcitonin, a peptide hormone, is a potent inhibitor of bone resorption, being used clinically in the drug therapy of osteoporosis (Raisz, 1999). It is regulated by the extracellular calcium level and has receptors on osteoclasts, preosteoclasts, monocytes and certain tumour cells (Safadi et al., 2009).

In the regulation and maintenance of bone tissue integrity, several systemic hormones, can be highlighted. Estrogen is a determinant in maintaining normal bone turnover. In its absence, an exaggerated remodelling in which resorption overlaps bone formation may occur (Raisz, 1999). Moreover, it exerts direct effects on the growth plate, being crucial for peripubertal growth and epiphyseal fusion (Karaplis, 2002). The growth hormone, acting in the systemic pathway, or locally through insulin-like growth factor (IGF), stimulates both bone formation and resorption (Raisz, 1999). The thyroid hormone, which has a similar effect, is also crucial for the homeostasis of bone remodelling (Raisz, 1999). During development,

glucocorticoid hormone is necessary for cell differentiation, especially for chondrocyte proliferation, maturation and differentiation earlier in life; after birth it inhibits bone formation (Karaplis, 2002).

Numerous local factors have been described in the last 30 years as having an important role in bone remodelling (Raisz, 1999). Cytokines, also called “osteoclastic-activating factors”, and prostaglandins, namely prostaglandin E<sub>2</sub>, are viewed as active stimulators of bone resorption (Raisz, 1999). Recently, some proteins and molecules linked to the function of these substances have been identified, such as TRANCE (produced by the osteoblast precursors), RANK (osteoclast differentiation factor) and OPG (osteoprotegerin), this last produced by the osteoblastic lineage and marrow cells (Raisz, 1999). Under the scope of the growth factors, the insulin-like growth factor (IGF) which is a determinant of local bone remodelling, and the platelet-derived growth factor and fibroblast growth factor, are crucial not only in physiologic remodelling, but also in skeletal repair (Raisz, 1999). Locally, the production of new bone may also be modulated by mechanical loading (Rauch et al., 2007). According to Robling et al. (2006), mechanical load is a powerful stimulus for bone cells, improving bone strength and preventing bone loss with age. In addition to the previous bone regulators, the concentration of some plasma ions such as calcium, phosphate and magnesium, can also affect bone metabolism. Calcium is the main mineral component of the skeleton; it simultaneously plays an important role in several physiological and biochemical processes, namely in the regulation of nerve excitability, muscle contraction, and blood coagulation (Civitelli et al., 1998). Calcium absorption occurs in the intestine and is regulated by vitamin D. In this process, the active metabolite of vitamin D, 1.25(OH)<sub>2</sub>D<sub>3</sub> is responsible for several steps of the calcium transport process (Civitelli et al., 1998). The estrogen hormone is also involved in the physiological regulation of calcium absorption (Civitelli et al., 1998). At the bone level, calcium can affect bone formation by controlling the secretion of calcium-regulating hormones, by mediating the intracellular effects of these hormones, by accelerating mineralisation, and by directly stimulating matrix formation and cell proliferation (Raisz and Kream, 1983b in Weston, 2004). Furthermore, the accumulation of high concentrations of calcium in the resorption lacunae during the reversal phase seems to have a direct control over osteoclast activity, causing cell retraction and in the long term, inhibiting bone resorption (Hill et al., 1998). Phosphate is not only the major component of apatite crystals but also a mediator of energy transfer, participating in numerous intracellular metabolic processes (Civitelli et al., 1998). In the skeleton, it stimulates both mineralisation and matrix formation, inhibiting bone resorption

when it occurs in high plasma concentrations (Raisz and Kream, 1983b in Weston, 2004). Magnesium is involved in many cellular functions, including production and utilization of energy, regulation of enzymatic activities, and control of intracellular and extracellular electrolyte concentration (Civitelli et al., 1998: 190). Magnesium seems to have an important role in bone mineralization: in high concentrations it decreases mineralisation; in lower concentrations it increases the rate of mineralisation (Raisz and Kream, 1983b in Weston, 2004).

Beyond normal development and remodelling, what are the pathological mechanisms of PNB? Richardson (2001) points out that PNB may be caused by any mechanism that breaks, tears, stretches, inflames, or even touches the periosteum. Here, three examples of interconnected factors that may induce PNB, such as stress injury, bone healing and bone inflammation will be given.

### **1. Stress Injury**

The overuse of bone may cause tissue damage, which, in turn, stimulates bone remodelling (Robling et al., 2006). The relationship between PNB and excessive mechanical load is documented in the clinical literature; particularly in relation to the medial tibial stress syndrome. This syndrome, also called shin splints, is a type of overuse stress injury frequently observed in recreational and competitive athletes, such as runners, occurring after repetitive and strenuous activities (Gaeta et al., 2006; Tweed et al., 2008). In addition to pain along the distal posterior-medial aspect of the tibia (Mubarak et al., 1982), the increased muscle and fascial tension also provokes stress-induced periosteal and marrow reactions (Jose et al., 2011). Identical bone response was reported by Nielsen et al. (1991) in twenty-two soldiers from the Royal Danish Lifeguard with lower leg pain. Although the mechanism that underlies the formation of bone lesions remains unknown, some studies pointed to the involvement of the soleus muscle. Disruption of the Sharpey fibers that connect the medial soleus fascia through the periosteum and into the bone, stress forces that eccentrically fatigue the soleus and/or microfractures have been advanced as possible aetiologies (Craig, 2008: 316).

### **2. Bone healing**

Acute bone trauma, such as fracture also stimulates the production of new bone. In fact, PNB is an important component of fracture healing. Unlike soft tissues that heal through the formation of scar tissue, bone recovers from injury through the synthesis of new bone in a

process that resembles embryonic skeletal formation (Ferguson et al., 1999; Arican et al., 2003; Sfeir et al., 2005).

The biology of bone fracture repair can be divided into three phases: inflammatory, reparative and remodelling (Figure 3.8) each of which is characterized by the presence of different cellular features and extracellular matrix components (Sfeir et al., 2005).

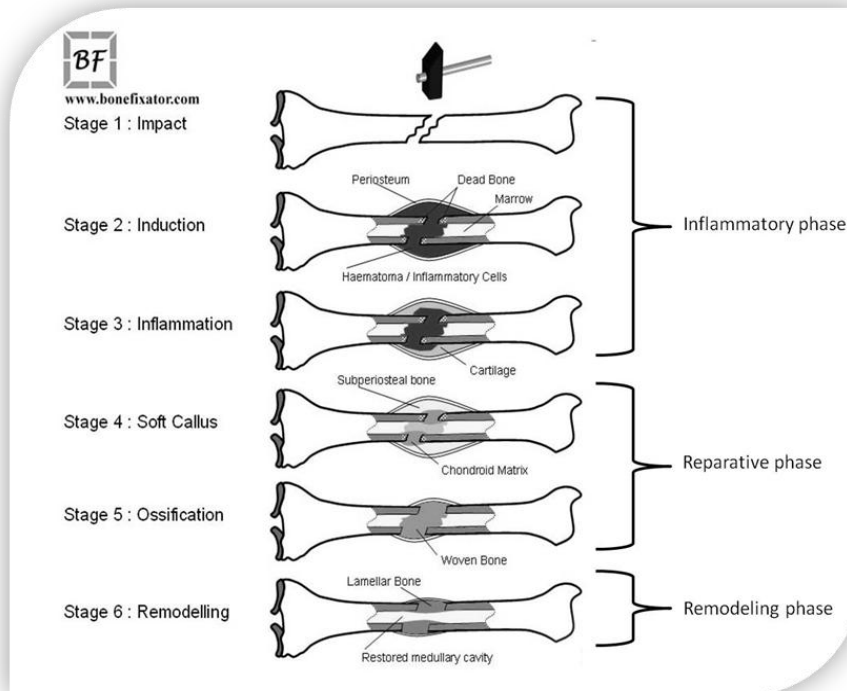


**Figure 3.8:** Schematic representation of the three phases of bone fracture healing (adapted from [www.bonfixator.com](http://www.bonfixator.com)).

Following the injury, an immediate or inflammatory bone response is activated mainly locally, and through the vascular system (McKibbin, 1978; Malizos and Papatheodorou, 2005; Bullough, 2010). In this process not only are the bone tissue, cells and blood vessels (vascular endothelial damage) involved, but also the surrounding soft tissues, such as muscle and nerves (McKibbin, 1978; Sfeir et al., 2005). The main function of the inflammatory reaction is the complete immobilization of the fractured bone ends (Sfeir et al., 2005; Bullough, 2010). In nature this immobilization is achieved in two ways: pain that unable disrupting movements, and swelling of the affected area (Sfeir et al., 2005; Bullough, 2010). Simultaneously, a cascade of cellular and biochemical events occur that include: platelet degranulation and release of growth factors; aggregation of polymorphonuclear leukocytes (PMNs), lymphocytes, blood monocytes, and tissue macrophages in the injured area to stimulate the release of cytokines

and subsequent angiogenesis, and the formation of a subperiosteal hematoma between the fracture ends to limit further blood loss (Malizos and Papatheodorou, 2005; Sfeir et al., 2005; Bielby et al., 2007). The release of platelet-derived growth factor (PDGF) and basic fibroblast growth factor (bFGF) from the disrupted platelets seems to stimulate the proliferation of periosteal and mesenchymal cells in the fracture haematoma (Malizos and Papatheodorou, 2005), which results in the formation of a reparative granuloma (Sfeir et al., 2005).

The reparative phase starts in the first days after injury and lasts for several weeks (Sfeir et al., 2005). This process is characterized by the development of a reparative callus in and around the fracture site, which will eventually be replaced by new bone (Sfeir et al., 2005). The function of this immature tissue is to guarantee the mechanical stability of the injured area (Bullough, 2010). According to Bullough (2010), the amount of callus produced depends of several factors including the degree of instability of the fracture and the vascularity of the affected bone. Unstable fractures tend to produce an increasing amount of callus, whereas in the poorly vascularised areas of the skeleton (e.g. midshaft of the tibia) the production of callus is scarce (Bullough, 2010). The reparative phase involves two antagonistic events: bone cells apoptosis and tissue necrosis, and new bone formation. The damage of the soft tissues, periosteum and marrow along with the death of osteocytes will induce local necrosis (McKibbin, 1978; Sfeir et al., 2005). With the resorption of the necrotic tissue, new cells, such as fibroblasts, chondroblasts, and osteoblasts are produced in the cambial layers of the periosteum (Sfeir et al., 2005), and from undifferentiated mesenchymal cells that populate the unaffected soft tissues around the fracture (Bullough, 2010). Besides periosteum, the bone marrow also contributes progenitor cells for inflammation, matrix remodelling, and for cartilage and bone formation (Colnot et al., 2006). The presence of pluripotent mesenchymal cells in the cambium layer of the periosteum in combination with growth factors regularly produced or released after injury, confers to this membrane an important role in the healing processes (Arican et al., 2003; Malizos and Papatheodorou, 2005; Bielby et al., 2007). In fact, numerous studies agree that periosteum contributes to the formation of a callus, which is normally composed of fibrous connective tissue, blood vessels, cartilage, woven bone, and osteoid (Sfeir et al., 2005).

During the reparative phase a recapitulation of the embryonic intramembranous and endochondral ossifications and chondrogenesis occurs (Ferguson et al., 1999; Arican et al., 2003). The intramembranous ossification begins in the first days of fracture healing and is characterized by the differentiation of osteoblasts directly from precursor cells, without the

formation of cartilage as an intermediate step (Sfeir et al., 2005). Osteoblastic activity in the woven bone opposed to the cortex and close to the fracture site also occurs (Sfeir et al., 2005). This type of bony formation occurs externally and compounds the hard callus. Experimental studies have revealed the importance of woven bone in the repair, synthesis and maturation of the new lamellar bone (Figure 3.9).

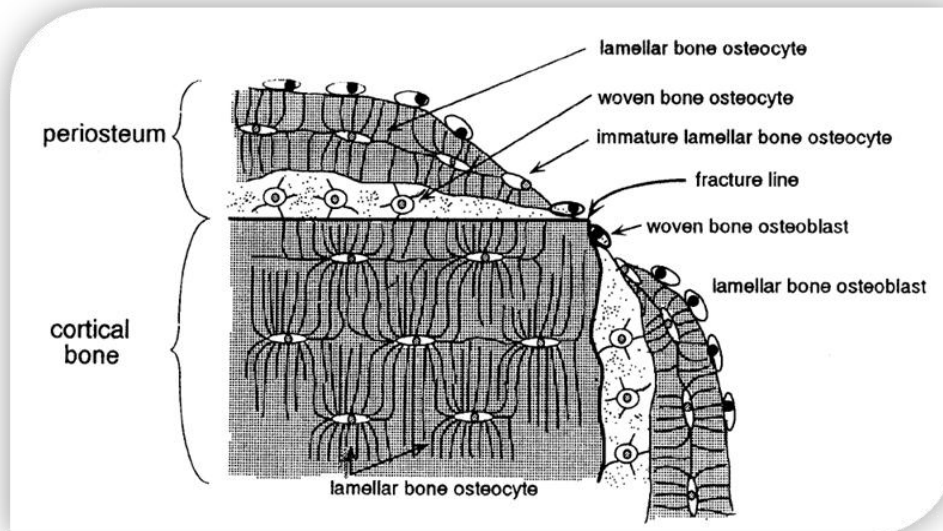


**Figure 3.9:** Schematic representation of bone canaliculi development by woven and lamellar osteocytes during fracture healing (after Kusuzaki et al., 2000: 658).

Kusuzaki and co-authors (2000) used a fracture-like simulation model of the rat femur to ascertain the development of bone canaliculi during the process of intramembranous ossification, concluding that woven bone osteocytes may be necessary for the induction of the lamellar bone osteocytes. Their results showed that in the early phase of bone repair (5 days after injury), the woven bone osteoblasts connect to the surface of the injured cortical bone, creating a scaffold for the attachment and maturation of lamellar bone osteoblasts, which afterward differentiate into immature lamellar bone osteocytes and then into mature lamellar osteocytes (Kusuzaki et al., 2000). After becoming embedded in the matrix, the woven bone osteocytes may operate as a mediator, via canaliculi, between the cartilage or injured bone matrix and the lamellar bone osteocytes, eventually supplying nutrients and communicating with them and with osteoblasts in the bone marrow (Kusuzaki et al., 2000). This gives woven bone osteocytes an important role in the synthesis of new bone during the intramembranous ossification process (Kusuzaki et al., 2000).

At the periphery of the hard callus, chondrogenesis also begins (McKibbin, 1978; Sfeir et al., 2005). Mesenchymal or undifferentiated cells from the periosteum and adjacent external soft tissue located over the fracture become larger and start to acquire the appearance of cartilage (Sfeir et al., 2005). This region composed of fibrous tissue that will eventually be replaced by cartilage is termed soft callus. In the second week of the fracture repair there is sufficient cartilage covering the fracture, which will stimulate endochondral ossification (Sfeir et al., 2005). At this stage cells and later osteoblasts will release membrane-derived vesicles that contain calcium phosphate complexes into the matrix, activating the process of mineralization. As the callus becomes rigid the fracture is internally immobilized (Sfeir et al., 2005). This callus will be invaded by capillaries from the adjacent bone and by osteoblasts which will form the primary spongiosa consisting of both cartilage and woven bone (McKibbin, 1978; Sfeir et al., 2005). The woven bone will then connect the two fractured ends, preparing the area for the remodelling phase (Sfeir et al., 2005).

The remodelling phase is characterized by the replacement of woven by lamellar bone and by the resorption of the remaining callus (McKibbin, 1978; Sfeir et al., 2005). This final stage is also responsible for the gradual modification of the fracture region under the influence of mechanical loads, and by the reestablishment of the skeletal integrity (Sfeir et al., 2005; Bielby et al., 2007). Contrary to foetal skeletogenesis, fracture bone repair is accompanied by inflammation and by the release of inflammatory cells which are an important source of osteoinductive signals for bone regeneration and healing (Ferguson et al., 1999). This means that inflammation of the periosteum or of the surrounding tissues may also induce PNBf.

### 3. Bone inflammation

Inflammation<sup>37</sup> is a primordial response that protects our body from internal and external aggressions such as infection, cancer and tissue injury, and restores the physiological function of the damaged tissues (Štvrtinová et al., 1995; Saylor, 2005; Gilroy and Laurence, 2008). This body response may be local or systemic depending on the type of the injurious agent (Bullough, 2010). Štvrtinová and co-authors (1995: 579) identify two categories of factors that may cause inflammatory responses: endogenous, that includes immunopathological reactions, and some neurological and genetic disorders; and exogenous,

---

<sup>37</sup> Incorrectly used as a synonym, it is important to highlight that inflammation and infection are distinct entities. Inflammation is an innate response of the body to tissue damage, whereas infection arises when the body is invaded by pathogenic organisms, such as bacteria. Normally infection is accompanied by an inflammatory response. In contrast, inflammation may occur in the absence of infection (Weston, 2004).

which can be divided into mechanical (traumatic injury); physical (temperature variation, ionising irradiation, microwaves); chemical (caustic agents, poisons, venoms, genotoxic and proteotoxic compounds); nutritive (deficiency of oxygen, vitamins and basic nutrients); and biological (viruses, microorganisms, protozoan, and metazoan parasites). According to Gilroy and Laurence (2008), our well-being and survival depends on a rapid and effective inflammatory response to these environmental aggressors. Normally, the inflammatory response is activated within minutes and resolves itself after a couple of hours. If the inflammation persists for weeks or months, it evolves into a chronic process (Tomkins, 2003; Gilroy and Laurence, 2008). According to Štvrtinová et al. (1995: 582), inflammation can be divided into four major phases:

- i. **Acute vascular response:** characterized by vasodilatation and vascular permeability that increases the blood supply to the affected area (hyperaemia), causing redness (erythema) and the entry of fluids into the tissues (oedema). This phase usually resolves after a few minutes<sup>38</sup>;
- ii. **Acute cellular response:** characterized by the appearance of granulocytes, particularly neutrophils, in the tissues. Following the retraction of the vascular endothelial cells, the blood vessels become permeable allowing the migration of different cell types such as neutrophils, monocytes and lymphocytes. Erythrocytes may also leak into the tissues leading to haemorrhages. When the vessels are damaged, fibrinogen, fibronectin and platelets are aggregated at the site of the injury to stop the bleeding and aid in clot formation. The death of cells will contribute to the formation of pus;
- iii. **Chronic cellular response:** occurs after severe damage and is characterized by the appearance of an infiltrate of mononuclear cells composed of macrophages and lymphocytes. These cells are involved in the destruction of microorganisms and in the cleaning of the affected area;
- iv. **Resolution:** occurs a few weeks after the injury and aims to restore the normal tissue architecture. During this phase the blood clots and other residual products are removed and the tissue acquires its original form and/or forms a scar.

---

<sup>38</sup> This initial response mirrors the four cardinal signs of inflammation first described by the ancient Roman Celsius: rubor (redness, caused by vasodilatation); calor (heat, the result of increased blood flow); tumor (swelling, caused by exudation of fluids and cells into the extravascular spaces) and dolor (pain, the result of irritation of the local nerve endings) (Bullough, 2010: 88).



The vascular and cellular responses are mainly observed during the acute stage of inflammation. The chronic cellular response and the resolution phases are characteristic of the chronic stage of inflammation. Chronic inflammation is more prolonged and indicates an incomplete elimination of residual and foreign materials such as in infections (e.g. tuberculosis) or following the deposition of crystals (e.g. urate crystals), culminating with granuloma formation (Štvrtinová et al., 1995). A granuloma is formed when macrophages and lymphocytes accumulate around the residual product, together with epithelioid and giant cells (Štvrtinová et al., 1995).

Inflammation of the bone and periosteum follows the same cascade of reactions observed in the soft tissues. According to the place of occurrence in the bone tissue, it may be classified as: (1) periostitis, when it affects the periosteum; (2) osteitis<sup>39</sup>, when it affects the cortical bone; and (3) osteomyelitis<sup>40</sup>, when it affects the medullar cavity.

Periostitis is an old clinical entity frequently mentioned in the treatises of surgery and pathology, especially from the 19<sup>th</sup> century. For example, in 1817 the surgeon Philip Crampton published a medical report entitled “On Periostitis, or Inflammation of the Periosteum”, where the aetiology, development and treatment of this condition is described and the lack of attention given by other physicians is criticized: «[i]nflammation of the periosteum, unconnected with any known constitutional disease, is an affection with which practical surgeons are well acquainted. It is remarkable, however, that a disease so important in its consequences, and of such frequent occurrence, should not have been noticed in any systematic work, nor have been made the subject of any separate inquiry» (Crampton, 1817: 331). Similar medical writings were also published by Usher Parsons (1839) and John Ashhurst (1871). In these medical compendia, periostitis is described as a reactive response of the periosteum to injury, infection and other inflammatory agents. It may be primary, when the injury directly affects the periosteum, or secondary, when the inflammation spreads from other locations, namely the cortical bone (osteitis) or medulla (osteomyelitis) (Ashhurst, 1871).

---

<sup>39</sup> Osteitis is a common complication of either periostitis or osteomyelitis and refers to an inflammation of the compact bone, including the Haversian canals, and the bone adjacent to the medullary cavity (Ortner, 2003b). It is characterized by a softening or medullization of the bone tissue, with absorption of the early constituents (Ashhurst, 1871). As a result, the bone becomes enlarged (though it loses weight), with the layers of the walls separated, and with a porous appearance (Ashhurst, 1871). If the inflammation progresses, it may lead to a necrotic state, or in other cases, to the formation of new bony matter giving bone an abnormally solid and heavy appearance with thickening and marrow-cavity encroachment (Ashhurst, 1871).

<sup>40</sup> Osteomyelitis refers to an inflammation of the medullary or marrow cavity of bone (Ashhurst, 1871). A complete description of this condition will be given in Table 3.8.

The pathological changes observed in periostitis may consist of swelling of the periosteum, followed by cell-proliferation of its cambium layer, and/ or a rapid accumulation of wandering cells, which allows the formation of inflammatory lymph (Ashhurst, 1871). Likely soft tissue inflammation, periostitis may occur either in the acute, or in the chronic form (Crampton, 1817). In the acute form, the residual products of inflammation are removed from the affected area and the structure of the periosteum is restored (Ashhurst, 1871). In some cases, a suppurative process may eventually develop (Crampton, 1817). The chronic form most frequently ends in cartilaginous thickening of the membrane, absorption of the subjacent bone, and/or formation of new bone upon its surface (Crampton, 1817). Expansion of the bone diaphysis is also a common finding (Druitt, 1860). The chronic form may also induce the formation of a granuloma under the periosteum containing osteoblasts (Weston, 2004). These bone forming cells will then produce a bony callus composed primarily of woven bone, which will gradually be converted into lamellar bone (Weston, 2004).

The response of the periosteum with respect to the acute and chronic forms of inflammation and the severity of injury was experimentally tested in the 19<sup>th</sup> century by physiologists and anatomists. Parsons (1839: 22/23) describes the findings of the French anatomist Cruveilhier of Montpellier: «(...) Mr. Cruveilhier detached it [periosteum] from the tibia, in a great number of hares, to two thirds at least of the circumference and extent of the bone. After ten, twenty, thirty, and sixty days, he found the periosteum reunited, and scarcely any perceptible difference between the surface of the bone and that of the opposite site, excepting a slight increase in thickness. A haren, upon which he separated the periosteum from the whole circumference of the bone (...), [showed that] the external wound was cicatrized, but the denuded bone was surrounded two thirds of its circumference with a copious deposition of matter of a caseous appearance. The anterior face of the bone was covered by a thick bed of new formation which shot forth irregular sprouts (...)». Through these experiments Cruveilhier confirmed the osteogenic potential of periosteum and its capacity to secrete and deposit osseous matter on the internal surface when detached from the underlying cortical bone (Parsons, 1839). Despite the chronological distance, these findings are surprisingly up-to-date. In fact, the physical elevation of the periosteum is frequently described as a prerequisite for PNB (Weston, 2004). Cruveilhier of Montpellier also presents an hypothesis based on the process of ossification to explain the physiological mechanism that underlies the new bone formation: «[t]he periosteum thus detached, swells and secretes from its internal face a small quantity of reddened fluid, at first very thin (...). Its quantity and

consistence gradually increase till that which was a limpid fluid becomes a jelly, which thickens daily and passes into a state of cartilage. In this, osseous fibres are deposited, and finally the fluid and cartilaginous substance disappear, leaving the new bone perfectly formed» (Parsons, 1839: 24). Since this very beginning, the clinical meaning of periostitis has practically not changed. It continues to be described as a bone condition characterized by infiltration of the periosteum by inflammatory cells, elevation and/or violation of the periosteal membrane, and new bone deposition in the periosteum or in the surrounding soft tissues (Spjut and Dorfman, 1981). Nevertheless, changes have occurred in the application of the concept of “periostitis”. As noted earlier, periostitis is used to describe an inflammatory process. However, it is now accepted that the periosteum has the capacity to respond to stimuli different from inflammation<sup>41</sup>. As a consequence, a broader term called “periosteal reactions” has been adopted in recent publications (e.g. Wenaden et al., 2005; Burgener et al., 2006; Rana et al., 2009) and is being used in this thesis under the designation of PNB (periosteal new bone formation) or PR (periosteal reaction).

Periosteal reactions may be caused by any pathological process or disturbing agent that separates the periosteum from the underlying bone such as blood, pus, granulation tissue, haematoma, abscess, or tumor cells (Kenan et al., 1993; Weston, 2004). Other factors can also be identified, namely the mechanical adaptation or compensation for weakness secondary to osteolysis, attempts at tumour containment, disruption of blood circulation, and bone stimulating products derived from tumours (Weston, 2004 after Ragsdale, 1993; Ragsdale et al., 1981). Physiologically, the response of the periosteum occurs in three basic steps: activation of the periosteal osteoprogenitor cells, differentiation in osteoblasts and subsequent production of osteoid, and mineralization of the subperiosteal osteoid (Kenan et al., 1993). The clinical list of pathologies associated with periosteal new bone deposition is extensive and includes many infections (e.g. osteomyelitis, syphilis, tuberculosis, leprosy), metabolic and hormonal disorders (e.g. hyperphosphatasia, hyperparathyroidism, hyperthyroidism, rickets, scurvy, hypervitaminosis A), tumours (e.g. leukemia, lymphoma, metastases, primary bone tumors, eosinophilic granuloma), skin conditions (e.g. urticaria pigmentosa, pyoderma, burns, chronic cellulitis), trauma, juvenile rheumatoid arthritis, sickle cell anemia, dactylitis, venous insufficiency, and other bone disorders such as pachydermoperiostosis, secondary hypertrophic osteoarthropathy, idiopathic cortical

---

<sup>41</sup> In paleopathology, several terms are used as synonymous, such as “periostitis” or “periostosis”. In order to clarify, Ortner (2003b; 2008) suggests the use of the term periostitis only when there is certainty about the infectious agent that underlies the bone response. In cases where the aetiology is unknown, the term periostosis is the most appropriate (Ortner, 2003b, 2008).

hyperostosis, fibrous dysplasia, and Paget's disease, amongst others (Kenan et al., 1993). Table 3.5 presents and describes by location, distribution and type, some of the conditions that exhibit periostitis in their clinical and radiographic spectrum.

**Table 3.5:** List of conditions that frequently manifests new bone deposition (after Kenan et al., 1993; Burgener et al., 2006).

Disease	Preferred Locations	Distribution	Periosteal reactions	Comments
<b>Developmental periostitis</b>				
Physiological periostitis in infants	Long bones	Generalized and symmetrical	Solid thin or thick	Develops in second or third month of life, especially in premature.
<b>Periosteal reaction in infectious conditions</b>				
Acute hematogenous osteomyelitis	---	Solitary, rarely multiple	Solid thin and thick, laminated or perpendicular, Codman's triangle	After 1 week: bone destruction After 2 weeks: PRs After 3 weeks: sequestrum formation.
Chronic hematogenous osteomyelitis	---	Solitary, rarely multiple	Solid thick, often undulating and cloaking	Thick PR with sclerosis. Scattered radiolucent areas which may contain a dense bone sequestrum.
Osteomyelitis contiguous infection source	Hands, feet	Localized	Solid thin or thick	PR, bone destruction and sclerosis. Common in diabetes mellitus, quadriplegia and vascular insufficiency.
Tuberculous osteomyelitis	---	Solitary, rarely multiple	Solid thin or thick	Pronounced osteopenia. PR and osteosclerosis less common.
Congenital syphilis	Long bones	Generalized, symmetrical	Solid thick or laminated	Transverse striping of metaphyses and destructive lesions, initially involving the corners of the metaphyses.
Acquired syphilis	Long bones, skull	Localized or generalized	Solid thin or thick, often undulating and with squat spicules, or laminated	Initial stages: extensive PR and cortical thickening. Tertiary stage: dense bony sclerosis with areas of destruction (gumma formation) – hallmark.
Leprosy	Hands, feet	Solitary or multiple	Solid thin or thick, or laminated	Some bone destruction. Neuropathic bone manifestations more common.
<b>Periosteal reaction in joint conditions</b>				
Rheumatoid arthritis (juvenile)	Peripheral and axial skeleton: periarticular, tendon and ligament insertion	Localized or generalized	Solid thin or thick or laminated	Common in juvenile rheumatoid arthritis; very rare in adults, and never a dominant feature.
Psoriatic arthritis	As above (mostly hands)	Localized or generalized	Solid thin or thick or laminated	PR not uncommon. Irregular bony excrescences common.

	Reiter's Syndrome	Calcaneus, short tubular bones of foot, tibia and fibula	Localized, seldom generalized	Solid thin or thick (often "fluffy") or laminated	Periosteal reactions common.
	Polyarteritis nodosa	Long tubular bones (+ lower limbs), metatarsals	Generalized and symmetrical	Solid thin or thick, characteristically undulating	Radiological features similar to HOA.
	<b>Periosteal reaction in metabolic conditions</b>				
	Dysproteinemia	Tubular bones, mandible	Generalized and symmetrical	Solid thin or thick, or laminated	In children: bone pain and fever. Hyperphosphatemia may be present.
	Hyper-Vitaminosis A	Tubular bones (+ ulna) metatarsals, clavicle, tibia, fibula (limited to diaphyses)	Generalized	Solid, undulating or occasionally laminated	In children (1-3 y.o.): associated with tender soft masses. Prostaglandin infusions in neonates and chronic administration of retinoid drugs in older children and adolescents may produce similar bony changes.
	Rickets (healing)	Long bones	Generalized	Solid thin, thicker laminated	Calcification of the subperiosteal osteoid. Appears as an irregular dense area in the epiphyseal cartilage, separated by a thin radiolucent line from the metaphysis.
	Scurvy (healing)	Long bones	Generalized	Solid thick	Caused by ossification of the subperiosteal haemorrhage.
	Fractures and stress fractures	---	Solitary or multiple	Solid thin or thick or laminated. Codman's triangle	Periosteal reactions similar in traumatic and pathologic fractures.
	Subperiosteal haemorrhage	Long tubular bones	Solitary or multiple	Solid thin or thick or laminated. Codman's triangle occurs	Traumatic and haemophilia.
	Electrical and thermal injury	Upper extremities	Localized	Solid thin	Osteolysis, osteosclerosis, periarticular calcifications and heterotopic bone formation.
II. True neoplasms	Osteosarcoma	Femur, tibia, humerus, and mandible	Localized	Solid thin, laminated, perpendicular (thin spicules) or amorphous. Codman's triangle	Periosteal sarcoma: limited to the cortex of long bone diaphyses (especially femur and tibia). Perpendicular PR and Codman's triangle are characteristic. Parosteal sarcoma: a large radiodense lesion with smooth lobulated or irregular to the external cortex.
	Ewing's sarcoma	Under 20 y.o.: tubular bones Over 20 y.o.: flat bones	Localized	Solid thin, laminated or perpendicular (thin spicules). Codman's triangle occurs	---

III. Miscellaneous	Other sarcomas: chondrosarcoma, fibrosarcoma. Primary bone lymphoma: reticulum cell sarcoma	Long bones, flat bones	Localized	Solid thin, thick or amorphous. Rarely solid thick, laminated, perpendicular or amorphous. Codman's triangle is unusual	PRs are rare in these conditions. Cortical thickening in a chondroid matrix tumor suggests low-grade chondrosarcoma rather than enchondroma.
	Leukemia and metastases	Long bones, ribs	Multiple	Solid thin or laminated. Perpendicular in skull. Rarely solid thick	Interrupted PRs are common in children (e.g. leukemia and metastases from neuroblastomas). Solid PR or localized cortical thickening is associated with metastases from prostatic and breast carcinomas.
	Osteoid osteoma	Femur, tibia, fibula, humerus, vertebral arch	Localized	Elliptical and dense. Rarely solid thin	Radiolucent intracortical with and without central calcification is classic, but not always demonstrated.
	Other benign tumors and cysts	---	Localized	Solid thin or thick	PR usually associated with bone expansions and/or pathological fractures.
	Bone infarct	Long tubular bones	Solitary or multiple	Solid thin or thick	In sickle cell disease PR may be caused by osteomyelitis. Hand-foot syndrome: infarctions of the short tubular bone causing PR that is indistinguishable from osteomyelitis. Occurs in young children (average age 18 months).
	DISH (diffuse idiopathic skeletal hyperostosis)	Spine, pelvis, lower extremity (commonly patella and calcaneus)	Multiple and often symmetrical	Solid thick	Particularly at tendon and ligament insertions ("whiskering").
	Eosinophilic granuloma (Langerhans cell histiocytosis)	---	Solitary or multiple	Solid thin or thick. Rarely laminated	Destructive bone lesions may contain bone sequestrum.
	Fluorosis	Tubular bones	Generalized and symmetrical	Solid thick, often undulating and cloaking	Osteosclerosis and ossification of ligaments and tendons at their insertion.
	Infantile cortical hyperostosis (Caffey's disease)	Mandible, clavicle, scapula, ribs, tubular bones (diaphyses)	Solitary or multiple	Solid thick or laminated	Clinically tender soft-tissue swellings are associated with the affected bone. Onset occurs in the first five months of life.
	Primary hypertrophic osteoarthropathy (HOA)	Long tubular bones: (+) radius, ulna, tibia and fibula. (-) innominate, ribs and clavicles	Generalized and symmetrical. From diaphyses into metaphyses and epiphyses	Solid thick, often with shaggy, irregular excrescence	Familiar condition with skin and cortical thickening. PNBf tends to blend with thickened cortex. Almost exclusively found in males. Onset in adolescence.

Secondary hypertrophic osteoarthropathy (HOA)	Diaphyses of tubular bones	Generalized and symmetrical	Solid thin or thick (often undulating and cloaking) or laminated	In patients with bronchogenic carcinoma, and occasionally with chronic diseases of lung, gastrointestinal tract, or cardiovascular system.
Renal osteodystrophy	Long tubular bones, metatarsal, pubic rami	Generalized and symmetrical	Solid thin and thick, occasionally laminated	Associated with hyperparathyroidism and osteosclerosis. Very rare in primary hyperparathyroidism.
Tuberous sclerosis	Tubular bones	Solitary or multiple	Solid thin or thick, often undulating	---
Vascular and lymphatic disease	Lower extremity	Localized or generalized	Solid thin or thick, often undulating	Any disease associated with venous and /or lymphatic stasis. Vascular calcifications and phleboliths may be associated.

It should be stated that the type and extension of the periosteal reactions depend not only on the nature of the stimuli, but also on a combination of factors that comprise the biological activity of the underlying process, the patient age and metabolic state, and the anatomical location (Kenan et al., 1993). For instance, only bones that are covered with periosteum can show PNBFs (Vigorita, 2008). Additionally, and since the periosteum ends at the perichondral ring, the deposition of new bone is only observed several millimetres short of the bone growth plate (Vigorita, 2008). Recent studies on rabbits have shown that the chondrogenic potential of periosteum varies, not only in different skeletal elements but also along the same bone (Vigorita, 2008). As an example, the chondrogenic potential of periosteum is higher in the ilium, followed by the scapula and tibia (Gallay et al., 1994). In the tibia, the upper portion is more chondrogenic than the lower part (Gallay et al., 1994). Other factors to consider include the intensity, aggressiveness and duration of the underlying insult or stimuli (Rana et al., 2009; Nogueira-Barbosa et al. 2010), as well as the patient response (Edeiken et al. 1966). According to Rana et al. (2009), processes that induce a rapid synthesis of woven bone over a short period of time produce more aggressive periosteal reaction. In contrast, conditions with a slow and less intense progression tend to develop periosteal reactions with a nonaggressive appearance. It is important to note that the appearance of the new bone may not be directly related to the malignancy of the condition. Burgener et al. (2006) note that a thin layer of new bone may signify an early stage of an aggressive lesion, or a chronic, benign process; whereas a thicker periosteal reaction usually suggests a benign condition. The individual's skeleton may also behave differently in relation to the same

pathology, with the bone response ranging from minor periosteal deposits to more aggressive and thicker reactions (Edeiken et al. 1966).

Focusing on the role of age, Kenan and co-authors (1993) and Vigorita (2008) state that periosteal lesions are more frequent in children, especially following fracture or infection (e.g. congenital syphilis) due to the nature of their periosteum (very thick, active and loosely attached to the cortical bone). In contrast, the less active and tightly attached periosteum of adults is responsible for a lower bone response (Wenaden et al., 2005; Rana et al., 2009). The relationship between age and the chondrogenic potential of periosteum has been extensively studied and tested in non-human (e.g. Gallay et al., 1994; O'Driscoll et al., 2001) and human bones (e.g. De Bari et al., 2001).

### 3.2.1.3. Classification and Types

PNBFs are diagnosed in the clinic through the application of radiographic techniques, such as conventional radiology, magnetic resonance imaging (MRI) and CT scan. However, this identification is only possible after mineralization of the new bone, a process that normally takes two to three weeks to occur after injury (Kenan et al., 1993; Wenaden et al., 2005; Burgener et al., 2006).

In the medical literature, PNBFs are classified according to their location and morphology. Regarding the tissue location, Kenan and co-authors (1993) considers three anatomical layers in the study of new bone formation: the cortical bone, the periosteum and the adjacent soft tissues. Accordingly, PNBFs may be grouped as:

- i. **Juxtacortical:** a broad concept applied to surface lesions of extracortical origin. It is used to classify those bony changes whose exact anatomical relation to the periosteum is unknown;
- ii. **Cortical:** describe those lesions that may break through the cortex, affecting the subperiosteal space (e.g. osteofibrous dysplasia, osteoid osteoma, intracortical osteosarcoma, or cortical metastatic carcinoma);
- iii. **Subperiosteal:** describes the processes that separate the periosteum from the cortex, resulting in subperiosteal bone formation. This type of new bone formation is observed in post-traumatic reparative processes, such as subperiosteal hematoma or abscess;
- iv. **Periosteal:** defines the processes that have their origin in the deep layer of the periosteum. These lesions, very common in tumours, are firmly attached to the cortex, showing no cleavage line between the two tissues. In slow growing tumors, the



periosteum is pushed away from the cortex, producing a peripheral wedge-shaped bony reaction (or buttress) (e.g. periosteal chondroma). In aggressive lesions, the periosteal reaction is lamellated (Codman's triangle). The presence of parallel and spiculated reaction (sunburst) indicates a rapid and aggressive process (e.g. periosteal osteosarcoma);

- v. **Parosteal:** describes the processes that originate from the outer fibrous layer of the periosteum (e.g. parosteal osteosarcoma). These lesions do not elevate the cambium layer and are separated from the cortex by a thin radiolucent periosteal membrane. Absence of peripheral periosteal reaction;
- vi. **Parosseous:** defines the processes that have their origin outside the periosteum. Separating the pathological mass from the adjacent cortex and periosteum, a cleavage plane of soft tissue is observed (e.g. myositis ossificans, soft tissue chondroma, and giant cell tumour).

Periosteal reactions can also be classified according to their morphology (Table 3.5). Different nomenclatures have been used in the clinical literature to describe the morphology of PRs, such as continuous versus interrupted forms, single versus multiple layers, and aggressive versus nonaggressive subtypes (Rana et al. 2009). For instance, Edeiken et al. (1966), de Santos (1980) and Burgener et al. (2006) classify periosteal abnormalities into two categories: solid (also termed continuous or uninterrupted) and interrupted reactions, which are then divided into subcategories. The solid type occurs classically in slow and indolent processes and includes four subcategories: thin and dense undulating periosteal reaction; dense, elliptic periosteal reaction; periosteal cloaking; and Codman triangle (Edeiken et al. 1966). The interrupted form is divided into three subcategories: lamellated periosteal reactions; perpendicular periosteal reactions (sunburst); and amorphous periosteal reactions (Edeiken et al. 1966; Burgener et al., 2006), and normally suggests the presence of a more aggressive process (Nogueira-Barbosa et al. 2010).

Highlighting the role of magnetic resonance (MR) imaging in the study of bone lesions, Greenfield and co-authors (1991) presented a simple classificatory system for PNBf composed of four types: solid, laminated, spiculated and Codman triangle (Figure 3.10). With small adaptations, this system has been replicated by other authors such as Wenaden et al. (2005), Rana et al. (2009), and Nogueira-Barbosa et al. (2010), and will be described in more detail in this thesis.

The solid periosteal reactions (Figure 3.10 B) are described as a nonaggressive form primarily observed in slow and benign processes (Rana et al., 2009). Nevertheless, they can also emerge in malignant conditions (Wenaden et al., 2005). A periosteal reaction appears as a well-defined line of periosteal density that forms after mineralization of the new bone produced by the cambium layer of the periosteum (de Santos, 1980). Morphologically, it may be thin (1mm or less) or thick (2mm or more), of any degree of density, straight or undulating (Edeiken et al. 1966; Greenfield et al., 1991; Burgener et al., 2006; Haun et al., 2006). The thin form is observed in both benign and malignant lesions. The thick periosteal reaction (more than 1 mm) is normally associated with benign conditions (Greenfield et al., 1991). De Santos (1980: 72) states that a «(...) homogeneous, usually thick (although not necessarily), occasionally granular, and variable in length (...)» is the pattern classically seen in infectious processes (e.g. hypertrophic osteoarthropathy, osteomyelitis, haemorrhage, vascular diseases), benign tumors (e.g. osteoid osteoma, osteoblastoma, eosinophilic granuloma, among others), and healing fractures. Despite some variations, PNBf with a uniform density and solid appearance that remains relatively unchanged for weeks is normally considered “the hallmark of benign process” (Edeiken et al. 1966: 710; Wenaden et al., 2005). This relationship has been proven through histological analysis. In a sample composed of 78 lesions with solid periosteal reactions, Wenaden et al. (2005) established a positive diagnosis in 15 (19.2%) with osteoid osteoma, and in 10 (12.8%) with osteomyelitis.

In laminated bone (Figure 3.10 E), a variable pattern composed of one single layer (linear-simple) or multilamellae may be observed (Edeiken et al., 1966; Wenaden et al., 2005; Nogueira-Barbosa et al. 2010):

- i. In the linear-simple type, a thin layer of new bone is formed in the space adjacent to the cortex (Wenaden et al., 2005). Morphologically, it appears as a well-defined, uniformly dense line of radiodensity (Wenaden et al., 2005). Despite being commonly observed in benign conditions, such as physiological periosteal reactions, early fracture healing and osteomyelitis, it is also present in malignant diseases (Wenaden et al., 2005). Apart from Ewing’s sarcoma, the single layer PR was histologically diagnosed in 23.6% (13/55) of individuals with osteosarcoma (Wenaden et al., 2005).
- ii. In the multilamellae type, numerous parallel layers of new bone are deposited concentrically around the cortex, originating from an “onionskin like” periosteal reaction (Wenaden et al., 2005; Rana et al., 2009; Nogueira-Barbosa et al., 2010). The layers of mineralized PNBf are normally separated by vascular dilations and loose connective

tissue. When associated with malignant tumours, these spaces may be filled or infiltrated by malignant cells (Nogueira-Barbosa et al., 2010). Multilamellae bone has been interpreted as the result of an intermittent or cyclic process that combines periods of rapid (no new bone is formed) and slow growth (a layer of bone similar to the involucrum of the infection is produced by the periosteum), as a result of the lifting of the periosteum by a tumour, pus or blood accumulation (Edeiken et al., 1966; Greenfield et al., 1991; Wenaden et al., 2005). This hypothesis is not supported by recent findings that show a space between layers free of tumour and normally filled by connective tissue and vessels (Wenaden et al., 2005). Other studies point out that the modulation of sheets of fibroblasts from the parosteal soft tissues, or the stimulation of the inner cambium layer may increase the osteoblastic potential leading to the formation of successive layers of new bone (Wenaden et al., 2005; Rana et al., 2009).

Despite the evidence it is accepted that a number of different mechanisms may induce the development of this type of PR (Wenaden et al., 2005). In general, laminated periosteal reactions are found in both benign (e.g. osteomyelitis, aneurysmal bone cyst) and malignant conditions (e.g. Ewing sarcoma, osteosarcoma, and chondroblastoma) (Wenaden et al., 2005; Rana et al., 2009; Nogueira-Barbosa et al., 2010).

Spiculated periosteal reaction is observed in rapid and aggressive conditions, most often in primary malignant bone tumours (Haun et al., 2006), being characterized by fine spicules of new bone that project from the underlying cortex (De Santos, 1980; Wenaden et al., 2005; Rana et al., 2009; Nogueira-Barbosa et al., 2010). Spicules are not neoplastic, originating from the ossification along periosteal vascular channels and fibrous bands (Sharpey fibers) which are stretched away from the cortex (Edeiken et al., 1966; Wenaden et al., 2005; Nogueira-Barbosa et al., 2010). A disruption of the reparative process that follows periosteal elevation is identified as the major cause (Greenfield et al., 1991). Depending on the size and orientation of the spicules, three subtypes may be identified: hair-on-end and sunburst pattern (Greenfield et al., 1991; Wenaden et al., 2005; Rana et al., 2009); velvet; and disorganised pattern (Wenaden et al., 2005).

- i. In the hair-on-end pattern (Figure 3.10 F), parallel bone spicules are projected perpendicularly from the cortex (Greenfield et al., 1991; Wenaden et al., 2005; Rana et al., 2009). These spicules develop along radially oriented blood vessels that emerge from the cortex in a honeycomb structure (Wenaden et al., 2005: 450). In some cases, the

space between spicules may be filled by tumour or other tissues (Nogueira-Barbosa et al., 2010). The spicules tend to be long and thin in the centre of the lesions, decreasing in height in the extremities (Wenaden et al., 2005). This type of PR is frequently observed in the aggressive forms of osteosarcoma and Ewing's sarcoma (86%, 6/7) (Wenaden et al., 2005). Some infections and healing fractures may also stimulate a hair-on-end PR pattern (Wenaden et al., 2005);

- ii. The sunburst subtype (Figure 3.10 G) is characterized by the development of spicules with a divergent orientation (Wenaden et al., 2005; Rana et al., 2009) that extends into an epicentre in the bone tissue (Nogueira-Barbosa et al., 2010). No perpendicular spicules are observed (Rana et al., 2009). This type of PR is normally perceived as a sign of malignancy (Nogueira-Barbosa et al., 2010). In fact, Wenaden et al. (2005) reported a high number of cases in osteosarcoma. Moreover, it can also be observed in haemangiomas and aggressive osteoblastic metastases, especially in those secondary to prostatic and bronchus cancer, and in advanced retinoblastoma (Lehrer et al., 1970; Wenaden et al., 2005). Less common is their occurrence in stress episodes or trauma;
- iii. Sloping or velvet periosteal reaction is composed of short and focal gently sloping spicules that give the lesion a smooth or "velvet" appearance (Wenaden et al., 2005);
- iv. The disorganized or complex periosteal reaction is formed by randomly distributed spicules that lead to a bizarre and disorganized appearance (Wenaden et al., 2005). It is associated with the acceleration of tumour growth, especially when malignant tumours originate from benign ones (Wenaden et al., 2005). The authors report a high number of cases associated with osteosarcoma (22.8%, 21/92); metastasis (15.2%, 14/92); and osteomyelitis (12%, 11/92).

The Codman's triangle PR (Figure 3.10 I) was firstly described by the surgeon Ernest Amory Codman (1869-1940, USA) and refers to a triangular-shaped elevation that develops away from the cortex in response to osseous destruction (Hwang and Schneider, 2010). It indicates an aggressive process in which bone resorption occurs faster than the capacity of the periosteum to regenerate it (De Santos et al., 1980). According to Nogueira-Barbosa et al. (2010), Codman's triangle PR is the interrupted version of the single or multiple layer lamellated bone. It probably results from anything that lifts the periosteum, such as the accumulation of pus, blood or a neoplastic lesion (Edeiken et al. 1966; Wenaden et al., 2005). Codman's triangle is frequently recorded in malignant tumours, namely osteosarcoma (56%,

48/85) and Ewing's sarcoma (14%, 12/85) (Wenaden et al., 2005). Nevertheless, it is also observed in benign conditions, such as osteomyelitis, subperiosteal haemorrhage, and fractures (Burgener et al., 2006).

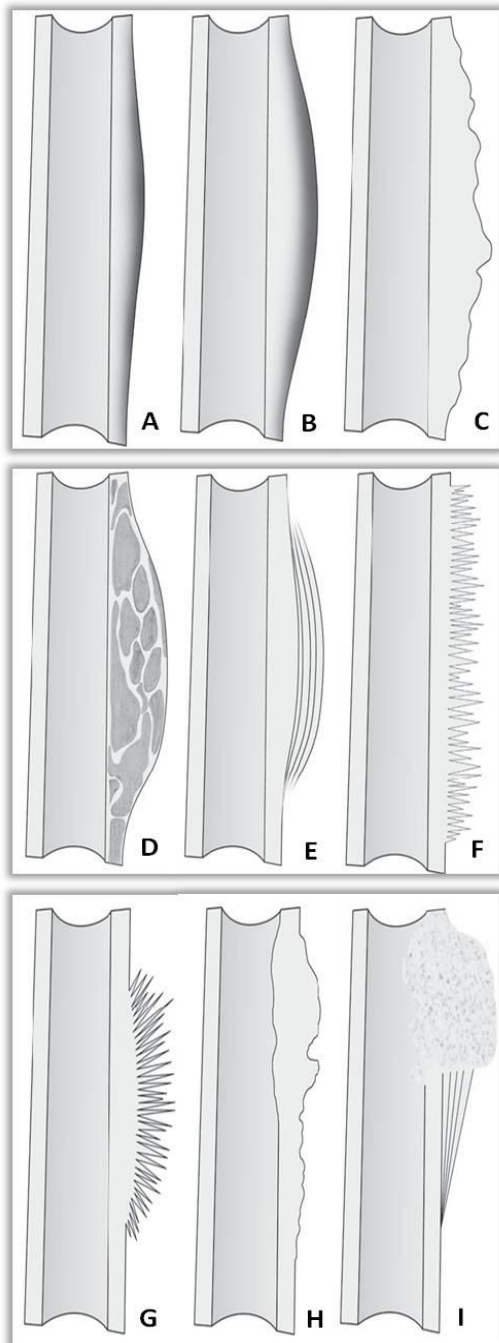


**Figure 3.10:** The various types of periosteal new bone formations. **(A)** Thin; **(B)** Solid; **(C)** Thick irregular; **(D)** Septated; **(E)** laminated (onionskin); **(F)** perpendicular (hair-on-end); **(G)** sunburst; **(H)** disorganized; **(I)** Codman triangle (adapted from Rana et al., 2009: w260).

## 3.2.2. PNB in the Paleopathological Literature

### 3.2.2.1. Macroscopic and Histological Manifestations

Periosteal new bone formation is a common occurrence in human skeletal remains from archaeological contexts (Ortner, 2008; Weston, 2008). It may affect individuals of both sexes and distinct age groups (Larsen, 1997). As for the clinics, several options must be considered in their differential diagnosis such as focal and systemic infections, trauma and tumours (Ortner, 2008). However, in the paleopathological literature there is some misunderstanding concerning its aetiology, since it is frequently associated with infectious conditions. In fact, many paleopathological studies consider PNB as an important index of health for past populations (e.g. Bennike et al., 2005; Buzon, 2006; DeWitte, 2010). Regarding this issue, Ortner (2003d: 209) advises that: «[a]lthough it is highly probable that the most common cause of periostitis is infection, we simply do not have a good basis for estimating what percentage of the cases in an archaeological skeletal sample is due to infection», which reinforces the need for a deep understanding of the nature of the PR.

In periosteal reactions two types of new bone can be observed. In acute conditions the new bone formed is the woven type (Ortner, 2008). Macroscopically, the woven bone shows a porous appearance increased by the proliferation of vascular channels, similar to froth (Ortner, 2003b and 2008). The presence of woven bone is normally indicative of an active condition at the time of the death (Roberts and Manchester, 2005; Ortner, 2008). In chronic conditions, woven bone tends to be remodelled into lamellar or compact bone, which is a stronger type of tissue (Ortner, 2008). Chronic conditions may also stimulate the formation of compact bone (Ortner, 2008). This type of bone is denser and less porous and may indicate a condition that was quiescent or overcome at the time of death (Roberts and Manchester, 2005). It should be pointed out that a chronic condition may have several episodes of acute new bone formation (Ortner, 2008). As observed in the radiographic characterization, PNB may also assume distinct patterns (Table 3.6) that range from solid layers of lamellar bone added directly to the cortical surface to fine spicules connecting a fairly solid layer of woven or lamellar bone (Aufderheide and Rodríguez-Martín, 1998; Ortner, 2008). Other manifestations include fine pitting, porosity, longitudinal striation and plaque-like new bone formation (Roberts and Manchester, 2005; Ortner, 2003b). In numerous conditions (e.g. tuberculosis, osteomyelitis and some carcinomas) PNBs develop in association with erosive lesions that may assume different configurations and sizes. These erosive lesions result from the abnormal interplay between osteoblasts and osteoclasts. Ortner (2003b: 50) identifies four common

manifestations/types: 1) an abnormal increase in osteoclast activity with normal osteoblast activity; 2) an abnormal decrease in osteoblast activity with normal osteoclast function; 3) a combination of increased osteoclast activity and decreased osteoblast activity; and 4) normal osteoclast and osteoblast function but an inability to mineralize the matrix. A summary of the most common types is described in the Table 3.6.

**Table 3.6:** Different types of abnormal bone formation and resorption.

<b>Macroscopic abnormal bone formation (after Ortner, 2003b: 50)</b>	
<b>Lesions composed of woven bone (fiberbone)</b>	General woven bone (no clear pattern of pores or striations, often transitional to compact bone)
	Porous bone
	Striated bone
	Spiculated bone
<b>Lesions composed of lamellar bone</b>	Smooth compact bone (lesions other than plaque, e.g. osteoma)
	Porous compact bone
	Striated compact bone
	Spiculated compact bone
	Plaque (relatively flat, thin areas of smooth compact bone on a normal bone surface)
<b>Lesions composed of spongy bone</b>	Enlargement of the diploë
<b>Radiographic abnormal bone resorption (after O'Donnell, 2003: 300-302)</b>	
<b>Geographic</b>	Bone destruction is confined to one area, within which all the bone tissue is destroyed. The lesion has a well-defined margin separating it from the surrounding normal bone. The sclerotic border that surrounds the lesions may have various thicknesses. This pattern may be found in infections, particularly granulomatous and benign tumours. Multiple myeloma and metastases may also show similar lesions.
<b>Moth-eaten</b>	Represent a poorly demarcated focus of bone destruction with a long zone of transition between normal and abnormal bone, which indicates its aggressiveness and rapid growth potential. It is frequently observed in malignant bone tumors, osteomyelitis and eosinophilic granuloma.
<b>Permeative</b>	Aggressive bone destruction with rapid growth. The lesion tends to merge almost imperceptibly with the normal bone. It is observed in highly malignant tumours infiltrating the bone marrow (e.g. Ewing's sarcoma and lymphomas). Other conditions include acute osteomyelitis and rapidly developing osteoporosis.
<b>No margin or clear border</b>	The distinction between normal and destroyed bone is ill-defined or well-demarcated, with a wide zone of transition. Radiographically, this pattern is associated with the process of rapid growth.
<b>Clear border but no repair (no sclerosis)</b>	The interface between normal and abnormal bone is sharply defined, but the new bone formed in response to the lesion is destroyed before it becomes radiographically visible.
<b>Clear border but evidence of repair (sclerosis)</b>	The host bone responds to a focal lesion through new bone formation. In this case there is a sharply defined interface between normal and abnormal bone with a well-defined transition zone.

PNBFs may occur as an isolated finding, affecting only a single element, or present a broader distribution. In both cases, the lesions may be localized to a particular bone segment or show a more diffuse distribution affecting a large portion of the shaft. The dispersion of lesions is sometimes interpreted as the result of a longstanding condition (Gall et al., 1951). Lesions with a symmetric and bilateral distribution can also be encountered (e.g. syphilis, hypertrophic osteoarthropathy). The same can be said for those with a randomly distributed pattern. Normally, the presence of PNBF in different bones may suggest a systemic condition (e.g. syphilis, leprosy, tumours). On the contrary, isolated occurrences are usually found in non-specific conditions, such as osteomyelitis, or in trauma and leg ulcers. The tibial diaphysis is the most common site of periosteal reactions in archaeological material (Aufderheide and Rodríguez-Martín, 1998; Ortner, 2003d). A complete explanation for this phenomenon has not yet been achieved; however several hypotheses have been advanced over time. One of the most commonly accepted relates PNBF to the fact that the tibia, especially its anterior surface, is closest to the skin surface and thus more exposed to blunt trauma than those bones enclosed in a heavy mass of muscles (Ortner, 2003d; Roberts and Manchester, 2005). In most cases, PNBF is not a disease by itself but part of a disease syndrome as in syphilis. In these cases, periosteal reactions are a secondary response to a specific disease process. Primary new bone formation is most commonly found in trauma (e.g. fracture and calcified haematomas) and in cases of primary infection of the periosteum (Ortner, 2003d).

According to Schultz (2001 and 2003), at the microscopic level different types of new bone formations may also be observed in response to the type of pathological stimuli (Table 3.7). In spite of the abnormalities depicted in Table 3.7, the author notes that PNBFs of hemorrhagic and circulatory origin do not normally affect the underlying cortical bone. On the contrary, an involvement of the cortex and of the deep structures of bone is seen in inflammatory and tumour lesions (Schultz, 2001 and 2003).



**Table 3.7:** Different types of new bone abnormalities observed at microscopic level (after Schultz, 2001 and 2003: 84).

<b>Histologic abnormal bone formation</b>	
<b>External periosteal reactions of the long bones and skull</b>	<b>Hemorrhagic origin</b> (e.g. subperiosteal haematoma or scurvy) <ul style="list-style-type: none"> <li>• Thin layer of new bone with a splitlike appearance (observed on the periphery of large lesions or in less severe cases)</li> <li>• Short, bulky trabeculae showing extensive bridging and, more rarely, deposition of several layers of new bone (observed in the centre of large lesions)</li> </ul>
	<b>Inflammatory origin</b> (e.g. nonspecific and specific PNBf) <ul style="list-style-type: none"> <li>• Thin layer of new bone with a splitlike appearance (observed on the periphery of large lesions or in less severe cases)</li> <li>• Relatively long and thin bone trabeculae that are irregularly oriented in parallel order. In some cases, several layers may develop with extensive bridging (observed in the centre of large lesions)</li> </ul>
	<b>Tumour origin</b> <ul style="list-style-type: none"> <li>• Similar to the inflammatory changes, however, the trabeculae present a more regular development</li> </ul>
	<b>Circulatory origin</b> (e.g. HOA) <ul style="list-style-type: none"> <li>• Presence of thick secondary layers of new bone over the original cortical surface. In some cases, short and bulky trabeculae may also be observed</li> </ul>

In the Table 3.8, a set of pathological conditions manifesting new bone formation will be reviewed and summarized. Since the record is extensive, only those disorders most frequently encountered in the archaeological remains, and that match with the skeletal sample under analysis (see Chapter 4) will be outlined. The paleopathological description will be complemented by paleohistopathological data.

In the Chapter 4, it will be presented and discussed the methods used to investigate the macroscopic and microscopic characteristics of the periosteal new bone formation among the skeletal samples considered.

**Table 3.8:** List of paleopathological conditions that frequently manifests new bone deposition.

<b>Paleopathological conditions</b>	
<b>Tuberculosis (TB)</b>	<b>Gross morphology</b> <sup>a, b, c, d</sup>
	<b>TB of the vertebral column:</b> <ul style="list-style-type: none"> <li>• Abscess formation;</li> <li>• Prevalence of bone destruction over bone formation;</li> <li>• Anterior portion of the vertebral bodies more affected than the spinous and transverse processes;</li> <li>• Minimal bone regeneration;</li> <li>• Sclerosis of the trabeculae that surround the tubercular abscess;</li> <li>• Collapse of one or more vertebrae: Pott's deformity.</li> </ul>
	<b>TB of the joints:</b> <ul style="list-style-type: none"> <li>• Lesions localized or diffuse and regularly symmetrical;</li> <li>• Osteopenia;</li> <li>• Marginal bone erosion and destruction of the subchondral bone;</li> <li>• Massive joint destruction, subluxation and ankylosis (severe cases);</li> <li>• Diaphyseal extension of the abscess;</li> <li>• Sequestration is infrequent and when present is smaller;</li> <li>• Presence of periosteal reactions.</li> </ul>
	<b>TB dactylitis:</b> <ul style="list-style-type: none"> <li>• Thickening of the periosteum of the metacarpals and phalanges, generating a fusiform appearance;</li> <li>• Destruction of the growth plate can induce bone shortening.</li> </ul>
	<b>Rib lesions:</b> <ul style="list-style-type: none"> <li>• Erosive lesions (head of the ribs);</li> <li>• New bone deposition (woven, lamellar or both) along the body of the rib.</li> </ul>
	<b>Paleohistopathological changes</b> <sup>e, f</sup>
<b>Congenital syphilis</b>	<b>Long bones PNBFs:</b> <ul style="list-style-type: none"> <li>• Slight periosteal changes on the external surface of long bones;</li> <li>• Mild osteoclast resorption revealed by the presence of Howship's lacunae.</li> </ul>
	<b>Rib Lesions:</b> <ul style="list-style-type: none"> <li>• Active deposition of new bone around a network of vascular grooves. These grooves exhibit different stages of enclosure;</li> <li>• Presence of superimposed layers of new bone;</li> <li>• Evidences of osteoblastic and osteoclastic (Howships lacunae) activity.</li> </ul>
	<b>Gross bone changes</b> <sup>a, b, d</sup>
	<b>Early osseous changes</b> (from birth to very young infants) <b>Skull</b> <ul style="list-style-type: none"> <li>• <b>Necrotizing osteitis and hypertrophic periostitis</b></li> </ul>
	<b>Long bones</b> <ul style="list-style-type: none"> <li>• <b>Syphilitic osteochondritis (also known as metaphysitis):</b> symmetrical involvement of the sites of endochondral ossification (e.g. epiphyseal-metaphyseal junction of the tubular bones, the costochondral region, the short and flat tubular bones, and the centres of ossification of the sternum and vertebrae) causing widening of the provisional calcification zone, serration, and adjacent osseous irregularities, especially in the growing metaphyses (saw-toothed metaphysis). In severe cases, irregular erosive lesions develop along the contours of the growth plates, with possible displacement of the epiphyses. The bones more affected are the tibia, followed by the ulna, radius, femur, humerus, and fibula.</li> <li>• <b>Diaphyseal osteomyelitis (osteitis):</b> granulation tissue may extend from the metaphysis into the diaphysis. Presence of osteolytic lesions overlying periostitis.</li> <li>• <b>Periostitis:</b> less frequent than the above conditions, however it can be observed in the long bones. It represents a reactive and reparative process characterized by the deposition of one or more layers of new bone over the affected region. This may be gradually converted into lamellar bone, leading to an increase in cortical thickening. The massive periosteal reaction is called "periosteal cloaking".</li> </ul>
	<b>Late osseous changes</b> (from infancy to adulthood - 5-20 y.o.) <b>Skull</b> <ul style="list-style-type: none"> <li>• <b>Destruction of the nasal bones ("saddle nose"), calvarial gumma, and Hutchinson's teeth</b></li> </ul>

	<p><b>Long bones</b></p> <ul style="list-style-type: none"> <li>• <b>Hyperplastic osteoperiostitis:</b> affects primarily the diaphysis of the long bones, rather than the metaphyses. Marked subperiosteal new bone production that is laid down parallel to the cortex and tends to remain separate from it. On the tibia, the new bone is deposited on the anterior surface (shin) of the shaft, creating a typical bending called “saber shin”. The thickening produced is usually fusiform, creating an enlarged, undulating and dense osseous contour that involves the middle third of the diaphyses. Endosteal bone proliferation with subsequent narrowing of the medullary cavity can also be observed. The original cortex may maintain its normal appearance or be affected by gummatous osteomyelitis.</li> <li>• <b>Gummatous osteomyelitis:</b> chronic and diffuse condition that produces dense and irregular trabeculae. Destructive foci are normally localized at the sites of gummata. Sequestrum and sinus formation are rarely seen. The tibia is the most frequently affected bone.</li> </ul>
Acquired syphilis	<p style="text-align: center;"><b>Gross bone changes<sup>a, b, d</sup></b></p> <p><b>Late stages of acquired syphilis</b></p> <p><b>Skull</b></p> <ul style="list-style-type: none"> <li>• <b>Cranial vault gumma:</b> starts almost invariably on the external surface of calvarium, especially in the frontal bone. It is characterized by multiple, scattered areas of destruction that may coalesce. Two processes are involved: bone destruction that can reach the diploë, forming cranial depressions; and bone remodelling that occurs around the eroded areas. After the complete resorption, a stellate lesion called “caries sicca” is left. Lesions may also affect the endocranial surface.</li> </ul> <p><b>Long bones</b></p> <ul style="list-style-type: none"> <li>• <b>Proliferative periostitis:</b> it is the most frequent bone lesion, especially in the tibia, skull, ribs, and sternum. Other bones can also be affected such as the clavicle, femur, fibula, and osseous structures of the hand and foot. It is characterized by subperiosteal new bone formation that starts at the metaphyseal portion of the long bones. The subperiosteal involvement may be limited to a part of the shaft (e.g. medial third of the clavicle or distal portion of the tibia) or diffuse, leading to an increased thickening and even deformation of the bones. The new bone deposited is not connected with the cortex, but with the progression of the condition it starts to merge with the underlying cortex.</li> <li>• <b>Osteitis and osteoperiostitis:</b> occurs when the infection extends from the periosteum to the underlying bone tissue. The major bone changes observed are: increased thickening with subsequent narrowing of the medullary cavity, especially in the tibia and femur; bone destruction in the form of pitting, namely on the surface of the skull and long bones; and a mixture of reactive and irregular new bone with destructive granulation produced by gummata.</li> <li>• <b>Formation of gummatous bone lesions:</b> the formation of gummata normally begins in the metaphyseal portion of long bones, constituting a mixture of necrotizing tissue with the toxic products of the treponema degeneration. Gummata are normally small, but may coalesce to form large masses that fill the medullary cavity. Despite the destruction generated by gummata, the surrounding necrotic cavity may exhibit some bone sclerosis. Osteophytic overgrowths may be formed as a result of the soft tissue gummata.</li> </ul> <p style="text-align: center;"><b>Paleohistopathological changes<sup>f, g</sup></b></p> <p><b>Venereal syphilis:</b></p> <ul style="list-style-type: none"> <li>• Presence of polsters: pillow-like newly built bone formations;</li> <li>• Presence of grenzstreifen: a very fine or a narrow, band-like structure that represents the original external surface of the bone shaft;</li> <li>• Presence of sinuous lacunae: similar to a resorption lacuna it is found between the cortical bone and the pathological periosteal deposition.</li> </ul>
	Leprosy

<b>Osteomyelitis</b>	<p><b>Primary and secondary bone involvement (tibia and fibula)</b></p> <ul style="list-style-type: none"> <li>• Irregular deposits of subperiosteal new bone: distal third of the tibia and fibula on adjacent surfaces;</li> <li>• The tibia is more affected than the fibula;</li> <li>• Prominent transverse striation and vascular grooves may cross the PNBf.</li> </ul>
	<p style="text-align: center;"><b>Paleohistopathological changes<sup>f</sup></b></p> <ul style="list-style-type: none"> <li>• Presence of grenzstreifen;</li> <li>• Presence of several layers of new bone deposition at the same place.</li> </ul>
	<p style="text-align: center;"><b>Gross bone changes<sup>a, b, c, d</sup></b></p> <p><b>Less severe cases:</b></p> <ul style="list-style-type: none"> <li>• New bone deposition limited to the metaphyseal area.</li> </ul> <p><b>Most severe cases:</b></p> <ul style="list-style-type: none"> <li>• Massive bone apposition along the bone surface forming an involucrum. This bony shell may have a lamellated appearance resembling Ewing's sarcoma or a bulky and very irregular outline;</li> <li>• Several cloacae perforating the involucrum may also be present;</li> <li>• Even in well-healed cases the bone exhibits irregularities characterized by different degrees of sclerosis and sharply defined cavities with lack of bone matrix.</li> </ul> <p><b>Following a compound fractures:</b></p> <ul style="list-style-type: none"> <li>• Sequestration due to infection or to the splintering of bone;</li> <li>• Involucrum and cloacae formation, as well as improper union of the broken ends.</li> </ul>
<b>Hypertrophic osteoarthropathy (HOA)</b>	<p style="text-align: center;"><b>Paleohistopathology changes<sup>h</sup></b></p> <ul style="list-style-type: none"> <li>• Extensive osteolytic bone loss and enormous osteoblastic bone reaction, a response to the rapid growth of the condition;</li> <li>• Presence of small foci of decayed bone matrix located within the region of the former original compact bone or in the area of the secondarily filled medullary cavity;</li> <li>• Osteolytic focus containing necrotic material;</li> <li>• Grenzstreifen and sinuous lacunae may be present;</li> <li>• Various layers of new bone may formed in the same place (similar to leprosy);</li> <li>• Presence of a clear line of separation between the periosteal new bone and the underlying cortical tissue;</li> <li>• Evidence of osteoclastic resorption previous to new bone deposition.</li> </ul>
	<p style="text-align: center;"><b>Gross bone changes<sup>b, c, d, i, j, k, l</sup></b></p> <ul style="list-style-type: none"> <li>• PNBf presents "a dense and lumpy" appearance with a multi layered laminated structure, being normally symmetrical;</li> <li>• New bone separated from the underlying cortex by a thin and fibrous layer;</li> <li>• The general appearance may range from a laminated or "onion-skin" shape, with smooth relief, to dense and irregular areas showing wavy contours;</li> <li>• New bone deposition occurs normally at both the ends and shafts of long and short tubular bones;</li> <li>• Absence of cortical involvement;</li> <li>• Skull, scapulae, patellae, ribs, and pubic and iliac bones are the bone elements less affected.</li> </ul>
	<p style="text-align: center;"><b>Paleohistopathology changes<sup>m</sup></b></p> <ul style="list-style-type: none"> <li>• Hypertrophic bone apposition with an irregular and scalloped border and constructed with fibrous layers;</li> <li>• A relatively clear demarcation between the newly formed bone and the original cortex;</li> <li>• New bone layers with a disorganized and woven nature;</li> <li>• Areas of bone resorption with widening of the Haversian canals indicating a chronic condition.</li> </ul>
<b>Skin ulcer</b>	<p style="text-align: center;"><b>Gross bone changes<sup>c, n</sup></b></p> <ul style="list-style-type: none"> <li>• Lesions are most frequently observed on the anterior and medial surface of the tibial diaphysis;</li> <li>• The margins of the lesions are frequently sharply demarcated with plaque-like deposition of periosteal bone of considerable thickness, roughly copying the outline of the ulcer. Lytic lesions may also be present;</li> <li>• Cortical thickening with thickened bark-like bone formation affecting a portion or all of the diaphysis may also develop;</li> <li>• Bone bridging between adjacent bones, such as the tibia and fibula may occur.</li> </ul>
	<p style="text-align: center;"><b>Paleohistopathology changes<sup>h</sup></b></p> <ul style="list-style-type: none"> <li>• Clear line of separation between the periosteal new bone and the underlying cortex (grenzstreifen), in some areas mimicking sinuous lacunae;</li> <li>• Presence of numerous osteocyte lacunae in the new bone formation.</li> </ul>

Subperiosteal hematoma	<b>Gross bone changes</b> <sup>b, c</sup>
	<ul style="list-style-type: none"> <li>• Subperiosteal haematomas are usually diaphyseal, of a moderate size and with an outer layer composed of lamellar bone (after healing);</li> <li>• Other skeletal elements frequently affected by subperiosteal haemorrhages are the skull, mandible, vertebrae, ribs and pelvis;</li> <li>• Subperiosteal hematomas of traumatic origin are formed by new bone whose shape may be solidly thin or thick, laminated or in Codman's triangle. In scorbutic individual the new bone is regularly solidly thick.</li> </ul>
	<b>Paleohistopathology changes</b> <sup>f, o</sup>
	<ul style="list-style-type: none"> <li>• Newly formed bone may range from thin layers in the form of a sliplike cover to relatively short, bulky bone trabeculae with extensive bridging formation and /or with multiple layers (rare);</li> <li>• Demarcated and radiating bone apposition perpendicular to the periosteal surface of bone may be observed. In completely remodelled hematomas, the distinction between the bone lesion and the underlying cortex is less clear;</li> <li>• Grenzstreifen and polsters may also be present.</li> </ul>
Fractures	<b>Gross bone changes</b> <sup>b, c</sup>
	<p><b>Early stage of fracture healing</b></p> <ul style="list-style-type: none"> <li>• Bone callus is mostly composed of woven bone with a porous appearance.</li> </ul> <p><b>Well-consolidated calluses</b></p> <ul style="list-style-type: none"> <li>• Bone callus formed by compact, lamellar bone. The periosteal bone produced may be solid, thin or thick, laminated or in Codman's triangle.</li> </ul>
	<b>Paleohistopathology changes</b> <sup>f</sup>
	<ul style="list-style-type: none"> <li>• Woven bone composed of trabeculae oriented parallel.</li> </ul>
Metastatic carcinoma	<b>Gross bone changes</b> <sup>b, c, p</sup>
	<ul style="list-style-type: none"> <li>• Bone metastases vary amongst solitary, or commonly, multiple osteolytic, osteoblastic or mixed osteolytic-osteoblastic lesions. Osteolytic metastases may be well or poorly marginated, whereas the osteoblastic ones may be focal or diffuse. Periosteal new bone deposition is highly unusual in metastatic disease, except in prostatic and breast carcinoma, gastrointestinal malignancies and neuroblastoma.</li> </ul>
	<b>Paleohistopathology changes</b> <sup>f, q, r, s, t, u</sup>
	<ul style="list-style-type: none"> <li>• Microscopic pattern characterized by the presence of Howship's lacunae formed by osteoclastic resorption, especially at trabeculae, in some cases combined with deposits of woven bone.</li> </ul>

Data retrieved from: (a) Steinbock (1976); (b) Aufderheide and Rodríguez-Martín (1998); (c) Ortner (2003e); (d) Resnick and Kransdorf (2005); (e) Wakely et al. (1991); (f) Schultz (1993; 2001; 2003; and 2012); (g) von Hunnius et al. (2006); (h) Weston (2004 and 2009); (i) Cavanaugh and Holman (1965); (j) Ali et al. (1980); (k) Balaji et al. (2006); (l) Martínez-Lavín (2007); (m) von Hunnius (2009); (n) Boel and Ortner (2011); (o) van der Merwe et al. (2010); (p) Burgener et al. (2006); (q) De La Rúa et al. (1995); (r) Wakely et al. (1995); (s) Mays et al. (1996); (t) Šeřčáková et al. (2001); (u) Luna et al., (2008).



---

# CHAPTER 4

---

*“(...) THERE IS AN INTIMATE LINK BETWEEN HOW WE COLLECT AND ANALYSE SKELETAL DATA, THE RESEARCH TRADITION WE WORK IN AND THE HISTORICAL MOMENT WE ARE WORKING AT. [...] INDEED, ONE GOAL OF DRAWING THE LINKAGE BETWEEN RESEARCH CONTEXTS AND METHODS EXPLICITLY IS TO MAKE US REALISE THAT ALTERNATIVE METHODS AND QUESTIONS ARE POSSIBLE.”*

(ROBB, 2000: 477)





## 4. MATERIALS AND METHODS

Based on an integrative approach that combines two complementary lines of enquiry – gross inspection and histology, this section aims to present and characterize the samples selected for study and to describe the procedures involved in the macroscopic and histological analysis of the specimens.

### 4.1. MATERIAL

#### 4.1.1. Macroscopic Analysis

For the macroscopic analysis an assemblage of 253 individuals, 138 males and 115 females, comprising individuals with an age at death ranging from 2.5 months to 94 years old, was chosen (Figure 4.1).

The sample was retrieved from the Lisbon Human Identified Skeletal Collection, also called the Luis Lopes Collection housed at the Bocage Museum, the official designation for the Department of Zoology and Anthropology of the National Museum of Natural History in Lisbon, Portugal (Cardoso, 2005 and 2006)<sup>42</sup>. This large identified human collection is made up of 1692 skeletons and is considered one of the most important in the country (Cardoso, 2005 and 2006) and worldwide. The skeletons were collected from five cemeteries from Lisbon and belong to individuals who passed away between 1880 and 1975 (Cardoso, 2005 and 2006). Despite its size, an almost complete biographic profile, including name, birthplace, sex, age-at-death, occupation and cause of death is available for only 699 (41.3 %) skeletons (Cardoso,

---

<sup>42</sup> It is important to note that the *Bocage* Museum possesses two collections (Cardoso, 2006). One is composed of the remnants of Ferraz de Macedo collection, almost completely consumed by a fire in 1978 (Cardoso, 2005 and 2006). This collection, consisting mainly of human skulls, was initiated in the 19th century by the Portuguese physician Francisco Ferraz de Macedo, and was donated to *Bocage* Museum by its collector in the beginning of the 20<sup>th</sup> century. The second human collection was started by Luis Lopes between 1981 and 1992 and was continued by Hugo Cardoso in 2000 (Cardoso, 2005 and 2006).

2006)<sup>43</sup>. At the Museum, the collection is organized in cabinets, and each skeleton is stored in a drawer. Most individuals were labelled with a collection number, and the bones, especially those of small size, were packed in plastic bags. All skeletons are accompanied by a paper form, containing the identifying data related to the individual's biological profile (Figure 4.2).

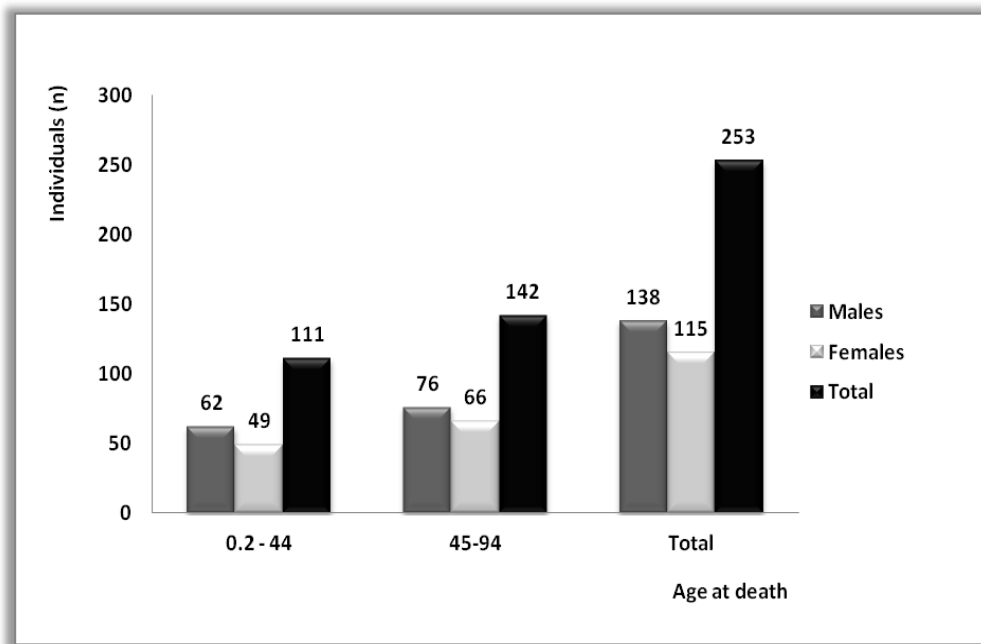


**Figure 4.1:** Sample distribution by sex and age at death.

Taking into account the major goal of the research, which consists of testing the differences in bone macro- and microstructure in distinct infectious and non-infectious nosologies, the criterion that guided the sample selection was the cause of death reported. Based on the Museum digital database, composed of data transcribed from the original paper forms, individuals who died from the following diseases were selected (table I.I, I.II, I.III; appendices):

- I. Tuberculosis, in its multiple expressions (i.e. pulmonary and extra-pulmonary);
- II. Non-TB infections (i.e. pneumonia, bronchitis, bronchopneumonia, leprosy, syphilis, typhoid fever, osteomyelitis, gangrene and septicaemia, among others);
- III. Other systemic conditions of different aetiologies (i.e. arteriosclerosis, diabetes, tumours, etc.) that potentially may have induced bone periosteal changes.

<sup>43</sup> There are individuals who possess only elementary data (i.e. name, sex, age at death and cause of death). In these cases, the data related to the birthplace, age of birth or occupations is missing.

Thus, the total sample was divided into three groups. Group 1 contained all individuals from the collection who suffered from TB (N=114). Group 2 consisted of 89 individuals, all of whom had a non-TB infectious disease as a cause of death. The remaining group, composed of 50 skeletons, was chosen randomly between different non-infectious pathological conditions. The sample distribution (N=253) by cause of death, sex and age at death is illustrated in Table 4.1.

**Table 4.1:** Distribution of individuals by cause of death, sex and age at death intervals.

Cause of death	Sex	Age classes (years)		Total
		0.2-44	45-94	
Group 1 - Tuberculous infections (TB)	F	40	12	52
	M	39	23	62
	<b>Subtotal</b>	<b>79</b>	<b>35</b>	<b>114</b>
Group 2 - Non-TB infections	F	8	32	40
	M	19	30	49
	<b>Subtotal</b>	<b>27</b>	<b>62</b>	<b>89</b>
Group 3 - Other pathological conditions	F	1	22	23
	M	4	23	27
	<b>Subtotal</b>	<b>5</b>	<b>45</b>	<b>50</b>
<b>Total</b>		<b>111</b>	<b>142</b>	<b>253</b>

Regarding the age at death averages, Group 1 had the lowest mean overall ( $\bar{x}$  =25.9), and the lowest mean for females ( $\bar{x}$ =19.1), whereas Group 3 had the highest mean for both sexes ( $\bar{x}$ = 60.6). The Group 2 (non-TB infections) had not only an intermediate mean age at death ( $\bar{x}$ =50.6), but also the greatest discrepancy between the minimum and maximum values per age, 0.2 and 89 years old respectively (Table 4.2).

**Table 4.2:** Maximum, minimum and mean age at death values by cause of death and sex groups.

Cause of death	Sex	Age classes (years)		
		Maximum value	Minimum value	Mean value ( $\bar{x}$ )
Group 1 - Tuberculous infections (TB)	F	66	9	19.1
	M	78	14	29.4
	<b>Subtotal</b>			<b>25.9</b>
Group 2 - Non-TB infections	F	89	0.3	60.5
	M	86	0.2	42.5
	<b>Subtotal</b>			<b>50.6</b>
Group 3 - Other pathological conditions	F	94	21	65.5
	M	86	26	56.1
	<b>Subtotal</b>			<b>60.6</b>

Concerning the chronological distribution of the sample, it was possible to ascertain this parameter based on the direct or indirect analysis of the birth date<sup>44</sup> and date of death for only 229 skeletons (Figure 4.3). For the remaining 24 individuals, this information was not available. From Figure 4.3 it is clear that the majority of the sampled individuals were born between the years of 1861 and 1900. The temporal period that recorded the largest number (54.1 %) of obituaries was the period from 1941 to 1960.

Despite the place of exhumation – the Lisbon cemeteries, not all individuals were born in Lisbon or even in Portugal. From the total sample (N=253), 230 (90.9%) were born in the Portuguese continental territory, two individuals were recorded as having their birthplace in the Portuguese former colonies (0.8%), namely Mozambique and São Tomé and Príncipe, one was born in Brazil (0.4%), and 7 (2.8%) were born in other European countries, such as Austria, France, Italy, and Spain. For 13 (5.1%) individuals it was impossible to infer the birthplace. Figure 4.4 shows the geographic provenience of the individuals from the assemblage, taking into account the administrative division of continental Portugal.

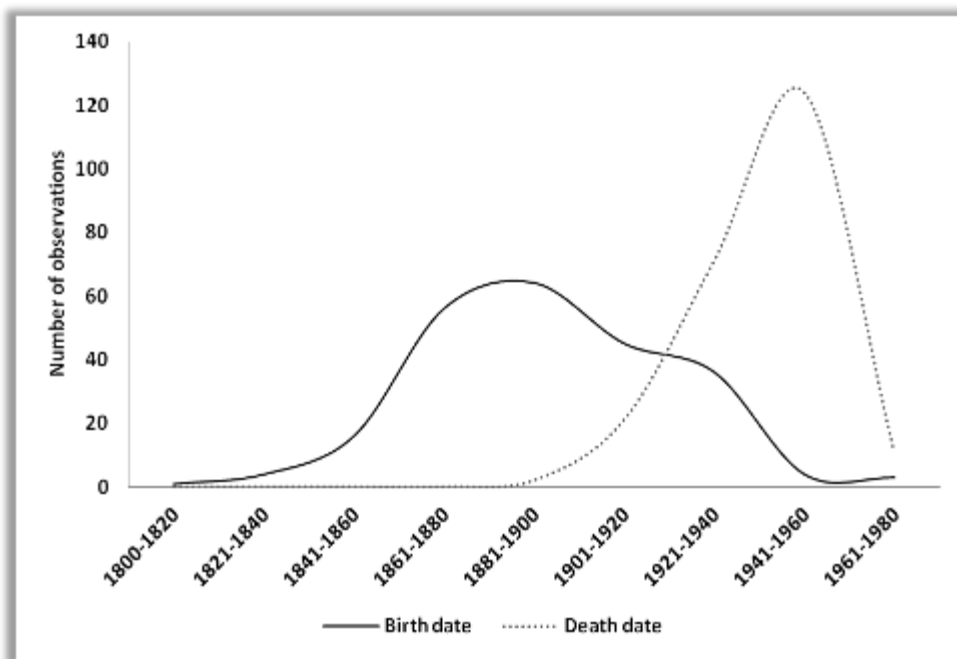


**Figure 4.3:** Chronological distribution of the individuals who show a complete record for birth and death dates (n=229).

<sup>44</sup> For the individuals who did not have the birth date recorded, this information was determined by subtracting the age at death from the year of death.

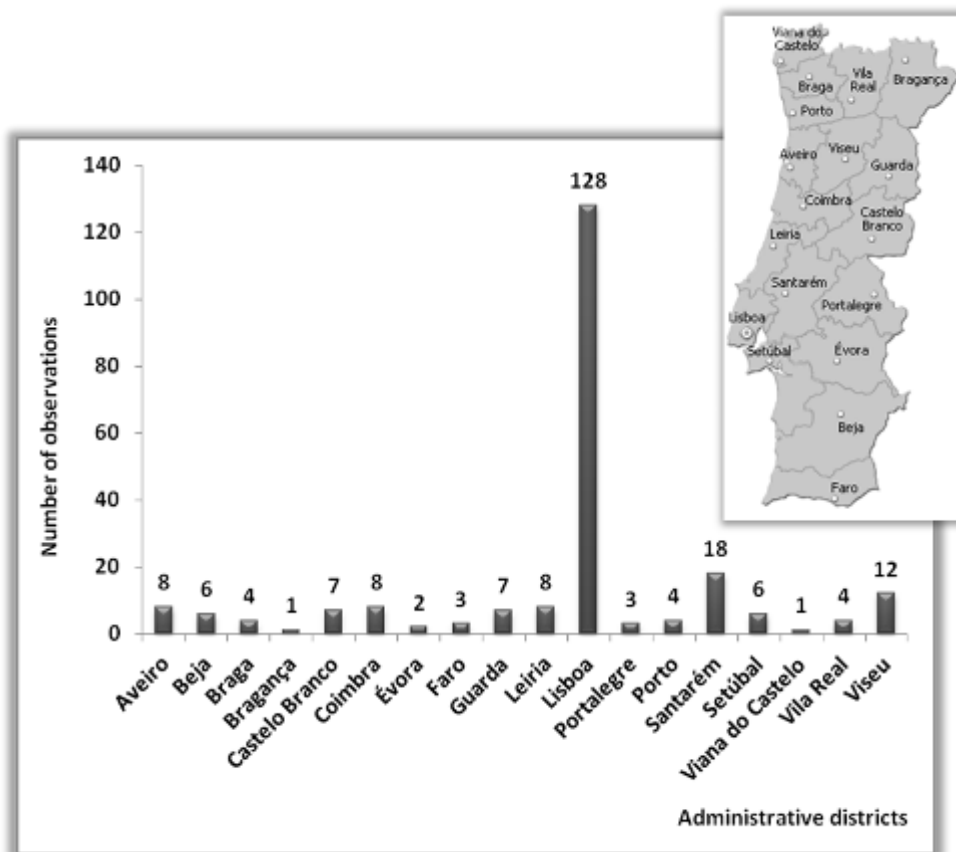


**Figure 4.4:** Geographic distribution of the sample by Portuguese districts.

As illustrated in the graph, the largest number of individuals in the sample (55.7%, 128/230) were born in the district of Lisbon, followed by the contiguous district of Santarém, (7.8%, 18/230), and the main districts from the centre of Portugal, namely, Viseu (5.2%, 12/230), Aveiro, Coimbra and Leiria, all of them with 3.5% (8/230). The lowest number of individuals came from the districts of Viana do Castelo and Bragança, in the Northwest of Portugal, both with (0.4%, 1/230) each.

#### 4.1.2. Paleohistological Analysis

For the histological analysis, 34 bone samples, 26 from the Lisbon Human Identified Skeletal Collection from the Bocage Museum and eight from archaeological skeletons were collected. The archaeological samples were selected to complement the comparative study of the identified sections, as well as to test the differences found in bone microstructure.

#### 4.1.2.1. Identified Bone Samples

The identified bone samples (n=26) were collected from the Bocage Museum and belong to 23 individuals (table I.IV, appendices). For skeleton numbers 1196 and 1534-A, permission was granted to take two samples from each of these individuals. Unfortunately, it was impossible to extract bone samples from all individuals studied, for two reasons: firstly, full access to the individuals was limited by the museum rules<sup>45</sup>; and secondly, bone sampling had to be adjusted based on time and supplies in order to avoid needless damage to the skeletons. As a consequence, the sectioning of specimens was done according to the following criteria:

- I. Only visible pathological lesions repeated in more than one bone piece and/or individual were considered;
- II. Only bones with taphonomic alterations and postmortem breakage were authorized for sampling;
- III. When possible the cutting procedures were taken close to damaged areas, avoiding zones of well preserved bone.

The above constraints have undoubtedly conditioned the sample selection. Therefore, 70.4% (19/27) of the bone pieces selected were exclusively ribs (Figure 4.5). Anatomically, the thoracic cage was the region that showed the highest number of deposits of new bone; furthermore it was also more affected by postmortem damage. For the remaining bones, namely the radius, femur, tibia, fibula and metatarsals, the percentage of sampling ranged between 3.7% (1/27) and 7.4% (2/27) (Figures 4.6 and 4.7).

The selection of bone samples for histological analysis followed some of the recommendations of Turner-Walker and Mays (2008: 124), such as: i) minimizing damage to the specimens; ii) avoiding critical bone features that may hinder other researchers' work, as in the case of morphometric studies; and iii) sectioning different skeletons in the same anatomical location to facilitate comparisons.

---

<sup>45</sup>According to the new policies from the Bocage Museum available at:

[http://www.mnhn.ul.pt/zoologia/col\\_form/Regulamento\\_de\\_Emprestimo\\_das\\_Coleccoes\\_Zoologicas\\_e\\_Anthropologicas.pdf](http://www.mnhn.ul.pt/zoologia/col_form/Regulamento_de_Emprestimo_das_Coleccoes_Zoologicas_e_Anthropologicas.pdf), accessed on 5<sup>th</sup> August, 2011, extraction of biological samples is conditional. The approval obtained for the present study was unprecedented since the formal application occurred during a transitional period in the museum's organizational model.

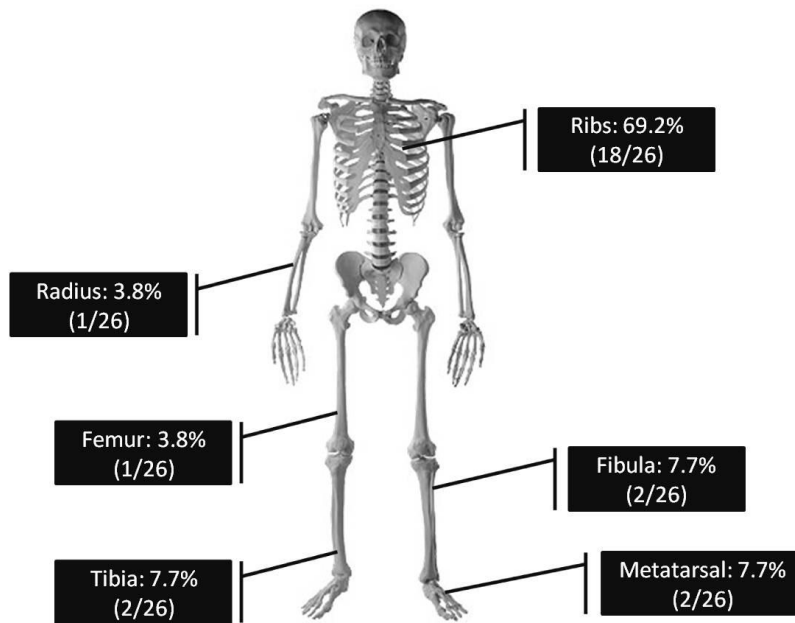


**Figure 4.5:** Anatomical distribution of the bone samples collected (skeletal frame obtained at Google images on 5<sup>th</sup> August, 2011).

In the course of the research, efforts were also made to obtain the same number of bone sections from each of the three pathological groups created. The sample distribution obtained was as follows (figure 4.8):

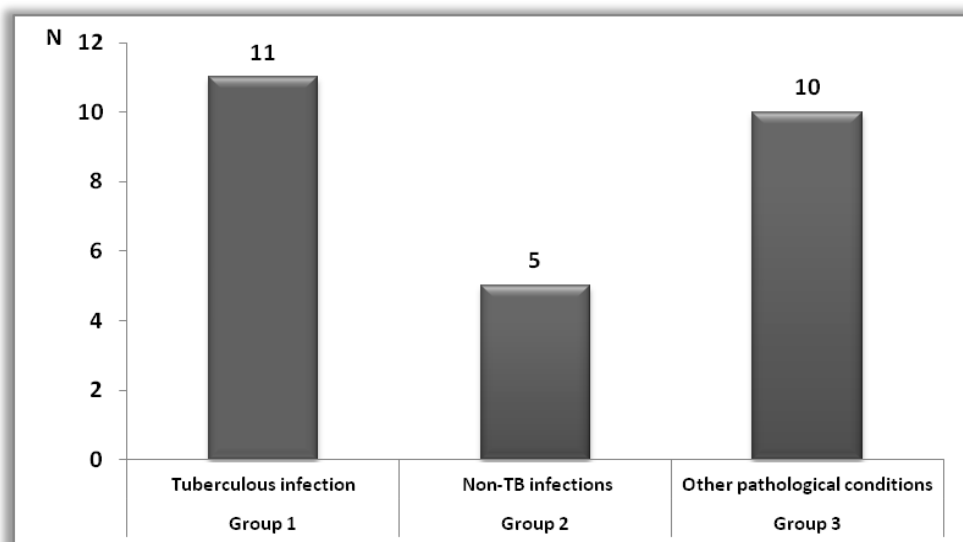


**Figure 4.8:** Distribution of bone samples by cause of death groups.

Each cause-of-death group includes bone segments without macroscopic evidence of periosteal reactions, as well as sections containing bone callus in different stages of healing that operates as control specimens (Group 1 = 1; Group 2 = 2; Group 3 = 3).

#### **4.1.2.2. Archaeological Bone Samples**

The archaeological bone samples (n=8) were retrieved from three distinct skeletal assemblages: Constância necropolis; the cemetery of the hospital of the Ordem do Carmo in Oporto, and the cemetery of the Royal Hospital of All Saints in Lisbon (Figure 4.9 and table I.V, appendices).

##### **1. Ancient necropolis of the Constância village**

Constância is a small village located in the centre of Portugal. In 2002 and 2003, during the environmental and urban renewal of the historical centre of the village, human skeletons were brought to light in the Alexandre Herculano's square, the area occupied in the past by the former necropolis and São Julião Church, both dated from the 14<sup>th</sup>-19<sup>th</sup> centuries (Assis, 2006). This finding led to an extensive archaeological excavation that resulted in the recovery of 151 skeletons: 106 adults and 45 non adults (Assis, 2006). From this skeletal series, three distinct individuals, designated PAH/C.02 SG24 E1, PAH/C.02 SG25-26 E2, and PAH/C.02 SG19 E7 were chosen for sampling. The criterion used was based on the pattern of bone lesions observed and respective differential diagnosis.

The skeleton PAH/C.02 SG24 E1 belongs to a young individual with an age at death estimated between 14 and 18 years old. New bone deposition was observed on the visceral surface of both left and right ribs. Similar lesions were noticed on the visceral surface of the sternum and on the anterior body of the vertebrae (Assis, 2006). The differential diagnosis proposed in this case points to a pulmonary infection, such as tuberculosis (Assis, 2006). From this young individual, a costal fragment of a right rib was extracted. The PAH/C.02 SG25-26 E2 skeleton belongs to a young female with an age at death estimated between 18 and 25 years old (Assis, 2006). Despite some postmortem damage, paleopathological lesions also compatible with a possible case of respiratory infection (e.g. TB) were observed, namely new bone deposition on the visceral surface of ribs, hypervascularization of the anterior surface of vertebrae, and the presence of *serpens endocrania symmetrica* (SES) (Assis, 2006). From this



individual a costal fragment of a left rib was collected<sup>46</sup>. The last skeleton used for sampling (PAH/C.02 SG19 E7) was that of a middle-aged to old female, which showed a distinct pattern of bone lesions distributed over several bone elements (Assis, 2006). This specimen, previously described in the literature (Assis and Codinha, 2010), has been diagnosed as a possible case of metastatic carcinoma. A fragment of a left rib was extracted for histological analysis.

## 2. Cemetery from the hospital from the *Ordem do Carmo* in Oporto

From the old hospital of the *Ordem do Carmo*, located in the Carlos Alberto Square in the city of Oporto, approximately 480 human skeletons were unearthed in 2006 (Menéndez and Teixeira, 2008). These remains belong to individuals who lived and died in Oporto between 1801 and 1869 (Menéndez and Teixeira, 2008). From this skeletal assemblage two samples with unspecific periosteal reactions were collected. Besides the presence of bone lesions, the criterion that guided sample selection was the existence of some degree of postmortem damage to reduce the amount of bone destroyed. From the adult individual Porto UE 5041-70<sup>47</sup> a portion of a massive bone outgrowth with a flowing appearance located near the site of attachment of the tibiofibular ligament of the left tibia was collected. Despite being detached from the remaining shaft by postmortem breakage, the bone piece showed a horizontal orientation, forming a crest. A case of talocalcaneal coalition on the left foot was also observed (Sardoeira, 2011). The other sample was retrieved from the middle diaphysis of the left fibula of the adult male - Porto UE 6451.65, which exhibited extensive periosteal bone reaction. This condition extended to the adjacent tibia and was thus asymmetrical in its distribution (Sardoeira, 2011).

## 3. Cemetery of the extinct Royal Hospital of All Saints in Lisbon

The remaining archaeological samples were collected from three adult individuals exhumed from the extinct Royal Hospital of All Saints in Lisbon. Similar to the previous assemblages described above, bone selection was based on the presence of bone lesions, as well as some degree of postmortem destruction.

The Royal Hospital of All Saints opened in 1504 with the aim of centralizing the Lisbon city's health services, replacing about 43 small hospitals as well as hostels, leper houses and

---

<sup>46</sup> Due to the pattern of bone lesions recorded and possible differential diagnosis, identical rib samples were collected from individuals PAH/C.02 SG24 E1 and PAH/C.02 SG25-26 E2, for ancient pathogen DNA analysis on the scope of the UK's project entitled "Biomolecular archaeology of tuberculosis in ancient Britain and Europe".

<sup>47</sup> This skeleton was fairly incomplete, represented only by the tibiae, fibulae and feet bones. Due to the scarcity of bone elements the sex and age at death were not estimated (Sardoeira, 2011).

hospices (Panarra, 1994; Ramos, 1994). The hospital was organized in three major wards, one of them focused on the care and treatment of syphilis patients (Panarra, 1994; Ramos, 1994). The building was severely damaged by a fire in 1750, and in 1755 as a consequence of the Lisbon earthquake it ceased to exist (Ramos, 1994). In its place the Figueira's Square was built. Between the years of 1999 and 2001, during an archaeological survey 14 skeletons representing both sexes and different age groups and dating from the 18<sup>th</sup> century were exhumed. From the skeleton of a young adult male with the designation Praça da Figueira [1492] a bone section was removed from the middle diaphysis of the left femur, which contained a calcified hematoma approximately 4 cm in length. From the skeleton Praça da Figueira [1429], also an adult male, a portion of fibula with unspecific periosteal bone deposition was collected. A similar bone sample was extracted from the left fibula of the skeleton Praça da Figueira [1310]. This individual, an adult female (< 40 years old), showed multiple bone lesions characterized by new bone deposition with a bilateral pattern in several bone pieces (skull, upper and lower limbs). The macroscopic, radiological and CT-scan analysis are compatible with a case of acquired syphilis (Assis et al., 2010)<sup>48</sup>.

## 4.2. METHODS

### 4.2.1. Macroscopic Analysis

All bones from the 253 individuals from the identified collection were scrutinized with the help of a magnifying lens. Due to the subtle nature of some of the bone lesions, a lamp was placed a few centimetres from the bone surface to look for the presence of irregularities or texture changes compatible with periosteal bone reactions. The data observed were documented in a visual recording form (Figure I.I, appendices) and later transferred to a Microsoft Office Excel 2007® database. In addition to the individual biological profile (i.e. sex, age at death, cause of death and collection number), the recording form contained specific data concerning the type, distribution and location of lesions in the bone shaft. Thus, the periosteal reactions were classified according to their presence or absence, symmetry, side affected, extent (localized/diffuse), type of new bone observed (woven/lamellar/ or both) and bone segment affected (Table 4.3).

---

<sup>48</sup>This paleopathological case was presented, in 2010, at the 18th European Meeting of the Paleopathology Association. Vienna, Austria (August 23rd – 26<sup>th</sup>).

**Table 4.3:** Grade system used to rank periosteal bone lesions by location and type.

General	Extent	Laterality	Symmetry	Bone type
0=absent	0=absent	0=absent	0=absent	1=woven
1=present	1=localized	1=unilateral	1=symmetric	2=lamellar
7=N.O. <sup>1</sup>	2=diffuse	2=bilateral	2=asymmetric	3=Both
9=B.A. <sup>2</sup>	7= N.O.	7= N.O.	7= N.O.	7= N.O.
12=N.A. <sup>3</sup>	9= B.A.	9= B.A.	9= B.A.	9= B.A.
---	12= N.A.	12= N.A.	12= N.A.	12= N.A.

<sup>1</sup>Non-observable (N.O.), when *postmortem* destruction has made the complete observation of periosteum impossible; <sup>2</sup>Bone absent (B.A.), when the bone piece was not available for study; <sup>3</sup>Non-applicable (N.A.), when the classificatory system could not be used, as occurred in the cases of asymmetrical and irregular bones.

Descriptive analysis of the resulting data was performed, and Chi-square and odds ratio testing data were carried out using SPSS 16.0 and Epi Info7, with the level of significance set at  $p < 0.05$ .

#### 4.2.2. Paleohistological Analysis

The methods used in paleohistological analysis were characterized by a particular sequence of steps that ran from the simple sample selection and finished with the digital record of all bone slides.

The archaeological samples were collected at the place where the skeletal assemblages are stored. Regarding the osteological material from Constância, the bone sampling was undertaken at the Department of Life Sciences (Anthropology) from the University of Coimbra. Since the bone elements targeted were already fragmented *postmortem*, no special saw was used to cut them off. The bone samples from the cemetery of the hospital of the Ordem do Carmo were collected at the Oporto head office of the archaeological company responsible for the excavation, Vessants arqueologia i cultura SL. The samples from the Royal Hospital of All Saints were gathered at the Faculty of Humanities and Social Sciences from the New University of Lisbon. In both cases, a hacksaw was used for sampling. In better preserved bones, the areas to be cut were first measured with a ruler and marked with a pencil. It is important to highlight that all bone pieces were recorded photographically before and after the appliance of the cutting measures. Each sample was later stored in a plastic bag previously identified with the individual designation, type of bone, laterality and possible differential diagnosis of the lesions observed.

The identified samples were exclusively collected from the Lisbon Human Identified Skeletal Collection located at the Bocage Museum. The procedures linked with sample

processing of both archaeological and identified samples took place in the Bioarchaeological Laboratory of the Department of Anthropology, Trent University, Peterborough - Ontario, Canada, under the direction of Prof. Anne Keenleyside (Figure 4.10).

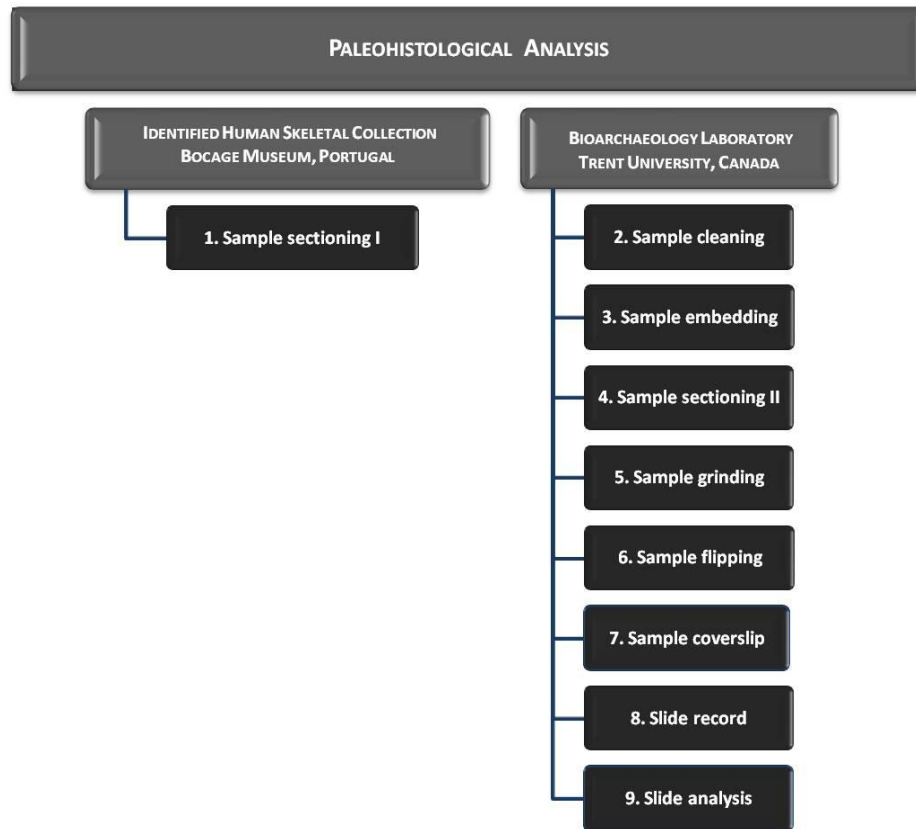


**Figure 4.10:** Summary of all procedures used in the production of bone histological sections for microscopic analysis.

Taking into account the characteristics of the sample selected in this study for histological analyses, a modified version of the protocol developed by Fitzgerald and Saunders (2007) for the preparation of undecalcified ground tooth sections was adopted. In spite of being more complex, requiring several technological devices, this protocol was chosen because it «(...) overcome the tendency for archaeological bone or tooth specimens to crumble or shatter during cutting and gridding (...) [since they are first] embedded in a penetrating resin with hardness similar to that of the mineralized tissue. Specimens thus embedded in epoxy or other resins can be sectioned by a variety of techniques (...)» (Turner-Walker and Mays, 2008: 124), producing samples with a more reduced thickness and therefore easy to grind and observe.

In the following section, all of the procedures used during the preparation of the bone samples will be described. It is important to note that a number of health and safety measures were adopted during the course of the laboratory work, such as the use of the fume hood, gloves, eye protection and dust masks every time hazardous substances were handled.

### 1. Sample sectioning I

- i. After marking the bone pieces to be sampled, the process of sectioning started with the measurement of the bony area to be cut. To accomplish this step a regular ruler was placed on the bone surface and a length of approximately 1-1.5 cm was measured, which corresponds to the estimated size chosen for each sample. Subsequently, and to help in the cutting process, a line delimiting the bone surface to be handled was drawn with the help of a soft pencil (Figure 4.11);
- ii. Finally, the bone samples were carefully extracted using a small hacksaw. In ribs the incision was made perpendicular to the bone shaft, whereas for the remaining bones a “V-shaped” cut was made. The samples extracted were then measured and stored in a previously identified plastic bag. It is important to note that all bone specimens, prior to and after sampling, were recorded photographically for future reference.

### 2. Sample cleaning

- i. Each sample was cleaned, first in tap water and then in alcohol using 100 ml grade glass beakers (Pyrex®); an ultrasonicator (Fisher Scientific 30®); tap water and 95% ethyl alcohol 95% (Figure 4.12);
- ii. The cleaning process started with three cycles of 20 minutes each in a sonic bath, where the bone samples were immersed in glass beakers containing tap water (50 ml). All glass beakers were labeled with the ID from the skeleton;
- iii. After drying at room temperature, they were dehydrated in ethyl alcohol (20 ml) and sonicated for 15 minutes. They were left to dry at room temperature for almost 12 hours.

### 3. Sample embedding

- i. The embedding procedures started with the preparation of the plastic medium substance. For this stage paper cups; plastic pipettes; wooden sticks; an electronic balance (Adventurer<sup>tm</sup> SL Ohaus®); mounting cups (Buehler® Samplkup®; 1<sup>1/4</sup>” ID); and

Epo-kwick® resin and hardener (Buehler®) were used. To help with the removal of the embedded blocks from the mounting cups, a release agent (Buehler®) was also applied (Figure 4.13);

- ii. The embedding solution was prepared by adding hardener to the epoxy resin following a 5:1 dilution ratio. To achieve this goal a paper cup was placed on the balance and its weight was adjusted so that the balance displayed zero weight. Using a disposable plastic pipette, the required quantity of resin was added to the paper cup. After that, and to achieve the exact proportion, the hardener was added using a clean pipette;
- iii. Next, the substances were mixed with a wooden stick until the mixture become transparent. To avoid bubble formation, the paper cup was tilted at a 45° angle. Before adding the embedding solution, the mounting caps were greased with the release agent. In the case of the small samples, the plastic moulds were divided in two equal portions;
- iv. After that, a small amount of epoxy was dropped into the cups until it covered 1 cm of the bottom. This process was conducted to avoid direct contact of the bone sample with the plastic container. The cups were left to dry overnight;
- v. The next step started with the preparation of a new mixture that was carefully poured over the sample, from the bottom to the top of the cup. The orientation of the bone samples in the cups is very important to allow a perpendicular cut in relation to the long axis of the bone. Efforts were made to remove all the air bubbles. The epoxy was left to cure overnight;
- vi. After they were completely hardened, the bone blocks were gently removed from the mounting cups. In the cases where the formation of a slight rim occurred, it was cut with an electric scalpel. All the procedures described were carried out under the fume hood.

#### 4. Sample sectioning II

- i. Since bone blocks are very hard, the thin sections were cut with a slow speed saw (IsoMet® 1000 precision saw). To maximize and to improve the sectioning, a wafer chuck device was used to attach the block against the IsoMet® blade. Thus, one of the surfaces of the embedded bone was fixed to the wafer chuck, and the opposite to a clean slide, using a generous amount of dental sticky wax (DENTSPLY® sticky wax) previously melted on a hot plate (figure 4.14);

- ii. After the wax had hardened, the chuck was attached to the saw arm and orientated parallel to the blade. The sample positioning knob was then rotated until the blade lay close to the “cutting-line”;
- iii. Next, the blade was reset to the zero position and the thickness of the section (1-2mm) was chosen rotating the sample knob. The speed of the saw (~100) and the loading used (~50-150) were also adjusted;
- iv. From each block three distinct slides were made<sup>49</sup>; however only two were completely processed. The cuts were made by adjusting the blade to the point of attachment between the embedded block and the slide;
- v. Then, the sample was positioned moving the knob until it reached 1.0 or 1.5 mm (the thicknesses selected for samples). After each cut, the chuck was dismantled from the saw and a new slide was glued to the embedding block;
- vi. Each slide was then labeled with the acronyms of the place from its provenience, as well as with the number of the skeleton;
- vii. When necessary, and to improve the cutting efficiency, the blade was dressed with a dressing stick<sup>50</sup> in order to remove epoxy resin and sticky wax deposits on the blade;
- viii. At the end of each work day the blade was dismantled and the Isomet® 1000 was cleaned.

## 5. Sample grinding

- i. The main purposes of the grinding process are twofold: firstly, to reduce the thickness of the bone samples to 100 µm (0.01 mm); and secondly, to eliminate possible scratch marks produced by the saw. To achieve this, the following equipment was used: a MiniMet® 1000 Grinder-Polisher (Buehler®); polishing bowls; glass plates for the bowls; Carbimet® paper discs (600 grift-P1200) (Buehler®); Carbimet® paper discs (400 grift-P600); Microcloth PSA 2-7/8” 20/PK (Buehler®); Aluminium Oxide (Al<sub>2</sub>O<sub>3</sub>) abrasive powders in 12.5 µm, 9.5 µm and 5.0 µm particle size powder in the form of slurry (a liquid containing indissoluble solids in suspension), three plastic water bottles for mixing slurry with distilled or milli-q water and a digital caliper (Figure 4.15);

---

<sup>49</sup> This methodological option had two purposes, firstly to describe the microstructure variance found in each bone sample, and secondly to guarantee the integrity of two samples, if some of them became damaged.

<sup>50</sup> A dressing stick is “ (...) a rectangular block made from carborundum-type material used to grind or sharpen blades” (FitzGerald and Saunders, 2007: 25).

- ii. The grinding process started with the attachment of a piece of 600 grit paper to the glass plate from the plastic bowl. Some care was taken to insure that the glass plate was completely clean and dry to guarantee a perfect attachment;
- iii. Before the attachment of the slide to the slide holder from the grinder, some measurements were taken using a digital caliper; firstly in a clean slide setting up the digital caliper to zero, and then in a slide sample. Three measures we made, two on each side of the specimen, and one on the bottom, avoiding touching the bone with the caliper extremities. All measures were then recorded individually in a Microsoft Office Excel 2007® database;
- iv. To hold the slide sample to the slide holder from the grinder, a bit of distilled water was dropped to create a suction effect. Another drop of water, about 1-2 cm in diameter, was also added to the grit paper. After that the MiniMet was turned on and the speed (between 3.0 and 3.5), force (between 0.02 and 0.05) and duration of each cycle (~4 min.) were adjusted. It is important to highlight that the running cycles were frequently interrupted and the sample slides removed to control their thickness;
- v. In the case of thick or asymmetrical samples, the polishing was made by hand adding a vacuum adaptor to the slide and using synchronized movements in the shape of a figure eight. The base for polishing was created by attaching the grid paper to a glass disc. This measure was also used to optimize the time available. For both manual and mechanical procedures, the grinding value expected for each slide was ranked between 0.86 and 0.76 mm. After reaching this mark, the grinding procedure moved to a 400 grit paper (more softly) and the process started all over again until a rank of 0.6 to 0.4 mm was reached;
- vi. Once desired thickness was obtained, the grid paper was replaced with a Microcloth, a type of paper with soft texture. At this stage, instead of using distilled water, a batch of slurry<sup>51</sup> was created to help in the polishing process, first with 12.5 powder grit and then moving sequentially to the 9.5 and to the 5.0 powder grit. In this phase of the grinding process a very small amount of the sample is removed; however, the scratch marks are

---

<sup>51</sup> Fitzgerald and Saunders (2007: 10) describe the preparation of slurry in four steps, all of them carried out under the fume hood or using a dust mask: firstly, to «[w]eight out the required quantity of Aluminium Oxide abrasive powder for the amount of slurry to be mixed (20 g Al<sub>2</sub>O<sub>3</sub> : 100 ml H<sub>2</sub>O); [secondly to], add the weighed quantity of Al<sub>2</sub>O<sub>3</sub> to the appropriate amount of distilled water measured into a glass or plastic bottle; [thirdly to] cap the bottle and agitate until well mixed; and [finally] a large batch may be made up and stored. For use, shake the mixture well before decanting an aliquot of the slurry into a refillable plastic “squeeze bottle”.



softened. Between each type of grit paper and slurry used, the specimens were ultrasonicated in a bath of tap water for 15 minutes to remove grit.

## 6. Sample flipping and grinding

- i. The flipping phase started with the transfer of the bone sample to a second (and final) glass slide, followed by additional grinding until the bone specimen reached the desirable thickness of 0.1 mm. The supplies required were the same as those used in the grinding and embedding process. Additional supplies included an electric scalpel, new slides, wooden tweezers, a diamond pencil and a transmitted light /polarized microscope Nikon Eclipse 80i® (Figure 4.16);
- ii. Firstly, a diamond pencil was used to mark the ID of the bone samples on the new slide. After that, the slide was cleaned with a soft paper soaked in alcohol to remove dust and glass particles, and then left to dry;
- iii. Secondly, a solution of resin mixed with hardener was prepared following the protocol for sample embedding. After finishing the mixture, a clean plastic pipette was used to drop a small quantity of epoxy onto the clean slide, avoiding the formation of bubbles. In the meantime, the respective slide containing the bone sample was left on the hot plate to melt the wax. After melting, the slide was held carefully with the help of tweezers and its bone sample was transferred gently to the second slide. In this delicate stage, particular attention was paid to removing air bubbles, since their presence may obscure one's view of it. To facilitate the attachment of the bone sample to the new slide, an electric scalpel was used to cut the excess resin on the sample edges;
- iv. After transferring all bone samples to the second slides, they were left to dry under the fume hood for 12 hours. When dried, the second set of samples was submitted to a new set of polishing, following the same steps described above. Since at this stage the samples were thinner, increased attention was paid during the grinding process by using a microscope to evaluate the thickness of the samples;
- v. Once the expected thickness was reached, grinding ceased and the samples were ready for the next step.

## 7. Sample cover slip

- i. The cover slip is the ultimate stage in the sample processing and the more time-consuming. The supplies needed at this phase were: 50 ml grade glass beakers (Pyrex®);

- ethyl alcohol 95%; a vacuum pump; Drierite – versatile desiccators of anhydrous calcium sulfate (Buehler®, Canada); a high vacuum grease Dow Corning® (a silicone lubricant for glass stopcocks; joints and glass-rubber connections); a bottle of xylene; mounting medium liquid; plastic pipette; wooden and metal tweezers and cover slips (figure 4.17);
- ii. The process started with dehydration of the final slides in three distinct sonic baths of ethyl alcohol (ETOH), each of them with distinct dilutions, for a total of 8 minutes following the diluting method outlined in the Fitzgerald and Saunders (2007) protocol;
  - iii. Meanwhile, the vacuum chamber was prepared and stabilized by adding Drierite to the plastic bottle, as well as covering the edges of the vacuum container with the vacuum grease;
  - iv. Following dehydration, the samples were immersed in xylene (in glass beakers without cover) under vacuum. Since xylene is highly hazardous to health, all procedures that involved its handling were carried out under the fume hood using gloves, eye protection and powder mask;
  - v. The chamber vacuum was sealed and the pump turned on until the pressure inside reached a value close to 96. When that rate was achieved, the pump was shut down and the chamber put on rest until no more air bubbles were seen emerging from the bone samples;
  - vi. After the removal of slides from the vacuum chamber, a small amount of mounting medium was put over the samples using a clean plastic pipette. Finally, and with the help of tweezers, a cover slip was gently put over the samples. Special care was taken to do this to prevent air bubbles from occurring between the sample and the cover slip. If this occurred it would hinder microscopic observation of the sample;
  - vii. All samples were then left to dry.

### 8. Slide record

- i. Because of the time scheduled for the histological analysis, the final slides were carefully observed under the microscope even prior to being completely dried (Figure 4.18);
- ii. The microscopic observation was made using a high resolution microscope with an incorporated digital camera - Nikon Eclipse 80i® and a computer. The observations were made first with transmitted light and then with polarized light<sup>52</sup>, by adjusting the

---

<sup>52</sup> Polarized light was used to compensate for some degree of glare or distortion of the object image associated with the use of transmitted light (Lovell, 2000). According to the same author (Lovell, 2000: 227): «[p]olarized light is generally considered more useful than ordinary light for obtaining a detailed picture of cell and

analyzer and the polarizer devices in the microscope. All samples were then scrutinized using magnifying objectives of 2X, 4X and 10X;

- iii. Stereologer 2000® software was used to capture the bone images. For each sample, individual folders were created to store all images taken in regular and polarized light. Once photographed, all samples were carefully packed in a slide storage box.

### 9. Slide analysis

Three distinct softwares were used to process the microscope images, namely: the IrfanView 4.33<sup>®</sup>, 1996-2012 (to convert multiple photos from BMP to JPEG format); the Autostitch V2.2<sup>®</sup>, 2004 (to merge multiple photos in a plan); and the Image J 1.44p<sup>®</sup> (to calibrate photos). Photographs from both light and polarized images were qualitatively analyzed for particularities in bone microstructure such as:

- a. Type of bone activity observed: resorption, formation, or both;
- b. Type of new bone produced: woven, lamellar or both;
- c. Location of microstructure changes: periosteum, cortex, endosteum;
- d. Microstructure of the periosteal new bone formation;
- e. Type of mineralized bone: normal versus presence of structural defects;
- f. Density and prevalence of osteocyte lacunae;
- g. Presence of Howship's lacunae, a sign of osteoclast activity;
- h. Signs of bone tissue remodelling: formation of secondary Haversian systems

Qualitative differences and similarities of the bone microstructure were recorded among control samples and in those affected by lesions. A comparative analysis was also undertaken between bone specimens exhibiting the same pathological condition and samples with distinct bone conditions. Additionally, the incorporation of fractured bones in distinct stages of healing allowed for the study of the mechanisms that mediate bone callus formation. A complete description of all taphonomic alterations observed in the bone samples, such as encrustation by mineral soil, bacterial activity, presence of fungus and microfractures, was also made. Concerning this topic, a qualitative comparison among archaeological and identified samples was also conducted.

---

tissue structure in transparent specimens by revealing the birefringence of long molecules, such as those characteristic of collagen fibers».



---

# CHAPTER 5

---

*"[T]HE BRIDGING OF MACROSCOPIC DATA WITH MICROSCOPIC DATA IS SEEN AS AN ESSENTIAL STEP  
TOWARD ADDRESSING DIFFERENTIAL HEALTH STATUS ACROSS AGE, SEX AND CULTURE"*

MARTIN (1991: 55)



## 5. RESULTS

This chapter will present the results of the investigation into the macroscopic and paleohistopathological characteristics of periosteal new bone formation (PNBF) conducted in an identified skeletal sample from the Bocage Museum, Lisbon (Portugal), as well as in bone specimens derived from archaeological contexts<sup>53</sup>. Since taphonomy has a deleterious effect on bone tissue integrity, the first step in the macroscopic analysis will be to consider the bone representativeness and preservation by individual and element. This analysis will be complemented by the description of the main diagenetic changes observed in the histological samples.

### 5.1. MACROSCOPIC ANALYSIS

Two hundred and fifty-three skeletons belonging to the Lisbon Human Identified Skeletal Collection were examined macroscopically and the characteristics of the PNBF were recorded as outlined in Chapter 4. The presence of skeletal lesions was investigated in the total number of affected bones and individuals in the sample, and the prevalence of bone involvement was analyzed by sex, age-at-death, cause of death, anatomical distribution, and type of new bone observed. All skeletal elements were systematically examined for pathological changes, and the data obtained were entered into a database specifically designed for this research.

---

<sup>53</sup>As pointed out in the previous chapter, the archaeological samples were only considered in the paleohistopathological study.

### 5.1.1. Representativeness and Preservation of the Skeletal Sample

#### *The rib cage*

In the sample under study, a total of 4895 well-preserved ribs were identified, which represents 80.6% of the total number expected if all individuals possessed twelve pairs of ribs (Table 5.1 and Figure 5.1).

**Table 5.1:** Distribution of the total number of ribs observed by side (P=bone present; NO=bone present but with taphonomic changes; A=bone absent) and for the overall sample (P=bone preserved/Exp=expected bone in each individual assuming 12 pairs of ribs).

Rib cage							
Bone element	Left			Right			Total P/Exp (%)
	P	NO	Absent	P	NO	Absent	
R1	214	6	33	216	7	30	430/506 (85.0)
R2	226	9	18	232	7	14	458/506 (90.5)
R3	216	8	29	227	5	21	443/506 (87.5)
R4	222	7	24	229	5	19	451/506 (89.1)
R5	218	10	25	214	7	32	432/506 (85.4)
R6	210	14	29	207	13	33	417/506 (82.4)
R7	213	14	26	210	15	28	423/506 (83.6)
R8	209	20	24	208	17	28	417/506 (82.4)
R9	204	23	26	205	22	26	409/506 (80.8)
R10	189	24	40	191	25	37	380/506 (75.1)
R11	190	23	40	192	23	38	382/506 (75.5)
R12	126	13	114	127	14	112	253/506 (50.0)
<b>Total</b>							<b>4895/6072 (80.6)</b>

In the rib cage, the first four pairs of ribs (R1→R4) were the best preserved on both sides. In this subgroup, the 2<sup>nd</sup> (90.5%), 4<sup>th</sup> (89.1%), and 3<sup>rd</sup> (87.5%) ribs displayed the highest preservation scores. In contrast, the ribs that were less well-preserved were those from the lower thorax (R10→R12), namely the 12<sup>th</sup> rib (50%, 253/506), a significant number of which were missing (n=226). The most poorly preserved ribs (<25% of preservation) were the 10<sup>th</sup> (in 429 observed bones, 49 were excluded due to postmortem damage), the 11<sup>th</sup> (in 428 observed bones, 46 were not considered), and the 9<sup>th</sup> rib (in 454 bones recovered, 45 were excluded from the analysis). Two factors may explain the above observations, namely the incomplete recovery of all bones during the individual's exhumation, and the severe damage imposed by taphonomic agents that made the correct identification of each element impossible. With regard to the low representativeness of the twelfth rib, the possibility of rib agenesis in some individuals should also be considered since it most frequently affects the last pair (see Chapter 3, section 3.1.6).



Superficial erosion on the visceral surface of ribs was the most common taphonomic change observed (Figure 5.2). Besides erosion, flaking of the periosteum affecting, in some cases, the entire rib with exposure of the cancellous bone at the sternal and vertebral ends was also recorded. Furthermore, postmortem fissuring along the rib shaft with total or partial displacement of both the visceral and dorsal surfaces was observed in some individuals. Other common alterations included color changes and presence of dried soft tissues and evidence of chirurgical procedures (e.g. autopsy cut marks).

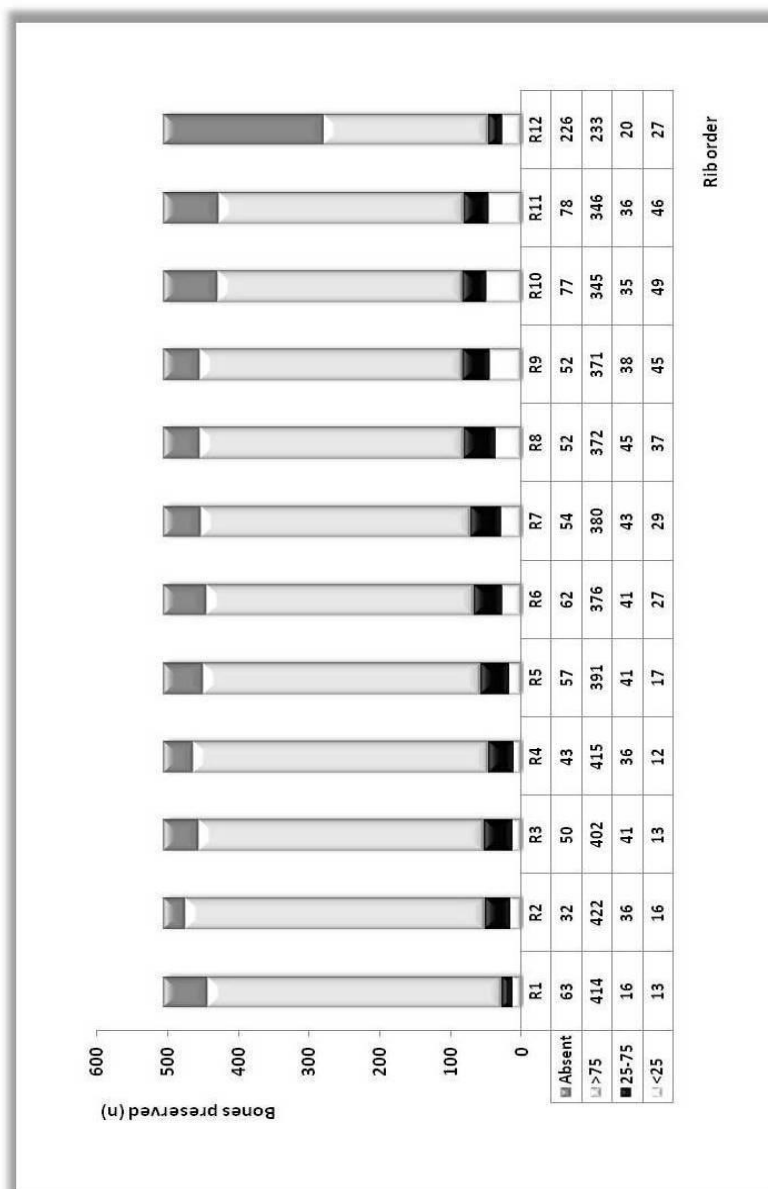


**Figure 5.1:** Classification of the ribs according to four grades of preservation (Grade 1 - >75% preserved; Grade 2 – 25-75% preserved; Grade 3 - <25% preserved; Grade 4 – bone absent). Only bones classified with grade 1 and 2 preservation were considered suitable for analysis.

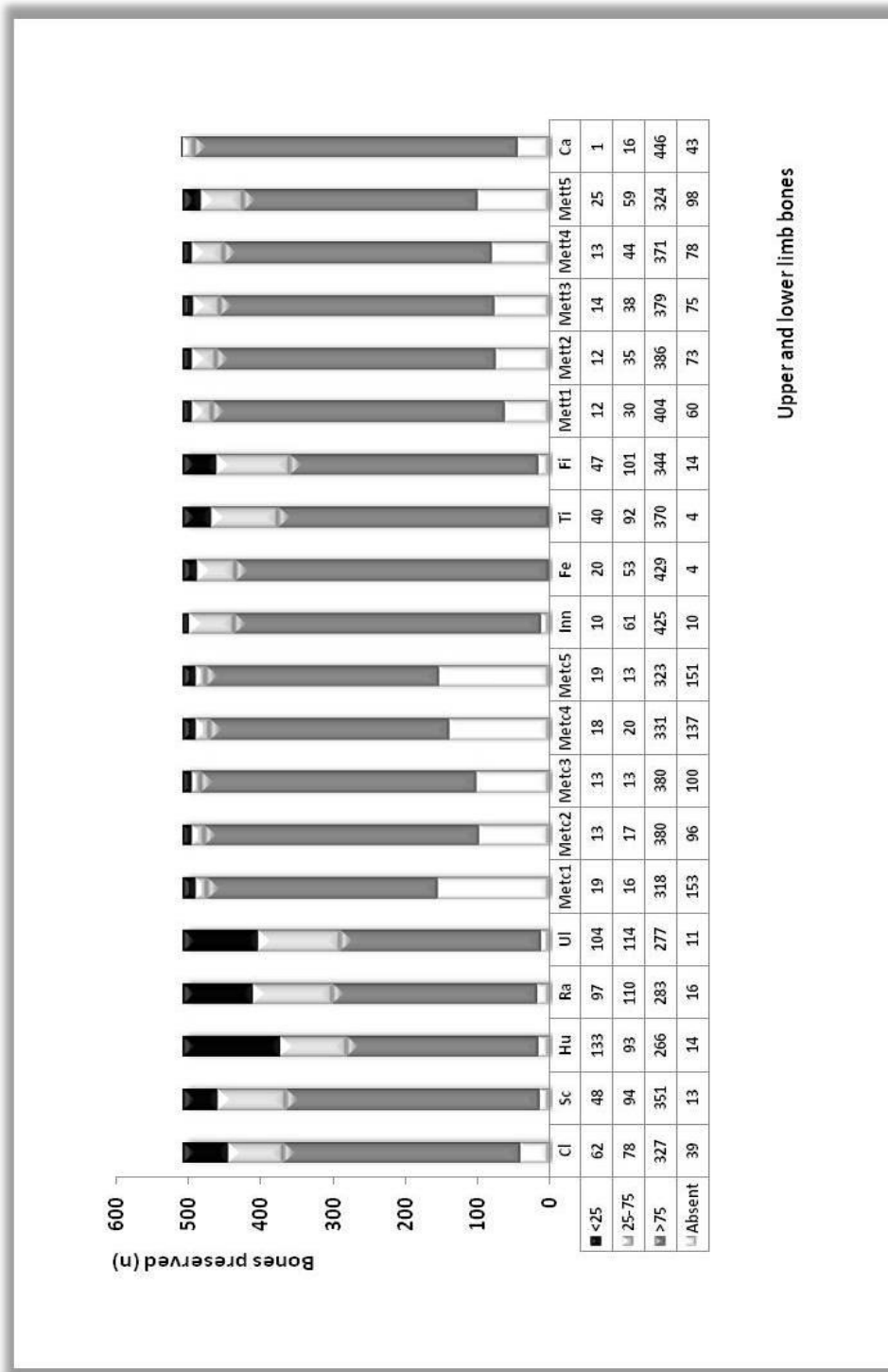
### Appendicular skeleton

In the 253 individuals that comprise the sample, only 8211 bones from the upper and lower limb were fully preserved, which corresponds to 81.1% of the total number expected if the skeletons were complete. Approximately 1189 bones were counted as absent and 720 were not included in the sample because they showed significant postmortem changes. When the preservation and representativeness of each bone element was scrutinized (Table 5.2 and Figure 5.3), the scapula (87.9%, 445/506) and the innominate (96%, 486/506) were more frequently represented and had fewer taphonomic changes than other bones in the sample, followed, in the upper limb, by the clavicle (80.0%) and the 2<sup>nd</sup> metacarpal (78.5%), and in the lower limb by the femur (95.3%), tibia and calcaneus (both with 91.3%). In contrast, the most poorly preserved bones were the remaining tubular bones of the hand, namely the 1<sup>st</sup> metacarpal (66%, 334/506), the humerus (70.9%, 359/506), the ulna (77.3%, 391/506), and the 5<sup>th</sup> metatarsal (75.7%, 383/506).

**Table 5.2:** Number of bones of the appendicular skeleton observed by side (P=bone present; NO=bone present but with significant taphonomic changes; A=bone absent) and in the overall sample (P=number of bones preserved/Exp= number of bones expected).

Upper limb							
Bone element	Left			Right			Total
	P	NO	Absent	P	NO	Absent	P/Exp (%)
Clavicle	203	32	18	202	30	21	405/506 (80.0)
Scapula	221	26	6	224	22	7	445/506 (87.9)
Humerus	177	66	10	182	67	4	359/506 (70.9)
Radius	197	46	10	196	51	6	393/506 (77.7)
Ulna	193	53	7	198	51	4	391/506 (77.3)
1 <sup>st</sup> Metc <sup>1</sup>	161	11	81	173	8	72	334/506 (66.0)
2 <sup>nd</sup> Metc	195	8	50	202	5	46	397/506 (78.5)
3 <sup>rd</sup> Metc	190	7	56	203	6	44	393/506 (77.7)
4 <sup>th</sup> Metc	173	9	71	178	9	66	351/506 (69.4)
5 <sup>th</sup> Metc	166	11	76	170	8	75	336/506 (66.4)
Lower Limb							
Innominate	242	6	5	244	4	5	486/506 (96.0)
Femur	241	10	2	241	10	2	482/506 (95.3)
Tibia	231	20	2	231	20	2	462/506 (91.3)
Fibula	224	22	7	221	25	7	445/506 (87.9)
1 <sup>st</sup> Mett <sup>2</sup>	215	8	30	219	4	30	434/506 (85.8)
2 <sup>nd</sup> Mett	210	7	36	211	5	37	421/506 (83.2)
3 <sup>rd</sup> Mett	207	7	39	210	7	36	417/506 (82.4)
4 <sup>th</sup> Mett	201	9	43	214	4	35	415/506 (82.0)
5 <sup>th</sup> Mett	185	15	53	198	10	45	383/506 (75.7)
Calcaneus	228	1	24	234	0	19	462/506 (91.3)
<b>Total</b>							<b>8211/10120 (81.1)</b>

<sup>1</sup>Metc= Metacarpal bones; <sup>2</sup>Mett= Metatarsal bones



Upper and lower limb bones

**Figure 5.3:** Classification of the bones of the upper and lower limb according to four grades of preservation (Grade 1 - >75% preserved; Grade 2 – 25-75% preserved; Grade 3 - <25% preserved; Grade 4 – bone absent). Only bones classified as having grade 1 and 2 preservation were considered suitable for analysis.

In some individuals complete destruction of the outer surface of the bones was observed, which made the analysis of PNBf impossible. Erosion and cortical detachment of the outer shell were the most visible postmortem changes (Figure 5.4 and Figure 5.5). These conditions were particularly apparent on the upper limb bones, namely the humerus (in 492 recovered bones, 133 were excluded due to the presence of significant taphonomic changes) and the ulna (in 495 recovered bones, 104 were not considered in the analysis due to their destruction). Additionally, some destruction of the bone epiphyses was also recorded (Figure 5.6). The skeletal elements that were less well-represented were the 1<sup>st</sup> metacarpal (n=153), the 5<sup>th</sup> metacarpal (n=151), and 4<sup>th</sup> metacarpal (n=137).

## 5.1.2. Periosteal New Bone Formation (PNBF): Gross Morphology

### 5.1.2.1. General Distribution by Sex and Age at Death

In the 253 individuals observed, 61.3% (155/253) presented periosteal new bone formation in one or more bones. Considering the overall prevalence by sex, more males (n=89) were affected than females (n=66) (Table 5.3), but the difference was not statistically significant. When the distribution of PNBf was examined by age at death, the frequency of cases was found to be significantly higher in the younger group (0.2 months to 44 years; mean=22.64 years old and SD=10.81) compared to the older group (45 to 94 years; mean=63.36 years old and SD= 12.71) ( $\chi^2 = 7.451$ , df =1, p= 0.006).

**Table 5.3:** Distribution of cases of periosteal new bone formation (PNBF) by sex and age at death (F=female, M=male).

PNBF	Sex	Age range (years)		Total
		0.2-44	45-94	
Absent	F	14	35	49
	M	18	31	49
	<b>Subtotal</b>	<b>32 (28.8%)</b>	<b>66 (46.5%)</b>	<b>98 (38.7%)</b>
Present	F	35	31	66
	M	44	45	89
	<b>Subtotal</b>	<b>79 (71.2%)</b>	<b>76 (53.5%)</b>	<b>155 (61.3%)</b>
<b>Total</b>		<b>111</b>	<b>142</b>	<b>253</b>

### 5.1.2.2. Distribution by Cause of Death

An examination of PNBf by cause of death (Table 5.4) revealed a higher prevalence of PNBf (82.5%, 94/114) in individuals who died from tuberculosis (TB) (Group 1), followed by those with other conditions (46%, 23/50) (Group 3) and non-TB infection (42.7%, 38/89)

(Group 2). These differences were highly significant ( $\chi^2 = 39.413$ ,  $df = 2$ ,  $p = 0.000$ ), and in fact, individuals who died from TB were 5.51 times more likely (OR=5.51, CI=95%: 2.6420 to 11.5223) to develop PNBf than those who died from other causes ( $\chi^2=20.8452$ ,  $df=1$ ,  $p=0.000$ ). Furthermore, the TB group (Group 1) also had a 1.79 times increased risk (RR=1.7925, CI=95%: 1.3121 to 2.4489) of developing PNBf than the Group 3. In contrast, no statistically significant association with PNBf was observed within the non-TB group (OR= 0.8747, CI=95%: 0.4357 to 1.7560) ( $\chi^2=0.0395$ ,  $df=1$ ,  $p=0.8426$ ). The relative risk of developing this type of bone lesion was also lower (RR=0.9282, CI=95%: 0.6317 to 1.3639). When combined, the TB and the non-TB infection groups revealed an association with PNBf 2.18 times higher (OR=2.1825, CI=95%: 1.1664 to 4.0836) than in the Group 3 ( $\chi^2=5.3433$ ,  $df=1$ ,  $p=0.02$ ). The relative risk of developing new bone lesions was calculated as 1.41 (RR=1.4136, CI=95%: 1.0297 to 1.9405).

**Table 5.4:** Distribution of individuals affected and unaffected by PNBf according to the cause of death.

Cause of death	PNBF		Unaffected		Total
	n	%	n	%	N
<b>Group 1. Tuberculosis infection (TB)</b>	94	82.5	20	17.5	114
<b>Group 2. Non-TB infection</b>	38	42.7	51	57.3	89
<b>Group 3. Other conditions</b>	23	46	27	54	50
<b>Total</b>	<b>155</b>	<b>61.3</b>	<b>98</b>	<b>38.7</b>	<b>253</b>

### 5.1.2.3. Distribution Pattern within the Skeleton

Amongst the 155 individuals affected with PNBf, 42.6% showed traits of the condition in the ribs (R), 31.6% in the bones of the appendicular skeleton (AB), and the remaining 25.8% in the ribs and appendicular bones (R+AB) (Figure 5.7).

The anatomical distribution of PNBf by age group revealed a high percentage of rib lesions in individuals younger than 45 years of age (56.8%), when compared with the older group (26.7%), a difference that was statistically significant ( $\chi^2=14.064$ ,  $df=1$ ,  $p=0.000$ ) (Table 5.5). Similarly, the frequency of lesions in the ribs and appendicular bones combined was significantly higher in younger individuals ( $\chi^2=7.714$ ,  $df=1$ ,  $p=0.005$ ). The frequency of individuals with PNBf in the appendicular bones was higher in the older age group (36/102, 35.3%); however this difference was not statistically significant.

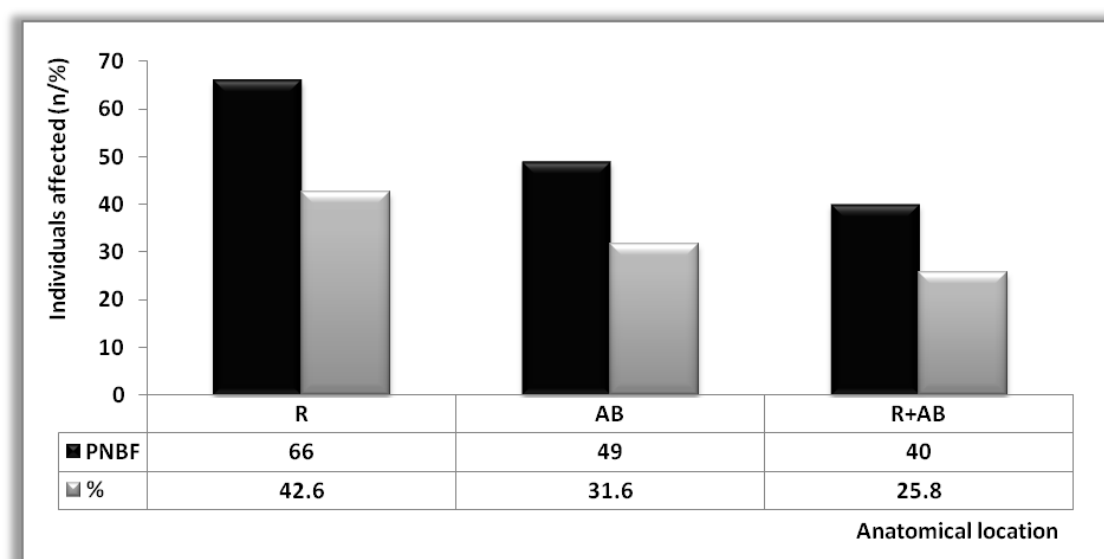


**Figure 5.7:** Number and frequency of individuals affected with PNBf by anatomical location (R: ribs, AB: appendicular bones; R+AB: ribs and appendicular bones).

**Table 5.5:** Distribution of individuals affected with PNBf by age and anatomical location (n=number of individuals affected; N=total number of individuals observed).

Anatomical region	Age range (years)						Chi-square	
	0.2-44		45-94		Total		$\chi^2$	P
	n/N	%	n/N	%	n/N	%		
R	42/74	56.8	24/90	26.7	66/164	40.2	14.064	0.000
AB	13/45	28.9	36/102	35.3	49/147	33.3	0.324	0.569
R+AB	24/56	42.9	16/82	19.5	40/138	29	7.713	0.005
Total	79		76		155		25.688	0.000

When the anatomical distribution of the lesions was examined by cause of death (Table 5.6), a significantly higher frequency of rib lesions was observed in individuals who died from TB infection (56.4%) in comparison with other conditions (18.4%) and non-TB infection (26.1%) ( $\chi^2=57.610$ ,  $df=2$ ,  $p=0.000$ ). Similarly, statistically significant differences ( $\chi^2=50.016$ ,  $df=2$ ,  $p=0.000$ ) were found in individuals who died from TB infection (Group 1) and showed PNBf in the ribs and appendicular bones (36.2%), in comparison with individuals from Group 2 and Group 3. The frequency of PNBf in the appendicular bones was higher in individuals who died from other conditions (69.6%) and lower in those who suffered from TB infection (7.4%); however, these differences were not statistically significant.

**Table 5.6:** Distribution of PNBf by cause of death and anatomical location (n=number of individuals affected; N=total number of individuals affected).

Cause of death	PNBF						Total
	R		AB		R+AB		
	n	%	n	%	N	%	
1. TB infection	53	56.4	7	7.4	34	36.2	94
2. Non-TB infection	7	18.4	26	68.4	5	13.2	38
3. Other conditions	6	26.1	16	69.6	1	4.3	23
<b>Total</b>	<b>66</b>		<b>49</b>		<b>40</b>		<b>155</b>

The anatomical distribution of lesions and its impact on the cause of death was measured by odds ratio. Regarding the presence of PNBf in the ribs, the results showed that individuals who died from TB infection had a 11.9 times greater risk (OR=11.93; CI=95%: 4.2860 to 33.1791) of developing rib lesions than those who died from other conditions, with a significance of  $\chi^2=25.112$  (df=1, p=0.000). The relative risk was calculated as 3.9 (CI=95%: 1.9102-8.3474). No statistically significant relationships were observed between the presence of rib lesions and non-TB causes of death (p=0.624).

When PNBf of the appendicular bone was considered, the analysis showed that its occurrence was less likely in individuals who died from TB infection (OR=0.5906, CI=95%: 0.2047-1.7045) with a  $\chi^2=0.514$  (df=1, p=0.473) when compared with other conditions. The presence of appendicular lesions was also less expected in individuals who perished from non-TB causes of death (OR=0.8603; CI=95%: 0.3951-1.8732), and the results were not statistically significant (p=0.857).

The risk of developing PNBf in the ribs and appendicular bones was 45.9 times higher in individuals who died from TB infection (OR=45.900, CI=95%: 5.786-364.105), and this difference was statistically significant ( $\chi^2=24.214$ , df=1, p=0.00) in comparison with other causes of death. The probability of exhibiting a broader distribution of lesions was also 17.6 times more likely in individuals with TB infection (RR=17.6296; CI=95%: 2.545-122.132) than in those with other conditions. The predicted odds for the individuals who presented bone lesions in the ribs and appendicular skeleton and died from non-TB infections was 2.6 times the odds (OR=2.6471; CI=95%: 0.2941-23.8221) of those who perished from other conditions, with a relative risk that was quite similar (RR=2.5000, CI=95%: 0.3066-20.3869). Despite that, the differences were not statistically significant ( $\chi^2=0.202$ , df=1, p=0.653).

### 5.1.2.3.1. Distribution of PNBf in the Ribs

#### *By individual*

In the 253 individuals who comprise the sample, 243 had preserved ribs that could be examined for PNBf. For the remaining ten individuals the analysis of PNBf was impossible due to the absence of ribs (n=7) or severe postmortem damage (n=3). In the 243 individuals considered, 106 (43.6%) exhibited deposits of new bone on at least one rib (Table 5.7). For the overall sample, the number of affected ribs ranged from 1 in 14 individuals to 22 in one individual, and the average number of ribs with lesions by individual was 2.77 (SD=4.35, Median=0.00). Regarding the frequency and the mean number of ribs affected by age and cause of death, a higher percentage of individuals who were younger than 45 years old and who had died from TB infection (80.3%) had rib lesions compared to older individuals and those who had died from other causes (Group 3). This age group also had a higher number of PNBf in ribs ( $\bar{x}$ =5.45, SD=4.78, Median=5.0). In contrast, a lower frequency (14%) of affected ribs was observed in older individuals who had died from other causes ( $\bar{x}$ =0.65, SD=3.36, Median=0.0).

**Table 5.7:** Frequency and average number of ribs affected with PNBf by individual, age group and cause of death (n=number of individuals affected, N= total number of individuals observed).

Cause of death	Age range (years)											
	0.2-44				45-94				Total			
	n/N	%	$\bar{x}$	SD	n/N	%	$\bar{x}$	SD	n/N	%	$\bar{x}$	SD
<b>Group 1</b>	61/76	80.3	5.45	4.78	26/34	76.5	4.85	4.86	87/110	79.1	<b>5.26</b>	<b>4.79</b>
<b>Group 2</b>	4/23	17.4	0.78	2.22	8/62	12.9	0.69	1.96	12/85	14.1	<b>0.72</b>	<b>2.02</b>
<b>Group 3</b>	1/5	20	1.0	2.24	6/43	14	0.65	3.36	7/48	14.6	<b>0.69</b>	<b>3.24</b>
<b>Total</b>	66/104	<b>63.5</b>	<b>4.20</b>	<b>4.70</b>	40/139	<b>28.8</b>	<b>1.70</b>	<b>3.75</b>	106/243	<b>43.6</b>	<b>2.77</b>	<b>4.35</b>

The results shown above are in agreement with those in Figure 5.8. Accordingly, individuals who died from TB infection (Group 1) were not only those most affected by rib lesions but also those who showed a broader involvement of the rib cage. For example, 12 individuals presented PNBf in seven ribs (11 died from pulmonary TB and one died from intestinal TB); eight individuals who suffered from pulmonary TB showed lesions in ten ribs, and three who also died from pulmonary TB exhibited lesions in 14 ribs. Finally, a young adult male (Sk. 1227, 21 y.o.) had diffuse lesions in eighteen ribs (Figure 5.9).



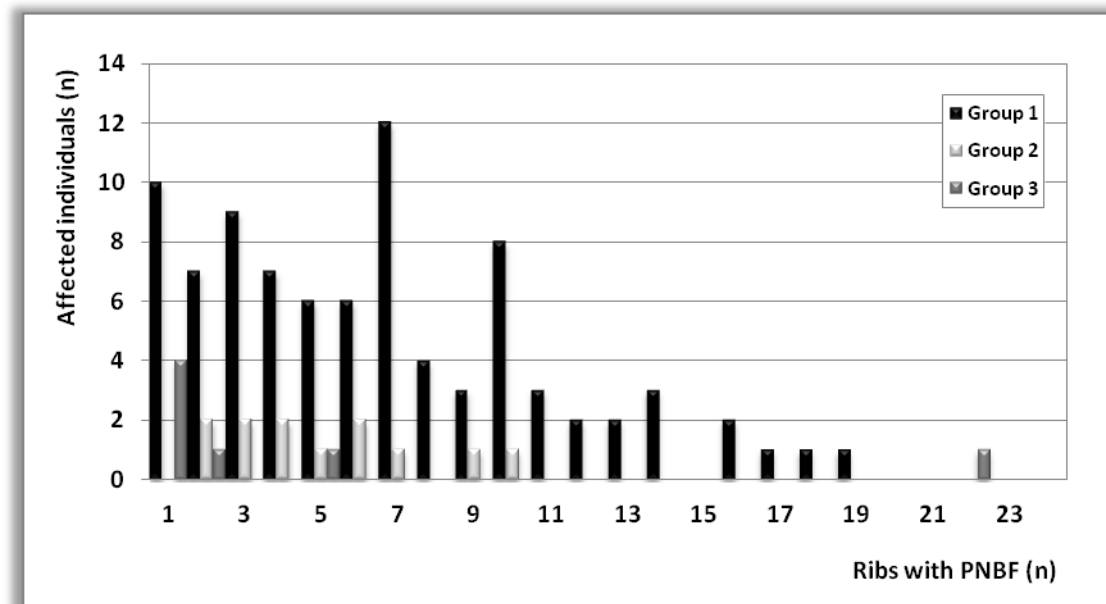


**Figure 5.8:** Number of ribs with PNB in individuals with varying causes of death.

In the non-TB infection group (Group 2), the most extensive involvement of the rib cage was recorded in a young male individual (Sk. 1534-A, 2 y.o.) who died from pneumonia (10 ribs affected), in a middle aged male (Sk. 270, 50 y.o.) who died from bronchopneumonia (9 ribs affected) (Figure 5.10), and in a middle aged male (Sk. 504, 59 y.o.) who died from bronchitis (7 ribs affected). The most widespread distribution in the entire sample (22 ribs affected) was an old male (Sk. 457, 66 y.o) who died from a rectum neoplasm (Group 3 cause of death) (Figure 5.11).

#### ***By ribs affected and side***

Periosteal new bone formation was recorded in 673 (15.9%) out of the 4222 ribs examined (Table 5.8). Similar to previous analysis, younger individuals (<45 years old) who died from TB infection exhibited a higher percentage of rib lesions (35.7%) compared to older individuals from Group 2 and Group 3 (3.4%). In the overall sample, the largest number of ribs showing PNB was recorded in the TB group (33.8%).

With respect to the distribution of PNB in the rib cage (Figure 5.12), the majority of cases involved the upper to middle segment (R1→R6, 60.2% [405/673]) compared to the lower segment (R7→R12, 39.8% [268/673]). A sharp increase in the number of lesions was observed from the first to the fourth and fifth ribs, followed by a more gradual decrease to the tenth rib. The least affected ribs were the first (n=7), eleventh (n=27) and twelfth (n=4) ribs.

**Table 5.8:** Number of rib lesions by age and cause of death [N(ob)=total number of ribs observed, n(PNBF)=total number of ribs affected with periosteal new bone formation].

Cause of death	Age range (years)								
	0.2-44			45-94			Total		
	N(ob)	n(PNBF)	%	N(ob)	n(PNBF)	%	N(ob)	n(PNBF)	%
<b>Group 1</b>	1161	414	35.7	551	165	30	1712	579	33.8
<b>Group 2</b>	372	18	4.8	1250	43	3.4	1622	61	3.8
<b>Group 3</b>	67	5	7.5	821	28	3.4	888	33	3.7
<b>Total</b>	1600	437	27.3	2622	236	9.0	4222	673	15.9

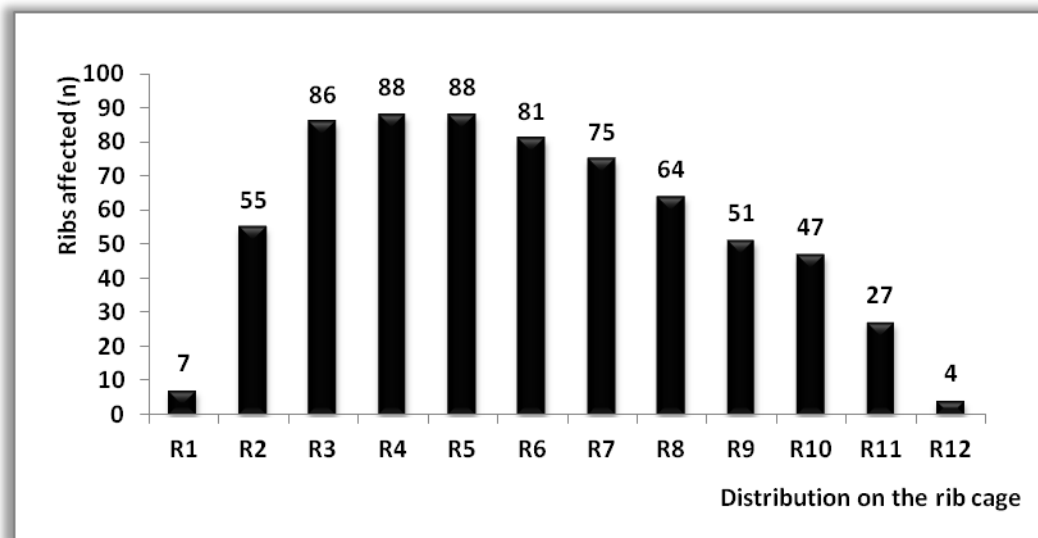


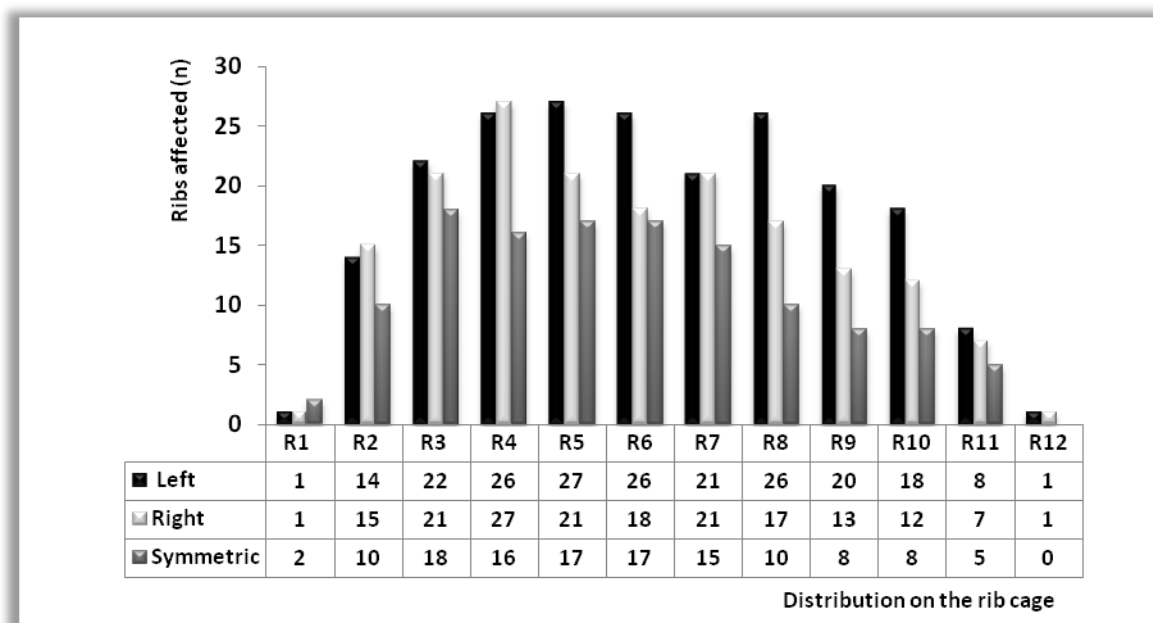
**Figure 5.12:** Distribution of ribs affected by PNBF (left and right ribs combined) by their anatomical order in the rib cage.

An examination of the distribution of bone lesions by side was conducted on only 2255 pairs of ribs (Table 5.9). Those pairs that were incomplete or showed at least one bone damaged postmortem by taphonomic processes were not included in the analysis. In the subgroup considered, PNBF was observed in 510 pairs of ribs, and was one-sided distributed in 75.3 % (384/510) of the cases, compared to symmetrically in 24.7% (126/510) of cases. In general, left-sided lesions (41.2%) were slightly more frequent than those from the right-side (34.1%). The cross tabulation analysis of PNBF by side and cause of death revealed a higher frequency of one-sided lesions in individuals who died from TB infection (Group 1) and non-TB infections (Group 2) [76.3% (338/443) and 83% (39/47), respectively]. In Group 1 the lesions were predominantly located on the left-side (42.9%), whereas in Group 2 they were more often observed on the right-side (46.8%). Regarding individuals who died from other conditions (Group 3), the lesions recorded were essentially symmetrical (65%).

**Table 5.9:** Distribution of ribs affected with PNBFB by side and cause of death [N(ob)= total number of ribs observed; n(PNBFB)= total number of ribs with periosteal new bone formation].

Cause of death	N(ob)	n (PNBFB)		Side and symmetry of the lesions					
		N	%	Left		Right		Symmetric	
				n	%	n	%	n	%
Group 1	1069	443	41.4	190	42.9	148	33.4	105	23.7
Group 2	775	47	6.1	17	36.2	22	46.8	8	17
Group 3	411	20	4.9	3	15	4	20	13	65
<b>Total</b>	<b>2255</b>	<b>510</b>	<b>22.6</b>	<b>210</b>	<b>41.2</b>	<b>174</b>	<b>34.1</b>	<b>126</b>	<b>24.7</b>

An analysis of lesions by their anatomical location and side in the rib cage (Figure 5.13) revealed a predominance of one-sided foci in the majority of ribs examined, with the exception of the first rib that displayed an equal number of one-sided and symmetrical occurrences. A dominance of left-sided lesions was also noted, especially in the fifth and sixth rib and between the eighth and tenth ribs. For example, left-sided lesions were observed in 26 pairs of rib number eight compared to right-sided lesions in only 17 pairs. More right-sided lesions were noted in the second rib (n=15) and the third rib had the highest frequency of symmetrical occurrences (n=18).

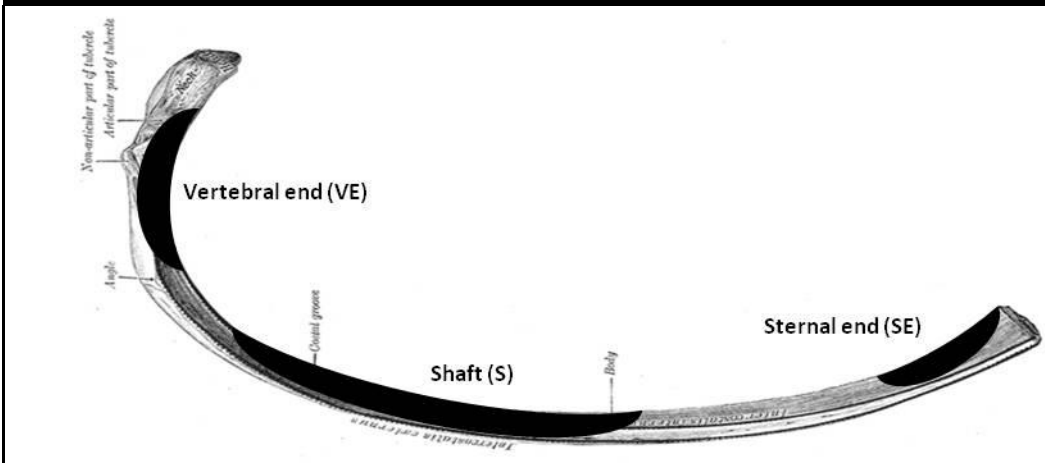
**Figure 5.13:** Distribution of rib lesions by side and anatomical location in the rib cage.

#### ***By ribs affected and anatomical location***

In the 673 affected ribs studied (Table 5.10), 48.9% exhibited intermittent or continuous deposits of new bone all along the visceral surface from the vertebral end (VE) to the sternal

end (SE). In comparison, 38.9% of ribs had PNBF at the vertebral end, and only 0.7% had lesions on the shaft. This general distribution was similar for each cause of death. However, individuals who died from TB infections (Group 1) exhibited a more varied distribution of lesions by bone segment. For example, rib lesions comprising the vertebral end and shaft (n=23), the sternal end and vertebral end (n=8), the sternal end and shaft (n=6), and the shaft (n=5) only were observed in individuals who died from TB infection.

In addition to the analysis of the general distribution of PNBF within the ribs and by cause of death, the location of PNBF by rib order (Figure 5.14) was also examined. Apart from the fourth (n=39) and fifth (n=41) ribs whose lesions were found on the vertebral end, in the remaining bones the deposits of new bone were most often observed alongside the rib shaft, especially of the third (n=40) and the seventh (n=39) ribs. A broader dispersion of the lesions regarding the anatomical segment affected was also observed between the 3<sup>rd</sup> and the 7<sup>th</sup> ribs. The first rib only exhibited diffuse lesions.

**Table 5.10:** Distribution of the lesions observed by rib segment and cause of death.


Anatomical location		Cause of death			
		Group 1	Group 2	Group 3	Total
VE	n	234	20	8	262
	%	89.3	7.6	3.1	38.9
S	n	5	0	0	5
	%	100	0	0	0.7
SE	n	34	6	0	40
	%	85	15	0	5.9
VE+S	n	23	0	0	23
	%	100	0	0	3.4
S+SE	n	6	0	0	6
	%	100	0	0	0.9
VE+SE	n	8	0	0	8
	%	100	0	0	1.2
VE↔SE	n	269	35	25	329
	%	81.8	10.6	7.6	48.9
Total	n	579	61	33	673
	%	86	9.1	4.9	100

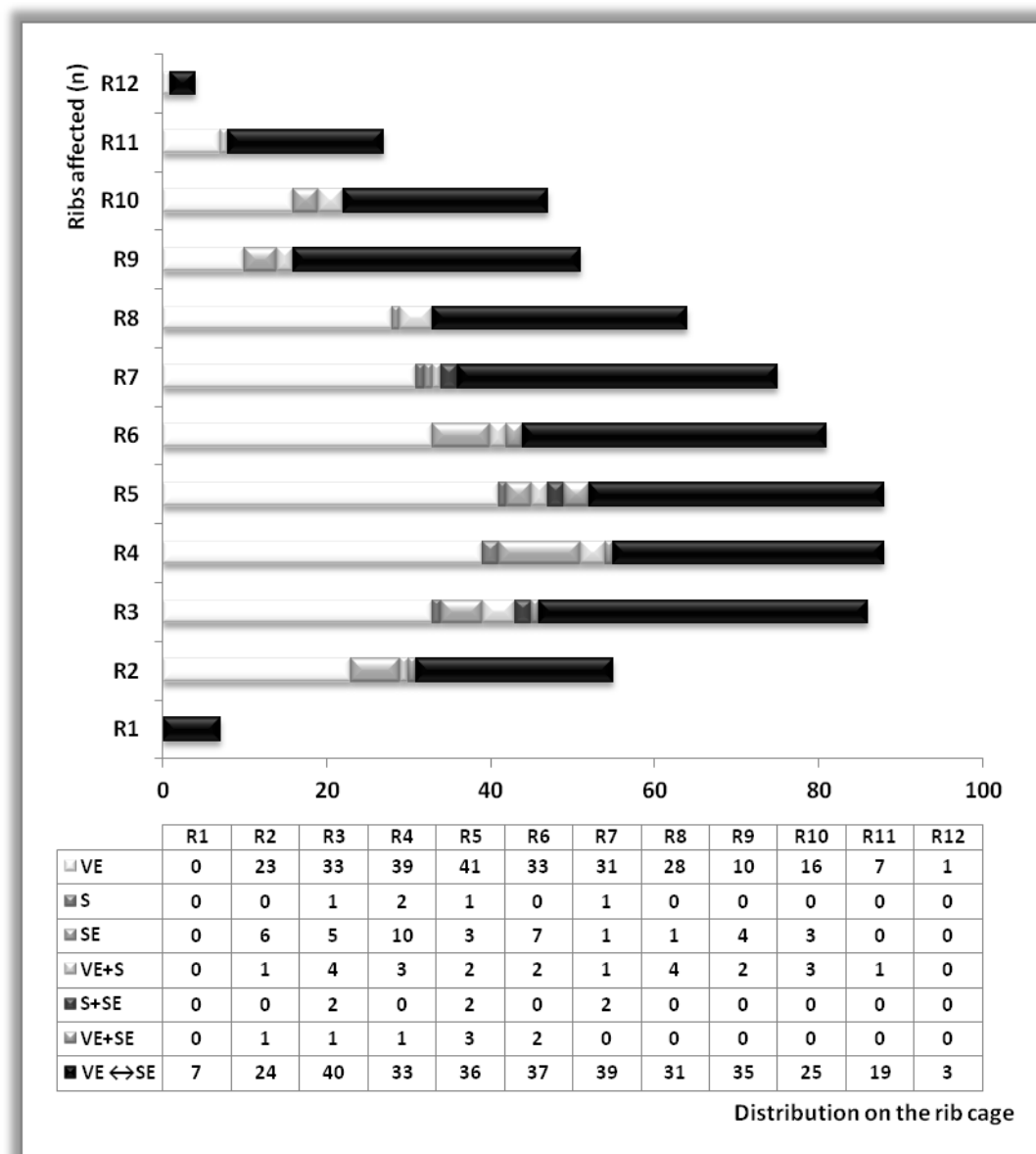


**Figure 5.14:** Distribution of rib lesions by bony segment and anatomical order in the rib cage.

#### ***By ribs affected and type of new bone***

On the ribs affected by PNBFs (n=673), a higher frequency of deposits of mixed woven and lamellar bone (50.7%, 341/673) was observed, followed by woven foci in 30.6% (206/673) of the cases. Lamellar deposition made up only 17.5% of the observations (Figure 5.15). In general, the type of bone reactions that had the lowest frequency (1.2%, 8/673) was proliferative (woven bone) and erosive lesions (Table 5.11).

When the type of bone reaction was examined by cause of death, some differences were found. In the individuals who died from TB infection (Group 1), a high number of ribs

with mixed woven and lamellar reactions (93.5%), as well as with solitary lamellar (90.7%) and woven deposits (70.4%) were recorded. The combination of osteolytic and osteoproliferative lesions was also observed in three tuberculous individuals: two adult males, one of them 68 years old (Sk. 470: one 6<sup>th</sup> left rib affected) (Figure 5.16) and the other one 53 years old (Sk. 332: one 5<sup>th</sup> left rib affected), and a younger female 9 years old (Sk. 1583: three affected pairs, 9<sup>th</sup> to 11<sup>th</sup> ribs). In this last case, the rib lesions observed seem to be associated with the bone changes observed in the thoracic column (Figure 5.17 and 5.18). Accordingly, from the 4<sup>th</sup> to 12<sup>th</sup> thoracic vertebrae, a spectrum of lesions was recorded which were characterized by the complete destruction of the body of the 4<sup>th</sup> to 9<sup>th</sup> vertebrae, ankylosis of the spinous process of the 4<sup>th</sup> to 7<sup>th</sup> vertebrae and subsequent kyphosis formation. In skeleton no. 314, which belongs to a young adult female (20 y.o.) who died of Pott's disease, similar lesions characterized by massive scalloping of the core of the vertebral body were observed in the first and second lumbar vertebrae. Moreover, new bone formation with a vascular and smooth appearance was observed on the lateral segment of the vertebral bodies. However, no signs of rib lesions were seen (Figure 5.19).

**Table 5.11:** Distribution of the type of lesions observed in the ribs by cause of death (W=woven bone; L=lamellar bone; W+L=woven and lamellar bone; W+LT=woven bone and lytic lesions).

Anatomical location		Cause of death			
		Group 1	Group 2	Group 3	Total
W	n	145	30	31	206
	%	70.4	14.6	15	30.6
L	n	107	11	0	118
	%	90.7	9.3	0	17.5
W+L	n	319	20	2	341
	%	93.5	5.9	0.6	50.7
W+LT	n	8	0	0	8
	%	100	0	0	1.2
Total	n	579	61	33	673
	%	86	9.1	4.9	100

A similar distribution was recorded in the non-TB infection group (Group 2), however without the presence of both lytic and proliferative lesions. Inverse results were obtained for Group 3; these individuals showed a high percentage of woven bone lesions (15%), when compared with the mixed pattern of woven/lamellar deposits (0.6%).

The distribution of the type of rib lesions by their anatomical order followed the tendency already mentioned, which was characterized by a predominance of woven/lamellar deposits over the other types, particularly in the 3<sup>rd</sup> to 8<sup>th</sup> ribs. Only the 3<sup>rd</sup> and 4<sup>th</sup> ribs showed more cases of woven bone (Figure 5.20).

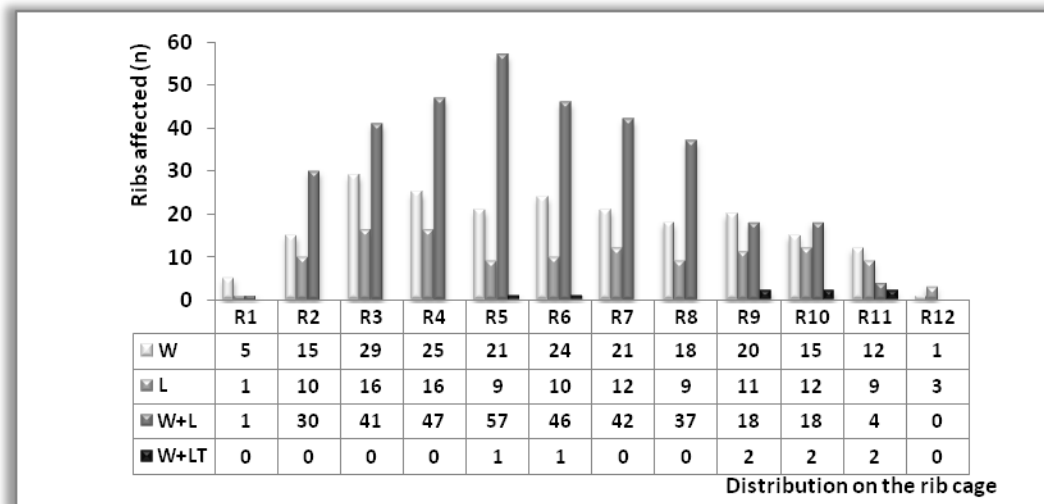


**Figure 5.20:** Distribution of the ribs affected by type of new bone formed and anatomical order in the rib cage (W=woven bone; L=lamellar bone; W+L=woven and lamellar bone; W+LT=woven bone and lytic lesions).

### 5.1.2.3.2. Distribution of PNB in the Appendicular Skeleton

#### *By total number of bones affected*

In the 253 individuals that comprise the sample, PNB was observed in 367 (4.7%) out of 7844 bones examined from the appendicular skeleton (Table 5.12).

In terms of the number of bones affected, a higher frequency of cases was observed in the lower limb (7.5%, 307/4100) in comparison with the upper limb (1.6%, 60/3744). In the lower limb, the lesions were recorded primarily in the tibia (23.5%), femur (16.1%), and fibula (9.9%), with minimal differences regarding the side of the condition. The bones least affected were the innominate (2.3%), the 4<sup>th</sup> metatarsal (2.7%), and the 3<sup>rd</sup> (3%) and 5<sup>th</sup> metatarsals (3.2%). In the upper limb, the humerus (3.2%) and the bones from the forearm (3.7%) and scapula (2.8%) presented more deposits of new bone than the other bones. A similar distribution with respect to the side of the lesions was also evident in the upper limb. The bones from the hands were less affected; for example, no evidence of periosteal reactions was observed in the 4<sup>th</sup> and 5<sup>th</sup> metacarpals.



**Table 5.12:** Distribution of the bones affected with PNBf in the upper and lower limbs by side and total sample (N=total number of individuals; n=number of individuals affected).

BONES	Upper limb						Total	
	Left			Right				
	N(o)	n(PNBF)	%	N(o)	n(PNBF)	%	n(PNBF)/N(o)	%
Clavicle	202	1	0.5	201	1	0.5	2/403	0.5
Scapula	214	7	3.3	219	5	2.3	<b>12/433</b>	<b>2.8</b>
Humerus	173	4	2.3	<b>175</b>	<b>7</b>	<b>4</b>	<b>11/348</b>	<b>3.2</b>
Radius	<b>190</b>	<b>7</b>	<b>3.7</b>	<b>189</b>	<b>7</b>	<b>3.7</b>	<b>14/379</b>	<b>3.7</b>
Ulna	<b>185</b>	<b>8</b>	<b>4.3</b>	192	6	3.1	<b>14/377</b>	<b>3.7</b>
1 <sup>st</sup> Metc <sup>1</sup>	160	1	0.6	172	1	0.6	2/332	0.6
2 <sup>nd</sup> Metc	193	2	1	200	2	1	4/393	1
3 <sup>rd</sup> Metc	190	0	0	202	1	0.5	1/392	0.3
4 <sup>th</sup> Metc	173	0	0	178	0	0	0/351	0
5 <sup>th</sup> Metc	166	0	0	170	0	0	0/336	0
<b>Subtotal</b>	<b>1846</b>	<b>30</b>	<b>1.6</b>	<b>1898</b>	<b>30</b>	<b>1.6</b>	<b>60/3744</b>	<b>1.6</b>
	Lower limb							
Innominate	236	6	2.5	239	5	2.1	11/475	2.3
Femur	<b>209</b>	<b>32</b>	<b>15.3</b>	<b>206</b>	<b>35</b>	<b>17</b>	<b>67/415</b>	<b>16.1</b>
Tibia	<b>187</b>	<b>44</b>	<b>23.5</b>	<b>187</b>	<b>44</b>	<b>23.5</b>	<b>88/374</b>	<b>23.5</b>
Fibula	<b>203</b>	<b>21</b>	<b>10.3</b>	<b>202</b>	<b>19</b>	<b>9.4</b>	<b>40/405</b>	<b>9.9</b>
1 <sup>st</sup> Mett <sup>2</sup>	205	10	4.9	208	11	5.3	21/413	5.1
2 <sup>nd</sup> Mett	201	9	4.5	197	14	7.1	23/398	5.8
3 <sup>rd</sup> Mett	202	5	2.5	203	7	3.4	12/405	3
4 <sup>th</sup> Mett	197	4	2	207	7	3.4	11/404	2.7
5 <sup>th</sup> Mett	180	5	2.8	191	7	3.7	12/371	3.2
Calcaneus	218	10	4.6	222	12	5.4	22/440	5
<b>Subtotal</b>	<b>2038</b>	<b>146</b>	<b>7.2</b>	<b>2062</b>	<b>161</b>	<b>7.8</b>	<b>307/4100</b>	<b>7.5</b>
							<b>Total:</b>	<b>367/7844</b>
								<b>4.7</b>

<sup>1</sup>Metc= Metacarpal bones; <sup>2</sup>Mett= Metatarsal bones

### *By individuals affected*

Periosteal reactions in the appendicular skeleton were recorded in 35.2% (89/253) of the individuals analyzed. In the individuals affected, the bones most frequently involved were those from the lower limb (Figure 5.21) such as the tibia (n=51,  $\chi^2=39.175$ , df=1, p=0.000), the femur (n=39,  $\chi^2=27.048$ , df=1, p=0.000), the fibula (n=24,  $\chi^2=15.123$ , df=1, p=0.000) and the 2<sup>nd</sup> metatarsal (n=19,  $\chi^2=10.908$ , df=1, p=0.001) and these results were statistically significant in comparison with the results obtained in the remaining bones. Fewer deposits of new bone were observed on the innominate, with only six individuals affected, and in the remaining foot bones, and none of the differences were statistically significant. In the upper limb the most frequently affected bones were the ulna (10 individuals), humerus and radius (eight and nine individuals, respectively); nevertheless, no statistic significance was found. The clavicle and metacarpals were the least affected bones in the individuals studied.

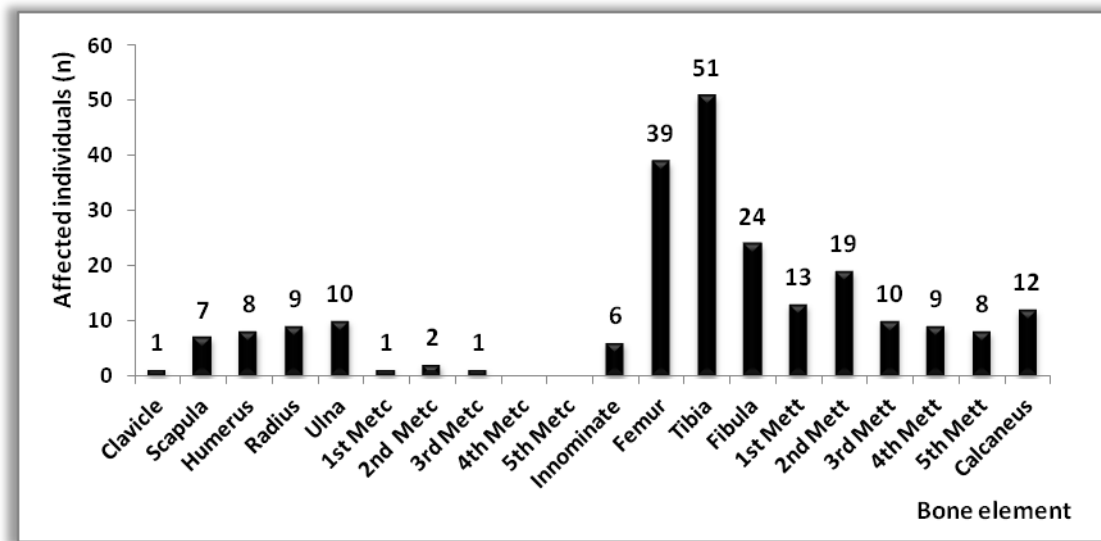


**Figure 5.21:** Distribution of the individuals affected with PNBf by bone type (upper and lower limb).

#### ***By age and cause of death of the individuals affected***

The frequency of PNBf in the appendicular bones by age of the individuals affected is illustrated in Table 5.13. In the individuals younger than 45 years of age, a higher prevalence of lesions was observed in the upper limb, with the highest rates recorded in the humerus (11.8%, 8/68), the radius and the ulna (both with 6.1%, 5/82). When compared with the older age group, however, no statistically significant differences were observed. On the tubular bones of the hands, lesions were mostly observed in the older group.

In the lower limb, a similar distribution of bone lesions among age groups was observed in the femur (younger age group, 18.3% and older age group, 19.1%). In contrast, significantly more tibiae (38.8%, 38/98 with a  $\chi^2=6.927$ ,  $df=1$ ,  $p=0.008$ ) and fibulae (17.5%, 20/114 with a  $\chi^2=6.403$ ,  $df=1$ ,  $p=0.011$ ) were affected in older individuals than in younger ones. In the younger group, other bones such as the 2<sup>nd</sup> metatarsal (10.7%) and the calcaneus (8.9%) were frequently affected, but the differences were not statistically significant ( $p>0.05$ ).

**Table 5.13:** Distribution of periosteal reactions in the bones from the upper and lower limb of the individuals affected by age groups (N=total number of individuals; n=number of individuals affected).

Bones	Age range (years)								P
	0.2-44			45-94			Total		
	N(o)	n(PNBF)	%	N(o)	n(PNB F)	%	n/N	%	
Clavicle	89	0	0	129	1	0.8	1/218	0.5	---
Scapula	92	4	4.3	131	3	2.3	7/223	3.1	---
Humerus	<b>68</b>	<b>8</b>	<b>11.8</b>	119	0	0	8/187	4.3	---
Radius	<b>82</b>	<b>5</b>	<b>6.1</b>	126	4	3.2	9/208	4.3	---
Ulna	<b>82</b>	<b>5</b>	<b>6.1</b>	125	5	4	10/207	4.8	---
1 <sup>st</sup> Metc <sup>1</sup>	81	0	0	116	1	0.9	1/197	0.5	---
2 <sup>nd</sup> Metc	88	1	1.1	134	1	0.8	2/222	0.9	---
3 <sup>rd</sup> Metc	87	0	0	132	1	0.8	1/219	0.5	---
4 <sup>th</sup> Metc	87	0	0	118	0	0	0/205	0	---
5 <sup>th</sup> Metc	80	0	0	121	0	0	0/201	0	---
<b>Total</b>	<b>836</b>	<b>23</b>	<b>2.8</b>	<b>1251</b>	<b>16</b>	<b>1.3</b>	<b>39/2087</b>	<b>1.9</b>	
Innominate	106	4	3.8	136	2	1.5	6/242	2.5	---
Femur	<b>93</b>	<b>17</b>	<b>18.3</b>	<b>115</b>	<b>22</b>	<b>19.1</b>	39/208	18.8	---
Tibia	<b>88</b>	<b>13</b>	<b>14.8</b>	<b>98</b>	<b>38</b>	<b>38.8</b>	51/186	27.4	<b>0.008</b> *
Fibula	97	4	4.1	<b>114</b>	<b>20</b>	<b>17.5</b>	24/211	11.4	<b>0.011</b> *
1 <sup>st</sup> Mett <sup>2</sup>	94	2	2.1	123	11	8.9	13/217	6	---
2 <sup>nd</sup> Mett	<b>84</b>	<b>9</b>	<b>10.7</b>	127	10	7.9	19/211	9	---
3 <sup>rd</sup> Mett	86	4	4.7	131	6	4.6	10/217	4.6	---
4 <sup>th</sup> Mett	89	3	3.4	127	6	4.7	9/216	4.2	---
5 <sup>th</sup> Mett	87	1	1.1	123	7	5.7	8/210	3.8	---
Calcaneus	<b>90</b>	<b>8</b>	<b>8.9</b>	136	4	2.9	12/226	5.3	---
<b>Total</b>	<b>914</b>	<b>65</b>	<b>7.1</b>	<b>1230</b>	<b>126</b>	<b>10.2</b>	<b>191/2144</b>	<b>8.9</b>	

\*Chi-square with continuity correction

<sup>1</sup>Metc= Metacarpal bones; <sup>2</sup>Mett= Metatarsal bones

The distribution of the bones affected by individual and cause of death (Table 5.14) revealed a high prevalence of PNBF in the ulna (7.9%), humerus (7.6%), and radius (6.5%) in the individuals who died of TB infection (Group 1), when compared with those who died from other causes (Group 3). In spite of the differences found among groups, the results were not significant. In the individuals who died from non-TB infections (Group 2), the most frequently affected bones in the upper limb were the radius (4.2%) and scapula (3.9%). Once again, no statistically significant differences were observed. For those who died of other conditions, the most frequently affected bones were the scapula (4.4%) and clavicle (2.3%), but the differences were not statistically significant. Regarding the bones from the lower limb, the femur showed a high percentage of lesions in individuals who died from other conditions (25%) compared to those who passed away from non-TB infections (20.8%) and TB infections (14.6); however, the differences were not statistically significant. The lesions of the tibia were more frequently observed in individuals from Group 3 (41.2%) and Group 2 (36.7%), than in those from Group 1 (16.3%), and the differences were statistically significant ( $\chi^2=6.596$ ,  $df=2$ ,

$p=0.037$ ). When the groups were compared separately for the presence of PNB in the tibiae, significant differences were found between Group 1 and Group 2 ( $\chi^2=4.059$ ,  $df=1$ ,  $p=0.044$ ), and between Group 1 and Group 3 ( $\chi^2=4.053$ ,  $df=1$ ,  $p=0.044$ ). In contrast, no significant differences were noted between the non-TB infectious group and the group comprising individuals who died from other conditions ( $\chi^2=0.007$ ,  $df=1$ ,  $p=0.933$ ). Similar results were obtained for the fibulae, which were most frequently affected in the individuals from Group 2 and Group 3 compared to those who died from TB infection ( $\chi^2=6.362$ ,  $df=2$ ,  $p=0.042$ ). Significant differences were also observed between Group 1 and Group 2 ( $\chi^2=4.509$ ,  $df=1$ ,  $p=0.034$ ), but not between Groups 1 and 3 or Groups 2 and 3 ( $p>0.05$ ).

**Table 5.14:** Distribution of periosteal reactions in the bones from the upper and lower limb of the individuals affected by cause of death (N=total number of individuals; n=number of individuals affected).

Bones	Cause of death									P
	Group 1			Group 2			Group 3			
	N(o)	n(PNB F)	%	N(o)	n(PNBF)	%	N(o)	n(PNBF)	%	
Clavicle	93	0	0	81	0	0	44	1	2.3	---
Scapula	102	2	2	76	3	3.9	45	2	4.4	---
Humerus	79	6	7.6	67	2	3	41	0	0	---
Radius	93	6	6.5	71	3	4.2	44	0	0	---
Ulna	89	7	7.9	73	2	2.7	45	1	2.2	---
1 <sup>st</sup> Metc	90	0	0	68	1	1.5	39	0	0	---
2 <sup>nd</sup> Metc	104	1	1	73	1	1.4	45	0	0	---
3 <sup>rd</sup> Metc	103	0	0	72	1	1.4	44	0	0	---
4 <sup>th</sup> Metc	99	0	0	64	0	0	42	0	0	---
5 <sup>th</sup> Metc	94	0	0	66	0	0	41	0	0	---
<b>Total</b>	<b>946</b>	<b>22</b>	<b>2.3</b>	<b>711</b>	<b>13</b>	<b>1.8</b>	<b>430</b>	<b>4</b>	<b>0.9</b>	
Innominate	112	0	0	83	4	4.8	47	2	4.3	---
Femur	96	14	14.6	72	15	20.8	40	10	25	---
Tibia	92	15	16.3	60	22	36.7	34	14	41.2	0.037
Fibula	101	5	5	69	12	17.4	41	7	17.1	0.042
1 <sup>st</sup> Mett	104	4	3.8	67	7	10.4	46	2	4.3	---
2 <sup>nd</sup> Mett	95	12	12.6	72	3	4.2	44	4	9.1	---
3 <sup>rd</sup> Mett	100	5	5	70	4	5.7	47	1	2.1	---
4 <sup>th</sup> Mett	101	3	3	69	5	7.2	46	1	2.2	---
5 <sup>th</sup> Mett	99	3	3	68	4	5.9	43	1	2.3	---
Calcaneus	103	7	6.8	76	4	5.3	47	1	2.1	---
<b>Total</b>	<b>1003</b>	<b>68</b>	<b>6.8</b>	<b>706</b>	<b>80</b>	<b>11.3</b>	<b>435</b>	<b>43</b>	<b>9.9</b>	

When the individuals in Groups 1 and 2 were combined and were compared with the individuals who died from other conditions (i.e. Group 3), no statistically significant differences were found in the distribution of bone lesions in the upper and lower limb.

***By individuals affected, laterality and symmetry***

The distribution of the bone lesions in the upper limb (Figure 5.22) by side and symmetry revealed that most of the individuals presented symmetric foci of new bone, more frequent in the scapula (n=5) and radius (n=5) (Figure 5.23). The only exceptions were recorded in the ulna of five individuals who exhibited more left lesions and in the 3<sup>rd</sup> metacarpal of one skeleton that only presented right lesions. In the humerus, only three individuals presented symmetric lesions (Figure 5.24), the majority exhibiting one-sided foci.

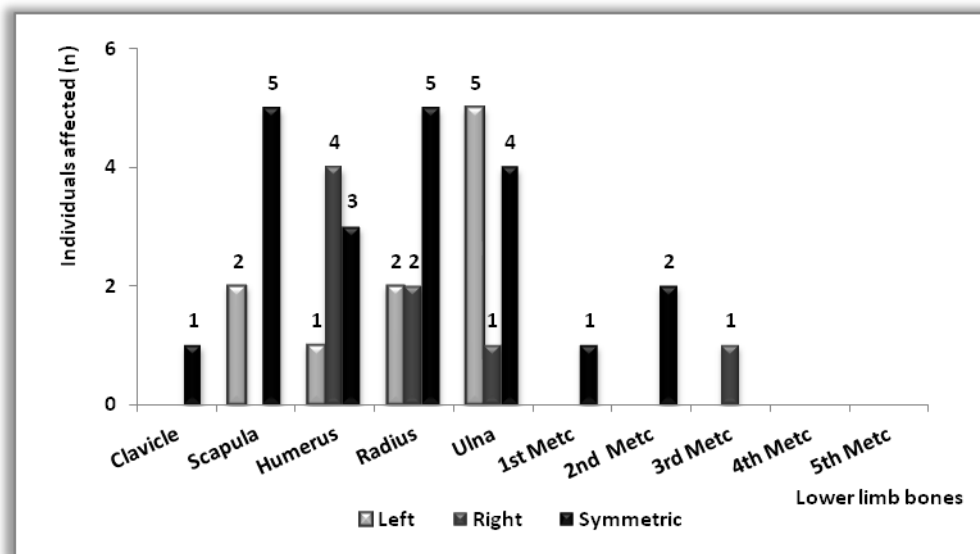


**Figure 5.22:** Distribution of the individuals affected with PNBf by the bones from the upper limb and laterality.

In the lower limb (Figure 5.25), a high frequency of symmetric bone lesions was observed in the tibiae of 37 individuals (Figure 5.26), in the femurs of 28 individuals, in the fibulae of fifteen, in the calcaneus of ten, and in the innominate of five skeletons. With the exception of the 1<sup>st</sup> and 5<sup>th</sup> metatarsal (Figure 5.27), the remaining foot bones showed a predominance of one-sided lesions, more common in the right-side. For the tibia, an equal number of individuals affected by right and left lesions was observed (Figure 5.28). No significant differences in side were observed when analyzed by cause of death.

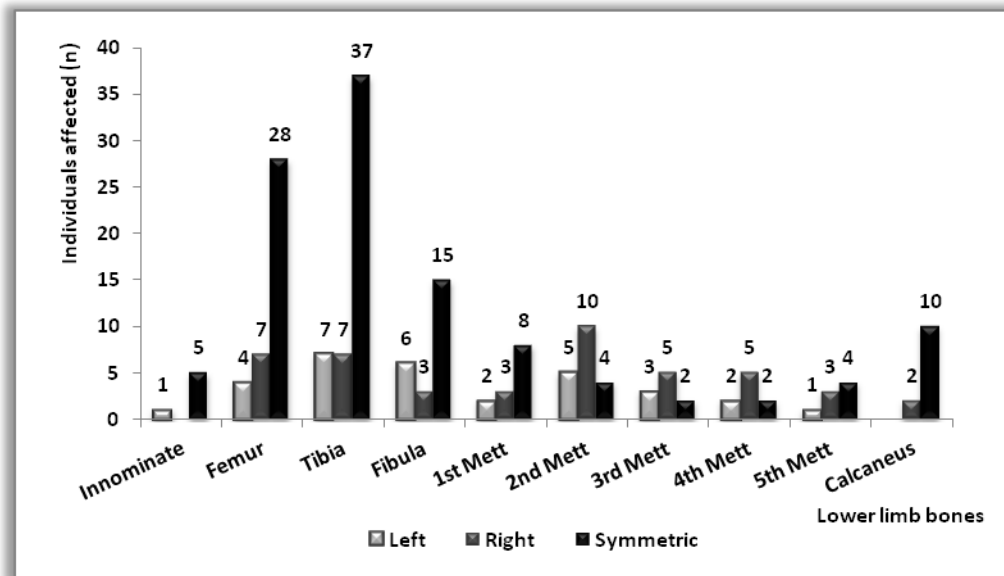


Figure 5.25: Distribution of individuals affected with PNB in the lower limb bones by side.

Identical results were obtained when the number of pairs of bones affected with symmetrical lesions per individual was investigated (Figure 5.29). Although the individuals who died of tuberculosis presented more pairs of bones affected in both categories (less and more than two symmetrical bones involved), the differences were not statistically significant in relation to other causes of death. Even when the two infectious groups (Groups 1 and 2) were combined and compared with Group 3, no statistically significant differences were found.

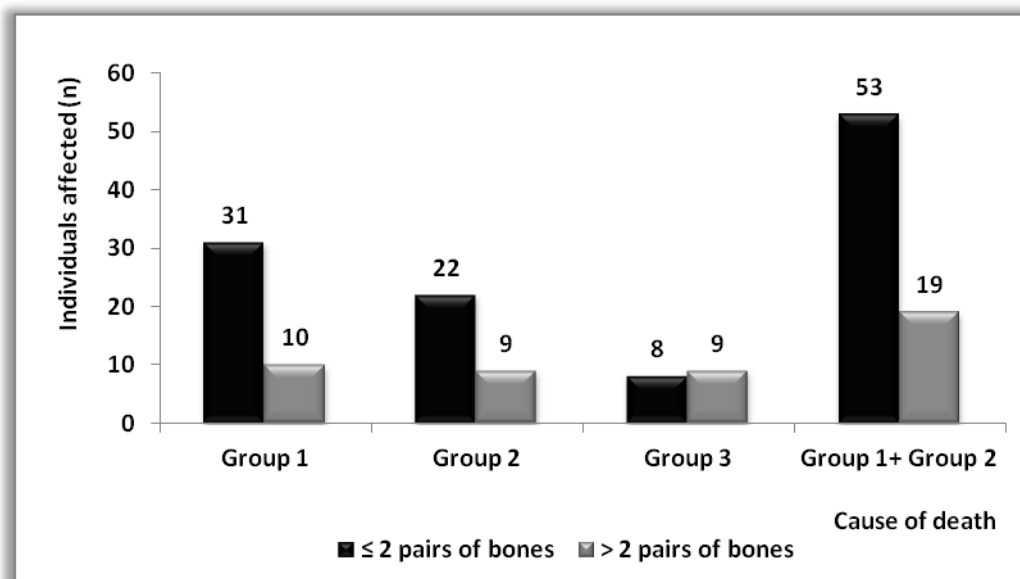


Figure 5.29: Distribution of individuals with two or less affected symmetrical bones by cause of death.

In fact, few differences were noticed amongst groups regarding individuals with a broader involvement of the skeleton. For example, in the TB infection group (Group 1), an extensive dispersion of lesions was observed in an adult female (Sk. 1604, 45 y.o.) who died of TB and who presented symmetrical involvement of the radius, ulna, femur, tibia, fibula, calcaneus and 1<sup>st</sup> and 5<sup>th</sup> metatarsals; in a young adult male (Sk. 684, 16 y.o.) who died of acute phthisis and showed symmetric lesions in the humerus, tibia, fibula and two asymmetric foci in the left ulna and in the 2<sup>nd</sup> right metatarsal; in a young male (Sk. 54, 23 y.o.) who died of pulmonary TB and exhibited symmetric lesions in the femur, tibia and calcaneus and an asymmetric foci in the right radius; and in an young adult male (Sk. 422, 21 y.o) who died of pulmonary TB and presented symmetric lesions in the ulna, femur and asymmetric foci in the left scapula and right humerus and radius.

In the non-TB group (Group 2) , a broader involvement of the skeleton was recorded in a non-adult male (Sk. 1534-A, 14 months) who died of pneumonia and showed symmetric bone lesions in the scapula, humerus, innominate, femur, tibia and fibula; in an adult male (Sk. 312, 69 y.o.) who died of pulmonary abscess and presented symmetric lesions in the radius, ulna, femur, tibia, 1<sup>st</sup> and 2<sup>nd</sup> metacarpals and 1<sup>st</sup> metatarsals; in an adult male (Sk. 507, 51 y.o.) who died of pulmonary emphysema and who exhibited symmetric new bone foci in the radius, femur, tibia, fibula and in the 1<sup>st</sup> metatarsals, and an asymmetric deposit on the left scapula (Figure 5.30). Slight new bone reactions with a symmetric involvement of the ulna, tibia and 1<sup>st</sup> metatarsal, and asymmetric distribution in the femur were observed in an adult male (Sk. 491, 66 y.o.) who died of syphilis (Figure 5.31 and 5.32). PNBf with a symmetrical pattern affecting the tibiae and fibulae equally was also observed in an adult male (Sk. 35, 47 y.o) who died of leprosy (Figure 5.33).

In the group of individuals who died of other causes, a major dispersion of the bone lesions was recorded in an adult male (Sk.457, 66 y.o) who died of rectum neoplasm, exhibiting symmetric lesions in the clavicle, scapula, innominate and femur, and in an adult male (Sk. 1484, 73 y.o) who died of gastric ulcer, presenting symmetric lesions in the femur, tibia and fibula (Figure 5.34 and 5.35). An identical dispersion was observed in two adult females who died from arteriosclerosis (Sk. 429 - 67 y.o. and Sk.971 - 74 y.o).

No significant differences were found when the distribution of individuals affected with symmetrical lesions was analyzed by age groups.

***By individuals, dispersion of lesions and bone segment affected***

Regarding the dispersion of lesions along the bone surface, a distinct pattern in the upper and lower limb was observed (Figure 5.36).

In the upper limb, a high number of individuals had localized lesions in the shaft of the ulna (n=9), radius (n=8) and humerus (n=6). The bone elements that exhibited more diffuse lesions were the scapula, present in five individuals, and the 2<sup>nd</sup> metacarpal, observed in only two individuals.

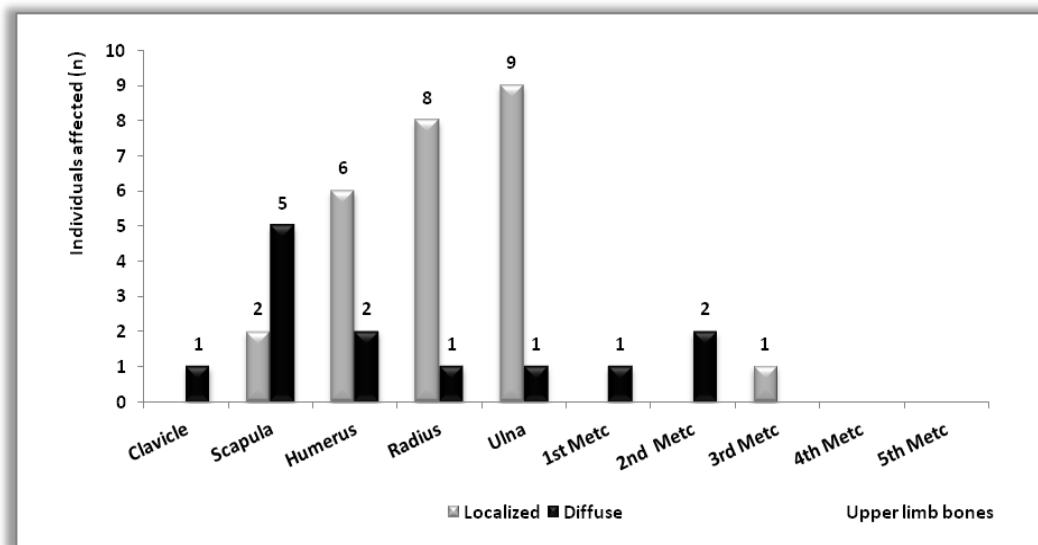


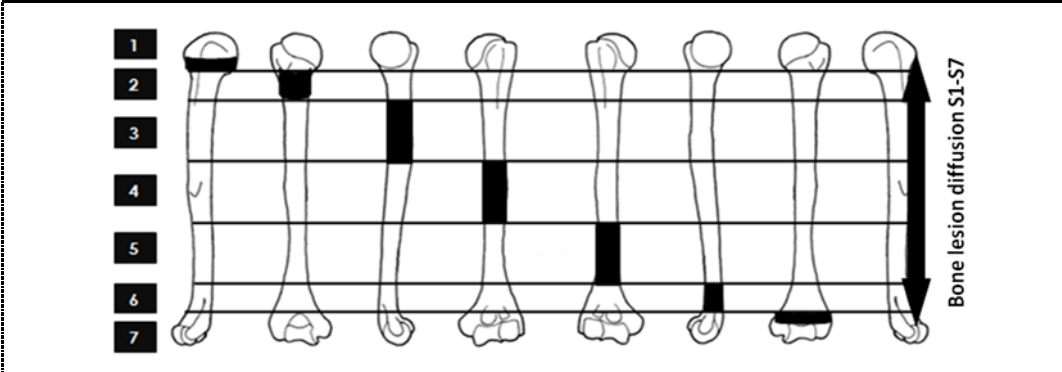
**Figure 5.36:** Distribution of individuals affected with PNBf of the upper limb bones, according to the extent of lesions.

A statistical comparison of the frequencies for each bone from the upper limb by age and cause of death did not yield any significant results.

When the distribution of lesions by long bone segment (humerus, radius, ulna) and cause of death was analyzed (Table 5.15), individuals who died of TB showed more deposits of new bone localized on the lower portion of the humerus (n=4) and radius (n=4), and on the upper portion of the ulna (n=3), in comparison to those who died of other conditions (Group 3). The lesions of the metacarpals were observed only on the medial portion of the diaphysis.



**Table 5.15:** Distribution of individuals affected with PNBf by cause of death (upper limb bones: humerus, radius and ulna) (S=bone segment; D=diffuse).



Bone	Number of segments affected (S)	Cause of death		
		Group 1 Location (n)	Group 2 Location (n)	Group 3 Location (n)
Humerus	One	S2 (1), S6 (4)	S6(1)	0
	Two	0	0	0
	Three or more	D(1)	D(1)	0
Radius	One	S6 (4), S7 (2)	S6(1), S7(1)	0
	Two	0	0	0
	Three or more	0	D(1)	0
Ulna	One	S1(3), S2(1)	0	S5(1)
	Two	S2+S3 (2) S4+S5(1)	S6+S7 (1)	0
	Three or more	0	D(1)	0

In contrast to the results obtained for the upper limb, a high frequency of diffuse lesions were found on the shaft of the tibia, observed in 31 individuals, on the diaphysis of the fibula, noticed in 19 individuals, and on the shaft of the 2<sup>nd</sup> metatarsal, recorded in 15 individuals (Figure 5.37). Diffuse lesions were also observed on the body of the calcaneus of eleven individuals. Only the femur showed a high prevalence of localized lesions, present in 28 individuals.

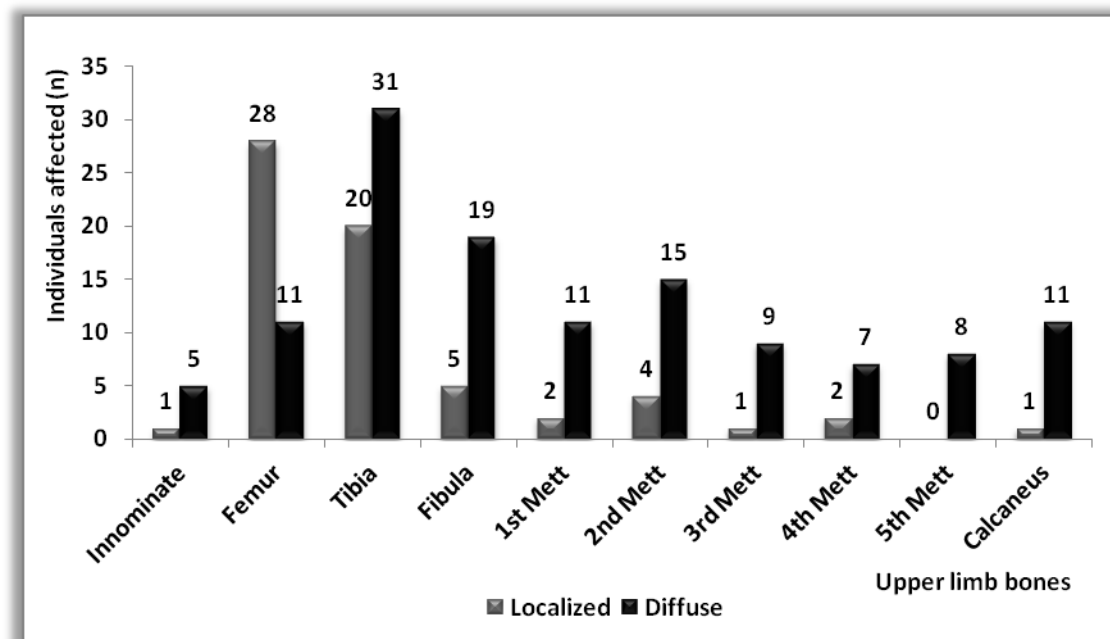


**Figure 5.37:** Distribution of individuals affected with PNBf in the lower limb bones, according to the extent of lesions.

The dispersion of lesions in the shaft of the bones from the lower limb was examined by age and cause of death of the individuals. As indicated in Table 5.16, high frequencies of both focal or localized and diffuse lesions were observed in individuals older than 45 years of age. The only exceptions were the innominate (66.7%) and calcaneus (58.3%) of individuals from the younger group, which showed a high percentage of diffuse lesions.

**Table 5.16:** Distribution of individuals affected with PNBf in the bones of the lower limb by age range (n=number of individuals with bone lesions).

Bone	Age range (years)								Total	P
	0.2-44				45-94					
	Localized		Diffuse		Localized		Diffuse			
n	%	n	%	n	%	n	%			
<b>Innominate</b>	0	0	4	66.7	1	16.7	1	16.7	6	---
<b>Femur</b>	14	35.9	3	7.7	14	35.9	8	20.5	39	---
<b>Tibia</b>	<b>7</b>	<b>13.7</b>	<b>6</b>	<b>11.8</b>	<b>13</b>	<b>25.5</b>	<b>25</b>	<b>49</b>	<b>51</b>	<b>0.011</b>
<b>Fibula</b>	1	4.2	3	12.5	4	16.7	16	66.7	24	---
<b>1st Mett</b>	0	0	2	15.4	2	15.4	9	69.2	13	---
<b>2nd Mett</b>	1	5.3	8	42.1	3	15.8	7	36.8	19	---
<b>3rd Mett</b>	0	0	4	40	1	10	5	50	10	---
<b>4th Mett</b>	2	22.2	1	11.1	0	0	6	66.7	9	---
<b>5th Mett</b>	0	0	1	12.5	0	0	7	87.5	8	---
<b>Calcaneus</b>	1	8.3	7	58.3	0	0	4	33.3	12	---

An equal number of individuals with focalized periosteal lesions in the femurs (35.9%) were observed in both age groups. In the older group, the bones most frequently affected with diffuse lesions were the 5<sup>th</sup> and 1<sup>st</sup> metatarsal (87.5% and 69.2%, respectively) and the fibula (66.7%). Although differences were observed between the age groups, only the results computed for the tibia were found to be statistically significant ( $\chi^2=9.011$ ,  $df=2$ ,  $p=0.011$ ).

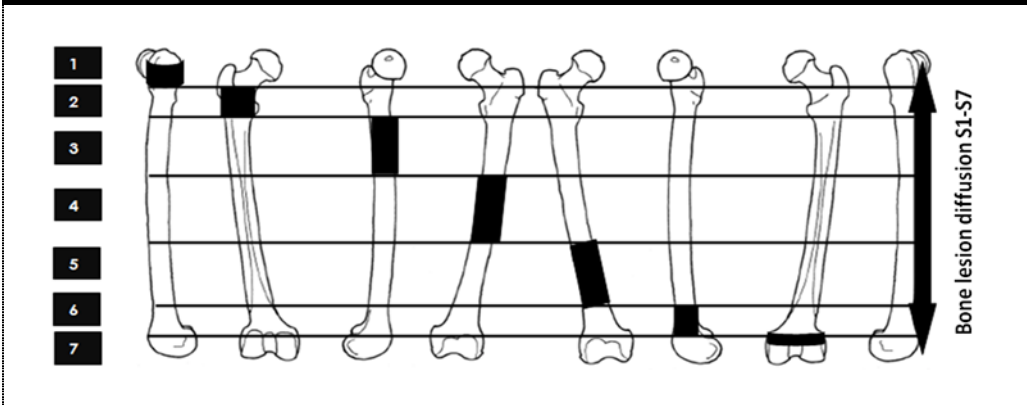
Apart from the femur that showed more focal lesions in individuals who died from TB infection (30.8%) and non-TB infection (25.6%), the general pattern was characterized by diffuse foci of new bone, especially in Group 2 (Table 5.17). For example, the innominate was affected in 66.7% of the individuals, the 4<sup>th</sup> metatarsal in 55.6%, the 5<sup>th</sup> metatarsal in 50%, and the 1<sup>st</sup> metatarsal in 46.2% of the subjects analysed. The calcaneus and the 3<sup>rd</sup> metatarsal were more frequently affected by diffuse periosteal reactions in Group 1 (both with 50%), whereas the fibula was more frequently involved in Group 3 (29.2%). Like the previous analysis, only the differences recorded for the tibia were found to be statistically significant ( $\chi^2=10.979$ ,  $df=4$ ,  $p=0.027$ ) among cause of death groups.

**Table 5.17:** Distribution of individuals affected with PNBf in the bones of the lower limb by cause of death (n=number of individuals with bone lesions).

Bone	Cause of death										Total	P		
	Group 1		Group 2				Group 3							
	Localized n	Diffuse %	Localized n	Diffuse %	Localized n	Diffuse %	Localized n	Diffuse %	Localized n	Diffuse %				
Innominate	0	0	0	0	4	66.7	1	16.7	1	16.7	6	---		
Femur	12	30.8	2	5.1	10	25.6	5	12.8	6	15.4	4	10.3	39	---
Tibia	<b>9</b>	<b>17.6</b>	<b>6</b>	<b>11.8</b>	<b>8</b>	<b>15.7</b>	<b>14</b>	<b>27.5</b>	<b>3</b>	<b>5.9</b>	<b>11</b>	<b>21.6</b>	<b>51</b>	<b>0.027</b>
Fibula	1	4.2	4	16.7	4	16.7	8	33.3	0	0	7	29.2	24	---
1st Mett	1	7.7	3	23.1	1	7.7	6	46.2	0	0	2	15.4	13	---
2nd Mett	3	15.8	9	47.4	0	0	3	15.8	1	5.3	3	15.8	19	---
3rd Mett	0	0	5	50	1	10	3	30	0	0	1	10	10	---
4th Mett	2	22.2	1	11.1	0	0	5	55.6	0	0	1	11.1	9	---
5th Mett	0	0	3	37.5	0	0	4	50	0	0	1	12.5	8	---
Calcaneus	1	8.3	6	50	0	0	4	33.3	0	0	1	8.3	12	---

As noted earlier, a high proportion of individuals with diffuse lesions in the tibia and fibula were observed in all three causes of death groups (Table 5.18). Focal lesions were essentially located on the lower third of the diaphysis of the tibia and fibula. For instance, three individuals who died from TB infections presented PNBf on the distal segment (S6) of the tibia. Regarding the femur, focal deposits of new bone were found to be randomly distributed, affecting almost equally the upper and lower third of the diaphysis.

**Table 5.18:** Distribution of individuals affected with PNBf by cause of death (lower limb bones: femur, tibia and fibula) (S= bone segment; D=diffuse).



Bone	Number of segments affected (S)	Cause of death		
		Group 1 Location (n)	Group 2 Location (n)	Group 3 Location (n)
Femur	One	S3 (3), S5 (1), S6 (1)	S1(1), S3(2), S5(2), S6(1), S7(2)	S5(1), S6(4)
	Two	S3+S4 (5) S5+S6 (2)	S4+S5(1) S5+S6 (1)	S6+S7(1)
	Three or more	D(2)	D(5)	D(4)
Tibia	One	S4(2), S5(1), S6(3)	S4(2), S6(1), S7(2)	S2(1), S6(1), S7(1)
	Two	S3+S4(1) S5+S6(2)	S2+S3(1) S3+S6(1) S4+S5(1)	0
	Three or more	D(6)	D(14)	D(11)
Fibula	One	0	S3(1), S5(1)	0
	Two	S4+S6(1)	S2+S3(1) S4+S6(1)	0
	Three or more	D(4)	D(8)	D(7)

In the metatarsals, the periosteal lesions were essentially diffuse with the central portion of the shaft being regularly affected.

***By individual and type of bone response observed***

A distinct pattern of bone response was observed in the skeleton of affected individuals when the upper and lower limb bones were compared. The lesions recorded in the bones from the upper limb were essentially of the woven type. As illustrated in Figure 5.38, the humerus and radius were most frequently affected by deposits of woven bone, observed in five individuals, followed by the scapula and ulna, recorded in four individuals. Deposits of lamellar

or compact bone were most frequently observed in the humerus of three individuals. In the scapula of one individual, a combination of osteolytic and osteoproliferative lesions was observed.

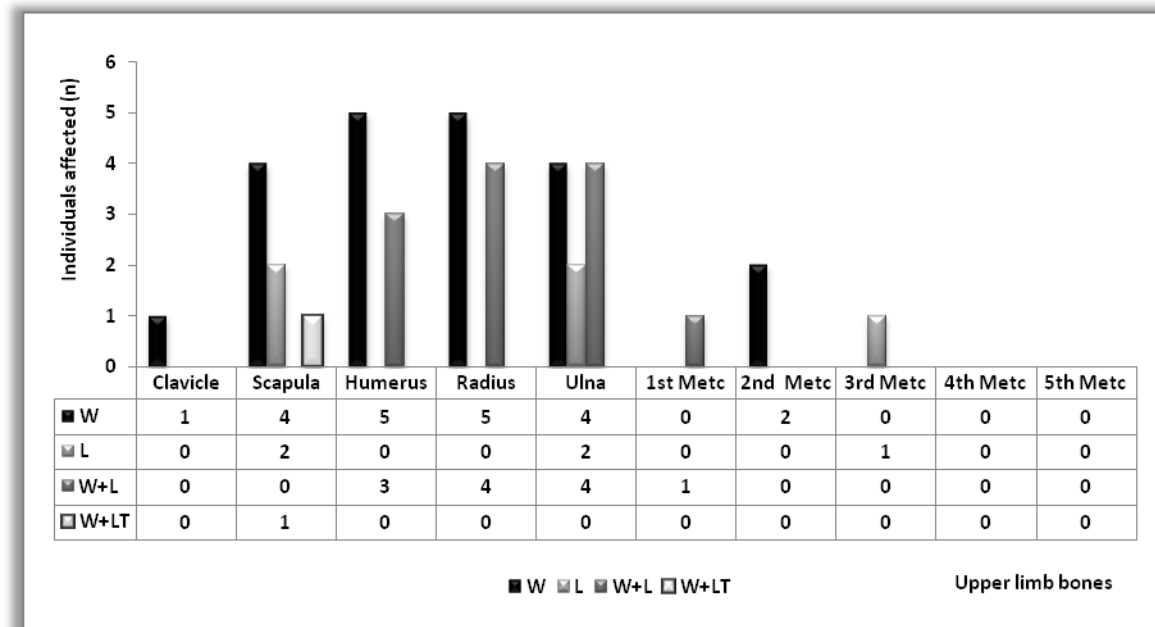


**Figure 5.38:** Distribution of the type of bone response in the bones from individuals affected (upper limb bones) (W=woven bone; L=lamellar bone; W+L=woven and lamellar bone; W+LT=woven bone and lytic lesions).

When the distribution of the type of bone response was analyzed by cause of death (Table 5.19), deposits of woven and of woven and lamellar bone were found to occur most frequently in the bones of the arm and forearm in the group of individuals who died from TB infection (Group 1). For example, woven bone deposits were observed in the radius of 44.4% (4/9) of individuals, and in the ulna of 40% (4/10). Lesions of the clavicle were only recorded in one individual from Group 3, whereas those in the 2<sup>nd</sup> and 3<sup>rd</sup> metacarpals were observed in Group 2. The woven foci of the 2<sup>nd</sup> metacarpal were recorded in individuals who died from tuberculous (Group 1) and from non-tuberculous infections (Group 2). Despite the differences found, the results were not statistically significant.

**Table 5.19:** Distribution of the type of bone lesions by cause of death (upper limb bones) (W=woven bone; L=lamellar bone; W+L=woven and lamellar bone; W+LT=woven bone and lytic lesions).

Bone	Type of bone reaction	Cause of death			Total N
		Group 1 n (%)	Group 2 n(%)	Group 3 n(%)	
Clavicle	W	0	0	1(100)	1
	L	0	0	0	
	W+L	0	0	0	
	W+LT	0	0	0	
Scapula	W	1(14.3)	2(28.6)	1(14.3)	7
	L	1(14.3)	1(14.3)	0	
	W+L	0	0	0	
	W+LT	0	0	1(14.3)	
Humerus	W	3(37.5)	2(25)	0	8
	L	0	0	0	
	W+L	3(37.5)	0	0	
	W+LT	0	0	0	
Radius	W	4(44.4)	1(11.1)	0	9
	L	0	0	0	
	W+L	2(22.2)	2(22.2)	0	
	W+LT	0	0	0	
Ulna	W	4(40)	0	0	10
	L	0	1(10)	1(10)	
	W+L	3(30)	1(10)	0	
	W+LT	0	0	0	
1 <sup>st</sup> Metc	W	0	0	0	1
	L	0	0	0	
	W+L	0	1 (100)	0	
	W+LT	0	0	0	
2 <sup>nd</sup> Metc	W	1 (50)	1 (50)	0	2
	L	0	0	0	
	W+L	0	0	0	
	W+LT	0	0	0	
3 <sup>rd</sup> Metc	W	0	0	0	1
	L	0	1 (100)	0	
	W+L	0	0	0	
	W+LT	0	0	0	
4 <sup>th</sup> Metc	W	0	0	0	0
	L	0	0	0	
	W+L	0	0	0	
	W+LT	0	0	0	
5 <sup>th</sup> Metc	W	0	0	0	0
	L	0	0	0	
	W+L	0	0	0	
	W+LT	0	0	0	

A high prevalence of combined woven and lamellar lesions was observed in the tibia of 28 individuals and in the femur and fibula of 15 and 14 individuals, respectively (Figure 5.39). Lamellar lesions were also frequent in the femur and in the tibia of 17 individuals. The calcaneus showed a high number of woven bone deposits, present in eleven of the individuals analysed. A mixture of lytic and proliferative lesions was encountered in the innominate of one individual and in the femurs of two more (Figure 5.40).

When considered by cause of death (Table 5.20), individuals who died of TB infection showed more lamellar and woven/lamellar lesions in the femurs and 2<sup>nd</sup> metatarsal and woven deposition in the calcaneus (50%) than those who died of other causes (Group 3). The woven/lamellar pattern was also frequent in the tibia (21.6%), fibula (20.8%), and in the 5<sup>th</sup> metatarsal (25%) in those individuals who died of non-TB infection (Group 2). An equal frequency of woven/lamellar lesions in the tibia (21.6%) was also observed in Group 3. Although differences were found, the results were not statistically significant.

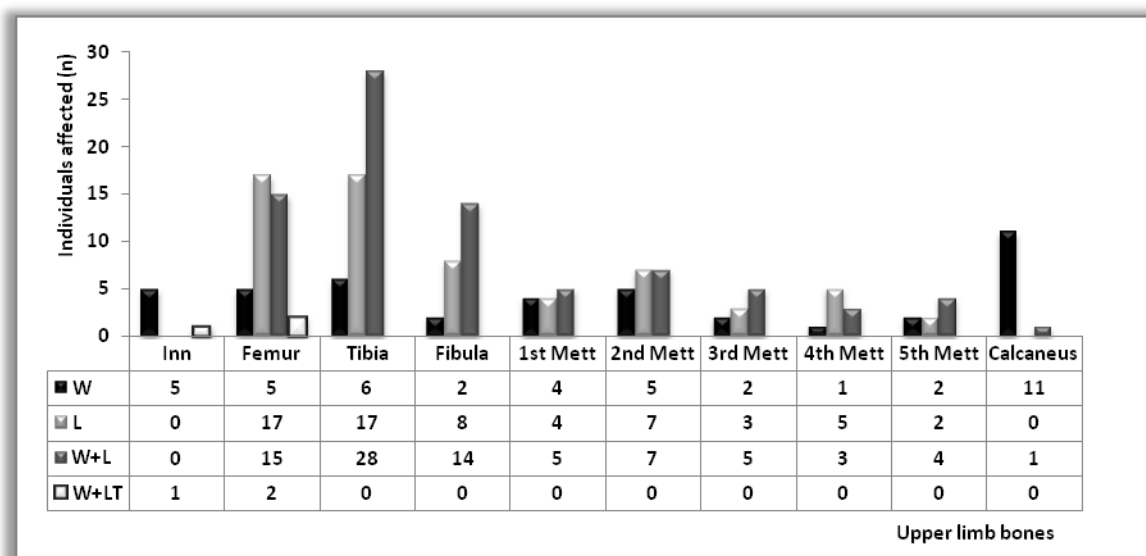


**Figure 5.39:** Distribution of the type of bone response in the bones from individuals affected (lower limb bones) (W=woven bone; L=lamellar bone; W+L=woven and lamellar bone; W+LT=woven bone and lytic lesions).

**Table 5.20:** Distribution of the type of bone lesions by cause of death (lower limb bones) (W=woven bone; L=lamellar bone; W+L=woven and lamellar bone; W+LT=woven bone and lytic lesions).

Bone	Type of bone reaction	Cause of death			Total N
		Group 1 n (%)	Group 2 n (%)	Group 3 n (%)	
Innominate	W	0	4(66.7)	1(16.7)	6
	L	0	0	0	
	W+L	0	0	0	
	W+LT	0	0	1(16.7)	
Femur	W	0	4(10.3)	1(2.6)	39
	L	7(17.9)	6(15.4)	4(10.3)	
	W+L	7(17.9)	5(12.8)	3(7.7)	
	W+LT	0	0	2(5.1)	
Tibia	W	2(3.9)	4(7.8)	0	51
	L	7(13.7)	7(13.7)	3(5.9)	
	W+L	6(11.8)	11(21.6)	11(21.6)	
	W+LT	0	0	0	
Fibula	W	0	2(8.3)	0	24
	L	2(8.3)	5(20.8)	1(4.2)	
	W+L	3(12.5)	5(20.8)	6(25)	
	W+LT	0	0	0	
1 <sup>st</sup> Mett	W	1(7.7)	2(15.4)	1(7.7)	13
	L	1(7.7)	3(23.1)	0	
	W+L	2(15.4)	2(15.4)	1(7.7)	
	W+LT	0	0	0	
2 <sup>nd</sup> Mett	W	4(21.1)	0	1(5.3)	19
	L	4(21.1)	0	3(15.8)	
	W+L	4(21.1)	3(15.8)	0	
	W+LT	0	0	0	
3 <sup>rd</sup> Mett	W	2(20)	0	0	10
	L	1(10)	1(10)	1(10)	
	W+L	2(20)	3(30)	0	
	W+LT	0	0	0	
4 <sup>th</sup> Mett	W	0	0	1(11.1)	9
	L	2(22.2)	3(33.3)	0	
	W+L	1(11.1)	2(22.2)	0	
	W+LT	0	0	0	
5 <sup>th</sup> Mett	W	1(12.5)	0	1(12.5)	8
	L	0	2(25)	0	
	W+L	2(25)	2(25)	0	
	W+LT	0	0	0	
Calcaneus	W	6(50)	4(33.3)	1(8.3)	12
	L	0	0	0	
	W+L	1(8.3)	0	0	
	W+LT	0	0	0	



Next, the results of the paleohistological investigation on the PNB microstructure will be presented.

## 5.2. PALEOHISTOPATHOLOGICAL ANALYSIS

For the paleohistopathological analysis, a total of 34 bone specimens, 26 belonging to 23 individuals from the Lisbon Human Identified Skeletal Collection, and eight extracted from archaeological skeletons, were sampled and prepared for histological examination as described in Chapter 4.

In the following pages, a detailed micrographic and descriptive analysis of the histological bone features observed will be provided. This illustrative approach will consider not only the normal and abnormal bone microstructure but also any diagenetic changes that are present. To summarize the most striking features observed, a general Table will follow the descriptions.

### 5.2.1. Group 1- Tuberculosis (TB)

From the group of individuals who died of tuberculosis eleven samples were taken, one with no macroscopic evidence of periosteal new bone formation (Sk. 1242) used as a control sample, and ten showing evidence of new bone formation and/or a combination of erosive and proliferative lesions. Ten samples were collected from ribs and one from the 5th left metatarsal of Sk. 1604.

A 2<sup>nd</sup> right rib with no visible lesions was sampled from the adult male Sk. 1242 (78 y.o.). Macroscopically, the rib specimen showed good preservation with minor taphonomic changes (Figure 5.41). Under polarized light, high levels of bone birefringence were recorded (Figure 5.42). The detailed analyses of the rib microanatomy revealed intact secondary osteons with their cement line, circumferential lamellae and Haversian canals, as well as preserved interstitial lamellae and osteocyte lacunae (Figure 5.42 A and A1). Spaces of bone resorption or Howship's lacunae were observed affecting the endosteal surface and/or the rib trabeculae (Figure 5.42 A). Figure 5.42 A1 exhibits a space of bone resorption due to osteoclastic activity that has destroyed half an osteon, as well as the contiguous interstitial lamellae. In spite of the features described that may be related to the regular process of bone remodelling, no deposits of new bone were observed on the pleural and cutaneous surfaces. For instance, Figure 5.42 B

presents the close-up appearance of the pleural-endosteal surface, in which only two rows of osteons and interstitial bone delimited by regular periosteal and endosteal circumferential lamellae are seen.

A 3<sup>rd</sup> right rib sample exhibiting woven and compact bone on the visceral surface was collected from the adult male Sk. 102 (48 y.o.). Apart from minor postmortem damage observed on the inferior border of the rib, the macroscopic and histological analyses revealed a relatively well-preserved thin section (Figure 5.43 and 5.44). Figure 5.44 also shows an increased thickness of the pleural-endosteal surface in relation to the cutaneous shell. In Figures 5.44 A and A1, the microstructure of the upper border of the pleural surface is shown. Here the rib cortex is composed of a row of secondary osteons and outlined by a dense layer of periosteal new bone. Dense agglomerates of osteocyte lacunae are also seen. From the upper to the lower borders of the pleural-endosteal surface, changes in the thickness and morphology of the newly built bone were observed. On the edges of the rib, no distinguishable features were observed separating the new bone from the underlying cortex (Figure 5.44 B and B1). As portrayed in Figure 5.44 B1, a dense layer of bone was deposited *de novo* partially submerging some cortical osteons. In this case, the innermost layers of periosteal bone are formed by collagen fibers and osteocyte lacunae structured in a lamellar fashion, whereas the outermost areas are composed of tissue with a random organization and erratic osteocyte lacunae. A different picture was gathered in the midsection of the pleural-endosteal surface. Accordingly, multiple foci of osteoclastic resorption were observed at the border between the newly formed bone and the underlying cortex (Figure 5.44 C, D and D1). Moreover, an increased thickness and high concentration of osteocyte lacunae without particular organization was noticed (Figure 5.44 C). At some points, a row of primary vascular canals is seen between the bulky body of the periosteal new bone and its outermost layers (5.44 D and D1). The different stages of tissue organization described at the periosteal level may suggest that the new bone was laid down in multiple episodes, in an almost appositional way. In the present rib sample, abnormal bone changes were only observed on the periosteal surface and/or at the interface between the newly formed bone and the cortex. The cortical tissue was maintained intact, with a structure composed of multiple rows of secondary osteons and interstitial lamellae. Regarding the cutaneous-endosteal surface, no particular changes were seen.

A 6<sup>th</sup> right rib exhibiting periosteal new bone of woven and compact appearance on the visceral surface was collected from the adult male Sk. 154 (35 y.o.). Macroscopically, the bone

specimen was in excellent state of preservation (Figure 5.45). Under polarized light, the microscopic examination revealed a deformed rib microstructure characterized by an enlarged pleural-endosteal surface in relation to the cutaneous-endosteal shell. This abnormal distribution was caused by massive periosteal new bone production whose thickness has surpassed almost three times the thickness of the underlying cortical bone (Figure 5.46). A detailed scrutiny of the microanatomy of the pleural-endosteal surface revealed a cortex formed by multiple rows of secondary osteons with intact Haversian canals and interstitial lamellae. Particularly noticeable was the large number of osteocyte lacunae seen (Figure 5.46 A). The considerable amount of interstitial lamellae observed in addition to the presence of secondary osteons with enlarged Haversian canals may indicate that remodelling was occurring (Figure 5.46 B, B1, C). In the sample under analysis, the main structural changes were recorded on the periosteal surface. On the edges of the pleural-endosteal surface the newly formed bone was characterized by a thick layer of primary lamellae with multiple osteocyte lacunae (Figure 5.46 B and B1). Figure 5.46 B1 provides a plain illustration of the orientation of the primary lamellae fibers and incorporated osteocyte lacunae. On the midsection of the pleural-endosteal surface, the periosteal new bone gained a tremendous thickness formed by multiple layers of deposition. Figures 5.46 B2 and C1 clearly exemplify the “appositional” layering of new bone with entrapped primary vascular canals. Here the innermost layers of bone present a more organized structure with a linear alignment of the collagen fibers. In contrast, the outermost areas of periosteal new bone appear more haphazard and populated by erratic osteocyte lacunae. Figure 5.46 D further elucidates the striking microstructure of the periosteal new bone composed of approximately ten distinct layers of deposition. In the Figure 5.46 C, the lack of organization of the new bone, indicative of its woven nature, and the proliferation of multiple osteocyte lacunae are evident. Primary vascular canals, some of them enlarged and with signs of bone resorption and/or coalescence, were seen separating distinct layers of bone. A clear line of demarcation formed by osteoclastic lacunae was recorded between the newly deposited bone and the underlying cortex (Figure 5.46 E). The microanatomy of the cutaneous-endosteal surface showed distended Haversian canals and large spaces of resorption that may have their origin in the coalescence of neighboring osteon canals (Figure 5.46 F). This process led to the formation of cortical bone composed of peripheral osteons and parallel rows of interstitial lamellae. Figure 5.46 F1 show a detail of the cutaneous-endosteal cortex formed by osteons with enlarged Haversian canals, interstitial lamellae and osteocyte lacunae with their branching canaliculi.

A 5<sup>th</sup> left rib<sup>54</sup> exhibiting erosive and proliferative lesions was collected from the adult male Sk. 332 (53 y.o.). The macroscopic analysis showed a well-preserved bone specimen (Figure 5.47). Under histological analysis, two thin sections with high bone birefringence were observed, which indicates good preservation of the bone tissue (Figure 5.48, 5.49 and 5.48 A). This assertion was broadly confirmed during the detailed analysis of the rib microanatomy. For instance, Figure 5.48 A shows a segment of the pleural surface under polarized light composed of a row of Haversian systems, with well-defined Maltese crosses, and layered by regular periosteal and endosteal circumferential lamellae. A set of bony abnormalities especially focused at the cortical and periosteal level were recorded on the rib midsections. On the pleural surface, a thick layer of newly formed bone with a dense and haphazard appearance was observed (Figure 5.48 B and 5.49). Figure 5.48 B1 highlights the periosteal new bone and the lack of alignment of the collagen fibers. The major microstructural changes were observed on the rib cortex. Here numerous foci of bone resorption (Howship's lacunae), digested Haversian systems, and large extensions of interstitial lamellae were observed (Figure 5.48 B, B1, C, C1 and C2). A similar phenomenon occurred at the endosteal and periosteal level (Figure 5.48 B and D, Figure 5.49 and Figure 5.50). Figure 5.48 C2 exemplifies the multiple bays of resorption formed by osteoclastic activity in the cortical bone and at the endosteal surface. In contrast, Figures 5.48 D, 5.49 and 5.50 A portray the bays of bone resorption produced on the pleural surface and cortical bone, identified macroscopically as osteolytic or erosive lesions. A mass of densely packed lamellae running parallel to the pleural surface and intersected by Howship's lacunae was observed on the rib cortex (Figure 5.48 and 5.50). These lamellar units separated at some points by cement-like lines may constitute remains of the periosteal primary lamella that now occupy an intracortical position adjacent to several Haversian systems (Figure 5.48 C, C1 and D). Earlier episodes of new bone deposition, now completely remodeled, may also justify the lamellar formations.

A rib fragment exhibiting erosive and proliferative lesions was sampled from the adult male Sk. 470 (68 y.o.). Macroscopically, no major diagenetic changes were noticed (Figure 5.51). Under the microscope lens, an increased thickness of the pleura-endosteal surface was recorded in comparison to the cutaneous-endosteal shell (Figure 5.52). The detailed analysis of the affected area showed a thick, dense and haphazard layer of periosteal new bone deposited upon the rib cortex (Figure 5.52 A). Figure 5.52 B illustrates the thickness of the new periosteal bone that has surpassed the volume of the cortex. No clear line of demarcation was noticed

---

<sup>54</sup> Since the two thin sections prepared from the rib sample presented important structural features, the microanatomy of both will be described.

between the newly built bone and the underlying cortical tissue (Figure 5.52 A1, A1.1, A2 and B). At some points the periosteal new bone seems to be an extension of the rib cortex, however without the mature structure that characterizes the last (Figure 5.52 A1.1). In general, multiple rows of well-defined osteons, Haversian canals, interstitial lamellae and osteocyte lacunae comprised the cortical bone (Figure 5.52 A1, A1.1. and A2). In fact, a large number of osteocyte lacunae dispersed throughout the newly periosteal bone, cortex and rib trabeculae was observed (Figure 5.52 A2). Figure 5.52 B shows an enlargement of the Haversian canals near the endosteal surface. Differences in the organization of the periosteal new bone were found in the thin section represented by Figure 5.53. With a wave-like morphology, the newly formed periosteal bone gave an irregular appearance to the pleural surface. Under transmitted and polarized light, a dense layer of new bone formed by fibers and osteocyte lacunae oriented linearly and separated from the supporting cortex by punctuated resorption spaces was observed (Figure 5.53 A). Figure 5.53 A1 better illustrates the microstructure of this bone layer that may have functioned as a substrate for the apposition of new bone sheets separated by primary vascular canals. A high concentration of osteocyte lacunae was seen in the outermost layer of the periosteal new bone formation (Figure 5.53 A2). A close-up of the microanatomy of the rib also exhibited an intact cortical bone formed by multiple rows of osteons, interstitial lamellae and populated by osteocyte lacunae. In Figures 5.53 A and A1, numerous osteons present an enlarged Haversian canal which may indicate that bone remodelling was taking place. Bays of bone resorption were seen on the endosteal surface (Figure 5.53 A).

A 5<sup>th</sup> left rib exhibiting new bone deposition of woven type on the visceral surface was sampled from the adult female Sk. 1383 (22 y.o.). Macroscopically, the sample was well-preserved (Figure 5.54). The histological examination also showed an intact and regular rib microstructure. Nevertheless, on the pleural surface a thin rim of newly deposited bone was observed (Figure 5.55). The detailed observation of the periosteal new bone under transmitted and polarized light showed a ruffled rim of bone with an arc-like structure attached to a substrate layer by pedestals. Between the new periosteal bone and the rib cortex a small line of demarcation was observed, however with no formation of resorption spaces (Figure 5.55 A, A\* and B). A proliferation of osteocyte lacunae was noticed, especially in the periosteal new bone (Figure 5.55 A\*1, B and C). Figure 5.55 C exemplifies the type of bone bridging formed within the periosteal reaction. The microstructure of the cortex was maintained intact. The cortical tissue appeared formed by multiple rows of osteons with their preserved Haversian

canal and interstitial lamellae. Some drifting osteons eccentrically formed and Volkmann's canals were noticed near the pleural surface, constituting remnants of the subadult cortex (Figure 5.55 B and B\*). Figure 5.55 D illustrates the cutaneous-endosteal surface composed of numerous rows of secondary osteons with their circumferential lamellae, Haversian canals, and osteocyte lacunae. Some enlarged Haversian canals were seen indicating that remodelling was probably occurring. In Figure 5.55 D1, well-preserved drifting osteons and interstitial lamellae are visible. On the endosteal surface bone resorption was taking place (Figure 5.55 D and D1).

A 7<sup>th</sup> left rib sample exhibiting new bone deposition of woven type was collected from the adult male individual Sk.1227 (21 y.o.). Macroscopically, some taphonomic changes were observed on the pleural surface (Figure 5.56). These changes gained expression at the microscopic level, especially in the thin section of Figure 5.57. For instance, some micro-cracks along the rib pleural-endosteal surface were noticed (Figure 5.57 A and B). The second thin section represented by Figure 5.58 appeared better preserved. In spite of the diagenetic changes, an increased thickness of the pleural-endosteal surface due to new bone deposition was observed. On the upper and lower edges of the pleural surface, numerous resorption spaces were signaled separating the cortical bone from the outermost layer of new bone formation (Figure 5.57 A and B). Figure 5.57 B shows a mass of dense intracortical lamellae deposited above a thin rim of periosteal new bone. A close-up view of the intracortical lamellae highlights the perfect arrangement of the mineralized collagen fibers, as well as the presence of Howship's lacunae that digested portions of the lamellar structure (Figure 5.57 B1). A plain illustration of the point of contact between the pleural and the cutaneous surfaces shows a branch-like layer of periosteal new bone populated by numerous osteocyte lacunae. Foci of bone resorption were noticed in the newly built bone and at the interface between the periosteal bone and the rib cortex (Figure 5.57 B2). Figure 5.57 C exemplifies the composition of the cutaneous-endosteal cortex formed by multiple rows of osteons (secondary and drifting) embedded in interstitial lamellae. Some Haversian canals appeared enlarged suggesting that bone remodelling was occurring (Figure 5.57 C1). The second thin section prepared from the Sk. 1227 rib revealed several abnormal changes mainly located at the periosteal level (Figure 5.58). In fact, a thick mass of periosteal bone combining well-defined mature lamellae with more haphazard new bone tissue was recorded. Figure 5.58 A shows the outermost layers of periosteal new bone exhibiting primary vascular canals. Between the newly formed bone and the underneath cortex, several resorption spaces with a horizontal distribution were observed

(Figure 5.58 and 5.58 A). The cortical bone was composed of multiple rows of osteons and interstitial lamellae (Figure 5.58 A).

A 5<sup>th</sup> right rib exhibiting new bone deposition of compact appearance was sampled from the adult male individual Sk. 1235 (50 y.o.). At first glance some taphonomic changes were noticed on the rib surface (Figure 5.59). A similar picture was gathered from the histological study. In fact a general lack of bone birefringence was found (Figure 5.60). Despite that, and through the analysis of the preserved microanatomy, two distinct layers of bone interconnected by pedestals are seen. The innermost layer corresponds to the rib cortex and is formed by Haversian canals and osteon shadows, whereas the outer layer is composed of periosteal new bone. Separating the two bone layers, resorption spaces were identified (Figure 5.60 A and B). In Figure 5.60 B, damage of the cortical bone is visible with the formation of small portions resembling clay particles. A regular microanatomy was identified on the cutaneous-endosteal surface; however only poor-defined osteons and interstitial lamellae were seen. Only the Haversian canals and the foci of endosteal resorption exhibited well-defined contours. Figure 5.60 C shows rib trabeculae with preserved osteocyte lacunae and mineralized collagen fibers, which indicates some degree of preservation.

A 4<sup>th</sup> right rib sample presenting new bone with a compact appearance on the visceral surface was collected from the adult male Sk. 1299 (26 y.o.). Macroscopically, some superficial postmortem damage was noticed (Figure 5.61). The histological inspection revealed a regular microanatomy; however with a slight increase in thickness of the pleural surface (Figure 5.62). A detailed analysis of the rib thin section showed additional features. For example, on the lower border of the pleural-endosteal surface, resorption lacunae were seen between the endosteal and the periosteal circumferential lamellae (Figure 5.62 A and A1). On the rib midsection, a dense layer of new bone was noticed above the cortex (Figure 5.62 B, C and C1). The cortical bone appeared composed of rows of osteons embedded in interstitial lamellae. Signs of endosteal resorption and Haversian remodelling were also evident (Figure 5.62 C and C1). Figure 5.62 D clearly shows the increased thickness observed on the rib midsection. Figures 5.62 D1 and D2 better illustrate the microanatomy of the newly formed bone on the pleural surface. Figure 5.62 D1 shows the periosteal new bone composed of two different layers and with an irregular and wavy-like contour. Distinct colorations and densities were also noticed. The inner layer presents a linear orientation, whereas the outermost layer is denser and less organized. A similar picture was obtained in Figure 5.62 D2. In this case, the outer layer also exhibited primary vascular canals and a denser concentration of osteocyte lacunae.

Erratic micro-cracks associated with diagenetic changes were occasionally seen. Contrary to previous samples, no resorption lacunae were observed on the interface between the periosteal new bone and the cortex of the rib.

An 11<sup>th</sup> right rib fragment showing lytic and productive lesions was sampled from the young female individual Sk.1583 (9 y.o.). The macroscopic and microscopic analysis showed some postmortem damage, especially around the lytic focus (Figure 5.63, 5.64 and 5.65). Figure 5.64 A highlights the differences between the cutaneous-endosteal surface and the pleural-endosteal shell. The cutaneous-endosteal surface is well-preserved. In contrast, the pleural-endosteal one is heavily destroyed not only by osteoclastic activity, but also by diagenetic changes. In the preserved remains of the pleural surface, an increased bone density incremented by the proliferation of osteocyte lacunae was seen. Multiple primary vascular canals of different sizes were observed near the surface. A similar bone microstructure was observed on the cutaneous-endosteal surface. Here the bone tissue presented the haphazard structure characteristic of woven bone, and a high concentration of osteocyte lacunae (Figure 5.64 A and B). Under polarized light, a general lack of bone organization is evident (Figure 5.65 A and B). Figure 5.65 A presents multiple bays of bone resorption associated with the process of trabecularization. The coexistence of intracortical primary lamellae with primary vascular canals was observed on the cutaneous surface (Figure 5.65 B and B1). A well-defined primary vascular canal (primary osteon) occupying a central position on the rib thin section was recorded. Under polarized light, thin circumferential lamellae were observed surrounding the Haversian canal (Figure 5.65 B1). Note the dispersion of osteocyte lacunae, at some points showing a linear organization. In contrast with the woven bone, the primary lamellar bone presented a well-defined structure (Figure 5.65 C). It is important to note that all the aforementioned features observed on the cutaneous-endosteal surface are considered normal taking into account the age of the individual (see Chapter 3).

A sample from the distal extremity of the 5<sup>th</sup> left metatarsal showing new bone deposition was collected from the adult female Sk. 1604 (45 y.o.). The macroscopic examination revealed a well-preserved bone sample (Figure 5.66). The histological analysis showed a thin section with good bone birefringence (Figure 5.67). Nevertheless, a detailed inspection of the bone sample revealed diagenetic changes such as micro-cracks, responsible for the detachment of the periosteal new bone (Figure 5.67 A). The cortical tissue was intact and composed of secondary osteons, interstitial lamellae and intracortical lamellar bone (Figure 5.67 A and A1). The intracortical lamellae were particularly evident on the endosteal



surface, being intersected by complete or partially complete Haversian systems (Figure 5.67 B and B1). Under polarized light, a clear demarcation was observed between the cortex and the periosteal new bone. Figures 5.67 B and B2 show the newly built bone composed of primary vascular canals.

To summarize (Table 5.21), in eleven samples studied from the TB group (Group 1), ten presented histological evidence of periosteal new bone formation. Only the sample used as a control (Sk.1242) did not show new bone deposition, corroborating the macroscopic inspection. In general, the samples were well-preserved and had good bone birefringence. One sample, Sk.1235, was particularly affected by diagenetic changes, which made the detailed analysis of its structure impossible. Regarding the bone microanatomy, a number of qualitative features were shared. Most bone samples presented a mature bone microstructure composed of multiple rows of secondary osteons (n=10) and interstitial lamellae (n=9). The only exception was found in Sk. 1583 rib specimen that presented an immature bone structure composed of primary lamellar bone, woven bone and erratic primary osteons. Despite the differences, the microstructure of Sk. 1583 is regular considering the age of the individual.

Drifting osteons were observed in Sk.1383 rib sample, which constitute a remnant of the subadult cortex. In numerous samples, the periosteal (n=5) and endosteal (n=5) circumferential lamellae were preserved. Eight specimens showed enlarged Haversian canals, which may suggest that bone remodelling was occurring. Signs of endosteal bone resorption were recorded in nine samples. Nevertheless, only Sk.332 specimen showed massive Howship's lacunae affecting the endosteal surface, cortical bone and periosteal surface. Bone resorption was also evident on the periosteal surface of Sk. 1583 sample, in this case associated with small foci of new bone. All foci of periosteal new bone were recorded on the pleural surface of ribs and in the diaphysis of the 5<sup>th</sup> metatarsal (Sk. 1604). When the appearance is considered, some differences were found in the organization and behavior of the PNB in relation to the underlying cortex.

Table 5.21: Summary of the histological analysis of Group 1 samples (<sup>1</sup>).

Skeleton / Sample	General microanatomy											Bone resorption											Periosteal new bone										
	PNBF	PCL	Cortical bone				ECL	PS	HC	CB	ES	Location			Distinct from cortex	Affecting cortex	Appearance			Organization													
			PO	DO	SO	IL						PS	CS	D			TL	A-L	A	L	W	M	OL										
Sk.1242 2 <sup>nd</sup> right rib	N	Y	N	N	Y	Y	N	N	N	Y	N	N	N	N	N	N	N	N	N	N	N	N	N	N	N	N							
Sk. 102 3 <sup>rd</sup> right rib	Y	Y	N	Y	Y	Y	N	N	N	N	Y	N	Y++	N	N	N	N	Y+	N	N	N	N	Y	Y	Y++	Y++							
Sk.154 6 <sup>th</sup> right rib	Y	N	N	Y	Y	N	N	Y	Y	N	Y	N	Y++	N	N	N	Y+	N	N	N	N	Y	Y	Y	Y++	Y++							
Sk. 332 5 <sup>th</sup> left rib	Y	Y	N	Y	Y	Y	Y+	Y	Y+	+	Y	N	N	N	N	Y	N	N	N	N	N	Y	N	N	N	N							
Sk. 470 Rib sample	Y	N	N	Y	Y	N	N	Y	N	Y	Y	N	Y++	N	N	N	Y+	N	N	N	N	Y	Y	Y	Y++	Y++							
Sk. 1383 5 <sup>th</sup> left rib	Y	N	N	Y	Y	N	N	Y	N	Y	Y	N	N	N	N	N	N	N	Y	N	N	Y	N	Y	Y++	Y++							
Sk. 1227 7 <sup>th</sup> left rib	Y	Y	N	Y	Y	Y	N	Y	Y	Y	Y	N	Y++	N	N	N	Y+	N	N	N	N	Y	Y	Y	Y++	Y++							
Sk. 1235 5 <sup>th</sup> right rib	Y	-	-	Y	-	-	N	Y	N	Y	Y	N	Y++	N	N	Y	N	-	-	-	-	-	-	-	-	-							
Sk. 1299 4 <sup>th</sup> right rib	Y	Y	N	Y	Y	Y	N	Y	Y	Y	Y	N	N	N	N	N	Y+	N	N	N	N	Y	Y	Y	Y++	Y++							
Sk. 1583 11 <sup>th</sup> right rib	Y	N	Y	N	N	N	Y	N	N	Y	Y	N	-	-	-	-	-	-	-	-	-	Y	N	Y	Y++	Y++							
Sk. 1604 5 <sup>th</sup> left Met.	Y	N	N	Y	Y	N	N	Y	N	Y	N	Y	N	N	N	Y	N	N	N	N	N	Y	N	Y	N	N							

Group 1- TB

**Legend (<sup>1</sup>):****General microanatomy**

PCL-periosteal circumferential lamellae  
 Cortical bone (PO-primary osteons, DO – drifting osteons, SO – secondary osteons, IL – interstitial lamellae)  
 ECL- endosteal circumferential lamellae

**Bone resorption**

PS – periosteal surface  
 HC – Haversian canals  
 CB – cortical bone  
 ES – endosteal surface

**Periosteal new bone**

Location (PS – periosteal surface, CS – cutaneous surface, D - diaphysis)  
 Appearance (TL – thick layer, A-L- arc-like structure, A – appositional bone)  
 Organization (L-lamellae, W-woven, M- mist, OL – osteocyte lacunae)

(+) isolated foci

(++) severe foci

Four samples shared a number of distinctive features characterized by multiple layers of appositional newly formed bone with a lamellar and woven appearance and separated from the underlying cortical tissue by resorption spaces. Sk. 1299 rib sample also presented appositional new bone formation; however no physical demarcation was recorded between the newly built bone and the cortex. In two samples, the periosteal new bone appeared as a thick and continuous layer of bone deposited upon the cortex, and in another two as an arc-like structure linked to the underlying bone by pedestal structures. A common finding was the proliferation of osteocyte lacunae in the newly formed bone.

### 5.2.2. Group 2 – Non-Tuberculosis (non-TB)

From the group of individuals who died from non-tuberculosis diseases, five samples exhibiting periosteal new bone formation were collected from four different individuals. Two samples were retrieved from the non-adult individual Sk. 1534-A, namely a vertebral portion of a right rib and a fragment of the diaphysis of the right fibula.

A 7<sup>th</sup> right rib specimen exhibiting new bone deposition of woven and compact type was sampled from the adult male Sk. 270 (50 y.o) who died from bronchopneumonia. Macroscopically, the sample was in a good state of preservation. Only a small layer of new bone was missing from the pleural surface (Figure 5.68). The microscopic view revealed a well-preserved microanatomy and good birefringence. The pleural-endosteal and cutaneous-endosteal surfaces were intact, and a thin rim of bone was observed on the pleural surface (Figure 5.69). The detailed analysis of the rib microstructure revealed multiple foci of bone resorption affecting the cortex and the underlying endosteal surface (Figure 5.69 A, B and C). Figure 5.69 B illustrates a portion of the pleural-endosteal surface formed by cortical osteons partially digested by osteoclastic activity and dense areas of disorganized bone with multiple

osteocyte lacunae. The outer layer of the cortical bone is visible, with new bone being laid down in some areas (Figure 5.69 B). In spite of the postmortem damage of the periosteal new bone, an almost arc-like structure composed of a unique layer of bone on the edges (Figure 5.69 A, C and C\*) and by two rows of new bone in the center (Figure 5.69 B) can be seen. Connecting the newly built structure and the underlying cortex, a set of bony columns were identified. Figures 5.69 B and C show the periosteal new bone composed of primary vascular canals. In Figures 5.69 C\* and D, the unaffected cortex of the pleural surface can be seen. In both Figures, the outer and inner cortical lamellae were maintained intact. Only small foci of bone resorption were noticed on the endosteal surface (Figure 5.69 C\*).

A left rib specimen presenting new bone of compact appearance was collected from the adult male Sk. 1429 (26 y.o) who died from pulmonary congestion. As in previous cases, the bony features observed in the two thin sections will be described since the differences found were remarkable. Macroscopically, the surface of the rib showed some postmortem erosion (Figure 5.70). The histological analysis revealed a well-preserved rib microanatomy and good bone birefringence (Figure 5.71). The detailed analysis of one of the thin sections showed a massive periosteal new bone formation with an amorphous appearance (Figure 5.71 A). In fact, a close-up of the affected area revealed a highly disorganized arrangement of the bone fibers intersected by multiple osteocyte lacunae. Between the newly built bone and the supporting cortex, no apparent line of demarcation was seen (Figure 5.71 B). The innermost cortex presented a regular structure composed of multiple rows of well-defined osteons embedded in interstitial lamellae (Figure 5.71 A). A more haphazard structure combining dense intracortical lamellae, interstitial lamellae and incomplete osteons was observed in the outer cortex (Figure 5.71 B and B1). A very different scenario was obtained from the analysis of the second thin section, mainly at the periosteal and cortical level (Figure 5.72). Accordingly, the study of the pleural-endosteal surface revealed cortical tissue affected by large spaces of osteoclastic resorption that have destroyed some Haversian systems and interstitial lamellae (Figure 5.72 A and 5.72 A\*). At some points in the pleural midsection, an unclear distinction between the original cortex and the newly built bone was evident due to massive invasion of osteocyte lacunae (Figure 5.72 A and 5.72 A\*). Above the rib cortex, five layers of appositional new bone separated by primary vascular canals and resorption lacunae were identified. The outer layers of the periosteal new bone presented a poor organization of the collagen fibers (Figure 5.72 A\*). An increased number of osteocyte lacunae were observed in all layers of the periosteal new bone. Figure 5.72 B highlights the microstructure of the distinct layers of new

bone: the innermost layers exhibit a better arrangement of the collagen fibers with parallel osteocyte lacunae and well-defined primary vascular canals; in contrast, the outermost layers of periosteal new bone are denser with a cotton-like appearance and less defined vascular canals.

Two distinct samples were collected from the non-adult male Sk. 1534-A (2 y.o.) who died from pneumonia: a right rib exhibiting new bone deposition of woven type on the visceral surface, and a fragment of the right fibula also showing new bone formation in the diaphysis. Regarding the rib sample, the macroscopic inspection showed a bone specimen in relatively good state of preservation. Nevertheless, some periosteal new bone detachment due to taphonomic factors was observed on the pleural surface (Figure 5.73). Microscopically, the thin section was well-preserved (Figure 5.74). The detailed histological analysis revealed a rib microstructure consistent with the age at death of the individual. This assertion is justified by the woven nature of the pleural-endosteal and cutaneous-endosteal cortices. For example, in Figures 5.74 A and A\*, the lack of components of the mature cortical bone, such as the secondary osteons and interstitial lamellae, is evident. In fact, only localized systems of primary lamellar bone were observed close to the endosteal surface (Figure 5.74 A\*). On the pleural-endosteal surface, only few primary vascular canals were seen. A large and circular focus of bone resorption was seen in the subadult cortex (Figure 5.74 A). The cutaneous-endosteal surface was formed by woven bone with an amorphous structure and numerous osteocyte lacunae. Multiple primary vascular canals and areas of bone resorption were seen randomly distributed (Figure 5.74 C). Although the microstructure of the pleural and cutaneous cortex was normal in appearance, an abnormal and dense ridge of periosteal new bone was recorded above the pleural surface (Figures 5.74 A and A\*). A close inspection of the newly built bone revealed a wavy-like structure with multiple primary vascular canals and osteocyte lacunae. The periosteal new bone was observed to be broadly attached to the cortical tissue (Figure 5.74 B).

Macroscopically, the right fibula was well-preserved (Figure 5.75). The histological study revealed the presence of some diagenetic damage (Figure 5.76). Under polarized light, a layer of periosteal new bone was observed on the surface of the fibula diaphysis. The edges of the newly formed bone present an arc-like structure (Figure 5.76 A and B). At the middle portion, a thick and branch-like microstructure is recorded (Figure 5.76 C). The presence of multiple osteocyte lacunae and the lack of lamellar organization point to a composition rich in woven bone. Figure 5.76 A better illustrates the structure of the periosteal new bone with numerous

primary vascular canals in the innermost layers. In Figures 5.76 B and C, resorption spaces are observed separating the periosteal new bone from the cortex. Some well-defined primary lamellae were observed on the endosteal surface (Figure 5.76 A).

A 5<sup>th</sup> left metatarsal sample showing periosteal reactions with a compact appearance was collected from the adult female Sk. 119 (64 y.o.) who died from bronchopneumonia. Macroscopically, the sample and the thin section prepared revealed good preservation (Figure 5.77). The same results were obtained during the histological study (Figure 5.78). The detailed analysis of the 5<sup>th</sup> metatarsal microanatomy showed cortical bone in excellent state of preservation and with good bone birefringence. Figure 5.78 A clearly shows the presence of several Maltese crosses intersecting the Haversian systems. Multiple rows of osteons with well-defined contours and embedded in interstitial lamellae were identified in the mature cortex (Figure 5.78 A and D). Enlargement of Haversian canals was regularly seen suggesting that bone remodelling was occurring (Figure 5.78 A, B, D and D1). Moreover, larger areas of localized resorption in the endosteal surface and in the interface zone between the cortical bone and the newly built bone were seen (Figure 5.78 C). Figures 5.78 B and D1 illustrate the structure of the periosteal new bone. Composed of a thick and dense layer of bone, the newly deposited bone was observed closely attached to the underlying cortex; however a clear line of demarcation was noticed between tissues (Figure 5.78 B, D and D1). Some newly formed primary vascular canals (Figure 5.78 B) and developed primary osteons (Figure 5.78 D1) were observed throughout the periosteal new bone.

To summarize, all Group 2 – non-TB samples presented histological evidence of periosteal new bone formation (Table 5.22). One sample (Sk. 1534-A, fibula) exhibited some diagenetic changes. The remaining specimens were in excellent state of preservation. Sk. 1534-A bone samples displayed an age-related microstructure mainly composed of woven bone and multiple primary vascular canals. A mature bone microstructure formed by secondary osteons and interstitial lamellae was observed in the remaining samples. Foci of bone resorption were observed affecting the Haversian canals (n=3), cortical bone (n=5) and endosteal surface (n=4). Major foci of osteoclastic activity were recorded in the cortical bone of specimens Sk. 270, Sk. 1429, and Sk. 1534-A. In ribs, new periosteal formation was observed on the pleural surface, whereas in the tubular/long bones the diaphysis was the area affected.

Table 5.22: Summary of the histological analysis of Group 2 samples (1).

Skeleton / Sample	General microanatomy											Bone resorption											Periosteal new bone									
	PNBF		PCL		Cortical bone			ECL			PS			HC		CB		ES		Location			Distinct from cortex		Affecting cortex		Appearance			Organization		
	PO	DO	SO	IL	ECL	PS	HC	CB	ES	PS	CS	D	PS	CS	D	PS	CS	D	TL	A-L	A	L	W	M	OL							
Sk. 270 7 <sup>th</sup> right rib	Y	N	Y	Y	Y	N	Y	Y++	Y	Y	N	N	Y	N	N	Y	Y	N	N	Y	N	N	N	Y	N	Y	N	Y				
Sk. 1429 Rib sample	Y	N	Y	Y	N	N	Y	Y++	Y	Y	N	N	Y	N	N	Y	Y	N	N	N	Y	N	N	N	Y	N	Y	Y				
Sk. 1534-A Rib sample	Y	N	N	N	N	N	Y	Y	Y	Y	N	N	Y	N	N	Y	Y	N	N	Y	N	N	N	Y	N	Y	N	Y				
Sk. 1534-A Fibula sample	Y	N	N	N	N	N	Y++	N	N	N	N	N	Y++	N	Y	N	N	N	N	Y++	N	N	N	Y	N	Y	N	Y				
Sk. 119 5 <sup>th</sup> left Met.	Y	N	Y	Y	Y	N	Y	Y	Y	N	N	Y	Y	N	Y	Y	N	N	N	N	N	N	N	Y	N	N	N	N				

Group 2- non TB

**Legend (1):**  
**General microanatomy**  
 PCL-periosteal circumferential lamellae  
 Cortical bone (PO-primary osteons, DO – drifting osteons, SO – secondary osteons, IL – interstitial lamellae)  
 ECL- endosteal circumferential lamellae  
**Bone resorption**  
 PS – periosteal surface  
 HC – Haversian canals  
 CB – cortical bone  
 ES – endosteal surface  
**Periosteal new bone**  
 Location (PS – periosteal surface, CS – cutaneous surface, D - diaphysis)  
 Appearance (TL – thick layer, A-L- arc-like structure, A – appositional bone)  
 Organization (L-lamellae, W-woven, M- mist, OL – osteocyte lacunae)  
 (+) isolated foci  
 (++) severe foci

Newly built bone with an arc-like structure was the more frequently observed type of deposition (n=3). In only two samples was a clear demarcation between the periosteal new bone and the underlying cortex observed (Sk. 270 and Sk. 1429). New bone formation of woven type and populated with multiple osteocyte lacunae was also common (n=3).

### 5.2.3. Group 3 – Other conditions

Group 3 is composed of samples collected from individuals who died from conditions other than TB and non-TB diseases (four samples), and of specimens that exhibited fractures in different stages of bone healing (six samples). In this last subgroup, three samples were taken from individuals who died from bronchopneumonia and pulmonary tuberculosis.

A lower third of a right fibula showing a bone callus was sampled from the adult male Sk.198 (68 y.o.) who died of urinary sepsis. Macroscopically, the bone fragment was in excellent state of preservation and the bone callus seemed to be almost completely remodeled (Figure 5.79). Under polarized light, a well-defined thin section formed by a network of lamellae, resembling trabeculae, and with good bone birefringence was seen. This observation was the same for the two thin sections observed (Figure 5.80 and 5.81). A detailed examination of the rib cortex showed an intricate system of lamellae, comparable to bone trabeculae, that probably was formed by resorption of previous Haversian systems and interstitial lamellae (Figure 5.80 A and B). The presence of partially digested osteons, large resorption spaces and enlarged Haversian canals may support this hypothesis. A thin rim of bone with a regular appearance forms the outermost layer of the cortical bone (Figure 5.80 A and B). No clear medullary cavity is seen. In fact, all of the internal bone microstructure seems to be formed by a network of lamellae and/or trabeculae in distinct stages of maturation. Figure 5.80 B exhibits a mesh of superimposed lamellae with no apparent organization above the periosteal edge that merges with remnants of mature lamellae and osteons. When compared, the mature lamellae are densely packed, whereas the most recent units show a poor alignment of their mineralized collagen fibers. Multiple spaces of osteoclastic resorption are visible. While some of these spaces are empty, others appeared totally or partially filled with a blue-grey substance. The origin of this substance is uncertain; however a correlation with the contiguous lamellae seems to exist. Figure 5.80 C exemplifies this apparent interaction. A similar appearance was evident in the second thin section prepared (Figure 5.81). For example, Figure 5.81 A presents the inner cortex formed by multiple branches and islands of old lamellae interconnected with immature bone and embedded in the blue-grey



substance. Figure 5.81 A1 shows the close-up microstructure of the immature bone, which at some points is almost indistinguishable from the surrounding substance. The absence of a clear lamellar structure and the presence of multiple osteocyte lacunae are indicative of the woven nature of the newly formed bone. In contrast with the inner cortex that is scarce in bone tissue, the outermost areas that border the periosteal surface are composed of a mesh of random lamellae (Figure 5.81 A).

A right tibia specimen exhibiting signs of a healed fracture was sampled from the young adult male Sk.54 (24 y.o.) who died from pulmonary tuberculosis. The macroscopic analysis revealed a thin section composed of dense cortical tissue and in good state of preservation (Figure 5.82). Under polarized light, a well-preserved microanatomy with good bone birefringence was seen. Nevertheless, some differences were found when the lateral and the medial surfaces of the bone callus were compared (Figure 5.83). The detailed analysis of the lateral portion of the healed callus revealed a cortical microstructure formed by multiple rows of osteons with different sizes and shapes embedded in interstitial lamellae. Separating the inner cortex from the outermost layers of bone, dense sheets of lamellae occupying an intracortical position were observed. At some points, erratic resorption lacunae parallel to the intracortical lamellae were seen (Figure 5.83 A and A1). Additionally, some foci of bone resorption due to osteoclastic activity were noticed at the periosteal level (Figure 5.83 A2). Figure 5.83 B clearly demonstrates the composition of the healed bone. Here the cortex is portrayed as a dense lattice of osteons, some of them with enlarged Haversian canals, interstitial lamellae and Volkmann's canals crossing multiple Haversian systems. This haphazard arrangement, in addition to the presence of enlarged vascular canals, clearly indicates that a great amount of remodelling was occurring and new Haversian systems were being formed or absorbed. Enclosing the cortical tissue a thin rim of periosteal circumferential lamellae was identified. In contrast to the lateral surface, the medial portion of the bone callus showed a thicker layer of periosteal bone and a more uneven organization of the cortical tissue (Figure 5.83 C). For example, Figure 5.83 C presents a cortex composed of multiple rows of well-defined osteons and interstitial lamellae, whereas Figure 5.83 D illustrates a more chaotic structure formed by osteons, resorption spaces and remnants of densely packed lamellae crossed by other randomly organized lamellar units. In spite of the increased thickness, the periosteal bone presented a regular appearance.

A sternal portion of the 9<sup>th</sup> right rib showing a remodeled bone callus was collected from the adult female Sk.119 who died from bronchopneumonia. Macroscopically, the bone sample

and the thin section prepared were in excellent state of preservation (Figure 5.84). Figure 5.85 and 5.86 provide an illustration of the general microanatomy of the rib, highlighting the good preservation as well as the abnormal enlargement of the pleural-endosteal surface in relation to the cutaneous-endosteal shell. This fact suggests that most of the structural changes related to the fracture healing were occurring on the pleural-endosteal surface, mainly at the cortical and periosteal level. In the upper border of the pleural-endosteal surface, a row of well-defined osteons flanked by endosteal and periosteal circumferential lamellae was observed. Above the periosteal lamellae, a thick deposit of new bone showing a high concentration of osteocyte lacunae was seen (Figure 5.85 A). Figure 5.85 B illustrates the arrangement of the cortical bone. Here differences between the inner and the outermost areas are found. The inner cortex is composed of multiple rows of osteons and interstitial lamellae, whereas the outer cortex is formed by individualized sheets of lamellae randomly interconnected by Haversian systems. A large number of osteocyte lacunae invading not only the periosteal new bone, but also the innermost areas of the cortex was observed throughout. Under polarized light, the level of organization of the bone tissue was even more apparent. In Figures 5.86 A and B, a chromatic division between the mature cortical bone (brown) and the newly formed bone (blue) appears to exist. Furthermore, a lack of alignment of the mineralized collagen fibers and a more abundant number of osteocyte lacunae seem to distinguish the periosteal new bone from the underlying cortex. Structural differences were also observed in the same bone tissue. Figure 5.86 B1 clearly illustrates this observation, showing a bulk of new bone with distinct levels of organization. Accordingly, the deepest layer is formed by densely packed lamellae with small erratic osteocyte lacunae. In the core of the periosteal formation, a poor lamellar arrangement accompanied by elongated osteocyte lacunae with their branching canaliculi is seen. The outer shell exhibits a random structure with no lamellar organization and densely populated by circular osteocyte lacunae. All the aforementioned differences seem to reflect distinct stages of remodelling of the bone callus.

A 4<sup>th</sup> right rib exhibiting an unhealed fracture was sampled from the adult male Sk.1138 (86 y.o.) who died from bronchopneumonia. The macroscopic analysis showed a well-preserved specimen with a thin layer of new bone near the edge of the fracture (Figure 5.87). In spite of the fracture and associated bone formation, no other lesions were recorded in the rib. Microscopically, an arc-like rim of newly built bone was observed on the pleural-endosteal surface. A profuse network of bone trabeculae with remnants of blood vessels was seen throughout the medullary cavity (Figure 5.88). Figure 5.88 A shows the arc-like structure of

new bone separated from the underlying cortex by resorption spaces. In another segment of the pleural-endosteal surface no spaces of bone resorption were recorded between tissues (Figure 5.88 B). In this particular case, the endosteal and periosteal circumferential lamellae remained intact. Below the periosteal reaction, enlarged Haversian canals were seen in the rib cortex (Figure 5.88 A and B). Figure 5.88 C exhibits a large micro-crack, probably of postmortem origin that caused a discontinuity in the rib cortex. Below the periosteal new bone deposition, enlarged Haversian canals and irregular resorption spaces occupy the cortical area (Figure 5.88 D and D1). A common observation in all segments analyzed was the existence of an intricate network formed by trabeculae and preserved blood vessels near the endosteal surface (Figure 5.88 A, B, D and D1).

From the adult female Sk.1196 (75 y.o.) who died from arteriosclerosis and hypertension, two bone specimens exhibiting healed bone callus were collected: a middle portion of a right rib and a distal portion of a right radius. Gross inspection of the rib sample showed a well-preserved specimen with a residual bone callus (Figure 5.89). A similar picture was obtained from the histological study. Figure 5.90 provides a plain illustration of the rib microanatomy, highlighting the thin pleural-endosteal and cutaneous-endosteal surfaces, as well as the lack of bone trabeculae. No evidence of the process of bone healing was observed. On both the pleural and endosteal surfaces the cortical tissue appeared to be formed by a unique row of osteons and interstitial lamellae (Figure 5.90 A and C). Figure 5.90 C shows a segment of the pleural-endosteal surface preserving the periosteal and endosteal circumferential lamellae. Another common observation along the rib thin section was the presence of multiple foci of bone resorption, mainly on the endosteal surface (Figure 5.90 B and C). The detailed analysis did not show any evidence of new bone deposition. The macroscopic analysis of the radius sample revealed a relatively well-preserved bone specimen. Nevertheless, some taphonomic changes, such as bone erosion, were recorded on the anterior surface (Figure 5.91). Figure 5.92 illustrates the general structure of the radius. While the anterior surface is formed by a thin rim of cortical tissue, a bulky network of trabeculae occupy the cortex on the posterior surface of the bone shaft. This network of sparse trabeculae forms the bone callus. In Figure 5.92 A, a close-up of the system of trabeculae that forms the bone callus is shown. In general, bone trabeculae are characterized by a haphazard arrangement of their mineralized collagen fibers, as well as by the presence of numerous osteocyte lacunae. Multiple foci of bone resorption were observed throughout the network of bone trabeculae. In particular segments of the radius diaphysis, especially in the interface between the bone callus

and the unaffected cortex, multiple sheets of new bone densely populated by osteocytes lacunae were seen. Intersecting the newly built bone, numerous primary vascular canals and enlarged resorption spaces were also recorded (Figure 5.92 B). Figure 5.92 B1 further elucidates the structure of the new bone formation, with a rudimentary system of aligned lamellae and osteocyte lacunae. The outermost areas appear more disorganized in appearance, lacking the lamellae structure and indicating the woven nature of the bone. In Figure 5.92 C, an impressive plain illustration of the anterior cortical bone is presented. Multiple horizons of lamellae, probably suggesting distinct levels of bone deposition were noticed. The outermost layers presented a compact appearance. The sheets of lamellae close to the endosteal surface exhibited a more disorganized structure and a more abundant number of osteocyte lacunae. Running parallel to the periosteal-endosteal surface, two microfractures not completely healed were seen separating layers of bone. No Haversian systems were observed in the anterior cortex of the radius.

A right rib sample with no evidence of bone lesions was collected from the adult male Sk. 1484 (73 y.o.) who died from a gastric ulcer. The general macroscopic and microscopic views showed a bone specimen relatively well-preserved and with bone birefringence (Figure 5.93 and 5.94). Under the microscope, the bone sample did not appear pathological. The regular rib microstructure formed by numerous rows of osteons and interstitial lamellae was maintained. The outer and inner lamellae of the cortical bone are visible in Figures 5.94 A and B. In Figure 5.94 C, diffuse diagenetic changes consisting of micro-cracks and generalized tissue disintegration are apparent. Major spaces of bone resorption, especially at the endosteal level, and enlarged Haversian canals were also recorded in Figures 5.94 D and D1.

A sternal end of the 5<sup>th</sup> left rib showing massive bone deposition with a sunburst pattern was sampled from the adult male Sk. 457 who died from rectal neoplasm (66 y.o.). The macroscopic examination revealed a bone specimen in good stage of preservation (Figure 5.95). The same picture was gathered through histological analysis (Figure 5.96). Under polarized light, a deformed rib microanatomy composed of multiple bone spikes of different sizes and shapes was recorded (Figure 5.96). Figures 5.96 A and C illustrate the appearance of the new periosteal bone, stressing the composition and orientation of the bony filaments formed. The spikes of new bone are organized in a parallel fashion, being thicker at the base and thinner at the extremity. No clear lamellar structure is present. A large number of osteocyte lacunae, equally distributed, were seen through the new bone formation. In contrast to the exuberant periosteal new bone, massive spaces of bone resorption were observed in

the rib cortex. Figure 5.96 B clearly illustrates the process of bone resorption that was occurring at the cortical level. At some points, the old structure composed of Haversian systems and interstitial lamellae was reduced to islands of partially digested osteons. Figure 5.96 D shows another example of the striking changes that were taking place in the rib cortex. Here vast areas of bone resorption due to osteoclastic activity are apparent. In the preserved cortical tissue, enlarged Haversian canals and multiple osteocyte lacunae are also visible.

A distal portion of the right femur combining proliferative and erosive lesions was sampled from the adult male Sk. 135 (86 y.o.) who died as a result of cachexia. The macroscopic and histological view revealed a relatively well-preserved reticulate microstructure (Figures 5.97 and 5.98). Figures 5.98 A and A1 illustrate the close-up appearance of fragments of the outer cortical lamellae interconnected with a network of newly built trabeculae. No clear system of osteons and interstitial lamellae was identified. Rather, multiple bays of bone resorption were seen in the femoral cortex. At some points, a geometric pattern made of trabeculae and resorption spaces was seen. Figures 5.98 B and B1 are a good example of this bone arrangement. Here multiple squared bays of osteoclastic activity are seen shaping the morphology of the bone trabeculae. Under polarized light, the trabecular bone is composed of remnants of densely packed lamellae crossed by layers of randomly organized new bone. Accompanying this immature or woven tissue is a proliferation of osteocytes lacunae (Figure 5.98 B1 and C).

A bone fragment of the distal portion of the right tibia showing a localized deposit of new bone was sampled from the adult female Sk. 1412 (81 y.o.) who died from arteriosclerosis. The gross inspection and the histological analysis revealed a thin section in good state of preservation (Figure 5.99 and 5.100). Figure 5.100 A further elucidates the well-preserved microstructure of the tibia cortex, with multiple rows of osteons embedded in interstitial lamellae. Figures 5.100 B and C exemplify the periosteal new bone production that occurred at the outer shell of the cortex. The periosteal new bone is firmly attached to the cortex and is composed of a thick layer of bone with a haphazard appearance. No lines of separation or resorption spaces were found between the periosteal new bone and the underlying cortex.

In summary, the histological analysis of Group 3 samples revealed striking results (Table 5.23). Regarding the subgroup formed by fracture callus, periosteal new bone formation was only visible in the Sk. 1138 sample. In this case the newly built bone presented an arc-like microstructure, being separated from the underlying cortex by resorption spaces. In the

remaining fracture samples (n=5), the bone callus exhibited a healed and remodeled appearance almost indistinct from the surrounding bone tissue. However, a very different picture was gathered through histological analysis. In fact, and below the bony shell, many changes related to the healing process and not visible to the naked eye were found. For instance, Sk. 198 and Sk. 1196 revealed a bone callus microstructure composed of an intricate network of trabeculae and lamellae in distinct stages of maturation. In contrast, the Sk.54 callus sample presented a more regular and mature structure, especially at the cortical level. Nevertheless, some evidence of fracture remodelling was observed. Features compatible with an incomplete healed fracture, such as the presence of a bulky mass of newly built bone in distinct stages of remodelling below the callus shell, were observed in the Sk. 119 sample. Another striking observation was made in the Sk.457 sample. In addition to the exuberant and spiky-like periosteal new bone formation, the histological analysis showed large bays of bone resorption that almost destroyed the cortical bone, not visible macroscopically. In the majority of the samples studied, the cortical bone appeared formed by multiple rows of secondary osteons and interstitial lamellae (n=8). Some evidence of Haversian remodelling (n= 7), and localized cortical (n=6) and endosteal resorption (n=4) were also observed.

Table 5.23: Summary of the histological analysis of Group 3 samples (<sup>1</sup>).

Skeleton / Sample	General microanatomy										Bone resorption										Periosteal new bone									
	PNBF		PCL		Cortical bone		ECL		PS		HC		CB		ES		Location		Distinct from cortex		Affecting cortex		Appearance		Organization					
	PO	DO	SO	IL	IL	PS	PS	PS	PS	PS	PS	PS	PS	PS	PS	CS	D	CS	D	CS	D	TL	A-L	A	L	W	M	OL		
Sk. 198 Right fibula	N	N	Y	Y	N	N	Y	Y	N	Y	Y	Y	N	N	-	-	-	-	-	-	-	-	-	-	-	Y	Y++			
Sk. 54 Right tibia	N	N	Y	Y	N	Y	Y	Y	N	Y	Y	Y	N	N	N	Y	N	N	N	N	Y	N	N	Y	N	N	N			
Sk. 119 9 <sup>th</sup> right rib	N	N	Y	Y	N	Y	Y	Y	N	Y	Y	Y	N	N	Y	N	N	Y	N	N	Y	N	N	N	Y	Y++				
Sk. 1138 4 <sup>th</sup> right rib	Y	N	Y	Y	N	Y	Y	Y	N	Y	Y	Y	N	N	Y	N	N	Y	N	Y	N	Y	N	N	Y	Y++				
Sk. 1196 Right rib	N	N	Y	Y	N	Y	Y	Y	N	Y	Y	Y	N	N	-	-	-	-	-	-	-	-	-	-	-	-	-			
Sk. 1196 Right radius	N	N	N	N	N	N	N	N	N	N	N	N	Y	N	-	-	-	-	-	-	-	-	-	-	Y	Y++				
Sk. 1484 Right rib	N	N	Y	Y	N	Y	Y	Y	N	Y	Y	Y	N	N	-	-	-	-	-	-	-	-	-	-	-	-	-			
SK.457 5 <sup>th</sup> left rib	Y	N	Y	Y	N	Y	Y	Y	N	Y	Y	Y	Y	N	Y	Y	N	N	N	N	Y	N	N	N	Y	Y++				
Sk. 135 Right femur	Y	Y	N	N	N	Y	Y	Y	N	Y	Y	Y	Y	N	N	Y	N	N	N	Y	N	-	-	-	N	Y	Y++			
SK. 1412 Right tibia	Y	Y	Y	Y	N	Y	Y	Y	N	N	N	N	N	N	N	Y	N	N	N	Y	N	Y	N	N	Y	Y++				

Group 3- Other conditions

**Legend (<sup>1</sup>):****General microanatomy**

PCL-periosteal circumferential lamellae  
 Cortical bone (PO-primary osteons, DO – drifting osteons, SO – secondary osteons, IL – interstitial lamellae)  
 ECL- endosteal circumferential lamellae

**Bone resorption**

PS – periosteal surface  
 HC – Haversian canals  
 CB – cortical bone  
 ES – endosteal surface

**Periosteal new bone**

Location (PS – periosteal surface, CS – cutaneous surface, D - diaphysis)  
 Appearance (TL – thick layer, A-L- arc-like structure, A – appositional bone)  
 Organization (L-lamellae, W-woven, M- mist, OL – osteocyte lacunae)

(+) isolated foci

(++) severe foci

### 5.2.4. Group 4 – Archaeological samples

Eight bone specimens exhibiting periosteal new bone formation were collected from human skeletal remains exhumed from three distinct archaeological sites: three samples were taken from two adults and from one non-adult individual unearthed from the ancient necropolis of the village of Constância (14<sup>th</sup>-19<sup>th</sup> centuries); three samples were collected from three adult individuals excavated from the necropolis of the extinct Royal Hospital of All Saints, Lisbon (18<sup>th</sup> century), and two samples were collected from two adult individuals exhumed from the cemetery of the hospital of the Ordem do Carmo, Oporto (19<sup>th</sup> century).

#### Ancient necropolis of the village of Constância

From the non-adult individual PAH/C-SG22-E4 (age at death estimated at 14-17 years old), a rib fragment exhibiting new bone deposition of woven type on the visceral surface was sampled.

Macroscopically, the tridimensional structure of the bone was intact without major taphonomic changes, as seen in Figure 5.101. The rib sample revealed a normal cortical thickness for an individual of this age (Figure 5.101). A localized rim of new bone with irregular contours was observed attached to the cortex of the pleural surface, however without compromising the underlying bone tissue. Multiple vascular holes corresponding to Haversian canals were found randomly distributed alongside the rib cortex, being larger and more numerous on the cutaneous surface. The cortical bone on the pleural surface showed a more dense appearance (Figure 5.101). Beyond the macroscopic view, a very distinct picture characterized by heavy diagenetic changes of the bone tissue was observed (Figure 5.102). In fact, several close-ups of the rib microstructure (Figure 5.102 A, B and C) did not allow for the identification of Haversian systems, interstitial bone, osteocyte lacunae and endosteal and



periosteal lamellae. Rather, the rib cortex appeared filled by an indistinguishable mass of composites probably resulting from bacterial activity or chemical action. Despite the absence of the basic bone units, the Haversian canals and major spaces of bone resorption associated with the normal bone remodelling are still visible (Figure 5.102 A). A close-up of the pleural surface using transmitted and polarized light provided a clearer picture of the periosteal reaction (Figure 5.102 B and C). In both pictures, a layer of new bone above the rib cortex can be easily identified. From this new substrate, another periosteal layer formed around large spaces and attached to the underlying surface by pedestals or arcade-like structures is apparent. As observed on the rib cortex, the new bone formation is also characterized by a lack of visible histological structures due to diagenesis. Nevertheless, and under polarized light some areas seem to maintain their birefringence in the blue spectrum (Figure 5.102 B\*) which may indicate some degree of preservation of the bone tissue and lamellae. An identical picture was noticed in small areas of the rib trabeculae (Figure 5.102 C).

A rib sample exhibiting lytic and osteoblastic lesions probably associated with a case of metastatic carcinoma was collected from an adult female (PAH/C-SG19 E7). The general macroscopic and microscopic view revealed massive bone resorption, mainly at the endosteal level, with destruction of the rib trabeculae (Figure 5.103 and 5.104). At some portions of the rib body, the cortical bone disappeared or was reduced to a thin rim of bone (Figure 5.104). In fact, abnormal bone resorption associated with the activity of osteoclasts was the most commonly noted phenomenon at the microscopic level. For instance, a close-up of a section of the pleural surface (Figure 5.104 A) and of the cutaneous surface (Figure 5.104 B and C) revealed multiple bays of bone resorption (Howship's lacunae) more numerous on the endosteal surface of the rib cortex. Some bone scalloping was also observed on the periosteal surface (Figure 5.104 A). A common occurrence in all segments analyzed was the presence of heavy diagenetic changes that prevented the identification of new bone deposits or other bone features (Figure 5.104 A, B, C and D). Figure 5.104 D shows a segment of the cutaneous surface with "shadows" of two Haversian systems. Here, only the contours of the osteons and their canals are visible. There is no evidence of the respective circumferential lamellae system. The application of polarized light revealed some trabecular birefringence which may indicate the preservation of some lamellae (Figure 5.104 D\*). Enlarged Haversian canals were signaled which may suggest that bone remodelling was simultaneously occurring (Figure 5.104 A, D, D\*).

A rib sample exhibiting new bone deposits with a woven appearance was collected from the skeleton of an adult female (PAH/C-SG25/26 E2). As observed in the previous cases, only the macroscopic tridimensional structure of the rib was preserved (Figure 5.105). The histological analysis showed severe diagenetic changes that have destroyed all of the structural units of bone (Figure 5.106). Accordingly, no Haversian systems, interstitial lamellae or osteocyte lacunae were observed. Nevertheless, it was possible to identify, at least, three distinct layers of new bone formed on the visceral surface (Figure 5.106 A, B and C). A close-up of the newly built bone revealed a primary layer that was denser and firmly attached to the underlying cortex by bone bridges (Figure 5.106 A). In other rib segment, a clear hiatus between the original rib structure and the newly deposited periosteal formation was seen (Figure 5.106 B). Multiple bridges or pedestal structures linking the different layers of new bone were observed (Figure 5.106 B and C). The pedestal structures were separated by large and irregular spaces (Figure 5.106 A, B and C). In the outermost layer, the periosteal new bone was essentially formed around small resorption spaces (Figure 5.106 B). This pattern of new bone formation is similar to the microstructure found in the sample of the PAH/C-SG22-E4 individual.

#### **Cemetery of the extinct Royal Hospital of All Saints in Lisbon**

A rib fragment exhibiting periosteal new bone formation was sampled from the adult individual P. Fig. 1429 exhumed from the ancient necropolis of the Royal Hospital of All Saints. The macroscopic and the full microscopic view revealed a bone thin section relatively well-preserved and with some signs of bone birefringence (Figure 5.107 and 5.108). In general, the rib sample is characterized by a thick pleural and cutaneous cortex, as well as by an intricate system of trabeculae (Figure 5.108). Several close-ups of the rib thin section allowed for the identification of some histological features, as well as areas of bone diagenesis. For example, in the cutaneous surface, some regions of bone birefringence, especially around the Haversian canals, were observed, which may indicate some degree of lamellae preservation. Numerous Haversian canals with different sizes and shapes were observed on the cutaneous surface. In Figures 5.108 A and B, an enlargement of the osteon canals is seen, suggesting that some degree of bone remodelling was taking place. A similar appearance was recorded on the pleural surface (Figure 5.108 C and D). Here, a thin layer of periosteal new bone is clearly distinguishable from the underlying cortex (Figure 5.108 D). Several enlarged Haversian canals were also noticed on the endosteal surface (Figure 5.108 C, D and E). Diagenetic changes

randomly distributed through the bone microstructure were a common observation in all rib segments considered. These changes were represented by diffuse (Figure 5.108 A and B) or localized micro-cracks (Figure 5.108 C), as well as by microbial tunneling in the form of continuous lines (Figure 5.108 C and D) or worm-like trails (Figure 5.108 E and F). Some black spots, probably resulting from fungal contamination, were also revealed (Figure 5.108 E and F).

A fibula sample showing remodeled foci of new bone compatible with a possible case of acquired syphilis was collected from the adult female (P. Fig. QT6 E3 1310). Macroscopically, the sample seemed well-preserved (Figure 5.109). An identical picture was retrieved from the general microscopic view that showed a well-defined bone contour at both the periosteal and endosteal surfaces (Figure 5.110). Nevertheless, the magnification of particular segments revealed massive diagenetic changes and a lack of bone birefringence (Figure 5.110 B and C). In agreement, the only microstructures preserved were Haversian canals, some of them presenting large spaces of bone remodelling (Figure 5.110 A, B, D and E), and a few recognizable shadows of Haversian systems (Figure 5.110 D and E). In spite of the described bone features, no system of lamellae or osteocyte lacunae was seen. Instead, the cortical bone was filled with an indistinct mass of composites probably resulting from microbial and fungal activity. Regarding the periosteal outline, a very different pattern of new bone formation was recorded. In a portion of the fibula diaphysis the new bone presented a wave-like and round morphology (Figure 5.110 A). In another section, new bone deposits with a finger-like or thorny morphology were seen (Figure 5.110 B). A wavy-like pattern of new bone packed between periosteal blood vessels and separated from the underlying cortex by resorption spaces was also identified (Figure 5.110 C and C\*).

A subperiosteal ossified haematoma located in the diaphysis of the left femur of an adult male (P. Fig. 1492) was sampled. The macroscopic and the general microscopic view under polarized light showed a well-preserved bone structure (Figure 5.111 and 5.112). In Figure 5.112, a large artifactual crack (probably resulting from the embedding process) was observed separating the large area of the subperiosteal haematoma from the original cortical bone. In Figures 5.112 A and 5.112 A1, the artifactual crack is clearly represented. The images also portray the structural differences observed between the cortical bone composed of well-preserved osteons and peripheral lamellae and the ossifying haematoma affected by diagenetic changes. Figure 5.112 B illustrates the good preservation of the cortical bone formed by secondary Haversian systems and interstitial lamellae. In the bulky portion that corresponds to the ossifying hematoma, only the outer layer of periosteal bone and the

Haversian canals were visible (Figure 5.112 C and D). Figure 5.112 D shows the presence of diffuse diagenetic changes such as micro-cracks throughout the pathological bone. Under transmitted light (Figure 5.112 E and E1), numerous “shadows” of osteons were identified. However, no preserved system of lamellae was seen around the vascular canals. Rather, the bodies of the osteons were formed by small fragments. These changes have affected equally the inner and the outermost layers of the ossifying haematoma (Figure 5.112 E1, F and F1).

### **Cemetery of the hospital of the *Ordem do Carmo* in Oporto**

A bone outgrowth located at the site of attachment of the tibiofibular ligament was sampled from the adult individual (Porto UE 5093) exhumed from the ancient necropolis of the hospital of the *Ordem do Carmo*. Macroscopically, the thin section was well-preserved (Figure 5.113). The microscopic view revealed a bony structure with an irregular morphology, combining smooth areas and thorny outlines (Figure 5.114). Looking closer into the bone, worm-like structures probably associated with fungal or bacterial activity were observed (Figure 5.114 A, B and C). Despite that, preserved vascular canals exhibiting some bone birefringence were seen (Figure 5.114 A and B). In some segments, signs of bone resorption were also recorded (Figure 5.114 C).

A left tibia sample showing non-specific periosteal new bone was collected from an adult male (Porto UE6451-65). As described for the previous samples, the macroscopic component is characterized by good preservation (Figure 5.115). The histological examination showed differential preservation of the bone tissue (Figure 5.116). The close-up appearance of particular segments revealed areas with relatively well-preserved osteons (Figure 5.116 A and B). Numerous enlarged osteon canals were observed which may signify that bone remodelling was occurring (Figure 5.116 B). Two distinct bone layers were observed at the periosteal level. However, the presence of diagenetic changes made it impossible to ascertain their microstructure. Despite this, two hypotheses can be advanced: the innermost layer may represent the periosteal circumferential lamellae and the outermost the newly built bone or, in contrast, both may indicate distinct episodes of periosteal new bone formation (Figure 5.116 A and B). Diagenetic changes were a common finding in the bony segments investigated (Figure 5.116 A1 and A2). Figure 5.116 A2 illustrates the detachment of Haversian systems in relation to the supporting cortex caused by micro-cracks and microbial tunnelling. Lamellate and linear longitudinal microscopic focal destruction were also recorded. The dark shadows observed throughout the bone thin section may be caused by fungal and bacterial

contamination (Figure 5.116 A1 and A2). In a thin section segment, massive osteoclastic tunnelling penetrating the periosteal and cortical bone was seen. The Howship's lacunae were intersected by lamellar bone that resembles bony trabeculae (Figure 5.116 C and D). The good preservation of lamellae allowed for the identification of primary vascular canals and osteocyte lacunae (Figure 5.116 C and D).

To summarize, the main feature shared by archaeological samples was the lack of preservation of the bone tissue. Despite the apparent macroscopic integrity, the histological analysis revealed bone samples completely affected by diagenetic changes and/or differentially preserved. These changes were particularly apparent in the specimens from Constância and Lisbon. In some samples, only Haversian canals and osteon shadows were visible. The tridimensional preservation of the bone envelope allowed for the identification of periosteal new bone formations (e.g. PAH/C-SG22-E4, P. Fig. QT6 E3 1310), as well as Howship's lacunae (e.g. PAH/C-SG19 E7). Nevertheless, the presence of diagenetic changes made it impossible to characterize the newly formed bone. The diagenetic changes most frequently observed were micro-cracks, microbial tunnelling and fungal contamination.



---

# CHAPTER 6

---

*"HUMAN SKELETAL DATA IS A BIOSOCIAL UNIT SHAPED DURING LIFE BY SOCIO-CULTURAL  
RELATIONSHIPS AND BIOLOGICAL FACTORS AND, AFTER DEATH, BY TAPHONOMIC CONSTRAINTS"*

ROBB (2000) AND DUTOUR (2008)





## 6. DISCUSSION

### 6.1. MACROSCOPIC ANALYSIS

More than half of the individuals studied presented periosteal new bone formation (PNBF) in at least one bone (61.3%, 155/253). The analysis of the distribution of periosteal lesions through the skeleton revealed different results with respect to the ribs and the appendicular bones, as it will be discussed below.

#### 6.1.1. Chest Wall: Ribs

For the overall sample, ribs were the bone elements most frequently affected by new bone deposition, mainly in individuals who died from TB (56.1%<sup>55</sup> - 87/155, Group 1), followed by those who passed away from non-TB diseases (7.7% - 12/155, Group 2) and other conditions (4.5% - 7/155, Group 3). Furthermore, individuals who showed rib lesions were always at a higher risk of developing TB, independently of having or not having corresponding foci in the appendicular bones, than those with other causes of death. Periosteal rib lesions were also most frequently seen in younger individuals (42.6% - 66/155), when compared with those older than 45 years of age (25.8% - 40/155). A combination of osteolytic and proliferative rib lesions was also observed in three individuals.

Tuberculosis is a multisystemic infection that can affect virtually any organ or system in the body (Harisinghani et al., 2000), including the musculoskeletal apparatus. Tuberculosis of the bone and joints is described as occurring in 1%-3% (Kuo et al., 2004) to 10% (Leonard and Blumberg, 2006) of patients with extra-pulmonary conditions. It is well accepted that the TB

---

<sup>55</sup> Percentages were estimated considering the individuals who showed only periosteal lesions on ribs, as well as those with PNBF on ribs and appendicular bones.

infection reaches the skeleton through the hematogenous route and from a primary focus, normally located in the lungs (Aufderheide and Rodríguez-Martín, 1998; Resnick and Kransdorf, 2005). Within the skeleton, the bacilli prefer areas of high circulatory and metabolic rate, such as the hematopoietic marrow, located in the cancellous bone (Ortner, 2003e). Accordingly, the bones most commonly targeted by the *Mycobacterium* are the vertebrae, ribs and sternum (Ortner, 2003e). The skeletal signs of tuberculosis manifest usually through focal and resorptive lesions, which may be followed by new bone formation (Aufderheide and Rodríguez-Martín, 1998; Roberts and Buikstra, 2003; Ortner, 2008).

Skeletal tuberculosis can be divided into spinal and extraspinal. Tuberculosis of the vertebral column (or tuberculous spondylitis) represents 25% to 50% of all cases of skeletal TB (Steinbock, 1976; Resnick and Kransdorf, 2005). The extraspinal form may affect the short tubular bones of the hands and feet (tuberculous dactylitis or spina ventosa), the synovial membrane of bursae, the tendons and tendon sheaths (tuberculous bursitis and tenosynovitis), the large joints (tuberculous arthritis) (Resnick and Kransdorf, 2005), and the chest wall (Pepper and Berinson, 1973; Ip et al., 1989; Asnis and Niegowska, 1997; Gupta et al., 2003; Ekingen et al., 2006; Bekci et al., 2010; Mourato et al., 2010; Grover et al. 2011; Kigera and Orwotho, 2011; Buonsenso et al., 2012).

Chest wall tuberculosis is uncommon and difficult to discern in clinical settings (Asnis and Niegowska, 1997; Faure et al., 1998; Kuzucu et al., 2004; Tuli, 2004; Bekci et al., 2010; Grover et al., 2011). Occasionally, it may affect the sternum, the sternoclavicular joint and the ribs, causing osseous destruction and localized abscess formation (Kim et al., 2001). With regard to the rib lesions, their frequency is relatively low, occurring in about 1% to 5% of cases of TB (Ip et al., 1989). For example, Tuli (2004) reports that of the 980 patients suffering from osteoarticular TB, 2% presented lesions in the ribs. Two principal causes are pinpointed to explain this low frequency: (1) its insidious development, which often occurs up to 18 months after infection and normally does not involve other organs (< 50% of patients have active pulmonary disease) (Asnis and Niegowska, 1997); and (2) the reduced sensitivity of chest radiography in detecting early signs of the condition (Ip et al., 1989; Asnis and Niegowska, 1997; Gupta et al., 2003)<sup>56</sup>. Furthermore, the differential diagnosis of chest wall TB is also challenging, as other infections (i.e. typhoid fever or paratyphoid fever, syphilis, infections due to *Streptococci*, *Straphylococci*, *Salmonella*, *Haemophilus influenza*, *Actinomycetes*, *Brucella*, and fungal infections such as coccidioidomycosis and blastomycosis), as well as benign and

---

<sup>56</sup> Ip and colleagues (1989) state that in most cases the diagnosis is delayed until osseous lesions become visible and/or palpable chest wall masses are identified.

malignant tumors (i.e. chondroma, osteochondroma, fibrous dysplasia, chondrosarcoma, multiple myeloma, Ewing's sarcoma, fibrosarcoma, and metastases of the liver, breast, thyroid and kidney carcinoma) (Bishara et al., 2000; Gupta et al.; 2003; Agrawal et al., 2008) may cause similar lesions. Tuberculosis of the ribs is more frequently found in males than females (about twice) and in patients between 15 and 30 years of age (Asnis and Niegowska, 1997). Most cases reported in the medical literature are uniformly lytic, with adjacent extrapulmonary soft tissue mass that may contain caseating or noncaseating granuloma (Pepper and Berinson, 1973; Chang et al., 1992; Grover et al., 2011). Periosteal activity is often described as absent (Johnson and Rothstein, 1952). A summary review of some clinical studies clearly illustrates the demographic and pathological distribution of tuberculous rib lesions (table 6.1).

**Table 6.1:** Summary of the literature review on cases of chest wall tuberculosis with rib lesions.

Authors	Case-Studies				
	Sex	Age (yrs)	Bone affected	Type of Lesions	Diagnosis
Johnson and Rothstein (1952)	M	26	2 <sup>nd</sup> and 4 <sup>th</sup> right ribs	2 <sup>nd</sup> right rib: destruction and widening at the costochondral junction; 4 <sup>th</sup> right rib: osteolytic lesion at the costovertebral extremity. Presence of a soft tissue abscess.	Chest wall TB
	M	26	8 <sup>th</sup> right rib	Osteolytic lesion with partial destruction of the rib. Presence of a soft tissue abscess.	Chest wall TB
	M	33	11 <sup>th</sup> right rib	Severe bone destruction of the posterior portion of the rib. Presence of a soft tissue abscess.	Chest wall TB
Pepper and Berinson (1973)	M	59	5 <sup>th</sup> right rib and tuberculous spondylitis	Osteolytic lesion of the vertebral end of the rib with extrapleural mass (tuberculous caseating granulomata). Extradural impression at T7 and a compression fracture.	Chest wall TB and tuberculous spondylitis
Ip et al. (1989)	F	30	6 <sup>th</sup> and 7 <sup>th</sup> left ribs	Thinning of the cortex of the ribs with adjacent soft tissue mass. Presence of an abscess with necrotic tissue.	Chest wall TB
	M	27	3 <sup>rd</sup> left rib	Osteolytic lesions with adjacent soft tissue mass. Presence of an abscess with granulation tissue.	Chest wall TB
Chang et al. (1992)	M	18	4 <sup>th</sup> right rib	Presence of a granuloma that partially destroyed the costal cartilage.	Chest wall TB and pulmonary TB
Asnis and Niegowska (1997)	M	46	6 <sup>th</sup> left rib	Destructive lesion: 3 cm Soft tissue mass overlying the lesion (noncaseating granuloma): 2 cm.	Chest wall TB
Afonso et al. (2001)	M	30	Several ribs (bilateral)	Osteolytic lesions in several ribs associated with bilateral soft tissue mass.	Chest wall TB and bilateral pseudogynecomastia
Gupta et al. (2003)	M	29	Left ribs	Multiple destructive foci with thickening of the left pleura. Presence of a caseating granulomatous lesion in the pleura.	Chest wall

<b>Shelat et al. (2005)</b>	F	65	4 <sup>th</sup> right rib	Posterior erosion of the rib with soft tissue mass.	Chest wall TB and tuberculous mastitis
<b>Ekingen et al. (2006)</b>	F	2	7 <sup>th</sup> left rib	Osteolytic lesion (4cm) with adjacent soft tissue mass.	Chest wall TB
<b>Bekci et al. (2010)</b>	M	22	Right ribs	Pleural thickening, destruction of the right ribs and pleural nodular lesions.	Chest wall TB "cold abscess"
<b>Mourato et al. (2010)</b>	M	36	5 <sup>th</sup> right rib	Osteolytic lesion with adjacent soft tissue swelling.	Chest wall TB
<b>Grover et al. (2011)</b>	M	26	Sternum	Osteolytic lesions with adjacent soft tissue swelling.	Chest wall TB
	M	25	Sternum	Osteolytic lesions with adjacent soft tissue swelling.	Chest wall TB
	M	7	Sternum	Osteolytic lesions with adjacent soft tissue swelling.	Chest wall TB
	F	53	sternoclavicular joint	Osteolytic lesions of the clavicular margin and soft tissue swelling.	Chest wall TB
	F	23	sternoclavicular joint	Osteolytic lesions of the clavicular margin and soft tissue swelling. Dense sclerosis of the articular surface.	Chest wall TB
	F	11	4 <sup>th</sup> left rib	Erosive lesions. Presence of a cold abscess with caseating material.	Chest wall TB
	M	2	3 <sup>rd</sup> right rib	Erosive lesions. Presence of a cold abscess with caseating material.	Chest wall TB
	F	9	10 <sup>th</sup> left rib	Mixed osteolytic and sclerotic lesions.	Chest wall TB
	F	8	3 <sup>rd</sup> and 4 <sup>th</sup> left ribs	Sclerosis and widening with ipsilateral empyema.	Chest wall TB
	F	25	4 <sup>th</sup> left rib	Erosive lesions.	Chest wall TB
M	23	---	Presence of a cold abscess with caseating material.	Chest wall TB	
M	9	---	Presence of a cold abscess with caseating material.	Chest wall TB	
<b>Kigera and Orwotho (2011)</b>	M	32	9 <sup>th</sup> left rib and tuberculous spondylitis	Hypodense lytic lesions in the thoracic vertebrae (T6-T9), with anterior collapse and kyphotic deformity. Lytic lesions in the posterior aspect of the 9 <sup>th</sup> left rib.	Chest wall TB and tuberculous spondylitis
<b>Buonsenso et al. (2012)</b>	F	15 months	10 <sup>th</sup> left rib	Well-circumscribed abscess adherent to the cartilagenous rib. Chest wall swelling.	Chest wall TB

TB is the second most common cause of destructive rib lesions after metastatic tumors (Buonsenso et al., 2012). Some clinicians classify erosive rib lesions into two types: tuberculous chondritis (more frequent), when the costal cartilage is affected, and tuberculous osteitis (rare), when the body of the rib is involved (Johnson and Rothstein, 1952). The first type is interpreted as the result of the formation of abscesses and sinus, as well as the spread of the infection from adjacent bones (Johnson and Rothstein, 1952). In contrast, Tatelman and Drouillard (1953) described four patterns of rib destruction: (1) costovertebral involvement generally associated with tuberculous spondylitis and paravertebral abscess; (2) costochondral involvement usually of a solitary rib associated with an extrapleural soft tissue mass; (3) shaft involvement with numerous areas of bone destruction associated with extrapleural soft tissue

mass; and (4) multiple cystic bone tuberculosis characterized by lesions of varying size and distinct zones of surrounding sclerosis and expansion of the shaft. One of the most frequently described sites of tuberculous involvement of ribs is the costovertebral joint, followed by the shaft (Johnson and Rothstein, 1952; Khalil et al., 1999). Clinically, the costovertebral involvement has been interpreted as secondary to spinal tuberculosis (Roberts and Buikstra, 2003). It is hypothesized that if an individual suffers from Pott's disease, the infections can be easily transferred from the vertebrae to the head of the ribs, causing the development of destructive foci (Roberts and Buikstra, 2003). For example, Khalil and colleagues (1999) observed costovertebral destruction of ribs associated with tuberculous spondylitis in 5 of 15 patients analyzed.

In the present study, only one individual who died from TB (Sk. 1583: 9 year old female) presented a mixture of proliferative and erosive lesions on ribs associated with severe destructive foci on thoracic vertebrae (T4-T12), ankylosis and gibbous formation, which resembles a case of tuberculous spondylitis, also termed Pott's disease (see Chapter 3, table 3.8) (Steinbock, 1976; Aufderheide and Rodríguez-Martín, 1998; Resnick and Kransdorf, 2005; Roberts and Manchester, 2005). A combination of proliferative and osteolytic foci was also seen in the costovertebral extremity of the 6<sup>th</sup> left rib (Sk. 470) and in the shaft of the 5<sup>th</sup> left rib (Sk. 332) of two adult males who died from TB; nevertheless there was no involvement of the vertebral column. Curiously, in skeleton no. 314, which belongs to a young adult female (20 y.o.) who died from Pott's disease and shows massive destruction of two lumbar vertebrae (L1 and L2), no destructive lesions in the contiguous thoracic ribs were recorded. In order to better understand the variability of skeletal involvement of tuberculosis, Pálfi and co-authors (2012) studied 1728 skeletons from the Terry Anatomical Collection (Smithsonian Institution, Washington, D.C., USA), dating from the first half of the 20<sup>th</sup> century. Of the cases studied, the authors describe the lesions observed in the spine of a young male (19 y.o.) who died from TB spondylitis. The lesions characterized by destructive foci of different sizes and spheroid shape were recorded in the thoracic, lumbar and sacral regions (Pálfi et al., 2012). Several ribs showed erosive lesions similar to those of the vertebrae, as well as evidence of remodelling on the visceral surface, resembling the pattern described for Sk. 1583. Extensive scalloping of some vertebral bodies, suggesting the preexistence of a granulomatous process was also reported (Pálfi et al., 2012). This last bone feature is identical to that observed in the lumbar vertebrae of Sk. 314. This evidence reinforces the hypothesis that the lytic involvement of the

spine and ribs may be an important indicator of TB in the paleopathological record (Roberts and Manchester, 2005).

In the clinical literature, three mechanisms of the pathogenesis of chest wall tuberculosis are frequently enunciated: (1) lymphohaematogeneous spread from a quiescent tuberculosis focus (e.g. gut, kidney, and tonsil); (2) direct extension from an underlying pleural or pulmonary parenchymal disease; and (3) direct extension from lymphadenitis of the chest wall (Ip et al., 1989; Chang et al., 1992; Khalil et al., 1999; Kim et al., 2001; Kigera and Orwotho, 2011). Musculoskeletal tuberculosis, namely of ribs and vertebrae, is believed to be caused by haematogeneous dissemination (Asnis and Niegowska, 1997; Khalil et al., 1999). The spread of the bacillus may occur via intercostal and lumbar arteries and/or Batson's plexus, as well as from affected contiguous para-aortic lymph nodes (Kigera and Orwotho, 2011). Direct spread from the nearest pleuropulmonary focus is described as less likely (Chang et al., 1992; Asnis and Niegowska, 1997).

As highlighted earlier, rib new bone formation is rarely identified in chest wall tuberculosis. The relative low sensitivity of chest radiography is seen as one of the major impediments to revealing early signs of the condition (Gupta et al., 2003). For example, Khalil and co-authors (1999), investigating the utility of computed tomography as opposed to conventional radiography found a spectrum of rib changes that included periosteal reactions. In a sample composed of 15 patients with documented TB, rib new bone formation was observed in eight individuals. Among these, an association between newly built bone, destructive foci and adjacent soft tissue mass was noticed in six patients. Periosteal reactions without osteolytic involvement were only observed in two individuals (Khalil et al., 1999).

Although the reported incidence in modern clinical settings is low, rib PNBf has been frequently reported in human skeletal remains from distinct temporal periods and geographic provenances (Roberts et al., 1998; Pálfi et al., 1999; Roberts and Buikstra, 2003), as isolated findings (i.e. Molto, 1990; Pfeiffer, 1984 and 1991b; Wakely et al., 1991; Lambert, 2002; Walker and Henderson, 2010), or associated with other bony changes, such as massive vertebral destruction (i.e. Haas et al., 2000; Suzuki and Inoue, 2007; Suzuki et al., 2008, Arrieta et al., 2011). With regard to its aetiology, numerous studies support a possible causal relationship between rib new bone formation and pulmonary disorders. Studying the radiographic records of a sample of 156 patients<sup>57</sup> with chronic pleural conditions, Eyler and

---

<sup>57</sup> The sample was subdivided in four groups: Group 1- mixed conditions (n=41, e.g. tuberculosis, bacterial empyema, hemothorax and lung cancer); Group 2 - tuberculosis (n=30); Group 3 - empyema (n=25); and Group 4 - healthy individuals (n=60, control subjects) (Eyler et al., 1996).

colleagues (1996) found a significant correlation between rib enlargement due to abnormal periosteal apposition and pulmonary tuberculosis. Similar compelling evidence comes from studies of morgue cadavers (Kelley and Micozzi, 1984; Roberts et al., 1994) and identified skeletal collections (Santos and Roberts, 2001; Matos and Santos, 2006; Santos and Roberts, 2006) (table 6.2).

**Table 6.2:** Comparative analysis of the distribution of PNBf on ribs of tuberculous individuals from different collections, according to frequency, age interval, anatomical location on the rib cage and rib morphology and side affected.

Study	IC	% individuals affected	Age interval (y.o.)	Location - rib cage	Side affected	Location – rib
Kelley and Micozzi (1984)	HTC <sup>1</sup>	8.8% (39/445)	20-50	R4-R8	Left >right (2:1)	Not specified
Roberts et al. (1994)	TC <sup>2</sup>	61.6% (157/255)	26-35	R1-R4	Both	Vertebral end
Santos and Roberts (2001)	CISC <sup>3</sup>	61.1% (11/18)	7-21	R4-R6	Both Left>right	Vertebral end
Santos and Roberts (2006)	CISC <sup>3</sup>	85.2% (69/81)	---	R3-R7	Left>right	Vertebral end
Matos and Santos (2006)	MBC <sup>5</sup>	90.5% (76/84)	12-30	R3-R8	Both Right>left	Vertebral end and shaft
Current study	MBC <sup>5</sup>	92.6% (87/94)	<45	R3-R8	Both Left>right	Vertebral end VE↔SE

<sup>1</sup>Hamman Todd Collection, Cleveland, Ohio, USA; <sup>2</sup>Terry Collection, Washington, DC, USA; <sup>3</sup>Coimbra Identified Skeletal Collection, Coimbra, Portugal; <sup>4</sup>Museum Bocage Collection, Lisbon, Portugal.

For instance, Kelley and Micozzi's (1984) analysis of the Hamann Todd Collection (USA) confirmed that 8.8% (39/445) of the individuals with rib PNBf had died of tuberculosis, especially of the pulmonary form, listed in 31 individuals as the cause of death. Identical results were obtained by Roberts et al. (1994) on the study of 255 individuals from the Terry Collection (USA). The authors concluded that of the individuals with periosteal rib lesions, 61.6% died from pulmonary TB. Investigations conducted on Portuguese collections revealed concordant results. Santos and Roberts (2001 and 2006) observed rib lesions in 61.1% (11/18) of the non-adults and in 85.2% (69/81) of the adults who died from pulmonary and extrapulmonary TB in the Coimbra Identified Collection. Regarding the Museum Bocage Collection (Lisbon), Matos and Santos (2006) confirmed the presence of rib lesions in 90.5% of the individuals with pulmonary TB. This general trend was also verified in the present investigation. Accordingly, in ninety four individuals with tuberculosis listed as the cause of death and affected with PNBf, rib lesions were observed on the visceral surface of 87

(92.6%)<sup>58</sup>. Periosteal rib lesions were most commonly observed at the vertebral end of ribs 3-8, mainly on the left side of the rib cage. As illustrated in table 6.2, these findings are consistent with the results obtained by other researchers not only in terms of frequency and age of the individuals affected, but also in the distribution and location of the lesions. Only Roberts et al. (1994) found a high number of rib lesion in the upper thorax. With regard to the side of the rib cage affected, a predominance of bilateral and left-sided lesions was observed among the comparative studies. In the investigation under discussion, a predominance of proliferative lesions of the woven and woven/lamellar type was observed in the individuals who died from TB. Matos and Santos (2006) also found a high number of woven lesions, especially at the vertebral end of ribs. In contrast, the majority of lesions reported by Roberts et al. (1994) were of the lamellar type.

While tuberculous rib lesions of the erosive type are believed to be generated by haematogeneous spread (Asnis and Niegowska, 1997; Khalil et al., 1999), the formation of new bone on the visceral surface of ribs has been associated with pulmonary infection disseminated from the lung tissue (via pleura) to the ribs (Roberts et al., 1994; Eyler et al., 1996; Roberts, 1999; Roberts and Buikstra, 2003; Roberts and Manchester, 2005). In spite of the apparent contributing role of TB in the development of proliferative rib lesions, its exclusiveness has not been completely proven (Roberts et al., 1998; Roberts and Buikstra, 2003). Two main factors can be put forward to explain this: firstly, the possible multifactorial origin of the bone lesions; and secondly, some limitations in the interpretation of data derived from identified collections.

Numerous studies have extensively emphasized the numerous possible diagnoses of rib lesions, which include tuberculosis, pneumonia, tumors, and blastomycosis (i.e. Kelley and Micozzi, 1984; Molto, 1990; Pfeiffer, 1991b; Santos and Roberts, 2006). In the current investigation, for example, periosteal rib lesions were observed in individuals who died from non-TB infections (31.6%, 12/38: i.e. bronchopneumonia, chronic bronchitis, pulmonary emphysema, pulmonary edema), as well as from other conditions (30.4%, 7/23: i.e. arteriosclerosis, rectal neoplasm, diabetes). These results are not surprising, since similar findings have already been described. Eyler and co-authors (1996) found some cases of rib enlargement due to new bone deposition in non-tubercular empyema, thoracic surgery, blunt trauma, and metastatic tumor. Of the 385 individuals from the Hamann-Todd collection listed as having pneumonia as the cause of death, two exhibited periosteal new bone on the visceral

---

<sup>58</sup> This general frequency was calculated summing up the individuals who died of TB and had lesions in the ribs and in the ribs and appendicular bones.



surface of ribs (Kelley and Micozzi, 1984). In the Terry Collection, Roberts et al. (1994) found that 22.2% (51/230) of the individuals listed as having died of non-TB pulmonary diseases and 15.2% (165/1086) of those who died from extrapulmonary conditions, displayed periosteal rib lesions. Proliferative lesions were also reported by Santos and Roberts (2001) in two juveniles (4.2%, 2/48) from the Coimbra Identified Skeletal Collection who died from chronic bronchitis, and osteoarthritis/septicemia. In adults from this sample, rib lesions were observed in 17.8% (16/90) of individuals listed as having died of pulmonary non-TB (i.e. pulmonary aspergillosis, purulent pleurisy, pulmonary gangrene), as well as of extrapulmonary conditions (i.e. peritonitis, brain hemorrhage, syphilis) (Santos and Roberts, 2006). In the Museum Bocage Collection, new bone deposition on the visceral surface of ribs was observed in 36.7% (18/49) of the individuals who died from pulmonary non-TB and in 25.0% (16/64) of those listed as having extrapulmonary non-TB as causes of death (Matos and Santos, 2006).

A factor that must be taken into account in the analysis of data derived from identified collections is the accuracy and completeness of the documentation available for each individual. Cadaver and identified skeletal collections have been important to better understand the distribution and possible etiology of periosteal rib lesions. Unfortunately, most collections present inherent limitations that may bias the interpretation of results. For example, the non-existence of a complete clinical historiography for each individual is a major impediment to the difficult task of corroborating the relationship between lesions and the cause of death. With respect to the cause of death listed, Roberts and co-authors (1998: 58) state that: « [it] may be incorrect for some individuals, and some people may have been suffering from tuberculosis and/or another pulmonary disease that was not the stated cause of death». In the sample studied, a young male individual (Sk. 587: 21y.o.) who died from myocarditis presented periosteal lesions on five ribs, which suggest a possible concomitant respiratory disorder. However, due to the non-existence of additional medical records it was impossible to determine whether this individual suffered from tuberculosis or from another chronic pleural condition during his life. One must bear in mind that living conditions and certain habits may also have played a role in the development of bone lesions. Walker and Henderson (2010) studied the harmful effects of smoking in a sample of 705 skeletons unearthed from the cemeteries of St. Mary and St. Michael (19<sup>th</sup> century, London, UK). Of the individuals analyzed, 42.4% (25/59) of males with dental evidence of pipe smoking had periosteal lesions on the visceral surface of ribs. Taking into account the harmful effects of tobacco consumption these days, the authors hypothesize that smoking may have increased

the frequency of lung disease and/or exacerbated preexisting infections, such as tuberculosis, in past populations.

An attempt to confirm the link between periosteal reactions on the visceral surface of ribs and TB was made by Mays and co-authors (2002) through the analysis of *M. tuberculosis* DNA in seven skeletons from the English Medieval burial site of Wharram Percy (10<sup>th</sup>-16<sup>th</sup> centuries AD). Of the individuals analyzed, only one showed a positive PCR for the presence of the infection, thus failing «(...) to demonstrate any convincing general association between visceral surface rib lesions and the presence of *M. tuberculosis* complex DNA» (Mays et al., 2002: 31). Different results were obtained by Raff and colleagues (2006) in the study of ribs from 221 individuals from the Schild Mississippian cemetery, West-Central Illinois (1000 to 1200 AD). In this investigation, all individuals identified with periosteal rib lesions (three males and two females) were confirmed as tuberculosis-positive through biomolecular analysis. In spite of the apparent relationship between periosteal rib lesions and TB, the inconsistency of results and the presence of similar lesions in individuals who died from other diseases does not allow for the establishment of a definitive association, suggesting that periosteal rib lesions is not pathognomonic for tuberculosis (Roberts et al., 1998).

### 6.1.2. Appendicular skeleton

Apart from the rib cage, a high frequency of periosteal lesions was observed in the lower limb bones when compared with the upper segments. For example, in the lower limb, 51 individuals showed new bone formation in the tibia and 39 in the femur. In contrast, PNBf was only recorded in the ulna of ten individuals, in the radius of nine and in the humerus of eight individuals. However, it should be emphasized that the frequencies recorded on the upper limb bones are probably underestimated due to the poorer preservation of the outer shell of these bones<sup>59</sup>. As noted earlier, the humerus and the ulna were the bones most affected by postmortem damage, which made the observation of lesions impossible. Several taphonomic factors linked with the funerary context (e.g. type of soil, humidity, presence of plant roots, insects or rodents), as well as with the handling of the skeletons during their recovery and storage may have contributed to the type of superficial damage observed. In addition to

---

<sup>59</sup> In the literature, long bones are described as relatively resistant to diagenetic changes due to their high cortical tissue content, being more easily recovered from archaeological and forensic contexts. In this study, the main difficulty encountered during the analysis of the long bones was imposed not by their representativeness, but instead by their poor preservation.

taphonomy, the location and type of new bone may also have contributed to these results. On the upper limb, PNBF was most frequently observed at the bone extremities, a location which is also most commonly affected by postmortem damage. Furthermore, lesions were composed mostly of woven bone and thus were easily detachable from the underlying cortex during cleaning and/or regular handling of the osteological material. A much higher frequency of periosteal lesions in the upper limb bones was observed by Assis and co-authors (2011) studying three hundred and twenty nine individuals from the Coimbra Human Identified Skeletal Collection. Of the individuals analysed, the authors observed deposits of new bone in the ulna and radius of 28 individuals and in the humerus of fourteen individuals.

On the upper limb, periosteal lesions were most frequently observed in the humerus, radius and ulna of individuals younger than 45 years of age, as well as among those who died from tuberculosis (Group 1). In Group 1, for example, the mean age of the individuals with PNBF in the humerus and radius was 20.2 and 30.5 years old, respectively (Table 6.3). In spite of the differences found in terms of age and cause of death, the results were not statistically significant.

**Table 6.3:** Frequency and average age at death of the individuals affected by PNBF in the upper and lower limb bones by cause of death (N=number of individuals affected,  $\bar{x}$ =mean age, SD=standard deviation).

Bone <sup>1</sup>	Age at death											
	All individuals			Group 1			Group 2			Group 3		
	N	$\bar{x}$	SD	% (n)	$\bar{x}$	SD	%	$\bar{x}$	SD	%	$\bar{x}$	SD
H	8	15.5	9.9	75(6)	20.2	5.9	25(2)	1.6	0.65	0	0	0
R	9	42.3	20.8	66.7(6)	30.5	10.5	33.3(3)	66	13.7	0	0	0
U	10	42.2	18.9	70(7)	33.6	14.9	20(2)	67.5	2.1	10(1)	52	---
F	39	42.9	27	35.9(14)	26.6	15	38.5(15)	42.1	32.2	25.6(10)	66.7	9.6
T	51	53.1	24.3	29.4(15)	43.8	18.7	43.1(22)	49.7	29.2	27.5(14)	68.6	11.6
FI	24	54.5	22	20.8(5)	42.4	18.3	50(12)	54.5	27.1	29.2(7)	63	9.3
RB	106	37.7	19.4	82.1(87)	34.4	16.2	11.3(12)	45.8	26.7	6.6(7)	63.9	21

<sup>1</sup>H-humerus, U- ulna, R-radius, F-femur, T-tibiae, F-fibula, RB-ribs.

With regard to the distribution of PNBF per side and location, a predominance of bilateral lesions was observed in the scapula and radius. Left-sided lesions were most frequently seen in the ulna, whereas right-sided ones were more numerous in the humerus. As pointed out previously, most lesions were located at the extremity of long bones. Only in the scapula of five individuals and on the 2<sup>nd</sup> metacarpals of another two were diffuse foci of new bone recorded. In general, a high frequency of lesions of the woven and woven/lamellar type was seen in the upper limb bones. In their investigation, Assis and co-authors (2011) found a

high frequency of individuals affected by symmetrical lesions in the radius and ulna (63.2%), followed by the scapula (23.1%). As in the present study, most lesions were localized on the distal thirds of the shaft of the humerus, radius and ulna. Similarly, a predominance of woven and lamellar compact lesions was seen in the upper limb bones, mainly in the radius and ulna (Assis et al., 2011).

When the results obtained from the upper limb bones were compared with those from the lower segments, a very different trend emerged. Accordingly, a significantly higher number of periosteal lesions were observed in the lower limb bones (tibiae and fibulae) of those individuals older than 45 years of age. For instance, the average age of the individuals with PNBf in the tibiae was 53.1 years old, and in the fibulae was 54.5 years old (Table 6.3). Furthermore, significantly more periosteal lesions in the tibia and fibula were seen in individuals who died from non-TB diseases (Group 2) and other conditions (Group 3) than in those who passed away from TB (Group 1), and the average age of the individuals with PNBf in the tibia and fibula was substantially higher in Groups 2 and 3 in comparison with Group 1 (Table 6.3). In spite of the similar distribution of bone lesions observed in the femur among age groups, the mean age of the individuals affected was lower (42.9 years old), when compared to the values obtained for the tibia and fibula, and similar to the values estimated for the ulna and radius. This resemblance was even more remarkable in the case of individuals with tuberculosis (26.6 years old). Focusing on the relationship between tuberculosis and the age of the individuals, Tatelman and Drouillard (1953) stated that in contemporary groups a high incidence of tuberculosis is seen among the 15-35 year age group. To a certain extent, the age distribution of lesions recorded in the present investigation for the upper limb and femur is consistent with this trend.

In spite of the lower frequency of lesions on the upper limb bones, their distribution by age and cause of death mirrors the pattern already described for ribs (Table 6.3). Few inferences can be derived from this trend; however, at a first sight it seems that the lesions observed in the bones from the upper limb may be more informative about the cause of death, such as tuberculosis, than the periosteal lesions on the lower leg. In addition to the distribution of lesions by age and cause of death, other differences were noted when the upper and lower limb bones were compared. With the exception of the femur, which showed a higher frequency of localized lesions, the bones from the leg and foot were characterized by diffuse foci of PNBf. For example, 19 individuals presented diffuse lesions in the fibulae in contrast to only five who exhibited localized foci of new bone. An identical distribution pattern

was reported by Assis et al. (2011) in the Coimbra Identified Skeletal Collection. In their study, localized PNBFB was most frequently observed in the femur, whereas a diffuse pattern was more often seen in the tibia and fibula.

In the current investigation, diffuse periosteal lesions were most commonly observed in the tibia of individuals from Group 2 (27.5%) and Group 3 (21.6%) as cause of death. Localized lesions in the femur were mostly seen in individuals from Group 1 (30.8%) and Group 2 (25.6%). With the exception of the innominate and calcaneus, which showed numerous lesions of the woven type, the remaining bones were characterized by lesions of the lamellar (i.e. femur) and woven/lamellar type (i.e. tibiae and fibulae). A predominance of both-sided and symmetric lesions was recorded, especially in the femur, tibiae and fibulae.

Of the eighty-nine individuals with periosteal lesions in the appendicular skeleton, 28 had more than two pairs of bones symmetrically affected. According to Larsen (1997), periosteal lesions may affect a single bone, which is most commonly observed, or involve multiple bones, suggesting the presence of a widespread or systemic infection. In the current investigation, however, the analysis of the distribution of individuals with multiple bone involvement by cause of death did not show significant results. Even when the two infectious groups (Group 1 and Group 2) were combined and compared with Group 3, the results revealed not to be statistically significant. In Group 1, the higher number of individuals with multiple bone involvement were listed as having died of pulmonary TB (n=9, out of a total of ten). Nevertheless, none of the bone lesions observed corresponds to the tuberculous pattern commonly observed outside the spine, such as: juxta-articular osteoporosis, peripherally located osseous erosion, destruction of the subchondral bone with gradual narrowing of the interosseous space (Aufderheide and Rodríguez-Martín, 1998; Roberts and Buikstra, 2003; Resnick and Kransdorf, 2005), and fibrous fixation or ankylosis, particularly of the hip and knee joints (Aufderheide and Rodríguez-Martín, 1998; Roberts and Manchester, 2005). Few studies have described PNBFBs as a possible manifestation of tuberculosis infections. Hsieh et al. (1934) studied twenty patients with tuberculosis of the shaft of the long bones in a Chinese hospital. According to the authors, four types of bone lesions were identified: tuberculous periostitis, characterized by the presence of rarefied, laminated new bone formation deposited over an apparently intact cortex; solitary tuberculous abscess (Brodie's type), formed by a single area of destruction normally located near the metaphysis; localized tuberculous osteomyelitis, characterized by a large area of bone destruction affecting the medullary and cortical portion of the bone shaft; and massive tuberculous osteomyelitis, formed by marked decalcification of

the cortical and medullary bone of the shaft with many scattered areas of destruction (Hsieh et al., 1934: 561). Hsieh et al. (1934), referring to the studies of Allison (1921), stated that in certain circumstances the tuberculous lesions may be characterized by a marked tendency for new bone production. In these cases, the resulting bone lesions seem to depend on the tissue reaction to the infectious process. When the tubercle bacillus invades the cancellous bone, there is a tendency to bone destruction. In contrast, when the periosteum is affected, bone proliferation takes place (Hsieh et al., 1934).

In spite of being uncommon, Assis et al. (2011) found a high frequency of symmetrical periosteal lesions in individuals who died of pulmonary TB (n=17), followed by those with pulmonary non-TB (n=4) and extrapulmonary non-TB (n=5) conditions. In their study, the presence of multiple foci of new bone in tuberculous individuals is discussed as possible evidence of hypertrophic osteoarthropathy (HOA) (for a review see Assis et al., 2011). In an osteological and biomolecular study, Mays and Taylor (2002) also concluded that pulmonary TB was the underlying factor in one medieval individual (10<sup>th</sup>-16<sup>th</sup> century AD) from Wharram Percy, England, with possible HOA. In their study, periosteal lesions were observed in the scapula, innominate, calcaneus and long and short bones from the upper and lower limbs. The new bone deposits were predominantly symmetrical and composed of both woven and compact bone of only a few millimetres thick (Mays and Taylor, 2002). In the present study, most of the periosteal lesions observed in Group 1 resemble the pattern observed by Assis et al. (2011) and Mays and Taylor (2002), and that are described in the clinical and paleopathological literature as being associated with HOA (i.e. Kelly et al., 1991), that is, multiple, symmetric foci of new bone clearly differentiated from the underlying cortex and normally located at the bone extremities (Aufderheide and Rodríguez-Martín, 1998; Resnick and Kransdorf, 2005; Martínez-Lavín, 2007).

In Group 2, multiple periosteal bone involvement was observed in eight individuals with different diseases as cause of death. Of these, six were listed as having died of non-tuberculous pulmonary conditions (i.e. bronchopneumonia, pneumonia, fetid bronchitis, pulmonary emphysema, pulmonary abscess), and among those, four presented periosteal lesions compatible with HOA. This may be a possible correlation, since numerous pulmonary diseases such as primary and secondary lung carcinoma, pulmonary fibrosis and emphysema, pleural fibroma and mesothelioma, bronchogenic carcinoma, pulmonary tuberculosis, and pulmonary abscesses are commonly involved in the pathogenesis of HOA (Poppe, 1947; Balaji et al., 2006; Armstrong et al., 2007; Harifi et al., 2008). Disseminated periosteal lesions were

also observed in a case of syphilis and leprosy. In an adult male (Sk.491, 66 y.o.) listed as having died of “syphilis”, slight new bone reactions with a symmetric involvement of the ulna, tibia and 1<sup>st</sup> metatarsal, and asymmetric distribution in the femur were observed. At some points of the proximal extremity, an abnormal expansion of the ulnar and tibial shafts was observed. Periosteal lesions have a remodelled appearance; nevertheless, multiple vascular holes were observed in the cortical surface. In both congenital and acquired syphilis, periostitis, osteitis and osteoperiostitis and gummatous osteomyelitis are the most common findings in the long bones (Steinbock, 1976). PNBFs may be composed of woven bone, but most frequently they consist of compact bone, reflecting the chronic nature of the condition (Ortner, 2008). A pattern consisting of reactive bone formation of lamellar type is commonly encountered in the tibia (Ortner, 2008). Syphilis affects more often the tibia, followed by the frontal and parietal bones (“caries sicca”), the nasal-palatal area, the sternum and clavicle, the vertebrae, femur, fibula, humerus, ulna and radius (Steinbock, 1976). In spite of the presence of periosteal reactions, it is impossible to confirm if the lesions observed in Sk. 491 were caused by syphilis, since none of the most distinctive traits were observed (i.e. caries sicca and sabre shin).

The adult male Sk. 35 (47 y.o.) who died of “leprosy” also showed symmetric periosteal lesions in the tibia and fibula. With an exuberant appearance formed by spiky bone projection, the periosteal reaction was mostly circumscribed to the tibia-fibular ligament insertion. Leprosy, especially in its lepromatous form, may also induce the formation of new bone. Periosteal reactions may develop by extension of the infection from the overlying soft tissues to the periosteum (leprosy periostitis), adjacent cortex, spongy bone and marrow (leprosy osteitis and osteomyelitis) (Resnick and Kransdorf, 2005). In this case, symmetrical periostitis of the tibia, fibula, and distal portion of the ulna is observed (Resnick and Kransdorf, 2005). Secondary involvement of the skeleton as a result of neural changes may also stimulate the development of periosteal lesions. For example, neurological problems of the foot with loss of sensation may induce injuries and the development of secondary infection. This infection may then spread to the adjacent tibia and fibula, leading to the formation of periosteal reactions (Ortner, 2003e). Accordingly, the tibia and fibula are the long bones most commonly affected by nonspecific periosteal thickening (Steinbock, 1976). Ulceration followed by secondary infection and pyogenic osteomyelitis and soft tissue calcification may also occur (Resnick and Kransdorf, 2005; Waldron, 2009). The symmetric lesions observed in the leg bones of individual Sk. 35 were more likely caused by secondary involvement due to their localization

and lack of specificity. However, the absence of the foot bones did not allow for the confirmation of this hypothesis.

In Group 3, ten individuals presented more than two pairs of bones affected with PNBFB. Lesions were observed in individuals who died of different diseases, such as uraemia, gangrene, hepatic cirrhosis, gastric ulcer, arteriosclerosis and tumours. PNBFBs were most commonly seen in individuals listed as having died of arteriosclerosis (n=3) and tumours (n=3). With regard to the individuals who died of tumours (gastric carcinoma, rectal neoplasm and prostate cancer), most periosteal lesions observed are probably the result of metastatic spread from the affected organs to the skeleton. The malignant diseases that show a higher incidence of bone metastases are cancer of the prostate (84%), breast cancer (72%), thyroid cancer (50%) and kidney cancer (37%) (Berná et al., 1991; Alcalay et al., 1995 after Rosenthal, 1997; Brage and Simon, 1992 after Rosenthal, 1997). These are followed by cancer of the lung, pancreas, bladder and uterus (Mundy, 1997; Campanacci, 1999). Bone metastases are particularly frequent in individuals over 50, which agrees with the age of the individuals affected (Sk. 358, female, 52 y.o – gastric carcinoma, Sk. 457, male, 66 y.o. – rectal neoplasm, Sk. 1298, male, 67 y.o. – prostate cancer), and can affect several bone elements, amongst them the vertebrae, the pelvis, the ribs, the sternum, and the metaphyseal portions of the humerus and the femur (Steinbock, 1976; Waldron, 1996; Mundy, 1997; Aufderheide and Rodríguez-Martín, 1998; Ortner, 2003f; Nöbauer and Uffmann, 2005; Resnick and Kransdorf, 2005). Metastatic lesions distal to the elbow and knee are rare (Steinbock, 1976; Waldron, 1996; Thillaud, 1996; Campanacci, 1999; Ortner, 2003f; Resnick and Kransdorf, 2005). Metastatic carcinoma can generate a variety of alterations in bone cell function that are lytic, osteoblastic or a combination of both (Steinbock, 1976; Waldron, 1996; Coleman, 1997; Mundy, 1997; Rosenthal, 1997; Aufderheide and Rodríguez-Martín, 1998; Coleman, 2001; Ortner, 2003f; Resnick and Kransdorf, 2005). In the case of kidney, lung and thyroid carcinoma, the main alterations are predominantly osteolytic, whereas those of the prostate are mainly osteoblastic (Burgener et al., 2006). In breast carcinoma, both the destruction and the production of new bone can be found (Coleman, 1997; Aufderheide and Rodríguez-Martín, 1998; Ortner, 2003f; Resnick and Kransdorf, 2005; Burgener et al., 2006).

Only proliferative lesions of both the woven and compact type were observed in the ulna (asymmetric) and in the tibia and fibula (symmetric) of individual Sk. 358 who died from gastric carcinoma. In contrast, a more diverse and exuberant spectrum of lesions was observed in individual Sk. 457 who died from rectal neoplasm. Accordingly, lesions of the woven type



were seen in the clavicles and in the scapulae (symmetric) and in the innominate bones (asymmetric), and those of the lytic/proliferative (woven) type were present in the femora. In some bones (i.e. innominate), multiple thin spikes of bone were seen above the cortex, which gave the periosteal lesion a spongy and/or sunburst appearance. In spite of being quite unusual, PNBf may occur in gastrointestinal malignancies (Burgener et al., 2006). When present, the bone lesions may range from purely lytic to purely osteoblastic (Burgener et al., 2006). Occasionally, the metastases from colon or rectal carcinoma may resemble an osteosarcoma exhibiting periosteal reaction with a sunburst pattern (Burgener et al., 2006). To some extent, the periosteal lesions observed in Sk. 457 agreed with the clinical descriptions advanced for some gastrointestinal malignancies, namely those associated with rectal carcinoma. In individual Sk.1298 who died from prostate carcinoma, multiple symmetric lesions were observed in the scapulae, innominate bones and femora (lytic/proliferative - woven), and in the 2<sup>nd</sup> left metatarsal and in the 3<sup>rd</sup> right metatarsal bones (lamellar type). As pointed out previously, bone metastases of prostate cancer are predominantly osteoblastic (Aufderheide and Rodríguez-Martín, 1998; Burgener et al., 2006) with the combination of osteolytic/osteoblastic foci being rare. However, as stated by Ortner (2003f after Greenspan and Remagen, 1998), mixed lesions can be associated with virtually any type of tumor.

Three individuals who died of arteriosclerosis (Sk. 429, female, 52 y.o.; Sk. 971, female, 74 y.o.; Sk. 1199, male, 52 y.o.) also presented PNBf in the femora, tibiae and fibulae. The lesions were characterized by slight deposits of new bone with a remodeled appearance. Other manifestations included porosity, longitudinal striation and smooth nodule formation. Venous imprinting, mostly in the anterior surface of the tibia, was also observed. Numerous conditions may induce the formation of new bone on the periosteal surface (for a review see Table 3.5, Chapter 3). Among these, vascular and lymphatic disorders are commonly enunciated in the clinical literature (Kenan et al., 1993; Burgener et al., 2006). According to Burgener et al. (2006) any disease associated with venous and /or lymphatic stasis can potentially stimulate new bone production. With an undulating appearance, the layers of new bone may be solid thin or thick, circumscribed or diffuse, and more often localized in the lower extremities. Although the appearance and distribution of bone lesions is suggestive, it is impossible to establish a direct association between arteriosclerosis, as cause of death, and PNBf. Direct evidence of deficient blood circulation in the extremities is normally obtained from the presence of venous ulcers. In skeletal remains, large chronic ulcers manifest through «(...) plaquelike deposition of periosteal bone of considerable thickness, roughly copying the

outline of the ulcer» (Ortner, 2003d: 207). Cortical thickening accompanied by periosteal reaction with thickened bark-like bone formation affecting a portion or all of the diaphysis may also develop. In severe conditions, bone bridging between adjacent bones, such as the tibia and fibula may occur (Ortner, 2003d; Ortner, 2008; Boel and Ortner, 2011). For example, Pinheiro et al. (2004) describe a massive ossification of the interosseous membrane of the tibia and fibula in a forensic case of venous chronic insufficiency. In the three individuals who died from arteriosclerosis, none of the bone features consistent with skin ulceration or with other pathologies were observed. Consequently, the relationship between cause of death and periosteal lesions remains unclear.

An exuberant case of PNBf affecting the femora, and more severely the lower third of the tibiae and fibulae was observed in an adult male (Sk. 1484, 73 y.o.) who died of gastric ulcer. For example, in the shaft of the right tibia, massive densification of the periosteal surface with plaque-like bone formations was observed. In both tibiae and fibulae, distinct bone formations characterized by dense and striated foci, spiky and plaque-like deposits and finger-like formations were seen. In the clinical and paleopathological literature, no apparent correlation between gastric ulcer and PNBfs seems to exist. This may suggest that other conditions distinct from the cause of death may have affected the individual during his life. The presence of both-sided lesions and the nonexistence of cloacae ruled out a case of osteomyelitis. Acquired syphilis seems less likely due to the location of lesions, circumscribed to the lower third of the shaft of the tibia and fibula, as well as the fact that the general morphology of the lesions differ from those of syphilitic osteitis and osteoperiostitis (Steinbock, 1976). The lack of involvement of other skeletal elements, such as the foot bones, renders the diagnosis of leprosy less probable. A severe circulatory condition or a lower leg skin infection (i.e. cellulitis) is more likely. However, the non-specificity of the periosteal lesions makes the differential diagnosis inconclusive.

As pointed out earlier, multiple periosteal lesions are frequently described as the result of a systemic condition (i.e. infection). In the present investigation, no statistically significant differences were found among cause of death groups. As exemplified above, PNBf was observed in a broader group of pathologies. That is, distinct individuals listed as having died of different conditions presented multiple foci of new bone formation. This agrees with previous studies that highlighted the non-specificity of periosteal lesions (i.e. Weston, 2008). Weston (2008) studied fifty-six bones (n=56) from two London (UK) pathology museums (12 from St. George's Hospital Pathology Museum and 44 from the Hunterian Museum) with different

pathologies: osteomyelitis, necrosis, leg ulcer, syphilis, rickets and “periostitis”. Focusing on the macroscopic and radiographic analysis of the bone lesions, Weston (2008) found that the size, type, vascularisation, severity, radiographic margination, and cortical and endosteal features were not specific to the distinct diseases studied. Furthermore, the author stated that «[...] periosteal reaction should be interpreted with extreme caution, as lesion characteristics overlap across disease categories» (Weston, 2008: 58). In the paleopathological literature, periosteal reactions, especially those observed in the tibial shaft, have been used as an important indicator of the health conditions of past populations. In fact, numerous studies combine PNBf with other “physiological stress markers”, such as the enamel hypoplasias, Harris lines and *cribra orbitalia* to evaluate and discuss measures of health inequality (i.e. Šlaus, 2008; DeWhite, 2010; Shuler, 2011). The apparent non-specificity of the periosteal reactions seems, however, to challenge the utility of this bone response in the difficult task of reconstructing ancient profiles of health and disease. Taking into account the results of the present investigation, two important questions can be addressed: firstly, what is the real meaning of periosteal reactions as indicators of physiological stress?, and secondly, what are the limitations of identified skeletal collections in the study of particular bone conditions?

#### **What is the real meaning of periosteal reactions as indicators of physiological stress?**

As indicated previously, periosteal reactions may be caused by any mechanism that inflames, tears, breaks, stretches or even touches the periosteum (Richardson, 2001). Accordingly, every biological or mechanical factor that disrupts or interferes with the normal functioning of the inner layer of the periosteum may stimulate the formation of new bone. However, it must be emphasised that this bone response may not be uniform or homogeneous for all individuals and conditions. This means that the same agent may cause different periosteal responses, or inversely, that distinct stimuli may produce an identical periosteal reaction on the bone surface, thus reinforcing its non-specificity. Weston (2008) states that independently of the nature of the agent (i.e. subperiosteal accumulation of pus, blood, granulation tissue, or tumour cells; mechanical adaptation; or disruption of blood circulation), periosteal reactions are formed as a type of healing mechanism. If this is true, a parallel can be drawn with other body injuries. As in a skin lesion, the morphology of the “periosteal scar” will depend not only on the nature of the “stimulus”, but also on local factors such as the anatomical location of the injury, the depth and extension of the area affected, and the composition and health of the tissues injured. The age and sex of the individuals, genetic predisposition, human behaviour, nutritional status, physiological and immune conditions, as

well as the co-existence of other diseases (Roberts and Manchester, 2005) may also play a part in the type and velocity of the bone response. As a consequence, the morphology of the periosteal lesions will depend more on the type of periosteal response than on the impact of pathological agents. Quoting Weston (2008: 56): «It appears that this lack of identifying traits [periosteal lesions] is due to the way in which bone and the periosteum responds pathologically. It is not the disease that determines how these tissues respond, it is the tissues themselves». Even if the lesions present a more “distinctive pattern”, a careful approach must be taken in its analysis. For example, Haun et al. (2006) report a case of stress-induced spiculated PR resembling a malignant tumour, observed in an adult female (54 years-old). The lesion was located on the medial margin of the metadiaphyseal region of the distal fibula and exhibited spiculation and irregularity of the periosteum. After discarding any sign of malignancy, the authors concluded that the lesion was caused by repetitive stress on the distal fibula and along the insertion of the interosseous membrane, possibly aggravated by a partial tear and tenosynovitis of the posterior tibial tendon (Haun et al., 2006). This study clearly illustrates how difficult the differential diagnose of periosteal lesions in the clinical practice is. In paleopathology, this difficulty increases exponentially, especially when the skeletal remains are not well preserved. A current statement in the paleopathological literature is that periosteal lesions may be etiologically correlated to infectious or traumatic conditions (Larsen, 1997; Ortner, 2003d). But is PNBFs evidence of a life threatening condition?

Referring to tibial periosteal lesions, Roberts and Manchester (2005: 130) pointed out that trauma or venous insufficiency may induce a superficial and insignificant inflammation of the lower leg and subsequent new bone formation, however «(...)without producing the debilitating and even crippling symptoms of the more severe osteomyelitis». In accordance, it is likely that many of the bone lesions observed resulted from mild inflammatory processes or localized trauma (i.e. shin splint) that did not endanger the individual's life. When studying periosteal reactions, one should also bear in mind that the lesions observed may not have resulted from a single process, but instead from multiple pathological conditions faced by individuals during live. For example, in an adult male (Sk. 1199, 52 y.o.) who died from arteriosclerosis, superimposed foci of new bone in distinct stages of healing were observed. Regarding the pattern of lesions, two interpretations can be made: it resulted from the intermittence of a particular condition or, in contrast, was a consequence of unrelated processes. Taking into account these possibilities, the study of PNBFs as an indicator of morbidity and mortality may be limited. Such a constraint increases substantially if we

consider that individual susceptibility to illness also varies during life (Wright and Yoder, 2003). Using periosteal lesions to ascertain the frailty of an individual, as broadly discussed with respect to the osteological paradox, is even more complex if the non-representativeness of samples, selective mortality and hidden heterogeneity of risk are considered (Wood et al., 1992; Wright and Yoder, 2003).

PNBF is also not considered a good indicator of “physiological stress”. Stress<sup>60</sup> can be defined as a «[...] state of disharmony, or threatened homeostasis» that occurs when the harmonious equilibrium of the body is disturbed by intrinsic or extrinsic forces, or stressors (Chrousos and Gold, 1992: 1245; Kassi et al., 2012). When a stress episode occurs, an adaptive behavioural and/or physiological response<sup>61</sup> is given by the organism in order to counteract and re-establish homeostasis (Chrousos and Gold, 1992; O’Connor et al., 2000; Kassi et al., 2012). This adaptive response is mediated by a complex neuroendocrine, cellular and molecular pathway called the stress system, which is partially located in the central nervous system (CNS) and in various peripheral organs and tissues (Chrousos, 2009; Kassi et al., 2012). Amongst the CNS effectors are the arginine-vasopressin (AVP) neurons of the paraventricular nuclei (PVN) of the hypothalamus, the corticotrophin-derived peptides  $\alpha$ -melanocyte-stimulating hormone and the  $\beta$ -endorphin (Chrousos, 2009; Kassi et al., 2012). The main peripheral effectors are the sympathoadrenal epinephrine and norepinephrine secreted by the adrenal medulla (Chrousos, 2009) and the glucocorticoids, whose synthesis is regulated by the hypothalamic-pituitary-adrenal axis (O’Connor et al., 2000; Chrousos, 2009).

Excessive and/or chronically imposed stressors may act negatively upon the growth, reproduction, metabolism and immune response of individuals, leading to the development of disorders namely in the skeletal system (Chrousos, 2009; Kassi et al., 2012). The disorders associated with chronic-stress episodes are induced by an excessive secretion of the major mediators of the stress response, whose action may affect the function of numerous body

---

<sup>60</sup> In 1936, the Canadian physiologist Hans Selye introduced the concept of “stress” to describe a nonspecific response of the organism to particular stimuli that he termed “stressors”, which are regulated by the adrenal glands (Chrousos and Gold, 1992, Fox, 1999). This physiological response was called general adaptation syndrome (GAS) and is composed of three stages: (1) the alarm reaction, when the adrenal glands are activated; (2) the stage of resistance, in which the readjustment of the body to the stress episode occurs; and (3) the stage of exhaustion, which may lead to disease and/or death if the body’s readjustment is incomplete (Fox, 1999).

<sup>61</sup> In acute stress situations, the CNS division is involved in the facilitation of vigilance, cognition and aggression, as well as in the inhibition of vegetative functions, such as reproduction, feeding and growth (Chrousos, 2009). Conversely, the sympathetic division of the autonomic nervous system prepares the body for intense physical activity, increasing the cardiovascular tone, the levels of blood glucose, the general metabolic functions and the detoxification rates of metabolic products and foreign substances, the suppression of the inflammatory/immune system, and the secretion of hormones from the adrenal medulla (epinephrine and norepinephrine or noradrenaline) responsible for the “fight-or flight” reaction (Fox, 1999; Chrousos, 2009).

systems (Chrousos, 2009). For example, under chronic stress conditions the hypothalamic-pituitary-adrenal axis (HPA) is stimulated to increase the synthesis of glucocorticoids (GC)<sup>62</sup>(Fox, 1999), which in turn acts to inhibit the secretion of growth hormone (GH), insulin-like growth factor I (IGF-I), interleukin 6 (IL-6), and tumour necrosis factor- $\alpha$  (TNF- $\alpha$ ), amongst other substances (Chrousos, 2009). Phenotypically, this shift in the metabolism may have an enormous impact on the well-being of the individuals.

Chronic stress and/or abnormal HPA axis stimulation is described as causing arrested or impaired growth in children due to the suppression of the growth hormone and subsequent inhibition of the insulin-like growth factor-1 (IGF-1) (O'Connor et al., 2000; Mushtaq and Ahmed, 2002). An abnormal synthesis and/or long-term administration of GCs is also described, in the clinical literature, as responsible for a decrease in bone mass, as well as suppression of the osteoblastic differentiation and maturation (Kassi et al., 2012). These changes will affect the synthesis of bone proteins (i.e. collagen type-I, osteocalcin, osteopontin, fibronectin,  $\beta$ -1 integrin, collagenase, and alkaline phosphatase), the mineralization of the bone-forming matrix, and the apoptosis of osteoblasts (Reid, 1998; Papierska and Rabijewski, 2007). GC-induced bone changes have been widely investigated in human and non-human *in vitro* experiments and in patients submitted to glucocorticoid therapy (Reid, 1998). A common clinical occurrence associated with glucocorticoid-therapy is the development of “crippling forms of osteoporosis” and increased risk of bone fractures (i.e. Cushing’s syndrome) (Reid, 1998, Cooper, 2004; Canalis, 2005; Kim et al., 2006: 2152; Papierska and Rabijewski, 2007). Another effect of GCs is the inhibition of the inflammatory/immune response through a change in the movement and function of leukocytes, a decrease in the synthesis of cytokines and mediators of inflammation, and the inhibition of the response of the target tissues (Chrousos and Gold, 1992; O'Connor et al., 2000; Kassi et al., 2012). O'Connor et al. (2000) state that GCs may potentially inhibit the function of all inflammatory cells, since they modulate the innate and adaptive response of the immune system (Kassi et al., 2012). As a result, glucocorticoids are frequently used in the treatment of numerous inflammatory and autoimmune disorders (Kim et al., 2006; Papierska and Rabijewski, 2007). For example, numerous clinical studies on the treatment of systemic

---

<sup>62</sup> In normal stress conditions, GCs have a catabolic effect upon the body tissues (i.e. increasing the blood levels of hepatic gluconeogenesis and plasma glucose, inducing lipolysis and causing protein degradation at multiple tissues, such as muscle, bone and skin) as a way to make available sufficient energy resources that would be used in the counterbalancing of challenges imposed by stressors (Kassi et al., 2012).

vasculitis<sup>63</sup> and associated periosteal new bone formation reported that the condition resolved after administration of corticosteroids. In these cases a moderate or complete reduction of the newly built bone and the clinical remission of the pathology were noticed after GC therapy (Ball and Grayzel, 1964; Short and Webley, 1984; Astudillo et al., 2001; Aries et al., 2005; Périchon et al., 2010; Rauch et al., 2010). This clinical evidence contradicts the usefulness of PNB as an indicator of stress in the skeletal record, since there is a tendency to bone resorption instead of its production. In a review of the interaction between inflammation and bone metabolism, Hardy and Cooper (2009) noted that almost any chronic inflammatory disease is associated with systemic bone loss. According to the authors, bone loss occurs as a direct extension of inflammation, poor nutrition, reduced lean body mass, immobility, as well as drug therapy, especially glucocorticoids. Systemic inflammation commonly impacts normal bone resorption/formation, leading to bone loss, but rarely to bone gain (Hardy and Cooper, 2009). Thus, periosteal lesions seem not to be a good indicator of physiological stress.

The non-specificity of periosteal lesions in relation to the cause of death was one of the major findings of this investigation, especially when the tibia was considered. But should these results be attributed only to the nature of bone tissue response or to the composition of the sample as well?

**What are the limitations of identified skeletal collections in the study of particular bone conditions?**

Over the last few decades, identified human skeletal collections derived from morgue cadavers or historical cemeteries have been used to test the relationship between particular bone lesions and the cause of death of the individuals. Nevertheless, the establishment of such a correlation is not as straightforward as it seems. In fact, most reference collections have similar drawbacks as archaeological samples. Komar and Grivas (2008), in their investigation of the representativeness of contemporary reference skeletal collections, highlight three major problems: the representativeness of the samples, the criteria used to assemble collection, and the source and completeness of the documentation available for each individual. According to the authors, a recurrent pitfall in the use of identified collections is the tendency to confound “documented” with “representative”, which are not equivalent (Komar and Grivas, 2008: 224).

---

<sup>63</sup>Despite being uncommon, periosteal new bone formation may occur in systemic vasculitis (necrotizing vasculitis or polyarteritis nodosa and systemic lupus erythematosus), in which the bones from the lower extremity are most frequently affected both symmetrically and asymmetrically (Ball and Grayzel, 1964). In most cases, the pathogenesis of the periosteal new bone formation is justified as a result of the local production of bone growth factors associated with vascular hypoxia.

The way in which the collection was assembled, the criteria used in the selection of the individuals, and/or the osteological material available at the time may render identified collections unrepresentative of the original population and produce a considerable source of bias (Komar and Grivas, 2008). Focusing on the history and demographic composition of the Terry Anatomical Collection (20<sup>th</sup> century), for example, Hunt and Albanese (2005) found that this particular collection does not represent the living population or the pattern of mortality and disease of that time period because of the criteria used in the assemblage of individuals. Komar and Grivas (2008) obtained similar findings for the Maxwell Museum collection, concluding that all the identifying criteria used in the analysis (i.e. sex, age cohorts, biological affinity, and cause and manner of death) presented some sort of bias and did not mirror the living population. Another confounding factor relates to the non-existence of additional records that allow the complete reconstruction of the individual's historiography in terms of health and disease. For most documented skeletal collections the cause of death is known, however this information does not clarify whether other conditions have affected the individuals and ultimately the skeleton. Similarly, it does not provide information about hidden conditions that may have contributed to the cause of death, or inaccuracies in its diagnosis (Santos and Roberts, 2001; Matos and Santos, 2006; Brickley and Ives, 2008). The following three cases clearly illustrate some of the limitations of using documented collections to study bone pathology:

**Case#1:** A young male individual (Sk. 684, 16 y.o.) showed multiple foci of new bone with symmetric involvement of the humerus, tibia, and fibula, and asymmetric involvement of the left ulna and 2<sup>nd</sup> right metatarsal. Surprisingly, acute phthisis was listed as the cause of death. In a medical report published in 1890, McCall described the characteristics of this respiratory condition: «By acute phthisis [...] I allude to cases of phthisis setting in suddenly, with high and continuous fever, great prostration, and profound involvement of the system, reminding one rather of typhus or a severe attack of typhoid fever than of a pulmonary affection. Indeed, in some instances it may be necessary to watch the course of the disease for some days before an absolute diagnosis can be made, so that the term "galloping consumption," used by many of our leading authorities, although not a scientific one, conveys to the mind a most accurate impression of the kind of disease with which we are dealing» (McCall, 1890: 1051). If acute phthisis has a sudden development and was lethal to Sk. 684, it seems unlikely



that the multifocal bone involvement observed was caused by it. As pointed out by Ortner (2003c), the skeletal manifestations of illness are normally associated with chronic responses to disease. Accordingly, one may suppose that an unreported longstanding condition may have affected this individual, leaving their marks in the skeleton. Nevertheless, the association between bone lesions and acute phthisis cannot be completely discarded because in a chronic systemic condition numerous acute episodes may occur (Ortner, 2008). Furthermore, the hypothesis of an incorrect diagnosis should also be considered.

**Case#2:** In an adult male (Sk. 27, 67 y.o.) who died of pulmonary tuberculosis, periosteal lesions were observed in the ribs. In addition to rib lesions, multiple osteolytic foci with a round-shaped and/or moth-eaten morphology and different sizes were seen, for example, in the body of the right scapula, innominate bones (iliac fossa and iliac crest) and sacrum (Figure 6.4). While the periosteal rib lesions may be related to the cause of death, as previously described, the presence of lytic foci appears to suggest the co-existence of a different condition at the time of the death. TB may also produce osteolytic lesions but they are normally located in the vertebral column and at the weight-bearing joints (Roberts and Manchester, 2005). Accordingly, it is more likely that the lytic foci observed were caused by some mycotic disease or neoplasm, such as metastatic carcinoma (Aufderheide and Rodríguez-Martín, 1998). This bone evidence suggests that in spite of the cause of death, other conditions not reported in the obituary record may also have been present.

**Case#3:** In an adult female (Sk. 1042, 73 y.o.) listed as having died of senile cachexia, numerous bone outgrowths were observed in the distal metaphyses of the femur and fibula and in the proximal and distal metaphyses of the tibia. Furthermore, a left-sided asymmetry was also seen. No evidence of bone trauma was recorded. The bone changes described seem to correspond to a probable case of multiple cartilaginous exostoses (MCE). MCE, also termed hereditary multiple exostoses (HME), diaphyseal aclasis, (multiple hereditary) osteochondromatosis or multiple osteochondromas (MO), is an autosomal-dominant disorder frequently associated with progressive skeletal deformities (Stieber et al., 2001; Bovée, 2008). The condition is characterized by multiple cartilage-capped bone outgrowths with a sessile or pedunculated appearance that forms during the individual's growth (Stieber et al., 2001, Bovée, 2008). The

multiple exostoses are most frequently observed at the metaphyseal portions of the most rapidly growing long bones (i.e. tibia and femur). Nevertheless, other bones such as the scapulae, ribs, vertebrae and pelvic bones may be affected (Stieber et al., 2001). Among the clinical manifestations of MCE are pain, often caused by soft tissue trauma over exostoses, bursitis, short stature, limb-length discrepancies, and valgus deformities of the knee and ankle (Stieber et al., 2001). The most important complication is the possible transformation of osteochondroma into secondary chondrosarcoma, which occurs in 0.5-5% of cases (Bové, 2008). Given the severity of the bone lesions and the lower limb asymmetry observed, it seems reasonable to think that the skeletal deformities were quite evident. However, no mention of this condition was made in the death certificate. The lack of knowledge about the condition and/or its non-involvement in the cause of death may explain its omission from the death records.

In spite of the usefulness of identified skeletal collections, studies that aim to better characterize bone lesions based on the cause of death of individuals must be used and interpreted with caution. There is always the possibility of inaccurate records of cause of death, or the coexistence of multiple conditions not identified in the obituary certificate.

In the present investigation, the lack of significant differences in the distribution of lesions by cause of death may be due not only to the non-specificity of periosteal lesions, but also to the composition of the sample. This last hypothesis may explain the high frequency of PNBF in individuals from Group 3 [other conditions of cardiovascular (i.e. chest angina, mitral disorder, arteriosclerosis), metabolic (i.e. diabetes, hepatic cirrhosis, hepatic coma), and tumour origin], especially in the tibia and fibula. Some of these conditions constitute risk factors for the development of circulatory disturbances and skin infections, such as chronic venous insufficiency and cellulitis, which, in turn, may contribute to localized bone inflammation (Eagle, 2007). Furthermore, Group 3 also presented a higher average age of individuals affected than Groups 1 and 2. If individuals live longer, the probability of developing chronic diseases or suffering traumatic episodes with direct or indirect involvement of the skeleton also increases. Accordingly, bones may exhibit a broader record of pathological events prior to the cause of death.

In summary, in the present investigation only periosteal rib lesions had a positive relationship with TB as the cause of death (Group 1). The tibia and fibula were most frequently affected by PNBF in Group 2 (non-TB infectious conditions) and Group 3 (other diseases), and

in individuals older than 45 years of age. On the upper limb, the humerus, radius and ulna showed more deposits of new bone, especially among younger individuals from Group 1. The analysis of the individuals with multiple periosteal bone involvement did not reveal significant differences among cause of death groups. This lack of association between new bone formation, particularly in the tibia and fibula, and the underlying cause of death seems to corroborate the non-specificity of periosteal lesions, challenging their usefulness as an indicator of physiological stress. Accordingly, paleopathologists should be careful when using lower limb periosteal lesions to ascertain the diagnosis of particular conditions. Special attention must be given to the presence of PNB on the upper limb bones and femur. In spite of the lack of statistical significance, the distribution of lesions by age and cause of death seems to mirror the pattern observed on the rib cage, that is, a possible association with TB infection. However, this relationship needs further investigation. The results of this study also revealed some of the limitations and possible misinterpretations found in the study of identified skeletal collections.

## **6.2. HISTOLOGICAL ANALYSIS**

As mentioned earlier, the selection of documented bone specimens for histological analysis followed specific criteria that did not allow for the sampling of all pathological cases observed macroscopically. Even so, an attempt was made to collect samples that were representative of each cause of death group. In order to broaden the spectrum of new bone formations, samples of fracture callus in distinct stages of healing were also collected and added to Group 3 cause of death. Pathological cases derived from archaeological contexts were selected to better determine the aetiology of bone lesions, as well as to investigate the impact of diagenetic changes on the bone microstructure. The histological study of 34 bone samples revealed striking results that reinforce the importance of applying histological techniques in the description and diagnosis of bone changes. The value of histology was observed at three main levels: 1) diagnosis of pathological conditions, 2) description of bone lesions, and 3), assessment of bone tissue quality.

### 1. Role of histology in the diagnosis of pathological conditions

Differences in the microstructure of PNB were seen between causes of death groups. These variations were more pronounced in the rib thin sections collected from individuals belonging to Group 1 and Group 2. Accordingly, multiple layers of “appositional bone” enclosing primary vascular canals and separated from the underlying cortex by resorption spaces were the “pattern” most frequently observed in Group 1-TB samples (n=4). In these samples, no bony changes were seen at the cortical level. A similar bone microstructure was recorded in a male individual from Group 2 (Sk. 1429, 26 y.o.) who died from pulmonary congestion. However, in this case multiple foci of bone resorption due to osteoclastic activity were seen below the PNB and affecting the cortex. Sk. 1299 rib sample (Group 1) also presented appositional new bone formation; however no physical demarcation was recorded between the newly built bone and the cortex. The resorption spaces observed in the interface between the new bone and the cortex may be associated with the remodelling of older periosteal lamellae into new cortical bone. In a thin section of an infant femoral mid-diaphysis, Maggiano (2012) observed a row of irregular resorption spaces. According to the author, these resorption bays were designed for expansion during endocortical resorption or to be infilled via BMU-based remodelling (Maggiano, 2012: 57). As pointed out previously, the remodelling process aims to replace the older bone with new bone through the coordinated action of bone-resorbing osteoclasts and bone-forming osteoblasts, collectively referred to as BMU, as a way to maintain bone tissue homeostasis (Stout and Crowder, 2012).

In two samples from Group 1, the periosteal new bone appeared as a thick and continuous layer of bone deposited upon the cortex. With regard to this type of microanatomy, two explanations can be put forward: 1) it is a different type of bone formation, or 2) it is the beginning of the appositional process. Through comparison with other thin sections, the second explanation seems to be the most probable. For example, the analysis of contiguous thin sections from Sk. 470 rib showed two different microstructures: one composed of a single thick layer of new bone and the other formed by numerous layers of periosteal new bone separated by primary vascular channels. The presence of a single layer of new bone may suggest that the stimulus to osteogenesis occurred only one time before the individual's death. This pattern of multiple layers of new bone on the pleural surface of ribs seems to mimic and amplify the appositional growth that characterizes the modelling process of the periosteal and endosteal membranes (PEM) during rapid growth periods of the skeleton: «[r]apid growth periods in humans can demonstrate laminar-like sets of pericortical

woven or lamellar bone separated by longitudinal primary vessel horizons locked within “generations” of lamellar apposition. However, even in the quickly growing infant human, laminar-like bone is typically limited to only one or two “layers” of the immature external periosteal cortex (...)» (Maggiano, 2012: 57). Maggiano (2012: 57), referring to the work of Currey (2002), also notes that the «(...) [p]eriosteal vessels overlain by primary lamellar diaphyseal apposition are typically longitudinal and are often referred to as primary vascular canals, or “primary osteons». The presence of multiple layers of new bone on the visceral surface of ribs is clear evidence of an abnormal stimulation of the periosteum. In some individuals, the formation of new bone appears to have occurred almost uninterrupted during a period of intense growth (Sk. 154). The observation of layers of bone in distinct stages of remodelling seems to indicate, on the contrary, that bone synthesis occurred at different rates during an undetermined period of time (Sk. 102). Despite the severe diagenetic changes, the rib thin section collected from the adult female individual PAH/C – SG 25/26 E2 unearthed from the ancient necropolis of Constância also displayed a pattern of multiple layers of new bone. Applying scanning electron microscopy to the study of periosteal rib lesions from British Roman and Medieval cemeteries individuals, Wakely and co-authors (1991: 186) also observed a similar bone microstructure: «[w]hile some affected ribs showed only one layer of new bone others showed up to four, super-imposed in a gallery-like formation, suggesting a repetitive deposition of bone in consecutive layers». As in the cases described, a clear separation between the newly built bone and the original rib cortex was also observed (Wakely et al., 1991). An inflammatory reaction in the pleura or lungs, possibly of tuberculous origin, was proposed as the possible stimulus for the synthesis of new bone on the visceral surface of ribs (Wakely et al., 1991).

Numerous local factors regulate new bone formation and turnover during growth, modelling and remodelling. Transforming growth factors type  $\beta$  (TGF  $\beta$ 1- $\beta$ 2 and  $\beta$ 3) are described as potent stimulators of bone formation, regulating chondrocyte, osteoblast, and osteoclast formation and function (Horner et al., 1998; Filvaroff et al., 1999). For example, TGF  $\beta$ 1 isoform seems to promote bone formation through the recruitment of osteoblasts progenitor cells and subsequent stimulation of their proliferation (Lakey et al., 2008). Studies in vitro revealed that TGF  $\beta$  isoforms and their receptors also play an important role in the regulation of endochondral and intramembranous ossification (Horner et al., 1998). The particular effect of TGF  $\beta$  on the process of endochondral ossification has been observed not only during the normal development of the skeleton, but also during fracture repair (Branton

and Kopp, 1999; Filvaroff et al., 1999). Among the TGF  $\beta$  superfamily of genes, bone morphogenetic proteins (BMPs) play a pivotal role in the control of bone induction, maintenance and repair, participating in the process of bone modelling and remodelling (Sykaras and Opperman, 2003; Lakey et al., 2008). As a consequence, BMPs have been investigated for therapeutic use in fracture healing, as well as to prevent osteoporosis (Lind et al., 1996; Sykaras and Opperman, 2003), and to promote the re-habilitation of critical-size bone defects (Chen et al., 2012). Vascular endothelial growth factor (VEGF) is one of the most potent mediators of vascular regulation in angiogenesis and vasculogenesis (Neufeld et al., 1999; Papaioannou et al., 2006; Lakey et al., 2008). VEGF has the capability of promoting proliferation, migration and survival of endothelial cells, playing a fundamental role in the development of new blood vessels (Wang et al., 2011). In adult animals, it mediates in the development of the cardiovascular and pulmonary systems, controls vascular permeability and homeostasis, and regulates the blood pressure and neoangiogenesis in numerous pathological conditions, such as the wound healing (Papaioannou et al., 2006; Shibuya, 2006; Lee et al., 2007; Wang et al., 2011). Moreover, it is identified as the most likely mediator of periosteal new bone formation (PNBF) associated with diverse pathological conditions (Lakey et al., 2008). Surprisingly, most of the local factors mentioned above are also present in the pathophysiology of tuberculosis. For example, Hirsch and co-authors (1996), after studying 20 patients with TB, found that the production of TGF-  $\beta$  plays an important role in suppressing potentially protective host effector functions, acting as a mediator of TB immunosuppression (Hirsch et al., 1996). In a study by Olobo and co-authors (2001), the presence of high levels of TGF  $\beta$  in the plasma of TB patients also indicated a possible association with the immunopathogenesis of the infection. Active TGF  $\beta$  was found to be produced by cultured monocytes of individuals with active tuberculosis, as well as by human macrophages infected with *M. tuberculosis* (Reed, 1999). Reed (1999: 1320) found that an increase in the production of TGF  $\beta$  led to a decrease in lymphocyte proliferation and production of IFN- $\gamma$  (interferon), a cytokine associated with protective immune responses in TB. In contrast, the neutralization of TGF  $\beta$  causes an increase in IFN- $\gamma$  production and a subsequent decrease in the number of bacterial replication in the cells affected (Hirsch et al., 1994; Reed, 1999). An association between TGF  $\beta$  overproduction in response to TB infection and protein malnutrition was also found in *in vivo* and *in vitro* studies (Reed, 1999). These investigations seem to confirm the hypothesis that TGF  $\beta$  increases the susceptibility to disease, contributing to and being the result of a weakened immune system (Reed, 1999).

Increased serum levels of VEGF have been recorded in the pathogenesis of pulmonary tuberculosis. In a study of 97 patients (43 with active pulmonary tuberculosis, 29 with old tuberculosis, and 25 with acute bronchitis), Matsuyama and colleagues (2000) found that the VEGF levels were significantly higher in patients with active pulmonary tuberculosis than among those with old tuberculosis. Furthermore, they observed a correlation between the decrease in the serum levels of VEGF and the clinical improvement of patients. The authors hypothesized that VEGFs were probably released by alveolar macrophages located around active tuberculous lesions (Matsuyama et al., 2000). In another study, Wang et al. (2011) observed a specific interaction between an important structural and functional protein of *M. tuberculosis* - ESAT-6, involved in the virulence, pathogenesis and proliferation of the pathogen and VEGF. Although the detailed molecular mechanism of TB is not completely known, Wang and co-authors (2011) presumed that VEGF might play a crucial role in the virulence, proliferation and pathogenesis of the bacillus. Given the possible relationship between VEGF and TB, Matsuyama et al. (2000) noted that VEGF may become a useful screening marker for active tuberculosis diagnosis; however, further studies are needed in this direction. High serum levels of VEGF were also found in patients with lung cancer (Papaioannou et al., 2006). In addition to TB and lung cancer, the expression of VEGF has been reported in other pulmonary condition, such as asthma, chronic obstructive pulmonary disease (COPD – emphysema and chronic bronchitis), obstructive sleep apnea, idiopathic pulmonary fibrosis (IPF), sarcoidosis, pulmonary hypertension, and pleural effusion, among others; nevertheless, the exact role of VEGF in the pathogenesis of these conditions remains unclear since contradictory results have been published for the same condition (Papaioannou et al., 2006). In some studies the VEGF seems to play an important role in the pathogenesis of a certain pulmonary disease, whereas in others an attenuating effect was observed (Papaioannou et al., 2006). It is important to note that the expression of these growth factors may be interlinked. For example, the production of VEGF may be stimulated by other growth factors, such as epidermal growth factor (EGF), TGF- $\beta$ , keratinocyte growth factor (KGF) and insulin like growth factor (IGF) (Neufeld et al., 1999). Local or systemic hypoxia (low blood oxygen) also seems to induce VEGF production and subsequently periosteal new bone formation.

In the clinical literature, no reports were found that clearly establish a direct association between growth factors, TB pathogenesis and periosteal new bone formation on the visceral surface of ribs. With regard to the remaining skeleton, the interaction between the three variables has been suggested in the development of HOA. The pathophysiology of HOA

remains unknown (Poppe, 1947; Rao et al., 1979; Ali et al., 1980; Kelly et al., 1991; Martínez-León et al., 1997; Vandemergel et al., 2004; Ddungu et al., 2006). Since its identification, several theories have been suggested. One of them – the arteriovenous shunt or circulatory theory – proposes that normal tissues are able to produce hormone-like substances capable of inducing the development of HOA (Cudkowicz and Armstrong, 1953). It has been proposed that in cases of congenital cyanotic heart disease, liver and pulmonary diseases, megakaryocytes may bypass the pulmonary circulation through arteriovenous shunting, avoiding fragmentation, and entering directly into the bloodstream. At distal extremities, these unfragmented megakaryocytes may stimulate the production of growth factors, such as platelet derived growth factor (PDGF) and vascular endothelial growth factor (VEGF), leading to angiogenesis and endothelial hyperplasia (Armstrong et al., 2007; Martínez-Lavin, 2007; Ntaios et al., 2008). As a result, a proliferation of connective tissue and of periosteal bone may occur (Gilliland, 2006). Bazar et al. (2004) have recently proposed a unifying theory that postulates the existence of autonomic stimulation in HOA formation, and propose that this mechanism may occur as part of a normal physiological process or by an abnormal process involving chemoreceptor activation. In a literature review, Lakey et al. (2008) stated that hypoxia has angiogenic properties. In the skeleton, it stimulates VEGF release from osteoblasts, enhancing human endothelial cell proliferation and blood vessel formation (Lakey et al., 2008). Furthermore, it participates in the remodelling of the vasculature and surrounding tissue. For example, hypoxia seems to play an important role in the process of fracture healing (Lakey et al., 2008). As in the pathogenesis of HOA, it is possible that an abnormal stimulation of growth factors, especially the VEGF – through hematogenous dissemination, direct extension from a pulmonary TB foci, or hypoxia may have induced new bone formation on the visceral surface of ribs. This hypothesis might explain not only the multiple layers of appositional bone observed, but also the proliferation of numerous primary vascular channels in the newly formed bone. As mentioned previously, VEGF plays an important role in the development of new blood vessels in numerous pathological conditions (Wang et al., 2011). The rib thin section collected from the adult male Sk. 154 who died from pulmonary tuberculosis is a clear example of an extensive hypervascularization associated with appositional bone growth. Unresolved angiogenesis was also advanced by Cole and Waldron (2012) as a possible mechanism to explain the development of syphilitic bone changes. The authors advanced the hypothesis that lesions might occur by abnormal angiogenic activity acting on the Haversian and Volkmann canals associated with the reparative inflammatory



response (Cole and Waldron, 2012). This mechanism is probably enhanced by the infiltration of lymphocytes and plasma cells in the affected tissues, as well as by the presence of endothelial growth factors, which play an important role in the formation of new vessels, monocytes and macrophages (Cole and Waldron, 2012). Since the expression of VEGF in pulmonary conditions other than TB or lung cancer is not clear, the appositional and hypervascularized periosteal reaction observed in the rib of the individual Sk. 1429 (Group 2, pulmonary congestion) may have been caused by hypoxia and subsequent VEGF production. As stated by Costello and co-authors (2008), pulmonary hypoxia is a common complication of numerous chronic pulmonary conditions.

Newly deposited periosteal bone with an arc-like structure and attachment to the underlying bone by pedestals was observed in Groups 1 and 2, and in the archaeological samples. In Group 1 this type of new bone formation was observed in two rib thin sections, whereas in Group 2 three samples exhibited a similar bone formation: a rib thin section from the adult individual Sk. 270, and a rib and a fibula thin section from the non-adult Sk. 1534-A. In the archaeological samples, this pattern of periosteal lesions was seen in one rib from the ancient necropolis of Constância (PAH/C-SG22-E4). In the paleopathological literature, this type of new bone microstructure is described as a non-specific response (Schultz, 2001), frequently associated with subperiosteal haematoma and other hemorrhagic phenomena (Schultz, 2001, 2003 and 2012). For example, the pattern of new bone formation observed in the rib thin sections of Sk. 1383 (Group 1) and PAH/C – SG22 E4 (Constância necropolis) resemble the periosteal lesion observed by Schultz (2001: 125, figure 7-B) in the left fibula of an adult skeleton (probably female, 25-39 y.o.) from the late Byzantine period and diagnosed as a subperiosteal haematoma. Although diagenetic changes were present, the contours of the new bone formation observed in the rib thin section of the Sk. 1235 individual (Group 1) also resemble those of a subperiosteal haematoma. With regard to the PNBf seen in the 7<sup>th</sup> right rib of the Sk. 270 individual (Group 2, bronchopneumonia), it is similar to the “separated periosteal callus” recorded by de Boer et al. (2012) in a fractured 3<sup>rd</sup> metacarpal, and defined as a new periosteal layer connected to the underlying cortex by small pillars of bone tissue. As mentioned earlier, the formation of new bone on the visceral surface of ribs has been frequently associated with pulmonary infection (i.e. TB) disseminated from the lung tissue (via pleura) to the ribs. Nevertheless, the lesions observed seem to suggest that a mechanism different from inflammation or hypoxia may have induced new bone formation on the pleural surface of ribs. Subperiosteal hematomas associated, for example, with repetitive trauma may

constitute a possible explanation. In young children, periosteal rib lesions have been interpreted as a secondary manifestation to chest wall physiotherapy. Wood (1987) described three cases of PNBF in the ribs of infants who received medical therapy performed by a gauze-padded electric-toothbrush handle. This device is used for thinning and mobilizing bronchial secretions, as well as to relax the musculature of the chest wall. However, its continuous application in pulmonary therapy has been associated with minor trauma on ribs and the formation of subperiosteal hemorrhages (Wood, 1987). Studying the relationship between rib fractures in children and chest physical therapy (CPT), Gorincour and co-authors (2004) found that recurring CPT (by continuous anterior cephalocaudal compression and provoked cough) is more likely to cause subperiosteal haemorrhages than real fractures. In adult ribs, the presence of subperiosteal haematomas has been normally found in association with rib fractures (i.e. Kara et al., 2003). Rib fracture may be caused by blunt trauma, bone fragility diseases or cough-induced stress trauma. Numerous studies have described the development of rib fractures after episodes of severe cough. Cohen (1949) reported seven cases of “spontaneous” cough-induced rib fractures in female patients (<35 years of age) with TB. According to the author, these fractures may be the result of an abnormal posture that produces an uneven action on the ribs during the violent expiratory effort of a cough or sneeze (Cohen, 1949). Analyzing 54 patients with cough-induced rib fractures, Hanak and co-authors (2000) concluded that this condition occurs most frequently in females with chronic cough and may be independent of the bone quality. Kiliç et al. (2007) reported the presence of spontaneous rib fractures in two male individuals with atypical-pneumonia and chronic bronchitis caused by vigorous coughing. Yeh and Su (2012) also described a case of rib fractures in a healthy young man (22 y.o.) affected by a 6-week intermittent cough. In the pathophysiology of cough-induced rib fractures, it is postulated that extreme changes in intrapleural pressure due to active contraction of the inspiration and expiratory muscles applied over ribs can cause biomechanical stress (Kiliç et al., 2007). When the stress forces exceed the elastic limit of the rib, deformation and fracture may develop (Kiliç et al., 2007). Another plausible explanation is advanced by Yeh and Su (2012), who suggest that cough-induced rib fractures may be the result of the opposite forces exerted by two antagonistic chest muscles: the serratus anterior and the external oblique. In his evaluation of 4726 ribs from 197 individuals belonging to the Human Identified Skeletal Collection (Bocage Museum, Lisbon), Matos (2009) found a frequency of broken ribs of 2.6% (n=124). Despite the high mean rate of rib fractures among individuals who died from pneumonia, no significant

differences in the prevalence of rib fractures were observed between individuals who died from respiratory conditions and those who passed away from non-respiratory conditions (Matos, 2009). In this study, the cough-induced rib fractures hypothesis was not confirmed, suggesting that other etiological factors may have led to bone trauma. Cases of stress fractures attributed to sudden and undue muscular strain, as in lifting heavy objects (i.e. Waxman and Geshelin, 1949), or associated with particular occupations/sports (i.e. Warden et al., 2002; Iwamoto and Takeda, 2003) have also been reported for ribs. If chronic or acute episodes of coughing or sneezing, vomiting, and even accidental or occupational muscular strain are able to affect the rib microstructure leading to bone fractures, it is reasonable to suggest that the same factor(s) may potentially damage the periosteum. As in infantile pulmonary physiotherapy, it can be hypothesized that any agent that causes intra-thoracic and intrapleural vibration or chest wall musculoskeletal stress (i.e. severe cough or sneezing), may induce the detachment of the periosteum, causing subperiosteal bleeding and hematoma formation. Once again, it is important to remember that besides inflammation, every mechanism that breaks, tears, stretches, or even touches the periosteum can potentially stimulate the production of new bone (Richardson, 2001).

In the rib of the non-adult Sk. 1534-A (male, 2 y.o.) who died from pneumonia, a stitched ridge of periosteal new bone clearly distinguishable from the supporting cortex was observed. A more exuberant bone formation was observed in the corresponding right fibula. In spite of the diagenetic changes visible through the cortex, numerous loosely arranged trabeculae of appositional bone were seen radiating from the surface. To some extent, this pattern of bone formation resembles the microanatomy of an immature ossified subperiosteal haematoma. Regardless of the histology of the subperiosteal hematomas, Schultz (2001, 2003 and 2012) points out that the newly formed bone may range from thin layers in the form of a sliplike cover to relatively short, bulky bone trabeculae with extensive bridging, arc-like formation and /or with multiple layers (rare). Van der Merwe et al. (2010), analysing seven archaeological cases of ossifying hematoma from Kimberley, South Africa (1897-1900), found that demarcated and radiating bone apposition perpendicular to the periosteal surface of bone was the most striking feature observed. The only differences found were related to the degree of ossification. According to Schultz (2012: 263), the orientation of trabeculae in subperiosteal haematomas depends not only on the size and the volume of the bleeding, but also on the physiological tonus and the tension of the muscles on the affected area.

Blunt trauma, most commonly on the anterior surface of the tibial diaphyses, the radius, fibula or ulna, may lead to the development of localized subperiosteal hematomas that almost invariably ossify, forming an elevation on the external surface of bone (Aufderheide and Rodríguez-Martín, 1998; Rodríguez-Martín, 2006). In addition to trauma, other pathological conditions that cause massive subperiosteal bleeding may induce the development of calcified hematomas. For example, Steenbrugge et al. (2001: 170) refer to the bone matrix defects (scurvy and osteogenesis imperfecta), severe periosteal trauma (battered child syndrome), or neuromuscular deficiencies (congenital insensitivity to pain or meningomyelocele). Circulatory diseases (i.e. primary and secondary HOA) and tumours may also cause subperiosteal bleeding (Schultz, 2012). In the paleopathological literature, scurvy is frequently described as increasing the likelihood of the formation of subperiosteal hematomas (Aufderheide and Rodríguez-Martín, 1998; Ortner, 2003; Brickley and Ives, 2008). For example, in Van der Merwe and co-authors' (2010) investigation, the presence of subperiosteal hematomas was attributed to possible cases of healed scurvy (Van der Merwe et al., 2010). It is important to mention that the lesions observed in SK.1534-A were not solely confined to the ribs and fibula. In fact, a widespread, multifocal involvement of the skeleton with patches of periosteal new bone symmetrically distributed through the endocranial surface, orbital roof, scapulae (supraspinous and infraspinous areas), ilium (anterior surface), humerus and femora (posterior lower third of the diaphysis), tibiae and fibulae (medial posterior surfaces of the shaft) were seen. Given the pattern and distribution of the bone lesions, it seems plausible to assume that this individual might have suffered from a more generalized and systemic condition, which allows for the exclusion of blunt trauma from its aetiology. Infantile cortical hyperostosis (ICH) or Caffey's disease seems unlikely since it is most commonly observed in individuals younger than one year of age. Furthermore, it affects most often the mandible and the clavicle, followed by the long tubular bones of the extremities and ribs (Ortner, 2003h). The ulna is the most frequently affected tubular bone with asymmetric deposits of new bone (Lewis and Gowland, 2009). The hypertrophic lesions of the scapula are generally believed to be one-sided and are most frequently seen in the first six months of life (Lewis and Gowland, 2009). None of the bone features that normally characterize rickets, for instance rachitic rosary, delayed maturation of the cranial bones, frontal bossing and dorsal curvature of the vertebrae or flaring of the long bone metaphyses (Parson, 1980; Zimmerman and Kelley, 1982; Ortner, 2003h; Stevenson, 2005; Waldron, 2009) were observed. Taking into account the possible relationship between pulmonary conditions, such as pneumonia, and HOA, this condition may

be considered in the present differential diagnosis. In spite of being more common in adults (Ortner, 2003g), HOA can affect individuals of all ages. Pineda et al. (1987) stated that the loosely attached periosteum of children may be more conducive to the development of periosteal reactions. The new bone deposition normally occurs at both the ends and shafts of long and short tubular bones and does not show cortical involvement (Cavanaugh and Holman, 1965). Nevertheless, other bones may be affected in a minor degree such as the skull, scapulae, patellae, ribs, and pubic and iliac bones (Ali et al., 1980). In most cases, the skeletal abnormalities are symmetrical in distribution (Pineda et al., 1987). Scurvy is another condition that may have caused the widespread deposits of new bone and the extensive porosity observed in SK.1534-A skeleton. Scurvy is a metabolic disease caused by a deficient intake in vitamin C, which has an important role in the formation of the collagen fibril precursors, as well as in the regulation of the osteoblastic activity and in the synthesis of osteoid (Aufderheide and Rodríguez-Martín, 1998; Ortner, 2003g; Brickley and Ives, 2008). As a consequence, there is a delay in skeletal growth and a possible increase in hemorrhagic phenomena in various cranial sites, as well as in the scapula and long bones (Aufderheide and Rodríguez-Martín, 1998; Brickley and Ives, 2006). These hemorrhagic episodes may be spontaneous or caused by minor trauma, and are more marked in nonadults than in adults (Ortner, 2003g; Mays, 2008). Differences between age groups are also found in the skeletal distribution of the subperiosteal haemorrhages (Aufderheide and Rodríguez-Martín, 1998). Since the adult periosteum has a more reduced response, the haemorrhages are usually diaphyseal, of a moderate size, and with an outer layer composed of lamellar bone (after healing). The inner layer normally is composed of a more porous bone (Aufderheide and Rodríguez-Martín, 1998). In contrast, subperiosteal haemorrhages in scorbutic infants cover a much greater area and volume, affecting more frequently the metaphyseal portion of long bones (Aufderheide and Rodríguez-Martín, 1998). The weight-bearing bones of the lower limb, namely the femur and tibia, are the skeletal elements most frequently affected by localized subperiosteal hematomas (Ortner, 2003g)<sup>64</sup>. In cases where porosity and new bone formation are visible on the orbital roof, the possible coexistence of scurvy and anaemia (co-morbidity) should also be considered (Brickley and Ives, 2006). Independently of the underlying cause, the microstructure of the periosteal lesions observed in the SK.1534-A rib and fibula seems to be compatible with a subperiosteal haematoma secondary to a haemorrhagic phenomenon that lifted the periosteum, stimulating the synthesis of new bone.

---

<sup>64</sup> Other skeletal elements frequently affected by subperiosteal haemorrhages are the skull, mandible, vertebrae, ribs and pelvis (Aufderheide and Rodríguez-Martín, 1998; Ortner, 2003g; Brickley and Ives, 2008).

The differences found in the microstructure of periosteal rib lesions seem to suggest that beyond pulmonary diseases other mechanisms may stimulate new bone formation on the visceral surface of ribs. As a consequence, when studying rib lesions from archaeological or forensic contexts, researchers should be aware and consider in their differential diagnosis other possible aetiologies, such as repetitive microtrauma and haemorrhagic conditions. More histological studies on periosteal rib lesions, especially in individuals with known cause of death are warranted to confirm the trends observed in the present investigation.

In two individuals from Group 1 and Group 2 that showed multifocal involvement of the skeleton resembling the pattern described for HOA (Group 1 - Sk. 1604, female, 45 y.o., TB; Group 2 – Sk. 119, female, 64 y.o., bronchopneumonia), two bone samples were collected from the 5<sup>th</sup> left metatarsal. With regard to the microanatomy of the periosteal lesions, no major structural differences were found between causes of death group samples. In both thin sections, the point of contact between the PNB and the cortex was visible. Additionally, no bone changes were noticed at the cortical level, which agrees with the radiographic descriptions of HOA (i.e. Cavanaugh and Holman, 1965). von Hunnius (2009), conducting a histological study of dry bone evidence of HOA in the remains of a 16<sup>th</sup> century Iroquoian dog, also found a relatively clear demarcation between the newly formed bone and the original cortex. In the case of HOA, the histological analysis did not reveal diagnostic differences among cause of death groups; however, this inference needs further testing. The periosteal lesions observed on Sk. 135 and Sk.1412 samples (Group 3) did not exhibit particular distinctive traits, but rather were classified as non-specific.

## **2. What is the role of histology in the description of bone lesions?**

In the present investigation, the histological analysis proved to be fundamental in the description and characterization of bone changes. With regard to the type of new bone formation, few correspondences were seen between what we consider macroscopically as woven and compact bone and the histological picture. In most samples, a haphazard arrangement of the mineralized collagen fibres with multiple osteocyte lacunae was seen in the outermost layers of new bone. This pattern of organization was most commonly seen in woven bone and was equally found in individuals classified macroscopically as having a mist pattern (woven/lamellar) and in those with a more compact pattern. A correspondence between the macroscopic appearance of the periosteal bone and the respective microstructure was found only for the 5<sup>th</sup> left metatarsal bone samples from Sk. 1604 (Group

1) and Sk. 119 (Group 2). Three individuals were classified macroscopically as having erosive and proliferative lesions (Group 1 – Sk. 332, Sk. 470, and Sk. 1583). In two of them (Sk. 332 and Sk. 1583), the pattern was confirmed through histological analysis. In a third case no correspondence was found. That is, no lytic foci affecting the periosteal layers or the cortical bone were recorded. This may suggest that the large holes observed on the visceral surface of the Sk. 470 rib thin section were not caused by osteoclastic activity, but probably were the result of the coalescence of minor vascular channels. The opposite was also found. One individual from Group 2 (Sk. 1429, pulmonary congestion) with no macroscopic evidence of bone resorption presented large Howship's lacunae in the cortical bone that led to the almost complete collapse of the cortical tissue. A similar case was recorded in Group 3 (Sk. 457, rectal neoplasm). In addition to the exuberant and spiky-like periosteal new bone formation (sunburst pattern), the histological analysis revealed large bays of bone resorption that roughly destroyed the cortical bone. For this individual, a mixed pattern of osteolytic and proliferative lesions was macroscopically observed in the femora. The remaining bones (clavicle, scapula, ribs, and innominate bones) were only classified as having proliferative lesions. However, when histological techniques were applied, lytic lesions affecting the cortex of a rib were uncovered. This case demonstrates that relying exclusively on gross inspection for pathological analysis may be problematic, since it may not give a complete view of the tissue's response to disease. For example, if ribs had been the only bones affected by PNB in this individual, the macroscopic analysis would have been insufficient to properly classify the type of lesions (proliferative, lytic or mixed) because the erosive ones were not visible to the naked eye. In the samples used as controls (Sk.1242 – Group 1, Sk. 1484- Group 3), no differences were noticed between the macro- and the microstructure.

A good description of bone lesions is an obligatory procedure in every paleopathological study. But is the macroscopic analysis sufficient for this job? Are we really seeing all of the components of the bone lesion? The answer is probably not. What we observe macroscopically may not correspond to the histological picture or give a complete understanding of the disease process. As illustrated above, in certain circumstances the gross inspection may confound the analysis, giving biased information about the composition of the bone lesions. The disparity between macroscopic and histological analysis was also observed in the study of bone callus. Of the five samples with an apparent "consolidated" bone callus, only two presented a truly mature and remodeled microstructure. The most striking example came from the analysis of the Sk.198 right fibula thin section. In spite of the macroscopic appearance that revealed an

apparently remodeled bone callus, the histological analysis showed a very different scenario. The sparse microstructure of the cortical tissue composed of thin branches of lamellae in distinct stages of maturation and resembling trabeculae, in addition to multiple foci of bone resorption and islands of new bone formation seems to suggest that, at the time of death, the last stage of fracture healing remodelling was not finished. In the paleopathological literature, no histological descriptions that support this observation were found. In contrast, some potential clues come from clinical descriptions and bone engineering experiments. For instance, Gerstenfeld and co-authors (2006: 1215), studying fracture callus morphogenesis in the femora and tibiae of rats and mice using histological techniques and three-dimensional reconstruction, showed that the «[r]emodelling of the calcified cartilage proceeded from the edges of the callus inward toward the fracture producing an inner-supporting trabecular structure over which a thin outer cortical shell forms». The authors found that during the endochondral process of fracture healing, an outer shell of new bone forms above the original cortex and cartilage. As remodelling takes place, the underlying cortex and cartilage undergoes resorption, being replaced by an intricate network of trabeculae. The main goal of this trabecular-like structure is to stabilize the fracture. According to the authors «[t]his represents an efficient mechanism, using minimal material, to rapidly restore biomechanical stiffness and strength and allows for remodelling on internal surfaces» (page 1227). Similarly, Marsell and Einhorn (2011) pointed out that during the remodelling stage, a second resorptive phase occurs in which the hard callus is converted into lamellar bone. These processes, which may take years, occur to restore the biomechanical properties of bone (Marsell and Einhorn, 2011). Regarding the blue-grey substance observed filling the gap between bone lamellae, it is almost impossible to confirm its nature. Nevertheless, it resembles preserved calcified cartilage. In an experiment to evaluate the degree of bone regeneration in osteoperiosteal mandibular defects induced artificially in sheep through surgical procedures, Ayoub et al (2007) observed a characteristic histological picture characterized by islands of newly built bone surrounded by cartilage. In some individuals, large areas of cartilage interspersed with areas of lamellar bone were observed, indicating that lamellar bone may have arisen through replacement of cartilage, which clearly suggests the occurrence of endochondral ossification (Ayoub et al., 2007).

Despite the compact appearances of the outer shell of the Sk. 119 rib callus, the histological study showed an unremodelled cortical and periosteal microstructure. Only the endosteal inner layers of the cortex presented a mature structure composed of numerous



rows of osteons and interstitial lamellae. On the pleural-cortical surface, differences in the organization of the tissues that comprise the callus were seen. For instance, the deepest layers were formed by densely packed lamellae with small erratic osteocyte lacunae, whereas the outermost ones were composed of a random structure with no lamellar organization and densely populated by circular osteocyte lacunae. These structural differences clearly indicate that the rib bone callus of SK. 119 was undergoing remodelling at the time of the death of the individual.

An apparently remodeled bone callus was observed in the right radius of Sk. 1196. The histological analysis showed, however, a microstructure composed of an intricate network of trabeculae. The absence of alignment of the trabecular collagen fibers seems to suggest a lack of maturation of the tissue. Multiple foci of bone resorption were also seen destroying the trabeculae. The regular structure of the cortical bone is absent from the bone callus, as well as from the opposite anterior surface. That is, no osteons, interstitial lamellae or Haversian canals were observed. The network of trabeculae that fills the medullary cavity was also absent. On the anterior surface, incompletely remodeled micro-fractures were seen crossing the cortical bone. Instead of the typical structure, the anterior cortex appeared to be formed by horizons of lamellar bone. It seemed that the bone was continuously laid down in a lamellar fashion without being converted into secondary Haversian systems, forming a microstructure that Ericksen (1991) termed unremodeled lamellar bone. In the adult skeleton, intracortical remodelling operates, removing and replacing areas of bone affected by microdamage. In the absence of intracortical remodelling, there is a propensity to microdamage accumulation, which increases the risk of stress fractures, compromising the mechanical properties of bone (Bentolila et al., 1998). It is difficult to determine if this abnormal intracortical organization is a consequence of the process of fracture remodelling, or inversely, part of the mechanism that predisposes the bone to trauma (e.g., osteoporosis). Paine and Brenton (2006: 490) stated that: «[m]etabolic disorders and dietary deficiencies have been suggested as causing either increased bone turnover rates leading to the production of more secondary osteons per area of bone than what is considered to be normal, or can lead to lower bone turnover rates resulting in fewer secondary osteons per volume of bone [...]». When bone turnover is low, there is more time for secondary mineralization to proceed; as a consequence, the bone tissue becomes hypermineralized and more brittle, requiring less energy to fracture (Martin and Correa, 2010). Furthermore, an excessive reduction of bone turnover may result in an inefficient microdamage repair, leading to the development of microcracks and, in severe

cases, to fractures (Martin and Correa, 2010). Independently of the underlying cause, it is clear that this female presented an unremodeled bone callus that contrasted with the compacted gross appearance. From the same individual, a rib bone callus exhibiting a completely consolidated outer shell was also collected. At the microscopic level a similar picture was seen; however, the predominance of bone resorption over new bone formation erased the exact locations where bone callus remodelling occurred. Moreover, few rib trabeculae were found preserved. The cortical bone appeared to be formed only by a thin rim of discrete osteons and interstitial lamellae, encompassing a general loss of bone tissue, probably associated with a metabolic condition such as osteoporosis. Through the degree of bone healing, it seems evident that Sk. 1196 individual suffered multiple traumatic episodes throughout her life. The exact mechanisms that induced it remain unclear.

A remodeled bone callus was observed in the right tibia of the male individual Sk. 54 who died of pulmonary TB. Similar to the previous cases, the major changes in the bone microstructure were found at the cortical level. In the lateral portion of the bone callus, the cortex presented a mature and non-pathological appearance, being composed of a haphazard arrangement of Haversian systems and interstitial lamellae. This observation may suggest that the process of fracture healing was complete. In contrast, the presence of lamellae randomly organized and in different stages of maturation may indicate that, at the time of the death, the medial portion of the bone callus was probably undergoing the process of remodelling. Nevertheless, the normal bone microstructure prior to fracture was almost achieved in this bone sample. Densely packed lamellae resembling the bone features described by Schultz (2001) as “Grenzstreifen” (see figure 8, Schultz, 2001: 127) were observed at the intracortical level. Grenzstreifen is defined as a boundary line of varying thickness located between the original cortical surface and the secondary pathological new bone deposition in a subperiosteal position (Schultz, 2001, 2003 and 2012). It is a remnant of the external circumferential lamellae that is preserved due to the relatively slow growth of the PNB (Schultz, 2012). Hence, it may present a reduction in their size and shape (Schultz, 2012). As pointed out in Chapter 3, this lamellar pattern has been associated with treponemal infections (e.g. Schultz, 2001 and 2003). For instance, von Hunnius et al. (2006) found a similar histological feature in pre-Columbian skeletons (UK) that show evidence of venereal syphilis (see figure 2D, von Hunnius et al., 2006: 563). As in the present case, von Hunnius et al. (2006) also saw resorption lacunae near the intracortical lamellae, referred to as sinuous lacunae. Resembling a resorption lacuna, the sinuous lacunae are normally observed between the cortical surface and

the new layer of PNB (Schultz, 1994). Nevertheless, no circular lamellar structure is observed in its outline (Schultz, 1994). Following the definition proposed by Schultz (2012), the retention of a densely packed system of lamellae in the Sk. 54 tibia may be due not to a chronic, inflammatory disease, but instead to the normal process of bone healing. Depending on the type of fracture and subsequent healing process, it may be hypothesized that not all of the original cortical bone was “absorbed” during the remodelling process, with some remnants becoming embedded in the new shell of bone produced. If this hypothesis is true, the role of “Grenzstreifen” as a distinctive diagnostic feature for treponemal infections must be reconsidered once more in future investigations (see Weston, 2009; Van der Merwe et al., 2010). It is important to highlight that all of the bone features recorded at the macroscopic and histological levels are independent from the cause of death and were delimited to the area of fracture healing. In addition to the cases already described, a 4<sup>th</sup> right rib fracture sample with unfused margins and new bone formation was collected from the adult male Sk. 1138 (bronchopneumonia). In the fracture outline, the most striking histological feature observed was the presence of an arc-like structure of new bone interlinked with the underlying cortex by bone pedestals. Numerous resorption spaces occupying an intracortical position were also seen. A similar pattern was recorded by de Boer et al. (2012) in their study of 31 bones specimens collected from 21 individuals with bone fractures and amputations. In an attempt to evaluate the healing features and associated post-traumatic time interval, Boer and co-authors (2012) concluded that a clear visible periosteal callus normally appears 15 days after the traumatic event. This occurrence may be accompanied by osteoporosis of the cortex that develops almost at the same time (12 days). The union of the cortical bone discontinuity tends to occur after 21-28 days. Since the margins of the Sk. 1138 rib fracture were unfused, it may be hypothesized that the traumatic event occurred prior to 20 days before death. Furthermore, the microanatomy of the affected area is compatible with the reparative phase of fracture healing (see Chapter 3, section 3.2.1.2). The earlier stages of fracture healing may explain the proliferation of remnants of blood vessels that are more numerous on the pleural-endosteal bone surface. Following the injury, one of the cellular and biochemical events is the release of cytokines that act on the stimulation of angiogenesis and haematoma formation (Malizos and Papatheodorou, 2005; Sfeir et al., 2005; Bielby et al., 2007). The network of blood vessels observed may be an additional testimony of the leading stages of bone healing.

### 3. What is the role of histology in the assessment of bone tissue quality?

In spite of the “apparent” good preservation of the bone samples, massive diagenetic and biological changes due to the action of bacteria and fungi were observed at the microscopic level, mainly in those samples belonging to archaeological material. Of the 26 bone specimens collected from the identified skeletons, only three (Group 1 – Sk. 1235; Group 2 – Sk. 1534-A; Group 3 - Sk.1483) showed areas of bone degradation. The remaining samples presented an intact histological appearance in which it was possible to recognize Haversian systems, interstitial lamellae, cement lines, and empty osteocytic lacunae. Under polarized light, a good bone birefringence with the characteristic “Maltese cross” was observed. As pointed out by von Hunnius et al. (2006: 560), Maltese crosses are an important indicator of the integrity of bone tissue since they denote good preservation of lamellae in Haversian structures. In contrast to the identified specimens, all samples collected from archaeological skeletons exhibited some form of postmortem modification. These changes were more evident in the specimens from the Constância and the Royal Hospital of All-Saints necropolis, and ranged from generalized destruction with disintegration, disaggregation and dissociation of osteons to focal destruction. In most of the samples a generalized lack of bone birefringence under cross polarized light was observed. As a consequence, the identification of Haversian systems, interstitial bone, osteocyte lacunae and endosteal and periosteal lamellae was impossible. Some archaeological thin sections (e.g. PAH/C-SG19 E7) exhibited “shadows” of Haversian systems or “ghost” osteons without evidence of the respective circumferential lamellar system. Despite the absence of the basic bone units, the Haversian canals and major spaces of bone resorption associated with normal bone remodelling were still visible. In the majority of the specimens, the rib cortex appeared to be filled with an indistinguishable mass of composites probably resulting from bacterial activity or chemical action. For example, in a subperiosteal ossified haematoma sampled from the left femur of an adult male (P. Fig. 1492), the osteons were formed by scattered fragments described by Jans (2008) as linear longitudinal microscopic focal destruction (MFD) associated with microbial activity. Similar findings were seen in a thin section of a left tibia collected from an adult male (Porto UE6451-65). In this particular case, detachment of Haversian systems in relation to the supporting cortex caused by micro-cracks and microbial tunnelling was the most common trait seen. Lamellate and linear longitudinal microscopic focal destruction, as described by Jans (2008) was also recorded. Worm-like structures probably associated with fungal or bacterial activity were seen focally distributed throughout the bone sample of an adult skeleton (Porto UE

5093). The postmortem bone changes observed had an enormous impact on the analysis and description of the lesions. Despite the intact contours of the bone samples, it was impossible to characterize the periosteal and intracortical microanatomy and infer or corroborate the aetiology of lesions. For example, in a rib sample showing lytic and proliferative lesions probably associated with a case of metastatic carcinoma from an adult female (PAH/C-SG19 E7) (Assis and Codinha, 2010), it was possible to observe the outline of the resorption spaces, both at the periosteal and endosteal surface, but not the microstructure of the newly built bone. In spite of some “ghost” osteons and Haversian canals, no particular bone structures were recognized. A similar phenomenon was observed in a fibula thin section of an adult female (P. Fig. QT6 E3 1310) that exhibited bone lesions compatible with a possible case of acquired syphilis. On the periosteal surface, new bone deposits ranging from a round to a thorny morphology were seen. Furthermore, a wavy-like pattern of new bone packed between spaces of former periosteal blood vessels and separated from the underlying cortex by resorption spaces was also identified. However, only the contours of the periosteal bone were preserved, which made confirmation of the orientation of the collagen fibers impossible. This last bone feature resembles “polster” structures described by Schultz (2001, 2003 and 2012) as being associated with venereal syphilis. The author defines polsters as a “pillow-like” structure of new bone that develops at the external surface of the long bones (periphery of the cross-section) and only within some parts of the circumference. In tertiary syphilis, these histological features are caused by a relatively slow growing process (Schultz, 2012). In spite of being observed in treponemal infections, the author recently stated that: «(...) polsters are not permanently present in any specific inflammatory process» (Schultz, 2012: 265). Apart from the atypical outline of the periosteal reaction, no further pathological bone features (e.g. *grenzstreifen* and *sinuous lacunae*) were observed in an intracortical position. An interesting phenomenon was observed in a subperiosteal ossified haematoma collected from the diaphysis of the left femur of an adult male (P. Fig. 1492). While the cortical bone appeared to be formed by well preserved osteons and peripheral lamellae with good birefringence, the ossifying haematoma was composed of osteons with an amorphous appearance and cracked circumferential lamellae. It appears that the subperiosteal ossified haematoma worked as a buffer, protecting the cortex against the destructive action of biological and chemical agents. In spite of the degradation observed, the presence of osteons seems to indicate that at the time of the death, the subperiosteal haematoma was remodeled. The multitude of histological evidence outlined above appears to suggest that gross preservation of bones may not find

correspondence at the microscopic level. That is, the macroscopic inspection of skeletal remains does not give a complete picture of all chemical, physical and biological changes that they undergo postmortem. As pointed out by Garland (1987), imprecise terms such as “well preserved”, “badly preserved” and “weathered”<sup>65</sup> are frequently used to describe the macroscopic appearance of bones. However, this type of classification provides little information about the interactions that have taken place between the destructive agents eventually present in the burial environment and the inhumed bones (Garland, 1987). Diagenesis<sup>66</sup>, a geological term that refers to «(...) the processes by which sediment is transformed into sedimentary rock under conditions of low temperature and pressure», has been used in paleopathology to describe the changes that skeletal remains experience in the burial environment (Turner-Walker, 2008: 4). Chemical diagenesis of bone and teeth is a multifactorial process that depends on several factors such as soil PH, soil drainage, and other interfering agents present in the burial space (Grupe and Dreses-Werringloer, 1993). In nature, water is an important mediator of almost all chemical reactions. Accordingly, the presence of water in the burial environment may affect the potential of survival of the skeletal remains, since it may induce pronounced physical-chemical changes (Turner-Walker, 2008). Garland (1987) noted that ground water can enter bones by diffusion, disrupting the internal protein-mineral bond and hydrolysing the protein components of bone. After dissolution, the mineral components of bone can be removed by the permeating soil water (Garland, 1987). Bone dissolution depends on numerous factors such as the porosity of bone and the rate and volume of water flow into and out of the bone tissues (Turner-Walker, 2008). In a burial environment composed of sediments that resist continuous fluctuation of soil water (e.g. clays), the liquid reaches bones via the network of vascular canals, fills the pores and becomes saturated in  $\text{Ca}^{2+}$  and  $\text{PO}_4^{2-}$ , which prevents the flow of water out of the bone and subsequent loss of mineral components. In these cases, bones tend to exhibit exceptionally good preservation (Turner-Walker, 2008). On the contrary, in burial places in which repeated cycles of wetting and drying occur, there will be a tendency to successive losses of calcium and phosphorous from the bone matrix, leading to badly preserved skeletal material (Turner-

---

<sup>65</sup> Weathering is a physical decomposition process that results in easily detachable microfissures and crackings (Grupe and Dreses-Werringloer, 1993). According to the author, they develop essentially by sediment pressure and temperature, but also by superficial trampling (Grupe and Dreses-Werringloer, 1993).

<sup>66</sup> By opposition, taphonomy aims to understand the postmortem processes that operate on bone survival or destruction, focusing on the transformations that guide the passage of the organisms from the living world to the lithosphere (Turner-Walker, 2008). It is the combination of taphonomic and diagenetic processes that determine whether a bone will decay and disappear from earth or preserve throughout archaeological and geological times (Turner-Walker, 2008: 4).

Walker, 2008). Well-drained soils (e.g. sands or gravels) that allow for the continuous flow of water throughout the bones and never become saturated also have a deleterious effect upon the bone microstructure. These last two factors may ultimately explain the lack of preservation of the archaeological remains unearthed from the Constância necropolis. The ancient necropolis of Constância was located in the vicinity of the Tagus River, in an area that is frequently affected by seasonal floods. Moreover, the soil is mostly formed by fine-grained and permeable sands which may also have contributed to the mineral and organic degradation of bones. The biological decomposition or bioerosion of bones is primarily caused by boring organisms such as bacteria, fungi and, in marine environments, by cyanobacteria (Grupe and Dreses-Werringloer, 1993; Jans, 2008). The action of these organisms upon the bone microstructure is normally recognized through the presence of different types of tunneling (Jans, 2008). With regard to the microbial action, Jans (2008) stated that fungal and cyanobacterial changes are indicative of the past burial environment, whereas the bacterial alterations are mediated by the early postmortem taphonomy. In their study of 50 bones from 41 different archaeological sites, Jans and co-authors (2004) found that skeletal remains (human and non-human) unearthed from complete burials are more often affected by bacterial degradation than scattered fragments that resulted from butchering or dismemberment. It seems that bacterial degradation is closely linked to putrefaction and the early stages of degradation<sup>67</sup>, not occurring in cases where the bacterial growth was inhibited (e.g. extreme temperatures, bactericidal chemicals – copper, mercury or lead, or the absence of endogenous bacteria – neonates) or prevented from reaching the bone (e.g., butchering or dismemberment) (Jans et al., 2004; Jans, 2008). The good preservation of the samples collected among the identified collection may be related to a reduced burial interval, the use of coffins and disinfectants, or with a particular condition of the burial environment.

In spite of being frequently ignored and under-rated in bioarchaeological and paleopathological studies<sup>68</sup>, it is the histological analysis of skeletal remains «(...) that provides the greatest potential source of information on long-term bone decomposition» (Garland, 1987: 110). Studying bone remains from the Terme del Sarno at Pompeii using light and scanning electron microscopy, Guarino and co-authors (2006) concluded that assessing the

---

<sup>67</sup> Endogenous bacteria, especially those located in the intestine, seem to play an important role not only in the decomposition of soft tissues, but also in the degradation of bone. For example, bones located in the abdominal area are more likely to be affected by microbial attack due to their proximity to the intestine where putrefaction starts than more distant bones (Child, 1995).

<sup>68</sup> As presented in Chapter 2, section 2.2 (Figure 2.1), of the 630 final candidate studies considered for analysis, only 82 focused on the impact of physical-chemical and biological agents on the bone microstructure.

preservation of bones based on their hardness or softness may be a source of bias, since it does not always reflect the real histological condition. This clearly suggests that gross inspection is not a good measure of bone tissue quality, which may have a serious impact on the application of biomolecular, radiological and chemical methods. For example, the dissolution of bone mineral and the movement of soluble salts into and from the bone microstructure may have a negative effect on the interpretation of radiodensitometry data amongst others (Turner-Walker, 2008). Likewise, bone diagenesis could also affect the preservation of endogenous ancient DNA (Guarino et al., 2006). In fact, some investigations (e.g., Marinho et al., 2006) have found a positive correlation between well preserved bone microstructure and the recovery of DNA molecules. After analysing 13 rib samples collected from different individuals exhumed from three Brazilian Sambaquis – Rio de Janeiro (Moa, Beirada and Zé Espinho), Marinho and colleagues (2006) concluded that bone samples with a better intracortical lamellar arrangement had a higher probability of preserving ancient DNA. In fact, histology has also been applied to quantify bone integrity in paleopathological and molecular studies. The study of Cipollaro et al. (1998) is a good example of this application. The authors successfully extracted and amplified aDNA in human remains from Pompeii whose diagenesis was previously confirmed by histological analysis (Cipollaro, 1998). Histological analysis is also essential to differentiate between pseudopathology and physiological or pathological signs. For example, in the microscopic study of an endocranial lesion of the occipital bone of a child aged 8-10 years, Garland (1993) demonstrated that the outgrowths of extra cortical bone observed were not the result of postmortem damage, as previously thought, but rather the result of antemortem pathology.

In this investigation, the use of microscopy revealed surprising results that justify a more systematic application of histology, especially in the description of bone lesions and healing processes, as well as in the evaluation of bone tissue quality prior to the application of other methods. Despite the limitations currently addressed in the literature, it is clear that histological investigation can provide important data that is normally unattainable through other lines of enquiry (Pfeiffer and Pinto, 2012).



---

# CHAPTER 7

---

*«(...) ITS SEEMS TIMELY FOR HISTOLOGY TO ENTER THE MAINSTREAM OF SKELETAL ANALYSIS IN ANTHROPOLOGY».*

**(MARTIN, 1991: 58)**



## 7. CONCLUSION

Four centuries have passed since the invention of the composite microscope. The contribution that this instrument has made to the development of science is enormous and difficult to express or quantify in numbers. Presently, cells, microorganisms, molecules, and nanoparticles are regarded as acquired evidence and used freely in the scientific discourse. We can hardly imagine the astonishment of the first “microscopists”, such as Anthon van Leeuwenhoek (1632-1723, Netherlands), when they first discovered that beyond the visible world another unexplored dimension populated by strange creatures and structures existed. The microscope changed the face of science and of previous beliefs, expanded the horizons of knowledge, and revolutionized philosophical and scientific thoughts. The role of the microscope in science is probably comparable to the beginning of spatial exploration in the 20<sup>th</sup> century or the invention of the computer and internet that allowed individuals to contact other realities without moving from the same place. But presently microscopy and histological analysis are not absent from the scientific domain. On the contrary, this tool continues to be fundamental for the development of human knowledge. Year after year, new, more sophisticated microscopes have been developed for use not only in biological and medical studies, but also in geology, paleontology, engineering and physics. In medicine, histopathological analysis is crucial in the characterization of lesions and subsequent differential diagnosis. Paleopathology shares a similar goal: the study of past disease. However, it is ironic that histology has been so often neglected in paleopathological analyses. This is even more surprising given the difficulties and interpretative dilemmas faced by paleopathologists, for example, those associated with the true meaning of lesions and their impact on the mortality and morbidity profiles of past populations. Gross inspection of skeletal lesions is important to assess their distribution, anatomical location and general appearance, but as the name suggests, it is a gross inspection. To reduce the limitations of paleopathology,

a series of recommendations for the macroscopic analysis of skeletal remains have been made. One of them reinforces the need for a descriptive summary of the morphology of bone lesions, describing the type of bone formed and its organizational structure (Ortner and Putschar, 1981; Lovell, 2000; Ortner, 2003; Roberts and Manchester, 2005; Grauer, 2008), as well as the need for developing a specific classificatory system in order to provide consistency between researchers and allow for comparative studies (Ortner, 1991). But, how can we determine the organizational structure of bone lesions based only in their macroscopic appearance?

Some of the results of the present investigation showed that gross inspection is not sufficient to describe and characterize bone lesions. In contrast, histology was useful for detecting, for example, signs of the bone cells' activity (e.g. Howship's lacunae) that were imperceptible to the naked eye. Thus, and beyond the visible world, new clues about the microstructure of periosteal new bone formations (PNBFs) were revealed through the microscope lens. Despite some restrictions in sampling all types of periosteal lesions, the analysis of the microstructure of new bone formation revealed some interesting results that broadly fulfill the chief goal of this investigation: *to develop diagnostic criteria that can be used to distinguish between infectious disease and other systemic conditions that potentially stimulate the development of periosteal reactions (e.g. tumours and bone trauma), with particular emphasis on the identification of fragmentary bone lesions unearthed from archaeological contexts*. For example, this study demonstrated that the formation of new bone on the visceral surface of ribs may occur through different processes. Accordingly, the study of the microanatomy of rib lesions can provide useful criteria to distinguish between periosteal lesions of infectious origin from those probably associated with repetitive microtrauma. Furthermore, this study showed that only histology can elucidate the microstructure of lesions, as well as the degree of bone healing. In this sense, the histological analysis proved to be more informative about the structure of periosteal lesions than the gross inspection. All of the evidence recorded can be easily applied to the study of archaeological bone remains, but only if they are well preserved. In fact, microscopy was crucial to determine the true preservation of the skeletal remains, as well as to ascertain the impact of diagenetic agents upon the bone microstructure.

In the following pages, answers will be provided for the main hypothesis tested in this research.

**1. Does new bone deposition manifest differently, both macroscopically and histologically, in the different cause-of-death groups? With respect to both TB and non-TB infectious groups, are there qualitative differences between pulmonary and non-pulmonary TB conditions that allow for a positive diagnosis?**

The macroscopic and histological analysis revealed different results when the presence of periosteal lesions in the chest wall (ribs) and in the remaining appendicular bones was considered. In this investigation, only ribs showed a positive association between the presence of periosteal lesions on the visceral surface and TB as cause of death (Group 1). In fact, individuals who died from TB presented a higher frequency of rib lesions when compared with other cause-of-death groups. In spite of the apparent relationship between periosteal lesions on ribs and TB, the presence of similar new bone foci among individuals who died from other conditions (e.g., non-TB pulmonary conditions – Group 2) did not permit the establishment of a definitive association. These results were not unexpected and are consistent with many others obtained by different authors in the study of identified and archaeological samples. Despite the impossibility of ascertaining the precise etiology of rib lesions, this proliferative phenomenon has been frequently interpreted as the result of an inflammatory/infectious pulmonary condition. However, the application of histological techniques revealed that some rib lesions may have had an origin different from infection. For example, some periosteal rib lesions (> Group 2, non-TB pulmonary conditions) presented a microstructure compatible with a subperiosteal haematoma ultimately caused by repetitive microtrauma (e.g. chest wall vibration). In contrast, those lesions from TB individuals were primarily formed by multiple layers of “appositional bone” probably associated with an abnormal stimulation of growth factors, such as the vascular endothelial growth factor (VEGF). In these last cases, a possible relationship with infection may exist, since many growth factors are involved in the pathogenesis of TB or are induced by hypoxia, a frequent manifestation of pulmonary conditions. The histological differences found may explain why some biomolecular studies based on periosteal rib lesions have failed to identify *M. tuberculosis* complex DNA (Mays et al., 2002). It is possible that in such cases the underlying mechanism was not an infection but rather repetitive microtrauma or some other non-infectious bone response. Taking into account the results of this research, one may conclude that periosteal lesions on ribs manifest differently, both macroscopically and histologically, among cause of death groups but also within the same group. For instance, one individual who died from TB also presented periosteal lesions compatible with a subperiosteal haematoma. Regarding the second

question, further studies of identified or autopsy collections are needed: (a) to test the strength of the association between multiple appositional bone growth and TB infection, and (b) to determine if subperiosteal haematomas are indeed more frequently associated with non-TB pulmonary conditions than with TB. These approaches should be conducted with careful consideration of the new discoveries in the field of bone physiology and response to infection, as well as the immune-pathogenesis of TB.

With respect to the appendicular skeleton, few macroscopic differences were found in the distribution of periosteal lesions among the three groups. The tibia and fibula were the long bones most frequently affected by PNBf in Group 2 (non-TB infectious conditions) and Group 3 (other diseases), and in individuals older than 45 years of age. In the upper limb, the humerus, radius and ulna showed more deposits of new bone, especially among the younger individuals from Group 1. The analysis of the individuals with multiple periosteal bone involvement did not reveal significant differences among cause of death groups. This lack of association between new bone formation and the underlying cause of death seems to corroborate the non-specificity of periosteal lesions, challenging their usefulness as an indicator of physiological stress. The lesions observed in the tibia and fibula proved not to be a good indicator at all. Accordingly, paleopathologists should be careful when using periosteal lesions of the lower limb to diagnose particular conditions. Special mention should be made of the new bone formation in the upper limb bones. In spite of the lack of statistical significance, the distribution of lesions by age and cause of death seems to mirror the pattern observed on the rib cage, denoting a possible association with TB infection. However, this relationship needs further investigation. The results of the macroscopic study also seem to reflect some of the limitations and possible misinterpretations associated with the study of identified skeletal collections. With regard to the histological analysis of long bone samples, non-specific differences in the architecture of periosteal lesions were found among cause of death groups. However, further studies are needed since the sample used for analysis consisted of few long bone specimens. In spite of the reduced number of samples, the results were not surprising since other authors (e.g. Weston, 2009) studying periosteal reactions in long bones also found a lack of correspondence between new bone formation and different pathological conditions.

**2. With respect to TB infections and *other systemic conditions*, are the *proliferative lesions of tuberculous origin different from those caused by tumours*? To what extent is the *new bone produced during fracture remodelling different from that of infectious origin*?**

Unfortunately, the microscopic study of the periosteal lesions associated with metastatic carcinoma was restricted to a single identified sample (rectal carcinoma), which did not allow for the evaluation of possible differences in the microstructure of proliferative, erosive or mixed bone metastasis. The metastatic periosteal lesion was characterized by a dense bulk of thin filaments of new bone with a sunburst pattern, and arranged perpendicularly to the cortex. In an intracortical position, large resorption lacunae secondary to osteoclastic activity were observed. This pattern of pathological bone response is completely different from the periosteal lesions observed, for example, in TB cases. As pointed out earlier, in the tuberculous rib samples the new bone was deposited in multiple layers parallel to the bone surface, crisscrossing numerous primary vascular canals. In most samples, the sign of pathological activity was circumscribed to the periosteal level, as well as to the interface between the newly built bone and the underlying cortex. Large resorption spaces were only seen in the periosteal surface and cortex of those samples with gross lytic lesions. Even in the specimens with evidence of subperiosteal haematomas, a dissimilar pattern of new bone formation was observed when compared with the metastatic case.

Considerable differences were found when the bone callus microstructure was compared with periosteal reactions of infectious and tumour origin. Apart from an unfused rib fracture whose new bone arrangement resembled a subperiosteal haematoma, all remaining callus presented a quite distinctive structure.

**3. Does bone microstructure remain unaffected in cases where no visible lesions are present?**

Yes. In those samples with no macroscopic evidence of new bone formation (control-samples), an intact and regular periosteal and cortical microstructure was observed. In cases where new bone formation was visible, the application of histological techniques was extremely important to characterize the type of periosteal reaction. This was the case with the metastatic carcinoma specimen whose inner lytic lesions were only made visible after histological analysis. The use of microscopy also demonstrated that gross inspection is sometimes insufficient to determine the range of variation of the bone response to disease (e.g. fractures).

**4. Do histological comparative studies aid in the differential diagnosis of archaeological remains? What major diagenetic differences are found and what are the implications for the differential diagnosis?**

Yes. Some of the histological differences recorded in distinct cause of death groups can be used in the study of archaeological remains but only if well preserved, which was not the case in the present study. In fact, most of the archaeological samples collected for analysis presented some form of diagenetic changes that made the study of the normal and pathological bone microstructure impossible. In numerous cases, only the contours of the lesions were observed, with the remaining “bone architecture” being formed by an amorphous mass of composites punctuated by “ghost” osteons and Haversian canals. The diagenetic changes noticed were most probably caused by the action of exogenous and endogenous agents present in the burial environment. It is imperative to highlight that all postmortem damage observed was only revealed after histological investigation. This means that microscopy is essential to assess the quality of bone tissues, which is necessary in the study and characterization of bone lesions.

In spite of the reduced number of samples used in the histological analysis, the results obtained in this investigation were enlightening. In fact, many of the advantages frequently addressed in the literature regarding the application of microscopy to the study of skeletal remains were verified, for example: (1) its role in distinguishing between lesions of infectious from those of traumatic origin (Van der Merwe et al., 2010); (2) its usefulness in the examination of the degree of bone healing (Wright and Yoder, 2003); and (3) its importance in ascertaining the impact of diagenetic factors on the architecture of normal and pathological bone (Bianco and Ascenzi, 1993).

This study showed that researchers should be careful in their macroscopic description and interpretation of bone fractures. That is, one can infer macroscopically that the extremities of a fractured bone are superficially consolidated, but not that the bone callus is completely remodeled, an assertion that can only be made through histological analysis. Furthermore, researchers should consider the application of histological techniques before any biomolecular, radiodensitometric or radiocarbon analysis, especially in archaeological bone remains, in order to infer the degree of bone tissue preservation and thus to avoid null results and unnecessary costs. To a certain extent, the benefits of applying histological techniques are overshadowed by the costs. Histology is frequently portrayed as an invasive procedure that



requires a great deal of expensive equipment and is time-consuming. As a consequence, other faster and more economical techniques such as radiography and CT-scanning are used to provide a glimpse into the structure and density of bone tissues. However, in certain circumstances these methods may not provide a complete picture of all bone features. For example, it is possible that lesions with a high bone density may obscure small lytic foci, making them invisible on X-ray. Furthermore, there are always the constraints imposed by diagenesis when working with ancient remains. We cannot guarantee that the tissue density portrayed on X-ray films corresponds to that of the original bone composition. With regard to this last issue, histology can be very useful in making the distinction between intact, normal, pathological and damaged bone tissue.

The present study also revealed evidence that highlights the role of histology in the characterization of periosteal bone lesions, such as those observed on the visceral surface of ribs; however, further research is needed to corroborate its relationship with the cause of death of the individuals. Future studies based on well-documented collections with accurate medical records and/or samples retrieved from clinical cases will eventually solve some of the problems and limitations detected in this investigation. Increasing the sample size will also improve our understanding of the entire spectrum of new bone variation associated with a particular condition. Nevertheless, a number of questions related to the pathophysiology of periosteal new bone formation (PNBF) cannot be fully understood presently. It is possible that further research in the field of bone biochemistry, immunology and cell communication will shed light on the exact mechanism (or mechanisms) behind this particular type of bone response.

As pointed out previously, the future of paleohistology depends on a more systematic application, on the development of uniform methods, as well as on the creation of a proper nomenclature to describe and characterize pathological bone at the microscopic level, as a way of reducing potential errors and biased interpretations (Pfeiffer and Pinto, 2012; Schultz, 2012; Stout and Crowder, 2012). Through investigations similar to this one, more anthropologists may come to realize the full potential of applying histological techniques in the study of bone conditions, such as those of infectious origin that manifest through PNBF.

We can shift a little bit further and extend this desire for change to the future of paleopathology. Paleopathology has developed side by side with medical improvements. The medical knowledge derived from orthopaedic pathology and radiology has been extremely helpful to our understanding of some bone conditions. However, orthopaedists and

paleopathologists share different perceptions about bones, lesions, and diseases. When studying bone conditions, paleopathologists only see the products of the cellular activity. Accordingly, more knowledge about bone dynamics is needed to fully understand the processes of lesion formation. More than applying new tools derived from the clinics, paleopathology needs to build its unique language and body of knowledge. For that, paleopathologists need to go “back to the basics” and understand what cellular, biomolecular, and mechanical factors underlie the development of bone lesions before moving to individual and populational studies. It is pointless to discuss the impact of certain bone lesions on the health of past populations when we are not certain about the exact origin of the lesions. Paleopathologists need to know what lesions really are. What mechanisms activate bone cells’ response and in what circumstances? What is the range of variation of the individual response to disease? What is the influence of genetics in the expression of certain proteins and bone growth factors? What microstructural and biomolecular markers may be unequivocally used in the study of pathological conditions? Paleopathologists need to know what is possible and what is not possible. What group of conditions and associated skeletal reactions can be used, or not, as indicators of health inequality? Biomechanics, tissue engineering, and bone prosthetic research has been making important discoveries concerning the reaction of bone to internal and external stimuli. Combining the new discoveries in bone dynamics, physiology and pathophysiology with a more systematic analysis of the bone microstructure and biomolecular data will certainly enhance the paleopathological knowledge. The application of noninvasive histological techniques, such as synchrotron radiation X-ray microtomography that limits the degree of bone intrusion will be highly valuable, not only in the study of pathological bone changes, but also to better understand the levels of microstructural and biomolecular bone diagenesis.

---

# CHAPTER 8

---



## 8. REFERENCES

### A

- Aaron, J.; Rogers, J.; Kanis, J. 1992. Paleohistology of Paget's disease in two medieval skeletons. *American Journal of Physical Anthropology*, 89(3): 325-331.
- Abbott, S.; Trinkaus, E.; Burr, D. 1996. Dynamic bone remodelling in later Pleistocene fossil hominids. *American Journal of Physical Anthropology*, 99(4): 585-601.
- Abou-Arab, M.; Thomsen, J.; Frohlich, B.; Lynnerup, N. 1995. Technical note: histological staining of secondary osteons. *American Journal of Physical Anthropology*, 98(3): 391-394.
- Afonso, N.; Jasti, H.; Alangaden, G. 2001. Tuberculosis of the ribs presenting as bilateral pseudogynecomastia. *Infectious Diseases in Clinical Practice*, 10(2): 125-126.
- Agrawal, V.; Joshi, M.; Jain, B.; Mohanty, D.; Gupta, A. 2008. Tuberculous osteomyelitis of rib – a surgical entity. *Interactive Cardiovascular and Thoracic Surgery*, 7(6): 1028-1030.
- Aiello, L.; Molleson, T. 1993. Are microscopic ageing techniques more accurate than macroscopic ageing techniques? *Journal of Archaeological Science*, 20(6): 689-704.
- Ali, A.; Tetelman, M.; Fordham, E.; Turner, D.; Chiles, J.; Patel, S.; Schmidt, K. 1980. Distribution of hypertrophic pulmonary osteoarthropathy. *American Journal of Roentgenology*, 134(4): 771-780.
- Allen, M.; Hock, J.; Burr, D. 2004. Periosteum: biology, regulation, and response to osteoporosis therapies. *Bone*, 35(5): 1003-1012.
- Alt, K.; Adler, C.; Buitrago-Téllez, C.; Lohrke, B. 2002. Infant osteosarcoma. *International Journal of Osteoarchaeology*, 12(6): 442-448.
- Altun, B. 2008. Periosteum: resorption or formation area? *Turkish Journal of Endocrinology and Metabolism*, 12(1): 28-31.

- Alunni-Perret, V.; Muller-Bolla, M.; Laugier, J.; Lupi-Pegurier, L.; Bertrand, M.; Staccini, P.; Bolla, M.; Quatrehomme, G. 2005. Scanning electron microscopy analysis of experimental bone hacking trauma. *Journal of Forensic Sciences*, 50(4): 796-801.
- An, Y.; Martin, K. 2003. *Handbook of histological methods for bone and cartilage*. New Jersey, Humana Press.
- An, Y.; Gruber, H. 2003. Introduction to experimental bone and cartilage histology. In: An, Y.; Martin, K. (Eds.). *Handbook of histological methods for bone and cartilage*. New Jersey, Humana Press: 3-31.
- An, Y.; Moreira, P.; Kang, Q.; Gruber, H. 2003. Principles of embedding and common protocols. In: An, Y.; Martin, K. (Eds.). *Handbook of histological methods for bone and cartilage*. New Jersey, Humana Press: 185-197.
- Anderson, T.; Wakely, J.; Carter, A. 1992. Medieval example of metastatic carcinoma: a dry bone, radiological, and SEM study. *American Journal of Physical Anthropology*, 89(3): 309-323.
- Anemone, R.; Moonet, M.; Siegel, M. 1996. Longitudinal study of dental development in chimpanzees of known chronological age: implications for understanding the age at death of Plio-Pleistocene hominids. *American Journal of Physical Anthropology*, 99(1): 119-133.
- Arican, M.; Ortatatll, M.; Yigitarslan, K.; Ceylan, C. 2003. Osteogenic ability of free perichondreal autografts in canine tibial defects: an experimental study. *Journal of Experimental Animal Science*, 42(4): 203-217.
- Aries, P.; Reuter, M.; Lamprecht, P.; Gross, W. 2005. Periostitis as the initial manifestation of systemic vasculitis. *Annals of the Rheumatic Diseases*, 64(2): 329-330.
- Armelagos, G.; Van Gerven, D. 2003. A century of skeletal biology and paleopathology: contrasts, contradictions, and conflicts. *American Anthropologist*, 105(1): 53-64.
- Armitage, P.; Clutton-Brock, J. 1981. A radiological and histological investigation into the mummification of cats from Ancient Egypt. *Journal of Archaeological Science*, 8(2): 185-196.
- Armstrong, D.; McCausland, E.; Wright, G. 2007. Hypertrophic pulmonary osteoarthropathy (HPOA) (Pierre Marie-Bamberger syndrome). Two cases presenting as acute inflammatory arthritis: description and review of the literature. *Rheumatology International*, 27(4): 399-402.

- Arnaud, G.; Arnaud, S. 1975. Luxation congénitale bilatérale de la hanche et manifestations d'hyperostose porotique sur un squelette d'époque paléochrétienne. *Bulletins et Mémoires de la Société d'Anthropologie de Paris*, 2(4): 307-326.
- Arnautou, J.-P.; Blondiaux, J.; Coindre, J.-M.; Duda, H. 2011. Aux origines de la maladie osseuse de Paget. Un nouveau cas néolithique dans le sud de la France. *Bulletins et Mémoires de la Société d'Anthropologie de Paris*, 23(1-2): 94-104.
- Arnold, J.; Jee, W. 1954. Embedding and sectioning undecalcified bone and its application to radioautography. *Stain Technology*, 29(5): 225-239.
- Arrieta, M.; Bordach, M.; Mendonça, O. 2011. Pre-Columbian tuberculosis in Northwest Argentina: skeletal evidence from Rincón Chico 21 cemetery. *International Journal of Osteoarchaeology*: DOI: 10.1002/oa.1300.
- Ashurst, J. 1871. *The principles and practice of surgery*. Philadelphia, Henry C. Lea.
- Asnis, D.; Niegowska, A. 1997. Tuberculosis of the rib. *Clinical Infectious Diseases*, 24: 1018-1019.
- Assis, S. 2006. Um olhar sobre o passado de Constância. Relatório técnico-científico referente ao estudo paleoantropológico de uma série de esqueletos exumados da necrópole de Constância. Coimbra, Departamento de Antropologia da Universidade de Coimbra [Unpublished].
- Assis, S.; Codinha, S. 2010. Metastatic carcinoma in a 14th-19th century skeleton from Constância (Portugal). *International Journal of Osteoarchaeology*, 20(5): 603 - 620.
- Assis, S.; Santos, A. L.; Roberts, C. 2011. Evidence of hypertrophic osteoarthropathy in individuals from the Coimbra Skeletal Identified Collection (Portugal). *International Journal of Paleopathology*, 1(3-4): 127-206.
- Assis, S.; Caldeira, D.; Gonçalves, S.; Nabo, A.; Nunes, J.; Soares, C.; Lopes, C.; Alves Cardosos, F. 2010. A possible case of venereal syphilis at the extinct Royal Hospital of All Saints - Lisbon, Portugal (18th century). Poster presented at the 18<sup>th</sup> European Meeting of the Paleopathology Association. Vienna, Austria 23<sup>rd</sup>-26<sup>th</sup> August.
- Astudillo, L.; Rigal, F.; Couret, B.; Arlet-Suau, E. 2001. Localized polyarteritis nodosa with periostitis. *The Journal of Rheumatology*, 28 (12): 2758-2759.
- Aubin, J.; Triffitt, J. 2002. *Mesenchymal stem cells and the osteoblasts lineage*. San Diego, Academic Press.
- Aufderheide, A. 2003. *The scientific study of mummies*. Cambridge, Cambridge University Press.

- Aufderheide, A. 2011. Soft tissue taphonomy: a paleopathology perspective. *International Journal of Paleopathology*, 1(2): 75-80.
- Aufderheide, A.; Rodríguez-Martín, C. 1998. *The Cambridge encyclopedia of human paleopathology*. Cambridge, Cambridge University Press.
- Aufderheide, A.; Ragsdale, B.; Buikstra, J.; Ekberg, F.; Vinh, T. 1997. Structure of the radiological “sunburst” pattern as revealed in an ancient osteosarcoma. *Journal of Paleopathology*, 9(2): 101-106.
- Ayoub, A.; Challa, S. R.; Abu-Serriah, M.; McMahon, J.; Moos, K.; Creanor, S.; Odell, E. 2007. Use of a composite pedicled muscle flap and rhBMP-7 for mandibular reconstruction. *International Journal of Oral and Maxillofacial Surgery*, 36(12): 1183-1192.

**B**

- Bagousse, A.; Blondiaux, J. 2002. Mortalité maternelle et périnatalité au premier millénaire à Lisieux (Clavados, France). *Bulletins et Mémoires de la Société d'Anthropologie de Paris*, 14(3-4): 295-309.
- Balaji, R.; Ramachandran, K.; Krishnakumar, A.; Venugopal, M. 2006. Radiological quiz – musculoskeletal. *Indian Journal of Radiology and Imaging*, 16(4): 931-932.
- Ball, J. 1910. *Andreas Vesalius, the reformer of anatomy*. Saint Louis, Medical Science Press.
- Ball, J.; Grayze, A. 1964. Arteritis and localized periosteal new bone formation. *The Journal of Bone and Joint Surgery*, 46 B(2): 244-250.
- Barbour, E. 1950. A study of the structure of fresh and fossil human bone by means of the electron microscope. *American Journal of Physical Anthropology*, 8(3): 315-330.
- Barnes, I.; Young, J.; Dobney, K. 2000. DNA-based identification of goose species from two archaeological sites in Lincolnshire. *Journal of Archaeological Science*, 27(2): 91-100.
- Barrie, J. M. 1916. *Peter Pan in Kensington Gardens*. New York, Charles Scribner's Sons.
- Bartelink, E.; Wiersema, J.; Demaree, R. 2001. Quantitative analysis of sharp-force trauma: an application of scanning electron microscopy in forensic anthropology. *Journal of Forensic Sciences*, 46(6): 1288-1293.
- Bass, W. 1979. Developments in the identification of human skeletal material (1968–1978). *American Journal of Physical Anthropology*, 51(4): 555-562.
- Bazar, K. A.; Yun, A. J.; Lee, P. Y. 2004. Hypertrophic osteoarthropathy may be a marker of underlying sympathetic bias. *Medical Hypotheses*, 63(2): 357–361.



- Beasley, A. 1982a. The origin of orthopaedics. *Journal of the Royal Society of Medicine*, 75(8): 648-655.
- Beasley, A. 1982b. Orthopaedic aspects of mediaeval medicine. *Journal of the Royal Society of Medicine*, 75(12): 970-975.
- Beasley, A. 1986. Orthopaedics: evolution of the speciality. *Journal of the Royal Society of Medicine*, 79(10): 607-610.
- Beasley, M.; Brown, W.; Legge, A. 1992. Incremental banding in dental cementum: methods of preparation for teeth from archaeological sites and for modern comparative specimens. *International Journal of Osteoarchaeology*, 2(1): 37-50.
- Beauchesne, P.; Saunders, S. 2006. A test of the revised Frost's 'rapid manual method' for the preparation of bone thin sections. *International Journal of Osteoarchaeology*, 16(1): 82-87.
- Bekci, T.; Tezcan, B.; Yaşar, S.; Kesli, R.; Maden, E. 2010. Tuberculous abscess of the chest wall. *European Journal of General Medicine*, 7(3): 326-329.
- Bell, L. 2012. Histotaphonomy. In: Crowder, C.; Stout, S. (Eds.). *Bone histology: an anthropological perspective*. Boca Raton, CRC Press: 241-251.
- Bell, L.; Jones, S. 1991. Macroscopic and microscopic evaluation of archaeological pathological bone: backscattered electron imaging of putative pagetic bone. *International Journal of Osteoarchaeology*, 1(3-4): 179-184.
- Bell, L.; Piper, K. 2000. An introduction to palaeohistopathology. In: Cox, M.; Mays, S. (Eds.). *Human osteology in archaeology and forensic sciences*. London, Greenwich Medical Media, Ltd: 255-274.
- Bell, L.; Skinner, M.; Jones, S. 1996. The speed of postmortem change to the human skeleton and its taphonomic significance. *Forensic Science International*, 82(2): 129-140.
- Bellard, F.; Cortés, J. 1991. A muscular parasite in a mummified girl. *International Journal of Osteoarchaeology*, 1(3-4): 215-218.
- Bello, S.; Soligo, C. 2008. A new method for the quantitative analysis of cutmark micromorphology. *Journal of Archaeological Science*, 35(6): 1542-1552.
- Ben-Menahem, A. 2009. *Historical encyclopedia of natural and mathematical sciences*. Berlin, Springer-Verlag.
- Bennike, P.; Lewis, M.; Schutkowski, H.; Valentin, F. 2005. Comparison of child morbidity in two contrasting medieval cemeteries from Denmark. *American Journal of Physical Anthropology*, 128(4): 734-746.

- Bentolila, V.; Boyce, T.; Fyhrie, D.; Drumb, R.; Skerry, T.; Schaffler, M. 1998. Intracortical remodelling in adult rat long bones after fatigue loading. *Bone*, 23(3): 275-281.
- Berná, L.; Germá, R.; Estorch, M.; Torres, G.; Blanco, R.; Carrio, I. 1991. Bone marrow regeneration after hormonal therapy in patients with bone metastases from prostate cancer. *The Journal of Nuclear Medicine*, 32(12): 2295–2298.
- Bianco, P.; Ascenzi, A. 1993. Palaeohistology of human bone remains: a critical evaluation and an example of its use. In: Grupe, G.; Garland, A. (Eds.). *Histology of ancient human bone: methods and diagnosis*. Berlin, Springer-Verlag: 157-170.
- Bianucci, R.; Mattutino, G.; Lallo, R.; Charlier, P.; Jouin-Spriet, H.; Peluso, A.; Higham, T.; Torre, C.; Massa, E. 2008. Immunological evidence of *Plasmodium falciparum* infection in an Egyptian child mummy from the Early Dynastic Period. *Journal of Archaeological Science*, 35(7): 1880-1885.
- Bichat, X. 1799. *Traité des membranes en general et de diverses membranes en particulier*. Paris, Richard, Caille et Ravier.
- Bielby, R.; Jones, E.; McGonagle, D. 2007. The role of mesenchymal stem cells in maintenance and repair of bone. *Injury*, 38(1): S26-S32.
- Bishara, J.; Gartman-Israel, D.; Weinberger, M.; Maimon, S.; Tamir, G.; Pitlik, S. 2000. Osteomyelitis of the ribs in the antibiotic era. *Scandinavian Journal of Infectious Diseases*, 32(3): 223-227.
- Blanchard, C. 1996. Atomic force microscopy. *The Chemical Educator*, 1(5): 1-8.
- Blondiaux, J. 1997. Étude ostéo-archéologique de sept sépultures sous la place de l'Hôtel de ville à Abbeville (Somme). *Revue Archéologique de Picardie*, 3-4: 213-218.
- Blondiaux, J.; Charlier, P. 2008. Palaeocytology in skeletal remains: microscopic examination of putrefaction fluid deposits and dental calculus of skeletal remains from French archaeological sites. *International Journal of Osteoarchaeology*, 18(1): 1-10.
- Blondiaux, J.; Duvette, J.-F.; Vatteoni, S.; Eisenberg, L. 1994. Microradiographs of leprosy from an osteoarchaeological context. *International Journal of Osteoarchaeology*, 4(1): 13-20.
- Blondiaux, G.; Blondiaux, J.; Secousse, F.; Cotton, A.; Danze, P.-M.; Flipo, R.- M. 2002. Rickets and child abuse: the case of a two year old girl from the 4th century in Lisieux (Normandy). *International Journal of Osteoarchaeology*, 12(3): 209-215.
- Blondiaux, J.; Cotton, A.; Fonatine, C.; Hänni, C.; Bera, A.; Flipo, R.- M. 1997. Two roman and medieval cases of symmetrical erosive polyarthropathy from Normandy: anatomico-

- pathological and radiological evidence for rheumatoid arthritis. *International Journal of Osteoarchaeology*, 7(5): 451-466.
- Blondiaux, J.; Baud, C.; Boscher-Barré, N.; Dardenne, C.; Deschamps, N.; Trocellier, P.; Buchet, L. 1992. Trace elements in palaeopathology: quantitative analysis of a case of hypertrophic osteoarthropathy by instrumental neutron activation analysis. *International Journal of Osteoarchaeology*, 2(3): 241-244.
- Boel, L.; Ortner, D. 2011. Skeletal manifestations of skin ulcer in the lower leg. *International Journal of Osteoarchaeology*. DOI: 10.1002/oa.1248.
- Boel, L.; Boldsen, J.; Melsen, F. 2007. Double lamellae in trabecular osteons: towards a new method for age estimation by bone microscopy. *HOMO - Journal of Comparative Human Biology*, 58(4): 269-277.
- Boivin, G.; Meunier, P. 1993. Histomorphometric methods applied to bone. In: Grupe, G.; Garland, A. (Eds.). *Histology of ancient human bone: methods and diagnosis*. Berlin, Springer-Verlag: 137-156.
- Bovée, J. 2008. Multiple osteochondromas. *Orphanet Journal of Rare Diseases*, 3: 3.
- Branton, M.; Kopp, J. 1999. TGF-  $\beta$  and fibrosis. *Microbes and Infection*, 1(15): 1349-1365.
- Brickley, M.; Ives, R. 2006. Skeletal manifestations of infantile scurvy. *American Journal of Physical Anthropology*, 129(2): 163-172.
- Brickley, M.; Ives, R. 2008. *The bioarchaeology of metabolic bone diseases*. Oxford, Academic Press.
- Brickley, M.; Mays, S.; Ives, R. 2007. An investigation of skeletal indicators of vitamin D deficiency in adults: effective markers for interpreting past living conditions and pollution levels in 18th and 19th century Birmingham, England. *American Journal of Physical Anthropology*, 132(1): 67-79.
- Bromage, T.; Boyde, A. 1984. Microscopic criteria for the determination of directionality of cutmarks on bone. *American Journal of Physical Anthropology*, 65(4): 359-366.
- Brothwell, D.; Sandison, A.; Gray, P. 1969. Human biological observations on a Guanche mummy with anthracosis. *American Journal of Physical Anthropology*, 30(3): 333-347.
- Bullington, J. 1991. Deciduous dental microwear of prehistoric juveniles from the lower Illinois River Valley. *American Journal of Physical Anthropology*, 84(1): 59-73.
- Bullough, P. 2010. *Orthopaedic pathology*. Maryland Heights, MO, Mosby/Elsevier.
- Buikstra, J. 2010. Paleopathology: a contemporary perspective. In: Larsen, C. (Ed.). *A companion to biological anthropology*. Malden, Blackwell Publishing Ltd.: 395-411.

- Buonsenso, D.; Focarelli, B.; Scalzone, M.; Chiaretti, A.; Gioè, C.; Ceccarelli, M.; Valentini, P. 2012. Chest wall TB and low 25-hydroxy-vitamin D levels in a 15-month-old girl. *Italian Journal of Pediatrics*, 38: 1-6.
- Burgener, F.; Korman, M.; Pudas, T. 1991. *Differential diagnosis in conventional radiology*. New York, Thieme.
- Burgener, F.; Korman, M.; Pudas, T. 2006. *Bone and joint disorders: differential diagnosis in conventional radiology*. Stuttgart, Georg Thieme Verlag.
- Burger, E.; Klein-Nulend, J. 1999. Mechanotransduction in bone – role of the lacuno-canalicular network. *The FASEB Journal*, 13(9001): 101-112.
- Burke, A.; Castanet, J. 1995. Histological observations of cementum growth in horse teeth and their application to archaeology. *Journal of Archaeological Science*, 22(4): 479-493.
- Buzon, M. 2006. Health of the non-elites at Tombos: nutritional and disease stress in New Kingdom Nubia. *American Journal of Physical Anthropology*, 130(1): 26-37.

**C**

- 
- Campanacci, M. 1999. *Bone and soft tissue tumours: clinical features, imaging, pathology and treatment*. Padova, Piccin Nuova Libreria.
- Canalis, E. 2005. Mechanisms of glucocorticoid action in bone. *Current Osteoporosis Reports*, 3(3): 98-102.
- Canci, A.; Marchi, D.; Caramella, D.; Fornaciari, G.; Borgognini Tarli, S. 2005. Coexistence of melorheostosis and DISH in a female skeleton from Magna Graecia (sixth century BC). *American Journal of Physical Anthropology*, 126(3): 305-310.
- Cannet, C.; Baraybar, J.; Kolopp, M.; Meyer, P.; Ludes, B. 2010. Histomorphometric estimation of age in paraffin-embedded ribs: a feasibility study. *International Journal of Legal Medicine*, 125(4): 495-502.
- Capasso, L. 1997. Osteoma: palaeopathology and phylogeny. *International Journal of Osteoarchaeology*, 7(8): 615-620.
- Capasso, L. 1999. Brucellosis at Herculaneum (79 AD). *International Journal of Osteoarchaeology*, 9(5): 277-288.
- Capasso, L. 2007. Infectious diseases and eating habits at Herculaneum (1st century AD, Southern Italy). *International Journal of Osteoarchaeology*, 17(4): 350-357.

- Cardoso, H. F. 2005. Patterns of growth and development of the human skeleton and dentition in relation to environmental quality. Ph.D. Thesis in Anthropology. Hamilton, Ontario, McMaster University.
- Cardoso, H. F. 2006. Brief communication: the Collection of Identified Human Skeletons housed at the Bocage Museum (National Museum of Natural History), Lisbon, Portugal. *American Journal of Physical Anthropology*, 129(2): 173-176.
- Caropreso, S.; Bondioli, L.; Capannolo, D.; Cerroni, L.; Macchiarelli, R.; Condo, S. 2000. Thin sections for hard tissue histology: a new procedure. *Journal of Microscopy*, 199(3): 244-247.
- Carter, D.; Beaupré, G. 2001. Skeletal function and form: mechanobiology of skeletal development, aging, and regeneration. Cambridge, Cambridge University Press.
- Castriota-Scanderbeg, A.; Dallapiccola, B. 2005. Abnormal skeletal phenotypes: from simple signs to complex diagnoses. Berlin, Springer Verlag.
- Cattaneo, C.; Porta, D.; Gibelli, D.; Gamba, C. 2009. Histological determination of the human origin of bone fragments. *Journal of Forensic Sciences*, 54(3): 531-533.
- Cavanaugh, J.; Holman, G. 1965. Hypertrophic osteoarthropathy in childhood. *The Journal of Pediatrics*, 66(1): 27-40.
- Chamberlain, A. 2000. Problems and prospects in paleodemography. In: Cox, M.; Mays, S. (Eds.). *Human osteology in archaeology and forensic sciences*. Cambridge, Cambridge University Press: 83-100.
- Chan, A.; Crowder, C.; Rogers, T. 2007. Variation in cortical bone histology within the human femur and its impact on estimating age at death. *American Journal of Physical Anthropology*, 132(1): 80-88.
- Chandler, N.; Fyfe, D. 1997. Root canals of buried teeth: radiographic changes due to crystal growth. *International Journal of Osteoarchaeology*, 7(1): 11-17.
- Chang, J.; Kim, S.; Kim, S.; Chung, K.; Shin, D.; Joo, S.; Choe, K. 1992. Tuberculosis of the ribs: a recurrent attack of rib caries. *Yonsei Medical Journal*, 33(4): 374-377.
- Chappard, D.; Baslé, M.; Legrand, E.; Audran, M. 2011. New laboratory tools in the assessment of bone quality. *Osteoporosis International*, 22(8): 2225-2240.
- Charles, D.; Condon, K.; Cheverud, J.; Buikstra, J. 1986. Cementum annulation and age determination in *Homo sapiens*. I. Tooth variability and observer error. *American Journal of Physical Anthropology*, 71(3): 311-320.

- Chen, G.; Deng, C.; Li, Y.-P. 2012. TGF- $\beta$  and BMP signaling in osteoblast differentiation and bone formation. *International Journal of Biological Science*, 8(2): 272-288.
- Child, A. 1995. Towards an understanding of the microbial decomposition of archaeological bone in the burial environment. *Journal of Archaeological Science*, 22(2): 165-174.
- Cho, H. 2012. The histology laboratory and principles of microscope instrumentation. In: Crowder, C.; Stout, S. (Eds.). *Bone histology: an anthropological perspective*. Boca Raton, CRC Press: 341-359.
- Cho, H.; Stout, S. 2011. Age-associated bone loss and intraskeletal variability in the Imperial Romans. *Journal of Anthropological Sciences*, 89: 109-125.
- Cho, H.; Stout, S.; Bishop, T. 2006. Cortical bone remodelling rates in a sample of African American and European American descent groups from the American Midwest: comparisons of age and sex in ribs. *American Journal of Physical Anthropology*, 130(2): 214-226.
- Chrousos, G. 2009. Stress and disorders of the stress system. *Nature Reviews Endocrinology*, 5: 374-381.
- Chrousos, G.; Gold, P. 1992. The concepts of stress and stress system disorders: overview of physical and behavioural homeostasis. *JAMA: The Journal of the American Medical Association*, 267(9): 1244-1252.
- Cipollaro, M.; Di Bernardo, G.; Galano, G.; Galderisi, U.; Guarino, F.; Angelini, F.; Cascino, A. 1998. Ancient DNA in human bone remains from Pompeii archaeological site. *Biochemical and Biophysical Research Communications*, 247(2): 901-904.
- Ciranni, R.; Fornaciari, G. 2004. Juvenile cirrhosis in a 16th century Italian mummy. *Current technologies in pathology and ancient human tissues. Virchows Archiv*, 445(6): 647-650.
- Ciranni, R.; Castagna, M.; Fornaciari, G. 1999. Goiter in an eighteenth-century Sicilian mummy. *American Journal of Physical Anthropology*, 108(4): 427-432.
- Civitelli, R.; Zimbaras, K.; Leelawattana, R. 1998. Pathophysiology of calcium, phosphate, and magnesium absorption. In: Avioli, L.; Krane, S. (Eds.). *Metabolic bone disease and clinically related disorders*. San Diego, Academic Press: 165-205.
- Cohen, M.; Wood, J.; Milner, G. 1994. The osteologic paradox reconsidered. *Current Anthropology*, 35(5): 629-637.
- Cohen, R. 1949. Cough fracture of ribs. *British Medical Journal*, 1(4594): 133-135.

- Cole, G.; Waldron, T. 2012. Is unresolved inflammatory angiogenesis a mechanism for the delayed development of skeletal lesions in syphilis? *International Journal of Osteoarchaeology*. DOI: 10.1002/oa.2230.
- Coleman, R. 1997. Skeletal complications of malignancy. *Cancer*, 80(8): 1588–1594.
- Coleman, R. 2001. Metastatic bone disease: clinical features, pathophysiology and treatment strategies. *Cancer Treatment Reviews*, 27(3): 165–176.
- Collins, M.; Nielsen-Marsh, C.; Hiller, J.; Smith, C.; Roberts, J.; Prigodich, R.; Wess, T.; Csapò, J.; Millard, A.; Turner-Walker, G. 2002. The survival of organic matter in bone: a review. *Archaeometry*, 44(3): 383-394.
- Colnot, C.; Huang, S.; Helms, J. 2006. Analyzing the cellular contribution of bone marrow to fracture healing using bone marrow transplantation in mice. *Biochemical and Biophysical Research Communications*, 350(3): 557-561.
- Cook, D.; Patrick, R. 2011. As the worm turns: an enigmatic calcified object as pseudopathology. *International Journal of Osteoarchaeology*. DOI: 10.1002/oa.1302.
- Cook, D.; Powell, M. 2006. The evolution of American paleopathology. In: Buikstra, J.; Beck, L. (Eds.). *Bioarchaeology: the contextual analysis of human remains*. Burlington, Academic Press: 281-322.
- Cook, M.; Molto, E.; Anderson, C. 1988. Possible case of hyperparathyroidism in a roman period skeleton from the Dakhleh Oasis, Egypt, diagnosed using bone histomorphometry. *American Journal of Physical Anthropology*, 75(1): 23-30.
- Cooper, D.; Thomas, C.; Clement, J. 2012. Technological developments in the analysis of cortical bone histology. In: Crowder, C.; Stout, S. (Eds.). *Bone histology: an anthropological perspective*. Boca Raton, CRC Press: 361-375.
- Cooper, M. 2004. Sensitivity of bone to glucocorticoids. *Clinical Science*, 107(2): 111-123.
- Cormier, J. 2003. Microstructural and mechanical properties of human ribs. Master of science in mechanical engineering. Virginia, Virginia Polytechnic Institute and State University [Unpublished].
- Costello, C.; Howell, K.; Cahill, E.; McBryan, J.; Konigshoff, M.; Eickelberg, O.; Gaine, S.; Martin, F.; McLoughlin, P. 2008. Lung-selective gene responses to alveolar hypoxia: potential role for the bone morphogenetic antagonist gremlin in pulmonary hypertension. *American Journal of Physiology – Lung Cellular and Molecular Physiology*, 295(2): L272-L284.

- Cox, M.; Bell, L. 1999. Recovery of human skeletal elements from a recent UK murder inquiry: preservational signatures. *Journal of Forensic Sciences*, 44(5): 945-950.
- Craig, D. 2008. Medial tibial stress syndrome: evidence-based prevention. *Journal of Athletic Training*, 43(3): 316-318.
- Crampton, P. 1817. On periostitis, or inflammation of the periosteum. *Dublin hospital reports and communications in medicine and surgery*. Dublin, Hodges and M'Arthur: 331-357.
- Croft, W. 2006. *Under the microscope: a brief history of microscopy*. New Jersey, World Scientific Publishing Co., Ltd.
- Croker, S.; Clement, J.; Donlon, D. 2009. A comparison of cortical bone thickness in the femoral midshaft of humans and two non-human mammals. *HOMO - Journal of Comparative Human Biology*, 60(6): 551-565.
- Crowder, C.; Rosella, L. 2007. Assessment of intra- and intercostal variation in rib histomorphometry: its impact on evidentiary examination. *Journal of Forensic Sciences*, 52(2): 271-276.
- Cudkowicz, L.; Armstrong, J. B. 1953. The blood supply of malignant pulmonary neoplasms. *Thorax*, 8(2): 152-156.
- Cuijpers, A. 2006. Histological identification of bone fragments in archaeology: telling humans apart horses and cattle. *International Journal of Osteoarchaeology*, 16(6): 465-480.
- Cule, J.; Evans, I. 1968. Porotic hyperostosis at the Gelligaer skull. *Journal of Clinical Pathology*. 21(6): 753-758.
- Cullinane, D.; Einhorn, T. 2002. Biomechanics of bone. In: Bilezikian, J.; Raisz, L.; Rodan, G. (Eds.). *Principles of bone biology*. San Diego, Academic Press: 17-32.

**D**

- 
- D'Anastasio, R.; Zipfel, B.; Moggi-Cecchi, J.; Stanyon, R.; Capasso, L. 2009. Possible brucellosis in an early hominin skeleton from Sterkfontein, South Africa. *PLoS One*, 4(7): e6439.
- Darnell, L.; Teaford, M.; Livi, K.; Weihs, T. 2010. Variations in the mechanical properties of *Alouatta palliata* molar enamel. *American Journal of Physical Anthropology*, 141(1): 7-15.
- Davies, T; Fearnhead, R. 1960. The neuro-histology of mammalian bone. *Archives of Oral Biology*, 2(4): 263-270.



- Ddungu, H.; Johnson, J. L.; Smieja, M.; Mayanja-Kizza, H. 2006. Digital clubbing in tuberculosis—relationship to HIV infection, extent of disease and hypoalbuminemia. *BioMed Central Infectious Diseases*, 6 (45): 1–7.
- De Bari, C.; Dell’Accio, F.; Luyten, F. 2001. Human periosteum-derived cells maintain phenotypic stability and chondrogenic potential throughout expansion regardless of donor age. *Arthritis and Rheumatism*, 44(1): 85-95.
- De Boer, H.; Aarents, M.; Maat, G. 2012a. Staining ground sections of natural dry bone tissue for microscopy. *International Journal of Osteoarchaeology*, 22(4): 379-386.
- De Boer, H.; van der Merwe, A.; Hammer, S.; Steyn, M.; Maat, G. 2012b. Assessing post-traumatic time interval in human dry bone. *International Journal of Osteoarchaeology*. DOI: 10.1002/oa.2267.
- De Boer, H.; Aarents, M.; Maat, G. 2013. Manual for the preparation and staining of embedded natural dry bone tissue sections for microscopy. *International Journal of Osteoarchaeology*, 23(1): 83-93.
- De Donno, A.; Santoro, V.; Di Fazio, A.; Corrado, S.; Urso, D.; Baldassarra, S.; Di Nunno, N.; Introna, F. 2009. Analysis of Neolithic human remains discovered in southern Italy. *Journal of Archaeological Science*, 37(3): 482-487.
- De La Rúa, C.; Baraybar, J.; Etxeberria, F. 1995. Neolithic case of metastasizing carcinoma: multiple approaches to differential diagnosis. *International Journal of Osteoarchaeology*, 5(3): 254-264.
- De Santos, L. 1980. The radiology of bone tumors: old and new modalities. *CA: A Cancer Journal for Clinicians*, 30(2): 66-91.
- De Silva, P.; Evans-Jones, G.; Wright, A.; Henderson, R. 2003. Physiological periostitis: a potential pitfall. *Archives of Disease in Childhood*, 88(12): 1124-1125.
- Delly, J. 2008. Selected topics from essentials of polarized light microscopy. Illinois, College of Microscopy.
- Den Heuvel, T.; Maltha, J.; Kuijpers-Jagtman, A. 1991. A histological and histometric study of the periosteum in mandibular ramal and condylar areas of the rabbit. *Archives of Oral Biology*, 36(12): 933-938.
- Denton, J. 2008. Slices of mummy: a histologist’s perspective. In: David, R. (Ed.). *Egyptian mummies and modern science*. Cambridge, Cambridge University Press: 71-82.
- DeWhite, S. 2010. Sex differentials in frailty in Medieval England. *American Journal of Physical Anthropology*, 143(2): 285-297.

- Dirks, W.; Reid, D.; Jolly, C.; Phillips-Conroy, J.; Brett, F. 2002. Out of the mouths of baboons: stress, life history, and dental development in the Awash National Park hybrid zone, Ethiopia. *American Journal of Physical Anthropology*, 118(3): 239-252.
- Dittmann, K. 2003. Histomorphometric analysis of primate and domesticated animal long bone microstructure. In: Grupe, G.; Peters, J. (Eds.). *Decyphering ancient bones: the research potential of bioarchaeological collections*. Leidorf, Verlag Marie Leidorf: 215-225.
- Dittmann, K.; Grupe, G.; Manhart, H.; Peters, J.; Strott, N. 2006. Histomorphometry of mammalian and avian compact bone. In: Grupe, G.; Peters, J. (Eds.). *Microscopic examinations of bioarchaeological remains: keeping a close eye on ancient tissues*. Leidorf, Verlag Marie Leidorf: 48-101.
- Djurić, M.; Milovanović, P.; Janović, A.; Drasković, M.; Djukić, K.; Milenković, P. 2008. Porotic lesions in immature skeletons from Stara Torina, late medieval Serbia. *International Journal of Osteoarchaeology*, 18(5): 458-475.
- Djurić, M.; Janović, A.; Milovanović, P.; Djukić, K.; Milenković, P.; Drasković, M.; Roksandic, M. 2010. Adolescent health in medieval Serbia: signs of infectious diseases and risk of trauma. *Homo – Journal of Comparative Human Biology*, 61(2): 130-149.
- Djurić-Srejić, M.; Roberts, C. 2001. Palaeopathological evidence of infectious disease in skeletal populations from later medieval Serbia. *International Journal of Osteoarchaeology*, 11(5): 311-320.
- Dobson, J. 1952. Pioneers of osteogeny: Clopton Havers. *The Journal of Bone and Joint Surgery*, 34 B(4): 702-707.
- Dore, B.; Pavan, F.; Masali, M. 2001. Histological techniques and microscopic analysis of biological agents for preservation of human bone remains. *Biotechnic & Histochemistry*, 76(2): 89-95.
- Drapeau, M.; Streeter, M. 2006. Modelling and remodelling responses to normal loading in the human lower limb. *American Journal of Physical Anthropology*, 129(3): 403-409.
- Druitt, R. 1860. *The principles and practice of modern surgery*. Philadelphia, Blanchard and Lea.
- Drusini, A. 1996. Sampling location in cortical bone histology. *American Journal of Physical Anthropology*, 100(4): 609-610.
- Duhing, C.; Strouhal, E.; Němečková, A. 1996. Case of a secondary carcinoma of Anglo-Saxon period from Edix Hill, Barrington, Cambridgeshire, England. *Journal of Paleopathology*, 8(1): 25-31.

- Dupras, T.; Schultz, J.; Wheeler, S. 2006. Forensic recovery of human remains: archaeological approaches. Boca Raton, CRC Press.
- Dutour, O. 2008. Archaeology of human pathogens: palaeopathological appraisal of palaeoepidemiology. In: Raoult, D.; Drancourt, M. (Eds.). Paleomicrobiology: past human infections. Berlin Heidelberg, Springer-Verlag: 125-144.
- Dwek, J. 2010. The periosteum: what is it, and what mimics it in its absence? *Skeletal Radiology*, 39(4): 319-3323.

---

**E**

- Eagle, M. 2007. Understanding cellulitis of the lower limb. *Wound Essentials*, 2: 34-44.
- Edeiken, J.; Hodes, P.; Caplan, L. 1966. New bone production and periosteal reaction. *American Journal of Roentgenology*, 97(3): 708-718.
- Ekingen, G.; Guvenc, B.; Kahraman, H. 2006. Multifocal tuberculosis of the chest wall without pulmonary involvement. *Acta Chirurgica Belgica*, 106(1): 124-126.
- Ellender, G.; Feik, S.; Carach, B. 1988. Periosteal structure and development in a rat caudal vertebra. *Journal of Anatomy*, 158: 173-187.
- El-Zaatari, S.; Grine, F.; Teaford, M.; Smith, H. 2005. Molar microwear and dietary reconstructions of fossil *Cercopithecoidea* from the Plio-Pleistocene deposits of South Africa. *Journal of Human Evolution*, 49(2): 180-205.
- Emmanuel, J. 1988. A rapid method for producing stained sections of plastic embedded undecalcified bone sections. *Stain Technology*, 63(5): 329-331.
- Erben, R. 2003. Bone-labeling techniques. In: An, Y.; Martin, K. (Eds.). *Handbook of histological methods for bone and cartilage*. New Jersey, Humana Press: 99-117.
- Ericksen, M. 1991. Histologic estimation of age at death using the anterior cortex of the femur. *American Journal of Physical Anthropology*, 84(2): 171-179.
- Ericksen, M. 1997. Comparison of two methods of estimating age at death in a Chilean Preceramic population. *International Journal of Osteoarchaeology*, 7(1): 65-70.
- Ericksen, M.; Stix, A. 1991. Histologic examination of age of the first African Baptist church adults. *American Journal of Physical Anthropology*, 85(3): 247-252.
- Eshed, V.; Latimer, B.; Greenwald, C.; Jellema, L.; Rothschild, B.; Wish-Baratz, S.; Hershkovitz, I. 2002. Button osteoma: its etiology and pathophysiology. *American Journal of Physical Anthropology*, 118(3): 217-230.

- Estebaranz, F.; Martinez, L.; Galbany, J.; Turbon, D.; Perez-Perez, A. 2009. Testing hypotheses of dietary reconstruction from buccal dental microwear in *Australopithecus afarensis*. *Journal of Human Evolution*, 57(6): 739-750.
- Everts, V.; Delaisse, J.; Korper, W.; Jansen, D.; Tigchelaar-Gutter, W.; Saftig, P.; Beertsen, W. 2002. The bone lining cell: its role in cleaning Howship's lacunae and initiating bone formation. *Journal of Bone and Mineral Research*, 17(1): 77-90.
- Eyler, W.; Monsein, L.; Beute, G.; Tilley, B.; Schultz, L.; Schmitt, W. 1996. Rib enlargement in patients with chronic pleural disease. *American Journal of Roentgenology*, 167(4): 921-926.

**F**

- 
- Fabbri, P.; Lonoce, N.; Masieri, M.; Caramella, D.; Valentino, M.; Vassallo, S. 2012. Partial cranial trephination by means of Hippocrates trypanon from 5th century BC Himera (Sicily, Italy). *International Journal of Osteoarchaeology*, 22(2): 194-200.
- Faerman, M.; Nebel, A.; Filon, D.; Thomas, M.; Bradman, N.; Ragsdale, B.; Schultz, M.; Oppenheim, A. 2000. From a dry bone to a genetic portrait: a case study of sickle cell anemia. *American Journal of Physical Anthropology*, 111(2): 153-163.
- Fairgrieve, S. 2008. *Forensic cremation: recovery and analysis*. Boca Raton, CRC Press.
- Fan, W.; Crawford, R.; Xiao, Y. 2008. Structural and cellular differences between metaphyseal and diaphyseal periosteum in different aged rats. *Bone*, 42(1): 81-89.
- Fang, J.; Hall, B. 1997. Chondrogenic cell differentiation from membrane bone periosteum. *Anatomy and Embryology*, 196(5): 349-362.
- Faure, E.; Souilamas, R.; Riquet, M.; Chehab, A.; Pimpec-Barthes, F.; Manac'h, D.; Debesse, B. 1998. Cold abscess of the chest wall: a surgical entity? *The Annals of Thoracic Surgery*, 66(4): 1174-1178.
- Ferguson, C.; Alpern, E.; Miclau, T.; Helms, J. 1999. Does adult fracture repair recapitulate embryonic skeletal formation? *Mechanisms of Development*, 87(1-2): 57-66.
- Filvaroff, E.; Erlebacher, A.; Ye, J.-Q.; Gitelman, S.; Lotz, J.; Heilman, M.; Derynck, R. 1999. Inhibition of TGF  $\beta$  receptor signaling in osteoblasts leads to decreased bone remodelling and increased trabecular bone mass. *Development*, 126(19): 4267-4279.

- FitzGerald, C.; Saunders, S. 2005. Test of histological methods of determining chronology of accentuated striae in deciduous teeth. *American Journal of Physical Anthropology*, 127(3): 277-290.
- FitzGerald, C.; Saunders, S. 2007. Preparing undecalcified ground tooth sections. Anthropology hard tissue and light microscopy laboratory. Hamilton, Ontario, McMaster University.
- FitzGerald, C.; Saunders, S.; Bondioli, L.; Macchiarelli, R. 2006. Health of infants in an imperial roman skeletal sample: perspective from dental microstructure. *American Journal of Physical Anthropology*, 130(2): 179-189.
- Flohr, S.; Schultz, M. 2009a. Osseous changes due to mastoiditis in human skeletal remains. *International Journal of Osteoarchaeology*, 19(1): 99-106.
- Flohr, S.; Schultz, M. 2009b. Mastoiditis— paleopathological evidence of a rarely reported disease. *American Journal of Physical Anthropology*, 138(3): 266-273.
- Flohr, S.; Witzel, C. 2011. Hyperostosis *frontalis* interna – a marker of social status? Evidence from the Bronze-Age “high society” of Qatna, Syria. *HOMO - Journal of Comparative Human Biology* 62(1): 30-43.
- Flohr, S.; Kierdorf, U.; Schultz, M. 2009. Differential diagnosis of mastoid hypocellularity in human skeletal remains. *American Journal of Physical Anthropology*, 140(3): 442-453.
- Franklin, R.; Martin, M.-T. 1980. Staining and histochemistry of undecalcified bone embedded in a water-miscible plastic. *Biotechnic & Histochemistry*, 55(5): 313-321.
- Franz-Odendaal, T.; Hall, B.; Witten, P. 2006. Buried alive: how osteoblasts become osteocytes. *Developmental Dynamics*, 235(1): 176-190.
- Foldes, A.; Moscovici, A.; Popovtzer, M.; Mogle, P.; Urman, D.; Zias, J. 1995. Extreme osteoporosis in a sixth century skeleton from the Negev desert. *International Journal of Osteoarchaeology*, 5(2): 157-162.
- Fox, C.; Frayer, D. 1997. Non-dietary marks in the anterior dentition of the Krapina Neanderthals. *International Journal of Osteoarchaeology*, 7(2): 133-149.
- Fox, S. 1999. *Human physiology*. Boston, WCB/McGraw-Hill.
- Frassico, F.; Inoue, N.; Virolainen, P.; Chao, E. 1997. Skeletal system: biomechanical concepts and relationships to normal and abnormal conditions. *Seminars in Nuclear Medicine*, 27(4): 321-327.
- Frost, H. 1958. Preparation of thin undecalcified bone sections by rapid manual method. *Biotechnic & Histochemistry*, 33(6): 273-277.

- Frost, H. 1968. Tetracycline bone labeling in anatomy. *American Journal of Physical Anthropology*, 29(2): 183-195.
- Frost, H. 1987. Secondary osteon populations: an algorithm for determining mean bone tissue age. *American Journal of Physical Anthropology*, 30(S8): 221-238.

**G**

- Gaeta, M.; Minutoli, F.; Vinci, S.; Salamone, I.; D'Andrea, L.; Bitto, L.; Magaudda, L.; Blandino, A. 2006. High-resolution CT grading of tibial stress reactions in distance runners. *American Journal of Roentgenology*, 187(3): 789-793.
- Gall, E. A.; Bennett, G. A.; Bauer, W. 1951. Generalized hypertrophic osteoarthropathy: a pathologic study of seven cases. *The American Journal of Pathology*, 27(3): 349-381.
- Gallay, S.; Miura, Y.; Commisso, C.; Fitzsimmons, J.; O'Driscoll, S. 1994. Relationship of donor site to chondrogenic potential of periosteum in vitro. *Journal of Orthopaedic Research*, 12(4): 515-525.
- Gallie, W.; Robertson, D. 1914. The periosteum. *Canadian Medical Association Journal*, 4(1): 33-36.
- Galloway Group. 2004. Atomic force microscopy: a guide to understand and using the AFM. <http://www.txstate.edu/>.
- Garland, A. 1987. A histological study of archaeological bone decomposition. In: Boddington, A.; Garland, A.; Janaway, R. (Eds.). *Death, decay and reconstruction: approaches to archaeology and forensic science*. Manchester, Manchester University Press: 109-126.
- Garland, A. 1993. An introduction to the histology of exhumed mineralized tissue. In: Grupe, G.; Garland, A. (Eds.). *Histology of ancient human bone: methods and diagnosis*. Berlin, Springer-Verlag: 1-16.
- Geist, E. 1928. Does periosteum form bone? *The Journal of Bone and Joint Surgery*, 10(4): 716-717.
- George, J.; Kuboki, Y.; Miyata, T. 2006. Differentiation of mesenchymal stem cells into osteoblasts on honeycomb collagen scaffolds. *Biotechnology and Bioengineering*, 95(3): 404-411.
- Gerstenfeld, L. C.; Alkhiary, Y. M.; Krall, E. A.; Nicholls, F. H.; Stapleton, S. N.; Fitch, J. L.; Bauer, M.; Kayal, R.; Graves, D. T.; Jepsen, K. J.; Einhorn, T. A. 2006. Three-dimensional

- reconstruction of fracture callus morphogenesis. *Journal of Histochemistry & Cytochemistry*, 54(11):1215-28.
- Gilliland, B. 2006. Fibromyalgia, arthritis associated with systemic diseases, and other arthritides. In: Fauci, A.; Langford, C. (Eds.). *Harrison's rheumatology*. New York; McGraw-Hill: 281–298.
- Gilroy, D.; Lawrence, T. 2008. The resolution of acute inflammation: a “tipping point” in the development of chronic inflammatory diseases. In: Rossi, A.; Sawatzky, D. (Eds.). *The Resolution of Inflammation*. Birkhäuser, Verlag Basel: 1-18.
- Gladkowska-Rzeczycka, J. 1998. Periostitis: cause, form and frequency in paleopathology. *Mankind Q*, 38(3): 217–236.
- Glass, R.; Norton, K.; Mitre, S.; Kang, E. 2002. Pediatric ribs: a spectrum of abnormalities. *Radiographics*, 22(1): 87–104.
- Goldman, H.; Kindsvater, J.; Bromage, T. 1999. Correlative light and backscattered electron microscopy of bone – Part I: specimen preparation methods. *Scanning*, 21(1): 40-43.
- Goodman, A. 1993. On the interpretation of health from skeletal remains. *Current Anthropology*, 34(3): 281-288.
- Goodman, A.; Rose, R. 1990. Assessment of systemic physiological perturbations from dental enamel hypoplasias and associated histological structures. *American Journal of Physical Anthropology*, 33(S11): 59-110.
- Gordon, K. 1982. A study of microwear on chimpanzee molars: implications for dental micro-wear analysis. *American Journal of Physical Anthropology*, 59(2): 195-215.
- Gordon, S.; Mwandumba, H. 2008. Respiratory tuberculosis. In: Davies, P.; Barnes, P.; Gordon, S. (Eds.). *Clinical Tuberculosis*. London, Hodder and Arnold: 145-162.
- Gorincour, G.; Dubus, J.-C.; Petiti, P.; Bourliere-Najean, B.; Devred, P. 2004. Rib periosteal reaction: did you think about chest physical therapy? *Archives of Disease in Childhood*, 89(11): 1078-1079.
- Gosman, J.; Ketcham, R. 2009. Patterns in ontogeny of human trabecular bone from Sun Watch Village in the Prehistoric Ohio Valley: general features of microarchitectural change. *American Journal of Physical Anthropology*, 138(3): 318-332.
- Gosman, J.; Stout, S. 2010. Current concepts in bone biology. In: Larsen, C. (Ed.). *A companion to biological anthropology*. Malden, Blackwell Publishing, Ltd.: 465-484.
- Graf, W. 1949. Preserved histological structures in Egyptian mummy tissues and ancient Swedish skeletons. *Acta Anatomica*, 8(3):236-250.

- Grauer, A. 2008. Macroscopic analysis and data collection in paleopathology. In: Pinhasi, R.; Mays, S. (Eds.). *Advances in human paleopathology*. Chichester, John Wiley & Sons, Ltd.: 57-76.
- Greenfield, G.; Warren, D.; Clark, R. 1991. MR imaging of periosteal and cortical changes of bone. *Radiographics*, 11(4): 611-623.
- Greenlee, D.; Dunnell, R. 2009. Identification of fragmentary bone from the Pacific. *Journal of Archaeological Science*, 37(5): 957-970.
- Gregory, C.; Prockop, J.; Spees, J. 2005. Non-hematopoietic bone marrow stem cells: molecular control of expansion and differentiation. *Experimental Cell Research*, 306(2): 330-335.
- Grévin, G.; Baud, C.-A.; Susini, A. 1990. Etude anthropologique et paléopathologique d'un adulte inhumé puis incinéré provenant du site de Pincevent (Seine-et-Marne). *Bulletins et Mémoires de la Société d'Anthropologie de Paris*, 2(3-4): 77- 87.
- Gross, T.; Bain, S. 1993. Skeletal adaptation to functional stimuli. In: Grabiner, M. (Ed.). *Current issues in biomechanics*. Champaign III, Human Kinetics Publisher: 151-169.
- Grover, S.; Jain, M.; Dumeer, S.; Sirari, N.; Bansal, M.; Badqujar, D. 2011. Chest wall tuberculosis – a clinical and imaging experience. *Indian Journal of Radiology and Imaging*, 21(1): 28-33.
- Grupe, G. 1988. Metastasizing carcinoma in a medieval skeleton: differential diagnosis and etiology. *American Journal of Physical Anthropology*, 75(3): 369-374.
- Grupe, G.; Dreses-Werringloer, U. 1993. Decomposition phenomena in thin sections of excavated human bones. In: Grupe, G.; Garland, A. (Eds.). *Histology of ancient human bone: methods and diagnosis*. Berlin, Springer-Verlag: 27-36.
- Grupe, G.; Garland, A. 1993. *Histology of ancient human bone: methods and diagnosis*. Berlin, Springer-Verlag.
- Guarino, F.; Angelini, F.; Vollono, C.; Orefice, C. 2006. Bone preservation in human remains from the Terme del Sarno at Pompeii using light microscopy and scanning electron microscopy. *Journal of Archaeological Science*, 33(4): 513-530.
- Gupta, P.; Gupta, K.; Gupta, R.; Agarwal, D. 2003. Progressive rib destruction: an unusual feature in a patient who had irregular anti-tuberculosis treatment. *Indian Journal of Tuberculosis*, 50: 109-112.
- Gupta, H.; Seto, J.; Wagermaier, W.; Zaslansky, P.; Boesecke, P.; Fratzl, P. 2006. Cooperative deformation of mineral and collagen in bone at the nanoscale. *Proceedings from the National Academy of Sciences of the USA*, 103(47): 17741-17746.



## H

- Haas, C.; Zink, A.; Mólnar, E.; Szeimies, U.; Reischl, U.; Marcsik, A.; Ardagna, Y.; Dutour, O.; Pálfi, G.; Nerlich, A. 2000. Molecular evidence for different stages of tuberculosis in ancient bone samples from Hungary. *American Journal of Physical Anthropology*, 113(3): 298-304.
- Hajdu, S. 2002. A note from history: the first use of the microscope. *Annals of Clinical & Laboratory Science*, 32(3): 309-310.
- Hall, B. 2005. *Bones and cartilage: developmental and evolutionary skeletal biology*. San Diego, Elsevier Academic Press.
- Han, S.-H.; Kim, S.-H.; Ahn, Y.-W.; Huh, G.-Y.; Kwak, D.-S.; Park, D.-K.; Lee, U.-Y.; Kim, Y.-S. 2009. Microscopic age estimation from the anterior cortex of the femur in Korean adults. *Journal of Forensic Sciences*, 54(3): 519-522.
- Hanak, V.; Hartman, T.; Ryu, J. 2005. Cough-induced rib fractures. *Mayo Clinic Proceedings*, 80(7): 879-882.
- Hanson, D.; Buikstra, J. 1987. Histomorphological alteration in buried human bone from the lower Illinois Valley: implications for palaeodietary research. *Journal of Archaeological Science*, 14(5): 549-563.
- Hanson, M.; Cain, C. 2007. Examining histology to identify burned bone. *Journal of Archaeological Science*, 34(11): 1902-1913.
- Hardy, R.; Cooper, M. 2009. Bone loss in inflammatory disorders. *Journal of Endocrinology*, 201(3): 309-320.
- Harifi, G.; Younsi, R.; Ouilki, I.; Belkhou, A.; El Hassani, S. 2008. Ostéoarthropathie hypertrophiante primitive chez un adolescent. *La Revue de Médecine Interne*, 29(4): 335-336.
- Harisinghani, M.; McCloud, T.; Shepard, J.-A.; Ko, J.; Shroff, M.; Mulelller, P. 2000. Tuberculosis from head to toe. *Radiographics*, 20(2): 449-470.
- Harrington, L. 2010. Ontogeny of postcranial robusticity among Holocene hunter-gatherers of southernmost Africa. Degree of Doctor in Philosophy. Toronto, University of Toronto [Unpublished].

- Harsányi, L. 1993. Differential diagnosis of human and animal bone. In: Grupe, G.; Garland, A. (Eds.). In: *Histology of ancient human bone: methods and diagnosis*. Berlin, Springer-Verlag: 79-94.
- Haun, D.; Kettner, N.; Bates, D. 2006. Stress-induced spiculated periosteal reaction appearing as a malignant bone tumor: a case report. *Journal of Manipulative and Physiological Therapeutics*, 29(7): 595.e591–595.e595.
- Haverkort, C.; Lubell, D. 1999. Cutmarks on Caspian human remains: implications for Maghreb Holocene social organization and palaeoeconomy. *International Journal of Osteoarchaeology*, 9(3): 147-169.
- Havill, L. 2003. Osteon remodelling dynamics in the Cayo Santiago *Macaca mulatta*: the effect of matriline. *American Journal of Physical Anthropology*, 121(4): 354-360.
- Havill, L. 2004. Osteon remodelling dynamics in *Macaca mulatta*: normal variation with regard to age, sex, and skeletal maturity. *Calcified Tissue International*, 74(1): 95-102.
- Haynes, S.; Searle, J.; Bretman, A.; Dobney, K. 2002. Bone preservation and ancient DNA: the application of screening methods for predicting DNA survival. *Journal of Archaeological Science*, 29(6): 585-592.
- Hays, J. 2009. *The burdens of disease: epidemics and human response in Western history*. New Brunswick, Rutgers University Press.
- Hedges, R.; Millard, A.; Pike, A. 1995. Measurements and relationships of diagenetic alteration of bone from three archaeological sites. *Journal of Archaeological Science*, 22(2): 201-209.
- Henning, C.; Cooper, D. 2011. Brief communication: the relation between standard error of the estimate and sample size of histomorphometric aging methods. *American Journal of Physical Anthropology*, 145(4): 658-664.
- Hermann, P. 1986. Two examples of biogenous dead bone decomposition and their consequences for taphonomic interpretation. *Journal of Archaeological Science*, 13(5): 417-430.
- Herrmann, B. 1977. On histological investigations of cremated human remains. *Journal of Human Evolution*, 6(2): 101-103.
- Herrmann, B. 1993. Light microscopy of excavated human bone. In: Grupe, G.; Garland, A. (Eds.). In: *Histology of ancient human bone: methods and diagnosis*. Berlin, Springer-Verlag: 17-26.

- Hershkovitz, I.; Greenwald, C.; Rothschild, B.; Latimer, B.; Dutour, O.; Jellema, L.; Wish-Baratz, S. 1999. Hyperostosis *frontalis* interna: an anthropological perspective. *American Journal of Physical Anthropology*, 109(3): 303-325.
- Hershkovitz, I.; Greenwald, C.; Latimer, B.; Jellema, L.; Wish-Baratz, S.; Eshed, V.; Dutour, O.; Rothschild, B. 2002. Serpens endocrania symmetrica (SES): a new term and a possible clue for identifying intrathoracic disease in skeletal populations. *American Journal of Physical Anthropology*, 118(3): 201-216.
- Hess, M.; Klima, G.; Pfaller, K.; Künzel, K.; Gaber, O. 1998. Histological investigations on the Tyrolean Ice Man. *American Journal of Physical Anthropology*, 106(4): 521-532.
- Heuck, F. 1993. Comparative histological and microradiographic investigations of human bone. In: Grupe, G.; Garland, A. (Eds.). *Histology of ancient human bone: methods and diagnosis*. Berlin, Springer-Verlag: 125-136.
- Hildebolt, C.; Bate, G.; McKee, J.; Conroy, G. 1986. The microstructure of dentine in taxonomic and phylogenetic studies. *American Journal of Physical Anthropology*, 70(1): 39-46.
- Hill, G.; Tabrisky, J.; Peter, M. 1976. Tuberculous enteritis. *Western Journal Medical*, 124(6): 440-445.
- Hill, P.; Tumber, A.; Papaioannou, S.; Meikle, M. 1998. The cellular actions of interleukin-II on bone resorption in vitro. *Endocrinology*, 139(4): 1564-1572.
- Hillier, M.; Bell, S. 2007. Differentiating human bone from animal bone: a review of histological methods. *Journal of Forensic Sciences*, 52(2): 249-263.
- Hillson, S.; Antoine, D. 2003. Ancient bones and teeth on the microstructural level. In: Grupe, G.; Peters, J. (Eds.). *Decyphering ancient bones: the research potential of bioarchaeological collections*. Leidorf, Verlag Marie Leidorf: 141-157.
- Hillson, S.; Bond, S. 1997. Relationship of enamel hypoplasia to the pattern of tooth crown growth: a discussion. *American Journal of Physical Anthropology*, 104(1): 89-103.
- Hirsch, C.; Yoneda, T.; Averill, L.; Ellner, J.; Toossi, Z. 1994. Enhancement of intracellular growth of *Mycobacterium tuberculosis* in human monocytes by transforming growth factor-beta 1. *The Journal of Infectious Disease*, 170(5): 1229-1237.
- Hirsch, C.; Hussain, R.; Toossi, Z.; Dawood, G.; Shahid, F.; Ellner, J. 1996. Cross-modulation by transforming growth factor  $\beta$  in human tuberculosis: suppression of antigen-driven blastogenesis and interferon  $\gamma$  production. *Proceedings National Academy of Sciences*, 93(8): 3193-3198.

- Hogg, J. 1854. *The microscope: its history, construction and applications*. London, The Illustrated London Library.
- Hogue, S.; Melsheimer, R. 2008. Integrating dental microwear and isotopic analyses to understand dietary change in East-central Mississippi. *Journal of Archaeological Science*, 35(2): 228-238.
- Holck, P. 2008. Two medieval 'trepanations' – therapy or swindle? *International Journal of Osteoarchaeology*, 18(2): 188-194.
- Hollund, H.; Jans, M.; Collins, M.; Kars, H.; Joosten, I.; Kars, S. 2012. What happened here? Bone histology as a tool in decoding the postmortem histories of archaeological bone from Castricum, The Netherlands. *International Journal of Osteoarchaeology*, 22(5): 537-548.
- Holden, J.; Phakey, P.; Clement, J. 1995. Scanning electron microscope observations of incinerated human femoral bone: a case study. *Forensic Science International*, 74(1): 17-28.
- Horner, A.; Kemp, P.; Summers, C.; Bord, S.; Bishop, N.; Kelsall, A.; Coleman, N.; Compston, J. 1998. Expression and distribution of transforming growth factor- $\beta$  isoforms and their signaling receptors in growth human bone. *Bone*, 23(2): 95-102.
- Horni, H. 2002. *The forensic application of comparative mammalian bone histology*. Master of Arts Thesis. Texas, Texas Technical University [Unpublished].
- Hoyte, D. 1968. Alizarin red in the study of the apposition and resorption of bone. *American Journal of Physical Anthropology*, 29(2): 157-177.
- Hsieh, C.; Miltner, L.; Chnag, C. 1934. Tuberculosis of the shaft of the large long bones of the extremities. *The Journal of Bone and Joint Surgery*, 16(3): 545-563.
- Hummel, S.; Schutkowski, H. 1993. Approaches to the histological age determination of cremated human remains. In: Grupe, G.; Peters, J. (Eds.). *Decyphering ancient bones: the research potential of bioarchaeological collections*. Leidorf, Verlag Marie Leidorf: 111-123.
- Hunt, D.; Albanese, J. 2006. History and demographic composition of the Robert J. Terry Anatomical Collection. *American Journal of Physical Anthropology*, 127(4): 406-417.
- Hutchinson, D. 1996. Brief encounters: Tatham Mound and the evidence for Spanish and Native American confrontation. *International Journal of Osteoarchaeology*, 6(1): 51-65.

Hwang, S.; Schneider, R. 2010. Eponyms of tumors and tumorlike lesions in the musculoskeletal system: who were the people and what are the lesions? Pictorial Review. *American Journal of Roentgenology*, 195(6): s50-s61.

I

Ip, M.; Chen, N.-K.; So, S.-Y.; Chiu, S.-W.; Lam, W.K. 1989. Unusual rib destruction in pleuropulmonary tuberculosis. *Chest*, 95(1): 242-244.

Ito, Y.; Fitzsimmons, J.; Sanyal, A.; Mello, M. A.; Mukherjee, N.; O'Driscoll, S. 2001. Localization of chondrocyte precursors in periosteum. *Osteoarthritis and Cartilage*, 9(3): 215-223.

Iwamoto, J.; Takeda, T. 2003. Stress fractures in athletes. *Journal of Orthopaedic Science*, 8(3): 273-278.

Iwaniec, U.; Crenshaw, T.; Schoeninger, M.; Stout, S.; Ericksen, M. 1998. Methods for improving the efficiency of estimating total osteon density in the human anterior mid-diaphyseal femur. *American Journal of Physical Anthropology*, 107(1): 12-24.

Iyo, T.; Maki, Y.; Sasaki, N.; Nakata, M. 2004. Anisotropic viscoelastic properties of cortical bone. *Journal of Biomechanics*, 37(9): 1433-1437.

J

Jackes, M. 2011. Representativeness and bias in archaeological skeletal samples. In: Agarwal, S.; Glencross, B. (Eds.). *Social bioarchaeology*. Malden, Blackwell Publishing, Ltd.: 107-146.

Jackes, M.; Sherburne, R.; Lubell, D.; Barker, C.; Wayman, M. 2001. Destruction of microstructure in archaeological bone: a case study from Portugal. *International Journal of Osteoarchaeology*, 11(6): 415-432.

Jankauskas, R.; Barakauskas, S.; Bojarun, R. 2001. Incremental lines of dental cementum in biological age estimation. *HOMO - Journal of Comparative Human Biology*, 52(1): 59-71.

Jans, M. 2008. Microbial bioerosion of bone – a review. In: Wisshak, M.; Tapanila, L. (Eds.). *Current developments in bioerosion*. Erlangen Earth Conference Series. Berlin, Springer-Verlag: 397-413.

Jans, M.; Nielsen-Marsh, C.; Smith, C.; Collins, M.; Kars, H. 2004. Characterization of microbial attack on archaeological bone. *Journal of Archaeological Science*, 31(1): 87-95.

- Jee, W. 2001. Integrated bone tissue physiology: anatomy and physiology. In: Cowin, S. (Ed.). Bone mechanics handbook. Boca Raton, CRC Press: 1-53.
- Jilka, R. 2002. Osteoblast progenitor fate and age-related bone loss. *Journal of Musculoskeletal and Neuronal Interactions*, 2(6): 581-583.
- Johnson, M.; Rothstein, E. 1952. Tuberculosis of the ribs. *The Journal of Bone and Joint Surgery*, 34(4): 878-882.
- Jose, J.; Fichter, B.; Clifford, P. 2011. Tibial stress injuries in athletes. *The American Journal of Orthopedics*, 40(4): 202-203.
- Jowsey, J. 1955. The use of the milling machine for preparing bone sections for microradiography and microautoradiography. *Journal of Scientific Instruments*, 32(5): 159-163.
- Józsa, L.; Fóthi, E. 2003. Juxtacortical osteosarcoma on tibia and fibula from medieval cemetery of Budapest. *Journal of Palaeopathology*, 15(1): 23-31.
- Junqueira, L.; Carneiro, J. 2005. *Basic histology: text and atlas*. New York, MacGraw-Hill Medical Companies, Inc.

**K**

- 
- Kagerer, P.; Grupe, G. 2001. Age-at-death diagnosis and determination of life-history parameters by incremental lines in human dental cementum as an identification aid. *Forensic Science International*, 118(1): 75-82.
- Kara, M.; Dikmen, E.; Erdal, H.; Simsir, I.; Kara, S. 2003. Disclosure of unnoticed rib fractures with the use of ultrasonography in minor blunt chest trauma. *European Journal of Cardio-thoracic Surgery*, 24(4): 608-613.
- Karaplis, A. 2002. Embryonic development of bone and the molecular regulation of intramembranous and endochondral bone formation. In: Bilezikian, J.; Raisz, L.; Rodan, G. (Eds.). *Principles of bone biology*. San Diego, Academic Press: 33-58.
- Kassi, E.; Tsigos, C.; Kyrou, I.; Chrousos, G. 2012. Stress, endocrine physiology and pathophysiology. In: Chrousos, G. (Ed.). *Adrenal physiology and diseases*. Endotext-org - the endocrine source: <http://www.endotext.org/adrenal/index.htm>.
- Kato, L. 1973. The centenary of the discovery of the leprosy bacillus. *Canadian Medical Association Journal*, 109(6): 628-629.

- Katzenberg, A.; Lovell, N. 1999. Stable isotope variation in pathological bone. *International Journal of Osteoarchaeology*, 9(5): 316-324.
- Katzenberg, A.; Herring, A.; Saunders, S. 1996. Weaning and infant mortality: evaluating the skeletal evidence. *Yearbook of Physical Anthropology*, 101(S23): 177-199.
- Katzenberg, A.; Oetelaar, G.; Oetelaar, J.; Fitzgerald, C.; Yang, D.; Saunders, S. 2005. Identification of historical human skeletal remains: a case study using skeletal and dental age, history and DNA. *International Journal of Osteoarchaeology*, 15(1): 61-72.
- Keene, H. 1982. The morphogenetic triangle: a new conceptual tool for application to problems in dental morphogenesis. *American Journal of Physical Anthropology*, 59(3): 281-287.
- Kelley, M.; Micozzi, M. 1984. Rib lesions in chronic pulmonary tuberculosis. *American Journal of Physical Anthropology*, 65(4): 381-386.
- Kelly, P.; Manning, P.; Corcoran, P.; Clancy, L. 1991. Hypertrophic osteoarthropathy in association with pulmonary tuberculosis. *Chest*, 99(3): 769-770.
- Kemkes-Grottenthaler, A. 2002. Aging through the ages: historical perspectives on age indicator method. In: Hoppa, R.; Vaupel, J. (Eds.). *Paleodemography: age distributions from skeletal samples*. Cambridge, Cambridge University Press: 48-66.
- Kenan, S.; Abdelwahab, I.; Klein, M.; Hermann, G.; Lewis, M. 1993. Lesions of juxtacortical origin (surface lesions of bone). *Skeletal Radiology*, 22(5): 337-357.
- Keough, N. 2007. Estimation of age at death from the microscopic structure of femur. PhD Thesis from School of Medicine, Faculty of Health Sciences. Pretoria, University of Pretoria [Unpublished].
- Kerley, E. 1965. The microscopic determination of age in human bone. *American Journal of Physical Anthropology*, 23(2): 149-163.
- Kerley, E.; Ubelaker, D. 1978. Revisions in the microscopic method of estimating age at death in human cortical bone. *American Journal of Physical Anthropology*, 49(4): 545-546.
- Khalil, A.; Breton, C.; Tassart, M.; Korzec, J.; Bigot, J.-M.; Carette, M.-F. 1999. Utility of CT scan for the diagnosis of chest wall tuberculosis. *European Radiology*, 9(8): 1638-1642.
- Kigera, J.; Orwotho, N. 2011. Multifocal tuberculous spondylitis with rib involvement: a case report and review of the literature. *SA Orthopaedic Journal*, 10(2): 44-47.
- Kiliç, D.; Findikcioğlu, A.; Hatipoğlu, A. 2007. Spontaneous rib fracture caused by coughing: report of two cases. *Turkiye Klinikleri Journal Medical Science*, 27(3): 468-470.

- Kim, H.; Song, K.-S.; Goo, J.; Lee, J.; Lee, K.; Lim, T.-H. 2001. Thoracic sequelae and complications of tuberculosis. *Radiographics*, 21(4): 839-860.
- Kim, H.-J.; Zhao, H.; Kitaura, H.; Bhattacharyya, S.; Brewer, J.; Muglia, L.; Ross, F.; Teitelbaum, S. 2006. Glucocorticoids suppress bone formation via the osteoclast. *The Journal of Clinical Investigation*, 116(8): 2152-2160.
- Kim, M.; Oh, C.; Lee, I.; Lee, B.; Choi, J.; Lim, D.; Yi, Y.; Han, W.; Kim, Y.; Bok, G.; Lee, S. 2008. Human mummified brain from a medieval tomb with lime-soil mixture barrier of the Joseon Dynasty, Korea. *International Journal of Osteoarchaeology*, 18(6): 614-623.
- Kim, Y.-S.; Kim, D.I.; Park, D.-K.; Lee, J.-H.; Chung, N.-E.; Lee, W.-T.; Hans, S.-H. 2007. Assessment of histomorphological features of the sterna end of the fourth rib for age estimation in Koreans. *Journal of Forensic Science*, 52(6): 1237-1242.
- King, T.; Humphrey, L.; Hillson, S. 2005. Linear enamel hypoplasias as indicators of systemic physiological stress: evidence from two known age-at-death and sex populations from postmedieval London. *American Journal of Physical Anthropology*, 128(3): 547-559.
- Klein-Nulend, J.; Bakker, A. 2007. Osteocytes: mechanosensors of bone and orchestrators of mechanical adaptation. *Clinical Review of Bone Mineral Metabolism*, 5(4): 195-209.
- Klepinger, L. 2006. *Fundamentals of forensic anthropology*. New Jersey, John Wiley & Sons.
- Knudson, D. 2007. *Fundamentals of biomechanics*. New York, Springer Science.
- Komar, D.; Grivas, C. 2008. Manufactured populations: what do contemporary reference skeletal collections represent? A comparative study using the Maxwell Museum Documented Collection. *American Journal of Physical Anthropology*, 137(2): 224-233.
- Kuhn, G.; Schultz, M.; Müller, R.; Rühli, F. 2007. Diagnostic value of micro-CT in comparison with histology in the qualitative assessment of historical human postcranial bone pathologies. *HOMO - Journal of Comparative Human Biology*, 58(2): 97-115.
- Kuo, C.-C.; Uang, C.-C.; Hsu, C.-J.; Hsu, H.-C. 2004. Tuberculosis bursitis with rice bodies. *Mid-Taiwan Journal of Medicine*, 9: 124-129.
- Kusuzaki, K.; Kageyama, N.; Shinjo, H.; Takeshita, H.; Murata, H.; Hashiguchi, S.; Ashihara, T.; Hirasawa, Y. 2000. Development of bone canaliculi during bone repair. *Bone*, 27(5): 655-659.
- Kuzucu, A.; Soysal, Ö.; Günen, H. 2004. The role of surgery in chest wall tuberculosis. *Interactive Cardiovascular and Thoracic Surgery*, 3(1): 99-103.



Kwon, D.; Spevak, M.; Fletcher, K.; Kleinman, P. 2002. Physiologic subperiosteal new bone formation: prevalence, distribution, and thickness in neonates and infants. *American Journal of Roentgenology*, 179(4): 985-988.

L

---

Lagier, R.; Baud, C. 1980. Some comments on paleopathology suggested by a case of myositis ossificans circumscripta observed on a medieval skeleton. *Journal of Human Evolution*, 9(1): 9-13.

Lagier, R.; Baud, C.-A.; Kramar, C. 1983. Brodie's abscess in a tibia dating from the Neolithic period. *Virchows Archiv A*, 401: 153-157.

Lagier, R.; Baud, C.; Arnaud, G.; Arnaud, S.; Menk, R. 1982. Lesions characteristic of infection or malignant tumor in Pale-Eskimo skulls. *Virchows Archiv A*, 395: 237-243.

Lahey, M.; Klein, M.; Faye-Peterson, O. 2008. A comprehensive clinicopathologic analysis suggests that vascular endothelial growth factor (VEGF) is the most likely mediator of periosteal new bone formation (PNBF) associated with diverse etiologies. *Clinical medicine Arthritis and Musculoskeletal Disorders*, 1: 43-58.

Lalueza, C.; Pérez-Pérez, A.; Turbón, D. 1996. Dietary inferences through buccal microwear analysis of Middle and Upper Pleistocene human fossils. *American Journal of Physical Anthropology*, 100(3): 367-387.

Lambert, P. 2002. Rib lesions in a prehistoric puebloan sample from Southwestern Colorado. *American Journal of Physical Anthropology*, 117(4): 281-292.

Lamendin, H. 1974. Observation with SEM of rehydrated mummy teeth. *Journal of Human Evolution*, 3(4): 271-274.

Larsen, C. 1997. *Bioarchaeology: interpreting behavior from the human skeleton*. Cambridge, Cambridge University Press.

Larsen, C. 2002. Bioarchaeology: the lives and lifestyles of past people. *Journal of Archaeological Research*, 10(2): 119-165.

Larsen, C. 2006. The changing face of bioarchaeology: an interdisciplinary science. In: Buikstra, J.; Beck, L. (Eds.). *Bioarchaeology: the contextual analysis of human remains*. Burlington, Academic Press: 359-374.

- Larsen, C. 2010. Bioarchaeology: health, lifestyle, and society in recent human evolution. In: Larsen, C. (Ed.). *A companion to biological anthropology*. Malden, Blackwell Publishing, Ltd.: 379-394.
- Lazenby, R.; Pfeiffer, S. 1993. Effects of a nineteenth century below-knee amputation and prosthesis on femoral morphology. *International Journal of Osteoarchaeology*, 3(1): 19-28.
- Lee, S.; Chen, T.; Barber, C.; Jordan, M.; Murdock, J.; Desai, S.; Ferrara, N.; Nagy, A.; Roos, K.; Iruela-Arispe, M. 2007. Autocrine VEGF signaling is required for vascular homeostasis. *Cell*, 130(4): 691-703.
- Leeuwenhoek, F. 1720. Observations upon the bones and the periosteum, in a letter to the Royal Society. *Proceedings of the Royal Society of London. Philosophical Transactions of the Royal Society (1683-1775)*, 31: 91-97.
- Lehrer, H.; Maxfield, W.; Nice, C. 1970. The periosteal "sunburst" pattern in metastatic bone tumors. *American Journal of Roentgenology, Radium Therapy, and Nuclear Medicine*, 108(1): 154-161.
- Leonard, M.; Blumberg, H. 2006. Musculoskeletal tuberculosis. In: Schlossberg, D. (Ed.). *Tuberculosis and nontuberculous mycobacterial infections*. New York, McGraw-Hill: 242-263.
- Lewis, B. 1994. Treponematoses and Lyme borreliosis connections: explanation for Tchefuncte disease syndromes? *American Journal of Physical Anthropology*, 93(4): 455-475.
- Lewis, M.; Gowland, R. 2009. Infantile cortical hyperostosis: cases, causes and contradictions. In: Lewis, M.; Clegg, M. (Eds.). *Proceedings of the ninth annual conference of the British Association for Biological Anthropology and Osteoarchaeology (Department of Archaeology, University of Reading 2007)*. Oxford, Archaeopress, BAR international Series 1918: 43-51.
- Lichter, J. 2005. Bronchiectasis. In: Bardow, R.; Ries, A.; Morris, T. (Eds.). *Manual of clinical problems in pulmonary medicine*. Philadelphia, Lippincott Williams & Wilkins: 306-316.
- Lieberman, D. 1997. Making behavioral and phylogenetic inferences from hominid fossils: considering the developmental influence of mechanical forces. *Annual Review Anthropology*, 26: 185-210.
- Lind, M.; Overgaard, S.; Ongpipattanakul, B.; Nguyen, T.; Bünger, C.; Søballe, K. 1996. Transforming growth factor –  $\beta$ 1 stimulates bone ongrowth to weight-loaded tricalcium phosphate coated implants. *The Journal of Bone and Joint Surgery*, 78-B(3): 377-382.

- Lloyd, J. 1898. *Croton tiglium*. Chicago, The Western Druggist.
- LoBue, P.; Perry, S.; Catanzaro, A. 2000. Diagnosis of tuberculosis. In: Reichman, L.; Hershfield, E. (Eds.). *Tuberculosis: a comprehensive international approach*. New York, Marcel Dekker, Inc.: 341-375.
- Lovell, N. 2000. Paleopathological description and diagnosis. In: Katzenberg, A.; Saunders, S. (Eds.). *Biological anthropology of the human skeleton*. New York, Wiley-Liss: 217-248.
- Lozano, M.; Bermudez de Castro, J.; Carbonell, E.; Arsuaga, J. 2008. Non-masticatory uses of anterior teeth of Sima de los Huesos individuals (Sierra de Atapuerca, Spain). *Journal of Human Evolution*, 55(4): 713-728.
- Lynne, S. 1990. Palaeopathology and diagenesis: an SEM evaluation of structural changes using backscattered electron imaging. *Journal of Archaeological Science*, 17(1): 85-102.
- Lynnerup, N. 2007. Mummies. *Yearbook of Physical Anthropology*, 134(s45): 162-190.
- Lynnerup, N.; Frohlich, B.; Thomsen, J. 2006. Assessment of age at death by microscopy: unbiased quantification of secondary osteons in femoral cross sections. *Forensic Science International*, 159(s1): s100-s103.
- Luna, L.; Aranda, C.; Bosio, L.; Beron, M. 2008. A case of multiple metastases in Late Holocene hunter-gatherers from the Argentine Pampean region. *International Journal of Osteoarchaeology*, 18(5): 492-506.
- Luu, B. 2005. Viral pneumonia. In: Bardow, R.; Ries, A.; Morris, T. (Eds.). *Manual of clinical problems in pulmonary medicine*. Philadelphia, Lippincott Williams & Wilkins: 180-184.

**M**

- 
- Ma, P.; Teaford, M. 2010. Diet reconstruction in Antebellum Baltimore: insights from dental microwear analysis. *American Journal of Physical Anthropology*, 141(4): 571-582.
- Maas, M. 1993. Enamel microstructure and molar wear in the greater galago, *Otolemur crassicaudatus* (mammalia, primates). *American Journal of Physical Anthropology*, 92(2): 217-233.
- Maas, M. 1994. Enamel microstructure in *Lemuridae* (mammalia, primates): assessment of variability. *American Journal of Physical Anthropology*, 95(2): 221-241.

- Maat, G. 1991. Ultrastructure of normal and pathological fossilized red blood cells compared with pseudopathological biological structures. *International Journal of Osteoarchaeology*, 1(3-4): 209-214.
- Maat, G. 2004. Scurvy in adults and youngsters: the Dutch experience. A review of the history and pathology of a disregarded disease. *International Journal of Osteoarchaeology*, 14(2): 77-81.
- Maat, G.; Van Den Bos, R.; Aarents, M. 2001. Manual preparation of ground sections for the microscopy of natural bone tissue: update and modification of Frost's 'rapid manual method'. *International Journal of Osteoarchaeology*, 11(5): 366-374.
- Maat, G.; Gerretsen, R.; Aarents, M. 2006a. Improving the visibility of tooth cementum annulations by adjustment of the cutting angle of microscopic sections. *Forensic Science International*, 159(s1): s95-s99.
- Maat, G.; Maes, A.; Aarents, M.; Nagelkerke, N. 2006b. Histological age prediction from the femur in a contemporary Dutch sample. *Journal of Forensic Sciences*, 51(2): 230-237.
- Macadam, R.; Sandison, T. 1969. The electron microscope in paleopathology. *Medical History*, 13(1): 81-85.
- Macchiarelli, R.; Bondioli, L.; Caropreso, S.; Mazurier, A.; Merceron, G.; Piana, E. 2006. The oldest human remains from the Beagle Channel region, Tierra del Fuego. *International Journal of Osteoarchaeology*, 16(4): 328-337.
- Macho, G.; Abel, R.; Schutkowski, H. 2005. Age changes in bone microstructure: do they occur uniformly? *International Journal of Osteoarchaeology*, 15(6): 421-430.
- Maggiano, C. 2012. Making the mold: a microstructural perspective on bone modelling during growth and mechanical adaptation. In: Crowder, C.; Stout, S. (Eds.). *Bone histology: an anthropological perspective*. Boca Raton, CRC Press: 45-90.
- Maggiano, C.; Dupras, T.; Schultz, M.; Biggerstaff, J. 2009. Confocal laser scanning microscopy: a flexible tool for simultaneous polarization and three-dimensional fluorescence imaging of archaeological compact bone. *Journal of Archaeological Science*, 36(10): 2392-2401.
- Maggiano, I.; Maggiano, C.; Tiesler, V.; Kierdorf, H.; Stout, S.; Schultz, M. 2011. A distinct region of microarchitectural variation in femoral compact bone: histomorphology of the endosteal lamellar pocket. *International Journal of Osteoarchaeology*, 21(6): 743-750.
- Magner, L. 1992. *A History of Medicine*. New York, CRC Press.

- Mahoney, P. 2006. Dental microwear from Natufian hunter-gatherers and early Neolithic farmers: comparisons within and between samples. *American Journal of Physical Anthropology*, 130(3): 308-319.
- Mahoney, P. 2007. Human dental microwear from Ohalo II (22,500–23,500 cal BP), Southern Levant. *American Journal of Physical Anthropology*, 132(4): 489-500.
- Malgosa, A.; Aluja, M.; Isidro, A. 1996. Pathological evidence in newborn children from the Sixteenth Century in Huelva (Spain). *International Journal of Osteoarchaeology*, 6(4): 388-396.
- Malizos, K.; Papatheodorou, L. 2005. The healing potential of the periosteum: molecular aspects. *Injury* 36 (3, Supplement 1): S13-S19.
- Mann, A.; Monge, J.; Lampl, M. 1991. Investigation into the relationship between perikymata counts and crown formation times. *American Journal of Physical Anthropology*, 86(2): 175-188.
- Mann, R.; Hunt, D. 2005. *Regional atlas of bone disease: a guide to pathologic and normal variation in the human skeleton*. Springfield, Charles C. Thomas Publisher, LTD.
- Marinho, A.; Miranda, N.; Braz, V.; Ribeiro-dos-Santos, Â.; Mendonça de Souza, S. 2006. Paleogenetic and taphonomic analysis of human bonés from Moa, Beirada, and Zé Espinho Sambaquis, Rio de Janeiro, Brazil. *Memórias do Instituto Oswaldo Cruz, Rio de Janeiro*, 101 (II): 15-23.
- Marks, M.; Rose, J. 1985. Scanning electron-microscopy of Wilson bands and enamel hypoplasias. *American Journal of Physical Anthropology*, 66(2): 202-202.
- Marks, M.; Rose, J.; Davenport, W. 1996. Technical note: thin section procedure for enamel histology. *American Journal of Physical Anthropology*, 99(3): 493-498.
- Marks, S.; Odgren, P. 2002. Structure and development of the skeleton. In: Bilezikian, J.; Raisz, L.; Rodan, G. (Eds.). *Principles of bone biology*. San Diego, Academic Press: 3-15.
- Marotti, G. 2000. The osteocyte as a wiring transmission system. *Journal of Musculoskeletal and Neuronal Interactions*, 1(2): 133-136.
- Marsell, R.; Einhorn, T. 2011. The biology of fracture healing. *Injury*, 42(6): 551-555.
- Martin, D. 1991. Bone histology and paleopathology: methodological considerations. In: Ortner, D.; Aufderheide, A. (Eds.). *Human paleopathology: current syntheses and future options*. Washington, Smithsonian Institution: 55-59.
- Martin, D.; Armelagos, G. 1979. Morphometrics of compact bone: an example from Sudanese Nubia. *American Journal of Physical Anthropology*, 51(4): 571-577.

- Martin, D.; Armelagos, G. 1985. Skeletal remodelling and mineralization as indicators of health: an example from prehistoric Sudanese Nubia. *Journal of Human Evolution*, 14(5): 527-537.
- Martin, D.; Armelagos, G.; Mielke, J. 1981a. Perte de matière osseuse et problèmes d'alimentation dans une population adulte de Nubie soudanaise (en anglais). *Bulletins et Mémoires de la Société d'Anthropologie de Paris*, 8(3): 307-319.
- Martin, D.; Goodman, A.; Armelagos, G.; Pfeiffer, S. 1981b. On the use of microstructural bone for age determination. *Current Anthropology*, 22(4): 437-438.
- Martin, D.; Magennis, A.; Rose, J. 1987. Cortical bone maintenance in an historic Afro-American cemetery sample from Cedar Grove, Arkansas. *American Journal of Physical Anthropology*, 74(2): 255-264.
- Martin, H. 1996. L'analyse du ciment dentaire et la détermination de l'âge des adultes: méthodes et limites. *Bulletins et Mémoires de la Société d'Anthropologie de Paris*, 8(3-4): 433-440.
- Martin R. 2003. Fatigue microdamage as an essential element of bone mechanics and biology. *Calcified Tissue International*, 73(2): 101-107.
- Martin, R.; Correa, P. 2010. Bone quality and osteoporosis therapy. *Arquivos Brasileiros de Endocrinologia & Metabologia*, 54(2): 186-199.
- Martin, S.; Guatelli-Steinberg, D.; Walker, P. 2008. Brief communication: comparison of methods for estimating chronological age at linear enamel formation on anterior dentition. *American Journal of Physical Anthropology*, 135(3): 362-365.
- Martínez-Lavín, M. 2007. Less common arthropathies. F. Hypertrophic osteoarthropathy. In: Klippel, J.; Stone, J.; Crofford, L.; White, P. (Eds.). *Primer on the rheumatic diseases*. Atlanta, Arthritis Foundation: 504–508.
- Martínez-León, J. I.; Sánchez-Guzmán, A. R.; Bohórquez-Sierra, J. C.; Bohórquez-Sierra, C.; Rodríguez-Piñero, M.; Arribas-Aguilar, F. N. 1997. Subperiosteal new bone formation in association with vascular graft sepsis. *Journal of Vascular Surgery*, 26 (5): 895–896.
- Martínez-Maza, C.; Rosas, A.; García-Vargas, S. 2006. Bone paleohistology and human evolution. *Journal of Anthropological Sciences*, 84: 33-52.
- Martínez-Maza, C.; Rosas, A.; Nieto-Díaz, M. 2010. Brief communication: identification of bone formation and resorption surfaces by reflected light microscopy. *American Journal of Physical Anthropology*, 143(2): 313-320.

- Martiniaková, M.; Vondrakova, M.; Omelka, R. 2006. Manual preparation of thin sections from historical human skeletal material. *Timisoara Medical Journal*, 56(1): 15- 17.
- Martiniaková, M.; Grosskopf, B.; Omelka, R.; Dammers, K.; Vondráková, M.; Bauerová, M. 2007. Histological study of compact bone tissue in some mammals: a method for species determination. *International Journal of Osteoarchaeology*, 17(1): 82-90.
- Martrille, L.; Irinopoulou, T.; Bruneval, P.; Baccino, E.; Fornes, P. 2009. Age at death estimation in adults by computer-assisted histomorphometry of decalcified femur cortex. *Journal of Forensic Science*, 54(6): 1231-1237.
- Massa, E. 1981. Etude de la peau des Égyptiens predynastiques. *Bulletins et Mémoires de la Société d'Anthropologie de Paris*, 8(3): 291-296.
- Matos, V.; Santos, A. L. 2006. On the trail of pulmonary tuberculosis based on rib lesions: results from the Human Identified Skeletal Collection from the Museu Bocage (Lisbon, Portugal). *American Journal of Physical Anthropology*, 130(2): 190-200.
- Matos, V. 2009. Broken ribs: paleopathological analysis of costal fractures in the Human Identified Skeletal Collection from the Museu Bocage, Lisbon, Portugal (late 19<sup>th</sup> to middle 20<sup>th</sup> centuries). *American Journal of Physical Anthropology*, 140(1): 25-38.
- Matsuyama, W.; Hashiguchi, T.; Matsumuro, K.; Iwamin, F.; Hirotsu, Y.; Kawabata, M.; Arimura, K.; Osame, M. 2000. Increased serum level of vascular endothelial growth factor in pulmonary tuberculosis. *American Journal of Respiratory and Critical Care Medicine*, 162(3 Pt1): 1120-1122.
- Maurer, A.; Gerard, M.; Person, A.; Barrientos, I.; del Carmen Ruiz, P.; Darras, V.; Durllet, C.; Zeitoun, V.; Renard, M.; Faugère, B. 2011. Intra-skeletal variability in trace elemental content of Pre-Columbian Chupicuaro human bones: the record of postmortem alteration and a tool for palaeodietary reconstruction. *Journal of Archaeological Science*, 38(8): 1784-1797.
- Mayr, E. 1982. *The growth of biological thought: diversity, evolution and inheritance*. Harvard, Harvard University Press.
- Mayr, E. 2004. *What makes biology unique? Considerations on the autonomy of a scientific discipline*. Cambridge, Cambridge University Press.
- Mays, S. 1998. *The archaeology of human bones*. London, Routledge.
- Mays, S. 2008. A likely case of scurvy from early Bronze Age Britain. *International Journal of Osteoarchaeology*, 18(2): 178-187.

- Mays, S.; Nerlich, A. 1997. A possible case of Langerhan's cell histiocytosis in a medieval child from an English cemetery. *Journal of Paleopathology*, 9(2): 73-81.
- Mays, S.; Taylor, G. 2002. Osteological and biomolecular study of two possible cases of hypertrophic osteoarthropathy from mediaeval England. *Journal of Archaeological Science*, 29(11): 1267-1276.
- Mays, S.; Turner-Walker, G. 2008. A possible case of renal osteodystrophy in a skeleton from Medieval Wharram Percy, England. *International Journal of Osteoarchaeology*, 18(3): 307-316.
- Mays, S.; Fysh, E.; Taylor, G. 2002. Investigation of the link between visceral surface rib lesions and tuberculosis in a medieval skeletal series from England using ancient DNA. *American Journal of Physical Anthropology*, 119(1): 27-36.
- Mays, S.; Brickley, M.; Ives, R. 2007. Skeletal evidence for hyperparathyroidism in a 19th century child with rickets. *International Journal of Osteoarchaeology*, 17(1): 73-81.
- Mays, S.; Strouhal, E.; Vyhnánek, L.; Němečková, A. 1996. A case of metastatic carcinoma of medieval date from Wharram Percy, England. *Journal of Paleopathology*, 8(1): 33-42.
- Mazzarello, P. 1999. A unifying concept: the history of cell theory. *Nature Cell Biology*, 1: E13-E15.
- McCall, A. 1890. A clinical lecture on the curability of acute phthisis (galloping consumption). *The British Medical Journal*, 2(1558): 1051-1053.
- McGuinnis, P. 1999. *Biomechanics of sport and exercise*. New York, Human Kinetics.
- McKibbin, B. 1978. The biology of fracture healing in long bones. *Journal of Bone and Joint Surgery, British*, 60-B(2): 150-162.
- McWhinney, L.; Carpenter, K.; Rothschild, B. 2001. Dinosaurian humeral periostitis: a case of a juxtacortical lesion in the fossil record. In: Tanke, D.; Carpenter, K. (Eds.). *Mesozoic Vertebrate Life*. Bloomington, Indiana University Press: 364-377.
- Mekota, A.; Vermehren, M. 2005. Determination of optimal rehydration, fixation and staining methods for histological and immunohistochemical analysis of mummified soft tissues. *Biotechnic & Histochemistry*, 80(1): 7-13.
- Mekota, A.; Grupe, G.; Zimmerman, M.; Vermehren, M. 2005. First identification of an ancient Egyptian mummified human placenta. *International Journal of Osteoarchaeology*, 15(1): 51-60.
- Meindl, R.; Russell, K. 1998. Recent advances in method and theory in paleodemography. *Annual Review of Anthropology*, 27: 375-399.



- Mendonça de Souza, S.; Carvalho, D.; Lessa, A. 2003. Paleoepidemiology: is there a case to answer? *Memórias do Instituto Oswaldo Cruz*, Rio de Janeiro, 98(1): 21-27.
- Menéndez, J.; Teixeira, S. 2008. *Catálogo do espólio fúnebre e funerário do cemitério da Ordem do Carmo*. Porto, Editora Vessants.
- Merceron, G.; Scott, J.; Scott, R.; Geraads, D.; Spassov, N.; Ungar, P. 2009. Folivory or fruit/seed predation for *Mesopithecus*, an earliest colobine from the late Miocene of Eurasia? *Journal of Human Evolution*, 57(6): 732-738.
- Merrill, R. 2010. *Introduction to epidemiology*. Sudbury, Jones and Bartlett Publishers, LLC.
- Miles, A. E. 2001. Microscopic configurations on the bare-bone surfaces of mammalian synovial joints. *International Journal of Osteoarchaeology*, 11(6): 406-414.
- Milner, G.; Wood, J.; Boldsen, J. 2008. Advances in paleodemography. In: Katzenberg, A.; Saunders, S. (Eds.). *Biological anthropology of the human skeleton*. New Jersey, John Wiley & Sons, Inc.: 561- 600.
- Minozzi, S.; Manzi, G.; Ricci, F.; di Lernia, S.; Borgognini Tarli, S. 2003. Non-alimentary tooth use in prehistory: an example from early Holocene in Central Sahara (Uan Muhuggiag, Tadrart Acacus, Libya). *American Journal of Physical Anthropology*, 120(3): 225-232.
- Molnar, S.; Gantt, D. 1977. Functional implications of primate enamel thickness. *American Journal of Physical Anthropology*, 46(3): 447-454.
- Molnar, S.; Przybeck, T.; Gantt, D.; Elizondo, R.; Wilkerson, J. 1981. Dentin apposition rates as markers of primate growth. *American Journal of Physical Anthropology*, 55(4): 443-453.
- Molto, J. 1990. Differential diagnosis of rib lesions: a case study from middle woodland southern Ontario Circa 230 A.D. *American Journal of Physical Anthropology*, 83(4): 439-447.
- Monsalve, M.; Humphrey, E.; Walker, D.; Cheung, C.; Vogl, W.; Nimmo, M. 2008. Brief communication: state of preservation of tissues from ancient human remains found in a glacier in Canada. *American Journal of Physical Anthropology*, 137(3): 348-355.
- Moodie, R. 1918a. *Studies in paleopathology. I. General consideration of the evidences of pathological conditions found among fossil animals*. Harvard, Harvard University.
- Moodie, R. 1918b. Paleontological evidences of the antiquity of disease. *The Scientific Monthly*, 7(3): 265-281.
- Moodie, R. 1921. *Studies in the palaeopathology of Egypt*. Chicago, The University of Chicago Press.

- Morris, A.; Rodgers, A. 1989. A probable case of prehistoric kidney stone disease from the Northern Cape Province, South Africa. *American Journal of Physical Anthropology*, 79(4): 521-527.
- Mourato, T.; Costeira, J.; Pina, J. 2010. Tuberculose musculoesquelética – a propósito de um caso clínico. *Revista Portuguesa de Pneumologia*, XVI(1): 171-176.
- Mubarak, S.; Gould, R.; Yu Fon, L.; Schmidt, D.; Hargens, A. 1982. The medial tibial stress syndrome: a cause of shin splints. *The American Journal of Sports Medicine*, 10(4): 101-205.
- Mulhern, D. 2000. Rib remodelling dynamics in a skeletal population from Kulubnarti, Nubia. *American Journal of Physical Anthropology*, 111(4): 519-530.
- Mulhern, D.; Ubelaker, D. 2003. Histologic examination of bone development in juvenile chimpanzees. *American Journal of Physical Anthropology*, 122(2): 127-133.
- Mulhern, D.; Ubelaker, D. 2009. Bone microstructure in juvenile chimpanzees. *American Journal of Physical Anthropology*, 140(2): 368-375.
- Mulhern, D.; Ubelaker, D. 2012. Differentiating human from nonhuman bone microstructure. In: Crowder, C.; Stout, S. (Eds.). *Bone histology: an anthropological perspective*. Boca Raton, CRC Press: 109-134.
- Mulhern, D.; van Gerven, D. 1997. Patterns of femoral bone remodelling dynamics in a medieval Nubian population. *American Journal of Physical Anthropology*, 104(1): 133-146.
- Mundy, G. 1997. Mechanisms of bone metastasis. *Cancer*, 80(8):1546–1556.
- Mushtaq, T.; Asmed, S. 2002. The impact of corticosteroids on growth and bone health. *Archives of Disease in Childhood*, 87(2): 93-96.

**N**

- 
- Nawrocki, S. 1995. Taphonomic processes in historic cemeteries. In: Grauer, A. (Ed.). *Bodies of evidence: reconstructing history through skeletal analysis*. Chicago, Loyola University of Chicago: 49-66.
- Neill, C. 1983. Review of the histological method for determining age at death in human skeletons. *NEXUS - The Canadian Student Journal of Anthropology*, 3(1): 106-161.
- Nelson, M.; Dinardo, A.; Hochberg, J.; Armelagos, G. 2010. Brief communication: mass spectroscopic characterization of tetracycline in the skeletal remains of an ancient

- population from Sudanese Nubia 350–550 CE. *American Journal of Physical Anthropology*, 143(1): 151-154.
- Neufeld, G.; Cohen, T.; Gengrinovitch, S.; Poltorak, Z. 1999. Vascular endothelial growth factor (VEGF) and its receptors. *Faseb Journal*, 13(1): 9-22.
- Nicholson, R. 1998. Bone degradation in a compost heap. *Journal of Archaeological Science*, 25(5): 393-403.
- Nielsen, M.; Hansen, K.; Hølmer, P.; Dyrbye, M. 1991. Tibial periosteal reactions in soldiers: a scintigraphic study of 29 cases of lower leg pain. *Acta Orthopaedica Scandinavica*, 62(6): 531-534.
- Nielsen-Marsh, C.; Hedges, R. 2000. Patterns of diagenesis in bone I: the effects of site environments. *Journal of Archaeological Science*, 27(12): 1139-1150.
- Nijweide, P.; Burger, E.; Klein-Nulend, J. 2002. The osteocyte. In: Bilezikian, J.; Raisz, L.; Rodan, G. (Eds.). *Principles of bone biology*. San Diego, Academic Press: 93-107.
- Nöbauer, I.; Uffmann, M. 2005. Differential diagnosis of focal and diffuse neoplastic diseases of bone marrow in MRI. *European Journal of Radiology*, 55(1): 2–32.
- Nogueira-Barbosa, M.; Sá, J.; Trad, C.; Oliveira, R.; Elias Júnior, J.; Engel, E.; Simão, M.; Muglia, V. 2010. Ressonância magnética na avaliação das reações periosteais. *Radiologia Brasileira*, 43(4): 266-271.
- Novack, D.; Teitelbaum, S. 2008. The osteoclast: friend or foe? *Annual Review of Pathology: Mechanisms of Disease*, 3(1): 457-484.
- Ntaios, G.; Adamidou, A.; Karamitsos, D. 2008. Hypertrophic pulmonary osteoarthropathy secondary to bronchial adenocarcinoma and coexisting pulmonary tuberculosis: a case report. *Cases Journal*, 1: 221.
- Nystrom, P.; Phillips-Conroy, J.; Jolly, C. 2004. Dental microwear in anubis and hybrid baboons (*Papio hamadryas*, sensu lato) living in Awash National Park, Ethiopia. *American Journal of Physical Anthropology*, 125(3): 279-291.

---

**O**

- O'Connor, T.; O'Halloran, D.; Shanahan, F. 2000. The stress response and the hypothalamic-pituitary-adrenal axis: from molecule to melancholia. *Q.J.M.: International Journal of Medicine*, 93(6): 323-333.

- O'Donnell, P. 2003. Evaluation of focal bone lesions: basic principles and clinical scenarios. *Imaging*, 15(4): 298-323.
- O'Driscoll, S.; Saris, D.; Ito, Y.; Fitzimmons, J. 2001. The chondrogenic potential of periosteum decreases with age. *Journal of Orthopaedic Research*, 19(1): 95-103.
- Oh, C.; Seo, M.; Chai, J.; Lee, S.; Kim, M.; Park, J.; Shin, D. 2010. Amplification and sequencing of *Trichuris trichiura* ancient DNA extracted from archaeological sediments. *Journal of Archaeological Science*, 37(6): 1269-1273.
- Olobo, J.; Geletu, M.; Demissie, A.; Eguale, T.; Hiwot, K.; Aderaye, G.; Britton, S. 2001. Circulating TNF- $\alpha$ , TGF- $\beta$ , and IL-10 in tuberculosis patients and healthy contacts. *Scandinavian Journal of Immunology*, 53(1): 85-91.
- Ormerod, P. 2008. Non-respiratory tuberculosis. In: Davies, P.; Barnes, P.; Gordon, S. (Eds.). *Clinical Tuberculosis*. London, Hodder and Arnold: 163-188.
- Orschiedt, J.; Häußler, A.; Haidle, M.; Alt, K.; Buitrago-Téllez, C. 2003. Survival of a multiple skull trauma: the case of an early Neolithic individual from the LBK enclosure at Herxheim (Southwest Germany). *International Journal of Osteoarchaeology*, 13(6): 375-383.
- Ortner, D. 1991. Theoretical and methodological issues in paleopathology. In: Ortner, D.; Aufderheide, A. (Eds.). *Human paleopathology: current syntheses and future options*. Washington, Smithsonian Institution: 5-11.
- Ortner, D. 2003. Identification of pathological conditions in human skeletal remains. Amsterdam, Academic Press.
- Ortner, D. 2003a. Introduction. In: Ortner, D. (Ed.). *Identification of pathological conditions in human skeletal remains*. Amsterdam, Academic Press: 1-10.
- Ortner, D. 2003b. Methods used in the analysis of skeletal lesions. In: Ortner, D. (Ed.). *Identification of pathological conditions in human skeletal remains*. Amsterdam, Academic Press: 45-64.
- Ortner, D. 2003c. Background data in paleopathology. In: Ortner, D. (Ed.). *Identification of pathological conditions in human skeletal remains*. Amsterdam, Academic Press: 37-44.
- Ortner, D. 2003d. Infectious diseases: introduction, biology, osteomyelitis, periostitis, brucellosis, glanders, and septic arthritis. In: Ortner, D. (Ed.). *Identification of pathological conditions in human skeletal remains*. Amsterdam, Academic Press: 179-226.

- Ortner, D. 2003e. Infectious diseases: tuberculosis and leprosy. In: Ortner, D. (Ed.). Identification of pathological conditions in human skeletal remains. Amsterdam, Academic Press: 227-271.
- Ortner, D. 2003f. Tumors and tumor-like lesions of bone. In: Ortner, D. (Ed.). Identification of pathological conditions in human skeletal remains. Amsterdam, Academic Press: 503-544.
- Ortner, D. 2003g. Circulatory disturbances. In: Ortner, D. (Ed.). Identification of pathological conditions in human skeletal remains. Amsterdam, Academic Press: 343-357.
- Ortner, D. 2003h. Metabolic disorders. In: Ortner, D. (Ed.). Identification of pathological conditions in human skeletal remains. Amsterdam, Academic Press: 383-418.
- Ortner, D. 2008. Differential diagnosis of skeletal lesions in infectious disease. In: Pinhasi, R.; Mays, S. (Eds.). Advances in human paleopathology. Chichester, John Wiley & Sons, Ltd.: 191-214.
- Ortner, D. 2011a. What skeletons tell us. The story of human paleopathology. *Virchows Archiv*, 459(3): 247-254.
- Ortner, D. 2011b. Human skeletal paleopathology. *International Journal of Paleopathology*, 1(1): 4-11.
- Ortner, D.; Putschar, W. 1981. Identification of pathological conditions in human skeletal remains. *Smithsonian contributions to Anthropology*, 28. Washington, Smithsonian Institution Press.
- Ortner, D.; Turner-Walker, G. 2003. The biology of skeletal tissues. In: Ortner, D. (Ed.). Identification of pathological conditions in human skeletal remains. Amsterdam, Academic Press: 11-35.
- Ott, S. 2002. Histomorphometric analysis of bone remodelling. In: Bilezikian, J.; Raisz, L.; Rodan, G. (Eds.). Principles of bone biology. San Diego, Academic Press: 303-320.
- Oyen, O.; Rice, R.; Samuel, M. 1979. Browridge structure and function in extant primates and Neanderthals. *American Journal of Physical Anthropology*, 51(1): 83-95.

**P**

- 
- Pabst, M.; Letofsky-Papst, I.; Bock, E.; Moser, M.; Dorfer, L.; Egarter-Vigl, E.; Hofer, F. 2009. The tattoos of the Tyrolean Iceman: a light microscopical, ultrastructural and element analytical study. *Journal of Archaeological Science*, 36(10): 2335-2341.

- Pahl, W. 1983. Medical and archaeological findings concerning an unusual lethal injury in an Ancient Egyptian. Part I: medical aspect. *Journal of Human Evolution*, 12(2): 213-229.
- Paine, R.; Brenton, B. 2006. Dietary health does affect histological age assessment: an evaluation of Stout and Paine (1992) age estimation equation using secondary osteons from the rib. *Journal of Forensic Science*, 51(3): 489-492.
- Pálfi, G.; Bereczki, Z.; Ortner, D.; Dutour, O. 2012. Juvenile cases of skeletal tuberculosis from the Terry Anatomical Collection (Smithsonian Institution, Washington, D.C., USA). *Acta Biologica Szegediensis*, 56(1): 1-12.
- Pálfi, G.; Dutour, O.; Deák, J.; Hutás, I. 1999. Tuberculosis: past and present. Budapest-Szeged: Golden Book Publisher – Tuberculosis Foundation: 608.
- Panarra, A. 1994. Na origem do Hospital Real de Todos os Santos. *Medicina Interna*, 1(3): 201-203.
- Papaoiannou, A.; Kostikas, K.; Kollia, P.; Gourgoulialis, C. 2006. Clinical implications for vascular endothelial growth factor in the lung: friends or foe? *Respiratory Research*, 7(1): 128.
- Papierska, L.; Rabijewski, M. 2007. Glucocorticoid-induced osteoporosis. *Polskie Archiwum Medycyny Wewnętrznej*, 117(8): 1-6.
- Paral, V.; Witter, K.; Tonar, Z. 2007. Microscopic examination of ground sections - a simple method for distinguishing between bone and antler. *International Journal of Osteoarchaeology*, 17(6): 627-634.
- Parsche, F.; Nerlicg, A.; Zink, A.; Wiest, I. 1994. Collagen immunohistology in paleopathology. Evidence for the active bone remodelling in a Peruvian tibia. *Journal of Paleopathology*, 6(1): 103-108.
- Parsons, U. 1839. Boylston prize dissertations on 1. Inflammation of the periosteum. 2. Eneuresis irritata. 3. Cutaneous diseases. 4. Cancer of the breast. Also remarks on malaria. Boston, Charles C. Little and James Brown.
- Parsons, V. 1980. A colour atlas of bone disease. London, Wolfe Medical Publications Ltd.
- Patrick, M. 2006. Microwear and morphology: functional relationships between human dental microwear and the mandible. *Journal of Human Evolution*, 50(4): 452-459.
- Pavón, M.; Cucina, A.; Tiesler, V. 2010. New formula to estimate age at death in Maya populations using histomorphological changes in the fourth human rib. *Journal of Forensic Sciences*, 55(2): 473-477.

- Pawlicki, R. 1978. Methods of preparation of fossil bone samples for light and transmission electron microscopy. *Biotechnic & Histochemistry*, 53(2): 95-102.
- Pearson, O.; Lieberman, D. 2004. The aging of Wolff's "law": ontogeny and responses to mechanical loading in cortical bone. *American Journal of Physical Anthropology*, 125(s39): 63-99.
- Peck, J.; Stout, S. 2007. Intraskkeletal variability in bone mass. *American Journal of Physical Anthropology*, 132(1): 89-97.
- Pepper, H.; Berinson, H. 1973. Extrapleural mass with neurologic signs. *Chest*, 64(3): 345-346.
- Perez, P. 2006. The paleopathological and taphonomical context in human evolution and its records. *International Congress Series*, 1296: 23-40.
- Pérez-Pérez, A.; Bermúdez de Castro, J.; Arsuaga, J. 1999. Nonocclusal dental microwear analysis of 300,000-year-old *Homo heilderbergensis* teeth from Sima de los Huesos (Sierra de Atapuerca, Spain). *American Journal of Physical Anthropology*, 108(4): 433-457.
- Périchon, S.; Pagnoux, C.; Seror, R.; Dassonville, L.; Mangouka, L.; Cohen, P.; Letellier, P.; Guillevin, L. 2010. Périostéite au cours des vascularites systémiques nécrosantes: à propos de 4 observations d'une atteinte méconnue at pourtant évocatrice. *La Presse Médicale*, 39(7/8): e165-e173.
- Perry, M.; Newnam, J.; Gilliland, M. 2008. Differential diagnosis of a calcified object from a 4th-5th century AD burial in Aqaba, Jordan. *International Journal of Osteoarchaeology*, 18(5): 507-522.
- Petrone, P.; Giordano, M.; Giustino, S.; Guarino, F. 2011. Enduring fluoride health hazard for the Vesuvius area population: the case of AD 79 *Herculaneum*. *PLoS One*, 6(6): e21085.
- Pfeiffer, S. 1980. Bone remodelling age estimates compared with estimates by other techniques. *Current Anthropology*, 21(6): 793-794.
- Pfeiffer, S. 1984. Paleopathology in an Iroquoian ossuary, with special reference to tuberculosis. *American Journal of Physical Anthropology*, 65(2): 181-189.
- Pfeiffer, S. 1991a. Is paleopathology a relevant predictor of contemporary health patterns? In: Ortner, D.; Aufderheide, A. (Eds.). *Human paleopathology: current syntheses and future options*. Washington, Smithsonian Institution: 12-17.
- Pfeiffer, S. 1991b. Rib lesions and New World tuberculosis. *International Journal of Osteoarchaeology*, 1(3-4): 191-198.

- Pfeiffer, S. 1998. Variability in osteon size in recent human populations. *American Journal of Physical Anthropology*, 106(2): 219-227.
- Pfeiffer S. 2000. Paleohistology: health and disease. In: Katzenberg, A.; Saunders, S. (Eds.). *Biological anthropology of the human skeleton*. New York, Wiley-Liss: 287–302.
- Pfeiffer, S. 2006. Cortical bone in juveniles. In: Grupe, G.; Peters, J. (Eds.). *Microscopic examinations of bioarchaeological remains: keeping a close eye on ancient tissues*. Leidorf, Verlag Marie Leidorf: 15-28.
- Pfeiffer, S.; Pinto, D. 2012. Histological analyses of human bone from archaeological contexts. In: Crowder, C.; Stout, S. (Eds.). *Bone histology: an anthropological perspective*. Boca Raton, CRC Press: 297-311.
- Pfeiffer, S.; Varney, T. 2000. Quantifying histological and chemical preservation in archaeological bone. In: Ambrose, S.; Katzenberg, A. (Eds.). *Biogeochemical approaches to paleodietary analysis*. New York, Kluwer Academic/Plenum Publishers: 141-158.
- Pfeiffer, S.; Lazenby, R.; Chiang, J. 1995. Cortical remodelling data are affected by sampling location. *American Journal of Physical Anthropology*, 96(1): 89-92.
- Pfeiffer, S.; Crowder, C.; Harrington, L.; Brown, M. 2006. Secondary osteon and haversian canal dimensions as behavioral indicators. *American Journal of Physical Anthropology*, 131(4): 460-468.
- Pickering, R.; Bachman, D. 2009. Special techniques: their value and limitations. In: Pickering, R.; Bachman, D. (Eds.). *The use of forensic anthropology*. New York, CRC Press: 121-136.
- Pickering, T.; Hensley-Marschand, B. 2008. Cutmarks and hominid handedness. *Journal of Archaeological Science*, 35(2): 310-315.
- Piessens, W.; Nardell, E. 2000. Pathogenesis of tuberculosis. In: Reichman, L.; Hershfield, E. (Eds.). *Tuberculosis: a comprehensive international approach*. New York, Marcel Dekker, Inc.: 241-260.
- Pineda, C. J.; Martínez-Lavín, M.; Goobar, J. E.; Sartoris, D. J.; Clopton, P.; Resnick, D. 1987. Periostitis in hypertrophic osteoarthropathy: relationship to disease duration. *American Journal of Roentgenology*, 148 (4): 773–778.
- Pinhasi, R.; Bourbou, C. 2008. How representative are human skeletal assemblages for population analysis? In: Pinhasi, R.; Mays, S. (Eds.). *Advances in human paleopathology*. Chichester, John Wiley & Sons, Ltd.: 31-44.
- Pinhasi, R.; Stefanovi, S.; Papathanasiou, A.; Stock, J. 2011. Variability in long bone growth patterns and limb proportions within and amongst Mesolithic and Neolithic populations



- from Southeast Europe. In: Pinhasi, R.; Stock, J. (Eds.). *Human bioarchaeology of the transition of agriculture*. Chichester, John Wiley & Sons, Ltd.: 177-202.
- Pinheiro, J.; Cunha, E.; Cordeiro, C.; Vieira, N. 2004. Bridging the gap between forensic anthropology and osteoarchaeology – a case of vascular pathology. *International Journal of Osteoarchaeology*, 14(2): 137–144.
- Pinto, D.; Stout, S. 2010. Paget's disease in pre-contact Florida? Revisiting the Briarwoods site in Gulf coast Florida. *International Journal of Osteoarchaeology*, 20(5): 572-578.
- Polo-Cerdá, M.; Romero, A.; Casabo, J.; De Juan, J. 2007. The Bronze Age burials from Cova Dels Blaus (Vall d'Uixo, Castello, Spain): an approach to palaeodietary reconstruction through dental pathology, occlusal wear and buccal microwear patterns. *Homo-Journal of Comparative Human Biology*, 58(4): 297-307.
- Poppe, J. 1947. The diagnostic significance of clubbed fingers. *Chest*, 13(6): 658–662.
- Post, P.; Daniels, F. 1969. Histological and histochemical examination of American Indian scalps, mummies, and a shrunken head. *American Journal of Physical Anthropology*, 30(2): 269-293.
- Powell, K.; Atkinson, P.; Woodhead, C. 1973. Cortical bone structure of the pig mandible. *Archives of Oral Biology*, 18(2): 171-180.
- Price, J.; Oyajobi, B.; Rusell, R. 1993. The cell biology of bone growth. In: Waterlow, J.; Schürch, B. (Eds.). *Causes and mechanisms of linear growth retardation*. Proceedings of an I/D/E/G/C Workshop. London, International Dietary Energy Consultancy Group: <http://archive.unu.edu/unupress/food2/UID06E/UID06E00.HTM>.
- Proff, P.; Römer, P. 2009. The molecular mechanism behind bone remodelling: a review. *Clinical Oral Investigations*, 13(4): 355-362.
- Puech, P.-F.; Albertini, H. 1984. Dental microwear and mechanisms in early hominids from Laetoli and Hadar. *American Journal of Physical Anthropology*, 65(1): 87-91.
- Pugh, M.; Savchuck, W. 1958. Suggestions on the preparation of undecalcified bone for microradiography. *Biotechnic & Histochemistry*, 33(6): 287-293.

**Q**

- Qin, L.; Zhang, M. 2005. Mechanical testing for bone specimens. In: Deng, H.-W.; Liu, Y.-Z. (Eds.). *Current topics in bone biology*. Singapore, World Scientific Publishing Co.: 177-212.

- Qing, H.; Bonewald, L. 2009. Osteocyte remodelling of the perilacunar and pericanalicular matrix. *International Journal of Oral Science*, 1(2): 59-65.
- Quintelier, K. 2009. Calcified uterine leiomyomata from a post-medieval nunnery in Brussels, Belgium. *International Journal of Osteoarchaeology*, 19(3): 436-442.

---

**R**

- Rabino-Massa, E.; Chiarelli, B. 1972. The histology of naturally desiccated and mummified bodies. *Journal of Human Evolution*, 1(3): 259-262.
- Raff, J.; Cook, D.; Kaestle, F. 2006. Tuberculosis in the New World: a study of ribs from the Schild Mississippian population, West-Central Illinois. *Memórias do Instituto Oswaldo Cruz, Rio de Janeiro*, 101(II): 25-27.
- Ragsdale, B.; Lehmer, L. 2012. A knowledge of bone at the cellular (histological) level is essential to paleopathology. In: Grauer, A. (Ed.). *A companion to paleopathology*. Malden, Blackwell Publishing Ltd.: 227-249.
- Ragsdale, B.; Madewell, J.; Sweet, D. 1981. Radiologic and pathologic analysis of solitary bone lesions. Part II: Periosteal reactions. *Radiologic Clinics of North America*, 19(4): 749-783.
- Raisz, L. 1999. Physiology and pathophysiology of bone remodelling. *Clinical Chemistry*, 45(8B): 1353-1358.
- Ramos, L. 1994. Do Hospital Real de Todos os Santos à história hospitalar. *Revista da Faculdade de Letras: História*, II(10): 333-350.
- Rana, R.; Wu, J.; Eisenberg, R. 2009. Periosteal reaction. *American Journal of Roentgenology*, 193(4): w259-w272.
- Rao, G. M.; Guruprakash, G. H.; Poulouse, K. P.; Bhaskar, G. 1979. Improvement in hypertrophic pulmonary osteoarthropathy after radiotherapy to metastasis. *American Journal of Roentgenology*, 133 (5): 944-946.
- Rauch, A.; Seitz, S.; Baschant, U.; Schilling, A.; Illing, A.; Stride, B.; Kirilov, M.; Mandic, V.; Takacz, A.; Schmidt-Ullrich, R.; Ostermay, S.; Schinke, T.; Spanbroek, R.; Zaiss, M.; Angel, P.; Lerner, U.; David, J.-P.; Reichardt, H.; Amling, M.; Schütz, G.; Tuckermann, J. 2010. Glucocorticoids suppress bone formation by attenuating osteoblast differentiation via monomeric glucocorticoid receptor. *Cell Metabolism*, 11(6): 517-531.
- Rauch, F.; Travers, R.; Glorieux, F. 2007. Intracortical remodelling during human bone development: a histomorphometric study. *Bone*, 40(2): 274-280.

- Reed, S. 1999. TGF-  $\beta$  in infections and infectious diseases. *Microbes and Infection*, 1(15): 1313-1325.
- Reiche, I.; Lebon, M.; Chadefaux, C.; Müller, K.; Hô, A.-S.; Gensch, M.; Schade, U. 2010. Microscale imaging of the preservation state of 5,000-years-old archaeological bones by synchrotron infrared microspectroscopy. *Analytical and Bioanalytical Chemistry*, 397(6): 2491-2499.
- Reid, D.; Dean, M. 2000. Brief communication: the timing of linear hypoplasias on human anterior teeth. *American Journal of Physical Anthropology*, 113(1): 135-139.
- Reid, I. 1998. Editorial: Glucocorticoid effects on bone. *Journal of Clinical Endocrinology and Metabolism*, 83(6): 1860-1862.
- Reinholt, L.; Burrows, A.; Eiting, T.; Dumont, E.; Smith, T. 2009. Brief communication: histology and micro-CT as methods for assessment of facial suture patency. *American Journal of Physical Anthropology*, 138(4): 499-506.
- Renz, H.; Radlanski, R. 2006. Incremental lines in root cementum of human teeth are reliable age marker? *HOMO - Journal of Comparative Human Biology*, 57(1): 29-50.
- Resnick, M.; Kransdorf, M. 2005. *Bone and Joint Imaging*. Philadelphia, Elsevier Saunders.
- Ricci, R.; Lama, R.; Di Tota, G.; Pietrangelo, F.; Vecchio, F.; Evangelista, A.; Capelli, A.; Capasso, L. 1994. Skull osteolytic lesions in a XV century child: a case of childhood malignancy. *Journal of Paleopathology*, 6(3): 151-159.
- Richardson, M. 2001. *Approaches to differential diagnosis in musculoskeletal imaging*. Seattle, University of Washington.
- Ricqlès, A. 1993. Some remarks on palaeohistology from a comparative evolutionary point of view. In: Grupe, G.; Garland, A. (Eds.). *Histology of ancient human bone: methods and diagnosis*. Berlin, Springer-Verlag: 37-77.
- Ripamonti, U. 1988. Paleopathology in *Australopithecus africanus*: a suggested case of a 3-million-year-old prepubertal periodontitis. *American Journal of Physical Anthropology*, 76(2): 197-210.
- Ritzman, T.; Baker, B.; Schwartz, G. 2008. A fine line: a comparison of methods for estimating ages of linear enamel hypoplasia formation. *American Journal of Physical Anthropology*, 135(3): 348-361.
- Rivals, F.; Schulz, E.; Kaiser, T. 2009. A new application of dental wear analyses: estimation of duration of hominid occupations in archaeological localities. *Journal of Human Evolution*, 56(4): 329-339.

- Robb, J. 2000. Analysing human skeletal data. In: Cox, M.; Mays, S. (Eds.). *Human osteology in archaeology and forensic sciences*. London, Greenwich Medical Media Limited: 475-490.
- Roberts, C. 1999. Rib lesions and tuberculosis: the current state of play. In: Pálfi, G.; Dutour, O.; Deák, J.; Hutás, I. (Eds.). *Tuberculosis: past and present*. Budapest-Szeged, Golden Book/Tuberculosis Foundation: 311–316.
- Roberts, C. 2010. Adaptation of populations to changing environments: bioarchaeological perspectives on health for the past, present and future. *Bulletins et Mémoires de la Société d'Anthropologie de Paris*, 22(1-2): 38-46.
- Roberts, C.; Buikstra, J. 2003. *The bioarchaeology of tuberculosis: a global view on a reemerging disease*. Gainesville, University Press of Florida.
- Roberts, C.; Manchester, K. 2005. *The archaeology of disease*. Gloucestershire, Sutton Publishing.
- Roberts, C.; Wakely, J. 1992. Microscopical findings associated with the diagnosis of osteoporosis in palaeopathology. *International Journal of Osteoarchaeology*, 2(1): 23-30.
- Roberts, C.; Lucy, D.; Manchester, K. 1994. Inflammatory lesions of ribs: an analysis of the Terry Collection. *American Journal of Physical Anthropology*, 95(2): 169–182.
- Roberts, C.; Boylston, A.; Buckley, L.; Chamberlain, A.; Murphy, E. 1998. Rib lesions and tuberculosis: the palaeopathological evidence. *Tubercle and Lung Disease*, 79(1): 55-60.
- Roberts, S.; Smith, C.; Millard, A.; Collins, M. 2002. The taphonomy of cooked bone: characterizing boiling and its physic-chemical effects. *Archaeometry*, 44(3): 485-494.
- Roberts, W.; Huja, S.; Roberts J. 2004. Bone modelling: biomechanics, molecular mechanisms, and clinical perspectives. *Seminars in Orthodontics*, 10(2): 123-161.
- Robling, A.; Stout, S. 2008. Histomorphometry of human cortical bone: applications to age estimation. In: Katzenberg, A.; Saunders, S. (Eds.). *Biological anthropology of the human skeleton*. New Jersey, John Wiley Sons: 149-171.
- Robling, A.; Castillo, A.; Turner, C. 2006. Biomechanical and molecular regulation of bone remodelling. *Annual Review of Biomedical Engineering*, 8: 455-498.
- Roches, E.; Blondiaux, J.; Cotten, A.; Chastanet, P.; Flipo, R.-M. 2002. Microscopic evidence for Paget's disease in two osteoarchaeological samples from early Northern France. *International Journal of Osteoarchaeology*, 12(4): 229-234.
- Rodríguez-Martín, C. 2006. Identification and differential diagnosis of traumatic lesions of the skeleton. In: Schmitt, A.; Cunha, E.; Pinheiro, J. (Eds.). *Forensic anthropology and*

- medicine: complementary sciences from recovery to cause of death. New Jersey, Humana Press Inc.: 197-221.
- Roksandic, M.; Vlak, D.; Schillaci, M.; Voicu, D. 2009. Technical note: applicability of tooth cementum annulation to an archaeological population. *American Journal of Physical Anthropology*, 140(2): 583-588.
- Rosado, M.; Capel, A.; Cuccia, K. 2007. Macroscopic and microscopic analysis of calcined bone, Early Archaic, site 28-CU-79, Cumberland County, New Jersey. Scientific program & abstracts thirty-fourth annual meeting (North America) Paleopathology Association, Philadelphia, Pennsylvania: 24.
- Rose, J. 1977. Defective enamel histology of prehistoric teeth from Illinois. *American Journal of Physical Anthropology*, 46(3): 439-446.
- Rose, J.; Armelagos, G.; Lallo, J. 1978. Histological enamel indicator of childhood stress in prehistoric skeletal samples. *American Journal of Physical Anthropology*, 49(4): 511-516.
- Rosenthal, D. 1997. Radiologic diagnosis of bone metastases. *Cancer*, 80(8): 1595–1607.
- Rühli, F.; Kuhn, G.; Evison, R.; Müller, R.; Schultz, M. 2007. Diagnostic value of micro-CT in comparison with histology in the qualitative assessment of historical human skull bone pathologies. *American Journal of Physical Anthropology*, 133(4): 1099-1111.
- Ryan, A. 1979. Wear striation direction on primate teeth: a scanning electron microscope examination. *American Journal of Physical Anthropology*, 50(2): 155-167.

## S

- 
- Safadi, F.; Barbe, M.; Abdelmagid, S.; Rico, M.; Aswad, R.; Litvin, J.; Popoff, S. 2009. Bone structure, development and bone biology. In: Khurana, J. (Ed.). *Bone pathology*. New York, Humana Press: 1-50.
- Sanchez, J.; Etxeberria, F. 1991. Renal and biliary calculi: a palaeopathological analysis. *International Journal of Osteoarchaeology*, 1(3-4): 231-234.
- Sandison, A. 1955. The histological examination of mummified material. *Biotechnic & Histochemistry*, 30(6): 277-283.
- Sandison, A. 1967. Sir Marc Armand Ruffer (1859-1917) pioneer of palaeopathology. *Medical History*, 11(2): 150-156.

- Santos, A. L.; Roberts, C. 2001. A picture of tuberculosis in young Portuguese people in the early 20th century: a multidisciplinary study of the skeletal and historical evidence. *American Journal of Physical Anthropology*, 115(1): 38-49.
- Santos, A. L.; Roberts, C. 2006. Anatomy of a serial killer: differential diagnosis of tuberculosis based on rib lesions of adult individuals from the Coimbra Identified Skeletal Collection, Portugal. *American Journal of Physical Anthropology*, 130(1): 38-49.
- Sardoeira, J. P. 2011. Análise do trauma numa amostra proveniente do antigo cemitério da Ordem do Carmo na cidade do Porto. Dissertação de Mestrado em Biologia e Evolução Humanas. Coimbra, Departamento de Ciências da Vida da FCTUC [Unpublished].
- Sayler, M. 2005. *The encyclopedia of the muscle and skeletal systems and disorders*. New York, Facts on File, Inc.
- Schaffler, M.; Burr, D. 1984. Primate cortical bone microstructure: relationship to locomotion. *American Journal of Physical Anthropology*, 65(2): 191-197.
- Schamall, D.; Teschler-Nicola, M.; Kainberger, F.; Tangl, St.; Brandstätter, F.; Patzak, B.; Muhsil, J.; Plenk, H. Jr. 2003. Changes in trabecular bone structure in rickets and osteomalacia: the potential of a medico-historical collection. *International Journal of Osteoarchaeology*, 13(5): 283-288.
- Scherf, H.; Tilgner, R. 2009. A new high-resolution computed tomography (CT) segmentation method for trabecular bone architectural analysis. *American Journal of Physical Anthropology*, 140(1): 39-51.
- Scheuer, L.; Black, S. 2000. *Developmental juvenile osteology*. London, Elsevier Academic Press.
- Schmidt, C. 2001. Dental microwear evidence for a dietary shift between two nonmaize-reliant prehistoric human populations from Indiana. *American Journal of Physical Anthropology*, 114(2): 139-145.
- Schmidt, C. 2007. The recovery and study of burned human teeth. In: Schmidt, C.; Symes, S. (Eds.). *The analysis of burned human remains*. Amsterdam, Elsevier Ltd.: 55-74.
- Schmidt, C. 2010. On the relationship of dental microwear to dental macrowear. *American Journal of Physical Anthropology*, 142(1): 67-73.
- Schmidt-Schultz, T.; Schultz, M. 2007. Well preserved non-collagenous extracellular matrix proteins in ancient bone and teeth. *International Journal of Osteoarchaeology*, 17(1): 91-99.

- Schultz, M. 1986. Die mikroskopische Untersuchung prähistorischer Skelettfunde. Anwendung und Aussagemöglichkeiten der differentialdiagnostischen untersuchung in der Paläopathologie. In: Amt für Museen und Archäologie and Anthropologische Forschungsinstitut Aesch (Eds.). Tagungsber Paläopathologischen Symposium in Liestal (Baselland). Liestal, Amt für Museen und Archäologie BL, 6: 1-140.
- Schultz, M. 1993. Initial stages of systemic bone disease. In: Grupe, G.; Garland, A. (Eds.). Histology of ancient human bone: methods and diagnosis. Berlin, Springer-Verlag: 185-203.
- Schultz, M. 1994. Comparative histopathology of syphilitic lesions in prehistoric and historic human bones. In: Dutour, O.; Pálfi, G.; Berato, J.; Brun, J.-P. (Eds.). L'origine de la syphilis en Europe. Avant ou après 1493? Toulon, Centre Archaeologique du Var: 63-67.
- Schultz, M. 1997. Microscopic investigation of excavated skeletal remains: a contribution to paleopathology and forensic medicine. In: Haglund, W.; Sorg, M. (Eds.). Forensic taphonomy: the postmortem fate of human remains. Boca Raton, CRC Press: 201-222.
- Schultz, M. 1999. Microscopic investigation in fossil *Hominoidea*: a clue to taxonomy, functional anatomy, and the history of diseases. The Anatomical Record, 257(6): 225-232.
- Schultz, M. 2001. Paleohistopathology of bone: a new approach to the study of ancient diseases. Yearbook of Physical Anthropology, 116 (s33): 106-147.
- Schultz, M. 2003. Light microscopic analysis in skeletal paleopathology. In: Ortner, D. (Ed.). Identification of pathological conditions in human skeletal remains. Amsterdam, Academic Press: 73-107.
- Schultz, M. 2012. Light microscopic analysis of macerated pathologically changed bones. In: Crowder, C.; Stout, S. (Eds.). Bone histology: an anthropological perspective. Boca Raton, CRC Press: 253-296.
- Schultz, M.; Parzinger, H.; Posdnjakov, D.; Chikisheva, T.; Schmidt-Schultz, T. 2007. Oldest known case of metastasizing prostate carcinoma diagnosed in the skeleton of a 2,700-years-old Scythian King from Arzhan (Siberia, Russia). International Journal of Cancer, 121(12): 2591-2595.
- Schwander, S.; Ellner, J. 2008. Human immune response to *M. tuberculosis*. In: Davies, P.; Barnes, P.; Gordon, S. (Eds.). Clinical Tuberculosis. London, Hodder and Arnold: 121-141.

- Scott, R.; Ungar, P.; Bergstrom, T.; Brown, C.; Childs, B.; Teaford, M.; Walker, A. 2006. Dental microwear texture analysis: technical considerations. *Journal of Human Evolution*, 51(4): 339-349.
- Šefčáková, A.; Strouhal, E.; Nemecková, A.; Thurzo, M.; Stassíková-Stukovská, D. 2001. Case of metastatic carcinoma from end of the 8th-Early 9th century Slovakia. *American Journal of Physical Anthropology*, 116(3): 216-229.
- Seeman, E. 2006. Osteocytes—martyrs for integrity of bone strength. *Osteoporosis International*, 17(10): 1443-1448.
- Seeman, E. 2007. The periosteum – a surface for all seasons. *Osteoporosis International*, 18(2): 123-128.
- Sfeir, C.; Ho, L.; Doll, B.; Azari, K.; Hollinger, J. 2005. Fracture repair. In: Lieberman, J.; Friedlaender, G. (Eds.). *Bone regeneration and repair: biology and clinical application*. New Jersey, Humana Press Inc.: 27-44.
- Shelat, V.; Pandya, G.; Dixit, R. 2005. Tuberculous mastitis with rib erosion. *Journal, Indian Academy of Clinical Medicine*, 6(1): 82-85.
- Shiel, W. S.; Stöppler, M. C.; Lee, D.; Marks, J.; Mathur, R. 2008. *Webster's New World Medical Dictionary*. New Jersey, Wiley Publishing, Inc.
- Shillito, L.-M.; Bull, I.; Matthews, W.; Almond, M.; Williams, J.; Evershed, R. 2011. Biomolecular and micromorphological analysis of suspected faecal deposits at Neolithic Catalhoyuk, Turkey. *Journal of Archaeological Science*, 38(8): 1869-1877.
- Shin, D.; Youn, M.; Chang, B. 2003. Histological analysis on the medieval mummy in Korea. *Forensic Science International*, 137(2-3): 172-182.
- Shipman, P.; Rose, J. 1983. Evidence of butchery and hominid activities at Torralba and Ambrona: an evaluation using microscopic techniques. *Journal of Archaeological Science*, 10(5): 465-474.
- Shopfner, C. 1966. Periosteal bone growth in normal infants: a preliminary report. *American Journal of Roentgenology, Radium Therapy, and Nuclear Medicine*, 97(1): 154-163.
- Short, D.; Webley, M. 1984. Periosteal new bone formation complicating juvenile polyarteritis nodosa. *Journal of the Royal Society of Medicine*, 77(4): 325-327.
- Shuler, K. 2011. Life and death on a Barbadian sugar plantation: historic and bioarchaeological views of infection and mortality at Newton plantation. *International Journal of Osteoarchaeology*, 21(1): 66-81.



- Squires, K.; Thompson, T.; Islam, M.; Chamberlain, A. 2011. The application of histomorphometry and Fourier Transform Infrared Spectroscopy to the analysis of early Anglo-Saxon burned bone. *Journal of Archaeological Science*, 38(9): 2399-2409.
- Shibuya, M. 2006. Differential role of vascular endothelial growth factor receptor-1 and receptor-2 in angiogenesis. *Journal of Biochemistry and Molecular Biology*, 39(5): 469-478.
- Shih, M.-S. 2009. Bone histomorphometry and undecalcified samples. In: Khurana, J. (Ed.). *Bone pathology*. New York, Humana Press: 129-138.
- Simmons, D. 1985. Options for bone aging with the microscope. *American Journal of Physical Anthropology*, 28(s6): 249-263.
- Singh, I.; Gunberg, D. 1970. Estimation of age at death in human males from quantitative histology of bone fragments. *American Journal of Physical Anthropology*, 33(3): 373-381.
- Skinner, R. 2003. Decalcification of bone tissue. In: An, Y.; Martin, K. (Eds.). *Handbook of histological methods for bone and cartilage*. New Jersey, Humana Press: 167-184.
- Šlaus, M. 2008. Osteological and dental markers of health in the transition from the Late Antique to the Early Medieval Period in Croatia. *American Journal of Physical Anthropology*, 136(4): 455-469.
- Spatola, B.; Damann, F.; Ragsdale, B. 2012. Bone histology collections of the National Museum of Health and Medicine. In: Crowder, C.; Stout, S. (Eds.). *Bone histology: an anthropological perspective*. Boca Raton, CRC Press: 313-326.
- Spjut, H.; Dorfman, H. 1981. Florid reactive periostitis of the tubular bones of the hands and feet. A benign lesions which may simulate osteosarcoma. *The American Journal of Surgical Pathology*, 5(5): 423-433.
- Spring, K. 2003. Fluorescence microscopy. In: Driggers, R. (Ed.). *Encyclopedia of optical engineering*. New York, Marcel Dekker, Inc.: 548-555.
- Squier, C.; Ghonein, S.; Kremenak, C. 1990. Ultrastructure of the periosteum from membrane bone. *Journal of Anatomy*, 171: 233-239.
- Steckel, R. 2003. What can be learned from skeletons that might interest economists, historians, and other social scientists? *The American Economic Review*, 93(2): 213-220.
- Steenbrugge, F.; Poffyn, B.; Uyttendaele, D.; Verdonk, R.; Verstraete, K. 2001. Neurofibromatosis, gigantism, elephantiasis neuromatosa and recurrent massive subperiosteal hematoma: a new case report and review of 7 case reports from the literature. *Acta Orthopaedica Belgica*, 67(2): 168-172.

- Steinbock, R. T. 1976. Paleopathological diagnosis and interpretation. CC Thomas, Springfield.
- Steiniche, T.; Hauge, E. 2003. Normal structure and function of bone. In: An, Y.; Martin, K. (Eds.). Handbook of histology methods for bone and cartilage. Totowa, Humana Press: 59-72.
- Sterchi, D.; Eurell, J. 1989. A new method for preparation of undecalcified bone sections. *Stain Technology*, 64(4): 201-205.
- Stevens, G.; Wakely, J. 1993. Diagnostic criteria for identification of seashell as a trephination implement. *International Journal of Osteoarchaeology*, 3(3): 167-176.
- Stevenson, R. 2005. Bowing of long bones. In: Stevenson R.; Hall, J. (Eds.). Human malformations and related anomalies. Oxford, Oxford University Press: 882-893.
- Stieber, J.; Pierz, K.; Dormans, J. 2001. Hereditary multiple exostosis: a current understanding of clinical and genetic advances. *The University of Pennsylvania Journal*, 14: 29-48.
- Stodder, A. 2008. Taphonomy and the nature of archaeological assemblages. In: Katzenberg, A.; Saunders, S. (Eds.). Biological anthropology of the human skeleton. New Jersey, John Wiley & Sons, Inc.: 71-114.
- Stout, S. 1978. Histological structure and its preservation in ancient bone. *Current Anthropology*, 19(3): 601-604.
- Stout, S.; Crowder, C. 2012. Bone remodelling, histomorphology, and histomorphometry. In: Crowder, C.; Stout, S. (Eds.). Bone histology: an anthropological perspective. Boca Raton, CRC Press: 1-21.
- Stout, S.; Gehlert, J. 1982. Effects of field size when using Kerley's histological method for determination of age at death. *American Journal of Physical Anthropology*, 58(2): 123-125.
- Stout, S.; Gehlert, S. 1979. Histomorphological identification of individuals among mixed skeletons. *Current Anthropology*, 20(4): 803-805.
- Stout, S.; Paine, R. 1992. Histological age estimation using rib and clavicle. *American Journal of Physical Anthropology*, 87(1): 111-115.
- Stout, S.; Stanley, S. 1991. Percent osteonal bone versus osteon counts: the variable of choice for estimating age at death. *American Journal of Physical Anthropology*, 86(4): 515-519.
- Stout, S.; Teitelbaum, S. 1976. Histological analysis of undecalcified thin sections of archeological bone. *American Journal of Physical Anthropology*, 44(2): 263-269.

- Stout, S.; Porro, M.; Perotti, B. 1996. Brief communication: a test and correction of the clavicle method of Stout and Paine for histological age estimation of skeletal remains. *American Journal of Physical Anthropology*, 100(1): 139-142.
- Streeter, M. 2005. Histomorphometric characteristics of the subadult cortex: normal patterns of dynamic bone modelling and remodelling during growth and development. Degree of Doctor of Philosophy. Columbia, University of Missouri [Unpublished].
- Streeter, M. 2012. Histological age-at-death estimation. In: Crowder, C.; Stout, S. (Eds.). *Bone histology: an anthropological perspective*. Boca Raton, CRC Press: 135-152.
- Strouhal, E. 1991. A case of primary carcinoma from Christian Sayala (Egyptian Nubia). *Journal of Palaeopathology*, 3(3): 151-166.
- Strouhal, E.; Němečková, A. 2004. Paleopathological find of a sacral neurilemmoma from ancient Egypt. *American Journal of Physical Anthropology*, 125(4): 320-328.
- Strouhal, E.; Němečková, A.; Kouba, M. 2003. Palaeopathology of Iufaa and other persons found beside his shaft tomb at Abusir (Egypt). *International Journal of Osteoarchaeology*, 13(6): 331-338.
- Strouhal, E.; Vyhnánek, L.; Horáčková, L.; Benešová, L.; Němečková, A. 1996a. Malignant tumors affecting the people from the ossuary at Křtiny (Czech Republic). *Journal of Paleopathology*, 8(1): 5-24.
- Strouhal, E.; Vyhnánek, L.; Horáčková, L.; Benešová, L.; Němečková, A. 1996b. Two unusual benign tumours in skulls from the Ossuary at Křtiny (Czech Republic). *International Journal of Osteoarchaeology*, 6(3): 289-299.
- Strouhal, E.; Vyhnánek, L.; Horáčková, L.; Benešová, L.; Němečková, A. 1997. A case of osteosarcoma in a late medieval-early modern skull from Kyjov (Czech Republic). *International Journal of Osteoarchaeology*, 7(1): 82-90.
- Stuart-Macadam, P. 1987. Porotic hyperostosis: new evidence to support the anemia theory. *American Journal of Physical Anthropology*, 74(4): 521-526.
- Stutz, A. 2002. Polarizing microscopy identification of chemical diagenesis archaeological cementum. *Journal of Archaeological Science*, 29(11): 1327-1347.
- Štvrtinová, V.; Jakubovský, J.; Hulín, I. 1995. Inflammation and fever. Bratislava, Academic Electronic Press. <http://staryweb.fmed.uniba.sk/patfyz/zapalweb/Inf fever.html>.
- Su, X.; Sun, K.; Cui, F.; Landis, W. 2003. Organization of apatite crystals in human woven bone. *Bone*, 32(2): 150-162.

- Sullivan, A. 2005. Prevalence and etiology of acquired anemia in medieval York, England. *American Journal of Physical Anthropology*, 128(2): 252-272.
- Suzuki, T. 1987. Paleopathological study on a case of osteosarcoma. *American Journal of Physical Anthropology*, 74(3): 309-318.
- Suzuki, T.; Inoue, T. 2007. Earliest evidence of spinal tuberculosis from the Aneolithic Yayoi period in Japan. *International Journal of Osteoarchaeology*, 17(4): 392-402.
- Suzuki, T.; Fujita, H.; Choi, J. 2008. Brief communication: new evidence of tuberculosis from Prehistoric Korea – population movement and evidence of tuberculosis in Far East Asia. *American Journal of Physical Anthropology*, 136(3): 357-360.
- Swinton, W. 1981. Sir Marc Armand Ruffer: one of the first palaeopathologists. *Canadian Medical Association Journal*, 15(124): 1388-1392.
- Sykaras, N.; Opperman, L. 2003. Bone morphogenetic proteins (BMPs): how do they function and what can they offer the clinicians? *Journal of Oral Science*, 45(2): 57-73.

**T**

- 
- Takahashi, N.; Udagawa, N.; Takami, M.; Suda, T. 2002. Cells of bone. In: Bilezikian, J.; Raisz, L.; Rodan, G. (Eds.). *Principles of bone biology*. San Diego, Academic Press: 109-126.
- Tamarit, L. 2003. Bases anatomopatológicas de diagnóstico en paleopatología: introducción a la paleohistopatología. In: Isidro, A.; Malgosa, A. (Eds.). *Paleopatología: la enfermedad no escrita*. Barcelona, Masson, SA: 107-122.
- Tamarit, L.; Herrerín, J.; Garralda, M. 2003. Exogenous versus hematogenous osteomyelitis of ancient adult skeletal remains: differential diagnosis and histopathologic approach. *Journal of Paleopathology*, 15(2): 77-90.
- Tatelman, M.; Drouillard, E. 1953. Tuberculosis of ribs. *American Journal of Roentgenology, Radium Therapy, and Nuclear Medicine*, 70(6): 923-935.
- Teaford, M.; Lytle, J. 1996. Brief communication: diet-induced changes in rates of human tooth microwear: a case study involving stone-ground maize. *American Journal of Physical Anthropology*, 100(1): 143-147.
- Teaford, M.; Robinson, J. 1989. Seasonal or ecological differences in diet and molar microwear in *Cebus nigrivittatus*. *American Journal of Physical Anthropology*, 80(3): 391-401.
- Teaford, M.; Runestad, J. 1992. Dental microwear and diet in Venezuelan primates. *American Journal of Physical Anthropology*, 88(3): 347-364.

- Teaford, M.; Maas, M.; Simons, E. 1996. Dental microwear and microstructure in early oligocene primates from the Fayum, Egypt: Implications for diet. *American Journal of Physical Anthropology*, 101(4): 527-543.
- Tersigni, M. 2007. Frozen human bone: a microscopic investigation. *Journal of Forensic Sciences*, 52(1): 16-20.
- Thalhammer, S.; Heckl, W.; Zink, A.; Nerlich, A. 2001. Atomic force microscopy for high resolution imaging of collagen fibrils - a new technique to investigate collagen structure in historic bone tissues. *Journal of Archaeological Science*, 28(10): 1061-1068.
- Thillaud, P. 1996. *Paléopathologie Humaine*. Paris, Kronos BY.
- Thomas, C.; Stein, M.; Feik, S.; Wark, J.; Clement, J. 2000. Determination of age at death using combined morphology and histology of the femur. *Journal of Anatomy*, 196(3): 463-471.
- Thomas, P. 2003. *Forensic anthropology: the growing science of talking bones*. New York, Facts on File, Inc.
- Tkocz, I.; Bierring, F. 1984. A medieval case of metastasizing carcinoma with multiple osteosclerotic bone lesions. *American Journal of Physical Anthropology*, 65(4): 373-380.
- Tomkins, A. 2003. Assessing micronutrient status in the presence of inflammation. *Journal of Nutrition*, 133(5): 1649s-1655s.
- Tong, A.; Ng, I.; Yeung, K. 2006. Osteomyelitis with proliferative periostitis: an unusual case. *Oral Surgery, Oral Medicine, Oral Pathology, Oral Radiology, and Endodontology*, 102(5): e14-e19.
- Travlos, G. 2006. Normal structure, function, and histology of the bone marrow. *Toxicologic Pathology*, 34(5): 548-565.
- Tucker, B.; Hutchinson, D.; Gilliland, M.; Charles, T.; Daniel, H.; Wolfe, L. 2001. Microscopic characteristics of hacking trauma. *Journal of Forensic Sciences*, 46(2): 234-240.
- Tuli, S. 2004. *Tuberculosis of the skeletal system (bones, joints, spine and bursal sheaths)*. New Delhi, Jaypee Brothers Medical Publishers (P) Ltd.
- Turner, P.; Holtom, D. 1981. The use of a fabric softener in the reconstitution of mummified tissue prior to paraffin wax sectioning for light microscopical examination. *Biotechnic & Histochemistry*, 56(1): 35-38.
- Turner-Walker, G. 2008. The chemical and microbial degradation of bones and teeth. In: Pinhasi, R.; Mays, S. (Eds.). *Advances in human paleopathology*. Chichester, John Wiley & Sons, Ltd.: 3-29.

- Turner-Walker, G.; Jans, M. 2008. Reconstructing taphonomic histories using histological analysis. *Palaeogeography, Palaeoclimatology, Palaeoecology*, 266(3-4): 227-235.
- Turner-Walker, G.; Mays, S. 2008. Histological studies on ancient bones. In: Pinhasi, R.; Mays, S. (Eds.). *Advances in human paleopathology*. Chichester, John Wiley & Sons, Ltd: 121-146.
- Tweed, J.; Avil, S.; Campbell, J.; Barnes, M. 2008. Etiologic factors in the development of medial tibial stress syndrome: a review of the literature. *Journal of the American Podiatric Medical Association*, 98(2): 107-111.

---

**U**

- Ungar, P.; Spencer, M. 1999. Incisor microwear, diet, and tooth use in three Amerindian populations. *American Journal of Physical Anthropology*, 109(3): 387-396.
- Ungar, P.; Grine, F.; Teaford, M.; El Zaatari, S. 2006. Dental microwear and diets of African early *Homo*. *Journal of Human Evolution*, 50(1): 78-95.
- Uytterschaut, H. 1993. Human bone remodelling and aging. In: Grupe, G.; Garland, A. (Eds.). In: *Histology of ancient human bone: methods and diagnosis*. Berlin, Springer-Verlag: 95-109.

---

**V**

- Väänänen, K.; Zhao, H. 2002. Osteoclast function. In: Bilezikian, J.; Raisz, L.; Rodan, G. (Eds.). *Principles of bone biology*. San Diego, Academic Press: 127-139.
- Väänänen, K.; Zhao, H.; Mulari, M.; Hallen, J. 2000. The cell biology of osteoclast function. *Journal of Cell Science*, 113(3): 377-381.
- Van der Merwe, A.; Maat, G.; Steyn, M. 2010. Ossified haematomas and infectious bone changes on the anterior tibia: histomorphological features as an aid for accurate diagnosis. *International Journal of Osteoarchaeology*, 20(2):227-239.
- Vandemergel, X.; Blocklet, D.; Decaux, G. 2004. Periostitis and hypertrophic osteoarthropathy: etiologies and bone scan patterns in 115 cases. *European Journal of Internal Medicine*, 15(6): 375-380.
- Varaine, F.; Henkens, M.; Grouzard, V. 2010. *Tuberculosis: practical guide for clinicians, nurses., laboratory technicians and medical auxiliaries*. Paris, Médecins Sans Frontières.

- Velasco-Vázquez, J.; González-Reimers, E.; Arnay-De-La-Rosa, M.; Barros-López, N.; Martín-Rodríguez, E.; Santolaria-Fernández, F. 1999. Bone histology of prehistoric inhabitants of the Canary Islands: comparison between El Hierro and Gran Canaria. *American Journal of Physical Anthropology*, 110(2): 201-213.
- Vigorita, V. 2008. *Orthopaedic pathology*. Philadelphia, Lippincott Williams & Wilkins.
- Villa, C.; Lynnerup, N. 2010. Technical note: a stereological analysis of the cross-sectional variability of the femoral osteon population. *American Journal of Physical Anthropology*, 142(3): 491-496.
- von Hunnius, T. 2009. Using microscopy to improve a diagnosis: an isolated case of tuberculosis-induced hypertrophic osteopathy in archaeological dog remains. *International Journal of Osteoarchaeology*, 19(3): 397-405.
- von Hunnius, T.; Roberts, C.; Boylston, A.; Saunders, S. 2006. Histological identification of syphilis in pre-Columbian England. *American Journal of Physical Anthropology*, 129(4): 559-566.
- Vyhnánek, L.; Strouhal, E.; Němečková, A. 1999. Kissing osteochondroma: a case from ancient Egypt. *International Journal of Osteoarchaeology*, 9(5): 361-368.

**W**

- 
- Wade, A.; Holdsworth, D.; Garvin, G. 2011. CT and micro-CT analysis of a case of Paget's disease (osteitis deformans) in the Grant Skeletal Collection. *International Journal of Osteoarchaeology*, 21(2): 127-135.
- Wakely, J.; Anderson, T.; Carter, A. 1995. A multidisciplinary case study of prostatic (?) carcinoma from medieval Canterbury. *Journal of Archaeological Science*, 22(4): 469-477.
- Wakely, J.; Manchester, K.; Roberts, C. 1991. Scanning electron microscopy of rib lesions. *International Journal of Osteoarchaeology*, 1(3-4): 185-189.
- Wakely, J.; Strouhal, E.; Vyhnánek, L.; Němečková, A. 1998. Case of a malignant tumour from Abingdon, Oxfordshire, England. *Journal of Archaeological Science*, 25(10): 949-955.
- Waldron, T. 1994. *Counting the dead: the epidemiology of skeletal populations*. Chichester, Wiley, John & Sons.
- Waldron, T. 1996. What was the prevalence of malignant disease in the past? *International Journal of Osteoarchaeology*, 6(5): 463-470.

- Waldron, T. 2007. *Palaeoepidemiology: the measure of disease in the human past*. Walnut Creek, Left Coast Press Inc.
- Waldron, T. 2009. *Paleopathology*. Cambridge, Cambridge University Press.
- Wallin, J.; Tkocz, I.; Kristensen, G. 1994. Microscopic age determination of human skeletons including an unknown but calculable variable. *International Journal of Osteoarchaeology*, 4(4): 353-362.
- Wallin, J.; Tkocz, I.; Levinsen, J. 1985. A simplified procedure for preparation of undecalcified human bone sections. *Biotechnic & Histochemistry*, 60(6): 331-336.
- Walker, D.; Henderson, M. 2010. Smoking and health in London's East End in the first half of the 19<sup>th</sup> century. *Post-Medieval Archaeology*, 44(1): 209-222.
- Walker, R.; Parsche, F.; Bierbrier, M.; McKerrow, J. 1987. Tissue identification and histologic study of six lung specimens from Egyptian mummies. *American Journal of Physical Anthropology*, 72(1): 43-48.
- Walsh, W.; Walton, M.; Warwick, B.; Yan, Y.; Gillies, R.; Svehla, M. 2003. Cell structure and biology of bone and cartilage. In: An, Y.; Martin, K. (Eds.). *Handbook of histology methods for bone and cartilage*. New Jersey, Humana Press: 35-58.
- Wang, Y.; Xiao, Y.; Li, Y.; Feng, Y.; Li, C.; Ma, H. 2011. The vascular endothelial growth factor interacts with *Mycobacterium tuberculosis* ESAT-6. *African Journal of Microbiology Research*, 5(28): 5071-5075.
- Wapler, U.; Schultz, M. 1996. Une méthode de recherche histologique appliquée au matériel osseux archéologique: l'exemple des *cribra orbitalia*. *Bulletins et Mémoires de la Société d'Anthropologie de Paris*, 8 (3-4): 421-431.
- Wapler, U.; Crubézy, E.; Schultz, M. 2004. Is *cribra orbitalia* synonymous with anemia? Analysis and interpretation of cranial pathology in Sudan. *American Journal of Physical Anthropology*, 123(4): 333-339.
- Warden, S.; Gutschlag, F.; Wajswelner, H.; Crossley, K. 2002. Aetiology of rib stress fractures in rowers. *Sports Medicine*, 32(13): 819-836.
- Warren, M. 2008. Detection of commingling in cremated human remains. In: Adams, B.; Byrd, J. (Eds.). *Recovery, analysis, and identification of commingled human remains*. New York, Human Press: 185-197.
- Waxman, A.; Geshelin, H. 1949. Fracture of the ribs by muscular action other than coughing or sneezing. *California Medicine*, 70(2): 131-132.



- Weinberger, S.; Cockrill, B.; Mandel, J. 2008. Principles of pulmonary medicine. Philadelphia, Saunders Elsevier.
- Weiner, S.; Traub, W.; Wagner, D. 1999. Lamellar bone: structure-function relations. *Journal of Structural Biology*, 126(3): 241-255.
- Weinstein, R.; Simmons, D.; Lovejoy, C. 1981. Ancient bone disease in a Peruvian mummy revealed by quantitative skeletal histomorphometry. *American Journal of Physical Anthropology*, 54(3): 321-326.
- Wenaden, A.; Szyszko, T.; Saifuddin, A. 2005. Imaging of periosteal reactions associated with focal lesions of bone. *Clinical Radiology*, 60(4): 439–456.
- Wendy, D. 1998. Histological reconstruction of dental development and age at death in a juvenile gibbon (*Hylobates lar*). *Journal of Human Evolution*, 35(4-5): 411-425.
- Weston, D. 2004. Approaches to the investigation of periosteal new bone formation in palaeopathology. Thesis submitted for the degree of doctor in Philosophy. Institute of Archaeology. London, University College London [Unpublished].
- Weston, D. 2008. Investigating the specificity of periosteal reactions in pathology museum specimens. *American Journal of Physical Anthropology*, 137(1): 48-59.
- Weston, D. 2009. Brief communication: paleohistopathological analysis of pathology museum specimens: can periosteal reaction microstructure explain lesion etiology? *American Journal of Physical Anthropology*, 140(1): 186-193.
- White, T. 1986. Cut marks on the Bodo cranium: a case of prehistoric defleshing. *American Journal of Physical Anthropology*, 69(4): 503-509.
- White, T.; Folkens, P. 2005. The human bone manual. Burlington, Elsevier Academic Press.
- Wilson, C. 1995. The invisible world: early modern philosophy and the invention of the microscope. Princeton, Princeton University Press.
- Whiting, W.; Zernicke, R. 1998. Biomechanics of musculoskeletal injury. Champaign, Human Kinetics.
- Wittwer-Backofen, U.; Gampe, J.; Vaupel, J. 2004. Tooth cementum annulation for age estimation: results from a large known-age validation study. *American Journal of Physical Anthropology*, 123(2): 119-129.
- Witzel, C.; Kierdorf, U.; Schultz, M.; Kierdorf, H. 2008. Insights from the inside: histological analysis of abnormal enamel microstructure associated with hypoplastic enamel defects in human teeth. *American Journal of Physical Anthropology*, 136(4): 400-414.

- Wolfe, C. 2010. Empiricist heresies in early modern medical thought. In: Wolfe, C.; Gal, O. (Eds.). *The body as object and instrument of knowledge: embodied empiricism in early modern science*. *Studies in History and Philosophy of Science* 25. Dordrecht, Springer Science and Business Media: 333-344.
- Wood, B. 1987. Infant ribs: generalized periosteal reaction resulting from vibrator chest physiotherapy. *Radiology*, 162(3): 811-812.
- Wood, J.; Milner, G.; Harpending, H.; Weiss, K.; Cohen, M.; Eisenberg, L.; Hutchinson, D.; Jankauskas, R.; Česnys, G.; Katzenberg, A.; Lukacs, J.; McGrath, J.; Roth, E.; Ubelaker, D.; Wilkinson, R. 1992. The osteological paradox: problems of inferring prehistoric health from skeletal samples [and comments and reply]. *Current Anthropology*, 33(4): 343-370.
- Woodruff, L.; Norris, W. 1955. Sectioning of undecalcified bone with special reference to radioautographic applications. *Stain Technology*, 30(4): 179-188.
- World Health Organization (WHO). 2010. *Global tuberculosis control*. Geneva, World Health Organization Press.
- Wright, L.; Chew, F. 1998. Porotic hyperostosis and paleoepidemiology: a forensic perspective on anemia among the ancient Maya. *American Anthropologist*, 100(4): 924-939.
- Wright, L.; Yoder, C. 2003. Recent progress in bioarchaeology: approaches to the osteologic paradox. *Journal of Archaeological Research*, 11(1): 43-70.
- Wu, X.-J.; Schepartz, L.; Trinkaus, E. 2011. Antemortem trauma and survival in the late Middle Pleistocene human cranium from Maba, South China, *PNAS*, 108(49): 19558-19562.
- Wynsberghe, D.; Noback, C.; Carola, R. 1995. *Human anatomy and physiology*. Boston, McGraw-Hill.

**Y**

- 
- Yeh, C.-F.; Su, S.-C. 2012. Cough-induced rib fracture in a young healthy man. *Journal of the Formosan Medical Association*, 111(3): 179-180.
- Young, B.; Lowe, J.; Stevens, A.; Heath, J. 2006. *Wheater's functional histology: a text and colour atlas*. Boulevard, Elsevier.

**Z**

- 
- Zaki, M.; Hussein, F.; Abd El-Shafy El Banna, R. 2009. Osteoporosis among ancient Egyptians. *International Journal of Osteoarchaeology*, 19(1): 78-89.
- Zias, J.; Mitchell, P. 1996. Psoriatic arthritis in a fifth-century Judean desert monastery. *American Journal of Physical Anthropology*, 101(4): 491-502.
- Zimmerman, M. 1979. Paleopathologic diagnosis based on experimental mummification. *American Journal of Physical Anthropology*, 51(2): 235-253.
- Zimmerman, M. 2004. Paleopathology and the study of ancient remains. In: Ember, C.; Ember, M. (Eds.). *Encyclopedia of medical anthropology: health and illness in the world's cultures*. New York, Springer: 49-58.
- Zimmerman, M.; Kelley, M. 1982. *Atlas of human palaeopathology*. New York, Praeger Publisher.
- Zimmerman, M.; Brier, B.; Wade, R. 1998. Brief communication: twentieth-century replication of an Egyptian mummy. Implications for paleopathology. *American Journal of Physical Anthropology*, 107(4): 417-420.
- Zweifel, L.; Büni, Th.; Rühli, F. 2009. Evidence-based palaeopathology: meta-analysis of PubMed-listed scientific studies on ancient Egyptian mummies. *HOMO - Journal of Comparative Human Biology*, 60(5): 405-427.



---

# Appendices

---



**Table I.I.** Description of the cases of tuberculous infection recorded as cause of death in the Bocage Museum digital database.

Tuberculous conditions	Description
Tuberculosis (TB)	Multisystem and highly contagious infection caused by <i>Mycobacterium tuberculosis</i> complex (Shiel et al., 2008; Varaine et al., 2010). According to WHO (2010), in 2009, 9.4 million of new cases of TB were recorded and 1.3 million of deaths by HIV-negative people were registered.
Primo TB infection	Also called primary TB, refers to the initial pulmonary infection that affects immunologically naive patients through mild or asymptomatic signs (LoBue et al., 2000; Gordon and Mwandumba, 2008).
Pulmonary TB	Focused on lungs, it is the most common form of active tuberculosis (Shiel et al., 2008), being highly contagious throughout the release of saliva infected droplets during coughing, sneezing, singing, talking and breathing (Gordon and Mwandumba, 2008).
TB adenopathy	Abnormal enlargement of lymph nodes caused by tuberculosis infection (Shiel et al., 2008).
Acute phthisis	Distinct nomenclature to pulmonary TB of acute development.
Purulent pleurisy and tuberculosis	Caused by pus accumulation in the pleural cavity. Tuberculous pleuritis is normally associated with primary TB and may result from a local immune response to <i>M. Tuberculosis</i> (Schwander and Ellner, 2008).
Renal TB	It is a "silent" disease whose onset and development can lead to a total unilateral renal damage before diagnosis (Ormerod, 2008).
Intestinal TB	A gastrointestinal type more common in the ileocaecal area, and rare in the upper gastrointestinal tract or perianal region. The infection occurs through <i>bacilli</i> ingestion (Ormerod, 2008).
Tuberculous enteritis	Another type of gastrointestinal TB, primarily caused by <i>Mycobacterium bovis</i> after ingestion of infected meat or milk, or secondarily to a pulmonary focus. It is more frequent in the ileocaecal area (Hill et al., 1976).
Pott's disease	A tuberculosis infection of the vertebral column characterized by abscess formation, vertebral body destruction and collapse, leading to an inward and outward curvature of the spine (Shiel et al., 2008).
Meningeal TB	Affects the meninges of the central nervous system, being responsible for significant morbidity and mortality. Frequently, meningeal infection is the result of a distant focus activated by the blood stream (Ormerod, 2008).
Miliary TB	Characterized by the presence of multiple foci of TB infection in the body, caused by bloodstream dissemination of infected material (LoBue et al., 2000; Shiel et al., 2008).
Ultero-caseous TB	A few months after tuberculous contamination, the lesions may be encapsulated by the immune cells, forming calcified structures or small necrotic areas also called ultero-caseous or ultero-necrotic areas where <i>bacilli</i> are stored (Piessens and Nardell, 2000; Varaine et al., 2010).
Pulmonary bacillose	A general term for tuberculous infection.

**Table I.II.** Description of the cases of pulmonary non-TB and other infectious conditions recorded as cause of death in the Bocage Museum digital database.

<b>Non-TB pulmonary conditions</b>	
Disease	Description
Acute pneumopathy	General concept that points to a pulmonary condition of short duration, rapid and abbreviated in onset (Shiel et al., 2008).
Bronchitis	Inflammation and swelling of the bronchi that may have an acute or chronic origin (Shiel et al., 2008).
Asthmatic bronchitis	Lung disorder characterized by inflammation of the bronchi and subsequent swelling and narrowing of the airway (Shiel et al., 2008). A prominent component of airway hyperactivity is also observed (Weinberger et al., 2008).
Chronic bronchitis	Chronic inflammation of bronchi characterized by narrowing and obstruction of the airways, as well as by mucus production, increasing the possibility of a bacterial lung infection (Shiel et al., 2008; Weinberger et al., 2008).
Fetid bronchitis	In severe cases of bronchiectasis (persistent dilatation, distortion, and thickening of the walls of medium-sized bronchi) a multilobar involvement with voluminous purulent or fetid sputum may occur (Lichter, 2005).
Bronchopneumonia	Characterized by prominent distal airway inflammation along with alveolar disease. The spread of inflammation and/or infection occurs through airway rather than by adjacent alveoli and acini (Weinberger et al., 2008).
Influenza	Illness of the respiratory tract caused by virus (Shiel et al., 2008). It is the most common cause of respiratory tract infection (Luu, 2005).
Influenza with pulmonary congestion	In patients with chronic obstructive pulmonary disease, viral influenza may evolve to influenza pneumonia (Luu, 2005).
Pleural emphysema	It is a form of pleural effusion, grossly infected, characterized by an excess of fluid between the visceral and the parietal pleurae that cover the lungs, separating lungs from the chest wall. It can be unilateral or bilateral (Shiel et al., 2008; Weinberger et al., 2008).
Pneumonia	Dense unilateral or bilateral inflammation of the pulmonary parenchyma of lungs (Weinberger et al., 2008). It can be associated with an infection, but it is not mandatory (Shiel et al., 2008). When it has an infectious origin it can be of bacterial, viral, fungal or parasitic origin. It can also have an acute progression (Shiel et al., 2008).
Pneumonia of giant cells	Also called Hecht's pneumonia, it is a rare and deadly complication of measles that affects immunodeficient children and is characterized by multinucleated giant cells lining the lung alveolar tissue (Shiel et al., 2008).
Pulmonary abscess	A localized accumulation of pus in the lung tissues (Shiel et al., 2008; Weinberger et al., 2008). Bacteria that cause significant tissue necrosis are the agents commonly associated with lung abscess formation (Weinberger et al., 2008).
Pulmonary emphysema	A lung condition characterized by an abnormal accumulation of air at the alveoli. With the continuous enlargement of alveoli, a tissue disruption with scar formation may occur (Shiel et al., 2008).
Pulmonary embolism	Also called <i>pulmonary thromboembolism</i> (Weinberger et al., 2008), is caused by obstruction of the pulmonary artery, or one of its branches, by a foreign substance or a blood clot carried out through the bloodstream (Shiel et al., 2008).
Pulmonary oedema/congestion	Accumulation of fluids in the lung tissues (Shiel et al., 2008).
Pulmonary pleuritis	Inflammation of the pleurae, the membrane tissue that surrounds the lungs (Shiel et al., 2008).
<b>Extrapulmonary non-TB infections</b>	
Leprosy	Infectious disease caused by the bacillus <i>Mycobacterium leprae</i> that affect the skin, nervous system, mucous membranes, and indirectly the skeleton (Shiel et al., 2008).
Syphilis	It is a sexually transmitted disease caused by <i>Treponema pallidum</i> (Shiel et al., 2008).
Typhoid fever	An acute disease caused by the bacterium <i>Salmonella typhi</i> and that is related to faecal contamination of drinkable water or food (Shiel et al., 2008).
Osteomyelitis	Refers to an inflammation of bone and bone marrow due to infection (Shiel et al., 2008).
Gangrene	Condition characterized by tissue death due to loss or inadequate bone supply. Gangrene progression can be accelerated by bacterial invasion. In this case, gas and pus formation occur, requiring antibiotic treatment and/or surgical removal (Shiel et al., 2008).
Septicaemia	Occur when infectious organisms or the toxins produced during their activity spread throughout body by the bloodstream (Shiel et al., 2008).



**Table I.III.** Distinct conditions of circulatory, metabolic and neoplastic origin recorded as cause of death in the Bocage Museum digital database.

<b>Other pathological conditions</b>	
<b>Cardiovascular diseases:</b> According to Shiel and co-authors (2008: 71), cardiovascular diseases are a large group of conditions that affect the heart and blood vessels and include: arteriosclerosis, coronary artery disease, heart valve disease, arrhythmia, heart failure, hypertension, orthostatic hypotension, shock, endocarditis, diseases of the aorta and its branches, disorders of the peripheral vascular system, and congenital heart disease.	
Chest angina	Also called angina pectoris, is a chest pain due to the inadequate supply of oxygen to the heart muscles (Shiel et al., 2008). In agreement with the same authors, angina pectoris may come with or be a sign of a heart attack.
Mitral disorder	Characterized by a malfunction of the mitral valve, which allows the backflow of blood from the left ventricle into the left atrium (Shiel et al., 2008).
Arteriosclerosis	A circulatory disease due to hardening and thickening of the walls of the arteries. This condition has distinct aetiologies such as medical calcification, hypertension or arteriolar sclerosis and may lead to heart attacks, strokes as well as peripheral vascular disease (Shiel et al., 2008).
Heart asystole	A type of cardiac arrest characterized by the absence of electrical activity in the heart and leading to total standstill of heart beatings (Shiel et al., 2008).
<b>Cancer diseases:</b> An umbrella term that refers to a vast group of conditions characterized by an abnormal growth and proliferation of cells, in an uncontrolled fashion, which in some cases may travel (or metastasize) to other regions of the body through the blood or lymphatic stream (Shiel et al., 2008). The same authors point out that cancer is not one disease but a host for more than 100 different conditions.	
Gastric carcinoma	Also called stomach cancer, it is a malignant tumour of the stomach that can develop in any part of it and spread to other organs (Shiel et al., 2008).
Larynx carcinoma	Or laryngeal cancer, it is a malignant tumour of the larynx or voice box, which frequently affects individuals over the age of 55, especially those who were heavy smokers (Shiel et al., 2008).
Prostatic cancer	A malignant tumour that develops in the prostate and that is responsible for a high rate of deaths among males (Shiel et al., 2008).
<b>Miscellaneous conditions</b>	
«Caquexia senil»	A general term for dementia which is characterized by a significant loss of intellectual abilities, such as memory capacity, impairment of attention, orientation, judgement, language and motor or spatial skills (Shiel et al., 2008). Besides Alzheimer's diseases Shiel et al. (2008) refer to other causes, namely, alcoholism, brain injury, vascular dementia, brain tumours, drug toxicity, brain infection, syphilis, meningitis, Creutzfeldt-Jacob disease, hypothyroidism, etc.
Diabetes	Generally, diabetes is a chronic condition associated with an abnormal level of glucose in the blood and urine (Shiel et al., 2008).
Diabetic coma	In extreme cases, the uncontrolled diabetes associated with ketones in the blood stream may lead to a deep unconsciousness or coma state (Shiel et al., 2008).
Hepatic cirrhosis	Or simply cirrhosis, it is a liver disease characterized by an irreversible scarring of this organ. Many aetiological factors can underlie it, such as alcohol and viral hepatitis (Shiel et al., 2008).

**Table I.IV:** List of all bone samples extracted for microscopic analysis from the Identified Human Collection from the Bocage Museum.

Groups	Individual profile				Bone sample			
	Sk.	Sex	Age at death	Cause of death	Bone laterality	Location	Size	Type
Group 1	102	M	48	Pulmonary TB	3 <sup>rd</sup> right rib	Middle portion	l=1.1cm w=1.5cm	P
	154	M	35	Pulmonary TB	6 <sup>th</sup> right rib	Vertebral portion	l=0.5cm w=1.5cm	P
	332	M	41	Pulmonary TB	5 <sup>th</sup> left rib	Sternal portion	l=2.5cm w=1.0cm	P
	470	M	68	Pulmonary TB	6 <sup>th</sup> right rib	Vertebral portion	l=2.0cm w=1.5cm	P
	1227	M	21	Pulmonary TB	7 <sup>th</sup> left rib	Sternal portion	l=2.1cm w=1.2cm	P
	1235	M	50	Pulmonary TB	5 <sup>th</sup> right rib	Sternal portion	l=1.3cm w=1.5cm	P
	1242	M	78	Pulmonary TB	2 <sup>nd</sup> right rib	Sternal portion	l=1.5cm w=1.0cm	C
	1299	M	26	Pulmonary TB	4 <sup>th</sup> right rib	Sternal portion	l=1.5cm w=1.5cm	P
	1383	F	22	Pulmonary TB	5 <sup>th</sup> right rib	Sternal portion	l=2.0cm w=1.4cm	P
	1583	F	9	Pulmonary TB	11 <sup>th</sup> right rib	Vertebral portion	l=1.0cm w=0.7cm	P
	1604	F	45	Pulmonary TB	5 <sup>th</sup> left mett.	Distal portion	l=1.0cm w=1.0cm	P
	Group 2	119	F	64	Bronchop.	5 <sup>th</sup> left Mett.	Distal portion	l=1.0cm w=1.0cm
270		M	50	Bronchop.	7 <sup>th</sup> right rib	Sternal portion	l=2.2cm w=1.0cm	P
1429		M	26	Pulmonary congestion	Ind. left rib	Vertebral portion	l=2.5cm w=1.0cm	P
1534A		M	2	Pneum.	Right fibula	Distal portion	l=1.2cm w=0.5cm	P
1534A		M	2	Pneum.	Left rib	Vertebral portion	l=2.0cm w=1.0cm	P
Group 3	54	M	24	Pulmonary TB	Right tibia	Lower portion	l=1.5cm w=0.5cm	P*f
	119	F	64	Bronchop.	9 <sup>th</sup> right rib	Distal portion	l=2.0cm w=1.5cm	P*f
	135	M	86	Decrepitude	Right femur	Distal portion	l=2.5cm w=2.5cm	P
	198	M	68	Urinary sepsis	Right fibula	Distal portion	l=2.0cm w=1.0cm	P*f
	457	M	66	Rectus carcinoma	5 <sup>th</sup> left rib	Sternal portion	l=3.0cm w=2.0cm	P
	1138	M	86	Bronchop.	4 <sup>th</sup> right rib	Middle portion	l=1.0cm w=1.5cm	P
	1196	F	75	Arterioscl.	Right radius	Distal portion	l=1.7cm w=2.0cm	P*f
	1196	F	75	Arterioscl.	Right rib	Sternal portion	l=6.0cm w=1.0cm	P
	1412	F	81	Arterioscl. Stroke	Right tibia	Distal portion	l=2.0cm w=2.0cm	P
	1484	M	73	Gastric ulcer	Ind. right rib	Sternal portion	l=2.0cm w=2.0cm	C

**Legend:** P, pathological samples; P\*f, pathological samples with bone fracture; C, control sample.

**Table I.V:** List of the bone samples collected from archaeological specimens for microscopic analysis.

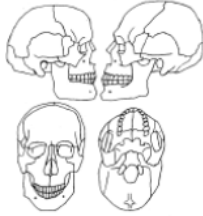
Catalogue number	Necropolis	Chronology	Profile	Bone sample	Diferential diagnosis
PAH/C_SG.24_SK.2	Constância, Portugal	14 <sup>th</sup> -19 <sup>th</sup> centuries	Young male	Rib	TB
PAH/C_SG.25_SK.2	Constância, Portugal	14 <sup>th</sup> -19 <sup>th</sup> centuries	Young female	Rib	TB
PAH/C_SG.19_SK7	Constância, Portugal	14 <sup>th</sup> -19 <sup>th</sup> centuries	Middle aged/old female	Rib	Metastatic carcinoma
Porto UE 5041-70	Porto, Portugal	19 <sup>th</sup> century	Adult	Left tibia Lower extremity	Massive bone outgrowths
Porto UE 6451.65	Porto, Portugal	19 <sup>th</sup> century	Adult male	Middle section of left fibula diaphysis	Non-specific periosteal bone reaction
Praça da Figueira [1492]	Lisboa, Portugal	18 <sup>th</sup> century	Adult male	Left femur	Calcified hematoma
Praça da Figueira QT6 E3 Sk.1310	Lisboa, Portugal	18 <sup>th</sup> century	Adult female	Left fibula	Acquired syphilis
Praça da Figueira Sk. 1429	Lisboa, Portugal	18 <sup>th</sup> century	Adult male	Fibula	Non-specific periosteal bone reaction

SKELETON – Visual record form

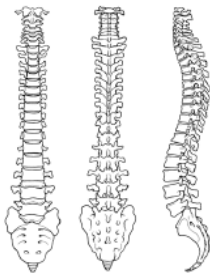
Skeleton Number # \_\_\_\_  
 Observation Number # \_\_\_\_  
 Date \_\_\_\_/\_\_\_\_/\_\_\_\_

3. Bone lesions labelling

Skull



Vertebrae



1. Skeleton Biological Profile			
Age at death	Sex	Place of death	Cause of death

2. Periosteal Bone Reaction – Macroscopical analysis									
Bone	Laterality	Distribution		Occurrence	Type 1 of 13	Severity 1 of 5	Type of new bone		
		Dispersion					Left	Right	
Skull	Unilateral <input type="radio"/> Bilateral <input type="radio"/>	Localized <input type="radio"/> Diffuse <input type="radio"/>		Regular <input type="radio"/> Heterogeneous <input type="radio"/>			Woven <input type="radio"/> Lamellar <input type="radio"/> Both <input type="radio"/>	Woven <input type="radio"/> Lamellar <input type="radio"/> Both <input type="radio"/>	
	Cervical	Unilateral <input type="radio"/> Bilateral <input type="radio"/>	Localized <input type="radio"/> Diffuse <input type="radio"/>		Regular <input type="radio"/> Heterogeneous <input type="radio"/>			Woven <input type="radio"/> Lamellar <input type="radio"/> Both <input type="radio"/>	Woven <input type="radio"/> Lamellar <input type="radio"/> Both <input type="radio"/>
Thoracic	Unilateral <input type="radio"/> Bilateral <input type="radio"/>	Localized <input type="radio"/> Diffuse <input type="radio"/>		Regular <input type="radio"/> Heterogeneous <input type="radio"/>			Woven <input type="radio"/> Lamellar <input type="radio"/> Both <input type="radio"/>	Woven <input type="radio"/> Lamellar <input type="radio"/> Both <input type="radio"/>	
Lumbar	Unilateral <input type="radio"/> Bilateral <input type="radio"/>	Localized <input type="radio"/> Diffuse <input type="radio"/>		Regular <input type="radio"/> Heterogeneous <input type="radio"/>			Woven <input type="radio"/> Lamellar <input type="radio"/> Both <input type="radio"/>	Woven <input type="radio"/> Lamellar <input type="radio"/> Both <input type="radio"/>	
Sacrum	Unilateral <input type="radio"/> Bilateral <input type="radio"/>	Localized <input type="radio"/> Diffuse <input type="radio"/>		Regular <input type="radio"/> Heterogeneous <input type="radio"/>			Woven <input type="radio"/> Lamellar <input type="radio"/> Both <input type="radio"/>	Woven <input type="radio"/> Lamellar <input type="radio"/> Both <input type="radio"/>	

\_\_\_\_\_

\_\_\_\_\_

\_\_\_\_\_

SKELETON – Visual record form

Skeleton Number # \_\_\_\_  
 Observation Number # \_\_\_\_  
 Date \_\_\_\_/\_\_\_\_/\_\_\_\_

1. Skeleton Biological Profile				
Age at death	Sex	Place of death	Cause of death	Additional data

2. Periosteal Bone Reaction – Macroscopical analysis													
Bone	Laterality	Distribution				Type 1 of 13		Metrics (mm)		Severity 1 of 7		Type of new bone	
		Dispersion		Occurrence		Left	Right	L W	L W	Left	Right	Left	Right
		Left	Right	Left	Right								
Os Coxae	Unilateral <input type="radio"/> Bilateral <input type="radio"/>	Localized <input type="radio"/> Diffuse <input type="radio"/>	Localized <input type="radio"/> Diffuse <input type="radio"/>	Regular <input type="radio"/> Heterogeneous <input type="radio"/>	Regular <input type="radio"/> Heterogeneous <input type="radio"/>			L W	L W			Woven <input type="radio"/> Lamellar <input type="radio"/> Both <input type="radio"/>	Woven <input type="radio"/> Lamellar <input type="radio"/> Both <input type="radio"/>
Scapula	Unilateral <input type="radio"/> Bilateral <input type="radio"/>	Localized <input type="radio"/> Diffuse <input type="radio"/>	Localized <input type="radio"/> Diffuse <input type="radio"/>	Regular <input type="radio"/> Heterogeneous <input type="radio"/>	Regular <input type="radio"/> Heterogeneous <input type="radio"/>			L W	L W			Woven <input type="radio"/> Lamellar <input type="radio"/> Both <input type="radio"/>	Woven <input type="radio"/> Lamellar <input type="radio"/> Both <input type="radio"/>
Clavicle	Unilateral <input type="radio"/> Bilateral <input type="radio"/>	Localized <input type="radio"/> Diffuse <input type="radio"/>	Localized <input type="radio"/> Diffuse <input type="radio"/>	Regular <input type="radio"/> Heterogeneous <input type="radio"/>	Regular <input type="radio"/> Heterogeneous <input type="radio"/>			L W	L W			Woven <input type="radio"/> Lamellar <input type="radio"/> Both <input type="radio"/>	Woven <input type="radio"/> Lamellar <input type="radio"/> Both <input type="radio"/>
Femora	Unilateral <input type="radio"/> Bilateral <input type="radio"/>	Localized <input type="radio"/> Diffuse <input type="radio"/>	Localized <input type="radio"/> Diffuse <input type="radio"/>	Regular <input type="radio"/> Heterogeneous <input type="radio"/>	Regular <input type="radio"/> Heterogeneous <input type="radio"/>			L W	L W			Woven <input type="radio"/> Lamellar <input type="radio"/> Both <input type="radio"/>	Woven <input type="radio"/> Lamellar <input type="radio"/> Both <input type="radio"/>

**SKELETON – Visual record form**

Skeleton Number # \_\_\_\_\_  
 Observation Number # \_\_\_\_\_  
 Date \_\_\_\_/\_\_\_\_/\_\_\_\_

**3. Bone lesions labeling**

Scapula  
Left / Right



Os Coxae  
Left / Right



Clavicle  
Left / Right



Patella  
Left/Right



**4. Bone Sampling**

Left Clavicle	Right Clavicle	Left Scapula	Right Scapula
<input type="radio"/> Yes <input type="radio"/> No	<input type="radio"/> Yes <input type="radio"/> No	<input type="radio"/> Yes <input type="radio"/> No	<input type="radio"/> Yes <input type="radio"/> No
Size (mm): L ____ / W ____	Size (mm): L ____ / W ____	Size (mm): L ____ / W ____	Size (mm): L ____ / W ____
Photo: <input type="radio"/> Yes <input type="radio"/> No	Photo: <input type="radio"/> Yes <input type="radio"/> No	Photo: <input type="radio"/> Yes <input type="radio"/> No	Photo: <input type="radio"/> Yes <input type="radio"/> No
Left Os Coxae	Right Os Coxae	Left Patella	Right Patella
<input type="radio"/> Yes <input type="radio"/> No	<input type="radio"/> Yes <input type="radio"/> No	<input type="radio"/> Yes <input type="radio"/> No	<input type="radio"/> Yes <input type="radio"/> No
Size (mm): L ____ / W ____	Size (mm): L ____ / W ____	Size (mm): L ____ / W ____	Size (mm): L ____ / W ____
Photo: <input type="radio"/> Yes <input type="radio"/> No	Photo: <input type="radio"/> Yes <input type="radio"/> No	Photo: <input type="radio"/> Yes <input type="radio"/> No	Photo: <input type="radio"/> Yes <input type="radio"/> No

\_\_\_\_\_  
 \_\_\_\_\_  
 \_\_\_\_\_

**SKELETON – Visual record form**

Skeleton Number # \_\_\_\_\_  
 Observation Number # \_\_\_\_\_  
 Date \_\_\_\_/\_\_\_\_/\_\_\_\_

**1. Skeleton Biological Profile**

Age at death	Sex	Place of death	Cause of death	Additional data

**2. Periosteal Bone Reaction – Macroscopical analysis**

Bone Portion	Laterality	Distribution				Type 1 of 13		Metrics (mm)		Severity 1 of 7		Type of new bone	
		Dispersion		Occurrence		Left	Right	Left	Right	Left	Right	Left	Right
		Left	Right	Left	Right								
1	Unilateral <input type="radio"/> Bilateral <input type="radio"/>	Localized <input type="radio"/> Diffuse <input type="radio"/>	Localized <input type="radio"/> Diffuse <input type="radio"/>	Regular <input type="radio"/> Heterogeneous <input type="radio"/>	Regular <input type="radio"/> Heterogeneous <input type="radio"/>	____	____	L ____ W ____	L ____ W ____	____	____	Woven <input type="radio"/> Lamellar <input type="radio"/> Both <input type="radio"/>	Woven <input type="radio"/> Lamellar <input type="radio"/> Both <input type="radio"/>
2	Unilateral <input type="radio"/> Bilateral <input type="radio"/>	Localized <input type="radio"/> Diffuse <input type="radio"/>	Localized <input type="radio"/> Diffuse <input type="radio"/>	Regular <input type="radio"/> Heterogeneous <input type="radio"/>	Regular <input type="radio"/> Heterogeneous <input type="radio"/>	____	____	L ____ W ____	L ____ W ____	____	____	Woven <input type="radio"/> Lamellar <input type="radio"/> Both <input type="radio"/>	Woven <input type="radio"/> Lamellar <input type="radio"/> Both <input type="radio"/>
3	Unilateral <input type="radio"/> Bilateral <input type="radio"/>	Localized <input type="radio"/> Diffuse <input type="radio"/>	Localized <input type="radio"/> Diffuse <input type="radio"/>	Regular <input type="radio"/> Heterogeneous <input type="radio"/>	Regular <input type="radio"/> Heterogeneous <input type="radio"/>	____	____	L ____ W ____	L ____ W ____	____	____	Woven <input type="radio"/> Lamellar <input type="radio"/> Both <input type="radio"/>	Woven <input type="radio"/> Lamellar <input type="radio"/> Both <input type="radio"/>
4	Unilateral <input type="radio"/> Bilateral <input type="radio"/>	Localized <input type="radio"/> Diffuse <input type="radio"/>	Localized <input type="radio"/> Diffuse <input type="radio"/>	Regular <input type="radio"/> Heterogeneous <input type="radio"/>	Regular <input type="radio"/> Heterogeneous <input type="radio"/>	____	____	L ____ W ____	L ____ W ____	____	____	Woven <input type="radio"/> Lamellar <input type="radio"/> Both <input type="radio"/>	Woven <input type="radio"/> Lamellar <input type="radio"/> Both <input type="radio"/>
5	Unilateral <input type="radio"/> Bilateral <input type="radio"/>	Localized <input type="radio"/> Diffuse <input type="radio"/>	Localized <input type="radio"/> Diffuse <input type="radio"/>	Regular <input type="radio"/> Heterogeneous <input type="radio"/>	Regular <input type="radio"/> Heterogeneous <input type="radio"/>	____	____	L ____ W ____	L ____ W ____	____	____	Woven <input type="radio"/> Lamellar <input type="radio"/> Both <input type="radio"/>	Woven <input type="radio"/> Lamellar <input type="radio"/> Both <input type="radio"/>
6	Unilateral <input type="radio"/> Bilateral <input type="radio"/>	Localized <input type="radio"/> Diffuse <input type="radio"/>	Localized <input type="radio"/> Diffuse <input type="radio"/>	Regular <input type="radio"/> Heterogeneous <input type="radio"/>	Regular <input type="radio"/> Heterogeneous <input type="radio"/>	____	____	L ____ W ____	L ____ W ____	____	____	Woven <input type="radio"/> Lamellar <input type="radio"/> Both <input type="radio"/>	Woven <input type="radio"/> Lamellar <input type="radio"/> Both <input type="radio"/>
7	Unilateral <input type="radio"/> Bilateral <input type="radio"/>	Localized <input type="radio"/> Diffuse <input type="radio"/>	Localized <input type="radio"/> Diffuse <input type="radio"/>	Regular <input type="radio"/> Heterogeneous <input type="radio"/>	Regular <input type="radio"/> Heterogeneous <input type="radio"/>	____	____	L ____ W ____	L ____ W ____	____	____	Woven <input type="radio"/> Lamellar <input type="radio"/> Both <input type="radio"/>	Woven <input type="radio"/> Lamellar <input type="radio"/> Both <input type="radio"/>

SKELETON – Visual record form

Skeleton Number # \_\_\_\_\_  
 Observation Number # \_\_\_\_\_  
 Date \_\_\_\_/\_\_\_\_/\_\_\_\_

**3. Bone lesions labelling**

LEFT HUMERUS                      RIGHT HUMERUS

1  
2  
3  
4  
5  
6  
7

lateral    posterior    medial    anterior    MEDIAL    LATERAL    DISTAL    MEDIAL

**4. Bone Sampling**

**Right Humerus**

Yes  No

Size (mm):  
L \_\_\_\_\_ / W \_\_\_\_\_

Photo:  
 Yes  No

**Left Humerus**

Yes  No

Size (mm):  
L \_\_\_\_\_ / W \_\_\_\_\_

Photo:  
 Yes  No

COMMENTS:

---

---

---

---

---

---

---

---

SKELETON – Visual record form

Skeleton Number # \_\_\_\_\_  
 Observation Number # \_\_\_\_\_  
 Date \_\_\_\_/\_\_\_\_/\_\_\_\_

**1. Skeleton Biological Profile**

Age at death	Sex	Place of death	Cause of death	Additional data

**2. Periosteal Bone Reaction – Macroscopical analysis**

Bone Portion	Laterality	Distribution				Type 1 of 13		Metrics (mm)		Severity 1 of 7		Type of new bone	
		Dispersion		Occurrence		Left	Right	Left	Right	Left	Right	Left	Right
		Left	Right	Left	Right								
1	Unilateral <input type="checkbox"/> Bilateral <input type="checkbox"/>	Localized <input type="checkbox"/> Diffuse <input type="checkbox"/>	Localized <input type="checkbox"/> Diffuse <input type="checkbox"/>	Regular <input type="checkbox"/> Heterogeneous <input type="checkbox"/>	Regular <input type="checkbox"/> Heterogeneous <input type="checkbox"/>	____	____	L _____ W _____	L _____ W _____	____	____	Woven <input type="checkbox"/> Lamellar <input type="checkbox"/> Both <input type="checkbox"/>	Woven <input type="checkbox"/> Lamellar <input type="checkbox"/> Both <input type="checkbox"/>
2	Unilateral <input type="checkbox"/> Bilateral <input type="checkbox"/>	Localized <input type="checkbox"/> Diffuse <input type="checkbox"/>	Localized <input type="checkbox"/> Diffuse <input type="checkbox"/>	Regular <input type="checkbox"/> Heterogeneous <input type="checkbox"/>	Regular <input type="checkbox"/> Heterogeneous <input type="checkbox"/>	____	____	L _____ W _____	L _____ W _____	____	____	Woven <input type="checkbox"/> Lamellar <input type="checkbox"/> Both <input type="checkbox"/>	Woven <input type="checkbox"/> Lamellar <input type="checkbox"/> Both <input type="checkbox"/>
3	Unilateral <input type="checkbox"/> Bilateral <input type="checkbox"/>	Localized <input type="checkbox"/> Diffuse <input type="checkbox"/>	Localized <input type="checkbox"/> Diffuse <input type="checkbox"/>	Regular <input type="checkbox"/> Heterogeneous <input type="checkbox"/>	Regular <input type="checkbox"/> Heterogeneous <input type="checkbox"/>	____	____	L _____ W _____	L _____ W _____	____	____	Woven <input type="checkbox"/> Lamellar <input type="checkbox"/> Both <input type="checkbox"/>	Woven <input type="checkbox"/> Lamellar <input type="checkbox"/> Both <input type="checkbox"/>
4	Unilateral <input type="checkbox"/> Bilateral <input type="checkbox"/>	Localized <input type="checkbox"/> Diffuse <input type="checkbox"/>	Localized <input type="checkbox"/> Diffuse <input type="checkbox"/>	Regular <input type="checkbox"/> Heterogeneous <input type="checkbox"/>	Regular <input type="checkbox"/> Heterogeneous <input type="checkbox"/>	____	____	L _____ W _____	L _____ W _____	____	____	Woven <input type="checkbox"/> Lamellar <input type="checkbox"/> Both <input type="checkbox"/>	Woven <input type="checkbox"/> Lamellar <input type="checkbox"/> Both <input type="checkbox"/>
5	Unilateral <input type="checkbox"/> Bilateral <input type="checkbox"/>	Localized <input type="checkbox"/> Diffuse <input type="checkbox"/>	Localized <input type="checkbox"/> Diffuse <input type="checkbox"/>	Regular <input type="checkbox"/> Heterogeneous <input type="checkbox"/>	Regular <input type="checkbox"/> Heterogeneous <input type="checkbox"/>	____	____	L _____ W _____	L _____ W _____	____	____	Woven <input type="checkbox"/> Lamellar <input type="checkbox"/> Both <input type="checkbox"/>	Woven <input type="checkbox"/> Lamellar <input type="checkbox"/> Both <input type="checkbox"/>
6	Unilateral <input type="checkbox"/> Bilateral <input type="checkbox"/>	Localized <input type="checkbox"/> Diffuse <input type="checkbox"/>	Localized <input type="checkbox"/> Diffuse <input type="checkbox"/>	Regular <input type="checkbox"/> Heterogeneous <input type="checkbox"/>	Regular <input type="checkbox"/> Heterogeneous <input type="checkbox"/>	____	____	L _____ W _____	L _____ W _____	____	____	Woven <input type="checkbox"/> Lamellar <input type="checkbox"/> Both <input type="checkbox"/>	Woven <input type="checkbox"/> Lamellar <input type="checkbox"/> Both <input type="checkbox"/>
7	Unilateral <input type="checkbox"/> Bilateral <input type="checkbox"/>	Localized <input type="checkbox"/> Diffuse <input type="checkbox"/>	Localized <input type="checkbox"/> Diffuse <input type="checkbox"/>	Regular <input type="checkbox"/> Heterogeneous <input type="checkbox"/>	Regular <input type="checkbox"/> Heterogeneous <input type="checkbox"/>	____	____	L _____ W _____	L _____ W _____	____	____	Woven <input type="checkbox"/> Lamellar <input type="checkbox"/> Both <input type="checkbox"/>	Woven <input type="checkbox"/> Lamellar <input type="checkbox"/> Both <input type="checkbox"/>

SKELETON – Visual record form

Skeleton Number # \_\_\_\_  
 Observation Number # \_\_\_\_  
 Date \_\_\_\_/\_\_\_\_/\_\_\_\_

**3. Bone lesions labelling**

**4. Bone Sampling**

<p><b>Right Radius</b></p> <p><input type="radio"/> Yes <input type="radio"/> No</p> <p>Size (mm): L ____ / W ____</p> <p>Photo: <input type="radio"/> Yes <input type="radio"/> No</p>	<p><b>Left Radius</b></p> <p><input type="radio"/> Yes <input type="radio"/> No</p> <p>Size (mm): L ____ / W ____</p> <p>Photo: <input type="radio"/> Yes <input type="radio"/> No</p>
---	--

COMMENTS:

---



---



---



---



---

SKELETON – Visual record form

Skeleton Number # \_\_\_\_  
 Observation Number # \_\_\_\_  
 Date \_\_\_\_/\_\_\_\_/\_\_\_\_

1. Skeleton Biological Profile				
Age at death	Sex	Place of death	Cause of death	Additional data

2. Periosteal Bone Reaction – Macroscopical analysis													
Bone Portion	Laterality	Distribution				Type		Metrics (mm)		Severity		Type of new bone	
		Dispersion		Occurrence		1 of 13		1 of 7		1 of 7		1 of 2	
		Left	Right	Left	Right	Left	Right	Left	Right	Left	Right	Left	Right
1	Unilateral <input type="radio"/> Bilateral <input type="radio"/>	Localized <input type="radio"/> Diffuse <input type="radio"/>	Localized <input type="radio"/> Diffuse <input type="radio"/>	Regular <input type="radio"/> Heterogeneous <input type="radio"/>	Regular <input type="radio"/> Heterogeneous <input type="radio"/>	___	___	L ___ W ___	L ___ W ___	___	___	Woven <input type="radio"/> Lamellar <input type="radio"/> Both <input type="radio"/>	Woven <input type="radio"/> Lamellar <input type="radio"/> Both <input type="radio"/>
2	Unilateral <input type="radio"/> Bilateral <input type="radio"/>	Localized <input type="radio"/> Diffuse <input type="radio"/>	Localized <input type="radio"/> Diffuse <input type="radio"/>	Regular <input type="radio"/> Heterogeneous <input type="radio"/>	Regular <input type="radio"/> Heterogeneous <input type="radio"/>	___	___	L ___ W ___	L ___ W ___	___	___	Woven <input type="radio"/> Lamellar <input type="radio"/> Both <input type="radio"/>	Woven <input type="radio"/> Lamellar <input type="radio"/> Both <input type="radio"/>
3	Unilateral <input type="radio"/> Bilateral <input type="radio"/>	Localized <input type="radio"/> Diffuse <input type="radio"/>	Localized <input type="radio"/> Diffuse <input type="radio"/>	Regular <input type="radio"/> Heterogeneous <input type="radio"/>	Regular <input type="radio"/> Heterogeneous <input type="radio"/>	___	___	L ___ W ___	L ___ W ___	___	___	Woven <input type="radio"/> Lamellar <input type="radio"/> Both <input type="radio"/>	Woven <input type="radio"/> Lamellar <input type="radio"/> Both <input type="radio"/>
4	Unilateral <input type="radio"/> Bilateral <input type="radio"/>	Localized <input type="radio"/> Diffuse <input type="radio"/>	Localized <input type="radio"/> Diffuse <input type="radio"/>	Regular <input type="radio"/> Heterogeneous <input type="radio"/>	Regular <input type="radio"/> Heterogeneous <input type="radio"/>	___	___	L ___ W ___	L ___ W ___	___	___	Woven <input type="radio"/> Lamellar <input type="radio"/> Both <input type="radio"/>	Woven <input type="radio"/> Lamellar <input type="radio"/> Both <input type="radio"/>
5	Unilateral <input type="radio"/> Bilateral <input type="radio"/>	Localized <input type="radio"/> Diffuse <input type="radio"/>	Localized <input type="radio"/> Diffuse <input type="radio"/>	Regular <input type="radio"/> Heterogeneous <input type="radio"/>	Regular <input type="radio"/> Heterogeneous <input type="radio"/>	___	___	L ___ W ___	L ___ W ___	___	___	Woven <input type="radio"/> Lamellar <input type="radio"/> Both <input type="radio"/>	Woven <input type="radio"/> Lamellar <input type="radio"/> Both <input type="radio"/>
6	Unilateral <input type="radio"/> Bilateral <input type="radio"/>	Localized <input type="radio"/> Diffuse <input type="radio"/>	Localized <input type="radio"/> Diffuse <input type="radio"/>	Regular <input type="radio"/> Heterogeneous <input type="radio"/>	Regular <input type="radio"/> Heterogeneous <input type="radio"/>	___	___	L ___ W ___	L ___ W ___	___	___	Woven <input type="radio"/> Lamellar <input type="radio"/> Both <input type="radio"/>	Woven <input type="radio"/> Lamellar <input type="radio"/> Both <input type="radio"/>
7	Unilateral <input type="radio"/> Bilateral <input type="radio"/>	Localized <input type="radio"/> Diffuse <input type="radio"/>	Localized <input type="radio"/> Diffuse <input type="radio"/>	Regular <input type="radio"/> Heterogeneous <input type="radio"/>	Regular <input type="radio"/> Heterogeneous <input type="radio"/>	___	___	L ___ W ___	L ___ W ___	___	___	Woven <input type="radio"/> Lamellar <input type="radio"/> Both <input type="radio"/>	Woven <input type="radio"/> Lamellar <input type="radio"/> Both <input type="radio"/>

SKELETON – Visual record form

Skeleton Number # \_\_\_\_\_  
 Observation Number # \_\_\_\_\_  
 Date \_\_\_\_/\_\_\_\_/\_\_\_\_

**3. Bone lesions labelling**

LEFT ULNA                      RIGHT ULNA

1  
2  
3  
4  
5  
6  
7

lateral    posterior    medial    anterior    medial    posterior    lateral

**4. Bone Sampling**

**Right Ulna**

Yes  No

Size (mm):  
L \_\_\_\_\_ / W \_\_\_\_\_

Photo:  
 Yes  No

**Left Ulna**

Yes  No

Size (mm):  
L \_\_\_\_\_ / W \_\_\_\_\_

Photo:  
 Yes  No

COMMENTS:

---

---

---

---

---

---

---

---

SKELETON – Visual record form

Skeleton Number # \_\_\_\_\_  
 Observation Number # \_\_\_\_\_  
 Date \_\_\_\_/\_\_\_\_/\_\_\_\_

1. Skeleton Biological Profile				
Age at death	Sex	Place of death	Cause of death	Additional data

2. Periosteal Bone Reaction – Macroscopical analysis													
Bone Portion	Laterality	Distribution				Type 1 of 13		Metrics (mm)		Severity 1 of 7		Type of new bone	
		Dispersion		Occurrence		Left	Right	Left	Right	Left	Right	Left	Right
		Left	Right	Left	Right								
1	Unilateral <input type="checkbox"/> Bilateral <input type="checkbox"/>	Localized <input type="checkbox"/> Diffuse <input type="checkbox"/>	Localized <input type="checkbox"/> Diffuse <input type="checkbox"/>	Regular <input type="checkbox"/> Heterogeneous <input type="checkbox"/>	Regular <input type="checkbox"/> Heterogeneous <input type="checkbox"/>	_____	_____	L _____ W _____	L _____ W _____	_____	_____	Woven <input type="checkbox"/> Lamellar <input type="checkbox"/> Both <input type="checkbox"/>	Woven <input type="checkbox"/> Lamellar <input type="checkbox"/> Both <input type="checkbox"/>
2	Unilateral <input type="checkbox"/> Bilateral <input type="checkbox"/>	Localized <input type="checkbox"/> Diffuse <input type="checkbox"/>	Localized <input type="checkbox"/> Diffuse <input type="checkbox"/>	Regular <input type="checkbox"/> Heterogeneous <input type="checkbox"/>	Regular <input type="checkbox"/> Heterogeneous <input type="checkbox"/>	_____	_____	L _____ W _____	L _____ W _____	_____	_____	Woven <input type="checkbox"/> Lamellar <input type="checkbox"/> Both <input type="checkbox"/>	Woven <input type="checkbox"/> Lamellar <input type="checkbox"/> Both <input type="checkbox"/>
3	Unilateral <input type="checkbox"/> Bilateral <input type="checkbox"/>	Localized <input type="checkbox"/> Diffuse <input type="checkbox"/>	Localized <input type="checkbox"/> Diffuse <input type="checkbox"/>	Regular <input type="checkbox"/> Heterogeneous <input type="checkbox"/>	Regular <input type="checkbox"/> Heterogeneous <input type="checkbox"/>	_____	_____	L _____ W _____	L _____ W _____	_____	_____	Woven <input type="checkbox"/> Lamellar <input type="checkbox"/> Both <input type="checkbox"/>	Woven <input type="checkbox"/> Lamellar <input type="checkbox"/> Both <input type="checkbox"/>
4	Unilateral <input type="checkbox"/> Bilateral <input type="checkbox"/>	Localized <input type="checkbox"/> Diffuse <input type="checkbox"/>	Localized <input type="checkbox"/> Diffuse <input type="checkbox"/>	Regular <input type="checkbox"/> Heterogeneous <input type="checkbox"/>	Regular <input type="checkbox"/> Heterogeneous <input type="checkbox"/>	_____	_____	L _____ W _____	L _____ W _____	_____	_____	Woven <input type="checkbox"/> Lamellar <input type="checkbox"/> Both <input type="checkbox"/>	Woven <input type="checkbox"/> Lamellar <input type="checkbox"/> Both <input type="checkbox"/>
5	Unilateral <input type="checkbox"/> Bilateral <input type="checkbox"/>	Localized <input type="checkbox"/> Diffuse <input type="checkbox"/>	Localized <input type="checkbox"/> Diffuse <input type="checkbox"/>	Regular <input type="checkbox"/> Heterogeneous <input type="checkbox"/>	Regular <input type="checkbox"/> Heterogeneous <input type="checkbox"/>	_____	_____	L _____ W _____	L _____ W _____	_____	_____	Woven <input type="checkbox"/> Lamellar <input type="checkbox"/> Both <input type="checkbox"/>	Woven <input type="checkbox"/> Lamellar <input type="checkbox"/> Both <input type="checkbox"/>
6	Unilateral <input type="checkbox"/> Bilateral <input type="checkbox"/>	Localized <input type="checkbox"/> Diffuse <input type="checkbox"/>	Localized <input type="checkbox"/> Diffuse <input type="checkbox"/>	Regular <input type="checkbox"/> Heterogeneous <input type="checkbox"/>	Regular <input type="checkbox"/> Heterogeneous <input type="checkbox"/>	_____	_____	L _____ W _____	L _____ W _____	_____	_____	Woven <input type="checkbox"/> Lamellar <input type="checkbox"/> Both <input type="checkbox"/>	Woven <input type="checkbox"/> Lamellar <input type="checkbox"/> Both <input type="checkbox"/>
7	Unilateral <input type="checkbox"/> Bilateral <input type="checkbox"/>	Localized <input type="checkbox"/> Diffuse <input type="checkbox"/>	Localized <input type="checkbox"/> Diffuse <input type="checkbox"/>	Regular <input type="checkbox"/> Heterogeneous <input type="checkbox"/>	Regular <input type="checkbox"/> Heterogeneous <input type="checkbox"/>	_____	_____	L _____ W _____	L _____ W _____	_____	_____	Woven <input type="checkbox"/> Lamellar <input type="checkbox"/> Both <input type="checkbox"/>	Woven <input type="checkbox"/> Lamellar <input type="checkbox"/> Both <input type="checkbox"/>



SKELETON – Visual record form

Skeleton Number # \_\_\_\_  
 Observation Number # \_\_\_\_  
 Date \_\_\_\_/\_\_\_\_/\_\_\_\_

**3. Bone lesions labelling**

**4. Bone Sampling**

	<b>Right Femur</b> <input type="radio"/> Yes <input type="radio"/> No Size (mm): L ____ / W ____ Photo: <input type="radio"/> Yes <input type="radio"/> No		<b>Left Femur</b> <input type="radio"/> Yes <input type="radio"/> No Size (mm): L ____ / W ____ Photo: <input type="radio"/> Yes <input type="radio"/> No
--	---	--	--

COMMENTS:

---



---



---



---



---

SKELETON – Visual record form

Skeleton Number # \_\_\_\_  
 Observation Number # \_\_\_\_  
 Date \_\_\_\_/\_\_\_\_/\_\_\_\_

**1. Skeleton Biological Profile**

Age at death	Sex	Place of death	Cause of death	Additional data

**2. Periosteal Bone Reaction – Macroscopical analysis**

Bone Portion	Laterality	Distribution				Type		Metrics (mm)		Severity		Type of new bone	
		Dispersion		Occurrence		1 of 13		1 of 7		Left		Right	
		Left	Right	Left	Right	Left	Right	Left	Right	Left	Right	Left	Right
1	Unilateral <input type="radio"/> Bilateral <input type="radio"/>	Localized <input type="radio"/> Diffuse <input type="radio"/>	Localized <input type="radio"/> Diffuse <input type="radio"/>	Regular <input type="radio"/> Heterogeneous <input type="radio"/>	Regular <input type="radio"/> Heterogeneous <input type="radio"/>	____	____	L ____ W ____	L ____ W ____	____	____	Woven <input type="radio"/> Lamellar <input type="radio"/> Both <input type="radio"/>	Woven <input type="radio"/> Lamellar <input type="radio"/> Both <input type="radio"/>
2	Unilateral <input type="radio"/> Bilateral <input type="radio"/>	Localized <input type="radio"/> Diffuse <input type="radio"/>	Localized <input type="radio"/> Diffuse <input type="radio"/>	Regular <input type="radio"/> Heterogeneous <input type="radio"/>	Regular <input type="radio"/> Heterogeneous <input type="radio"/>	____	____	L ____ W ____	L ____ W ____	____	____	Woven <input type="radio"/> Lamellar <input type="radio"/> Both <input type="radio"/>	Woven <input type="radio"/> Lamellar <input type="radio"/> Both <input type="radio"/>
3	Unilateral <input type="radio"/> Bilateral <input type="radio"/>	Localized <input type="radio"/> Diffuse <input type="radio"/>	Localized <input type="radio"/> Diffuse <input type="radio"/>	Regular <input type="radio"/> Heterogeneous <input type="radio"/>	Regular <input type="radio"/> Heterogeneous <input type="radio"/>	____	____	L ____ W ____	L ____ W ____	____	____	Woven <input type="radio"/> Lamellar <input type="radio"/> Both <input type="radio"/>	Woven <input type="radio"/> Lamellar <input type="radio"/> Both <input type="radio"/>
4	Unilateral <input type="radio"/> Bilateral <input type="radio"/>	Localized <input type="radio"/> Diffuse <input type="radio"/>	Localized <input type="radio"/> Diffuse <input type="radio"/>	Regular <input type="radio"/> Heterogeneous <input type="radio"/>	Regular <input type="radio"/> Heterogeneous <input type="radio"/>	____	____	L ____ W ____	L ____ W ____	____	____	Woven <input type="radio"/> Lamellar <input type="radio"/> Both <input type="radio"/>	Woven <input type="radio"/> Lamellar <input type="radio"/> Both <input type="radio"/>
5	Unilateral <input type="radio"/> Bilateral <input type="radio"/>	Localized <input type="radio"/> Diffuse <input type="radio"/>	Localized <input type="radio"/> Diffuse <input type="radio"/>	Regular <input type="radio"/> Heterogeneous <input type="radio"/>	Regular <input type="radio"/> Heterogeneous <input type="radio"/>	____	____	L ____ W ____	L ____ W ____	____	____	Woven <input type="radio"/> Lamellar <input type="radio"/> Both <input type="radio"/>	Woven <input type="radio"/> Lamellar <input type="radio"/> Both <input type="radio"/>
6	Unilateral <input type="radio"/> Bilateral <input type="radio"/>	Localized <input type="radio"/> Diffuse <input type="radio"/>	Localized <input type="radio"/> Diffuse <input type="radio"/>	Regular <input type="radio"/> Heterogeneous <input type="radio"/>	Regular <input type="radio"/> Heterogeneous <input type="radio"/>	____	____	L ____ W ____	L ____ W ____	____	____	Woven <input type="radio"/> Lamellar <input type="radio"/> Both <input type="radio"/>	Woven <input type="radio"/> Lamellar <input type="radio"/> Both <input type="radio"/>
7	Unilateral <input type="radio"/> Bilateral <input type="radio"/>	Localized <input type="radio"/> Diffuse <input type="radio"/>	Localized <input type="radio"/> Diffuse <input type="radio"/>	Regular <input type="radio"/> Heterogeneous <input type="radio"/>	Regular <input type="radio"/> Heterogeneous <input type="radio"/>	____	____	L ____ W ____	L ____ W ____	____	____	Woven <input type="radio"/> Lamellar <input type="radio"/> Both <input type="radio"/>	Woven <input type="radio"/> Lamellar <input type="radio"/> Both <input type="radio"/>

SKELETON – Visual record form

Skeleton Number # \_\_\_\_\_  
 Observation Number # \_\_\_\_\_  
 Date \_\_\_\_/\_\_\_\_/\_\_\_\_

**3. Bone lesions labelling**

	LEFT TIBIA				RIGHT TIBIA			
1								
2								
3								
4								
5								
6								
7								
	lateral	posterior	medial	anterior	inferior	medial	posterior	lateral

**4. Bone Sampling**

	<b>Right Tibia</b> <input type="checkbox"/> Yes <input type="checkbox"/> No Size (mm): L _____ / W _____ Photo: <input type="checkbox"/> Yes <input type="checkbox"/> No		<b>Left Tibia</b> <input type="checkbox"/> Yes <input type="checkbox"/> No Size (mm): L _____ / W _____ Photo: <input type="checkbox"/> Yes <input type="checkbox"/> No
--	---	--	--

COMMENTS:

---



---



---



---



---

SKELETON – Visual record form

Skeleton Number # \_\_\_\_\_  
 Observation Number # \_\_\_\_\_  
 Date \_\_\_\_/\_\_\_\_/\_\_\_\_

**1. Skeleton Biological Profile**

Age at death	Sex	Place of death	Cause of death	Additional data

**2. Periosteal Bone Reaction – Macroscopical analysis**



Bone Portion	Laterality	Distribution				Type		Metrics (mm)		Severity		Type of new bone	
		Dispersion		Occurrence		Left	Right	Left	Right	Left	Right	Left	Right
		Left	Right	Left	Right								
1	Unilateral <input type="checkbox"/> Bilateral <input type="checkbox"/>	Localized <input type="checkbox"/> Diffuse <input type="checkbox"/>	Localized <input type="checkbox"/> Diffuse <input type="checkbox"/>	Regular <input type="checkbox"/> Heterogeneous <input type="checkbox"/>	Regular <input type="checkbox"/> Heterogeneous <input type="checkbox"/>	___	___	L ___ W ___	L ___ W ___	___	___	Woven <input type="checkbox"/> Lamellar <input type="checkbox"/> Both <input type="checkbox"/>	Woven <input type="checkbox"/> Lamellar <input type="checkbox"/> Both <input type="checkbox"/>
2	Unilateral <input type="checkbox"/> Bilateral <input type="checkbox"/>	Localized <input type="checkbox"/> Diffuse <input type="checkbox"/>	Localized <input type="checkbox"/> Diffuse <input type="checkbox"/>	Regular <input type="checkbox"/> Heterogeneous <input type="checkbox"/>	Regular <input type="checkbox"/> Heterogeneous <input type="checkbox"/>	___	___	L ___ W ___	L ___ W ___	___	___	Woven <input type="checkbox"/> Lamellar <input type="checkbox"/> Both <input type="checkbox"/>	Woven <input type="checkbox"/> Lamellar <input type="checkbox"/> Both <input type="checkbox"/>
3	Unilateral <input type="checkbox"/> Bilateral <input type="checkbox"/>	Localized <input type="checkbox"/> Diffuse <input type="checkbox"/>	Localized <input type="checkbox"/> Diffuse <input type="checkbox"/>	Regular <input type="checkbox"/> Heterogeneous <input type="checkbox"/>	Regular <input type="checkbox"/> Heterogeneous <input type="checkbox"/>	___	___	L ___ W ___	L ___ W ___	___	___	Woven <input type="checkbox"/> Lamellar <input type="checkbox"/> Both <input type="checkbox"/>	Woven <input type="checkbox"/> Lamellar <input type="checkbox"/> Both <input type="checkbox"/>
4	Unilateral <input type="checkbox"/> Bilateral <input type="checkbox"/>	Localized <input type="checkbox"/> Diffuse <input type="checkbox"/>	Localized <input type="checkbox"/> Diffuse <input type="checkbox"/>	Regular <input type="checkbox"/> Heterogeneous <input type="checkbox"/>	Regular <input type="checkbox"/> Heterogeneous <input type="checkbox"/>	___	___	L ___ W ___	L ___ W ___	___	___	Woven <input type="checkbox"/> Lamellar <input type="checkbox"/> Both <input type="checkbox"/>	Woven <input type="checkbox"/> Lamellar <input type="checkbox"/> Both <input type="checkbox"/>
5	Unilateral <input type="checkbox"/> Bilateral <input type="checkbox"/>	Localized <input type="checkbox"/> Diffuse <input type="checkbox"/>	Localized <input type="checkbox"/> Diffuse <input type="checkbox"/>	Regular <input type="checkbox"/> Heterogeneous <input type="checkbox"/>	Regular <input type="checkbox"/> Heterogeneous <input type="checkbox"/>	___	___	L ___ W ___	L ___ W ___	___	___	Woven <input type="checkbox"/> Lamellar <input type="checkbox"/> Both <input type="checkbox"/>	Woven <input type="checkbox"/> Lamellar <input type="checkbox"/> Both <input type="checkbox"/>
6	Unilateral <input type="checkbox"/> Bilateral <input type="checkbox"/>	Localized <input type="checkbox"/> Diffuse <input type="checkbox"/>	Localized <input type="checkbox"/> Diffuse <input type="checkbox"/>	Regular <input type="checkbox"/> Heterogeneous <input type="checkbox"/>	Regular <input type="checkbox"/> Heterogeneous <input type="checkbox"/>	___	___	L ___ W ___	L ___ W ___	___	___	Woven <input type="checkbox"/> Lamellar <input type="checkbox"/> Both <input type="checkbox"/>	Woven <input type="checkbox"/> Lamellar <input type="checkbox"/> Both <input type="checkbox"/>
7	Unilateral <input type="checkbox"/> Bilateral <input type="checkbox"/>	Localized <input type="checkbox"/> Diffuse <input type="checkbox"/>	Localized <input type="checkbox"/> Diffuse <input type="checkbox"/>	Regular <input type="checkbox"/> Heterogeneous <input type="checkbox"/>	Regular <input type="checkbox"/> Heterogeneous <input type="checkbox"/>	___	___	L ___ W ___	L ___ W ___	___	___	Woven <input type="checkbox"/> Lamellar <input type="checkbox"/> Both <input type="checkbox"/>	Woven <input type="checkbox"/> Lamellar <input type="checkbox"/> Both <input type="checkbox"/>

SKELETON – Visual record form

Skeleton Number # \_\_\_\_\_  
 Observation Number # \_\_\_\_\_  
 Date \_\_\_\_/\_\_\_\_/\_\_\_\_

**3. Bone lesions labelling**

**4. Bone Sampling**

	<b>Right Fibula</b> <input type="radio"/> Yes <input type="radio"/> No Size (mm): L _____ / W _____ Photo: <input type="radio"/> Yes <input type="radio"/> No		<b>Left Fibula</b> <input type="radio"/> Yes <input type="radio"/> No Size (mm): L _____ / W _____ Photo: <input type="radio"/> Yes <input type="radio"/> No
---	--	---	---

COMMENTS:

---



---



---



---



---

SKELETON – Visual record form

Skeleton Number # \_\_\_\_\_  
 Observation Number # \_\_\_\_\_  
 Date \_\_\_\_/\_\_\_\_/\_\_\_\_

**1. Skeleton Biological Profile**

Age at death	Sex	Place of death	Cause of death	Additional data

**2. Periosteal Bone Reaction – Macroscopical analysis**

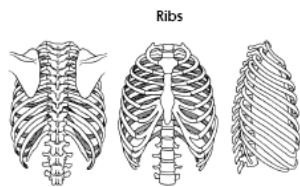
Bone Portion	Laterality	Distribution				Type		Metrics (mm)		Severity		Type of new bone	
		Dispersion		Occurrence		1 of 13		1 of 7		Left		Right	
		Left	Right	Left	Right	Left	Right	Left	Right	Left	Right	Left	Right
1	Unilateral <input type="radio"/> Bilateral <input type="radio"/>	Localized <input type="radio"/> Diffuse <input type="radio"/>	Localized <input type="radio"/> Diffuse <input type="radio"/>	Regular <input type="radio"/> Heterogeneous <input type="radio"/>	Regular <input type="radio"/> Heterogeneous <input type="radio"/>	____	____	L _____ W _____	L _____ W _____	____	____	Woven <input type="radio"/> Lamellar <input type="radio"/> Both <input type="radio"/>	Woven <input type="radio"/> Lamellar <input type="radio"/> Both <input type="radio"/>
2	Unilateral <input type="radio"/> Bilateral <input type="radio"/>	Localized <input type="radio"/> Diffuse <input type="radio"/>	Localized <input type="radio"/> Diffuse <input type="radio"/>	Regular <input type="radio"/> Heterogeneous <input type="radio"/>	Regular <input type="radio"/> Heterogeneous <input type="radio"/>	____	____	L _____ W _____	L _____ W _____	____	____	Woven <input type="radio"/> Lamellar <input type="radio"/> Both <input type="radio"/>	Woven <input type="radio"/> Lamellar <input type="radio"/> Both <input type="radio"/>
3	Unilateral <input type="radio"/> Bilateral <input type="radio"/>	Localized <input type="radio"/> Diffuse <input type="radio"/>	Localized <input type="radio"/> Diffuse <input type="radio"/>	Regular <input type="radio"/> Heterogeneous <input type="radio"/>	Regular <input type="radio"/> Heterogeneous <input type="radio"/>	____	____	L _____ W _____	L _____ W _____	____	____	Woven <input type="radio"/> Lamellar <input type="radio"/> Both <input type="radio"/>	Woven <input type="radio"/> Lamellar <input type="radio"/> Both <input type="radio"/>
4	Unilateral <input type="radio"/> Bilateral <input type="radio"/>	Localized <input type="radio"/> Diffuse <input type="radio"/>	Localized <input type="radio"/> Diffuse <input type="radio"/>	Regular <input type="radio"/> Heterogeneous <input type="radio"/>	Regular <input type="radio"/> Heterogeneous <input type="radio"/>	____	____	L _____ W _____	L _____ W _____	____	____	Woven <input type="radio"/> Lamellar <input type="radio"/> Both <input type="radio"/>	Woven <input type="radio"/> Lamellar <input type="radio"/> Both <input type="radio"/>
5	Unilateral <input type="radio"/> Bilateral <input type="radio"/>	Localized <input type="radio"/> Diffuse <input type="radio"/>	Localized <input type="radio"/> Diffuse <input type="radio"/>	Regular <input type="radio"/> Heterogeneous <input type="radio"/>	Regular <input type="radio"/> Heterogeneous <input type="radio"/>	____	____	L _____ W _____	L _____ W _____	____	____	Woven <input type="radio"/> Lamellar <input type="radio"/> Both <input type="radio"/>	Woven <input type="radio"/> Lamellar <input type="radio"/> Both <input type="radio"/>
6	Unilateral <input type="radio"/> Bilateral <input type="radio"/>	Localized <input type="radio"/> Diffuse <input type="radio"/>	Localized <input type="radio"/> Diffuse <input type="radio"/>	Regular <input type="radio"/> Heterogeneous <input type="radio"/>	Regular <input type="radio"/> Heterogeneous <input type="radio"/>	____	____	L _____ W _____	L _____ W _____	____	____	Woven <input type="radio"/> Lamellar <input type="radio"/> Both <input type="radio"/>	Woven <input type="radio"/> Lamellar <input type="radio"/> Both <input type="radio"/>
7	Unilateral <input type="radio"/> Bilateral <input type="radio"/>	Localized <input type="radio"/> Diffuse <input type="radio"/>	Localized <input type="radio"/> Diffuse <input type="radio"/>	Regular <input type="radio"/> Heterogeneous <input type="radio"/>	Regular <input type="radio"/> Heterogeneous <input type="radio"/>	____	____	L _____ W _____	L _____ W _____	____	____	Woven <input type="radio"/> Lamellar <input type="radio"/> Both <input type="radio"/>	Woven <input type="radio"/> Lamellar <input type="radio"/> Both <input type="radio"/>

SKELETON – Visual record form

Skeleton Number # \_\_\_\_  
 Observation Number # \_\_\_\_  
 Date \_\_\_\_/\_\_\_\_/\_\_\_\_

2. Periosteal Bone Reaction – Macroscopical analysis													
Bone Portion	Laterality	Distribution				Type		Metrics (mm)		Severity		Type of new bone	
		Dispersion		Occurrence		1 of 13				1 of 7			
		Left	Right	Left	Right	Left	Right	Left	Right	Left	Right	Left	Right
8	Unilateral <input type="radio"/> Bilateral <input type="radio"/>	Localized <input type="radio"/> Diffuse <input type="radio"/>	Localized <input type="radio"/> Diffuse <input type="radio"/>	Regular <input type="radio"/> Heterogeneous <input type="radio"/>	Regular <input type="radio"/> Heterogeneous <input type="radio"/>	____	____	L ____ W ____	L ____ W ____	____	____	Woven <input type="radio"/> Lamellar <input type="radio"/> Both <input type="radio"/>	Woven <input type="radio"/> Lamellar <input type="radio"/> Both <input type="radio"/>
9	Unilateral <input type="radio"/> Bilateral <input type="radio"/>	Localized <input type="radio"/> Diffuse <input type="radio"/>	Localized <input type="radio"/> Diffuse <input type="radio"/>	Regular <input type="radio"/> Heterogeneous <input type="radio"/>	Regular <input type="radio"/> Heterogeneous <input type="radio"/>	____	____	L ____ W ____	L ____ W ____	____	____	Woven <input type="radio"/> Lamellar <input type="radio"/> Both <input type="radio"/>	Woven <input type="radio"/> Lamellar <input type="radio"/> Both <input type="radio"/>
10	Unilateral <input type="radio"/> Bilateral <input type="radio"/>	Localized <input type="radio"/> Diffuse <input type="radio"/>	Localized <input type="radio"/> Diffuse <input type="radio"/>	Regular <input type="radio"/> Heterogeneous <input type="radio"/>	Regular <input type="radio"/> Heterogeneous <input type="radio"/>	____	____	L ____ W ____	L ____ W ____	____	____	Woven <input type="radio"/> Lamellar <input type="radio"/> Both <input type="radio"/>	Woven <input type="radio"/> Lamellar <input type="radio"/> Both <input type="radio"/>
11	Unilateral <input type="radio"/> Bilateral <input type="radio"/>	Localized <input type="radio"/> Diffuse <input type="radio"/>	Localized <input type="radio"/> Diffuse <input type="radio"/>	Regular <input type="radio"/> Heterogeneous <input type="radio"/>	Regular <input type="radio"/> Heterogeneous <input type="radio"/>	____	____	L ____ W ____	L ____ W ____	____	____	Woven <input type="radio"/> Lamellar <input type="radio"/> Both <input type="radio"/>	Woven <input type="radio"/> Lamellar <input type="radio"/> Both <input type="radio"/>
12	Unilateral <input type="radio"/> Bilateral <input type="radio"/>	Localized <input type="radio"/> Diffuse <input type="radio"/>	Localized <input type="radio"/> Diffuse <input type="radio"/>	Regular <input type="radio"/> Heterogeneous <input type="radio"/>	Regular <input type="radio"/> Heterogeneous <input type="radio"/>	____	____	L ____ W ____	L ____ W ____	____	____	Woven <input type="radio"/> Lamellar <input type="radio"/> Both <input type="radio"/>	Woven <input type="radio"/> Lamellar <input type="radio"/> Both <input type="radio"/>

3. Bone lesions labelling



4. Bone Sampling

Yes  No

Rib n°: \_\_\_\_\_

Size (mm):  
L \_\_\_\_ / W \_\_\_\_

Photo:  
 Yes  No

SKELETON – Visual record form

Skeleton Number # \_\_\_\_  
 Observation Number # \_\_\_\_  
 Date \_\_\_\_/\_\_\_\_/\_\_\_\_

1. Skeleton Biological Profile				
Age at death	Sex	Place of death	Cause of death	Additional data

2. Periosteal Bone Reaction – Macroscopical analysis													
Bone Portion	Laterality	Distribution				Type		Metrics (mm)		Severity		Type of new bone	
		Dispersion		Occurrence		1 of 13				1 of 7			
		Left	Right	Left	Right	Left	Right	Left	Right	Left	Right	Left	Right
1 <sup>st</sup> Metacarpal													
1	Unilateral <input type="radio"/> Bilateral <input type="radio"/>	Localized <input type="radio"/> Diffuse <input type="radio"/>	Localized <input type="radio"/> Diffuse <input type="radio"/>	Regular <input type="radio"/> Heterogeneous <input type="radio"/>	Regular <input type="radio"/> Heterogeneous <input type="radio"/>	____	____	L ____ W ____	L ____ W ____	____	____	Woven <input type="radio"/> Lamellar <input type="radio"/> Both <input type="radio"/>	Woven <input type="radio"/> Lamellar <input type="radio"/> Both <input type="radio"/>
2	Unilateral <input type="radio"/> Bilateral <input type="radio"/>	Localized <input type="radio"/> Diffuse <input type="radio"/>	Localized <input type="radio"/> Diffuse <input type="radio"/>	Regular <input type="radio"/> Heterogeneous <input type="radio"/>	Regular <input type="radio"/> Heterogeneous <input type="radio"/>	____	____	L ____ W ____	L ____ W ____	____	____	Woven <input type="radio"/> Lamellar <input type="radio"/> Both <input type="radio"/>	Woven <input type="radio"/> Lamellar <input type="radio"/> Both <input type="radio"/>
3	Unilateral <input type="radio"/> Bilateral <input type="radio"/>	Localized <input type="radio"/> Diffuse <input type="radio"/>	Localized <input type="radio"/> Diffuse <input type="radio"/>	Regular <input type="radio"/> Heterogeneous <input type="radio"/>	Regular <input type="radio"/> Heterogeneous <input type="radio"/>	____	____	L ____ W ____	L ____ W ____	____	____	Woven <input type="radio"/> Lamellar <input type="radio"/> Both <input type="radio"/>	Woven <input type="radio"/> Lamellar <input type="radio"/> Both <input type="radio"/>
2 <sup>nd</sup> Metacarpal													
1	Unilateral <input type="radio"/> Bilateral <input type="radio"/>	Localized <input type="radio"/> Diffuse <input type="radio"/>	Localized <input type="radio"/> Diffuse <input type="radio"/>	Regular <input type="radio"/> Heterogeneous <input type="radio"/>	Regular <input type="radio"/> Heterogeneous <input type="radio"/>	____	____	L ____ W ____	L ____ W ____	____	____	Woven <input type="radio"/> Lamellar <input type="radio"/> Both <input type="radio"/>	Woven <input type="radio"/> Lamellar <input type="radio"/> Both <input type="radio"/>
2	Unilateral <input type="radio"/> Bilateral <input type="radio"/>	Localized <input type="radio"/> Diffuse <input type="radio"/>	Localized <input type="radio"/> Diffuse <input type="radio"/>	Regular <input type="radio"/> Heterogeneous <input type="radio"/>	Regular <input type="radio"/> Heterogeneous <input type="radio"/>	____	____	L ____ W ____	L ____ W ____	____	____	Woven <input type="radio"/> Lamellar <input type="radio"/> Both <input type="radio"/>	Woven <input type="radio"/> Lamellar <input type="radio"/> Both <input type="radio"/>
3	Unilateral <input type="radio"/> Bilateral <input type="radio"/>	Localized <input type="radio"/> Diffuse <input type="radio"/>	Localized <input type="radio"/> Diffuse <input type="radio"/>	Regular <input type="radio"/> Heterogeneous <input type="radio"/>	Regular <input type="radio"/> Heterogeneous <input type="radio"/>	____	____	L ____ W ____	L ____ W ____	____	____	Woven <input type="radio"/> Lamellar <input type="radio"/> Both <input type="radio"/>	Woven <input type="radio"/> Lamellar <input type="radio"/> Both <input type="radio"/>

SKELETON – Visual record form

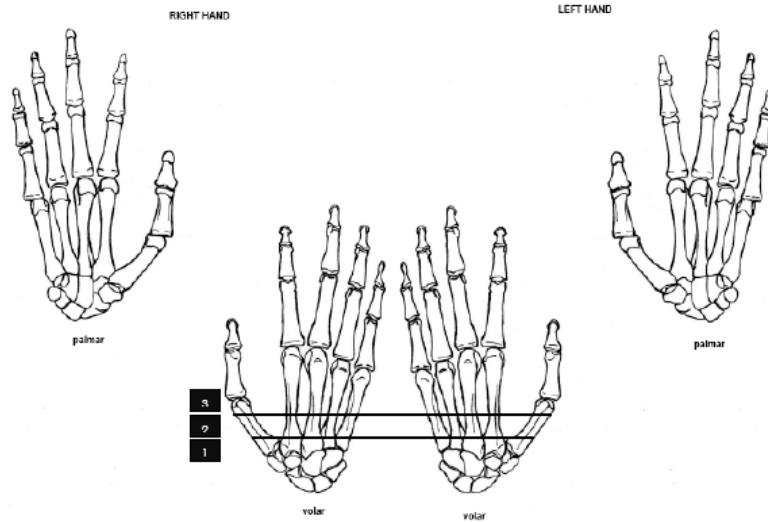
Skeleton Number # \_\_\_\_\_  
 Observation Number # \_\_\_\_\_  
 Date \_\_\_\_/\_\_\_\_/\_\_\_\_

2. Periosteal Bone Reaction – Macroscopical analysis															
Bone Portion	Laterality	Dispersion		Distribution		Occurrence		Type 1 of 13		Metrics (mm)		Severity 1 of 7		Type of new bone	
		Left	Right	Left	Right	Left	Right	Left	Right	L	W	L	R	Left	Right
<b>3<sup>rd</sup> Metacarpal</b>															
1	Unilateral <input type="radio"/> Bilateral <input type="radio"/>	Localized <input type="radio"/> Diffuse <input type="radio"/>	Localized <input type="radio"/> Diffuse <input type="radio"/>	Regular <input type="radio"/> Heterogeneous <input type="radio"/>	Regular <input type="radio"/> Heterogeneous <input type="radio"/>	___	___	___	___	L W	L W	___	___	Woven <input type="radio"/> Lamellar <input type="radio"/> Both <input type="radio"/>	Woven <input type="radio"/> Lamellar <input type="radio"/> Both <input type="radio"/>
2	Unilateral <input type="radio"/> Bilateral <input type="radio"/>	Localized <input type="radio"/> Diffuse <input type="radio"/>	Localized <input type="radio"/> Diffuse <input type="radio"/>	Regular <input type="radio"/> Heterogeneous <input type="radio"/>	Regular <input type="radio"/> Heterogeneous <input type="radio"/>	___	___	___	___	L W	L W	___	___	Woven <input type="radio"/> Lamellar <input type="radio"/> Both <input type="radio"/>	Woven <input type="radio"/> Lamellar <input type="radio"/> Both <input type="radio"/>
3	Unilateral <input type="radio"/> Bilateral <input type="radio"/>	Localized <input type="radio"/> Diffuse <input type="radio"/>	Localized <input type="radio"/> Diffuse <input type="radio"/>	Regular <input type="radio"/> Heterogeneous <input type="radio"/>	Regular <input type="radio"/> Heterogeneous <input type="radio"/>	___	___	___	___	L W	L W	___	___	Woven <input type="radio"/> Lamellar <input type="radio"/> Both <input type="radio"/>	Woven <input type="radio"/> Lamellar <input type="radio"/> Both <input type="radio"/>
<b>4<sup>th</sup> Metacarpal</b>															
1	Unilateral <input type="radio"/> Bilateral <input type="radio"/>	Localized <input type="radio"/> Diffuse <input type="radio"/>	Localized <input type="radio"/> Diffuse <input type="radio"/>	Regular <input type="radio"/> Heterogeneous <input type="radio"/>	Regular <input type="radio"/> Heterogeneous <input type="radio"/>	___	___	___	___	L W	L W	___	___	Woven <input type="radio"/> Lamellar <input type="radio"/> Both <input type="radio"/>	Woven <input type="radio"/> Lamellar <input type="radio"/> Both <input type="radio"/>
2	Unilateral <input type="radio"/> Bilateral <input type="radio"/>	Localized <input type="radio"/> Diffuse <input type="radio"/>	Localized <input type="radio"/> Diffuse <input type="radio"/>	Regular <input type="radio"/> Heterogeneous <input type="radio"/>	Regular <input type="radio"/> Heterogeneous <input type="radio"/>	___	___	___	___	L W	L W	___	___	Woven <input type="radio"/> Lamellar <input type="radio"/> Both <input type="radio"/>	Woven <input type="radio"/> Lamellar <input type="radio"/> Both <input type="radio"/>
3	Unilateral <input type="radio"/> Bilateral <input type="radio"/>	Localized <input type="radio"/> Diffuse <input type="radio"/>	Localized <input type="radio"/> Diffuse <input type="radio"/>	Regular <input type="radio"/> Heterogeneous <input type="radio"/>	Regular <input type="radio"/> Heterogeneous <input type="radio"/>	___	___	___	___	L W	L W	___	___	Woven <input type="radio"/> Lamellar <input type="radio"/> Both <input type="radio"/>	Woven <input type="radio"/> Lamellar <input type="radio"/> Both <input type="radio"/>
<b>5<sup>th</sup> Metacarpal</b>															
1	Unilateral <input type="radio"/> Bilateral <input type="radio"/>	Localized <input type="radio"/> Diffuse <input type="radio"/>	Localized <input type="radio"/> Diffuse <input type="radio"/>	Regular <input type="radio"/> Heterogeneous <input type="radio"/>	Regular <input type="radio"/> Heterogeneous <input type="radio"/>	___	___	___	___	L W	L W	___	___	Woven <input type="radio"/> Lamellar <input type="radio"/> Both <input type="radio"/>	Woven <input type="radio"/> Lamellar <input type="radio"/> Both <input type="radio"/>
2	Unilateral <input type="radio"/> Bilateral <input type="radio"/>	Localized <input type="radio"/> Diffuse <input type="radio"/>	Localized <input type="radio"/> Diffuse <input type="radio"/>	Regular <input type="radio"/> Heterogeneous <input type="radio"/>	Regular <input type="radio"/> Heterogeneous <input type="radio"/>	___	___	___	___	L W	L W	___	___	Woven <input type="radio"/> Lamellar <input type="radio"/> Both <input type="radio"/>	Woven <input type="radio"/> Lamellar <input type="radio"/> Both <input type="radio"/>
3	Unilateral <input type="radio"/> Bilateral <input type="radio"/>	Localized <input type="radio"/> Diffuse <input type="radio"/>	Localized <input type="radio"/> Diffuse <input type="radio"/>	Regular <input type="radio"/> Heterogeneous <input type="radio"/>	Regular <input type="radio"/> Heterogeneous <input type="radio"/>	___	___	___	___	L W	L W	___	___	Woven <input type="radio"/> Lamellar <input type="radio"/> Both <input type="radio"/>	Woven <input type="radio"/> Lamellar <input type="radio"/> Both <input type="radio"/>

SKELETON – Visual record form

Skeleton Number # \_\_\_\_\_  
 Observation Number # \_\_\_\_\_  
 Date \_\_\_\_/\_\_\_\_/\_\_\_\_

3. Bone lesions labelling



4. Bone Sampling

Yes  No

Metacarpal bone:

Size (mm):  
 L \_\_\_\_\_ / W \_\_\_\_\_

Photo:  
 Yes  No

COMMENTS:  
 \_\_\_\_\_  
 \_\_\_\_\_  
 \_\_\_\_\_

SKELETON – Visual record form

Skeleton Number # \_\_\_\_\_  
 Observation Number # \_\_\_\_\_  
 Date \_\_\_\_/\_\_\_\_/\_\_\_\_

1. Skeleton Biological Profile				
Age at death	Sex	Place of death	Cause of death	Additional data

2. Periosteal Bone Reaction – Macroscopical analysis													
Bone Portion	Laterality	Distribution				Type		Metrics (mm)		Severity		Type of new bone	
		Dispersion		Occurrence		1 of 13		1 of 7		1 of 7		1 of 7	
		Left	Right	Left	Right	Left	Right	Left	Right	Left	Right	Left	Right
<b>1<sup>st</sup> Metatarsal</b>													
1	Unilateral <input type="radio"/> Bilateral <input type="radio"/>	Localized <input type="radio"/> Diffuse <input type="radio"/>	Localized <input type="radio"/> Diffuse <input type="radio"/>	Regular <input type="radio"/> Heterogeneous <input type="radio"/>	Regular <input type="radio"/> Heterogeneous <input type="radio"/>	___	___	L W	L W	___	___	Woven <input type="radio"/> Lamellar <input type="radio"/> Both <input type="radio"/>	Woven <input type="radio"/> Lamellar <input type="radio"/> Both <input type="radio"/>
2	Unilateral <input type="radio"/> Bilateral <input type="radio"/>	Localized <input type="radio"/> Diffuse <input type="radio"/>	Localized <input type="radio"/> Diffuse <input type="radio"/>	Regular <input type="radio"/> Heterogeneous <input type="radio"/>	Regular <input type="radio"/> Heterogeneous <input type="radio"/>	___	___	L W	L W	___	___	Woven <input type="radio"/> Lamellar <input type="radio"/> Both <input type="radio"/>	Woven <input type="radio"/> Lamellar <input type="radio"/> Both <input type="radio"/>
3	Unilateral <input type="radio"/> Bilateral <input type="radio"/>	Localized <input type="radio"/> Diffuse <input type="radio"/>	Localized <input type="radio"/> Diffuse <input type="radio"/>	Regular <input type="radio"/> Heterogeneous <input type="radio"/>	Regular <input type="radio"/> Heterogeneous <input type="radio"/>	___	___	L W	L W	___	___	Woven <input type="radio"/> Lamellar <input type="radio"/> Both <input type="radio"/>	Woven <input type="radio"/> Lamellar <input type="radio"/> Both <input type="radio"/>
<b>2<sup>nd</sup> Metatarsal</b>													
1	Unilateral <input type="radio"/> Bilateral <input type="radio"/>	Localized <input type="radio"/> Diffuse <input type="radio"/>	Localized <input type="radio"/> Diffuse <input type="radio"/>	Regular <input type="radio"/> Heterogeneous <input type="radio"/>	Regular <input type="radio"/> Heterogeneous <input type="radio"/>	___	___	L W	L W	___	___	Woven <input type="radio"/> Lamellar <input type="radio"/> Both <input type="radio"/>	Woven <input type="radio"/> Lamellar <input type="radio"/> Both <input type="radio"/>
2	Unilateral <input type="radio"/> Bilateral <input type="radio"/>	Localized <input type="radio"/> Diffuse <input type="radio"/>	Localized <input type="radio"/> Diffuse <input type="radio"/>	Regular <input type="radio"/> Heterogeneous <input type="radio"/>	Regular <input type="radio"/> Heterogeneous <input type="radio"/>	___	___	L W	L W	___	___	Woven <input type="radio"/> Lamellar <input type="radio"/> Both <input type="radio"/>	Woven <input type="radio"/> Lamellar <input type="radio"/> Both <input type="radio"/>
3	Unilateral <input type="radio"/> Bilateral <input type="radio"/>	Localized <input type="radio"/> Diffuse <input type="radio"/>	Localized <input type="radio"/> Diffuse <input type="radio"/>	Regular <input type="radio"/> Heterogeneous <input type="radio"/>	Regular <input type="radio"/> Heterogeneous <input type="radio"/>	___	___	L W	L W	___	___	Woven <input type="radio"/> Lamellar <input type="radio"/> Both <input type="radio"/>	Woven <input type="radio"/> Lamellar <input type="radio"/> Both <input type="radio"/>

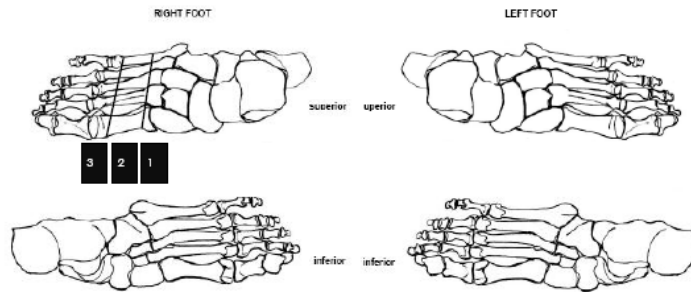
SKELETON – Visual record form

Skeleton Number # \_\_\_\_\_  
 Observation Number # \_\_\_\_\_  
 Date \_\_\_\_/\_\_\_\_/\_\_\_\_

2. Periosteal Bone Reaction – Macroscopical analysis													
Bone Portion	Laterality	Distribution				Type		Metrics (mm)		Severity		Type of new bone	
		Dispersion		Occurrence		1 of 13		1 of 7		1 of 7		1 of 7	
		Left	Right	Left	Right	Left	Right	Left	Right	Left	Right	Left	Right
<b>3<sup>rd</sup> Metatarsal</b>													
1	Unilateral <input type="radio"/> Bilateral <input type="radio"/>	Localized <input type="radio"/> Diffuse <input type="radio"/>	Localized <input type="radio"/> Diffuse <input type="radio"/>	Regular <input type="radio"/> Heterogeneous <input type="radio"/>	Regular <input type="radio"/> Heterogeneous <input type="radio"/>	___	___	L W	L W	___	___	Woven <input type="radio"/> Lamellar <input type="radio"/> Both <input type="radio"/>	Woven <input type="radio"/> Lamellar <input type="radio"/> Both <input type="radio"/>
2	Unilateral <input type="radio"/> Bilateral <input type="radio"/>	Localized <input type="radio"/> Diffuse <input type="radio"/>	Localized <input type="radio"/> Diffuse <input type="radio"/>	Regular <input type="radio"/> Heterogeneous <input type="radio"/>	Regular <input type="radio"/> Heterogeneous <input type="radio"/>	___	___	L W	L W	___	___	Woven <input type="radio"/> Lamellar <input type="radio"/> Both <input type="radio"/>	Woven <input type="radio"/> Lamellar <input type="radio"/> Both <input type="radio"/>
3	Unilateral <input type="radio"/> Bilateral <input type="radio"/>	Localized <input type="radio"/> Diffuse <input type="radio"/>	Localized <input type="radio"/> Diffuse <input type="radio"/>	Regular <input type="radio"/> Heterogeneous <input type="radio"/>	Regular <input type="radio"/> Heterogeneous <input type="radio"/>	___	___	L W	L W	___	___	Woven <input type="radio"/> Lamellar <input type="radio"/> Both <input type="radio"/>	Woven <input type="radio"/> Lamellar <input type="radio"/> Both <input type="radio"/>
<b>4<sup>th</sup> Metatarsal</b>													
1	Unilateral <input type="radio"/> Bilateral <input type="radio"/>	Localized <input type="radio"/> Diffuse <input type="radio"/>	Localized <input type="radio"/> Diffuse <input type="radio"/>	Regular <input type="radio"/> Heterogeneous <input type="radio"/>	Regular <input type="radio"/> Heterogeneous <input type="radio"/>	___	___	L W	L W	___	___	Woven <input type="radio"/> Lamellar <input type="radio"/> Both <input type="radio"/>	Woven <input type="radio"/> Lamellar <input type="radio"/> Both <input type="radio"/>
2	Unilateral <input type="radio"/> Bilateral <input type="radio"/>	Localized <input type="radio"/> Diffuse <input type="radio"/>	Localized <input type="radio"/> Diffuse <input type="radio"/>	Regular <input type="radio"/> Heterogeneous <input type="radio"/>	Regular <input type="radio"/> Heterogeneous <input type="radio"/>	___	___	L W	L W	___	___	Woven <input type="radio"/> Lamellar <input type="radio"/> Both <input type="radio"/>	Woven <input type="radio"/> Lamellar <input type="radio"/> Both <input type="radio"/>
3	Unilateral <input type="radio"/> Bilateral <input type="radio"/>	Localized <input type="radio"/> Diffuse <input type="radio"/>	Localized <input type="radio"/> Diffuse <input type="radio"/>	Regular <input type="radio"/> Heterogeneous <input type="radio"/>	Regular <input type="radio"/> Heterogeneous <input type="radio"/>	___	___	L W	L W	___	___	Woven <input type="radio"/> Lamellar <input type="radio"/> Both <input type="radio"/>	Woven <input type="radio"/> Lamellar <input type="radio"/> Both <input type="radio"/>
<b>5<sup>th</sup> Metatarsal</b>													
1	Unilateral <input type="radio"/> Bilateral <input type="radio"/>	Localized <input type="radio"/> Diffuse <input type="radio"/>	Localized <input type="radio"/> Diffuse <input type="radio"/>	Regular <input type="radio"/> Heterogeneous <input type="radio"/>	Regular <input type="radio"/> Heterogeneous <input type="radio"/>	___	___	L W	L W	___	___	Woven <input type="radio"/> Lamellar <input type="radio"/> Both <input type="radio"/>	Woven <input type="radio"/> Lamellar <input type="radio"/> Both <input type="radio"/>
2	Unilateral <input type="radio"/> Bilateral <input type="radio"/>	Localized <input type="radio"/> Diffuse <input type="radio"/>	Localized <input type="radio"/> Diffuse <input type="radio"/>	Regular <input type="radio"/> Heterogeneous <input type="radio"/>	Regular <input type="radio"/> Heterogeneous <input type="radio"/>	___	___	L W	L W	___	___	Woven <input type="radio"/> Lamellar <input type="radio"/> Both <input type="radio"/>	Woven <input type="radio"/> Lamellar <input type="radio"/> Both <input type="radio"/>
3	Unilateral <input type="radio"/> Bilateral <input type="radio"/>	Localized <input type="radio"/> Diffuse <input type="radio"/>	Localized <input type="radio"/> Diffuse <input type="radio"/>	Regular <input type="radio"/> Heterogeneous <input type="radio"/>	Regular <input type="radio"/> Heterogeneous <input type="radio"/>	___	___	L W	L W	___	___	Woven <input type="radio"/> Lamellar <input type="radio"/> Both <input type="radio"/>	Woven <input type="radio"/> Lamellar <input type="radio"/> Both <input type="radio"/>

SKELETON – Visual record form

**3. Bone lesions labelling**



Skeleton Number # \_\_\_\_  
 Observation Number # \_\_\_\_  
 Date \_\_\_\_/\_\_\_\_/\_\_\_\_

**4. Bone Sampling**

<input type="checkbox"/> Yes <input type="checkbox"/> No
Metatarsal bone:
Size (mm): L ____ / W ____
Photo: <input type="checkbox"/> Yes <input type="checkbox"/> No

COMMENTS:

---



---



---



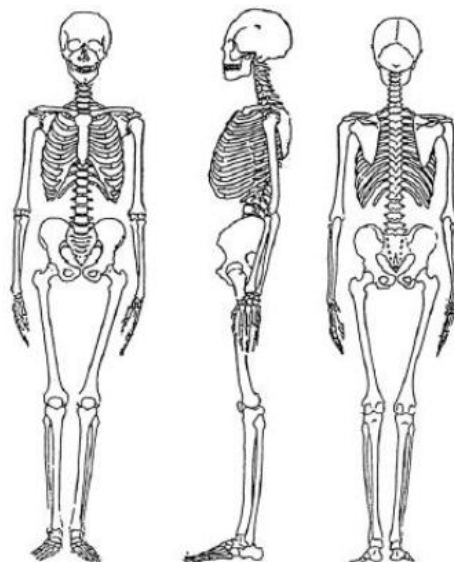
---



---

SKELETON – Visual record form

ADULT SKELETON



Skeleton Number # \_\_\_\_  
 Observation Number # \_\_\_\_  
 Date \_\_\_\_/\_\_\_\_/\_\_\_\_

Figure I.I: Skeleton's record form used to collect data.





